



The  
University  
Of  
Sheffield.



**E-Futures**

# Salt Stress in Two *Chlamydomonas* Species: Novel Insights into Biofuel Production from Microalgae

---

By: Emily Hounslow (MBiolSci)

Thesis submitted for the degree of Doctor of Philosophy (PhD)

Department of Chemical and Biological Engineering and Department of  
Molecular Biology and Biotechnology  
University of Sheffield

Submitted June 2016



## Summary

This thesis aims to find ways of increasing lipid content in algal biomass for biofuel production, by using complimentary metabolomic and proteomic data to increase understanding of the mechanisms that control lipid accumulation. Salt stress was investigated as a potential lipid trigger in two microalgae: a starchless mutant (CC-4325) of the model species *Chlamydomonas reinhardtii* and the snow alga *Chlamydomonas nivalis*. Gas chromatographic fatty acid (FA) analysis of both algae grown in a range of salt concentrations revealed a complex relationship between salinity and lipid accumulation in the two species. iTRAQ proteomic analysis was used to study the molecular mechanisms of each species under salt stress. *Chlamydomonas reinhardtii* showed little accumulation of lipids under salt stress, but some changes in lipid profile. Part of these analyses have been published in a study by Hounslow et al. (2016a).

*Chlamydomonas nivalis* cells showed a large increase over time of the monounsaturated FA C18:1*cis* when grown in 0.2 M NaCl. As monounsaturated FAs are one of the best FA types for biofuel properties, an increase in this FA is ideal for biofuel production. Use of *C. nivalis* as a homologous species to *C. reinhardtii* revealed novel proteomic analysis of lipid accumulation in this species, and a comparison of the proteomic responses of both species under salt stress was used to elucidate why salt triggers lipid accumulation in one species but not the other. Most notably, the rate-limiting enzyme in the fatty acid biosynthesis pathway, acetyl CoA-carboxylase, was found to be down-regulated in *C. reinhardtii* cultures in 0.2 M NaCl, but was not affected in *C. nivalis* cultures in 0.2 M NaCl. A number of enzymes involved in the availability of acetyl CoA for fatty acid synthesis were differently affected by salt stress in the two species. Halotolerance appears to play an important role in the ability of cultures to accumulate lipids under salt conditions.

The work in this thesis has contributed to two recent publications. The problem of reliable lipid quantification techniques for microalgae was discussed using experimental data and is addressed in a comprehensive published review by Hounslow et al. (2016b). This review

includes analysis of method requirements and construction of decision trees to guide future researchers.

## Acknowledgements

Many thanks to the University of Sheffield for giving me this opportunity to earn my PhD, to my supervisors Dr Jim Gilmour and Professor Phillip Wright for not only their academic guidance but also their support and understanding throughout the process. Working with two supervisors with such expertise in Chemical and Biological Engineering and in Molecular Biology has been a privilege. I came to be doing this PhD through the Energy Futures Doctoral Training Centre, which EPSRC has funded, and whom I would both like to thank. Energy Futures and everyone who was part of it inspired me in the area of Renewable Energy research and led me to this project on algal biofuels. I worked between two laboratories in Chemical and Biological Engineering and in Molecular Biology and Biotechnology, and both teams were fantastic to work with.

There were a great many people who worked with me in the laboratories and taught me many of the skills I needed to complete this work. Dr Jim Gilmour first introduced me to algal research and taught me algal culturing, gravimetric lipid analysis and chlorophyll analysis techniques. Dr Joseph Longworth guided me in algal culturing, Nile Red analysis, proteomic techniques and proteomic data processing; Dr Caroline Evans has given me great guidance in the processing and understanding of proteomic data; Dr Narciso Couto has taught me a great deal about both protein extraction and preparation techniques and principles, and mass spectrometry, and he has also dedicated a great number of hours to helping me carry out these techniques in the laboratory. Dr Rahul Kapoore taught me techniques in transesterification of fatty acids and analysis through gas chromatography, and Mark Jones gave me many hours of help in running the GC. Richard Smith taught me to use the oxygen electrode for photosynthesis and respiration analysis. Dr Krys Bangert gave me a great deal of help in many aspects of algal culturing during the first couple of years of the project, and taught me colorimetric techniques for lipid measurement. Dr

Esther Karunakaran taught me to use the Tecan plate reader. To all these great researchers, thank you for your time and expertise.

I'd like to thank all members of the Algal Biotechnology Sheffield network for their support and good company, especially those I have worked closely with in the laboratory, including Richard Smith, Joseph Longworth, Danying Wu, David Russo, Thomas Sydney, Dr Jagroop Pandhal, Gloria Padmaperuma, Maria Huete-Ortega and Katarzyna Okurowska.

I'd like to thank all those at Colorado State University in the algal proteomics research group for having me as a visiting researcher to study their techniques, especially Dr Seijin Park, Tara Schumacher and Professor Kenneth Reardon. My time working with this group was so valuable and a great experience.

Many thanks to Dr Josselin Noirel for helping me with statistics and for data mining for the review of lipid measurement papers. Many thanks to Andrew Landels and Dr Khoa Pham for help with processing proteomics data. Thank you to Michael De Selincourt, Martin De Selincourt, Gideon Jones, Alister Harlow, Penny Hounslow, Thomas Sydney and Katherine Fish for proof reading.

Thanks to my friends for keeping me going through this process, especially to my second family "Undermind", the "Lydgate Ladies", Alex Williams, Dr Katharine Fish, Kate Davis, Steph Thompson, Deya Brown, and to my wonderfully supportive boyfriend Thomas Sydney.

Finally thank you to my family (Penny, Fred, John, Katharine, Kevin, Carla, Will and Alex), who gave me so much love and support throughout this project. I owe all the opportunities I had that led to me carrying out this project to my parents, Fred and Penny Hounslow, who have always supported and encouraged me in my work. I dedicate this thesis to them, and thank them so much for being the most wonderful, loving and supportive parents I could wish for.

## Table of Contents

Summary .....	3
Acknowledgements.....	5
Table of Contents .....	7
List of abbreviations and acronyms .....	12
1 Introduction, background and literature review .....	16
1.1 Introduction to algal biofuels .....	16
1.2 Literature review .....	22
1.3 Aims of this PhD thesis .....	59
2 Chapter 2: Materials and Methods.....	62
2.1 Experimental design .....	62
2.2 Algal species .....	68
2.3 Algal culturing.....	68
2.4 Biological parameters.....	74
2.5 Algal lipids.....	79
2.6 Proteomics.....	84
2.7 18S rDNA sequencing .....	93
3 Chapter 3: Salt stress experiments in <i>C. reinhardtii</i> using different lipid measurement techniques.....	96
3.1 Summary.....	96

3.2	Preliminary data for wild type <i>C. reinhardtii</i> grown in a range of salt media (0, 0.05, 0.1, 0.15, 0.2 and 0.25 M NaCl).....	96
3.3	Discussion of lipid analysis techniques tested .....	115
3.4	Discussion of salt conditions and strains used .....	116
3.5	Conclusions.....	118
4	Chapter 4: The Effect of Salt Stress on Lipid Metabolism of <i>Chlamydomonas reinhardtii</i> (CC-4325) A Starchless Mutant .....	119
4.1	Summary.....	119
4.2	Introduction.....	119
4.3	Results and Discussion .....	120
4.4	iTRAQ investigation of the effect of 0.2 M NaCl on the proteome of <i>C. reinhardtii</i> 151	
4.5	Chapter Discussion and Conclusions.....	188
5	Chapter 5: The Effect of Salt Stress on Lipid Metabolism of <i>Chlamydomonas nivalis</i> .....	193
5.1	Summary.....	193
5.2	Introduction.....	193
5.3	Preliminary data .....	195
5.4	Response of <i>C. nivalis</i> to high salt (1.4 M NaCl).....	202
5.3.6	Photosynthesis and respiration activity in <i>C. nivalis</i> under 1.4 M NaCl conditions .....	211
5.5	Effect of 0.2 M NaCl on <i>C. nivalis</i> .....	213

5.6	Conclusions from 0.2 M NaCl experiment.....	238
5.7	Genetic identification in <i>C. nivalis</i> .....	240
5.8	Proteomic investigation of <i>C. nivalis</i> under lipid triggering 0.2 M NaCl salt conditions using iTRAQ.....	248
5.9	Chapter Discussion and Conclusions .....	282
6	Chapter 6: Comparison of <i>C. nivalis</i> data and <i>C. reinhardtii</i> proteomic data and discussion .....	285
6.1	Summary.....	285
6.2	Introduction.....	285
6.3	Results and Discussion .....	288
6.4	Discussion of important lipid metabolism proteins .....	303
6.5	Conclusions.....	305
7	Chapter 7: Thesis discussion, conclusions and future work .....	308
7.1	Overview.....	308
7.2	Data summary .....	308
7.3	Discussion of thesis aims .....	309
7.4	How iTRAQ has helped to address the question of which mechanisms are controlling lipid production under salt stress .....	313
7.5	Discussion of the use of lipid measurement methods.....	314
7.6	Implications of salt stress for biofuels production generally and in temperate Europe .....	314

7.7	Limitations of the research .....	317
7.8	Questions raised by the research.....	317
7.9	Conclusions.....	318
7.10	Future work .....	320
8	References .....	323
9	Appendix A: protocols .....	354
9.1	Growth media protocols .....	354
9.2	PBS 1x Buffer solution protocol .....	356
10	Appendix B: Lipid quantification techniques for screening oleaginous species of microalgae for biofuel production .....	357
10.1	Abstract .....	357
10.2	<i>Introduction</i> .....	358
10.3	Table 1 Summary of lipid quantification techniques in microalgae.....	363
10.4	<i>Prevalence of lipid techniques in literature</i> .....	366
10.5	<i>Choosing a suitable lipid measurement technique</i> .....	368
10.6	<i>Characteristics of lipid quantification techniques</i> .....	370
10.7	<i>Fluorescent lipid probes</i> .....	371
10.8	<i>Gravimetry</i> .....	378
10.9	<i>Direct (In-situ) transesterification</i> .....	383
10.10	<i>Raman spectroscopy</i> .....	386

10.11	<i>Chromatography and Mass Spectrometry</i> .....	389
10.12	<i>Colorimetric techniques</i> .....	397
10.13	<i>NMR</i> .....	399
10.14	<i>FTIR</i> .....	400
10.15	<i>Miscellaneous techniques</i> .....	402
10.16	<i>Conclusions</i> .....	403
10.17	Acknowledgements .....	404
10.18	References .....	404
10.19	Appendix 1 .....	441
11	Appendix C: Supplementary material from Chapter 4 .....	445
11.1	<i>C. reinhardtii</i> Experiment 1 data .....	445
11.2	Bradford protein quantification .....	454
11.3	Protein changes between phenotypes in iTRAQ experiment .....	454
12	Appendix D: Supplementary Material from Chapter 5.....	476
12.1	Cell count data.....	476
12.2	FAME profile for <i>C. nivalis</i> grown in 0.2 M NaCl conditions .....	480
12.3	Preliminary investigation of proteomic identification of <i>C. nivalis</i> proteins using <i>C. reinhardtii</i> and <i>chlorophyta</i> databases .....	481
12.4	Protein changes for iTRAQ experiments .....	486

## List of abbreviations and acronyms

2-DE	Two dimensional electrophoresis
ACCase	Acetyl CoA carboxylase
ACN	Acetonitrile
ADP	Adenosine diphosphate
ASTM	American Society for Testing and Materials
ATP	Adenosine triphosphate
BAE	Biomass accumulation efficiency
BD	Bligh and Dyer
BODIPY	Boron-dipyrromethene
BSA	Bovine albumin serum
CID	Collision induced dissociation
cICAT	Cleavable isotope-coded affinity tags
CS	Cequier-Sánchez
DAG	Diacylglyceride
DCW	Dry cell weight
DGDG	Digalactosyldiacylglycerol
DGTS	Diacylglyceryl trimethylhomoserine
DIGE	Difference gel electrophoresis
DMSO	Dimethyl sulfoxide
DNA	Deoxyribonucleic acid
DT	Direct transesterification
EC	Enzyme commission
EDTA	Ethylenediaminetetraacetic acid
EI-MS	Electron ionisation mass spectrometry

EST	Expressed sequence tag
FA	Fatty acid
FAAE	Fatty acid acyl ester
FAME	Fatty acid methyl ester
FDR	False discovery rate
FFA	Free fatty acids
FID	Flame ionisation detector
FM	Folch method
FTIR	Fourier transform infrared spectroscopy
GC	Gas chromatography
GC-GC	Two-dimensional gas chromatography
GCMS	Gas chromatography coupled mass spectrometry
GM	Garcia method
HILIC	High-resolution hydrophobic interaction chromatography
HPLC	High performance liquid chromatography
ID	Identification
iTRAQ	Isobaric tag for relative and absolute quantification
KEGG	Kyoto Encyclopedia of Genes and Genomes
LC	Liquid chromatography
LC-MS	Liquid chromatography coupled mass spectrometry
LHCI	Light harvesting complex I
LHCII	Light harvesting complex II
LRC	Lepage and Roy method
M	Molarity
MALDI	Matrix-assisted laser desorption ionization
MGDG	Monogalactosyl diacylglycerol

MLDP	Major lipid droplet protein gene
MMTS	Methyl methane-thiosulfonate
MS	Mass spectrometry
MTBE	Methyl tert-butyl ether
MUFA	Monounsaturated fatty acid
NADH	Nicotinamide adenine dinucleotide
NMR	Nuclear magnetic resonance
OD	Optical density
PAGE	Polyacrylamide gel electrophoresis
PBR	Photobioreactor
PBS	Phosphate buffered saline
PCA	Principle component analysis
PE	Phosphatidylethanolamine
PG	Phosphatidylglycerol
PI	Phosphatidylinositol
PPM	Parts per million
PSI	Photosystem I
PSII	Photosystem II
PSM	Peptide spectrum match
PTM	Post translational modification
PUFA	Polyunsaturated fatty acid
Q-TOF	Quadrupole time of flight
RNA	Ribonucleic acid
ROS	Reactive oxygen species
SCX	Strong cation exchange
SDS	Sodium dodecyl sulfate

SFA	Saturated fatty acid
SILAC	Stable isotope labeling by amino acids in cell culture
SPV	Sulfo-phospho-vanillin
SQDG	Sulfoquinovosyldiacylglycerol
TAG	Triacylglyceride or Triacylglycerol
TAP	Tris acetate phosphate
TCA	Trichloroacetic acid
TCEP	Tris-(2-carboxyethyl)-phosphine
TD-NMR	Time domain nuclear magnetic resonance
TEAB	Tetraethylammonium bromide
TEA-Cu	Triethanolamine-copper salts
TEMED	Tetramethylethylenediamine
TFA	Total fatty acids
TL	Total lipid
TLC	Thin layer chromatography
TOF	Time of flight
VOC	Volatile organic compound
VSN	Variance stabilization normalisation

# 1 Introduction, background and literature review

As fossil fuels continue to deplete, the search for ways to utilise the energy in natural resources to meet the electricity and fuel demands of our world continues. A clean renewable energy source is required to prevent further rises in greenhouse gases. Atmospheric carbon dioxide has been increasing steadily since 1750, and is now 142% of the 1750 levels. It increased by 2.9 ppm (parts per million) from 2012 to 2013, a relative increase of 0.74% for that year (World Meteorological Organization, 2014). One essentially unlimited source of energy is light from the sun. Photosynthetic organisms provide a natural and abundant mechanism for converting sunlight into chemical energy, and therefore provide an obvious choice in the search for new energy sources. This chapter introduces and explores the potential for biofuels from microalgae to help meet the requirement for a clean renewable energy source.

## 1.1 Introduction to algal biofuels

The first generation of biofuels was based on crop plants as the feedstock and bioethanol as the product. First generation biofuels were modelled on the successful bioethanol industry in Brazil using sugar cane, which has existed since the 1970s (Goldemberg, 2007). Subsequently the US and Europe have adopted first generation biofuels from about 2003 onwards using corn/maize as the feedstock. However, it became apparent that there were a number of problems with first generation biofuels including a negative impact on food security, the requirement for large amounts of high quality agricultural land and a Greenhouse Gas balance that was not favourable once full life cycle analyses had been carried out (Mohr and Raman, 2013). Second generation biofuels were developed in response to the problems associated with first generation biofuels and utilize non crop plants such as switchgrass or willow, or by-products of agriculture such as straw (Mohr and Raman, 2013). The main drawback of second generation biofuels is the recalcitrance of cellulose, hemi-cellulose and lignin to being broken down into suitable substrates for

fuel production (Himmel *et al.*, 2007). Due to the problems associated with first and second generation biofuels, research is now focussing on the possibilities of third generation biofuels based on microalgae (Leite *et al.*, 2013).

"Microalgae" are normally defined as microscopic (often single celled) photosynthetic organisms, which can be either prokaryotic (cyanobacteria) or eukaryotic (Li *et al.*, 2008b). It is estimated that more than 50,000 species exist, and that they are present in every ecosystem on Earth (Richmond, 2004), demonstrating the huge diversity within the group. Microalgae are highly efficient at converting sunlight into useful products such as lipids, which can be converted into biofuels. A lipid is defined as an organic compound that is insoluble in water but soluble in organic solvents; these comprise fatty acids and their derivatives. A triacylglyceride (TAG) is a lipid comprising three fatty acids and a glycerol backbone (see Figure 1.1) (Merchant *et al.*, 2012).

Microalgae can produce TAGs in abundance under certain conditions, and this is highly desirable because TAGs can be easily converted by transesterification to biodiesel (Fjerbaek *et al.*, 2009), the process for which is demonstrated in Figure 1.2. There are thousands of species, and many are highly oleaginous, producing different types of lipids (Harwood and Guschina, 2009). The vast number and diversity of extant species allows for a high diversity of lipid profiles that can be selectively screened to find desirable strains for biodiesel production.

[Image removed for copyright reasons]

Figure 1.1 Chemical structure of TAG, comprising 3 fatty acid chains and a glycerol backbone. Image taken from Merchant *et al.* (2012).

[Image removed for copyright reasons]

Figure 1.2 Chemical reaction of transesterification of TAG to fatty acid methyl esters (FAME) or biodiesel. Image taken from Scott *et al.* (2010).

Microalgae are better candidates for biofuel sources than land crops; they provide a lower demand for land and intensive agricultural practices (Chisti, 2008), and a higher efficiency of overall oil content per biomass of crop (Chisti, 2007). They may also provide a more feasible opportunity for genetic engineering than higher plants, due to the relative simplicity of biosynthesis and glycerolipid assembly in algae species, for example in *Chlamydomonas* sp., compared to that of higher plants such as *Arabidopsis* (Riekhof *et al.*, 2005). To date, the state of genetic engineering of microalgae is still in its infancy, however, engineering tools continue to be developed and validated in *Chlamydomonas reinhardtii* (Rasala *et al.*, 2014). Microalgae can use only sunlight, carbon dioxide and some vital nutrient sources as inputs, though many species can also grow

heterotrophically on carbon sources or mixotrophically (Liang *et al.*, 2009; Moon *et al.*, 2013).

No biofuel has yet achieved price parity with petroleum derived fuels, including algal biodiesel (Gallagher, 2011). Despite their many advantages, microalgae are not currently a feasible source of biodiesel, due to TAG yields being too low (Vasudevan and Briggs, 2008) and the production being economically unsustainable because it is not competitive with petrol products (Chisti, 2007; Chisti, 2013; Gallagher, 2011; Sheehan *et al.*, 1998). With improvements in algal oil yields, it would be possible to address both of these issues, as increases in productivity will improve economic sustainability (Beal *et al.*, 2011; Gallagher, 2011; Slade and Bauen, 2013).

There is a long history of scientific investigation into improving the yield of algal biofuels. The fuel crisis of the 1970s sparked off the Aquatic Species Program, a smaller subsection of the U.S. Department of Energy's Biofuels Program (Sheehan *et al.*, 1998). This program investigated the use of aquatic photosynthetic organisms to produce biofuels, and naturally progressed to a focus on microalgae as a potential source of biodiesel. They screened and characterized over 3000 species of microalgae, and initiated a body of work that investigated the "lipid trigger" of environmental stress to induce TAG production. They began to branch into genetic investigation by creating a strain with up-regulated acetyl CoA carboxylase (ACCase) – a key enzyme in lipid biosynthesis, but this was unsuccessful in stimulating TAG synthesis (Sheehan *et al.*, 1998) and soon after, in 1995, funding was cut and the project abandoned (Sheehan *et al.*, 1998). Many studies have tried to increase lipid accumulation via an increase in enzymes involved in lipid biosynthesis, but the majority have been unsuccessful (reviewed in Courchesne *et al.* (2009)). Blatti *et al.* (2013) describe the published efforts to date in engineering of fatty acid biosynthesis in algae, some of which change the fatty acid profile, but none of which change the yields, and most being unsuccessful in having any effect. There have, however, been demonstrations of altering the lipid profile of microalgae, and of engineering cells to excrete lipids (reviewed in Chisti (2013)). A review by De Bhowmick *et al.* (2015) describes

a few studies which show that targeted genetic engineering can result in changes in lipid yields in some species of green algae and diatoms.

A renewed feeling of urgency in the 21<sup>st</sup> century concerning the need for biofuels has reignited interest in algal biofuels, as they remain the best option for a photosynthetic source of biofuels (Chisti, 2008; Dismukes *et al.*, 2008; Oncel, 2013). The ideal microalgae species would have the following characteristics: it would be both prolific in biomass production, and have a very high TAG content, therefore resulting in high lipid productivity (Griffiths and Harrison, 2009); it would be able to dominate all other microorganisms in an open pond system, would grow well in additional nutrient sources such as wastewater streams (Pittman *et al.*, 2011) and industrial CO<sub>2</sub> emissions (Benemann, 1993), and be able to cope with seasonal and diurnal fluctuations in both sunlight and temperature (Goldman, 1977). The reason for these latter characteristics is that the ideal algae cultivation system is low energy input and low maintenance, in order to make it energetically and economically sustainable, and therefore the algae culture should be able to thrive in an outdoor open pond system, as these have a higher energy balance than photobioreactors (Jorquera *et al.*, 2010). Open pond systems are also more economical than PBRs, providing the significantly higher 10% economic return of \$18.10 gal<sup>-1</sup> versus \$8.52 gal<sup>-1</sup> for PBRs (Davis *et al.*, 2011).

No algae species like this is currently known. Finding a species through continuing screening processes may be possible; many studies have screened various algae species for their oil content, and some show greater oil producing capacity than others, with lipid contents between 4 and 65% being reported in different species (Gouveia and Oliveira, 2009). The Department of Energy's Aquatic Species Program (mentioned above) collected and screened more than 3000 strains, but due to funding cutbacks many strains were lost and the number retained at the University of Hawaii was reduced to 300 (Sheehan *et al.*, 1998). This screening process yielded about a dozen promising strains (all of which were green algae or diatoms) with suitable characteristics for biofuels production, but none that was ideal, leading them to the conclusion that genetically manipulating the dominant

strains within algae cultures may be necessary for increased lipid production (Sheehan *et al.*, 1998). Indeed, the answer to the search for the perfect algae strain for biofuels is likely to lie in the realm of biological engineering, and the need for a genetically engineered algae strain has been recognised repeatedly by researchers (Chisti, 2013; Hu *et al.*, 2008; Radakovits *et al.*, 2010; Sheehan *et al.*, 1998).

This thesis investigates the limitations and the possible solutions to increasing algal oil yields with the aim to increase triacylglyceride and overall lipid yields in algae. The following literature review is a description of how this PhD project has pinpointed environmental manipulation, proteomics and biosynthetic pathway study as the main tools in creating an algal species with a high lipid output. The study of systems biology (Kitano, 2002; Smolke and Silver, 2011) helps in understanding the processes by which organisms produce substances, and subsequently, the manipulation of these systems can take place through synthetic biology and metabolic engineering changes (Schwille, 2011; Stephanopoulos, 1999).

For algal biodiesel to become a successful replacement fuel for oil-derived liquid fuels, several advances need to be made in algal biofuels research. Firstly, lipids must be made on a large enough scale to be able to meet the demand for liquid fuels. The liquid fuels consumption around the world in 2016 is 95.26 million barrels per day (U.S. Energy Information Administration), and is projected to rise. Secondly, biodiesel prices must be able to compete with fossil fuel prices (Kovacevic and Wesseler, 2010). Biodiesel yields from algal cultures are currently limited by lipid percentage of dry weight of algae, which has a large impact on price; Jorquera *et al.* (2010) show that algae biodiesel would be economically competitive with oil or petroleum if the oil percentage content was increased from around 30% to 60%. By using proteomics and biological engineering techniques, it may be possible to increase lipid yields enough to meet algal biodiesel demand in an economically competitive manner, and solve the first problem. By employing the use of species suitable for growth in low-energy input systems, it may be possible to solve the second problem. Lowering production costs is also very important

because currently algal biodiesel is not able to compete economically with rapeseed biodiesel and fossil fuels (Chisti, 2013; Kovacevic and Wesseler, 2010).

## 1.2 Literature review

### 1.2.1 Biological and energetic limitations to algal biofuels production

More broadly speaking, the aims are to overcome the biological and energetic limitations that currently hamper lipid yields. For this, a deeper understanding of lipid synthesis and algae cell function is imperative. Figure 1.3 shows the lipid biosynthetic pathway within plants and microalgae (Yu *et al.*, 2011).

[Image removed for copyright reasons]

Figure 1.3 Lipid biosynthetic pathway in plants and microalgae, image taken from Yu *et al.* (2011).

The biggest problem encountered in increasing TAG production is that it has been repeatedly demonstrated that conditions which induce high TAG contents also decrease algal biomass productivity (Li *et al.*, 2008a; Lv *et al.*, 2010; Su *et al.*, 2011), thus causing an overall decrease in TAG productivity in a growth system. This is because there is an intrinsic inverse relationship between algal growth rate and oil content; carbon is redirected into storage compounds when it is not being used for growth (Williams and Laurens, 2010). The basic premise that environmental stress causes retarded cell growth and lipid accumulation within a cell is well established.

Fan *et al.* (2011) conducted investigations of the metabolic origins of lipid synthesis in *C. reinhardtii*. They found that under three different stress conditions - nitrogen deprivation, high salt, and high light - fatty acid synthesis was *de novo*, and located in the chloroplasts and cytosol. This major pathway is known as the Kennedy pathway (Dubini, 2011). The fatty acids were then used to synthesise TAG in the endoplasmic reticulum (see Figure 1.3). Concordantly, Miller *et al.* (2010) found that the acetate carbon source added to algal growth medium was used for *de novo* fatty acid biosynthesis, demonstrating that the

cell carbon sources, whilst possibly being diverted away from cell growth functions, are not acquired by breaking down other parts of the cell, at least not solely. The discovery that the fatty acids are synthesised *de novo* is important, as it indicates that these fatty acids are not being converted from other deconstructed components of the cell that are used in the cell functioning, but from the fixation of carbon. Therefore, in theory, there is no reason why algae cannot both produce lipids and continue to function and grow in a healthy state, if carbon is being directed towards both areas in adequate quantities. At the moment, carbon is only directed towards storage compounds when growth is restricted by stressors, and there is a complex set of constraints that govern carbon partitioning (Johnson and Alric, 2013). By manipulating the natural pathways in the cell, it may be possible to partition carbon into both storage compounds, and also into growth and cell maintenance, although a large part of the constraint is the energy losses involved in directing carbon into oil production (Johnson and Alric, 2013).

It is possible that with the availability of the right nutrients and cell components, the ideal biofuels producing algal cell, the “healthy obese cell”, can be created. However, the requirement for a carbon source in addition to CO<sub>2</sub> (in this case acetate) may restrict the algae that can be utilized to produce TAG during active growth to those that grow mixotrophically, like many *Chlamydomonas* strains. Photoautotrophic algal strains that utilize CO<sub>2</sub> as a sole source of carbon may not be able to carry out large amounts of TAG synthesis during active growth.

Some physical laws do impose firm upper limits on the ability of algae to produce biodiesel (Weyer *et al.*, 2010). These limits include the amount of sunlight that is available to the cell, the ability of the algae to capture the light energy, and the biomass accumulation efficiency (BAE). The latter term refers to the amount of energy that is used in maintaining cellular functions rather than stored directly in biomass. Knowing exactly how much energy is needed to maintain cellular functions and growth would give a better indication of exactly how much carbon would potentially be available for oil storage as TAG, and therefore what the theoretical limits of TAG production in algae really are.

Dubinsky and Berman-Frank (2001) describe the main processes that use carbon in a cell. These are respiration and production of new cells. They highlight that respiration is increased under high population growth, and that stressors increase respiration. However, this report provides no quantification of such carbon fluxes. Weyer *et al.* (2010) attempt to give a numerical value to energy required for maintaining the cell, but they do so in percentage form. They state a BAE of 50%, but this seems rather arbitrary, since the possible values these authors discuss - based on varying assumptions - range from 11% to 100%, and the choice seems to have been made on a “middle ground” basis rather than use of verified data.

In practice, the energy that a cell uses to maintain its functions is one of the main restrictions that this body of research faces (Leite *et al.*, 2013); it would be ideal to have a cell that is both good at maintaining its vital functions and therefore growing prolifically, but also at producing the much desired TAG product. Theoretical limits cannot properly be calculated without understanding exactly what is controlling energy flows and biological pathways within an algal cell. This is where the study of the complex fluxes is vital, and where state of the art laboratory techniques such as proteomics (the large scale study of proteins, particularly in their structures and functions) need to be employed. Current estimates on "return on investment" for synthesis of fatty acids is 60.7% (Johnson and Alric, 2013).

One aim of engineering and manipulation of algal cells is to induce the lipid synthesis at a high rate, whilst maintaining normal cell function and biomass productivity (i.e. the ability to grow and multiply), by balancing the allocation of cellular resources between these two processes. Alternatively, manipulation can be used to induce lipid synthesis in an already dense and productive culture, thereby converting algal biomass into a more lipid-rich product, if the first approach is not possible. As the lipid synthesis pathways interact with stress inducers, chlorophyll and photosynthesis efficiency, starch synthesis and TAG synthesis, this understanding needs to stretch beyond the mechanisms of lipid production,

into regulation of the cell metabolic pathway interactions, and particularly about how the cell pathways change in reaction to stress.

Walker (2009) highlights the pitfalls of imposing theoretical but practically implausible maxima on the calculations for the biofuels output it is possible to achieve. For example, predicting unfeasibly high growth rates of algal cultures or an unrealistic photosynthetic efficiency value will only project false hopes for algal biofuels. The absolute maximum photosynthetic efficiency attainable under ideal laboratory conditions is 11.9% (Radmer and Kok, 1977). The realistic photosynthetic efficiency that can be achieved over significant lengths of time (days to a few weeks) is about 4.5% (Walker, 2009). However, microalgal photosynthetic efficiencies of up to 21.6% are quoted in the literature (Brennan and Owende (2010), plus references therein) and used as a basis for microalgae biofuel yield projections. However, there are areas in which engineering may be able to extend the current limits of algae to produce oil, such as pathway efficiency in the cell.

Algae use TAG as an energy storage product when growth is curtailed by the absence of a key nutrient, such as nitrogen (Chen et al., 2011b; Longworth et al., 2012) or phosphorus (Khozin-Goldberg and Cohen, 2006), or by environmental stress such as high salinities (Siaut *et al.*, 2011). Under stress conditions, the photosynthetically fixed carbon supply exceeds the ability of the cell to multiply, causing the build up of carbon in storage molecules (Pal *et al.*, 2011). It is therefore not only the TAG production that needs to be investigated, but also the ability of the cell to continue to photosynthesise and multiply under stress conditions. The formation, pathways, and composition of different lipid types within algae are thoroughly researched and documented (Guschina and Harwood, 2006; Harwood and Guschina, 2009), and now the challenge lies in comprehensively linking these to the genes, metabolic pathways, proteins, and environmental conditions that trigger their synthesis. The understanding and manipulation of these aspects of a cell to make a new unique organism for a specific purpose is known as synthetic biology (Drubin *et al.*, 2007), and it is this area which this research has pursued.

### 1.2.2 The need for a low energy system

One problem with algal biofuels is the current energy inputs required for cultivation. Under certain conditions, it is possible for an algal population to grow exponentially, known as algal bloom (Chen *et al.*, 2009a). In practice, algal growth is subject to abiotic factors – such as light and temperature (Moheimani and Borowitzka, 2007), pH (Sogaard *et al.*, 2011) and nutrient levels (Smith, 1986) - and to biological interactions with other species, and with population limit factors (Titman, 1976).

The ability to dominate the population is imperative for open pond systems prone to contamination. For this reason, the ability of a species to dominate, and the conditions under which they do it, are important. Abis and Mara (2005) tested operational parameters of primary facultative ponds in the UK on algal populations. Although average ammonia removal was approximately 50% during both summer and winter, initially the algal populations were significantly decreased during the midwinter in all test loadings of effluent, demonstrating that temperature is a key issue in population maintenance. Furthermore, different species dominate the population at different points in the year. *Chlamydomonas* species flourished in one pond at the end of January, and *Chlorella* species dominated another throughout the winter.

Robustness to changes is therefore very important. Bhatnagar *et al.* (2011) evaluated the robustness of an algal consortium to climatic changes and compositional changes in wastewater content. Their results showed that an open raceway pond was consistently dominated by a few algal species, even during harsh winter conditions including freezing. The three different algae species isolated from the consortia (*Chlamydomonas globosa*, *Chlorella minutissima* and *Scenedesmus bijuga*) showed contrary responses in biomass and chlorophyll content in response to added nitrogen and type of wastewater. This demonstrates that every system and algal species is unique, and therefore finding the ideal algal species for a system is a unique solution.

It therefore follows, when searching for an algal species for a particular country's conditions, that using data from tests carried out in different climates will not be

sufficient. The current research takes place in temperate Europe, where it is hoped that the aim of using outdoor algal ponds for biofuels production will be realised. To do this, algae suitable for cold and temperate climates must be found.

Two main issues must be addressed: the first is that a species suitable to the temperature and light levels in temperate Europe must be found and secondly, the species must be able to dominate in an open environment. Buhr and Miller (1983) used mathematical models to find the limitations on yield of both algae and bacteria in a high-rate wastewater treatment pond, based on stoichiometric analysis and growth kinetics. They found that operating parameters changed on a diurnal pattern. They found the limiting factors that determined yield to be sunlight or substrate availability, but proposed that if sufficient carbon source is provided, and flow rates do not exceed the washout rate, the growth will only be limited by sunlight. Providing sufficient carbon sources may be something we are able to control by adding more substrate in the form of wastewater, carbon dioxide, or another carbon rich waste source. The limitation of sunlight, however, remains a problem, and this is where the search for algae with low optimal sunlight needs becomes a possible solution. The importance of fixed carbon is reinforced by Bhatnager *et al.* (2011), who found that supplementing wastewater sources with nitrogen did not increase biomass production, but that addition of glucose and nitrogen caused an increase in biomass of 3-8 times.

Baliga and Powers (2010) researched and modelled different scenarios for algae cultivation and conversion to biodiesel in upstate New York. Due to the challenging aspects of the short days and cold temperatures during the winter months, their scenarios involved insulation, greenhouses, artificial lighting and heating facilities. Out of their two locations within upstate New York, the one which had higher natural light levels and temperature used 18-20% less energy and yielded 12% more biomass output. They found that when natural light was insufficient, the consequences of boosting the light levels with artificial light powered by electricity counteracted the energy benefits of utilising waste heat. Temperature control was also very energy intensive. If natural light and waste heat

are absent, the energy consumption of algal biodiesel production is significantly increased and the emissions from fossil fuel derived energy are increased. Furthermore, in an open pond system, heating would result in large water losses through evaporation (Pfromm *et al.*, 2011), causing the need for a higher water input.

*Chlamydomonas reinhardtii*, an important model algal species, has been tested for its suitability to treat wastewater coupled with biofuels production (Kong *et al.*, 2010). This involved the experimental culture of *C. reinhardtii* in both biocoil-type photobioreactors (PBR) and flasks, wastewaters with added trace elements were used as the media. Growth in the biocoil PBR produced a maximum of 2.0 g biomass per litre per day and a maximum of 25.25% oil content. In the flasks, the biomass content was just 0.82 g per litre per day, and the oil content reached a maximum of 16.6%. The effect of greater light exposure in the biocoil PBR is thought to attribute to the higher productivity, demonstrating that light is a strong limiting factor, but both oil contents are lower than the desired 60% oil content quoted by Jorquera *et al.* (2010) to make algal biofuel feasible. What this study demonstrates is that *C. reinhardtii* can successfully uptake nitrogen and phosphorus to treat wastewater, and this causes a productivity boost in the algal population. However, the biomass and oil contents are both less than desirable even with wastewater supplementation, and this supports the need to investigate engineering techniques to boost oil contents and productivity.

The conclusions we can draw from this section are that heating and lighting inputs are necessary for many species to reach their full productivity, but that these inputs make the process energetically, economically, and environmentally unsustainable. Finding a species with low light and heat requirements would be extremely beneficial, especially in temperate Europe. This species also needs to be very productive and have high lipid-producing capabilities, and it needs to be able to dominate in the unique conditions of an outdoor open pond system with wastewater streams for low cost nutrient input, in temperate Europe.

### 1.2.3 A history of lipid manipulation in algae

Many species have been screened for oil content (Gouveia and Oliveira, 2009; Griffiths and Harrison, 2009; Sheehan *et al.*, 1998). Since algae, even with nutrient supplements, naturally yield insufficient oil contents for commercial exploitation, typically achieving less than half of the desired 60% (Gouveia and Oliveira, 2009; Jorquera *et al.*, 2010), finding ways to increase this oil content is imperative to successful biodiesel production.

As previously described, the Aquatic Species Program (Sheehan *et al.*, 1998) was the main body of work in trying to find or produce an algal species with high lipid productivity. Their techniques included environmental manipulation, known as biochemical engineering (Courchesne *et al.*, 2009), and an attempt at genetic engineering (Sheehan *et al.*, 1998). Applying a form of stress, such as high salinity (Takagi *et al.*, 2006), nitrogen deprivation (Li *et al.*, 2008a), and CO<sub>2</sub> aeration (Chiu *et al.*, 2009) to microalgal cells has consistently been shown to increase the lipid content of the cells, although the most common method is nitrogen deprivation. Usually one stress method is applied at a time, although Pal *et al.* (2011) investigated the effects of combined stress upon *Nannochloropsis* sp., using nitrogen deprivation, salt stress, and light variation. They found that unlike nitrogen-replete conditions, this species showed a significant reduction in lipid productivity overall under high light, high salinity and nitrogen depleted conditions. This demonstrates that nitrogen deprivation may not be the best method of inducing lipid production, because nutrient deficiency reduces the resources that can be put into growth and TAG. The stress used in exploring TAG and lipid accumulation in the current study is salt stress, because there has been very little exploration of this stress in the model species *C. reinhardtii*, and studying the model species allows lipid stress triggers to be linked with "-omics" strategies for understanding lipid production (see Section 1.2.5). It is likely that salt stress has not been employed as a lipid trigger in this species because it is a freshwater species with limited salt tolerance. However, freshwater species *Chlamydomonas mexicana* has been grown under salt stress and found to have a significant increase in lipid content under 0.05 M NaCl (Salama *et al.*, 2013), demonstrating that the salt stress method of lipid trigger can be used in freshwater species. This thesis also explores the effect of salt stress on lipid

yield in *C. nivalis*, a related snow algae species with a greater salt tolerance than *C. reinhardtii*, which could deepen the understanding gleaned from omics studies of salt stress in *Chlamydomonas*.

Unfortunately, the stress conditions which induce high lipid contents within cells also severely hamper the ability of the population to multiply. Algae halt growth and redirect the carbon they fix into storage organelles as oil and starch (Li et al., 2011). The result of this can be an overall decrease in lipid productivity in the culture (Griffiths and Harrison, 2009). Adams *et al.* (2013) explore the relationship between growth and lipid productivity in green algae, using high and low nitrogen stress as the lipid triggers, finding different responses in different species due to sensitivity to stress. Concurrent growth and lipid production give higher lipid yields than if growth and lipid productivity do not occur at the same time. One issue is that during nitrogen deprivation, the most common lipid inducer, photosynthetic capacity is lost - as well as cell growth being arrested due to the inability to synthesize proteins without a nitrogen source - so cell metabolism cannot rely on carbon fixation from photosynthesis (Johnson and Alric, 2013). An inhibition of photosynthesis is a limiting factor to the potential lipid yield, since a greater availability of fixed or assimilated carbon provides a greater resource for lipid accumulation. Ideally then, a stress lipid trigger would not reduce photosynthetic ability.

Since the desired effect is to turn on the “lipid trigger” (Sheehan *et al.*, 1998), research has turned to examining the cell pathways to find out how to apply the lipid trigger without needing to apply the stress that decreased productivity. The first example was the identification of ACCase as the committing step in lipid biosynthesis, and an experimental up-regulation of this enzyme, but this was unsuccessful in that it did not increase lipid production (Sheehan *et al.*, 1998).

Radakovits *et al.* (2010) reviewed different targets of pathway manipulation for improving biofuels production from microalgae. These include inducing lipid biosynthesis, preventing lipid catabolism, and blocking metabolic pathways that lead to other energy rich storage compounds such as starch.

This latter method has been found to be successful in increasing lipid contents of cells. Blocking starch synthesis in *C. reinhardtii* by inactivating ADP-glucose phosphorylase blocks the pathway to starch synthesis and switches the photosynthetic carbon partitioning into TAG synthesis, resulting in a 10-fold increase in TAG (Li *et al.*, 2010a). This has been achieved in the starchless mutant BAFJ5 which, in comparison with low-starch mutants which did not show as strong an increase in TAG production, showed an 8-fold increase in neutral lipid under high light and nitrogen starvation conditions, but still demonstrated some growth impairment (Li *et al.*, 2010b). Wang *et al.* (2009) similarly demonstrated that when starch synthesis is blocked in *C. reinhardtii*, the lipid body accumulation under nitrogen deprivation rises from 15-fold in wild type to 30-fold in the starch-less mutant. These mutants still require stress to induce lipid production, but it has been shown that carbon can be more efficiently partitioned within the cell for enhanced TAG production. A comparison of a wild type and starch-less mutant also indicated that the TAG biosynthetic pathway is not modified under inactivation of starch biosynthesis (Fan *et al.*, 2011), showing that it is possible to remove unnecessary pathways for the purposes of biofuels production.

The challenge still remains in inducing TAG biosynthesis under non-stress conditions. This is where study of cell pathways using “-omic” techniques is vital. Previous experimentation on ACCase demonstrated that changing one enzyme in the pathway was not enough to affect the lipid content of algae (Sheehan *et al.*, 1998), and therefore a successful transformation may rely on identifying several proteins that control the ability of a cell to produce lipids. Lv *et al.* (2013) did, however, use a proof of concept knock out of lyso-phosphatidic acid acyltransferase and diacylglycerol transferase to decrease neutral lipid production in *C. reinhardtii*, showing that by removal of key enzymes in lipid production that it can be genetically modified, even if not up-regulated successfully yet. Furthermore, their transcriptomic study of *C. reinhardtii* under induced lipid production demonstrated expression changes in 2500 genes including 30 related to lipid metabolism,

supporting the theory that single gene changes are not enough to make the required change in the alga for higher lipid production.

#### **1.2.4 Development of lipid analysis techniques**

Measuring the neutral lipid content of algal cultures accurately is essential for finding the conditions at which TAG production is at its highest rate. It is a problematic area, and no one single technique is perfect. Upon deeper investigation this area appeared to be a bottleneck in research progress in accurately assessing and analysing algal lipids, so a full review of algal lipid measurement techniques was carried out. This full review was published as a guide for researchers who encountered this issue of choosing appropriate techniques from the plethora available (Hounslow et al., 2016b), and has been included for reference in Appendix B. A summary of techniques available is displayed in Table 1.1 below. Broadly speaking, these are gravimetric, fluorescence, colorimetric, chromatographic and mass spectrometry techniques.

Table 1.1 Summary of lipid quantification techniques in microalgae. I=in situ. E=extraction. N=quantitative, L=qualitative, S=quantitative with standards, H=semi quantitative.

Technique type	Technique variation	Sensitivity	Lipid detection type	In situ or extraction	Qualitative/quantitative	Advantages	Disadvantages/ problems	References
<b>Gravimetric</b> Use of cell lysis and a solvent to extract lipids from biomass, followed by drying and weighing lipid extract.	Bligh and Dyer: 1:2 chloroform methanol.	500 mg wet biomass	"Crude" lipid	E	N	Direct measurement.	Extracts other compounds than lipids. Requires large amounts of culture Solvent type favours certain lipid types.	(Bligh and Dyer, 1959; Kumari <i>et al.</i> , 2011)
	Folch: 2:1 chloroform methanol.	500 mg wet biomass	"Crude" lipid	E	N	Direct measurement.	Solvent type favours certain lipid types.	(Kumari <i>et al.</i> , 2011)
	Soxhlet: Hexane and use of Soxhlet extractor.	1 g dry biomass	"Crude" lipid	E	N	Direct measurement.	Solvent type favours certain lipid types.	(Go <i>et al.</i> , 2012; Li <i>et al.</i> , 2008a)
	Cequier-Sánchez: Dichloromethane instead of chloroform.	500 mg wet biomass	"Crude" lipid	E	N	Less toxic solvents used.	Solvent type favours certain lipid types.	(Kumari <i>et al.</i> , 2011)
<b>Fluorescent lipid dye</b> Dye is applied to whole cells to penetrate in and bind to lipids. Excitation and emission filters are used to read dye fluorescence as a relative measure of lipids.	Nile Red: binds to neutral lipids.	0.2 to 1 x 10 <sup>6</sup> cells mL <sup>-1</sup> : 5 µL for microplate method	Neutral lipids	I	L, S	In situ. Relatively fast procedure. Can process many samples at once.	Varies between species as penetration of cell wall and concentration of dye must be optimised. Doesn't distinguish between neutral lipid types Relative measure unless using standards.	(Chen <i>et al.</i> , 2009b; Cirulis <i>et al.</i> , 2012)
	BODIPY: Binds to a range of lipids and fluoresces when excited at 488nm.	0.2 to 1 x 10 <sup>6</sup> cells mL <sup>-1</sup>	Fatty acids, phospholipids, ceramides, cholesterol and cholesteryl ethers	I	L	In situ. Relatively fast procedure Can process many samples at once. Has no chlorophyll interference.	Shows lower quantification correlation with other methods compared to Nile Red.	(Cirulis <i>et al.</i> , 2012)
	DiO: Binds to phospholipids.	0.2 to 1 x 10 <sup>6</sup> cells mL <sup>-1</sup>	Phospholipids	I	L	In situ. Relatively fast procedure Can process many samples at once.	Suitable for phospholipids only.	(Cirulis <i>et al.</i> , 2012)
<b>Colorimetric</b>	Phospho-vanillin (SPV)	5-120 µg dried	Fatty acids	E	S	Can be done on small	Relies on extraction.	(Cheng <i>et al.</i> ,

Extraction of lipids and reaction with a colour developer. Degree of colour change is proportional to lipid concentration.		lipid				volumes lipid.	Signal decreases with chain length of less than 12 carbons so hard to detect smaller chains. No structural information gained.	2011b)
	TFA-Cu salts: Triethanolamine and copper	2 mL at OD <sub>680</sub> 0.06-1.2	Fatty acids	E	S		No structural information gained.	(Chen and Vaidyanathan, 2012a)
	TFA-metal	1-2 mL (OD not specified)	Fatty acids	E	S		No structural information gained.	(Wawrik and Harriman, 2010)
<b>Raman microscopy</b> Lasers alter the vibrational state of a sample and the shift in energy is specific to chemical bonds and structures, yielding information about the sample content.	N/A	1 cell	Lipid type and degree of unsaturation	I	H	Small samples needed In situ and non destructive Detailed information of lipid properties.	Photosynthetic pigments can interfere with signal. Components in low abundance can't be detected.	(Samek <i>et al.</i> , 2010; Wu <i>et al.</i> , 2011)
<b>Density equilibrium</b> Samples are centrifuged in a 10-80% (w/v) sucrose gradient to find in vivo buoyant densities. An equation is used to convert the density values to lipid content values.	N/A	2 mL sample or 5 mg dry biomass	Lipid, hydro-carbon or biopolymer	I	N	Rapid, In situ.	Indirect, relies on the relationship density and lipid content being constant between all samples.	(Eroglu and Melis, 2009)
<b>Direct transesterification/ In situ esterification</b> Direct conversion of lipids in biomass to FAMES using a solvent and catalyst and measurement with GC	Lepage and Roy: Acetyl chloride/methanol reagent	500 mg wet biomass	FAME	E	N	Measures true potential of algal biomass to be converted to FAME.		(Kumari <i>et al.</i> , 2011)
	Garcia: Toluene and 5% methanolic HCl reagent	500 mg wet biomass	FAME	E	N	Detailed information on molecular structure of lipids.		(Kumari <i>et al.</i> , 2011)
	In situ esterification	4-7 mg wet biomass	FAME	I	N	Detailed information on molecular structure of lipids.		(Laurens <i>et al.</i> , 2012a)
<b>NMR</b> Applying magnetic field to sample and measuring the resonant frequency emitted to provide spectra of chemical shifts and information about molecule structure.	Time domain: This method is based on relaxation time of lipids' hydrogen nuclei in different phases of the samples.	1 g dried biomass	Specific targeted lipid compounds and molecular structure	I or E	S	Detailed information on molecular structure of lipids.	Can be interference from other compounds, which is not consistent between samples. Water can interfere so to exclude this samples must be freeze-dried.	(Gao <i>et al.</i> , 2008)
	Liquid state	1 g wet biomass	Specific	I	S	Detailed information on	Can be interference from other	(Beal <i>et al.</i> ,

			targeted lipid compounds and molecular structure			molecular structure of lipids.	compounds, which is not consistent between samples.	2010)
<b>Mass Spectrometry</b> Fatty acid extraction, derivatization, separation via chromatography, electron ionization, and measurement of the mass to charge ratio of the compound in a mass spectrometer.	GCMS	5 mg dry biomass	Lipid classes and chain types	E	N	Lipid classes obtained as well as quantitation.	Relies on the assumption that derivatized fatty acids can correctly identify all the lipid portions in the correct proportions. Assumes that all lipid types will ionize at the same rate.	(Barupal et al., 2010; Gu et al., 2011b)
	LCMS	500 mg dry biomass	Lipid classes and chain types	E	N	Detailed identification of lipid composition.	Detection of lipids is dependent on lipid type.	(Maddougall et al., 2011)
<b>FTIR</b> Measurements of infrared absorption and molecular vibrational modes are used to identify and quantify ester groups at wavelength $1740\text{cm}^{-1}$ in dried cells. Relative lipid content is determined by calculating the ratio of the lipid band ( $1740\text{cm}^{-1}$ ) to the amide I band.	N/A	0.15-2 mL culture (OD not specified)	Ester groups	I	L	No extraction needed.	Not specific to TAGs or lipids.	(Dean et al., 2010; Stehfest et al., 2005)

The techniques summarised in Table 1.1 vary in their specificity in terms of: the level of information about lipids they reveal (e.g. gravimetric showing total lipids versus Nile Red showing the presence of neutral lipids versus GC-MS identifying the chain length of hydrocarbons identified); the type of lipids they are suited to detecting (e.g. some solvents in gravimetric methods favour certain classes of lipids over others or Nile Red only shows neutral lipids); and the accuracy of the results. Even within types of methods, there is diversity in how the protocols are performed and how suited they are to different algal species.

#### ***1.2.4.1 Choice of lipid techniques for this thesis***

Only a few of the techniques covered in the published review (see Appendix B) have been chosen for use in this research. Gravimetric was chosen as a starting point for total lipid content, with Bligh and Dyer technique (which uses chloroform and methanol) being able to extract a wide range of lipids and therefore very suitable for quantifying the total lipid in an algae samples. As this technique used large amounts of biomass, Nile Red fluorescence and microcolorimetric SPV techniques were used on smaller algae samples over time course experiments. Lastly transesterification of lipid extract followed by GC-FID techniques allowed detailed investigation of lipid profiling without needing to use high power multidimensional chromatographic techniques or MS for absolute identification of all lipid compounds. In this case, information on the major FAME types was sufficient to inform the research. Exploration of data obtained with these methods is described in Chapter 3.

#### **1.2.5 “-Omics” tools in understanding lipid synthesis**

Approaching the manipulation or engineering of an organism requires a comprehensive knowledge of how it functions. There are several approaches to analysing the pathways, fluxes and functions of a cell, including genomic analysis, transcriptomic analysis, proteomic analysis and metabolomic analysis. These each map out the functions of an organism, but do so by analysing different components of the cell. Proteomics, the tool used as the focus of this study, is the systematic analysis of the proteins in a cell or tissue sample (Domon and Aebersold, 2006). This section will evaluate advantages and disadvantages and the progress made to date by different “-omics” tools.

“-Omics” tools have been used in a lot of biotechnology research. The most well known tool, genome or genetic manipulation, has been used to improve the yields of targeted compounds in microorganisms. For example, genomic analysis and manipulation has led to improvements of 23.5 fold increase in beta carotene production in *Escherichia coli* (Scaife *et al.*, 2009), and an increase of 1.57 fold of shikimic acid in a modified strain of *E. coli* (Fu *et al.*, 2007); antithrombotic hirudin production was increased 2.5 fold in genetically modified *Saccharomyces cerevisiae* yeast cells (Kim *et al.*, 2003); and ethanol concentrations were increased from 5 mM to 92 mM by disrupting  $\beta$ -hydroxybutyryl-CoA dehydrogenase gene in *Clostridium butyricum* (Cai *et al.*, 2011). This corresponded to a decrease in hydrogen production, suggesting that hydrogen and ethanol production pathways may compete for NADH. This is an example where cell dynamics can be streamlined away from one pathway and focussed into another (Cai *et al.*, 2011). However, since genomic manipulation attempts haven’t resulted in TAG increase (Sheehan *et al.*, 1998), other “-omic” tools may be necessary for analysis.

The following section describes advances made in “-omics” strategies in the study of *C. reinhardtii*. Miller *et al.* (2010) focussed on transcriptomic analysis of *C. reinhardtii* under nitrogen deprivation and lipid accumulation. Their study yielded a vast amount of information on the up-regulation and down-regulation of identified genes. The first point of note is that the changes in transcript abundance are numerous, since the changes in the cell during nitrogen deprivation are complex and affect many different aspects of cell function. More specifically, this study showed that genes involved in carbon fixation and reduction dropped in transcriptome abundance to 25% of that under nitrogen replete conditions. It also showed that genes associated with photosynthesis and DNA replication tended to be down regulated, and those associated with lipid metabolism tended to be up regulated. This technique has the advantage of identifying the genes involved during stress, and quantifying their expression. Although the quantity of transcripts would represent the quantity of proteins being up and down regulated, the disadvantages of transcriptomics lie in not being able to examine how post-translational modifications of proteins could have important effects on cell pathways and function. In this case, Miller *et al.* (2010)

verified that the RNA abundance did reflect changes in the activities of the relevant pathways. However, they also acknowledge that gene expression in the form of proteins may be subject to post-translational modifications, and therefore the expression may not directly translate to metabolic fluxes.

Genomic analysis also has its limitations. Riekhof *et al.*, (2005) in their exploration of gene annotation in glycerolipid biosynthesis in *C. reinhardtii*, highlighted that a single gene may code for enzymes that have dual targets within a cell. It is therefore vital to study the location and state of the protein that is acting within the pathway, and this demonstrates the importance of using proteomics in this study. Knowing the genes is not enough in itself, regulation is paramount.

Moellering and Benning (2010) conducted proteomic analysis of *C. reinhardtii* lipid droplets, by disrupting cells and extracting the lipid droplets from the resulting suspension. These were then analysed using mass spectrometry. Their investigation yielded the identification of the major lipid droplet protein gene (MLDP), and subsequent repression of the gene resulted in increased lipid droplet size. This is thought to be because creation of lipid droplet membranes is decreased, requiring the need for more efficient use of the membranes in fewer, larger lipid droplets (a lower surface area per volume ratio). TAG content was not affected. Although the lipid content was not affected, this successful use of proteomic techniques to examine and manipulate lipid droplets shows the potential of proteomics to identify the key elements that regulate the cell function. Recently developed tools, such as strong cation exchange (SCX) chromatography, have enabled analysis of post translational modifications (Mohammed and Heck, 2011), meaning a precise identification of the protein state can be obtained – perhaps vital information when investigating whether transformations of a cell can successfully yield the desired protein expression.

Proteomic analysis is the only analysis that can provide a full picture of how cell function changes its regulation. This knowledge can lead to successful genetic manipulation for a physiological change in the cell, as demonstrated by Moellering and Benning (2010). Proteomics was therefore chosen as the analytical tool in the current

research. Quantitative proteomics can give comprehensive data that is vital for informing systems biology (Cox and Mann, 2011).

#### *1.2.5.1 Shotgun proteomics*

Mass spectrometry based proteomics uses protein samples digested into peptides using a sequence specific enzyme, usually trypsin (Olsen *et al.*, 2004), to form peptides. The peptides are then processed by mass spectrometry to determine their molecular mass by ionising the peptides and then measuring their mass to charge ratios. These peptide ions can then be further fragmented and their mass to charge ( $m/z$ ) ratios measured to determine the sequence of the peptide. This is known as tandem MS, MS/MS or MS<sup>2</sup> (Steen and Mann, 2004). The resulting spectra are then used to identify the peptide, and the protein it is from, by using databases of known protein and peptide sequences via processing software such as Maxquant, PEAKS and Mascot.

Through this method, the presence of peptides, and therefore proteins, can be determined; when comparing samples and phenotypes, it is important to make quantitative measurements of protein abundance changes, or "fold changes" (Ong and Mann, 2005).

There are different methods of proteomic investigation, namely shotgun, directed and targeted approaches (Domon and Aebersold, 2010). Shotgun proteomics is used in this thesis, meaning that a complex sample is studied without targetting the analysis towards particular proteins, and it is preferable to detect and analyse as many proteins as possible (Wu and MacCoss, 2002). There are issues in underdetection when using shotgun proteomics, since the complex sample can produce background noise that leads to some peptides being discounted when they are not high enough above the signal-to-noise ratio (Domon and Aebersold, 2010). Detection limit, sample reproducibility and dynamic range are all negatively affected when the complexity of the sample increases (Domon and Aebersold, 2010). However, shotgun proteomics allows for complex sample analysis to look for key differences in protein expression that may be linked to differences in phenotype worth pursuing, without limiting the investigation to particular proteins (Wu and MacCoss, 2002). This is important when trying to identify individual or groups of proteins associated with particular changes.

When comparing samples via shotgun proteomics, a method of measuring and comparing the amount of proteins between samples needs to be employed. The methods available are discussed below.

#### ***1.2.5.2 Methods for quantification of peptides in a proteomic sample***

There are several methods for quantifying and comparing proteins in different samples. These include, but are not limited to, 2D-DIGE (difference gel electrophoresis), iTRAQ (isobaric tags for relative and absolute quantification), cICAT (cleavable isotope-coded affinity tags) (Wu *et al.*, 2006), SILAC (stable isotope labelling by amino acids in cell culture) (Ong *et al.*, 2002), label-free (Griffin *et al.*, 2010), metabolic labeling (e.g.  $^{15}\text{N}$ ) and tandem mass tag (TMT) (Elliott *et al.*, 2009).

Elliott *et al.* (2009) fully discuss the range of methods available for relative and absolute quantification, and this is summarised in the following discussion.

Absolute quantification will determine protein quantities as a concentration in a known amount of a sample, such as a known amount of tissue (Brönstrup, 2004). Samples can then be compared to assess the difference in proteome between the two samples. For this, internal standards of spiked proteins or peptides are desirable, to account for any variations in machine performance between samples (Elliott *et al.*, 2009). Although label free methods avoid the limitations of relative quantification methods (discussed below), there are also issues with this: to directly compare the quantities of a peptide, it must be detected in both sample runs; isotopically labelled samples however, are quantified in the same MS/MS run so each selected peptide is detected and quantified for every sample being compared. Consequently in label-free, very high resolution MS machines are required to resolve peptides enough to detect enough peptides for reliable quantitation (Elliott *et al.*, 2009).

Relative quantification uses the introduction of mass tags to samples to bind to peptides and quantify them through the relative ratios of the tags being detected by a mass spectrometer (Ross *et al.*, 2004). This means that two or more samples are labelled and then combined at a certain point during the sample preparation process (this varies depending on which labelling method is used), and then the isotopic labels of each peptide or protein can be quantified (Ong and Mann, 2005). Some labels are

introduced at the peptide level (after extraction and digestion of proteins into peptides), some at the protein level (before protein digestion or before extraction) (Elliott et al., 2009).

After consideration of the methods available, iTRAQ labelling was chosen for quantitation. A discussion of this choice and the advantages and disadvantages follows.

#### 1.2.5.2.1 Comparison of iTRAQ to alternative labelling methods for proteomic profiling

There are several points during the proteomic sample preparation process when a label could be introduced, and it varies depending on the method. These methods can broadly be divided into metabolic labelling and chemical labelling (Bantscheff et al., 2007). Metabolic labelling takes place before protein extraction as it uses isotopes of chemical elements in amino acids to label proteins during protein synthesis (Beynon and Pratt, 2005).

Whilst labelling during growth of cultures using metabolic labelling techniques such as SILAC could in theory allow a larger number of samples to be analysed than other metabolic labelling strategies (Bantscheff et al., 2007), the uptake rate of stable isotope labelled arginine is affected by culture conditions, including salt (Mastrobuoni *et al.*, 2012), which would make it unsuitable for the current work. SILAC is also not ideal for autotrophic organisms like algae, as they are less likely to incorporate amino acids from growth media than if  $^{15}\text{N}$  labelling is used, because algae synthesise their own amino acids.  $^{15}\text{N}$  limits the comparison to just two samples, however (Elliott et al., 2009). Metabolic labelling is also subject to issues of protein turnover rates and possible incomplete labelling (Beynon and Pratt, 2005).

Use of chemical mass tags allows multiple samples to be labelled and compared without the limitations discussed so far, and is therefore a more suitable method for an experimental design which compares several proteomic samples from photosynthetic organisms, as in the case of this research project.

Although other methods are available for isobaric labelling, such as ICAT, there are limitations to these methods that lead to iTRAQ being chosen. ICAT bind specifically

with cysteine residues, so that any peptide lacking these will not be labelled (Fuller and Morris, 2012), which could exclude more than half of the peptides in a sample (Vaughn et al., 2006).

One of the limitations of chemical mass tag labelling is the number of isotopes available and therefore the number of samples that can be compared in one experiment. Using a labelling system with as many sample channels as possible is therefore advantageous in an exploratory experiment (Pottiez et al., 2012). iTRAQ 8-plex kits have the largest number of sample channels available, whilst TMT is available in 2-plex or 6-plex, and iTRAQ is also available in 4-plex (Pichler et al., 2010).

iTRAQ was concluded to be the most suitable quantification technique for this investigation, although factors affecting data acquisition in iTRAQ must still be considered, so these are discussed below. It must also be considered that every quantitation method has its pitfalls and limitations, so method choice must match suitability to experimental design, and take limitations into account during data analysis (Elliott et al., 2009).

#### 1.2.5.2.2 Principles of iTRAQ

In this study, iTRAQ was employed for relative quantification of proteins between samples. This method allows shotgun proteomic analysis of up to 8 samples, using an 8-plex kit, by labelling peptides with isobaric tags (Wiese *et al.*, 2007). Each 8-plex kit contains 8 different isobaric tag labels. Each isobaric tag consists of a reporter group (for which the mass is different for each of the 8 different labels), a balance group, and an amine specific peptide reactive group (Sadowski et al., 2006). The structure of this is shown in Figure 1.4.

[Image removed for copyright reasons]

Figure 1.4 Chemical structure of iTRAQ label (image taken from Sadowski et al. (2006)).

Proteins are extracted and digested into peptides during preparation for the mass spectrometry process, and the digestion of proteins into peptides by trypsin results in free amines at the N-terminus of each peptide, since trypsin cleaves at the carboxyl side of the amino acids lysine and arginine (Olsen et al., 2004). During the labelling

process, the free amine of the N-terminus on the peptide replaces the peptide reactive group of the isobaric tag, and each peptide is labelled with the isobaric tag containing a reporter group and a balance group (Elliott et al., 2009). The aim of the labelling process is to obtain full coverage and label every peptide in a sample with the isobaric tags. Once each of the 8 samples is labelled with the 8 different reporter groups, the samples can be mixed together and the rest of the proteomic processing (fractionation, clean up, identification via mass spectrometry, data processing) can take place on one "sample", but the presence of the tags allows the relative quantities of the peptides in each sample to be calculated (Bantscheff et al., 2007).

As each reporter group has an attached balance group, so each peptide in the sample has the same mass upon entering the mass spectrometer, regardless of which tag label is attached, hence being isobaric. As the sample is processed in the mass spectrometer, peptides are selected for fragmentation. Each peptide is fragmented into  $\gamma$ -type and b-type sequence ions, and the reporter ions are released from the peptide (Unwin, 2010). The intensity of each of these reporter ions and fragment ions is detected by the mass spectrometer, thus a spectrum of a peptide will appear as in the simplified example diagram in Figure 1.7. Through the relative intensities of the reporter ions, it is therefore then possible to calculate the relative quantities of that peptide in each of the 8 samples. Unique peptides that are identified can then be used to calculate the relative quantities of a particular protein in each of the 8 samples (Ross et al., 2004).

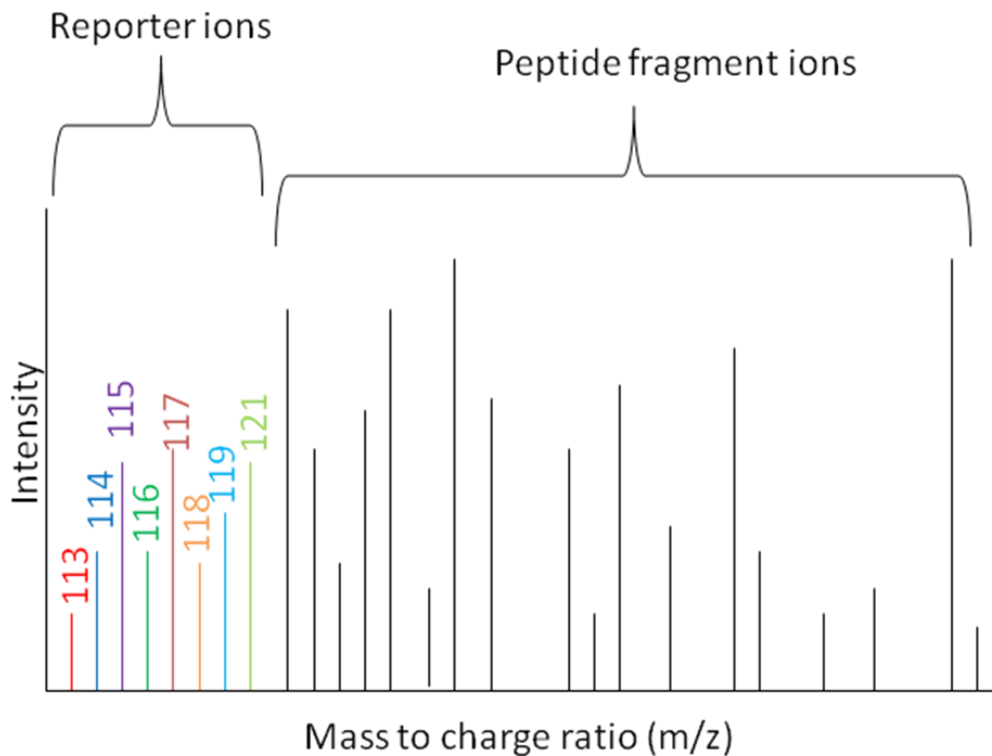


Figure 1.5 Basic layout of a peptide spectrum (with iTRAQ tags) after fragmentation and detection by MS.

#### 1.2.5.2.3 Advantages of iTRAQ labelling

This quantification approach was chosen for several reasons. Labelling the samples means that all digested samples can be mixed and analysed by the mass spectrometer at the same time. Therefore, variation in the performance of the mass spectrometer will not affect the outcome of sample detection in an unequal way (Elliott et al., 2009). Using labelling is also suitable for samples that require prefractionation before sample injection into MS, since there will not be variations in fractionation between samples as samples are already combined (Wang et al., 2012). A labelling method that allowed several samples to be compared was preferred, since this maximises the number of conditions and biological replicates that can be analysed, and the iTRAQ 8-plex kit is one of the largest multi-channel resources available (Pichler et al., 2010). This makes it highly suitable for comparing multiple conditions, or for comparisons of samples in a time course experiment (Wang et al., 2012).

iTRAQ has been shown to be highly efficient in peptide labelling, for example Nogueira et al. (2012) showed that 99.8% of all identified unique peptides. The quantification values detected by mass spectrometry have also been shown to be reliable, with

multiple injections showing good reproducibility of relative quantities (Chong et al., 2006). iTRAQ is also highly suitable for shotgun proteomics where a complex protein sample is analysed (Aggarwal et al., 2006).

#### 1.2.5.2.4 Current limitations and disadvantages of iTRAQ

iTRAQ has been shown to have systematic issues with underestimation of ratios of peptides between samples, because the normalization of the sample compresses ratios further towards the value 1 (Karp et al., 2010). This occurs for a number of reasons, namely: isotope impurities, statistical correction of each sample to contain the same mass of protein, and co-fragmented MS/MS (Evans et al., 2012). Although protein samples are quantified to get an equal estimated quantity of each sample for labelling, there will be small variations between the amount of sample loaded, which must be accounted for (Fuller and Morris, 2012). There may also be other variations like the efficiency of the label to bind to the sample, however experimental testing showed the variation caused at the point of iTRAQ labelling to be much lower than other technical or biological sources of variation in a workflow (Gan et al., 2007). These differences are accounted for in quantification software by adjusting all detected amounts so that the total amount detected is equal in each sample. This adjustment can compress the detected ratio differences (Evans et al., 2012). There are also issues of isotope contamination in separate labels at the point of manufacture (Evans et al., 2012).

This can also cause problems with peptides that are present in low abundance: their relative amount can be changed a lot by these normalization changes, and therefore there is a cut off in intensity applied for peptides, so that differences between sample groups are not over-magnified. This may mean that many proteins would be excluded from analysis of differences between samples, and that only high abundance proteins would be accurately quantified (Ow et al., 2009). It is possible to avoid this issue by using variance-stabilizing normalization (VSN) (Karp et al., 2010). Another way of accounting for this is to spike in known quantities of a specific protein to each sample and apply a correction factor (Karp et al., 2010).

Another issue may occur during selection of precursor ions; if two different peptides have similar enough  $m/z$  ratios, they may be selected together and the reporter ions would be from two different peptides with different relative quantities (Fuller and Morris, 2012). This can be solved in part by high resolution fractionation (Ow et al., 2011), and fractionating samples using HPLC prior to LC-MS/MS will be an important part of methodology in the experimental design used in this thesis.

The ratio of abundance between phenotypes is calculated by using an average of the detected peptide ratios used to identify a protein. If one of these peptide ratios is not accurate, this will affect the quantification of the whole protein (Fuller and Morris, 2012). Peptides may also only be relatively quantified if they appear in all of the iTRAQ channels, otherwise ratios cannot be drawn between samples, since an unquantified peptide will have a value of 0 (Gan et al., 2007).

These limitations of the technique mean that there are possible pitfalls in the analysis and interpretation of data gathered in iTRAQ experiments. However, taking care to employ suitable statistical analysis will overcome some of these. Other limitations will have to be acknowledged during reporting of iTRAQ data.

#### 1.2.5.2.5 Use of iTRAQ in literature for shotgun proteomics of algal samples

8-plex iTRAQ methods have been successfully used to study the effects of environmental stresses on eukaryotic algae to identify key changes in the proteome. Longworth et al. (2012) used iTRAQ 8-plex for a time course experimental study on *C. reinhardtii* subjected to nitrogen stress to accumulate lipids. Gao et al. (in press) studied *Chlorella vulgaris* exposed to pesticide Cypermethrin using four different phenotypes. Du et al. (2014) studied silicon starvation and metabolism in the diatom *Thalassiosira pseudonana*. Wase et al. (2014) studied the effects of nitrogen deprivation on *C. reinhardtii* over time. This shows that iTRAQ 8-plex kits are suitable to the purpose and experiments employed in this thesis, which will aim to explore the effect of salt stress on the proteome of *Chlamydomonas*.

#### 1.2.6 Choice of species for study

This study uses two known species to investigate oil production. The species were chosen for two different but complementary reasons. In Section 1.1 it was explained

that two possible avenues for making algal biofuels energetically and economically viable were to use biological and genetic engineering of algae to increase TAG output, and to use algae with low energetic requirements for culture. Two species of *Chlamydomonas* were chosen as suitable to tackle these two challenges. The first is *Chlamydomonas reinhardtii*. This was chosen for the first part of the research because it is one of the most suitable algae species for engineering purposes. Whilst this is not a highly oleaginous algal species, researchers have recognised its suitability as a model organism for investigating systems biology in green algae (Rupprecht, 2009). It is the model organism for microalgae (Harris, 2001). It is a highly tractable microalgal species (Grossman *et al.*, 2003) and therefore suitable for proteomic and genetic investigation and manipulation, and it has an already existing large body of information on the proteome (Longworth *et al.*, 2012; Stauber and Hippler, 2004), and phosphoproteome (Wagner *et al.*, 2006). There is already a good knowledge base on lipid biosynthesis in *C. reinhardtii* from previous studies (Giroud *et al.*, 1988) and success in proteomic identification and engineered up-regulation of a lipid droplet protein (Moellering and Benning, 2010). It has also been successfully genetically engineered with smaller PSII antennae resulting in improved photon conversion efficiency and increased growth rates in high light conditions (Beckmann *et al.*, 2009). There is a comprehensive online database, The Chlamydomonas Centre, of strain variants and tools for growing and analysing the species ([www.chlamy.org](http://www.chlamy.org)). The availability of information and manipulation tools is the key aspect in choosing this species, as the ultimate aim of the research is to engineer an algae species with enhanced oil producing capabilities. Using this highly tractable species may allow methods of increasing lipid production and accumulation through the successful execution of genetic modification. Additionally, a large number of mutants are available, meaning that strains with enhanced lipid producing abilities have been developed and can be used to target cell processes further towards becoming the ideal biofuel producer. The proteomic analysis of this species may give indicators as to which proteins need to be over-expressed or under-expressed in order to achieve this.

Among the mutants of *Chlamydomonas* sp. that are available, are starchless mutants, which show higher lipid accumulation levels than wild type strains (Li *et al.*, 2010a; Li *et*

*al.*, 2010b; Work *et al.*, 2010). Strains CC-4325 *sta1-1 mt-* [Ball 17] and CC-4323 137c *mt-* [Ball wild-type background for starch mutants] were ordered from the Chlamydomonas Centre ([www.chlamy.org](http://www.chlamy.org)), as a low starch producing mutant and a wild type strain were required for experimentation. A cell wall defective mutant was used in some preliminary experimentation (CCAP 11/32CW15+) and obtained from the Culture Collection of Algae and Protozoa (CCAP, Oban, UK).

The second part of the research was to find ways of reducing the energy input into algal biofuels by employing a species with low temperature growth requirements, and to investigate ways of increasing lipid content in that species. For this the species *Chlamydomonas nivalis* was selected. This is a snow alga and is a primary coloniser in frozen and snowy environments (Remias *et al.*, 2010), as it has the ability to grow in extremely cold places with limited light, with the temperature for cell division being 0-2°C (Hoham, 1975), although the optimum temperature for growth has also been reported as 15-20°C (Hoham, 1975). This species was chosen as it is close phylogenetically to *C. reinhardtii*, and may therefore prove an organism also well suited to proteomic investigation using the same techniques as with *C. reinhardtii*. It is necessary to either have a sequenced organism for proteomic investigation, or to use homology-based sequence-similarity finding tools; identification of proteins for proteomic investigations rely on matching peptide sequences to databases of known proteins (Liska *et al.*, 2004). If a genome is not available, the transcriptome can be sequenced and used as a reference point (Guarnieri *et al.*, 2011), but this supports the point that proteomic data cannot be gained without the use of sequence information of some kind. Sharing the same genus as *Chlamydomonas reinhardtii* may mean that although *C. nivalis* is not sequenced, it can be proteomically investigated using homology searches against the *C. reinhardtii* databases. Being able to grow in low levels of sunlight and low temperatures is extremely useful for algal biofuels development, as irradiance may be a limiting factor in theoretical yield calculations (Weyer *et al.*, 2010), and as outdoor algal cultures in temperate climates must be able to grow in low temperatures during winter; a further reason that *C. nivalis* may prove a desirable biofuel producer. Furthermore, *C. nivalis* has a greater tolerance for environmental changes than *C. reinhardtii*, especially for salt conditions and

temperature (Lu et al., 2012a; Lu et al., 2012c; Lukes et al., 2014). This means that a greater range of environmental stress conditions can be used in lipid investigation with *C. nivalis* than *C. reinhardtii*. This may reveal a greater capacity for lipid producing mechanisms as a defence mechanism against these environmental stresses in *C. nivalis* than in *C. reinhardtii*. *C. nivalis* has already been shown to increase lipid content under certain salt concentrations, as shown by a Nile Red staining experiment (Lu et al., 2012c).

Combining the two advantages of investigating salt induced lipid production in a model, sequenced, highly tractable species and a closely related halotolerant and psychrophilic species will allow this study to compare the response of a little-investigated species of interest which shows the potential for high lipid production under salt stress, with the response of a well known species for which we have a good platform for genetic engineering. It may be possible to use the mechanisms investigated in the snow algae species in a modified version of the model species for an alga designed for greater lipid production. Alternatively, the manipulation techniques applied to *C. reinhardtii* might be used in *C. nivalis* if they are similar enough.

### **1.2.7 Proteomic studies in *Chlamydomonas reinhardtii***

*Chlamydomonas reinhardtii* has been the subject of many proteomic investigations. There have been two reviews that summarize and explain the findings in *C. reinhardtii* (Rolland *et al.*, 2009; Stauber and Hippler, 2004), although these are from a few years ago and subsequently there has been a lot more research on *C. reinhardtii* proteomics, which will be discussed subsequently. Broadly speaking the two reviews cover advantages of *C. reinhardtii* as a candidate for proteomic research, the tools that have advanced the study of the *C. reinhardtii* proteome, and the aspects of the proteome that have been investigated and better understood due to proteomic research. These focus on the eyespot apparatus, redox signalling, mitochondrial proteins, the chloroplast, basal body and flagella proteins and circadian oscillators, with the review by Stauber and Hippler (2004) having a main focus on the sub-proteomes of *Chlamydomonas*. Neither review contains information specifically on the study of the

proteome for lipid metabolism. Ndimba *et al.* (2013) reviewed the proteomics of bioenergy crops, including algae. MLDP, high CO<sub>2</sub> conditions and hydrogen production under anaerobic conditions are the main findings summarized by this review for algal proteomic specific information, although they also state that most studies to date have either been subcellular compartments or stress response investigations. Algal sample preparation needs to be done carefully, since polysaccharide-rich sample species can hinder SDS-PAGE separation (Ndimba *et al.*, 2013).

Heat stress has also been investigated in *C. reinhardtii* using shotgun proteomics (Muhlhaus *et al.*, 2011). In this study chaperone proteins were up-regulated, whilst proteins concerned with photosynthetic and photorespiratory carbon metabolism, acetate metabolism, nitrogen metabolism, C<sub>1</sub> metabolism and cytosolic ribosomes were down-regulated. Proteins detected involved with glycerolipid and carbohydrate synthesis were also down-regulated. Gene Ontology enrichment was used to detect the differences between protein down regulation and protein degradation due to damage.

Proteomic investigations in *C. reinhardtii* have covered a wide range of research focuses, but for the purposes of this study, those concerned with lipid metabolism will be discussed. Table 1.2 summarises the experimental conditions and key findings from a number of proteomic investigations of lipid production in *C. reinhardtii*. This is not an exhaustive list but provides an indication of the breadth of existing research in this field.

**Table 1.2 Examples of proteomic analysis carried out on *C. reinhardtii*.**

Investigation purpose, methods used, and key findings	Reference
Nitrogen deprivation in CC124 and sta6-1. 2D-GEL and MALDI-TOF.  Periplasmic L-amino acid oxidase (LAO1) upregulation (control protein in carbon-nitrogen intergration). Glutathione S transferases and esterase inducement (lipid metabolism and lipid body associated proteins). Changes in major chlorophyll enzymes and carbon fixation and uptake enzymes.	Velmurugan <i>et al.</i> (2014)
Nitrogen deprivation in mutated strain selected for lipid production. 2D-gel ad MALDI-TOF.	Lee <i>et al.</i> (2014)

Upregulation of beta-subunit of mitochondrial ATP synthase. Upregulation of two-component response regulator PilR, a protein involved in response mechanisms of environmental stresses.	
Lipid-producing strains created by random mutagenesis. Comparison of wild-type with mutants at exponential and early stationary phase. 2D-PAGE and MALDI-TOF.	Choi <i>et al.</i> (2013)
Iron deficiency in cell wall-less strain. LC-MS/MS.  Down-regulation of proteins involved in PSI, chlorophyll biosynthesis and the cyt b <sub>6</sub> f complex. Inducement of a bifunctional alcohol and acetaldehyde dehydrogenase (ADH1). Inducement of proteases and redox and oxidative stress related enzymes.	Hohner <i>et al.</i> (2013)
Micronutrient deficiency (copper, iron, zinc, manganese). Label-free quantification. LC-MS.	Hsieh <i>et al.</i> (2013)
Nitrogen deprivation, iTRAQ quantification, LC-MS/MS.  Changes in activity balance between photosystems I and II. Increase in cell wall production and energy metabolism. Decrease in translation machinery.	Longworth <i>et al.</i> (2012)
Ammonium (nitrogen) deprivation. LC-MS, label free spectral counting.  Calvin cycle, acetate uptake and chlorophyll biosynthesis were altered. Increase in enzymes for lipid biosynthesis and accumulation of short chain free fatty acids.	Lee <i>et al.</i> (2012)

The majority of proteomic investigations of lipid production with *C. reinhardtii* have been done with nitrogen deprivation. James *et al.* (2011) investigated the lipid profile of starch-less mutants BAF-J5 and I7 under nitrogen deprivation, and found a shift in the lipid profile but the only major protein found in the lipid oil fraction was MLDP (not even oleosin or caleosin proteins were found, which would be expected as they are major structural proteins in lipid bodies). However, Nguyen *et al.* (2011) found 248 proteins associated with the lipid bodies in *C. reinhardtii* (2 or more peptides) under nitrogen stress, 33 of which were involved in lipid metabolism. These included key steps of the TAG synthesis pathway. They also found a number of proteins showing similarity to lipases and suggest that down regulation of these could be a route to boosting oil accumulation under non-stress conditions; although, it may also be due to degradation of plastidial membranes, which occurs when oil accumulation is triggered (Nguyen *et al.*, 2011). Longworth *et al.* (2012) investigated the proteomic changes in *C. reinhardtii* under increased lipid production from nitrogen stress. 135 proteins across all functional groups were found to be significantly altered under the lipid producing

conditions, and two of these were specifically to do with fatty acid production: up-regulation in acetyl-CoA carboxylase and a predicted protein with homology to long chain acyl-CoA synthase.

Nitrogen sparing mechanisms have been studied and it has been shown that respiration is prioritized over photosynthesis, and ribosomes were reduced. High abundance proteins are decreased and low abundance proteins are increased, and TAGs (which contain no nitrogen) are increased (Schmollinger *et al.*, 2014). Eckardt (2014) suggest that thylakoid membranes are reduced in TAG synthesis, rather than *de novo* fatty acid biosynthesis, as they found that proteins involved with the early stages of fatty acid metabolism were reduced under nitrogen deprivation.

### **1.2.8 Salt stress and lipid accumulation in microalgae and cyanobacteria**

Salt stress (an induction of increased salt level) has been shown to cause TAG increase in *Nannochloropsis salina* (Bartley *et al.*, 2013), as well as decreased membrane lipid content. Xia *et al.* (2014) have also shown that addition of high NaCl to a freshwater algal species (*Desmodesmus abundans*) induced higher lipid productivity, demonstrating that salt stress is not just relevant to halophile or halotolerant species. *Botryococcus braunii* shows increases in the relative proportions of oleic acid and palmitic acid under increased salinity (from 34 mM to 85 mM) (Rao *et al.*, 2007). Venkata Mohan and Devi (2014) also find higher lipid productivity under salinity induction than under normal growth phases in their mixed microalgal culture. *Dunaliella salina* has also been shown to increase lipid content in response to high salt concentrations (Takagi *et al.*, 2006).

In cyanobacteria, salt stress results in the inactivation of photosynthetic machinery (Hu *et al.*, 2014). To counter the effects of salt stress, halotolerant cyanobacteria have protection mechanisms; namely the formation of compatible solutes, and the desaturation of lipid membranes (Singh *et al.*, 2002). The desaturation of lipid membranes in salt stressed cyanobacteria is theorised to regulate the movement of ionic salts in and out of the cell, thereby helping to prevent osmotic shock by maintaining a low cellular salt content (Singh *et al.*, 2002). The mechanisms of lipid membrane desaturation that are used to counter salt stress are also used in low-

temperature stress (Sakamoto and Murata, 2002). Cyanobacteria at low temperatures have increased membrane lipid desaturation, as this makes the membrane more fluid and aids low temperature stress tolerance (Yuzawa *et al.*, 2014). The increase in membrane fluidity due to lipid desaturation at low temperatures has also been found in green alga *Nannochloropsis salina* (Van Wagenen *et al.*, 2012).

It has also been found that cyanobacteria downregulate activity in photosystem II under salt stress but upregulate it in photosystem I (Zhang *et al.*, 2010). This is suggested to be to protect photosystem II from excess excitation energy. The upregulation of photosystem I activity has also been suggested to provide energy for synthesising organic osmolytes to protect against osmotic stress (Zhang *et al.*, 2010). Proteomic analysis of cyanobacteria under salt stress reveals upregulation of synthesis of compatible solutes glucosylglycerol and sucrose (Chen *et al.*, 2014). ADP-glucose phosphorylase upregulation was observed by Pandhal *et al.* (2008), this provides the precursors for glucosylglycerol biosynthesis.

Whilst salt has been shown to induce lipid changes in cyanobacteria and microalgae, as demonstrated in these studies, only one study investigated the effect of salt stress on lipid content in *C. reinhardtii* (Siaut *et al.*, 2011), and this did not study lipid profile.

## **1.2.9 *Chlamydomonas reinhardtii*: lipid knowledge and manipulation**

### **1.2.9.1 Stress manipulation**

Nitrogen deprivation has been the main focus in lipid manipulation in *C. reinhardtii*. Sulphur stress has also been investigated and shown to be a lipid trigger (Cakmak *et al.*, 2012). According to Fan *et al.* (2011), light levels are important factors in the TAG levels, as well as acetate availability. Sharma *et al.* (2012) provide a full description of different stresses used to investigate the lipid profile in different species. *C. reinhardtii* is to date documented to respond with a TAG increase to nitrogen deprivation and sulphur deprivation. The effect of nitrogen stress and its interaction with culture growth and metabolism has been discussed by Johnson and Alric (2013), who describe how nitrogen deprivation induces cell growth arrest and loss of photosynthetic apparatus. To explore the unknown pathways involved with carbon relocation to lipids, they discuss the conditions known to lead to lipid production, namely: nitrogen

deprivation; lack of cell wall; sufficient acetate availability; and sufficient light availability. A full discussion of the known metabolic constraints of lipid production is detailed in this review (Johnson and Alric, 2013).

#### **1.2.9.2 Salt stress in *C. reinhardtii***

There have been a few studies of salt stress in *C. reinhardtii*, although only one that investigates the effect of salt on lipid content (Siaut *et al.*, 2011), and four studying the proteome (Mastrobuoni *et al.*, 2012; Neelam and Subramanyam, 2013; Subramanyam *et al.*, 2010; Yokthongwattana *et al.*, 2012). Neelam and Subramanyam (2013) studied the effect of salinity (50, 100, 150 mM) on the protein profile of Photosystem II and Light Harvesting Complex II, and found inhibitory effects on their functioning, as well as flagella motility inhibition. The inactivation of reaction centres in PSII increased as salinity increased, with a decrease of donor and acceptor side proteins and slower electron transport. This data was supported by a loss of chlorophyll pigments in the cells and changes in morphology. Similarly Subramanyam *et al.* (2010) targeted PSI and LHCI proteins in cells grown under 100 mM NaCl conditions, as this was the less well studied of the two photosystems with regards to salt stress. Electron transfer activity is reduced under these conditions, as there is evidence that PSI-LHCI is damaged by reactive oxygen species (ROS) under high salt conditions. This, in turn, impairs cell growth.

Yokthongwattana *et al.* (2012) used 300 mM NaCl with an exposure time of 2 hours to see the effect of short term sudden salt stress on the proteome. They used a 2D-gel-based method for this and exclusively investigated proteins that were present in only either the control or the salt stress group. 18 proteins appeared only in the control group, including the only spot that was seen associated with fatty acid metabolism. In contrast, 99 proteins were found in only the salt stressed sample. From these, a large number were associated with carbohydrate (11%) and amino acid (12%) metabolism, TCA cycle and energy metabolism (10%), photosynthesis (8%), protein folding, sorting and degradation (9%), and stress related proteins (15%). Broadly Yokthongwattana *et al.* (2012) concluded that: antioxidant enzymes are required to scavenge the ROS; the cells require a lot of energy to maintain homeostasis, from the glycolytic and energy-

producing metabolic pathways; and heat shock and chaperone proteins are required to renature misfolded or aggregated proteins. Yokthongwattana *et al.* (2012) provide some evidence that many changes to salt stress specific proteins could be from post translational modifications (PTMs) (as an active role in countering salinity stress) rather than *de novo* synthesis, although this was not proven. The alternative conclusion is that proteins are inactivated by the toxic level of salt stress and lose their function via PTMs.

Mastrobuoni *et al.* (2012) used SILAC labelling to measure proteomic changes under 100 mM and 150 mM NaCl over time points 1, 3, 8 and 24 hours, and combined this with metabolomic analysis. This study focused on protein dynamics, namely half-life of proteins and relative synthesis rates of proteins. They found proline accumulation as functional response to salt stress, as it can aid resistance to salt stress and freezing. They also found that amino acid metabolism is induced under salt stress. The metabolite changes occurred sooner in the 150 mM salt stress, with the 100 mM salt stress taking an additional 23 hours to reach the same metabolite pattern. The changes in patterns in metabolites were not reflected in the proteome, and the two salt conditions gave rise to very similar proteomes. It is suggested that the metabolome regulation is post translational.

It has also been found that *C. reinhardtii* produces volatile organic compounds (VOCs) in response to salt stress to mitigate against ROS. These VOCs induce a decrease in cell density, but an increase in chlorophyll content and antioxidant enzyme activity (Zuo *et al.*, 2012). Salt stress is enhanced by high illumination, as demonstrated by production of oxidative stress indicator lipid hydroperoxide in salt treated *C. reinhardtii* (Yoshida *et al.*, 2004). It has also been shown to enhance photoinhibition of photosynthesis, by preventing cell repair from photodamage (León and Galván, 1999; Neale and Melis, 1989). The production of glycerol to mitigate against osmotic stress is limited by illumination levels (León and Galván, 1999).

#### **1.2.10 Lipid research in *Chlamydomonas nivalis***

There are currently three published studies on lipid biomarkers in *C. nivalis* under salt conditions (Lu *et al.*, 2012a; Lu *et al.*, 2012b, c). Lu *et al.* (2012c) found that under a

range of salt stresses, using Nile Red as their screening technique, the highest lipid content was found at 1.00% NaCl (0.17 M NaCl) at 7 hours and 1.25% NaCl (0.21 M NaCl) at 5 hours. The use of UPLC/Q-TOF-MS has shown that certain lipids are biomarkers for salt stress; some appear during salt stress and others disappear under salt stress, as the need for membrane stability changes (Lu *et al.*, 2012a; Lu *et al.*, 2012c). The results from these previous studies can be summarised thus: the studies address the types of lipid component and their relative proportions rather than comparing relative levels of different fatty acid chains. The lipid types are sulfolipids (sulfoquinovosyldiacylglycerol or SQDG), galactolipids (monogalactosyl diacylglycerol or MGDG, and digalactosyldiacylglycerol or DGDG, collectively known as DAGs or diacylglycerols) and phospholipids (phosphatidylglycerol or PG, phosphatidylethanolamine or PE, and phosphatidylinositol or PI) and diacylglyceryl trimethylhomoserine (DGTS). The different lipid types can contain different fatty acid chains and these change depending on the conditions the algae are grown in. Both the relative proportions of the lipid groups change, as well as the chain types of fatty acids within the different lipid types (Lu *et al.*, 2012a; Lu *et al.*, 2012c). It is therefore difficult to draw apart exactly how the relative proportions of chain types as a whole change, but these studies describe how certain lipid types change in response to salt stress; regulation of galactolipid and the DGDG/MGDG ratio may be a response to salt stress and protecting the function of the cell (Lu *et al.*, 2012a). All of these lipid types are polar, and therefore not the main group of lipids that are interesting for biofuels research: TAGs are neutral lipids. However, the polar lipids are also the only lipids investigated in the study of nutrient deprivation in *C. nivalis* carried out by Lu *et al.* (2013), showing that, to date, there is no research focussing solely on the neutral lipids or TAGs in this species, that accumulate in lipid bodies. One study into a related Antarctic *Chlamydomonas* species studied lipid accumulation under salt stress (An *et al.*, 2013) and found a 23% lipid content (w/w) under 16% NaCl, and a strong influence of salinity on lipid profile.

No proteomic studies on *C. nivalis* exist to date. There has been a proteomic study (using 2-DE and subsequent MALDI-ToF-MS) on the effect of low temperature stress (4-6°C compared with control condition 6-8°C) on a related Antarctic "*Chlamydomonas*

sp." (Kan *et al.*, 2006), which identifies newly expressed enzymes that are important for the transport and metabolism of amino acids (homocitrate, isopropylmalate and citramalate synthases) and help the cells to maintain normal metabolism under temperature induced decreases. The second newly expressed protein was glutathione S-transferase, associated with free radical, active oxygen and noxious metabolite scavenging, which is necessary under low temperature stress. This paper references Palmisano and Sullivan (1982) on the role of increased fat in protecting ice diatoms from freezing, and Devos *et al.* (1998) for the role of Rubisco in adaptation to cold in psychrophilic algae. The authors also highlight the importance of protein sample preparation in Antarctic species with thick cell walls and a large amount of high-molecular weight substances (lipid, starch, polysaccharide pigments and salts) that need to be removed with TCA-acetone precipitation.

Non genome sequenced algae can be used for proteomic work using *do novo* sequencing or EST databases (Ndimba *et al.*, 2013), but the information obtained will be limited. Investigating an unsequenced species may require cross-species investigation (Wright *et al.*, 2010). This is made possible by shared peptides between species, which can be high even in species not in the same genus, as demonstrated by 30-50% shared peptides between *Mus musculus* and *Homo sapiens* (Snijders *et al.*, 2007). Pandhal *et al.* (2008) have demonstrated the successful use of this technique in a quantitative proteomic study of salt concentration on an unsequenced cyanobacterium, and identified 383 proteins using a combination of sequenced organism databases (although 82.5% of the identifications came from one closely related species). Pereira-Medrano *et al.* (2012) have also demonstrated this in a quantitative proteomic study of unsequenced psychrophilic bacterium *Pedobacter cryoconitis*. The number of identifications that can be made in cross-species investigation is limited by differences in amino acid sequences (and therefore peptide masses) between species, and therefore this method does not yield as many successful peptide identifications as when using a sequenced species (Wright *et al.*, 2010).

### 1.2.11 Gaps in research and opportunities for investigation

The lack of full lipid investigation into *C. reinhardtii* under salt stress provides an opportunity to investigate this model species under a new stress condition that could provide further understanding of lipid metabolism changes under stress. Unlike nitrogen stress, salt stress does not necessarily have the same limits on protein synthesis and cell division, and therefore might address the issues that affect overall lipid productivity in a culture. Coupling lipid investigation with proteomic analysis improves the chances of understanding these mechanisms within the cells, which as yet has not been carried out on lipid studies in *C. reinhardtii*.

Although lipid biomarkers have been investigated in *C. nivalis*, lipid productivity and suitability of the species to biofuel production has not been carried out in full, despite its advantages in robustness to environmental changes, and its low temperature requirements. This species has not been sequenced, so to date no proteomic studies have been carried out on it.

These areas have been chosen to explore the aim of this thesis - to explore ways to enhance microalgal biofuel production - and these are explained in more detail in the project aims in Section 1.3.

### 1.3 Aims of this PhD thesis

The aim of this research, broadly speaking, is to find ways of increasing the useful output from microalgae for renewable energy purposes. There are potentially several angles for doing this spanning over the range of upstream and downstream processes, but this project focusses specifically on the ways that biological understanding can influence both biological engineering of algal species and also the culturing of species to improve the oil content of those algae. Knowing that "lipid triggers" are a proven way to increase the overall oil content of algal biomass, this path was pursued.

The first aim was to establish whether salt stress was a lipid trigger in *Chlamydomonas reinhardtii* and if so, how this influenced the lipid profile of the species. It was important to know how the many different aspects of the biology interacted together, so the aim was not just to assess lipid content and profiling, but also aspects of carbon partitioning, growth data, and ability to carry out photosynthesis. This knowledge of exactly how different salt concentrations affect *C. reinhardtii* in these aspects informs research on how we can engineer algal cultures using lipid trigger understanding. Prior work has shown that these mechanisms are not simple and that making an algal cell produce more lipid suitable for biofuel may be a complex multifaceted problem. Understanding the lipid profiling in response to salt stress is also important for understanding the ability for cultures to function under fluctuating salinity, as may occur in open pond environments, and how the cells regulate their necessary processes for growth and maintenance with the desired process of creating lipids.

The second aim was to identify proteomic changes in the regulation of proteins associated with these key biological processes in response to salt, most importantly the regulation of lipid production, accumulation and regulation of different fatty acids. The quantitative difference between proteomes of treatment types, under normal and altered (ideally elevated) lipid producing conditions would demonstrate which proteins were responsible in the regulation of these lipids and for all processes associated with coping with increased salinity stress.

The third aim was to take a closely related species *C. nivalis* and investigate these same biological processes and regulation of lipid production under salt stress, with respect

to proteomic changes, as described for *C. reinhardtii* in aims 1 and 2. *C. nivalis* has different growth conditions so the influence of carbon source presence and temperature and species may have a different outcome to that of *C. reinhardtii*. Furthermore, it has a higher salt stress tolerance (1.2 versus 0.1 M NaCl). Part of this aim will be to explore the genetic and proteomic similarity of the two species.

By exploring these aims together, the suitability of *C. reinhardtii* and *C. nivalis* as biofuel producers could be evaluated and compared. Linking this research to proteomic data on the response of the species to a potential and unexplored lipid trigger could aid bio-engineering of algal cultures in the future to improve algal biofuel yields as much as possible. By comparing the proteomic studies from two species, we may be able to gain molecular information on the differences in lipid responses to salt from the two species.

The original contribution of this thesis is to provide in depth analysis of the effect of salt stress on the lipid profiles of two *Chlamydomonas* species, coupled to proteomic investigation of the lipid metabolism under salt stress. To date, there has been no detailed lipid profiling of *C. reinhardtii* under salt stress and therefore no clear evidence of whether or not this provides a lipid trigger in this species. Whilst there has been some lipid biomarker study of *C. nivalis* under salt stress in previous studies, there has been no proteomic investigation of the lipid changes using this un-sequenced species, and little investigation into its suitability to biofuel production. Therefore, these gaps in scientific knowledge are the areas that this thesis addresses. The flow chart displayed in Figure 1.6 outlines how this thesis will address these areas of investigation. Overall, the investigations into salt stress in microalgae may provide crucial information into its effects on producing biodiesel from algae on an industrial scale, since salt conditions have the potential to enhance or reduce yields.

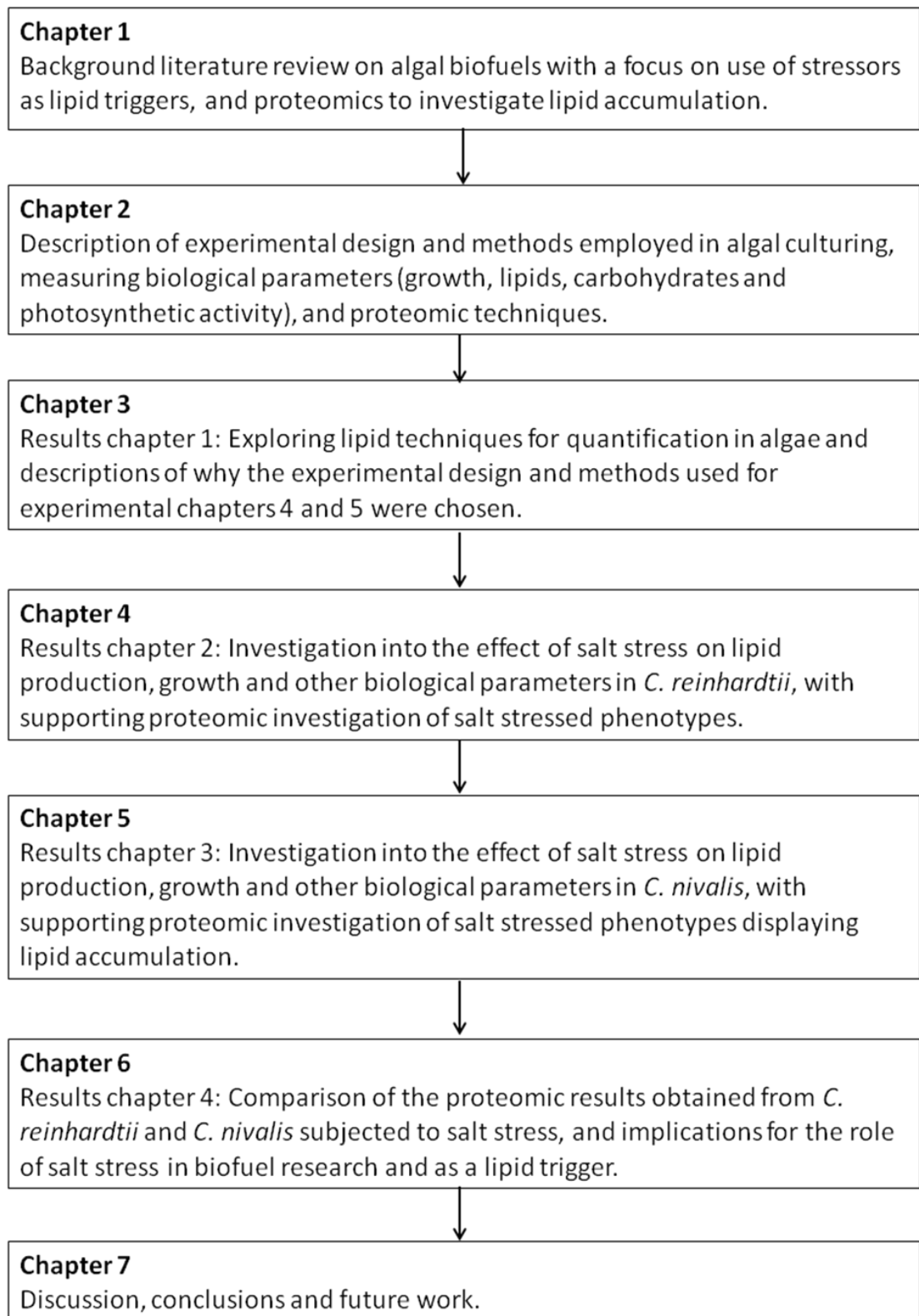


Figure 1.6 Flow diagram of chapters and thesis structure.

## 2 Chapter 2: Materials and Methods

The methods used in this thesis are designed to investigate various biological parameters of two algal species in laboratory cultures. The main areas of investigation are growth (both in terms of biomass production and cell numbers), lipid production, carbohydrate production, chlorophyll production, cell morphology and photosynthesis/respiration rates. The second main aim is to quantify the proteome of the different algal species and comparing the proteomes under lipid producing conditions.

This chapter sets out the methods that have been tested and developed, and describes the final methods that were used to gather data for the project. Additionally, the experimental design of the thesis is outlined below.

### 2.1 Experimental design

This section outlines the list of experiments undertaken and the reasons for choosing these experimental designs. The aim of the experiments in this thesis are to reveal the effect of salt stress on the lipid production of two species of algae, through lipid analysis and subsequent proteomic analysis. The broad workflow of the experiments is shown in Figure 2.1, although the details of the experimental design (e.g. exact culture conditions, lipid measuring techniques, salt conditions) developed as the research progressed. The list of experiments undertaken is summarised and explained in Table 2.1. The reasons for the developments in experimental design are further expanded in Chapter 3; this chapter presents the data obtained from preliminary lipid experiments and how this informed the choice of experimental design that forms the main body of investigation for this thesis (Chapters 4-6). All preliminary work (Experiments 1-8 in Table 2.1) was carried out on *C. reinhardtii*, whilst the full investigations of lipid profile and subsequent proteomic analysis (Experiments 9-16 in Table 2.1) were carried out

on both species. The choice of salt concentrations is described and explained in Section 2.3.1.

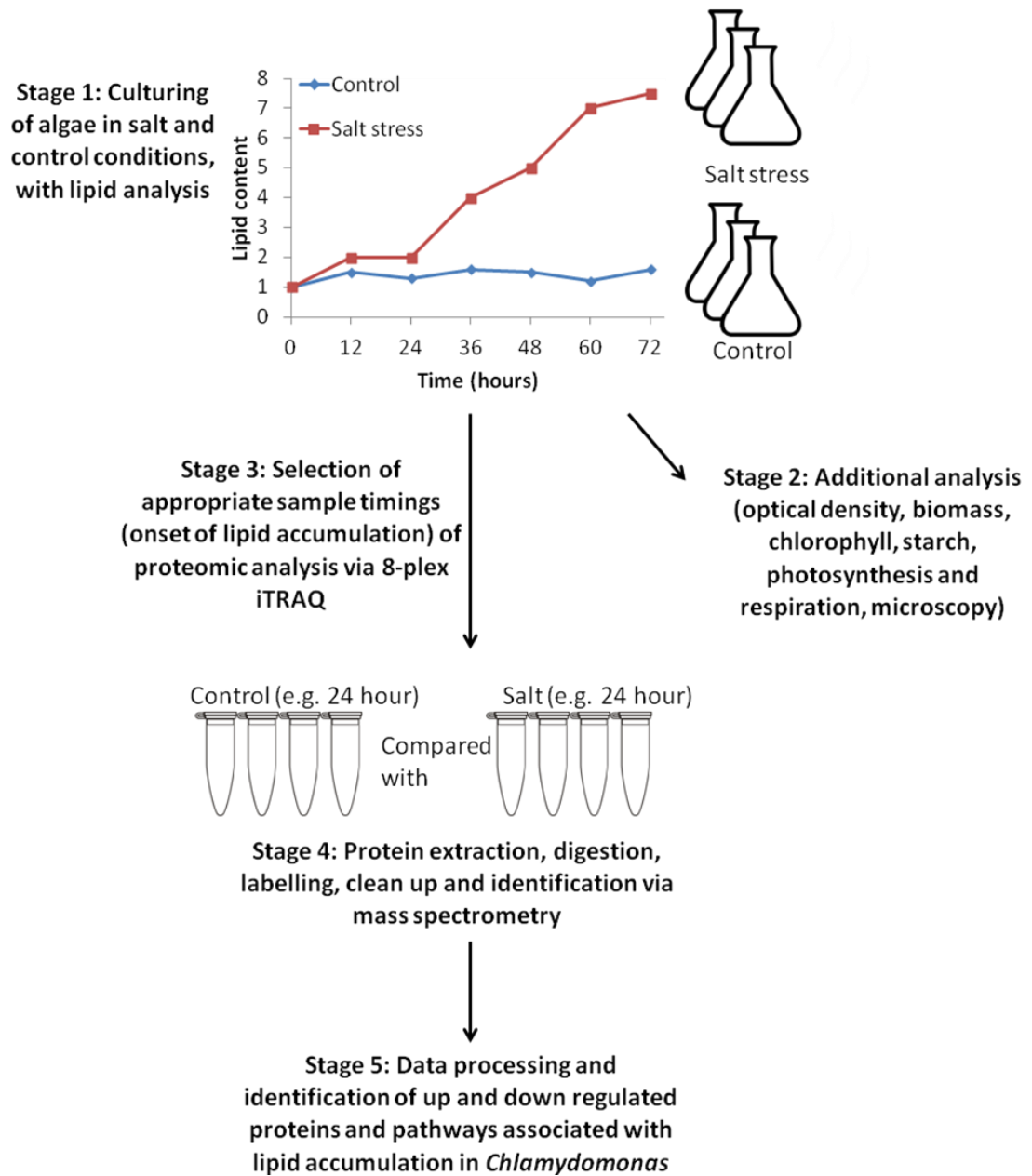


Figure 2.1 Experimental design workflow for investigating the effect of salt on lipid metabolism in *Chlamydomonas* species.

**Table 2.1 Summary table of experiments carried out for this thesis. Experiments are ordered chronologically and include rationale for changes in experimental design to show development of methods and experimentation.**

Experiment number	Experiment description	Species used	Salt conditions tested	Methods used	Aims and desired outcomes of experiment	Alterations (with rationale) to experimental design from previous experiment
1	1 mL seeding culture in 100 mL of TAP media containing a salt concentration. 1 replicate. Sampling took place at late log phase of growth curve (time point different for each condition).	<i>C. reinhardtii</i> wildtype CC-4323 137c mt-	0, 0.05, 0.1, 0.15, 0.2 and 0.25 M NaCl	Gravimetric lipid analysis	To determine the optimum salt concentration for increasing lipid content in wild type <i>C. reinhardtii</i> by measuring lipid content in each culture. Growth measured via OD and cell counts.	N/A
2	1 mL seeding culture in 100 mL of TAP media containing a salt concentration, or containing only TAP media and introducing salt later to the culture at different time points. 1 replicate. Sampling took place at different time points for each set of cultures.	<i>C. reinhardtii</i> wildtype CC-4323 137c mt-	0, 0.05, 0.1, 0.15, 0.2 M NaCl	Gravimetric lipid analysis	To determine if sampling early or later in the growth cycle affected the lipid content. Also to determine if adding salt to a culture partway through, rather than at the start, affected lipid content.	Introducing salt at later stages as well as at the point of seeding to look at the effect of stress addition timing on the lipid content. Loss of 0.25 M NaCl condition due to contaminated culture.
3	1 mL seeding culture in 100 mL of TAP media containing a salt concentration. 3 replicates. Sampling took place at late log phase of growth curve (time point different for each condition).	<i>C. reinhardtii</i> wildtype CC-4323 137c mt-	0, 0.05, 0.1, 0.15, 0.2 M NaCl	Gravimetric lipid analysis	To confirm results obtained from experiment 1 were consistent (determining optimum salt concentration and to make them more scientifically rigorous by using three biological replicates.)	Repeat of experiment 1, with 3 biological replicates.
4	Using samples from experiments 1 and 2 gravimetric lipid extracts to test the accuracy of the microcolorimetric method.	<i>C. reinhardtii</i> wildtype CC-4323 137c mt-	0, 0.05, 0.1, 0.15 and 0.2 M NaCl	Microcolorimetric lipid analysis	To test accuracy and suitability of microcolorimetric techniques. Comparisons of results obtained with gravimetric results.	Testing of microcolorimetric method against gravimetric results to see if this method would allow lipid analysis using smaller sample sizes.
5	Cultures grown in TAP media (no added salt) until log phase and resuspended using salt media to OD <sub>750</sub> 0.44. Multiple time points obtained and lipid analysis via Nile Red.	<i>C. reinhardtii</i> cell wall mutant CCAP 11/32CW15+	0 and 0.15 M NaCl. Also Nitrogen deprivation.	Nile Red lipid analysis	Nile Red samples are small enough to take multiple time points in a time course. Aim to compare lipid content over time in salt stress conditions, control conditions, and established lipid trigger nitrogen deprivation.	Use of 0.15 M NaCl, it was determined from experiment 2 that this was likely to yield the highest lipid content. Comparison against the known stress (nitrogen deprivation) shown to increase lipid in cell wall mutant.

6	Cultures grown in TAP media (no added salt) until log phase and resuspended using salt media to OD <sub>750</sub> 0.44. Multiple time points obtained and lipid analysis via Nile Red.	<i>C. reinhardtii</i> starchless mutant CC-4325 sta1-1 mt- [Ball I7]	0, 0.15 and 0.2 M NaCl	Nile Red lipid analysis	Compare lipid content over time in starchless mutant strain under control, 0.15 and 0.2 M NaCl.	Results from experiment 5 did not yield increase in Nile Red fluorescence, so starchless mutant and higher salt conditions of 0.2 M NaCl were tested.
7	Cultures grown in TAP media (no added salt) until log phase and resuspended using salt media to OD <sub>750</sub> 0.44. Multiple time points obtained and lipid analysis via Nile Red. PBS buffer used.	<i>C. reinhardtii</i> starchless mutant CC-4325 sta1-1 mt- [Ball I7]	0, 0.2 and 0.3 M NaCl	Nile Red lipid analysis	Compare lipid content over time in starchless mutant strain under control, 0.2 and 0.3 M NaCl.	Experiment 6 did not yield a high increase in Nile Red fluorescence. Salt may have been interfering with Nile Red so PBS buffer was used to wash samples. Higher salt conditions were also used.
8	Cultures grown in TAP media (no added salt) until log phase and resuspended using salt media to OD <sub>750</sub> 0.44. Multiple time points obtained and lipid analysis via Nile Red. PBS buffer used. Protein samples obtained at multiple time points.	<i>C. reinhardtii</i> starchless mutant CC-4325 sta1-1 mt- [Ball I7]	0, 0.2 and 0.3 M NaCl	Nile Red lipid analysis and protein extractions	Compare lipid content over time in starchless mutant strain under control, 0.2 and 0.3 M NaCl, and take protein samples for proteomic analysis of lipid producing conditions. (iTRAQ data not included in results chapters).	Repeat of experiment 7 but with protein samples also obtained to compare proteomes of cultures under control and high lipid producing conditions.
9	Cultures grown in TAP media (no added salt) until log phase and resuspended using salt media to OD <sub>750</sub> 0.44. Multiple time points obtained and lipid analysis via GC analysis of FAME. PBS buffer used.	<i>C. reinhardtii</i> starchless mutant CC-4325 sta1-1 mt- [Ball I7]	0, 0.2 and 0.3 M NaCl	GC analysis	Use samples from experiment 8 to compare FAME profile over time in starchless mutant strain under control, 0.2 and 0.3 M NaCl.	Same samples as experiment 8, but tested via GC analysis to compare FAME to Nile Red result.
10	Cultures grown in TAP media (no added salt) until log phase and resuspended using salt media to OD <sub>750</sub> 0.44. Multiple time points obtained and lipid analysis via GC analysis of FAME. PBS buffer used.	<i>C. reinhardtii</i> starchless mutant CC-4325 sta1-1 mt- [Ball I7]	0 and 0.1 M NaCl	GC analysis	Examine FAME profile over time in starchless mutant strain under control and 0.1 M NaCl.	Lower salt concentration than experiment 9, to compare the effects of high salt (0.2 M and above) and low salt (0.1 M) on FAME profile.
11	Cultures grown in TAP media (no added salt) until log phase and resuspended using salt media to OD <sub>750</sub> 0.44. Multiple time points obtained and lipid analysis via GC analysis of FAME.	<i>C. reinhardtii</i> starchless mutant CC-4325 sta1-1 mt- [Ball I7]	0, 0.2 and 0.3 M NaCl	GC lipid analysis and iTRAQ proteomic analysis	Carry out iTRAQ proteomic experiment of short term salt stress (at 3 hours exposure), comparing 3x control samples, 2x 0.2 M NaCl samples, and 3x 0.3 M NaCl samples.	Repeat of experiment 9 but with fewer time points (as already established FAME profile in experiment 9) and with protein samples obtained for proteomic

	PBS buffer used. Protein samples obtained at multiple time points.					analysis.
12	Single replicate preliminary data. Cultures grown in 3N-BBM-V media (no salt) until log phase and salt was added to media. Multiple time points obtained and lipid analysis via GC analysis of FAME. PBS buffer used.	<i>C. nivalis</i>	0, 0.2, 0.5, 1.0 and 1.5 M NaCl	GC lipid analysis	Compare FAME profile over time in <i>C. nivalis</i> under different salt conditions to establish the best salt concentration to increase lipids in this species.	Preliminary tests on <i>C. nivalis</i> . Different salt concentrations used to <i>C. reinhardtii</i> because <i>C. nivalis</i> has a higher salt tolerance.
13	Cultures grown in 3N-BBM-V media (no salt) until log phase and resuspended using salt media to OD <sub>750</sub> 0.44. Multiple time points obtained and lipid analysis via GC analysis of FAME. PBS buffer used. Protein samples obtained at multiple time points.	<i>C. nivalis</i>	0 and 1.4 M NaCl	GC lipid analysis and iTRAQ proteomic analysis	Carry out iTRAQ proteomic experiment of short term salt stress (at 3 hours exposure), comparing 3x control samples <i>C. nivalis</i> , 3x 1.4 M NaCl samples <i>C. nivalis</i> , and 2x 0.3 M NaCl samples <i>C. reinhardtii</i> (used as 2 additional 8-plex channels were available). (iTRAQ data was not able to be obtained for results chapters).	3x biological replicates of control and high salt conditions. High salt conditions had been used in <i>C. reinhardtii</i> for a short term lipid response to salt stress, so salt conditions beyond the salt tolerance of <i>C. nivalis</i> were used to try to achieve the same effect.
14	Cultures grown in 3N-BBM-V media (no salt) until log phase and resuspended using salt media to OD <sub>750</sub> 0.44. Multiple time points obtained and lipid analysis via GC analysis of FAME. PBS buffer used.	<i>C. nivalis</i>	0 and 0.2 M NaCl	GC lipid analysis	Compare FAME profile over time of control conditions and of 0.2 M NaCl conditions (found from preliminary experiment 12 to be the most suitable for lipid increase from long term salt stress).	3x biological replicates of control and 0.2 M NaCl salt conditions. Preliminary results from experiment 12 and literature data suggested this salt condition would achieve high lipid contents in <i>C. nivalis</i> .
15	Cultures grown in 3N-BBM-V media (no salt) until log phase and resuspended using salt media to OD <sub>750</sub> 0.7. Multiple time points obtained and lipid analysis via GC analysis of FAME. PBS buffer used.	<i>C. nivalis</i>	0 and 0.2 M NaCl	GC lipid analysis	Compare FAME profile over time of control conditions and of 0.2 M NaCl conditions when carrying out resuspension at later phase in growth curve.	Repeat of experiment 14 but grown to higher OD before resuspension to ensure a thick starting culture to obtain biomass.
16	Cultures grown in 3N-BBM-V media (no salt) until log phase and resuspended using salt media to OD <sub>750</sub> 0.35. Multiple time points obtained and lipid analysis via GC analysis of FAME. PBS buffer used. Protein samples obtained at	<i>C. nivalis</i>	0 and 0.2 M NaCl	GC lipid analysis and iTRAQ proteomic analysis	Carry out 8-plex iTRAQ proteomic experiment of 0.2 M NaCl salt stress, comparing 2x 0.2 M NaCl samples at 3 hours, 2x 0.2 M NaCl samples at 82 hours, 2x 0.2 M NaCl samples at 170 hours, and 2x control samples at 170 hours.	Repeat of experiment 14, but with protein samples taken at multiple time points for subsequent proteomic investigation.

	multiple time points.					
17	Genetic analysis	<i>C. nivalis</i>	Control	18S sequencing	To establish strength of genetic relatedness of <i>C. nivalis</i> to <i>C. reinhardtii</i> .	N/A
18	Cultures grown in TAP media (no added salt) until log phase and resuspended using salt media to OD <sub>750</sub> 0.35. Multiple time points obtained and lipid analysis via GC analysis of FAME. PBS buffer used. Protein samples obtained at multiple time points.	<i>C. reinhardtii</i>	0, 0.1, 0.15 and 0.2 M NaCl	GC lipid analysis and iTRAQ proteomic analysis	Carry out 8-plex iTRAQ proteomic experiment of 0.2 M NaCl salt stress, comparing 2x 0.2 M NaCl samples at 3 hours, 2x 0.2 M NaCl samples at 11 hours, 2x 0.2 M NaCl samples at 18 hours, and 2x control samples at 18 hours.	Repeat of experiment 11, but with protein samples taken at multiple time points for subsequent proteomic investigation.

## 2.2 Algal species

Algal species *Chlamydomonas reinhardtii* strain CC-4323 137c mt- (Ball background strain nit1 nit2) and strain CC-4325 sta1-1 mt- [Ball I7] were obtained from the Chlamydomonas Resource Centre ([www.chlamycollection.org](http://www.chlamycollection.org)). The Ball I7 strain is deficient in the catalytic (small) subunit of ADP-glucose pyrophosphorylase and was obtained by X-ray mutagenesis of the wild type strain CC-4323.

Snow algal species *Chlamydomonas nivalis* (strain number CCAP 11/128) was obtained from the Culture Collection of Algae and Protozoa, Scottish Marine Institute, Oban. This strain was originally collected from rocks below a snowfield near Saddlebag Lake, Sierra, USA.

## 2.3 Algal culturing

*Chlamydomonas reinhardtii* was used for the majority of experiments, due to its more highly tractable nature for genetic transformations (Leon-Banares *et al.*, 2004). Cultures were grown in TAP medium, for mixotrophic growth. The composition of TAP medium is shown in Appendix A. Cultures were grown in 24 hour light, at 25°C (monitored and kept constant by the Seasons Air Conditioning unit in the growth room) and at light intensity displayed in Figure 2.2. The cultures were grown without shaking initially (the shaker in this room was Stuart Orbital Shaker SSL1, Serial Number R000101087, Barloworld Scientific Limited, Stone, Staffordshire, UK), and all cultures were seeded from 1 mL culture in 100 mL media in 250 mL conical flasks, sealed with 55 x 50 mm polyurethane foam sponges (Fisherbrand Scientific, UK, product code 12904301) to allow some air, and therefore carbon dioxide, to enter the flask.

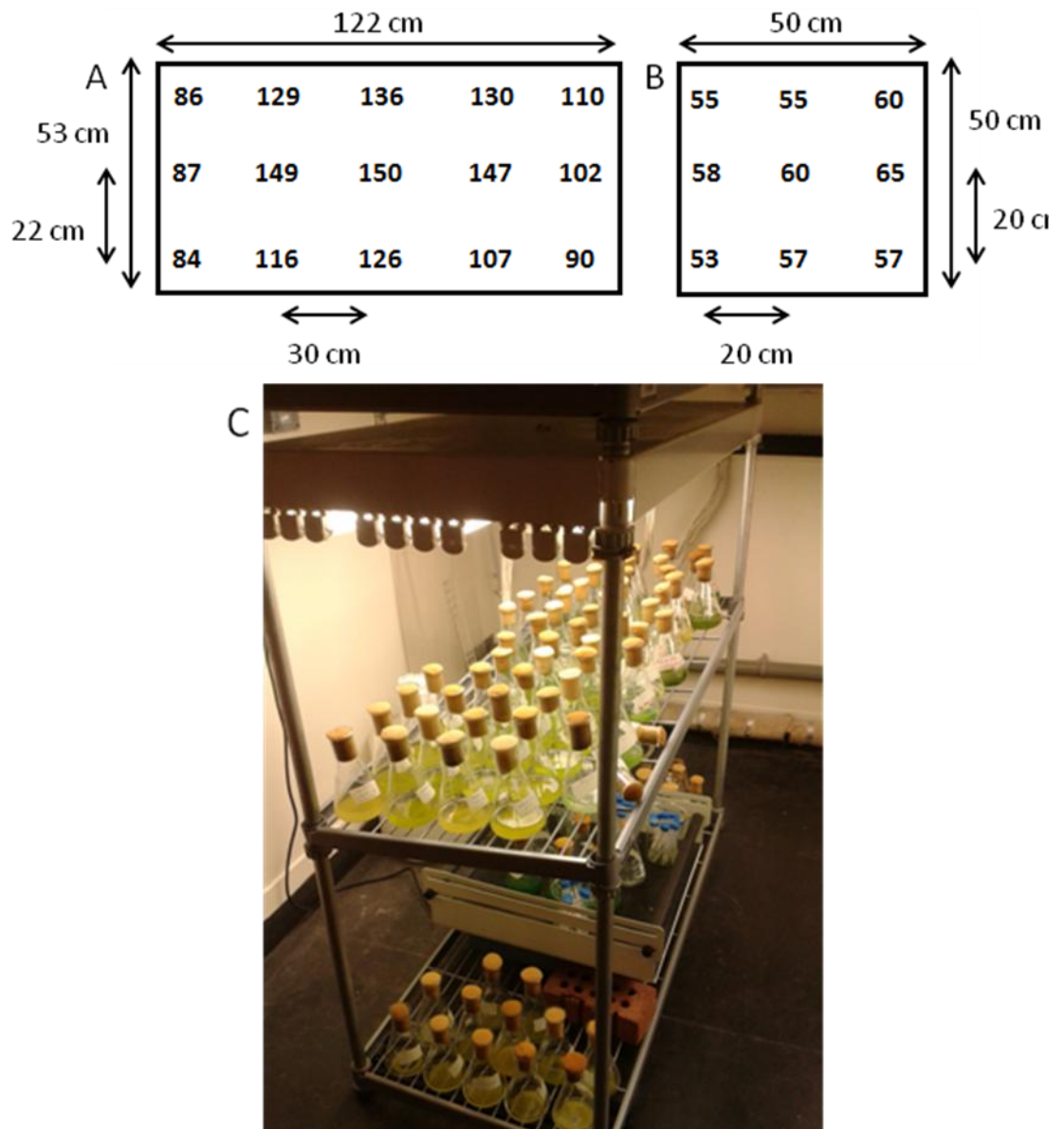


Figure 2.2 | Light intensity across the top shelf (A) and bottom shelf shaker (B) of the growth room (C). Light intensity measured in micro-Einsteins/m<sup>2</sup>/second ( $\mu\text{Em}^{-2}\text{s}^{-1}$ ). Cultures on the top shelf were 40 cm from the light source. Cultures on the bottom shelf were 90 cm from the light source. Lights were Osram Lumilux cool white L36W/840 fluorescent bulbs (Germany).

After initial experiments, it was noted that the cultures would need to be shaken to ensure homogeneity of the culture, both in terms of the proteomic activity and for biological activity generally. Cultures were, from this point forward, grown in a Sanyo Versatile Environmental Test Chamber Model MLR-351H on shakers at 100 rpm. The light intensity was recorded across the different shakers and displayed in Figure 2.3. The temperature was 25°C and light was 24 hour constant cycle.

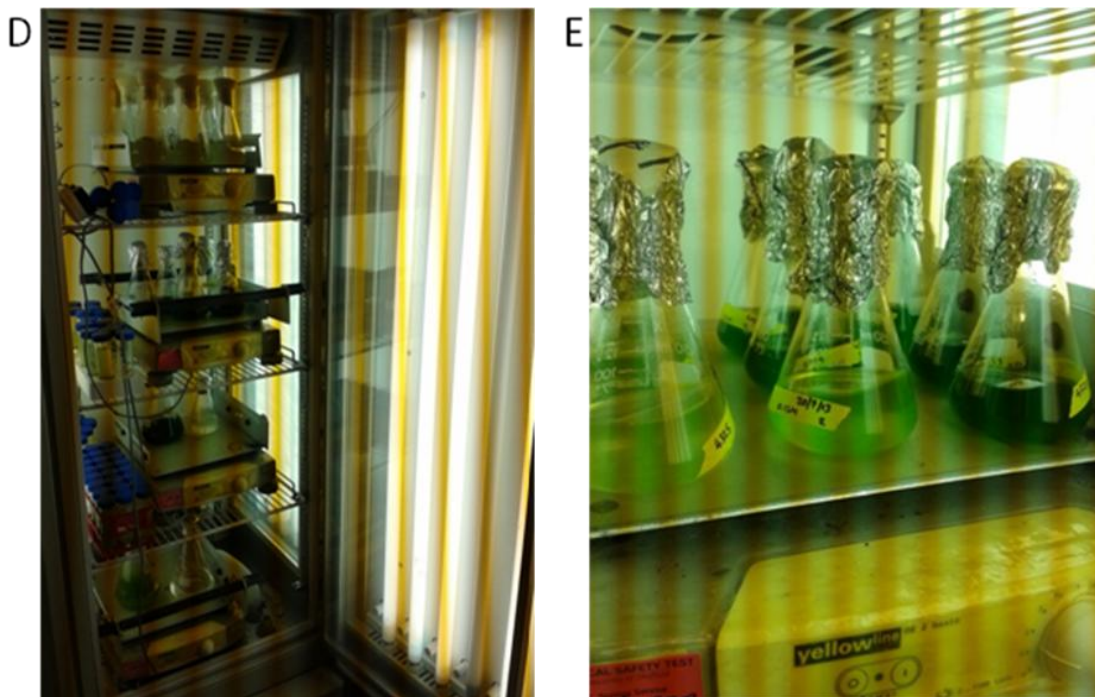
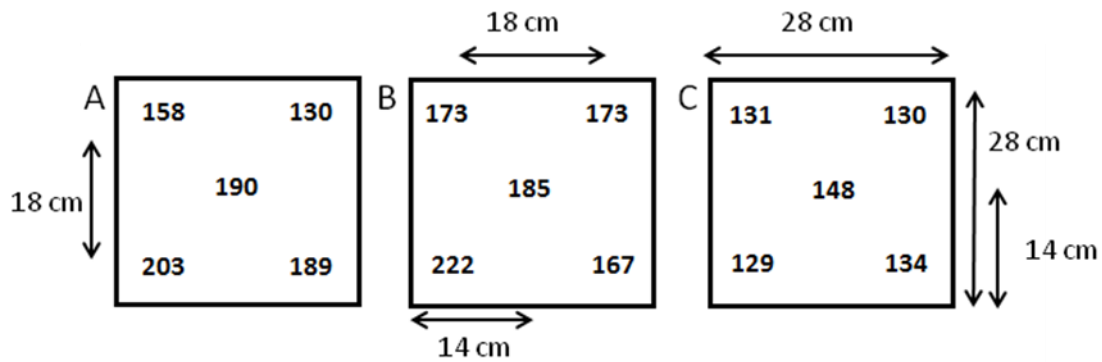


Figure 2.3 | Light intensities on different levels of the Sanyo Versatile Environmental Test Chambers (D and E). Chamber contains 4 levels. The first level was not used in this experiment. The light intensities on the shakers placed on the second (A), third (B) and fourth (C) levels. Light measured in micro-Einsteins/m<sup>2</sup>/second ( $\mu\text{Em}^{-2}\text{s}^{-1}$ ). Shakers were Yellowline 052 basic (Scientific Laboratory Supplies, IKA-Werke, Germany).

Two different approaches were taken to seeding the cultures with salt medium. Initially the cultures were seeded with 1 mL seeding stock in 100 mL fresh medium. In this approach, the culture takes a long time to reach high culture density at high salinities but the cells in the culture were viable and intact, since the cells will only grow in the culture if they are able to withstand the culture conditions. The second approach was to grow the culture for 48 hours in normal TAP medium and then

centrifuge and re-suspend the culture at an early-to-mid log growth phase (in this case measured as 0.44 OD at 750 nm) in either normal TAP medium or TAP medium with NaCl added to the desired concentration.

A second species, *C. nivalis*, a snow alga, was also investigated. This species naturally occurs in meltwater from ice and snow. It was grown in 3N-BBM-V medium, the composition for which can be found in Appendix A. It requires a relatively low temperature in order to grow, so a water bath at 16°C was set up with 250 mL conical flasks (containing 100 mL of culture) held in place with clamp stands. The water in the bath was heated by Tempette TE-8A heating element (Techne, Cambridge, UK, Serial No. 2200417) and cooled by P Selecta cooling element (Serial no. 116580). The light intensities (measured with a Scalar PAR Irradiance Sensor, Biospherical Instruments Inc, Serial number QSL-2100), for the growth of *C. nivalis* are shown in Figure 2.4A, B and C. Since the medium does not have a carbon source in it, the algae required carbon dioxide as the carbon source. Filtered sterile air was bubbled into the cultures using a pump and tubing with Whatman hepa-vent filters (Cat. no. 6723-5000, GE Healthcare Life Sciences, UK). The flow rate of air for the cultures was between 61.0 and 71.8 mL min<sup>-1</sup>. The air was at room temperature (approximately 21°C). Although the bubbling encouraged growth of the cultures, the system of tubing and sponge bungs did not completely seal the system and thus the cultures did not remain sterile. In addition, greater volumes of culture were required. Instead, a culturing system using 500 mL measuring cylinders and rubber bungs to seal them was used. Each bung had three holes drilled into it to allow three sets of tubing to enter the cylinders. One tube, for air inlet, reached the bottom of the culture and ended in a 1 mL pipette tip, which was used to bubble the air. It was connected to a filter and a pump. The second tube reached 3 cm into the cylinder, above the medium level, facilitating air outlet. A filter was attached to the air outflow, to ensure the system was sealed and that no contamination could enter via the outlet tube. The third tube reached to the bottom of the culture. This was for sampling, so that the system would not have to be opened each time a sample was taken. The sampling tube was clamped shut with a metal clamp. During sampling it was opened and syringes were used to draw out the sample through this tube. The set up is shown in Figure 2.4E and F.

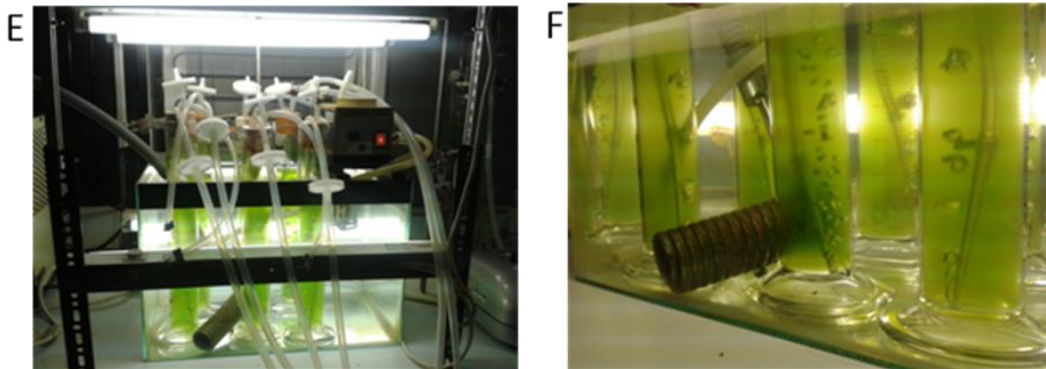
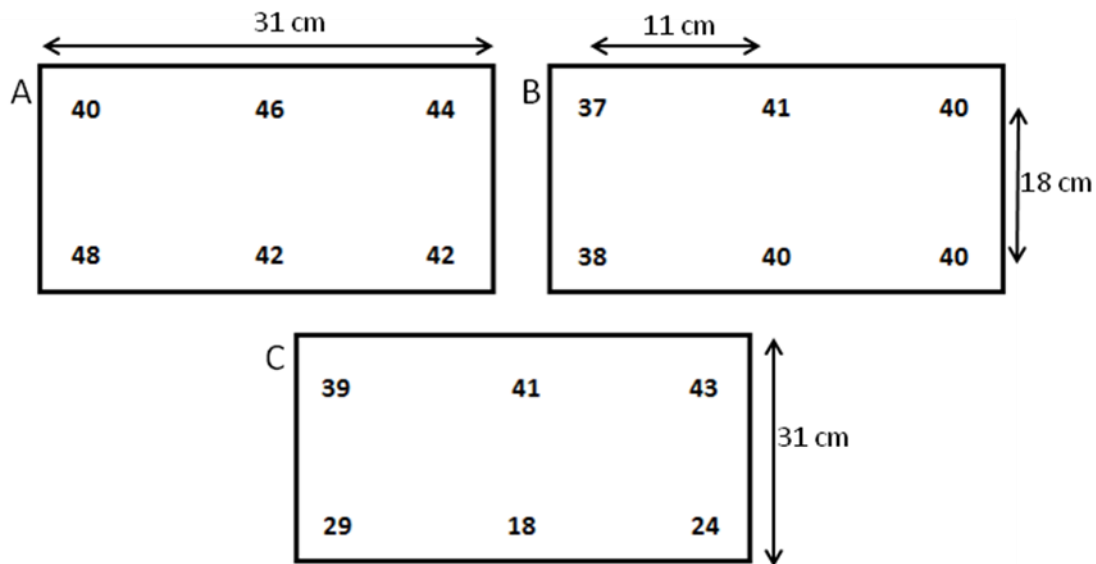


Figure 2.4 | Light distribution in the growth set up for *Chlamydomonas nivalis*, as pictured from the top of the tank. Diagrams show light intensity at the surface of the water (A), halfway down the tank (B), and at the bottom of the tank (C). All values measured in micro-Einsteins/m<sup>2</sup>/second ( $\mu\text{Em}^{-2}\text{s}^{-1}$ ). Growth set up (E, F) demonstrates light rig which contains 4 fluorescent tube lights (Wickes 18W, 57 cm length).

### 2.3.1 Application of salt stress

In *C. nivalis*, the cultures were grown to mid-log phase, at OD between 0.35 and 0.6 (750 nm), then salt stress was introduced. In the preliminary experiment, 4 different salt concentrations (one replicate only, due to space restrictions) were applied as well as a control. These were 0.2, 0.5, 1.0 and 1.5 M NaCl, and were added in as undissolved salt. After this preliminary experiment, two salt concentrations were chosen for subsequent experiments. The first was 1.4 M, as this was a high salt level beyond the *C. nivalis* salt tolerance level of 1.2 M. The sudden shock response of the algae

immediately after high salt stress application was of interest, as high osmotic shock would reveal a clear response in this halotolerant species. The high level of osmotic shock would also show how algae respond on a short term basis to dealing with very saline conditions, and also how a large change in salinity from the original growth conditions would affect the lipid response. Three replicates of control and salt stressed cultures were grown. To make up 1.4 M salt in 500 mL solution, 4 M salt 3N-BBM-V media was made and 175 mL of this was added to 325 mL of grown culture. The same was applied to the control cultures using normal 3N-BBM-V medium. Most tubes lost some volume due to evaporation (approximately 100 mL), therefore culture volume and salinity was maintained by topping up with the appropriate medium at the start of the experiment.

The second main salt concentration investigated in *C. nivalis* was 0.2 M NaCl. This was chosen as a low level salt stress that is well within the tolerance of the species. There is literature to show that this concentration of NaCl can evoke a lipid increase response in this species (Lu et al., 2012c), and preliminary testing of the FAME profile confirmed this to be the case. This salt concentration is therefore of interest particularly for a low level, long-term response to salt stress that can accumulate lipid content over time.

In *C. reinhardtii*, preliminary experiments grew the cultures in TAP medium made up to the appropriate NaCl molarity from the start of the culture. In later experiments, salt was added into the cultures by simply adding in the appropriate amount of undissolved salt. Finally the approach was used of growing the cultures in normal TAP medium to late log phase, spinning the cultures down at 3000 *g* for 5 minutes and re-suspending them in TAP medium with NaCl dissolved in the media at the appropriate amounts, and this was the approach used for the majority of experiments. *Chlamydomonas reinhardtii* has been reported to tolerate salt concentrations of up to 200 mM NaCl (Leon and Galvan, 1994), so initial experiments used a range of salt concentrations to establish the limit of salinity tolerance in this species. A range of salt concentrations (0, 50, 100, 150, 200 and 250 mM NaCl) was used, with each culture condition grown in triplicate. Later in the final experiments, the salt concentrations

100, 200 and 300 mM were used. These were chosen because the research is testing the response of the model species both within the bounds of tolerance (100 mM) to see the long term response of low level salt stress, and on the boundary of (200 mM) and beyond the bounds of salt tolerance (300 mM). Long term low level salt stress may reveal how a growing culture adapts and responds to salt stress over time, whilst short term extreme responses may reveal different mechanisms at play in lipid metabolism. The development of the chosen salt stress conditions for experiments is explained further in Table 2.1.

## 2.4 Biological parameters

### 2.4.1 Growth

To measure growth, initially cell counts were measured against optical density (OD). Cell counts were taken using a Helber Cell Counting chamber, taking 10 cell counts for each sample and using an average to establish the final cell count number. The algal cells were prepared in a solution of 9:1 algae culture: Grams Iodine solution. 20  $\mu$ L was pipetted onto the Helber Slide counting chamber and the heavy coverslip firmly placed on top. The cells were counted in four of the large squares, on each of the four corners of the counting chamber. This process was repeated 10 times with fresh algal culture and Grams Iodine solution.

Correlation curves were made between cell counts and OD, and afterwards OD was used as a measure of culture growth. The OD originally used was 600 nm and this is what was used for the cell count correlations. However, later, OD at 750 nm was used as the measure of growth phase, since a wavenumber scan of a *Chlamydomonas* culture across a wide range of wavelengths showed that this OD was far enough away from pigment peaks (680 nm) and peaks that would also include bacterial cells (600 nm) to be a good representation of the culture growth (see Figure 2.5). However, OD at all three of these wavelengths was recorded for subsequent growth experiments. OD was measured on an Ultraspec 2100 Pro spectrophotometer (Serial no. 88446, Biochrom Ltd, Cambridge, UK), using 1 mL cuvettes, and using deionised water as a blank.

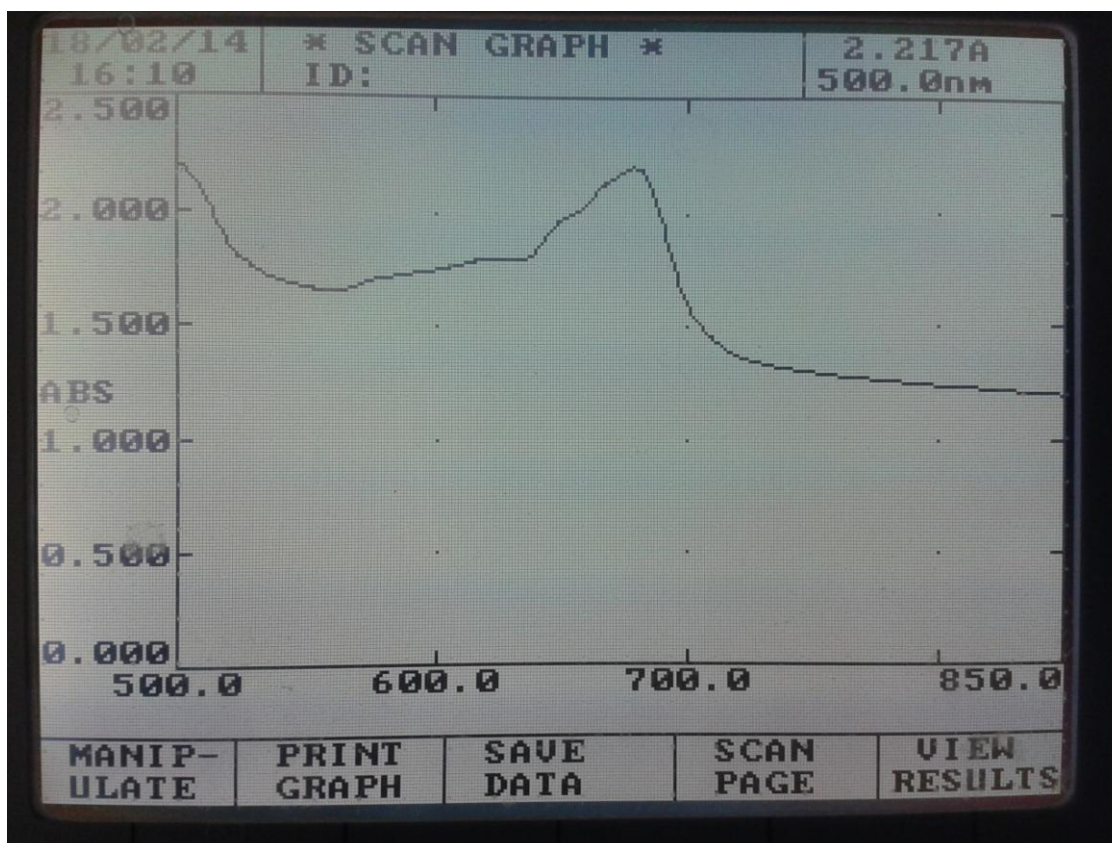


Figure 2.5 | Wavescan of *C. nivalis* taken on a spectrophotometer. This was the same shape for *C. reinhardtii*.

The last indication of culture growth used is dry cell weight (DCW). This is a normalising measure of culture growth and volume. Dry cell weight is important to know, since all other aspects of the culture can then be measured against it in terms of an overall percentage of the culture yield. This can be used as a normalising basis for lipid content, carbohydrate and chlorophyll content. Dry weight was measured by centrifuging a sample from the culture using a Hermle Z400K centrifuge (Labnet International Inc., New Jersey, USA) at 1,200 *g* for 10 minutes at 4°C, and transferring the pellet to a pre-weighed 1.5 mL Eppendorf tube. The sample was frozen, first at -20°C, then at -80°C, and then freeze-dried. The new tube and sample weight was used to obtain the DCW of the culture.

## 2.4.2 Carbohydrate analysis

Anthrone solution was made up by adding 25 mg anthrone to 500  $\mu\text{L}$  ethanol and 12 mL 75% (v/v)  $\text{H}_2\text{SO}_4$ . From a  $10 \mu\text{g} \mu\text{L}^{-1}$  algal suspension, 50  $\mu\text{L}$  was pipetted to fresh 1.5 mL Eppendorf tube and diluted with 950  $\mu\text{L}$  deionised water to make  $0.5 \mu\text{g} \mu\text{L}^{-1}$  algal suspension. 200  $\mu\text{L}$  of the  $0.5 \mu\text{g} \mu\text{L}^{-1}$  algal suspension was transferred to a glass tube (75 x 10 mm, Fisher Scientific, Serial no: 12347279), then 400  $\mu\text{L}$  of 75% (v/v)  $\text{H}_2\text{SO}_4$  was added, followed by 800  $\mu\text{L}$  anthrone solution. Samples from triplicate cultures were vortexed and placed in  $100^\circ\text{C}$  heating block for 15 minutes. They were left to cool at room temperature for 15 minutes, vortexed again and then absorbances were read at 620 nm in an Ultraspec 2100 Pro spectrophotometer (Serial no. 88446, Biochrom Ltd, Cambridge, UK). A blank was used consisting 200  $\mu\text{L}$  deionised water instead of algal suspension for one sample. A standard curve was made up using known quantities of glucose put through the same protocol.

## 2.4.3 Chlorophyll analysis

### 2.4.3.1 Acetone method

A method based on MacKinney (1941) was developed. 5 mL algal culture was centrifuged at 5000  $g$  for 10 minutes. The supernatant was drained off and the sample was re-suspended in 1 mL distilled water and 4 mL acetone, and centrifuged at 5000  $g$  for 5 minutes. The optical density of the supernatant was measured at 645 nm and 663 nm. The following equations were used to determine chlorophyll content:

$$\text{OD}_{645} \times 202 = y$$

$$\text{OD}_{663} \times 80.2 = x$$

$$(y+x)/5 = \mu\text{g chlorophyll mL}^{-1}$$

### 2.4.3.2 Wellburn based method

A second method, based on Wellburn (1994), was also used for chlorophyll analysis. Phosphate buffer ( $\text{H}_3\text{PO}_4$ , pH 7.4, 0.05 M) was made up by adding 0.3 g  $\text{NaH}_2\text{PO}_4$  to 50 mL deionised water, then using 1 M NaOH solution to adjust the pH to 7.4.

Samples were analysed from triplicate cultures. From a  $10 \mu\text{g } \mu\text{L}^{-1}$  algal suspension, 50  $\mu\text{L}$  was pipetted to fresh Eppendorf tube and centrifuged at 2000  $g$  for 2 minutes. Supernatant was removed and the solution was centrifuged again at 10000  $g$  for 5 minutes and supernatant was removed. The pellet was re-suspended in 150  $\mu\text{L}$  phosphate buffer and vortexed for 1 minute. 100  $\mu\text{L}$  glass beads (425-500  $\mu\text{m}$ ) from Sigma (G8772) were added. A Disruptor Genie bead beater (Scientific Industries, New York, USA, Serial No. D68-10198 and D48-1014) was used to break the cells for 10 minutes in dark conditions by covering the samples with foil. 800  $\mu\text{L}$  pure acetone was added, and sample was vortexed for 1 minute. Samples were incubated at room temperature in the dark for 10 minutes, then centrifuged at 1000  $g$  for 1 minute. 110  $\mu\text{L}$  of the resulting solution was pipetted into a 400  $\mu\text{L}$  quartz cuvette and read at 663, 646 and 470 nm (using 80% acetone as a reference).

#### **2.4.4 Photosynthesis and respiration analysis using oxygen electrode**

Photosynthesis and respiration were measured using a Hansatech oxygen electrode set up connected to Picolog software. The oxygen electrode (S1 Oxygen Electrode Disc, Hansatech Instruments) was set up with 5 drops (approximately 30  $\mu\text{L}$ ) of 2.3 M KCl solution pipetted to equally cover the electrode well and dome (one on each corner and one on the dome) and covered using a 1 cm square of cigarette paper and a 2.5 cm square of Teflon, which were fixed in place with the o-rings. The electrode was placed into the chamber which was connected to the light source (type L52A, Serial No. 108556, Hansatech Ltd, Kings Lynn, England), O<sub>2</sub> Electrode Control Box CB2D (Hansatech, type CB2-D, Serial no. 8813), CO<sub>2</sub> Light Source Control Box (Hansatech, L52B, serial no: 108556) and DrDAQ converter which connected the instrument to computer. A magnetic stirrer (Hansatech, Serial no. H.2815) was used to ensure fast and equal mixing.

Water was used to check the stability of the voltage readings and the membrane stability for 30 minutes. All measurements were taken at 1 second intervals. The equipment was then calibrated by using water with oxygen saturation (the lid off the

sample chamber) as the 100% value and by adding a small amount of sodium dithionite to reduce to a 0% value. The voltages were measured at both of these for 6 minutes and used for calibration. The data was analysed using Microsoft Excel to find a stable period of the voltage reading on both of these. An average of this period was used to find voltage values equivalent to 100% and 0% oxygen. These were then used to program the parameters for the voltage conversion with the equation:

$$(536 / (100\% \text{ Voltage value} - 0\% \text{ Voltage value})) * (A - 0\% \text{ Voltage value}) = \text{mmoles of oxygen}$$

Where 536 is the number of moles of oxygen in 100% saturation, and A is the value recorded by the electrode during sample runs.

Once the electrode was calibrated and washed, a 2 mL sample was pipetted into the electrode chamber. The voltage was measured for 6 minutes without the light source to get the stable "start" reading. Then the voltage was measured for 6 minutes with the light source switched on to obtain a value of the oxygen evolution during photosynthesis. The voltage was then measured for 6 minutes with the light source switched off to obtain a value of oxygen uptake during respiration. From each of these data sets, a period of stable voltage was found to create a linear equation of the rate of oxygen increase (photosynthesis) or decrease (respiration) within the sample. The OD of the sample was used to normalise for culture density. This method was taken from Smith *et al.* (in press).

#### **2.4.5 Microscopy and cell morphology**

Cells were photographed under x1000 magnification using an Olympus BX51 microscope (Smcs Limited), with ProgRes® C5 camera attachment (Jenoptik, Germany) and ProgRes® CapturePro 2.6 imaging software. Photographs were used as a visual reference to examine cells.

## 2.5 Algal lipids

Lipid techniques have been thoroughly investigated in this thesis and a full discussion of the suitability of the techniques in assessing algal lipid content are set out in Appendix B. This discussion was a result of issues with various lipid techniques being used and then found to not be suitable for the overall purpose. The following is a description of how lipid techniques were chosen and investigated for the purposes of this study.

### 2.5.1 Gravimetric method

The method was adapted from Bligh and Dyer (1959) and Chiu *et al.* (2009). Four samples of 15 mL were taken from each flask. Samples were centrifuged at 1,200 *g*, at 4°C for 10 minutes. The supernatant was discarded and the pellet was re-suspended in 5 mL of distilled water and centrifuged again for five minutes at 1,200 *g*. Supernatant was discarded and the pellet re-suspended in 5 mL of distilled water. Sample was centrifuged again for five minutes at 1,200 *g*, supernatant was discarded and each pellet was re-suspended in 1 mL of distilled water. Samples were transferred to four pre-weighed and labeled Eppendorf tubes. Lids were removed from another four Eppendorfs and holes made in the top using a dissecting needle. These lids were then put on the Eppendorf tubes containing the samples. The samples were put in -80°C freezer overnight and then freeze-dried for 48 hours. The tubes were weighed to obtain the dry cell weight of the biomass. 500 µL of methanol:chloroform solution (2:1 v/v) was added to samples and sonicated using a probe sonicator (Soniprep 105) at an amplitude of 15 microns for 1 minute on ice. Samples were centrifuged at 1,200 *g* for 5 minutes and supernatant was transferred to a fresh Eppendorf. The volume was estimated using a Gilson pipette. Chloroform and 1% NaCl solution was added to make a 2:2:1 methanol:chloroform:water solution. Samples were centrifuged for two minutes at 1,200 *g*, and chloroform phase was transferred to new pre-weighed and labeled Eppendorf tubes. Tubes were left open in a fume cupboard to evaporate. The tubes were weighed to obtain the dry weight of the lipids recovered.

The effect of the timing of both salt introduction and of measurement was investigated. Two sets of cultures were set up with salt introduced at 0 hours. One of these was measured after 7 days (168 hours), and the other was measured after 4 weeks (672 hours). Two sets of cultures were set up with salt introduced part way through the growth cycle: one with salt introduced at 48 hours, and measurements taken at 96 hours, and one with salt introduced at 120 hours, and measurements taken at 168 hours. Results for these experiments are displayed in Appendix B.

### 2.5.2 Colorimetric method

A micro-colorimetric method was also tested, as authors have concluded that it is highly suitable for lipid determination (Cheng et al., 2011b; Inouye and Lotufo, 2006), particularly in algae (Cheng et al., 2011b). The method was carried out using aliquots of 25, 50 and 100  $\mu\text{L}$  for each sample. The method used extracted lipid as in the gravimetric method detailed in Section 2.5.1. A range of lipid standards was made using a stock solution of 5  $\text{mg mL}^{-1}$  corn oil in 2:1 chloroform methanol and then pipetting 5  $\mu\text{L}$ , 10  $\mu\text{L}$ , 15  $\mu\text{L}$ , 20  $\mu\text{L}$  and 25  $\mu\text{L}$  with replicates into wells of a 96 well plate to give 25  $\mu\text{g}$ , 50  $\mu\text{g}$ , 75  $\mu\text{g}$ , 100  $\mu\text{g}$  and 125  $\mu\text{g}$  lipid respectively. Samples were also pipetted into wells of the 96 well plate, with three technical replicates for each sample. The plate was incubated at 90°C to evaporate the solvent. 100  $\mu\text{L}$  concentrated sulphuric acid was added to each well and incubated at 90°C for 20 minutes. The 96 well plate was cooled to room temperature using ice water and background absorbance was measured at 540 nm on a Genios Tecan plate reader (Tecan, Austria, Model: Genios Basic, Serial no. 502000016). 50  $\mu\text{L}$  vanillin-phosphoric acid reagent (0.2 mg vanillin per mL of 17% v/v phosphoric acid) was added to each well and allowed 10 minutes for colour development. The absorbance was measured again at 540 nm on the Tecan plate reader. Concentration curves were drawn based on the standards to calculate the amounts in extracted lipid samples.

### 2.5.3 Nile Red measurement method

A Nile Red method was adopted for a large amount of initial experimentation in this research. This method was that used by Longworth *et al.* (2012), originally adapted from Chen *et al.* (2009b). 10 mL was taken at each time point from the culture, centrifuged at 1,200  $g$  for 10 minutes at 4°C and transferred to a pre-weighed labelled

1.5 mL Eppendorf tube. This was frozen at  $-20^{\circ}\text{C}$ . When all samples were gathered, they were transferred to  $-80^{\circ}\text{C}$  and freeze dried. Samples were weighed again to find dry cell weight.

The dried algal samples were resuspended in deionised water to  $10\text{ mg mL}^{-1}$  and sonicated for five minutes in a pulse sonicator water bath.  $50\text{ }\mu\text{L}$  of this was taken and added to  $950\text{ }\mu\text{L}$  water to make a solution of  $0.5\text{ mg mL}^{-1}$  algal suspension. A Black Walled Micro Assay 96 well plate (Greiner Bio-one, UK, ref. 655076) was used. Each sample had six technical replicates (6 wells of the plate). To each well,  $125\text{ }\mu\text{L}$  deionised water was added, followed by  $100\text{ }\mu\text{L}$  diluted algal sample and  $50\text{ }\mu\text{L}$  dimethyl sulphoxide (DMSO). The plate was shaken for three minutes at  $37^{\circ}\text{C}$  and read five times at thirty-second intervals in a Genios Tecan plate reader (Tecan, Austria, Model: Genios Basic, Serial no. 502000016), at excitation  $530\text{ nm}$  and emission  $580\text{ nm}$ . From this the background autofluoresence was recorded. To each well,  $25\text{ }\mu\text{L}$  Nile Red solution in DMSO (concentration  $9\text{ }\mu\text{g mL}^{-1}$ ) was added. The plate was read again on the Tecan plate reader on an 8 hour program with 32 reads at fifteen-minute intervals.

From the two sets of readings, the maximum readings for each well were calculated, to ensure full permeation of the Nile Red. The background fluorescence was subtracted from the final Nile Red reading and an average of the six technical replicates was taken to give a final Nile Red reading. This reading, in units of fluorescence, can give a relative comparative measure of lipid measurement when comparing strains.

Measurements for Nile Red and GC were taken at 3 hours and then at 12 hour time intervals after re-suspension. Sampling continued up to 288 hours, depending on the species used. This allowed monitoring of the effect of salt shock on the cultures over time.

## 2.5.4 Direct Transesterification and Gas Chromatography Protocol for FAME analysis

### 2.5.4.1 Sample preparation

Samples were harvested, washed in 1 x PBS buffer and pelleted. They were stored in -20°C freezer, and freeze dried. The dry cell weight was calculated and dilution of 10 mg mL<sup>-1</sup> was made using distilled water. 100 µL sample was taken and added to 2 mL Eppendorf tube. 500 µL glass beads (425-600 µm) were added to the sample, with 1.2 mL of methanol:chloroform (1:2) solution and the first internal standard (detailed below in Section 2.5.4.2). The samples were bead beaten using a Disruptor Genie bead beater (Scientific Industries, New York, USA, Serial No. D68-10198 and D48-1014) on a 2 minute disruption and 2 minute interval on ice cycle. There were 10 cycles. The samples were centrifuged at 16,000 g at 4°C for 5 minutes. The supernatant was transferred to a new Eppendorf tube. 400 µL chloroform (Fisher Scientific UK) and 400 µL HPLC grade ultrapure water (Fisher Scientific UK, code: W/0106/17) were added to each sample. Samples were centrifuged for 15 minutes at 7000 g at 4°C. The organic phase, or bottom layer, was transferred to a glass vial and evaporated to dryness under inert nitrogen gas. 250 µL chloroform:methanol (1:1) solution and 100 µL BF<sub>3</sub>:methanol solution were added to each sample. Samples were incubated at 80°C for 90 minutes, then cooled at room temperature for 10 minutes. To each sample 300 µL ultrapure water (Fisher Scientific UK, code: W/0106/17) and 600 µL hexane (Fisher Scientific UK) with the second internal standard (detailed in Section 2.5.4.2 below) were added and samples were transferred to a fresh Eppendorf tube. They were vortexed for 1 minute and centrifuged at 7000 g for 5 minutes at 4°C. The top organic layer was transferred to a fresh glass vial and evaporated to dryness under inert nitrogen gas before re-suspending in hexane ready for injection into the gas chromatograph.

### 2.5.4.2 Internal standard to check transesterification efficiency

To check the transesterification efficiency, a known quantity of a fatty acid was spiked into each sample after the organic phase (containing the lipids) was separated from

the rest of the algal sample. This fatty acid was chosen as it does not appear in the *Chlamydomonas* lipid extracts, but is in the 37 FAME Mix standard. In this case tricosanoic acid C23:0 (obtained from Sigma-Aldrich, T6543-100MG) and methyl tetracosanoate C24:0 (obtained from Sigma-Aldrich, L6766-100MG) were chosen since they did not appear in any of the preliminary GC investigations of *C. reinhardtii*. 100 µg was spiked into 1 mg biomass, with tricosanoic acid (suspended in methanol:chloroform (1:2) solution) added to the biomass pellet at the point of solvent addition. Methyl tetracosanoate was added (suspended in hexane) after the extraction and transesterification. The transesterification efficiency was then calculated. This method was adapted from Laurens et al. (2012a).

#### **2.5.4.3 Gas Chromatography**

Analysis was carried out on a Thermo Scientific Trace 1310 Gas Chromatographer with FID detector and autosampler (Thermo Scientific, USA), and a TRACE TR-FAME Column (obtained from Thermo) (dimensions 25m x 0.32µm x 0.25mm). The oven ramp was held at 150°C for 1 minute, and increased by 10°C min<sup>-1</sup> up to 250°C, then held at 250°C for 1 minute. Split injection was carried out at split ratio 50, split flow 75 mL min<sup>-1</sup> and carrier flow 1.5 mL min<sup>-1</sup>. The FID detector was set to 250°C, air flow 350 mL min<sup>-1</sup> and hydrogen flow 35 mL min<sup>-1</sup>. The GC was calibrated using Supelco 37 Component FAME mix (Supelco, Bellefonte, PA).

#### **2.5.4.4 Data Analysis**

This data contained analytical replicates (3 injections of the same sample) and three biological replicates. In some cases analytical replicates showed the presence of FAMES in one but not in another. Therefore the average of the available replicates was taken, but if a value was missing it was discounted and not recorded as a "0".

The biological replicates also sometimes showed FAMES in one replicate but not another. In this case, missing values were recorded as "0", therefore there were always 3 biological replicates for each sample.

## 2.6 Proteomics

The recovery of the proteome can be greatly affected by the choice of protein and peptide preparation methods. In some instances, more than one method was tried before the final protocol was selected for this project.

### 2.6.1 Sample Washing

In these experiments, the salt must be removed, as well as any debris in the sample medium, in order to be compatible with the iTRAQ procedure. For this, a sucrose based wash buffer was used (50 mM Tris, pH 7.5; 100 mM EDTA, pH 8.0) with sucrose adjusted to the salt concentration of the culture to create an isotonic solution (values found in Weast (1976-77)): For 0.2 M NaCl samples, 0.335 M sucrose is added. For 0.3 M NaCl cultures, 0.464 M sucrose was added. For 1.4 M NaCl samples, 1.456 M sucrose was added.

### 2.6.2 Cell lysis and extraction

#### 2.6.2.1 Lysis buffer

Lysis buffers were tested to try out the chemical lysis methods on *C. reinhardtii* and *C. nivalis*. However, the buffer the sample was re-suspended in must be compatible with iTRAQ labeling techniques, and have no free amines. Urea and SDS detergent cause problems with iTRAQ, even if they help with chemical disruption of cell walls, and therefore 0.5 M tetraethylammonium bromide (TEAB) buffer is the most suitable, with 1% plant protease inhibitor cocktail (obtained from Sigma-Aldrich, product number 9599) added.

#### 2.6.2.2 Grinding with liquid nitrogen

A pestle and mortar, wiped with 70% ethanol and then cleaned with 100% ethanol which was burned off to leave the surface clear of ethanol, was pre-chilled using liquid

nitrogen. More liquid nitrogen was added and the sample was pipetted into the mortar. Once the nitrogen had evaporated, the sample was ground with a pestle for 15 minutes. Liquid nitrogen addition and grinding were repeated twice more, then the sample was collected with a spatula and placed in a 1.5 mL Lo-Bind Eppendorf tube.

### **2.6.2.3 Sonication**

After grinding and collecting in an Eppendorf tube, the samples were sonicated in an ice cold water bath for five minutes. A probe sonicator was used to sonicate for two cycles (a cycle being a single burst) using a Micro tip Branson sonifier (Enerson, Danbury, CT). Between cycles the samples were placed on ice. After sonication the samples were centrifuged at 18,000 *g* for 30 minutes at 4°C to separate the insoluble pellet from the soluble protein fraction. The soluble fraction was pipetted off and used for subsequent analysis, whilst the insoluble fraction in the pellet was stored at -80°C, in case it was required for further extraction processing later.

### **2.6.3 Acetone Precipitation**

Extracted protein was added to ice-cold acetone (pre-chilled to -20°C). Four parts acetone were added to 1 part protein extract and kept at -20°C for 12 hours. Samples were spun down at 21,000 *g* at 4°C for 30 minutes, the acetone was removed and precipitated protein samples were left open in a fume hood to let the last of the acetone evaporate, but not to let the samples go completely dry. The precipitated protein was then reconstituted in 0.5 M TEAB. If samples failed to reconstitute, they were sonicated in an ice cold water bath.

### **2.6.4 Protein quantification**

#### **2.6.4.1 Bradford**

The Bradford Ultra Detergent Compatible Coomassie-based protein quantification method was used. A standard curve of protein was created using Bovine Albumin Serum (BSA) (obtained from Sigma, Cat no. A9056-50G), using concentrations 1, 0.5,

0.25, 0.125, 0.0625, 0.03125 and 0 mg mL<sup>-1</sup>. 20 µL of samples and standards were pipetted into separate 1 mL cuvettes. The test was done in duplicate. 980 µL Bradford reagent was added to each cuvette. The cuvettes were vortexed briefly and then absorbance was read at 595 nm on a Ultraspec 2100 pro spectrophotometer (Serial no. 88446, Biochrom Ltd, Cambridge, UK), using the 0 mg mL<sup>-1</sup> sample as a blank.

A standard curve was plotted using a regression calculation in Excel and protein concentrations in samples were calculated using the resulting equation. The duplicate repeats were used to calculate an average for the protein quantification.

#### *2.6.4.2 RCDC*

Protein quantification assay using BioRad RC-DC Protein Assay Kit was also used. A standard curve of protein was created using BSA at concentrations 2, 1.5, 1.2, 0.8, 0.4, 0.2 and 0 mg mL<sup>-1</sup>.

5 µL DC Reagent S was added to each 250 µL DC Reagent A that is needed for the run, to make Reagent A'. 25 µL of standards and samples were pipetted into separate clean 1.5 mL Eppendorf tubes. 125 µL RC Reagent I was added to each tube, vortexed and incubated for 1 minute at room temperature. 125 µL RC Reagent II was added to each tube and vortexed. Tubes were centrifuged at 15,000 *g* for 5 minutes. Tubes were opened and inverted on clean absorbent tissue, to discard the supernatant and remove all liquid from the tubes. 127 µL Reagent A' was added to each tube, vortexed, and incubated at room temperature for 5 minutes, ensuring the precipitate had completely dissolved. Tubes were vortexed, then 1 mL of DC Reagent B was added to each tube and vortexed again immediately. They were incubated at room temperature for 15 minutes. Absorbance was read at 750 nm on a spectrophotometer, using the 0 mg mL<sup>-1</sup> standard as a blank.

A standard curve was constructed using a regression calculation in Excel, and from this the sample protein concentrations were calculated.

### 2.6.5 1D-SDS-PAGE

Gels were used for visualization of proteins. To make 1D-SDS-PAGE, a clean dry gel casting stand was used, cleaned with 100% methanol. Stock solutions were made as follows:

1.5 M Tris-HCl (pH 8.8): 27.23 g Tris Base with 80 mL deionised water, adjusted to pH 8.8 using HCl, and then the volume total was brought up to 150 mL.

0.5 M Tris-HCl (pH 6.8): 6 g Tris Base with 60 mL deionised water, adjusted to pH 6.8 using HCl, and then brought up to volume 100 mL.

10% w/v SDS: 10 g SDS with 90 mL water, dissolved and the total brought up to 100 mL.

10% APS solution: 100 mg ammonium persulphate (BioRad Cat. no. 161-0700), dissolved in 1 mL deionised water.

Laemelli buffer (2x): 62.5 mM Tris-HCl pH 6.8, 2% SDS, 25% glycerol, 0.01% Bromophenol Blue. 5%  $\beta$ -mercaptoethanol was added just before use.

12% resolving gels were used and made (10 mL) from 3.4 mL deionised water, 4 mL of 30% Acrylamide/Bis solution (BioRad Cat. no. 161-0158), 2.5 mL 1.5 M Tris-HCl pH 8.8 solution, 0.1 mL 10% w/v SDS solution.

10 mL of 4% stacking gel solution was made using 6.1 mL deionised water, 1.3 mL 30% Acrylamide/Bis solution, 2.5 mL 0.5 M Tris-HCl pH 6.8 solution and 0.1 mL 10% w/v SDS solution.

Immediately prior to gel casting, 50  $\mu$ L 10% APS solution and 5  $\mu$ L TEMED (BioRad cat. no. 161-0800) was added to the resolving gel. Resolving gel was pipetted in to the

assembled gel cassette up to 1 cm below where the comb teeth sat when inserted. After the resolving gel was pipetted in, isopropanol was pipetted in to level out gel and reduce evaporation. Gel was left to polymerize for 1 hour. Gel surface was rinsed with deionised water and then dried. Stacking gel was pipetted on top up to the top of the short plate, after 50  $\mu$ L 10% APS solution and 10  $\mu$ L TEMED was added to the stacking gel solution. Comb was inserted between the two plates and gel was left to polymerise for 45 minutes.

Gel cassette was loaded into electrode assembly and then into mini tank. 100 mL of 10x running buffer was mixed with 900 mL deionised water to make 1x running buffer. Running buffer was added in the central chamber up to the top, and approximately 200 mL was added to the outer chamber. The comb was removed immediately prior to sample loading.

50  $\mu$ L  $\beta$ -mercaptoethanol was added to 950  $\mu$ L sample buffer. Samples were mixed with 2x Laemelli buffer in a 1:1 ratio. A protein standard ladder was used as a marker; SigmaMarker™ (wide range, molecular weight 6,500 to 200,000 Da, obtained from Sigma Aldrich, Cat. no. S8445). For this, 1  $\mu$ L marker standard was added to 19  $\mu$ L sample buffer. Samples and marker were then heated to 95°C for 5 minutes, using a heat block. Samples were vortexed briefly and pipetted into the wells.

Electrophoresis module and chamber (BioRad) was connected to electrodes and VWR Power Source (Model: 300V, Serial No. 101004476) and run at 80 V for 15 minutes, then 180 V for 45 minutes. After completing the run, the gel was removed from the electrophoresis module and cassette and washed in deionised water. It was put in a tray of Coomassie stain solution which covered the gel. The gel was placed on a rocker and left overnight to stain. The stain was then removed and gel washed with deionised water. The gel was left on a rocker in de-staining solution (5% methanol, 7% acetic acid, 88% deionised water) to remove the stain.

## 2.6.6 Clean up

### 2.6.6.1 C18 column

Pierce C18 Spin Columns (Thermo Scientific Catalogue number 89870) were used for clean up. Samples were suspended in 20  $\mu\text{L}$  0.5% trifluoroacetic acid (TFA) in 5% acetonitrile.

The following solutions were made: Activation solution (50% acetonitrile); Equilibrium solution (0.5% TFA in 5% acetonitrile (ACN)); Sample buffer (2% TFA in 20% ACN); Wash solution (0.5% TFA in 5% ACN); Elution buffer (70% ACN).

200  $\mu\text{L}$  pure ACN was used to wash the walls of the column, and centrifuged at 1000  $g$  for 30 seconds at 25°C. Columns were placed in receiver tubes and 200  $\mu\text{L}$  Activation Solution was added to rinse walls of the spin column. Columns were centrifuged at 1000  $g$  for 30 seconds and the flow through was discarded. The Activation Solution step was repeated once more with the centrifugation step lasting 1 minute. 200  $\mu\text{L}$  Equilibrium solution was added to the column, then the column was centrifuged at 1000  $g$  for 1 minute. The flow-through was discarded, and this Equilibrium solution step was repeated once more.

Samples were loaded into the column and the receiver tube was placed on the column for binding. Columns were centrifuged at 1000  $g$  for 1 minute. The flow-through was recovered from the receiver tube and re-loaded into the column to repeat centrifugation step and ensure complete binding. Flow-through was retained in case it was needed later.

The column was placed in a new clean Eppendorf Lo-Bind tube for washing. 200  $\mu\text{L}$  Wash solution was added to column and centrifuged for 1 minute at 1000  $g$ . The flow-through was discarded, and this step was repeated once more.

The column was placed on a new receiver tube for elution. 25  $\mu\text{L}$  Elution buffer was added to the column and centrifuged at 1500  $g$  for 1 minute. The step was repeated

using the same receiver tube. The samples were dried using a vacuum centrifuge evaporator.

## 2.6.7 Digestion

### 2.6.7.1 *In-solution*

In solution digestion was carried out on labeled samples using iTRAQ compatible reagents. Sample (of 20-100  $\mu\text{g}$ ) was suspended in 20  $\mu\text{L}$  of 0.5 M TEAB. At each solution addition, the sample was vortexed and spun in a microfuge for 30 seconds to ensure contents were well mixed. Reduction was performed by adding 10% volume of 50 mM Tris-(2-carboxyethyl)-phosphine (TCEP) and incubated for 1 hour at 60°C. Sample was alkylated by adding 5% volume of 200 mM methyl methane-thiosulfonate (MMTS) and incubating for 10 minutes in the dark. A solution of 0.5  $\text{mg mL}^{-1}$  trypsin in TEAB was prepared, and a ratio of 1:20 ( $\mu\text{g } \mu\text{g}^{-1}$ ) trypsin to protein was added to sample. The sample was vortexed and spun down for 30 seconds in a microfuge to pull the contents to the bottom and ensure thorough mixing. The samples were then incubated for 16 hours at 37°C to digest the proteins into peptides.

## 2.6.8 iTRAQ labeling

Digested samples were dried down and reconstituted in 30  $\mu\text{L}$  1 M TEAB. iTRAQ 8 plex kit was obtained from ABSciex (Warrington, UK). iTRAQ labeling reagents were removed from the freezer immediately prior to labeling, allowed to come to room temperature, and spun in a microfuge to bring vial contents to the bottom. 100  $\mu\text{L}$  isopropanol was added to each reagent vial, and vial was vortexed and spun. Each iTRAQ reagent was added to a separate protein sample using a pipette set to 125  $\mu\text{L}$ , vortexed and spun. The pH was tested using 0.5  $\mu\text{L}$  of the sample on pH paper to ensure the pH was between 7.5 and 8.5. The tubes were incubated at room temperature in the dark for 2 hours. The contents of each tube were added together in one tube to combine the iTRAQ reagents, vortexed to mix and spun at 1000  $g$  for 15 seconds in an AccuSpin Micro 17 microfuge (Fisher Scientific, Germany, Serial No.

41263115). Once mixed, the contents were split equally into 2 Lo-bind Eppendorf tubes and dried down in a vacuum centrifuge overnight.

### 2.6.9 Separation via Hypercarb Column HPLC

Buffer A was made up of 3% ACN and 0.1% TFA. Buffer B was made up of 97% ACN and 0.1% TFA. The Hypercarb™ separation was carried out on Dionex UltiMate 3000 Autosampler linked to Dionex UltiMate 3000 Flow Manager and Pump system (Thermo Scientific, UK). Wash Buffer C was 20% ACN. Samples were re-suspended in 120 µL Buffer A and loaded onto Hypercarb™ Porous Graphitic Carbon LC reversed phase Analytical Column (Cat no. 35003-052130, ThermoFisher Scientific, UK), with 3 µm particle size, 50 mm length, 2.1 mm diameter and 250 Å pore size. Buffer A was exchanged with Buffer B with a flow rate of 0.2 mL min<sup>-1</sup> with the following gradient: 2% B at 0-15 minutes, 2-30% B at 15-80 minutes, 30-60% B at 80-130 minutes, 60-90% B at 130-131 minutes, 90% B at 131-136 minutes, 2% B at 137-145 minutes. The fractions were collected every two minutes from 20 minutes to 120 minutes. The fractions were dried for 20 hours on a Scavac vacuum centrifuge (Labogene, Denmark, Serial no. GVS23511110026) connected to a Vacuubrand Vacuum Pump (Vacuubrand, Germany) ready for recombining and mass spectrometry analysis.

This separation method has the advantage of not needing de-salting clean up after fractionation. Samples were collected every two minutes from the HPLC elution. The fractions were then recombined into 6 samples to run on the MS. The fractions were dried down, re-suspended in 20 µL Loading Buffer (3% ACN, 0.1% TFA, 96.9% ultrapure water), and 5 µL from each fraction was combined in 6 samples combined in the following order:

F1: minutes 40-46 and 100-106, F2: 48-56, F3: 58-66, F4: 68-74, F5: 76-86, F6: 88-98.

Samples before 40 minutes were not injected as these are mainly excess labelling molecules, which are undesirable for MS sample running. From each of the six pooled samples, 10 µL was injected into the Q Exactive HF MS.

## 2.6.10 Mass Spectrometry

### 2.6.10.1 AmaZon MS

AmaZon ETD MS was used to test a small aliquot of digested proteins to check for miscleavages and incomplete digestion. AmaZon ion-trap ETD MS was connected to Dionex UltiMate 3000 Autosampler linked to Dionex UltiMate 3000 Flow Manager and Pump system (Thermo Scientific, UK). HyStar and Chromeleon software was used to control the loading and running of samples, and recording of data. Data was analysed using DataAnalysis software and searched in Mascot.

### 2.6.10.2 Q Exactive HF MS

LC MS/MS was performed and analysed by nano-flow liquid chromatography (U3000 RSLCnano, Thermo Scientific) coupled to a hybrid quadrupole-orbitrap mass spectrometer (Q Exactive HF, Thermo Scientific). iTRAQ-peptides were separated on an Easy-Spray C<sub>18</sub> column (75 µm x 50 cm) using a 2-step gradient from 97% solvent A (0.1% formic acid in water) to 10% solvent B (0.08% formic acid in 80% acetonitrile) over 5 min then 10% to 50% B over 75 min at 300 nL/min. The mass spectrometer was programmed for data dependent acquisition with 10 product ion scans (resolution 15000, automatic gain control 5e4, maximum injection time 20 ms, isolation window 1.2 Th, normalised collision energy 32, intensity threshold 2.5e5) per full MS scan (resolution 60000, automatic gain control 3e6, maximum injection time 100 ms).

### 2.6.10.3 Data analysis

Data was run through in-house programs uTRAQ and Signifiquant. Comparisons were made between treatment groups in the iTRAQ, and Signifiquant gave outputs for the proteins which were significantly up and down regulated between groups. A false discovery rate (FDR) of 1% was used, multiple test correction was off, and at least two unique peptides required to accept a protein identification as genuine.

The accession numbers of up and down regulated proteins were checked against the Uniprot database ([www.uniprot.org](http://www.uniprot.org)) to identify the function of the proteins.

Functional group analysis of the proteins was carried out using DAIVD Functional Annotation Tool (<https://david.ncifcrf.gov/summary.jsp>). This groups proteins, using

accession numbers as protein identifiers, into their functional groups based on their biological process (BP) annotation at levels 3 (BP3) and 4 (BP4) of the 5 possible annotation levels.

Identified and up and down regulated proteins were mapped onto pathways in *C. reinhardtii* using the KEGG ([www.kegg.jp](http://www.kegg.jp)) "Search&Colour Pathway" tool, and using ChlamyCyc metabolic pathway mapping tool (<http://pmn.plantcyc.org/CHLAMY/class-tree?object=Pathways>).

## **2.7 18S rDNA sequencing**

### **2.7.1 Genomic DNA extraction using ZR Soil Microbe DNA Microprep kit**

20 mL of algal sample was centrifuged at 3000 *g* for 10 minutes, and supernatant was discarded. 750  $\mu$ L Lysis solution was added to each pellet and transferred to Benchmark Prefilled tube with zirconium beads. Tubes were shaken at 3000 rpm for 90, 180 and 270 seconds, accordingly, in Bead Bug beadbeater. Tubes were centrifuged at 10,000 *g* for 1 minute. 400  $\mu$ L of supernatant was transferred to Zymo-spin™ filter in a collection tube and centrifuged at 7000 *g* for 1 minute. 1,200  $\mu$ L Soil DNA binding buffer was added to the filtrate in the collection tube from the last step. 800  $\mu$ L of the collected solution was transferred to a Zymo-spin™ IS Column in a collection tube and centrifuged at 10,000 *g* for 1 minute. Flow through was discarded and the step was repeated. 200  $\mu$ L DNA Pre-wash Buffer was added to the Zymo-spin™ IC Column in a new collection tube and centrifuged at 10,000 *g* for 1 minute. 500  $\mu$ L Soil DNA Wash Buffer was added to Zymo-spin™ IC Column and centrifuged at 10,000 *g* for 1 minute. The Zymo-spin™ IC Column was transferred to a fresh 1.5 mL microcentrifuge tube and 50  $\mu$ L DNA Elution Buffer was added to the column, and eluted at 10,000 *g* for 30 seconds.

### **2.7.2 Gel electrophoresis of DNA to visualise DNA samples**

1% agarose gel was prepared with 0.6 g agarose powder, 60 mL distilled water, 1.2 mL 50x TAE buffer and 7  $\mu$ L ethidium bromide. 1x TAE running buffer was prepared using 20 mL 50x TAE buffer and 980 mL distilled water.

10  $\mu$ L of each DNA sample was mixed with 2  $\mu$ L 6x DNA loading dye before loading onto agarose gel. 6  $\mu$ L of 1 kb DNA ladder was used as a marker. Electrophoresis tank was run at 80 V for 45 minutes. Bands were visualised with Uvidoc UV Lamp.

### 2.7.3 PCR amplification

PCR amplifications were carried out in a Bio-Rad MyCycler thermal cycler using 18S primers (Lim et al., 2012) shown in Tables 2.2, 2.3 and 2.4 below.

**Table 2.2 Primer names and sequences.**

Primer	Sequence
18S rDNA Forward Lim	5'- gcg gta att cca gct cca ata gc -3'
18S rDNA Reverse Lim	5'- gac cat act ccc ccc gca acc -3'
18S rDNA Forward Sheehan	5'- aat tgg ttg atc ctg cca gc -3'
18S rDNA Reverse Sheehan	5'- tga ttc tgt gca ggt tca cc -3'

**Table 2.3 Solution volumes for adding primers to samples.**

Solution	18S Lim	18S Lim control	18S Sheehan	18S Sheehan Control
Master mix	20	20	20	20
Forward Primer	4	4	4	4
Reverse Primer	4	4	4	4
Distilled Water	12	22	12	22
Genomic DNA	10	0	10	0

**Table 2.4 PCR protocol for 18S gene amplification.**

Cycle step	Temperature °C	Time (minutes)
Initial Denature	94	5
30 Cycles:		
Denature	95	0.5
Anneal	58	0.5
Elongation	72	1
Final Elongation	72	10

Following PCR amplification, samples were visualised on 1% agarose gel and positive results were purified.

Volumes of samples were determined and adjusted to 100  $\mu$ L with sterile water. 500  $\mu$ L Buffer PCR were added and mixed. Samples were cleaned by loading onto a column

and collection tube and centrifuged at 10,000 *g* for 1 minute and flow through was discarded. Columns were washed with 750  $\mu$ L Wash Buffer and centrifuged at 10,000 *g* for one minute, and flow through was discarded. Columns were centrifuged at 10,000 *g* for 1 minute to remove residual ethanol. Columns were placed in clean Eppendorf tubes and 80  $\mu$ L Elution Buffer was added onto column membrane and allowed to stand for 2 minutes. DNA was eluted into tube by centrifuging at 10,000 *g* for 1 minute. An aliquot was used for electrophoresis imaging, and an aliquot was sent to Eurofins for sequencing. The rest was stored at 4°C. Obtained sequences were compared to the Genbank nucleotide collection using BLAST (Basic Local Alignment Search Tool).

### **3 Chapter 3: Salt stress experiments in *C. reinhardtii* using different lipid measurement techniques**

#### **3.1 Summary**

The first investigations into salt stress in the model species were carried out using different lipid analysis techniques, with a progression through techniques suitable to the purposes of this study. This chapter aims to determine if salt stress can be used as a lipid trigger in *C. reinhardtii*. Results obtained were inconclusive due to the limitations of different measurement techniques, causing changes in experimental design and to the choice of lipid measurement technique used in subsequent chapters' experimentation. Firstly gravimetric techniques were used, followed by microcolorimetric, Nile Red, and GC FAME analysis techniques. What follows is a description of the data obtained from preliminary experiments undertaken on *C. reinhardtii* to establish the best strains and salt conditions to use for investigating potential lipid induction. Experimental design is detailed in Table 2.1 in Chapter 2. GC-FID analysis was ultimately chosen for lipid measurement in the main experiments in Chapters 4 and 5, as it was identified as the most suitable technique to conclusively establish whether salt stress is a lipid trigger in *C. reinhardtii*.

#### **3.2 Preliminary data for wild type *C. reinhardtii* grown in a range of salt media (0, 0.05, 0.1, 0.15, 0.2 and 0.25 M NaCl)**

All data in the following growth, gravimetric and colorimetric sections was from cultures seeded at a low density of 1 mL seeding culture in 100 mL of the appropriate salt media from the start, as described in Section 2.3, (as opposed to growing in normal TAP media and then resuspending in appropriate salt media), therefore cultures were acclimated rather than exposed to sudden salt shock.

The first experiments were carried out on "wild type" strain CC-4323 137c mt- (Ball background strain nit1 nit2) of *C. reinhardtii*.

These experiments focused on microscopy, growth (measured by OD, cell counts and biomass) and lipid content as shown through gravimetric techniques. The aim was to

establish the best conditions for inducing lipid production in *C. reinhardtii*. The range was 0, 0.05, 0.1, 0.15, 0.2 and 0.25 M NaCl. One replicate of each condition was used, as this was preliminary data only to inform full future experiments.

### 3.2.1 Culture growth (cell counts and optical density)

OD was originally done at 600 nm, and only in later experiments was 750 nm also recorded (as a wavescan showed this OD to be highly suitable for measuring algal culture density, although either is a good proxy measure of culture growth without much interference from factors like chlorophyll pigmentation). Therefore all OD data discussed in this section used wavelength 600 nm.

Figure 3.1 and Figure 3.2 show the effect of salt conditions on growth of this species. Both OD and cell count show that the rate of growth was affected negatively by all salt concentrations. 0.05 M NaCl did not affect the growth at first, but then the cell counts plateaued around 120 hours when the control cultures continued to climb. Similarly, the final OD for 0.05 M NaCl was not as high as the control, despite the initial growth rate being the same up until about 100 hours. The difference between 0.05 M and 0.1 M NaCl was much bigger. The culture in 0.1 M NaCl took longer to move from lag phase to log phase, and the culture growth, measured through both cell count and OD, show that 0.1 M NaCl significantly reduced both the growth rate and final culture density. The same was demonstrated in 0.15 M NaCl culture, with the lag phase being even longer and the final OD even lower. Cell counts were similar between 0.15 and 0.1 M NaCl conditions, by the final timepoint, but the difference in lag phase was still shown. 0.2 and 0.25 M NaCl showed that growth at these conditions was extremely slow. The OD suggests that no culture growth took place at all, but cell counts demonstrated a small amount of culture growth in 0.2 M NaCl conditions. 0.25 M NaCl was too high a salt condition to allow culture growth, even in these acclimated cultures.

Cell counts and OD were correlated to see how well OD represented the growth of a culture (Figure 3.3). The correlation is high in 0, 0.05 and 0.1 M NaCl, with  $R^2$  of above 0.9. The correlation is lower in 0.15 M NaCl, and lower still in 0.2 M NaCl. The nature of the culture is different in these two conditions to those in lower salt concentrations,

since microscopy (Figure 3.4) reveals that the shape of the cells at these higher salt concentrations is very different, being larger than the cells grown in control conditions and lower salt concentrations. The cells in 0.15 and 0.2 M NaCl are also irregular shapes, unlike the control cells which are a regular oval shape. This appears to be because the cells in 0.2 and 0.15 M NaCl conditions are contained in a membrane known as a coenobium and therefore clustered together, causing distortion of their shape.

In 0.25 M NaCl the correlation is very low ( $<0.2$ ), but this culture became infected with bacteria at any early stage of growth, which caused some cloudiness in the culture and affected the OD. This correlation curve is therefore not well representative of algal culture correlation between cell count and OD.

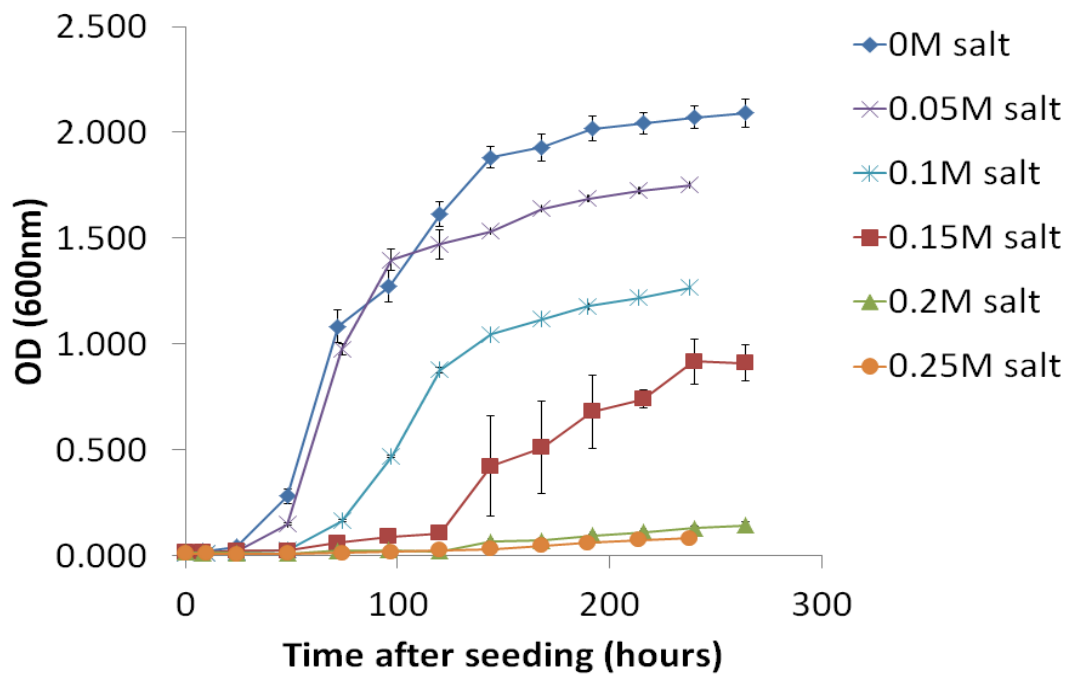


Figure 3.1 Optical density of wild type *C. reinhardtii* cultures grown in varying TAP salt media concentrations (n=3).

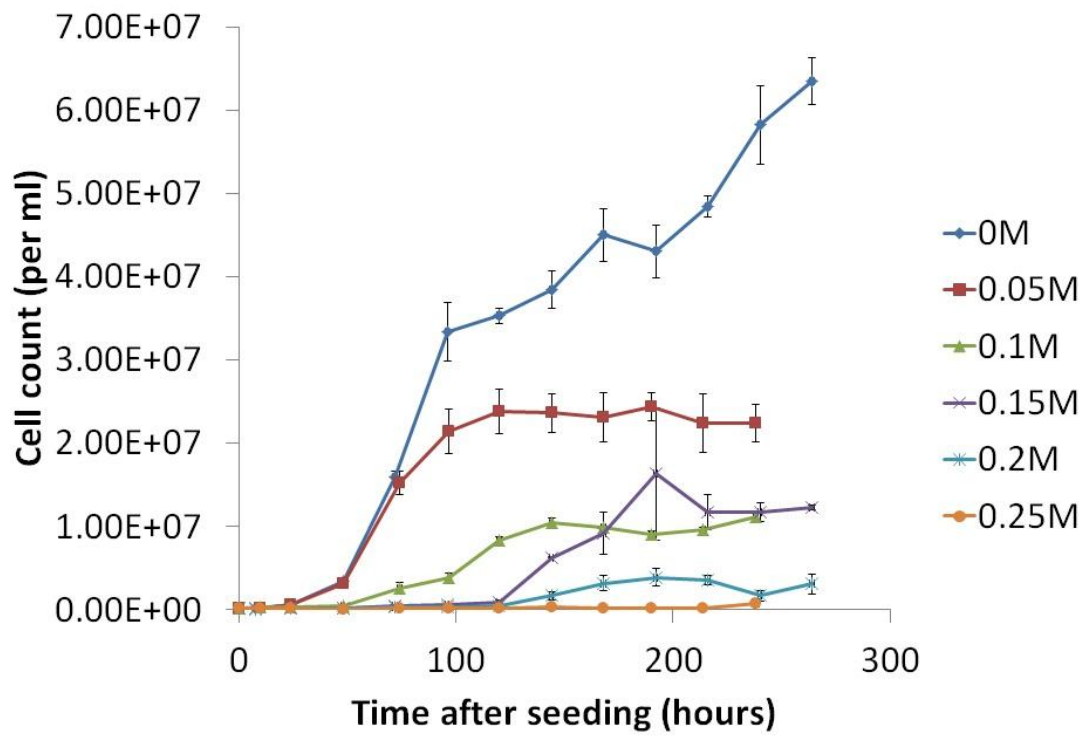


Figure 3.2 Cell counts of wild type *C. reinhardtii* cultures grown in varying TAP salt media concentrations (n=3).

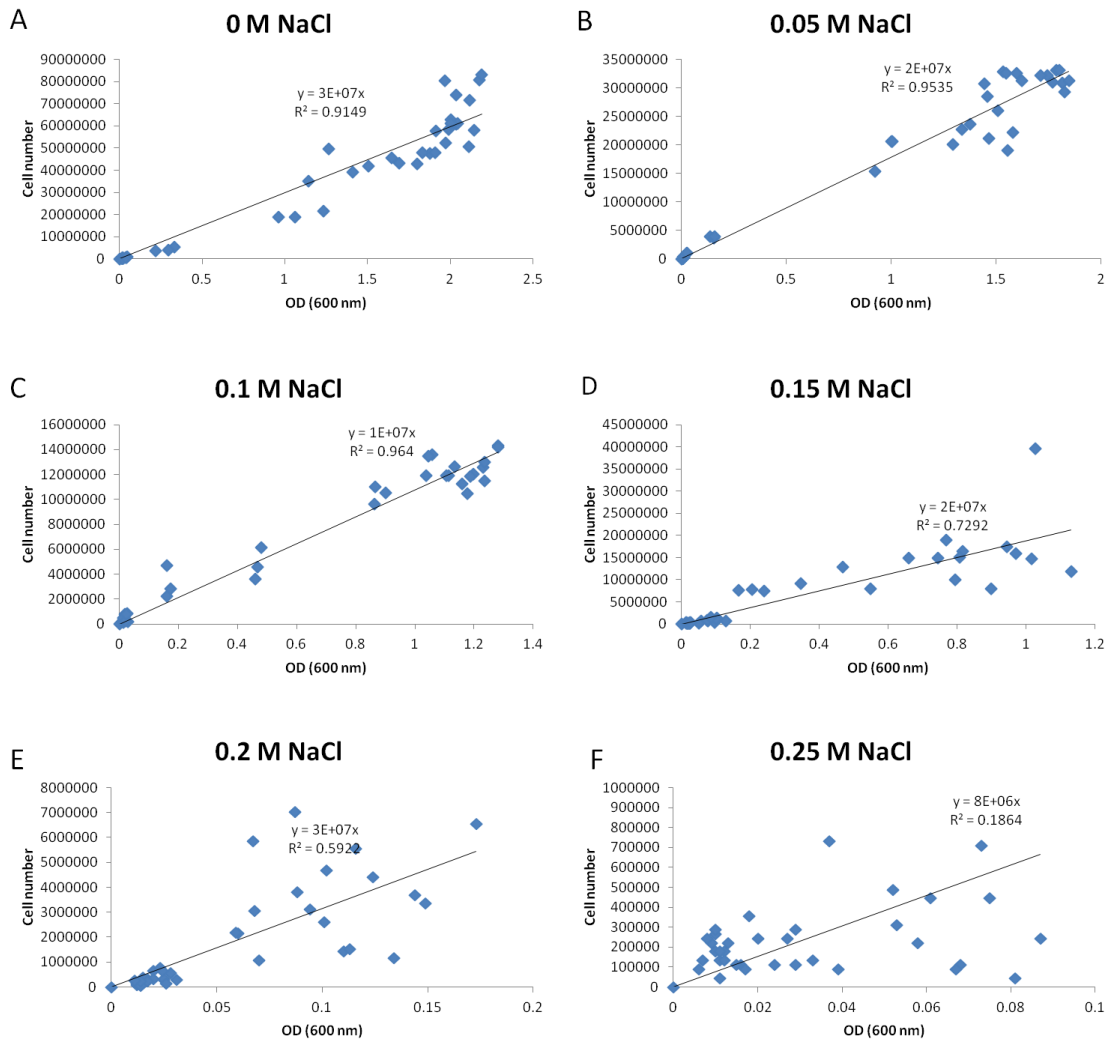
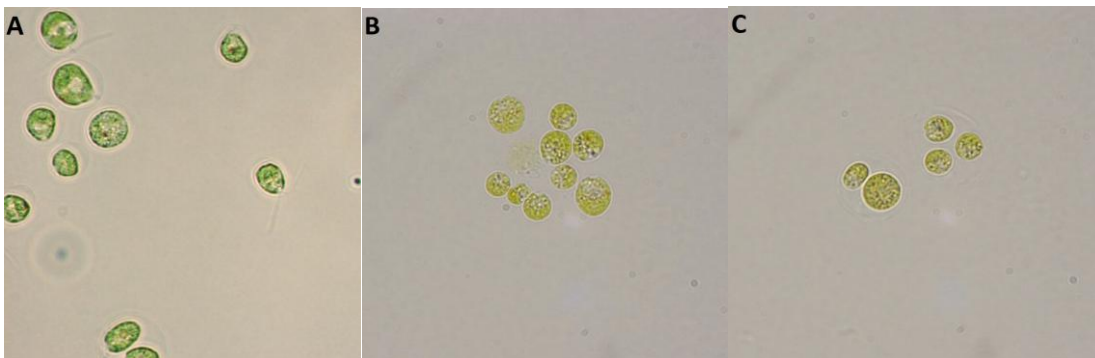


Figure 3.3 Cell counts versus OD (600nm) in wild type *C. reinhardtii* under different concentrations of salt in the media. The correlation decreases as the molarity increases. This is likely due to changes in cell morphology as demonstrated in Figure 3.4.



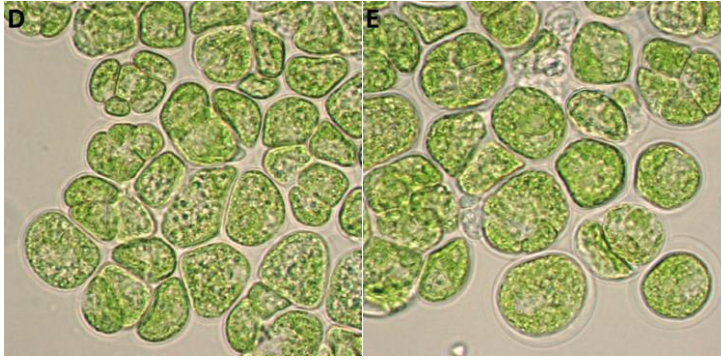


Figure 3.4 *C. reinhardtii* wild type cells under different NaCl salt concentrations. 0 M (A), 0.05 M (B) 0.1 M (C), 0.15 M (D), 0.2 M (E). Images show clear swelling of cells under higher salt concentrations (magnification x1000). Cells grown to mid-log phase or equivalent time for slow growing cultures.

### 3.2.2 Gravimetric data, lipid content and chlorophyll content

Gravimetric analysis of these cultures was carried out. Since the gravimetric method used 60 mL culture for one sample, only one time point per experiment could be taken. In this case the experiment was run multiple times, to test the effect of sampling and introducing salt at different time points. Four experiments like this were set up. Two had culture seeded in TAP media made up to the appropriate molarity of NaCl. Two experiments used normal TAP media for all the conditions, and then added in pure NaCl (to the appropriate amount to achieve desired molarity) at a particular time point (detailed in Table 3.1). The salt concentrations 0, 0.05, 0.1, 0.15 and 0.2 M NaCl were tested for each condition (0.25 M NaCl was too high to allow any culture growth). The time points of adding salt at 0 hours, 48 hours and 120 hours were chosen since these time points demonstrated the effect of adding salt from the start of the culture, from the start of culture exponential phase, and at the end of the growth phase, when the culture was reaching stationary phase.

The biomass contents, lipid contents and chlorophyll contents of these cultures are displayed in Table 3.1. The 0.2 M NaCl conditions did not allow enough growth of biomass to test the lipid or chlorophyll content. From this set of conditions, the highest lipid content as a percentage of biomass was 45.6% found in cultures seeded with 0.15 M NaCl TAP medium, and grown to 168 hours. It should be noted that due to the low biomass level in the 0.15 M NaCl cultures, overall lipid production was not increased. Nevertheless, 0.15 M NaCl was identified as a suitable lipid inducer for *C. reinhardtii*.

This salt condition was subsequently used for follow up experiments testing *C. reinhardtii* for lipid content.

Table 3.1 Table of results displaying biomass, total lipid, and chlorophyll contents of wild type *C. reinhardtii* cultures grown in TAP medium with varying concentrations of NaCl. All biomass and lipid contents were sampled using a method based on Bligh-Dyer (Bligh and Dyer, 1959) (n=1).

NaCl concentration (M)	Time of NaCl addition (hours)	Time of sampling (hours)	Biomass content ( $\mu\text{g mL}^{-1}$ )	Lipid content ( $\mu\text{g mL}^{-1}$ )	Percentage lipid content of DCW (%)	Chlorophyll content ( $\mu\text{g mL}^{-1}$ )
0	0	168	715.0	221.7	31.1	31.7
0.05	0	168	890.0	266.7	30.0	38.2
0.1	0	168	491.7	166.7	33.9	16.3
0.15	0	168	205.0	90.0	45.6	4.4
0.2	0	168	NA	NA	NA	NA
0	48	96	640.0	141.7	21.8	26.6
0.05	48	96	576.7	113.3	19.7	23.5
0.1	48	96	403.3	80.0	20.1	12.4
0.15	48	96	283.3	85.0	30.1	6.0
0.2	48	96	233.3	61.7	26.8	4.7
0	120	168	715.0	221.7	31.1	31.7
0.05	120	168	686.7	203.3	29.6	34.3
0.1	120	168	516.7	171.7	33.7	20.3
0.15	120	168	511.7	136.7	26.8	14.9
0.2	120	168	398.3	80.0	20.4	9.1
0	0	672	666.7	195.6	29.3	NA
0.05	0	672	1036.7	283.3	27.3	NA
0.1	0	672	875.0	246.7	28.2	NA
0.15	0	672	783.3	221.7	28.3	NA
0.2	0	672	NA	NA	NA	NA

A repeat experiment was performed (Figure 3.5), to replicate the data using 3 biological replicates. However, this experiment gave differing results to the previous data, as in this experiment 0.05 M NaCl induced the highest percentage lipid in biomass terms. The difference between these two sets of data was sample timings. In this repeat experiment, measurements were taken at different times in each culture, since the stage of growth cycle is important in determining lipid content (Fidalgo et al., 1998). The OD was monitored for each culture and then samples were taken towards the end of the log phase of each culture. The vast difference in these two results demonstrated the need for a method that could carry out a lipid measurement test on multiple time points by using much smaller amounts of culture for testing.

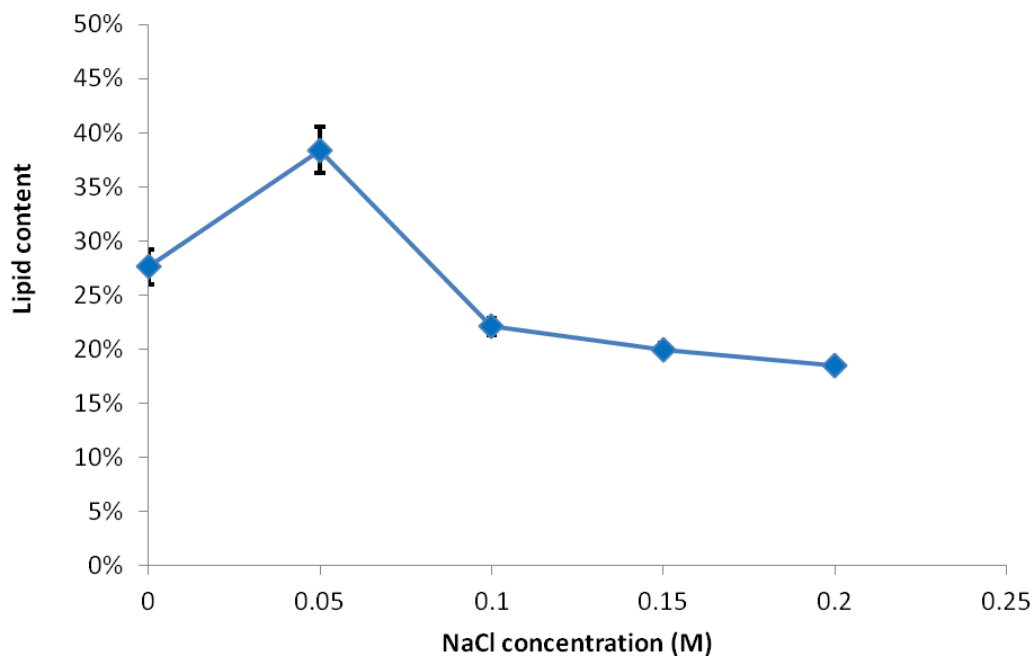


Figure 3.5 Gravimetric lipid content of *C. reinhardtii* wild type cultures grown in TAP media with varying concentrations of additional NaCl, sampled at a single time point (n=3).

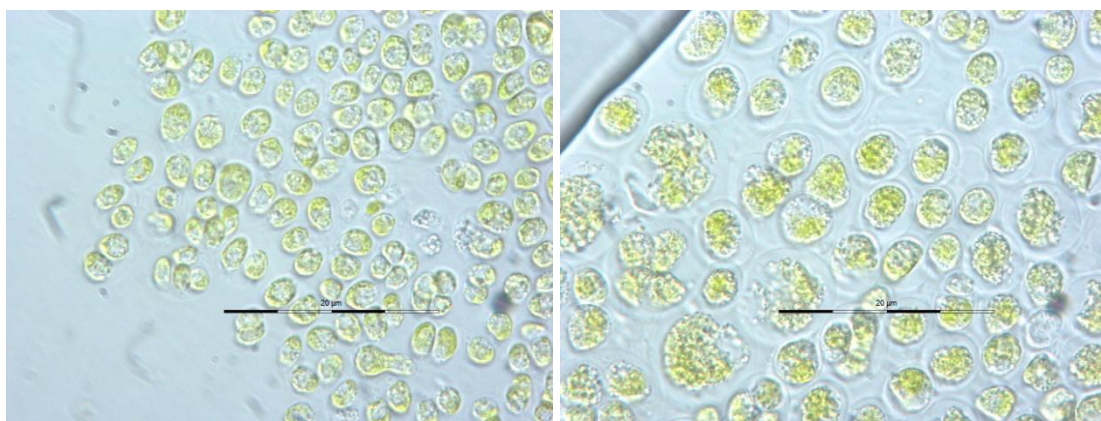


Figure 3.6 *C. reinhardtii* (wild type) growth in TAP medium (left) and 0.15M NaCl TAP medium (right) to 7 days (x1000 magnification).

### 3.2.3 Colorimetric data

A new method of microcolorimetric lipid analysis was trialed. This method is outlined in Section 2.5.2, and was adapted from Cheng et al. (2011b). This method only requires very small amounts of sample so it had potential for a better way to analysis lipid content in algal samples. The sulfo-phospho-vanillin reagent shows good correlation with pure oil and corn oil (Figure 3.7), however the two different types of oil do show a different correlation slope, showing that estimates of lipid content may vary depending on the standard used.

To test how well this method matched up to results found from gravimetric results, some of the dried lipid samples from the gravimetric method were taken and tested, varying some of the parameters of the assay to see if results were consistent. The results are laid out in Table 3.2. The size of the lipid sample aliquot, the ratio of solvents used, and the type of oil used as a standard were all varied and tested in a microplate format. Cells where "overflow" is stated are those where the absorbance reading was too high for the plate reader to record. The results in Table 3.2 demonstrate that the assay produces a wide variation in results depending on the solvent used for extraction, the standard used, and the size of the aliquot used for testing. There also did not appear to be any similarity to the previously obtained results from the gravimetric method. Because of this, and due to the long-winded

extraction procedure that precedes testing, this method was not pursued further as a lipid measurement assay.

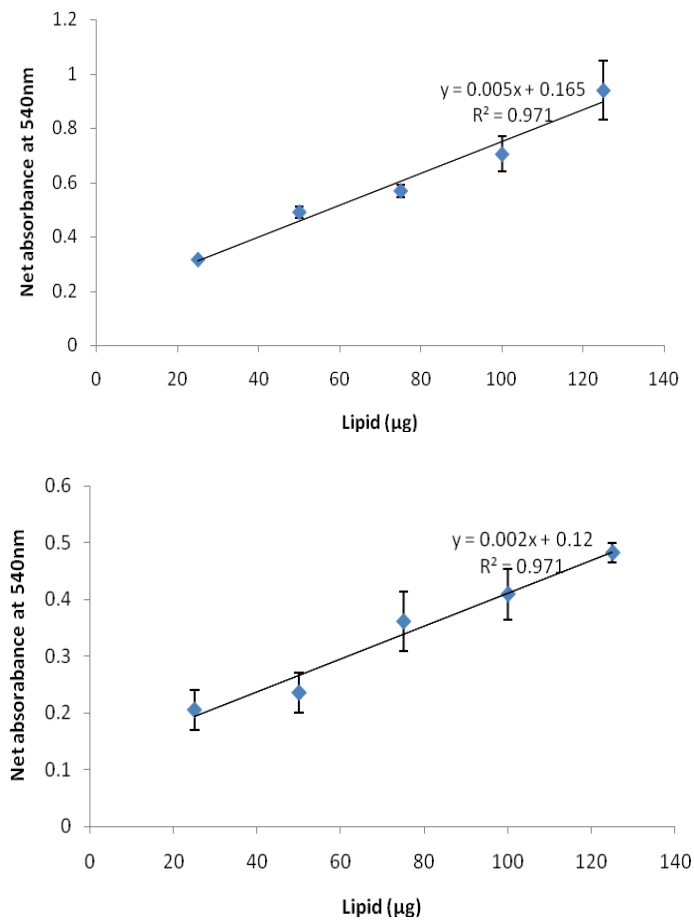


Figure 3.7 Net absorbance curves for standard quantities of vegetable oil (left) and corn oil (right), measured using the microcolorimetric microplate format.

Table 3.2 Lipid measurements obtained from microcolorimetric method, with comparison to values obtained from gravimetric method. Two sets of values were calculated, based on the calibration curve obtained from the corn oil and vegetable oil. Overflow – absorbance reading too high for plate reader.

Media	Solvent	Gravimetric result lipid content ( $\mu\text{g mL}^{-1}$ )	Corn oil equation			Vegetable oil equation		
			Lipid content ( $\mu\text{g mL}^{-1}$ (25 $\mu\text{L}$ aliquot))	Lipid content ( $\mu\text{g mL}^{-1}$ (50 $\mu\text{L}$ aliquot))	Lipid content ( $\mu\text{g mL}^{-1}$ (100 $\mu\text{L}$ aliquot))	Lipid content ( $\mu\text{g mL}^{-1}$ (25 $\mu\text{L}$ aliquot))	Lipid content ( $\mu\text{g mL}^{-1}$ (50 $\mu\text{L}$ aliquot))	Lipid content ( $\mu\text{g mL}^{-1}$ (100 $\mu\text{L}$ aliquot))
Standard Tap	1:2 Chloroform: Methanol	195.6	915.1	694.8	Overflow	375.7	282.7	Overflow
Standard Tap	Chloroform	195.6	214.1	179.2	143.5	95.3	76.5	Overflow
Tap 0.05 M NaCl	1:2 Chloroform: Methanol	283.3	1165.3	Overflow	Overflow	475.7	Overflow	Overflow
Tap 0.05 M NaCl	Chloroform	283.3	475.4	250.5	178.6	199.8	105.0	73.8
Tap 0.1 M NaCl	1:2 Chloroform: Methanol	246.7	1049.0	791.8	Overflow	429.2	321.5	Overflow
Tap 0.1 M NaCl	Chloroform	246.7	453.4	211.1	139.0	191.0	89.2	58.0
Tap 0.15 M NaCl	1:2 Chloroform: Methanol	221.7	721.6	668.1	Overflow	298.3	272.0	Overflow
Tap 0.15 M NaCl	Chloroform	221.7	358.5	197.3	162.3	153.0	83.7	67.3
Tap 0.05 M NaCl	2:1 Chloroform: Methanol	266.7	1177.8	Overflow	Overflow	352.1	155.3	146.7
Tap 0.2 M NaCl	2:1 Chloroform: Methanol	80.0	595.3	Overflow	Overflow	200.0	169.6	120.1

### 3.2.4 Nile Red

A method that required a small amount of sample for time course analysis of a culture was still required, so Nile Red was used as a lipid assay.

From previous experiments (Table 3.1), it was seen that 0.15 M NaCl could produce a high lipid content in *C. reinhardtii* cells, therefore this was pursued as a likely lipid trigger. At this time a new way of seeding cultures was also adopted. As high molarities slow down culture growth and reduce biomass accumulation significantly, a new method was carried out, of seeding all cultures with normal TAP media to mid to late log phase and then resuspending them at OD 0.44 (750 nm) in the appropriate salt media. The first experiment of this nature was carried out on a strain known to respond to nitrogen deprivation under these exact growth conditions, as it has been demonstrated in the literature (Longworth et al., 2012). This strain was a cell wall mutant of *C. reinhardtii* (CCAP 11/32CW15+). At the same time as testing the nitrogen deprivation, a culture resuspended in 0.15 M NaCl TAP was tested, and results are presented in Figure 3.8. Time points denote time after re-suspension and no standard was used so results are in arbitrary fluorescence units. The results show that whilst nitrogen deprivation very clearly causes a Nile Red fluorescence increase in this strain, the salt condition did not, apart from a slight increase at the last salt stress time point. This contradicted previous data from gravimetric tests that suggested that 0.15 M NaCl would cause a lipid increase in *C. reinhardtii*. This demonstrates that Nile Red and gravimetric data can show very contradictory results, and it was unclear whether salt was causing a lipid response, so further experiments were performed to investigate this.

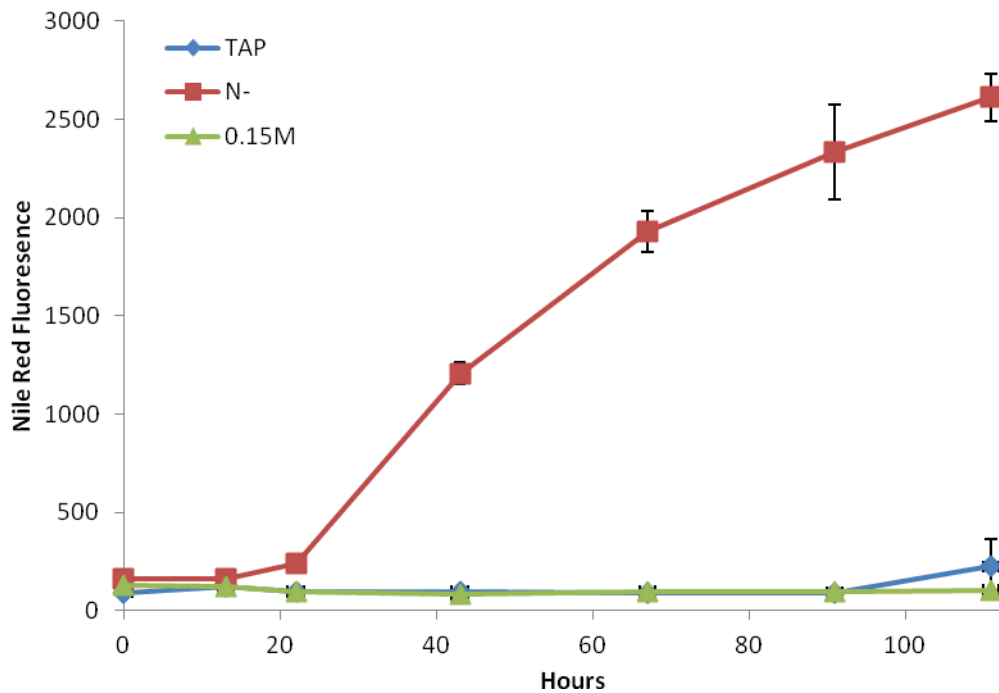


Figure 3.8 Cell-wall mutant of *C. reinhardtii* under nitrogen deprived (N-), non-stressed (TAP) and salt stressed (0.15 M) conditions. Nile Red Fluorescence expressed in arbitrary units.

As 0.15 M NaCl did not cause an increase in Nile Red fluorescence in the cell wall mutant, a starchless mutant strain of *C. reinhardtii* (CC-4325) was used to test the effect of 0.15 M NaCl, and also an increased salt concentration of 0.2 M NaCl, on lipid production, as measured by Nile Red response (Figure 3.9). This strain was used because starchless mutants have been shown to have elevated lipid production under stress conditions compared with wild types (James et al., 2011), and are therefore more likely to reveal a result if salt stress is a suitable lipid trigger. The second salt concentration was used to test if the reason for lack of lipid response in the previous Nile Red experiment (Figure 3.8) was due to too low a salt concentration. The results from this (Figure 3.9) show that 0.2 M NaCl had a slightly elevated Nile Red response over the control conditions and 0.15 M NaCl, which did not vary much from each other. After some literature research and consideration of the interaction of the Nile Red with the experimental conditions that were being used, it was postulated that the salt conditions were causing interference with the Nile Red assay.

Pick and Rachutin-Zalogin (2012) investigated the kinetic interactions of Nile Red in algae. NaCl has been shown to retard the interactions of Nile Red with lipid globules in

the algae cells. Studies with *Dunaliella salina* show that high NaCl medium concentrations significantly affect the emission spectrum and the uprise kinetics of Nile Red fluorescence (Pick and Rachutin-Zalagin, 2012). Therefore, care must be taken to remove substances that could interfere, like salt, particulates, precipitates or cell fragments (Cirulis *et al.*, 2012), using isotonic wash buffers (Pick and Rachutin-Zalagin, 2012) or flow cytometry for "gating" off these substances (Cirulis *et al.*, 2012).

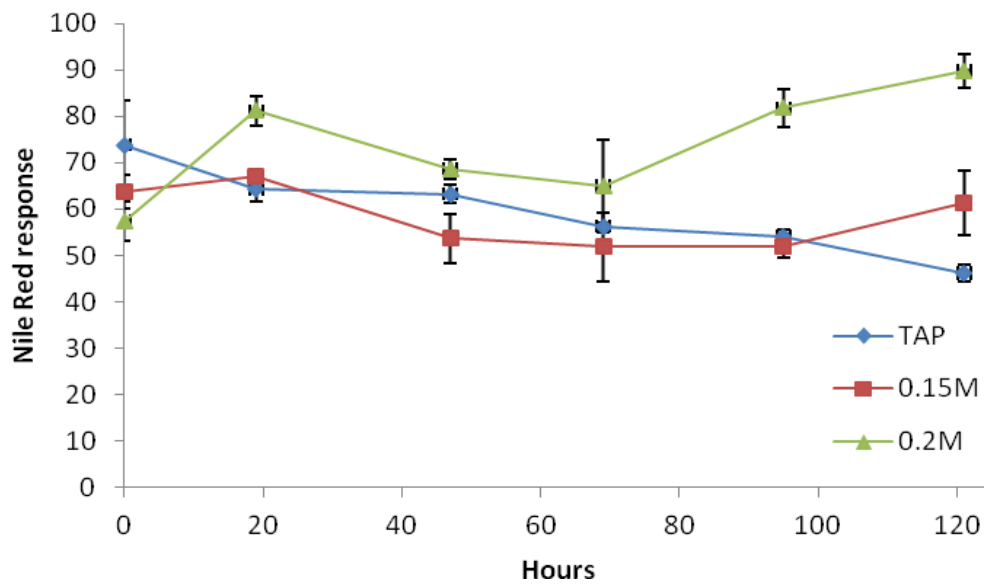


Figure 3.9 Nile Red fluorescence in starch-less mutant strain of *C. reinhardtii* (CC-4325) under control conditions (TAP), 0.15 M NaCl salt stress and 0.2 M NaCl salt stress (no PBS buffer used).

Because of this, 1x PBS buffer was used to wash samples at the point of sampling, and the assay was run again using the starchless mutant under control conditions, 0.2 and 0.3 M NaCl. The higher salt concentration was used to determine whether the salt level needed to be further increased to have an effect on lipid production in this strain.

Figure 3.10 shows the results of this experiment. Compared with the previous data that used 0.2 M NaCl on the starchless mutant strain and showed fluorescence units of less than 100, this data shows a markedly elevated Nile Red response that goes to above 700 in 0.2 M NaCl. This response is even higher in 0.3 M NaCl, which goes to approximately 1300 fluorescence units. It was demonstrated that the use of PBS buffer makes a large difference to the results obtained, and that the use of salt can mask the

interaction between lipid and Nile Red that is the basis of the Nile Red quantification method. Use of PBS was therefore employed for the remainder of the experimentation, as it removed the detrimental effect of salt on the protocols employed.

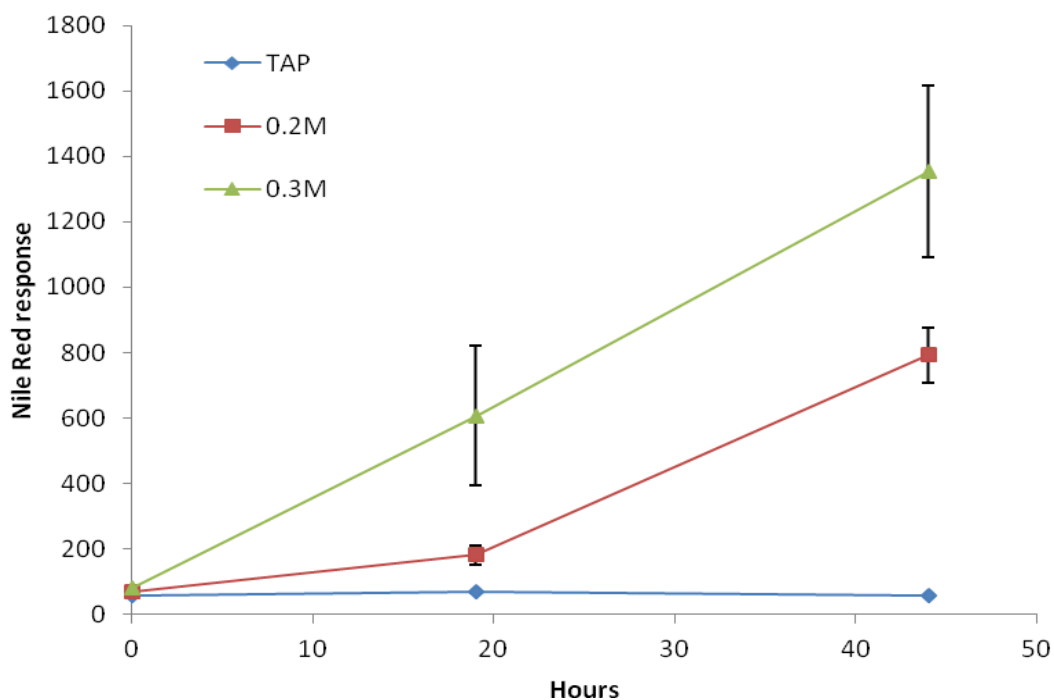


Figure 3.10 Nile Red fluorescence in starch-less mutant strain of *C. reinhardtii* (CC-4325) under control conditions (TAP), 0.2 M NaCl salt stress and 0.3 M NaCl salt stress (PBS buffer used).

These data from Nile Red analysis show an elevated Nile Red response under high salt conditions. Using salt concentrations of 0.2 and 0.3 M NaCl with the starchless mutant strain CC-4325 was therefore pursued for proteomic analysis.

A new set of samples were grown under the same conditions of control, 0.2 and 0.3 M NaCl, with samples for protein extraction taken at the later time points, since this is where the Nile Red response was highest. The results are presented in Figure 3.11.

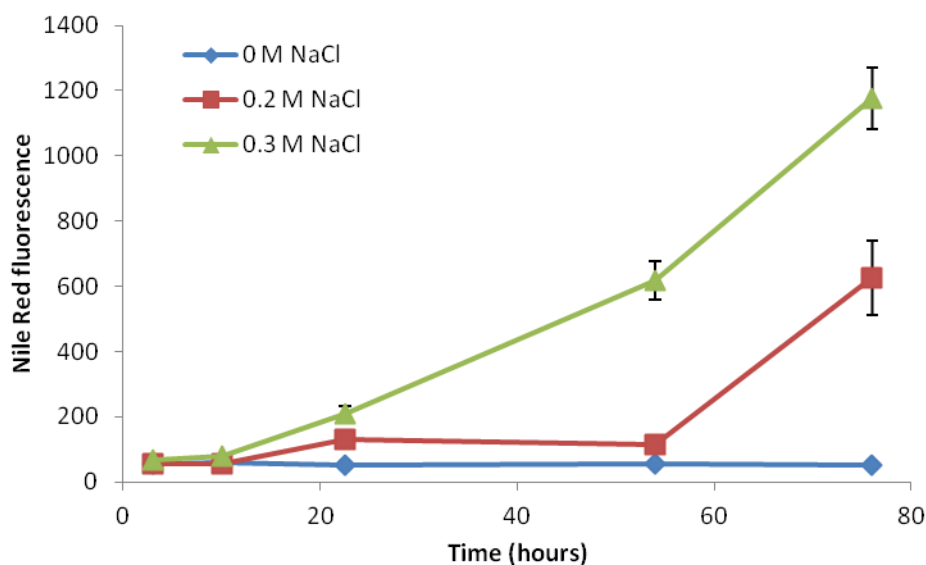


Figure 3.11 Nile Red fluorescence in *C. reinhardtii* starchless mutant (CC-4325) grown in 0, 0.2 and 0.3 M NaCl TAP media (n=3).

Fluorescence is displayed in arbitrary units and is used as a relative measure of neutral lipid content. Whilst the control condition stayed flat, the salt stressed cultures showed a large increase in fluorescence. Therefore, these results suggested that the cultures undergoing salt stress accumulated lipid in high quantities towards 76 hours culture time, especially at 0.3 M NaCl stress. The time point of 76 hours was chosen for proteomic analysis and protein extractions were carried out. However, the protein extractions of salt stressed samples had very little or no measurable protein in them (Table 3.3).

Table 3.3 Protein contents of samples taken at 76 hours in control, 0.2 M and 0.3 M NaCl conditions.

Salt concentration (M)	Biological replicate	Protein concentration (mg mL <sup>-1</sup> )	Acetone precipitated protein concentration (mg mL <sup>-1</sup> )	Estimated amount of total volume of sample (non precipitated) (μL)	Total amount of protein in non precipitated sample in theory (mg)
0	1	1.265	0.565	1200	1.518
0	2	1.463	0.570	1200	1.756
0	3	0.461	0.501	1100	0.507
0.2	1	0.010	0.010	1100	0.011
0.2	2	0	0	1100	0
0.3	1	0.144	0.129	1100	0.158
0.3	2	0.119	0	400	0.048
0.3	3	0	0	900	0

The samples were photographed using microscopy at x1000 magnification to observe physiological changes in them. It appeared from visual observation of the salt stressed cells that they were "ghosts" at that time point, making them unlikely to have a large quantity of lipid droplets within them.

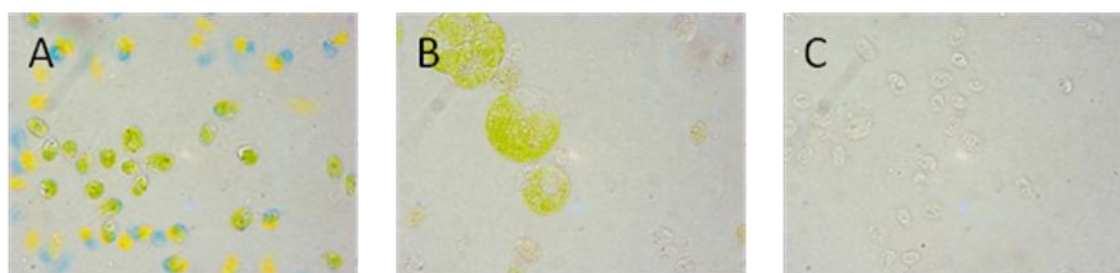


Figure 3.12 *C. reinhardtii* starchless mutant cells under control 0 M NaCl (A), 0.2 M NaCl (B) and 0.3 M NaCl (C) TAP conditions at 76 hours. Magnification at x1000.

The much lower protein contents of these salt stressed samples, combined with visual inspection of the cells at this time point, made it necessary to check the lipid content of the samples with a second method. For this, transesterification of extracted lipid followed by gas chromatography for FAME analysis was used. The results for the total FAME content are displayed in Figure 3.13. These results are performed on the exact same samples as those in Figure 3.11 yet they directly contradict one another.

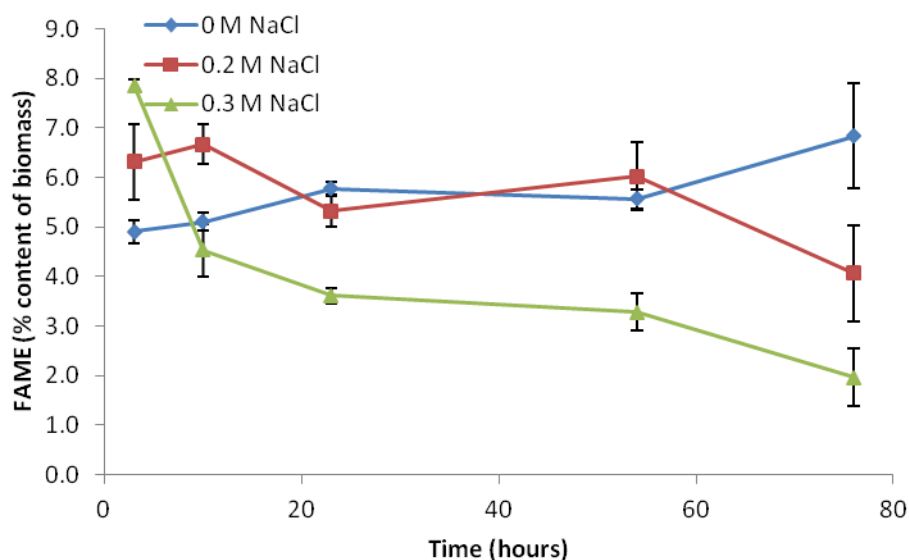


Figure 3.13 Overall FAME content of biomass in *C. reinhardtii* under 0, 0.2 and 0.3 M conditions (n=3).

### 3.2.5 Comparison of Nile Red and GC techniques

The discrepancy between Figure 3.11 and Figure 3.13 is important in thinking about the role of a lipid assay in obtaining accurate and reliable results. As discussed in the full review of lipid analysis techniques in microalgae in Appendix B, also found in the publication by Hounslow et al. (2016b), all lipid analysis techniques have limitations and using two measurement techniques is a good way to check the reliability of obtained data. The GC data is more reliable in this case because the measurement method is much more specific and it is harder to create false positives than with a method like Nile Red. Nile Red can have interfering substances that alter the fluorescence reading obtained (Cirulis *et al.*, 2012). In this experiment, a PBS buffer was used, so salt should not have been an interfering substance. The breakage of cells, however, is likely to be the cause of the high reading obtained in these experiments. The method cannot be used on broken cells because these are thought to have higher fluorescence readings due to the high contact with membrane lipids and other lipids, which are more accessible than those in an intact cell. The much higher contact of internal lipids with Nile Red dye is in contrast to an intact cell where the dye must permeate through cell walls and membranes into the lipid droplets. This is a finely balanced method, requiring optimal solvents and dye concentrations for penetration;

any aspect that affects this process will skew the data obtained (Chen et al., 2009b). GC relies on standards and can also have its limitations (see full discussion of this technique in Appendix B), but its quantitative and highly selective properties (all detected substances must correspond directly to a known standard) make it more suitable for the purposes of this thesis.

### **3.3 Discussion of lipid analysis techniques tested**

The data presented in this chapter shows the logical progression through the choices of strains, lipid analysis techniques and growth media salt conditions that were tested and then selected for the main part of experimentation for this thesis; the main part of experimentation being the detailed lipid analysis under salt conditions, combined with proteomic investigation of the algal strains under salt-induced high lipid conditions.

The gravimetric results revealed problems in a couple of ways. The first was that the protocol required so much biomass that more than one time point could not be tested in these small scale laboratory tests. The second was the potential interference of pigments, which can cause overestimation of the lipid content. In this case the lipid samples were extremely green from chlorophyll, and a review of the literature revealed that this is a common problem in gravimetric analysis (Appendix B).

The colorimetric analysis, as discussed, was found to be unreliable for the samples tested here, and also had more steps in the protocol than the gravimetric technique. This was therefore not used in primary analysis of any of the samples in this thesis, although it was originally considered for this purpose.

Nile Red analysis is a very common method in algal screening for biofuels research, as shown by analysis of the popularity of lipid quantification techniques in algae (Hounslow et al., 2016b). Whilst this method can be useful for screening lipid content in microalgae, literature research reveals a number of factors that can influence the result of a Nile Red lipid measurement (see Appendix B). The results obtained in this chapter demonstrate that Nile Red can be interfered with by the presence of salt, and therefore wash buffer must be used to ensure salt is removed before the test.

Nile Red also revealed conflicting results here with GC data. What this revealed was a false positive result that directly conflicted with GC measurements. Because cells were broken open in the high salt concentrations, the Nile Red reading was artificially high due to a higher surface area interaction between the cell lipids in cell fragments, and the dye. For the purposes of this thesis, it was found that Nile Red tests were not suitable for measuring lipids under high salt conditions.

After a full investigation into the available methods for lipid analysis (now published in the review by Hounslow et al. (2016b)) and the data that was obtained in the current chapter, transesterification combined with GC analysis was chosen to carry out the remaining lipid investigations in this work. Gravimetric, colorimetric and Nile Red had all been found to be unsuitable. There is a large variety of other methods available, but GC was chosen because of a few advantages. Firstly, the lipids detected have to directly match up to a standard peak detected, and therefore it is not likely to give false positives. Secondly, the method is highly quantitative, since known standards are used. Thirdly, the information obtained is very detailed, as the information is given in individual FAME types which are each quantified in the sample. This can then be used to measure total FAME. Since the current research is pursuing ways to increase lipid production in microalgae for biofuels production, knowing this information about lipid sample composition is advantageous, since some fatty acid chain types are more suitable for biofuel than others.

### **3.4 Discussion of salt conditions and strains used**

Following the use of a range of salt conditions and strains in this chapter, the strain that was selected for the remainder of the experimentation was the starchless mutant. Although the data in this chapter had not conclusively shown salt to be a lipid trigger in any of the strains tested, due to the issues encountered with the various lipid quantification techniques, this strain has the potential for higher lipid production than the wild type and therefore any changes in lipid production would be more stark in the starchless mutant than in the wild type in continuing *C. reinhardtii* experiments.

A variety of salt ranges had been used and two different ways of exposing the algal cultures to salt stress had also been used.

In this chapter, both sudden salt stress introduced at log phase and acclimated salt stress introduced at the seeding point were investigated. For the purposes of this thesis work, it was necessary to be able to test a wide range of salt conditions, including those at the limit of *C. reinhardtii*'s salt tolerance, and to be able to obtain a large amount of biomass to test. The method of accumulating biomass under control conditions and then introducing salt stress at log phase was therefore chosen for the remainder of the research work described in this thesis, because this method would ensure high biomass samples could be obtained for those at high salt conditions as well as the conditions that allow *C. reinhardtii* to grow at a high rate. This also follows the idea that by accumulating biomass and then introducing stress to the culture, more lipid can be accumulated in the culture overall (Takagi et al., 2006). Thus the effect of turning on this lipid trigger stress response part way through the growth cycle is of great interest. It is also important to be able to test the effect of salt on the lipid content and proteome of the biomass at different stages, post salt application, and so having a large amount of testable biomass is important at the early as well as the later stages of salt stress application. This response may vary over time, post salt application. As this thesis looks to explore the proteome of *C. reinhardtii* under lipid inducing salt stress, the onset and continuation of lipid production is the state that the samples must be studied, using the correct time points.

There are advantages to studying acclimated cultures growing under salt stress from the beginning, such as knowing that all the acclimated biomass has the ability to grow in salt stress and is therefore adapted to it, perhaps with mechanisms linked to lipid metabolism. However, the lack of testable biomass was a large part of the reason that the cultures seeded with salt media from the start were not used for the remainder of the work described in this thesis.

The salt conditions chosen for investigation in *C. reinhardtii* were chosen to be around the limit of the tolerance, according to the results obtained in this chapter. The salt conditions of 0.1, 0.15, 0.2 and 0.3 M NaCl were used for the following chapter's investigation of salt effect on FAME profile of *C. reinhardtii* starchless mutant. 0.1 M NaCl introduced a lower salt stress to the culture, which is likely to be tolerated by the

culture and allow it to grow well. 0.2 and 0.3 M NaCl are at and beyond the tolerance of *C. reinhardtii*, according to this chapter's testing. Using this range will provide information on how the strain responds to both moderate and high introduction of salt stress.

### 3.5 Conclusions

The lipid quantification techniques used in this chapter demonstrated many pitfalls that can lead the researcher astray, including the occurrence of false positives in Nile Red. The importance of a quantitative and reliable method in lipid measurement is highlighted, since these results can give conflicted data or misleading data that does not tell the full story. Consequently, a full list of techniques available for algal lipid measurement was drawn up and put into decision trees to show how a researcher can tackle the issue of choosing a suitable technique (Appendix B). In this case, GC data was found to be the most reliable method, and also highly suitable to the purpose of measuring the FAME profile for biofuels production.

Through experimentation, methods for growing and applying salt stress to a lipid producing strain of *C. reinhardtii* were selected to provide the best data for measuring the effect of salt stress on the lipid content and proteome of this species. Sudden salt shock was chosen to be more useful in this case, and the range of salt concentrations to be tested was narrowed down to three which would be within, at, and beyond the salt tolerance of *C. reinhardtii* (0.1, 0.2 and 0.3 M NaCl respectively). The chapter that follows will show the detailed results of applying these techniques to the investigation of salt stress on the lipid content of *C. reinhardtii*, and will go further in exploring what can be learned from these experiments.

## 4 Chapter 4: The Effect of Salt Stress on Lipid Metabolism of *Chlamydomonas reinhardtii* (CC-4325) A Starchless Mutant

### 4.1 Summary

This chapter describes a full investigation of salt stress on a *C. reinhardtii* starchless mutant strain. FAME analysis was carried out firstly on a range of 0.1 to 0.3 M NaCl cultures, with results demonstrating some small changes in lipid abundance and profile. A second experiment using a range of 0.1 to 0.2 M NaCl was then used to find a set of conditions where salt halted growth but did not kill the cells, since the arrest of cell division can often coincide with lipid triggering conditions in algae. 0.2 M NaCl cultures caused significant growth rate decreases and were used to investigate the effect of salt stress on the proteome of *C. reinhardtii* using iTRAQ peptide quantification. Supporting metabolomic data from this experiment showed no significant effect of salt stress on lipid abundance, leading to the conclusion that lipids are not accumulated under 0.2 M NaCl salt stress conditions in this strain. The proteomic data revealed that salt stressed cultures down-regulate acetyl CoA carboxylase, the rate limiting committing step to fatty acid synthesis, suggesting that this non halotolerant species diverts resources away from fatty acid synthesis and uses resources for cell maintenance instead. Up-regulation of citrate synthase also plays a key role in favouring the TCA cycle over fatty acid biosynthesis in salt stress conditions. Overall salt stress limits the availability of acetyl CoA for fatty acid synthesis in this species.

### 4.2 Introduction

This chapter explores the effects of salt stress on growth, lipid profile, carbohydrate content, cell morphology, chlorophyll content and photosynthesis activity of *Chlamydomonas reinhardtii* CC-4325 (a starchless mutant). In particular this chapter aims to establish whether salt stress can increase lipid production in *C. reinhardtii* CC-4325 cultures, and how the lipid profile changes under these conditions. Knowing how the growth, carbohydrates and pigments of the cells also respond help to give context to the lipid response of *C. reinhardtii* CC-4325 under high salt conditions, and how this

affects the suitability of this mutant strain as a candidate species for biofuel production.

Experimental design is detailed in Table 2.1 in Chapter 2. Two sets of experiments were carried out. In the first, 0.1, 0.2 and 0.3 M NaCl TAP media are used to show the effect of salt stress on growth and lipid accumulation. This provides information on how this strain responds to increasing levels of salt stress. As this strain is very sensitive to salt stress, small changes in salt concentration can provide vastly different results. Following this first set of experiments, a second set of experiments was undertaken using a smaller range of salinities (0.1, 0.15 and 0.2 M NaCl) in order to find the best salinity to induce lipid production by *C. reinhardtii* CC-4325.

## 4.3 Results and Discussion

### 4.3.1 Effect of 0.1, 0.2 and 0.3 M NaCl on growth of *C. reinhardtii* CC-4325

The initial growth experiments were carried out in three parts: the first was a comparison of growth in 0.1 M NaCl TAP against a control in normal TAP medium with no added NaCl. The second was to use TAP medium containing 0.2 and 0.3 M NaCl with a control (no added NaCl), to explore the effect of higher salt conditions. The third type of experiment used 0.2 and 0.3 M NaCl and a control again, but with only 2 time points (to cut down sampling), and in particular to investigate a potential lipid trigger in this strain under 0.3 M NaCl conditions.

In these growth experiments, cultures were grown to mid log phase and then re-suspended in control or higher salinity TAP media to a final OD<sub>750</sub> of 0.44. This is based on the idea of introducing stress part way through the growth phase in order to maximise the lipid yield of a culture (Takagi et al., 2006). The advantage is that the culture will be at a high level of biomass when the stress is applied, and therefore testing of the culture can take place at early as well as later stages of stress application along a time course; the problems of low biomass yield in lipid analysis were discussed in Chapter 3.

Figure 4.1 shows the optical density, taken as a measure of culture density and productivity, of this strain under salt conditions. The difference between the effects of

0.1 M NaCl and of 0.2 and 0.3 M NaCl are very distinct, with 0.1 M NaCl causing only a slight decline in growth rate of the culture, and ultimately achieving similar density, whilst the 0.2 and 0.3 M NaCl cause complete arrest of culture proliferation, indicated by the slight and steady decline of culture OD under these conditions. Between 0.1 M and 0.2 M NaCl, there must be a critical level of salt tolerance beyond which the cells cease to be able to carry out their normal biological functions. Growth was measured using OD<sub>600</sub> and OD<sub>750</sub> and the growth trends were the same at both optical densities.

The lowest salt tested (0.1 M NaCl) has an impact on the algal physiology and biological responses, but does not severely hamper the culture's ability to grow and survive. This demonstrates that a low level of salt can be tolerated by this strain, but that no added salt in the medium is a more suitable growth condition for reaching high cell density quickly.

In each case the first (3 hour) time point optical density was at a higher value in the higher salinities than in the 0 M NaCl control conditions. Salinity increases therefore must have an immediate effect on the culture density. This seems unlikely to be due to a spike in cell division at this point, therefore it may be due to an effect on cell morphology that makes the culture appear denser. These cultures were not washed with PBS buffer when taking the OD, therefore we must consider that there may be a slight difference due to medium composition, however, the dissolved salts should give a negligible effect on optical density. When comparing the OD<sub>750</sub> of 0 M NaCl TAP and 0.2 M NaCl TAP sterile medium, both gave an OD of 0.000.

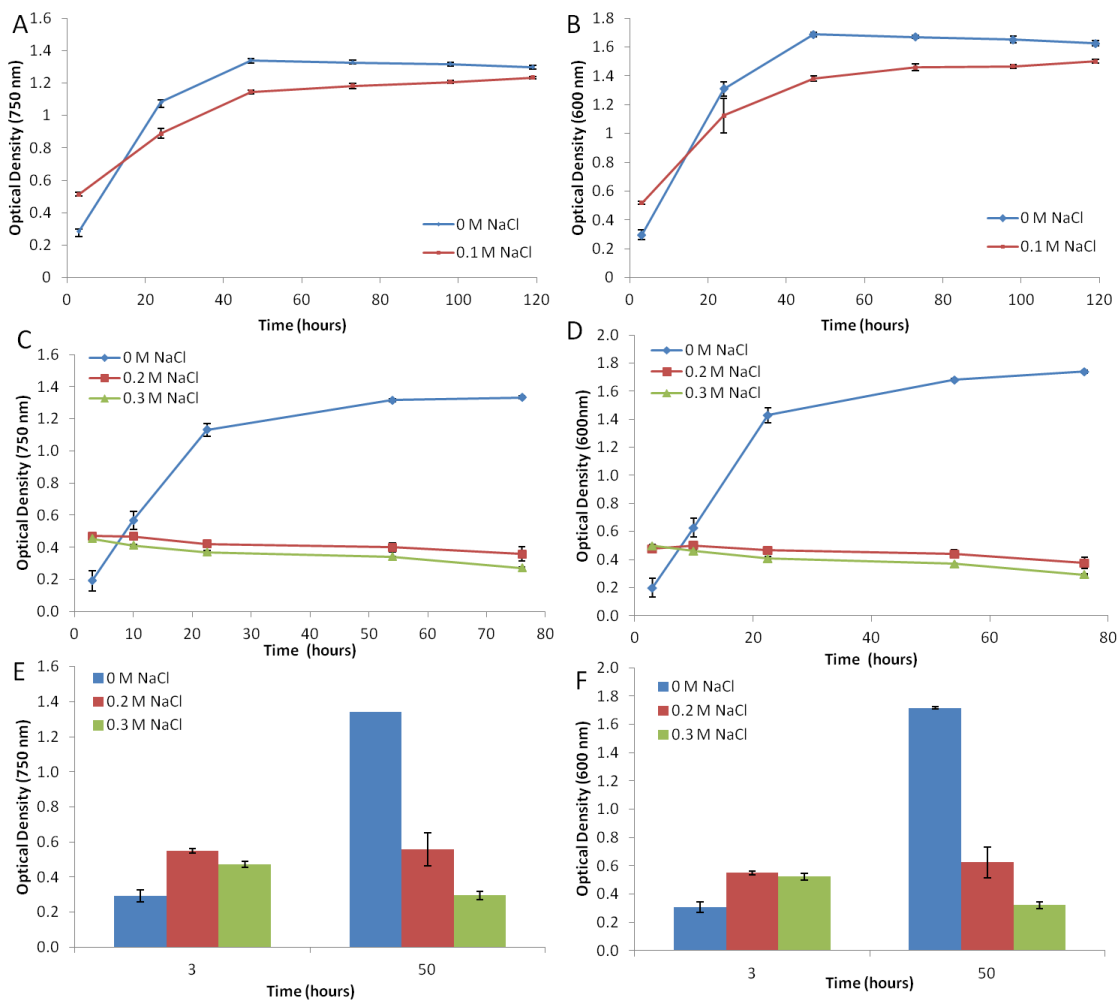


Figure 4.1 Optical density of cultures grown in 0 and 0.1 M NaCl (A and B) and 0, 0.2 and 0.3 M NaCl conditions (C, D, E, F). Optical densities taken at 750 nm (A, C, E) and 600 nm (B, D, F) (n=3).

Figure 4.2 shows that under all salt conditions, the biomass of the culture starts at the same level as the control conditions. This is a contrast to the OD data, therefore there is something affecting the OD at this time point that is not affecting the biomass or dry cell weight of the culture.

The biomass concentration demonstrates a slightly shallower growth curve in dry cell weight in 0.1 M NaCl, compared to normal TAP medium, perhaps due to slightly slower cell division. The biomass productivity of the 0.1 M culture beyond 45 hours then overtakes the TAP culture slightly, with both cultures showing a large increase within the first 24 hours. This shows that ultimately, 0.1 M NaCl does not impact the biomass productivity of the *C. reinhardtii* CC-4325, it just initially causes some decline in growth

rate. In contrast, 0.2 and 0.3 M NaCl completely arrest the proliferation of biomass in the culture. This supports the evidence from the optical density data that between 0.1 and 0.2 M NaCl, there is a critical tolerance level beyond which the culture is not able to carry out normal functions and be productive.

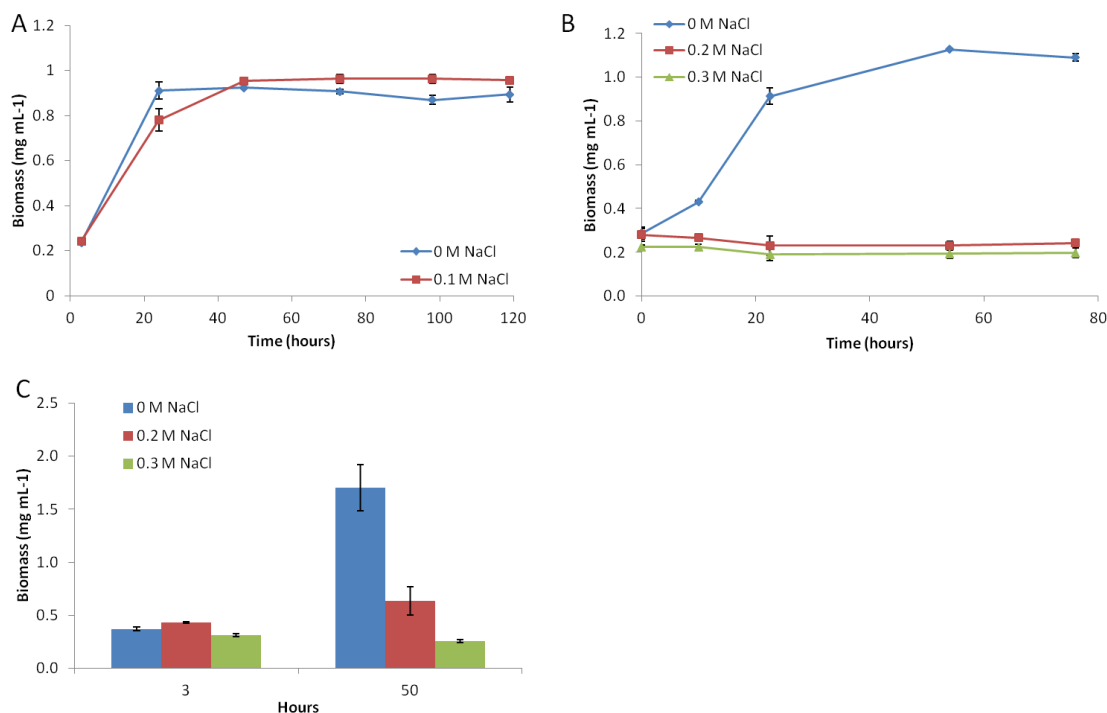


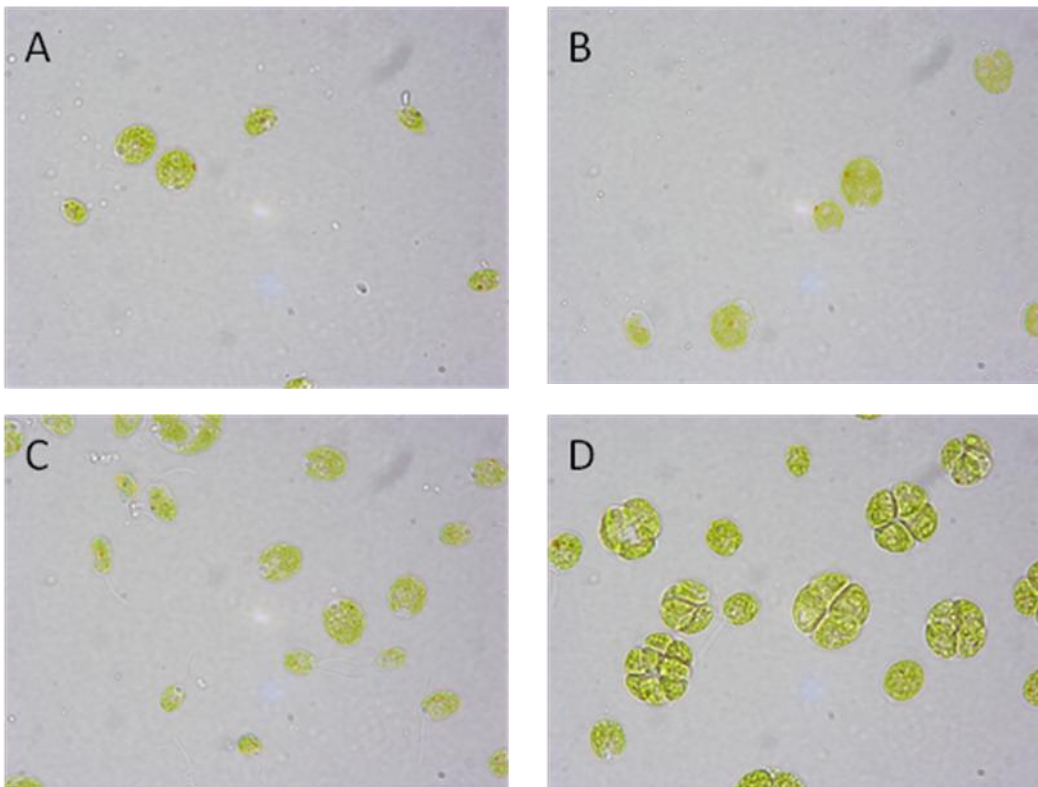
Figure 4.2 Biomass contents of cultures under 0.1 M NaCl and control (A), 0.2 and 0.3 M NaCl and control (B, C) (n=3).

#### 4.3.2 Effect of 0.1 M, 0.2 M and 0.3 M NaCl on Cell Morphology of *C. reinhardtii* CC-4325

Figure 4.3 shows the morphology of the cells grown in normal TAP medium and in TAP medium with 0.1 M NaCl over time. The cells grown in 0.1 M NaCl medium (B, D, F, H, J, L) show signs of being in abnormal cell division stages, clustered together in groups of four, rather than individual cells as seen in the control TAP medium (A, C, E, G, I, K). This occurs less in the latter stages (beyond time 98 hours) of the culture growth, and it was not evident either at the initial time point of three hours. The colour of the cells does not appear to be adversely affected by the presence of salt with all cells showing healthy pigmentation. The main difference is that cells grown in the 0.1 M NaCl TAP medium are clustered together in a membrane known as a coenobium, possibly as a

result of abnormal cell division. Cell division is often affected by the growth conditions, with the rate of growth altering the number of G1 phases (where the cell grows in size before dividing) the mother cell goes through (Bišová and Zachleder, 2014).

Having sufficient energy to divide is important in the commitment stages of cell division and producing high numbers of daughter cells. Therefore the ability of the cultures to supply energy will affect the cell division process (Zachleder and Vandenende, 1992). It is suggested that starch reserves are a critical supply of energy for cell division (Vítová et al., 2010), therefore having a starchless mutant may affect the ability of this strain to divide under stress conditions.



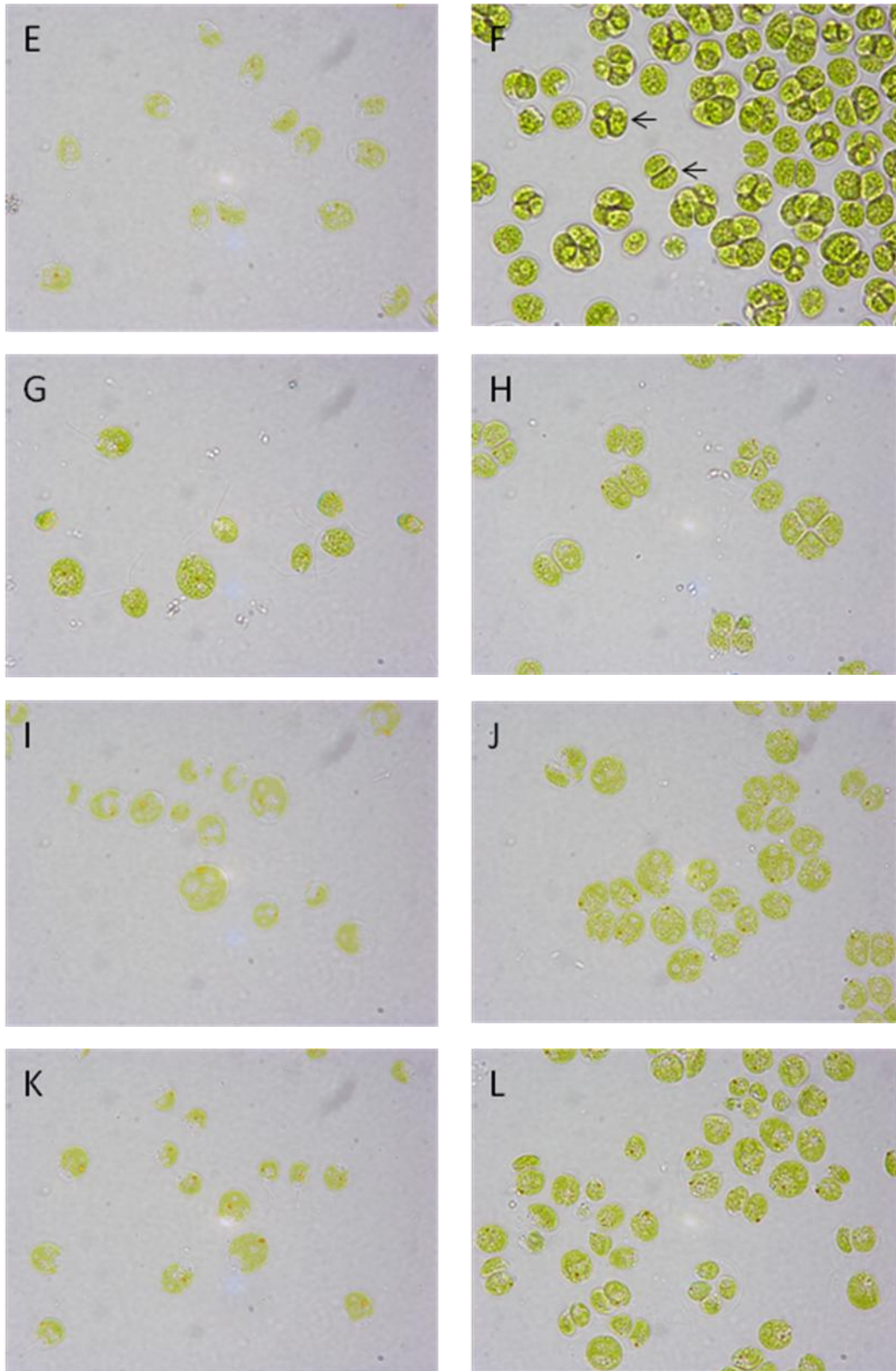
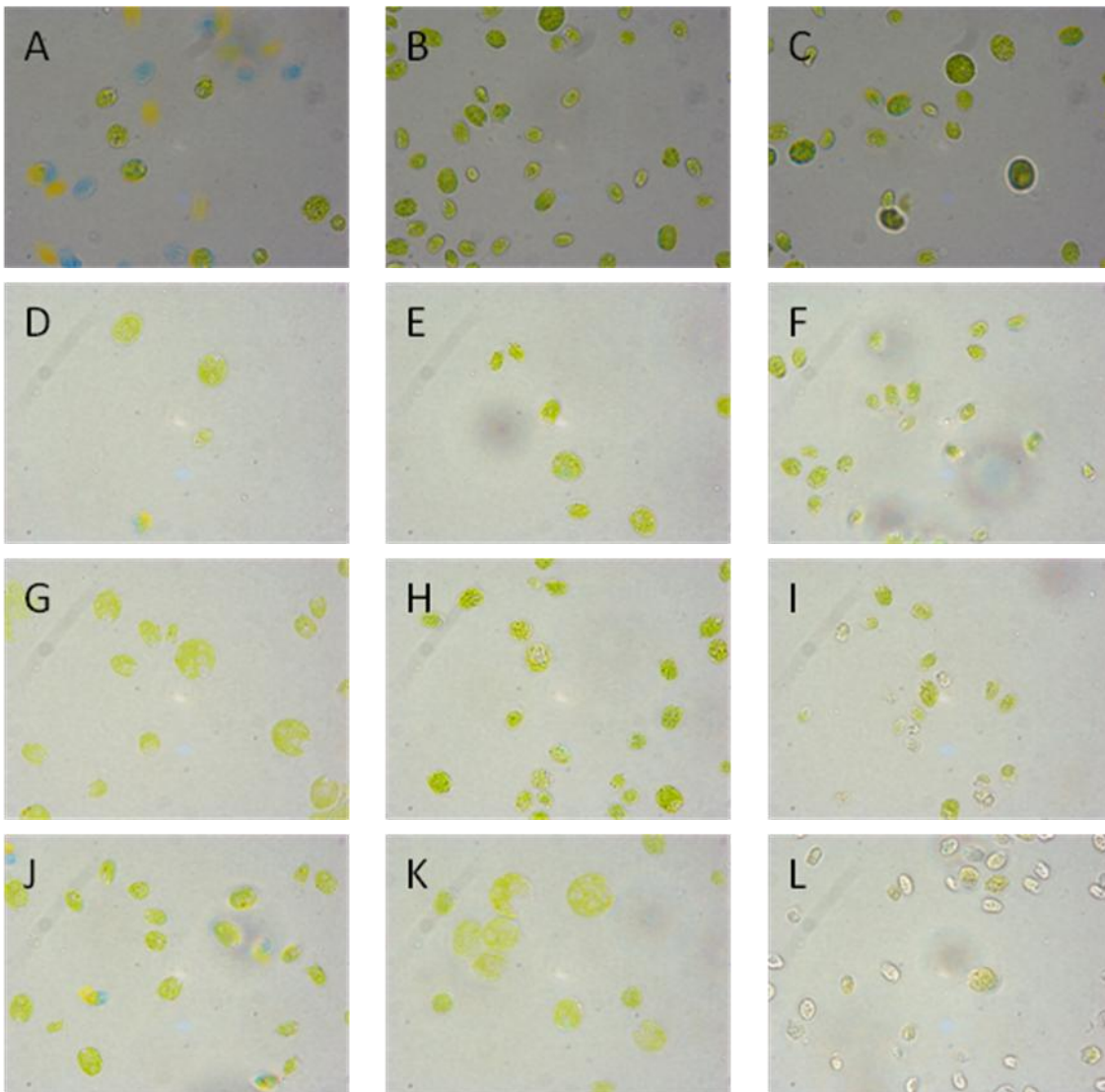


Figure 4.3 Optical microscopy of *C. reinhardtii* under TAP conditions (A, C, E, G, I, K) and 0.1 M salt conditions (B, D, F, H, J, L) At 3 (A, B), 24 (C, D), 47 (E, F), 73 (G, H), 98 (I, J), 119 (K, L) hours. All pictures taken at x1000 magnification. Arrows in F indicate cell clusters.

Figure 4.4 shows the effect of adding 0.2 and 0.3 M NaCl on cell morphology in comparison to normal TAP medium with no added salt. In 0.2 M NaCl cells retain a

significant amount of green pigmentation, although chlorophyll content is reduced compared to the control culture. Towards the end of the growth period some cells start to lyse and become "ghosts" and those which are still green become much bigger and change drastically in morphology (Figure 4.4 K and N). In comparison, adding 0.3 M NaCl appears to cause the cells to shrink after the initial time point (Figure 4.4 F), and after this the cells start to degrade and become "ghosts" (Figure 4.4 L and O). A salt concentration of 0.3 M NaCl is clearly a condition under which this strain cannot survive.



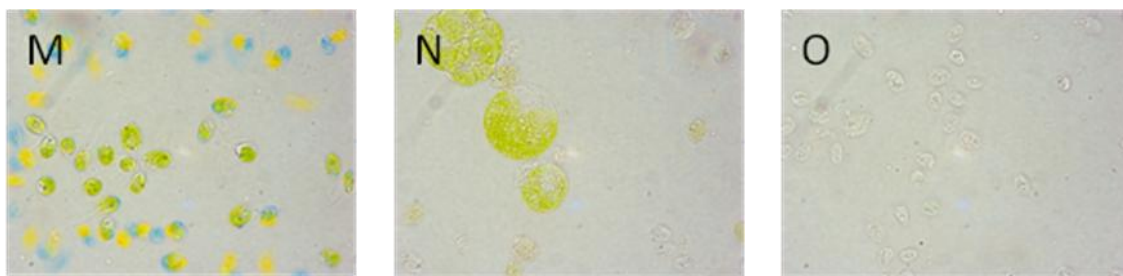


Figure 4.4 Microscopy of *C. reinhardtii* grown in TAP (A, D, G, J, M), 0.2 (B, E, H, K, N) and 0.3 (C, F, I, L, O) M salt TAP medium at time points 3 (A, B, C), 10 (D, E, F), 23 (G, H, I), 54 (J, K, L), 76 (M, N, O) hours at x1000 magnification.

A loss of pigmentation is an expected response in green algae under high salt stress, although they may also respond with an increase in cell size rather than a decrease (Batterto and Vanbaale, 1971), as seen in Figure 4.4 N. The cells in the 0.2 and 0.3 M NaCl conditions do not display the same multiple fission that 0.1 M NaCl cultures do, since cell division is completely halted. This may be autophagic cell death, which has been shown to occur in other algae species (Affenzeller *et al.*, 2009).

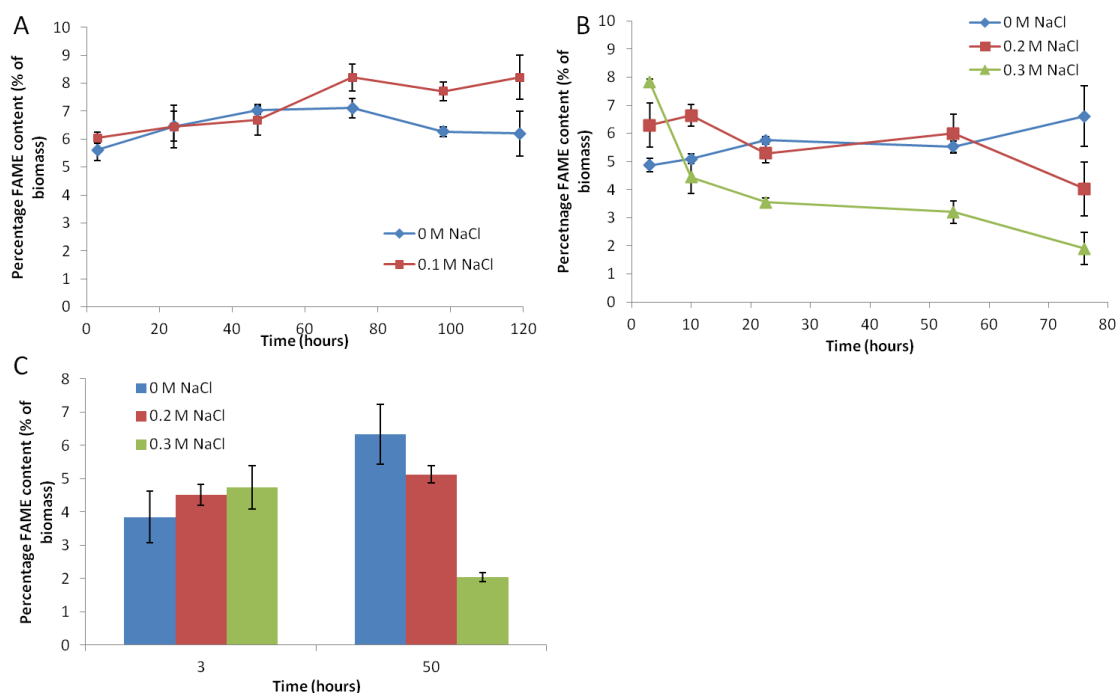
#### 4.3.3 Effect of 0.1, 0.2 and 0.3 M NaCl on Neutral Lipid (FAME) Accumulation by *C. reinhardtii* CC-4325

Figure 4.5 shows the overall FAME content measured by GC tests on *C. reinhardtii* cells grown in the different salinities. These figures are obtained by adding together all the detected FAME weights in a run and calculating it as a percentage weight of the total biomass. There are no large increases in lipid content caused by salt stress, with all cultures showing between 2% and 9% total FAME content of biomass (Figure 4.5).

The total FAME content of *C. reinhardtii* CC-4325 cells increased in the presence of 0.1 M NaCl after 50 hours incubation, whereas the FAME content decreased slightly in the control conditions after this time point (Figure 4.5 A). For the 0.1 M NaCl cultures, this is also the point at which stationary phase was reached, showing that the increase in FAMES coincided with the culture ceasing to proliferate (Figure 4.1). The increase in FAME may therefore be due to diverting of carbon that is no longer being used for growth.

Cultures of *C. reinhardtii* CC-4325 grown in 0.2 and 0.3 M NaCl TAP medium show a different FAME response to that of 0.1 M NaCl grown cells. Although cell division is arrested - a condition under which TAG is accumulated over time when caused by

nitrogen deprivation, due to an imbalance between energy supply and demand (Klok et al., 2013) - there is not an increase of lipid over time (Figure 4.5 B). However, at the initial time point of 3 hours, salt stress does increase the overall FAME content compared with the control conditions, and this increase is especially marked in the 0.3 M NaCl. A second independent experiment taking measurements of FAME only after 3 and 50 hours confirmed this observation, but the salt induced FAME increase was smaller in this experiment and not statistically significant (Figure 4.5 C). Nevertheless, this time point (t=3) is therefore of particular interest as it demonstrates a distinct (although small) increase in lipid content under salt stress conditions. In the time course experiment (Figure 4.5 B), the FAME content then decreases dramatically over time in the higher salinities especially in the 0.3 M NaCl cultures. This can be explained by the fatty acids in the cells degrading as the cells start to lyse and break down. There is some fluctuation in the FAME content of cells grown in 0.2 M NaCl rather than a continuous decline, suggesting that some of the cells are still functioning and altering their fatty acid content even though the culture is not dividing. This culture then shows a sharp decrease at the last time point, when the cells are starting to lose their shape, as demonstrated in Figure 4.4 N, suggesting the cells are breaking down in both structure and fatty acid content at this stage.



**Figure 4.5** Total FAME content of cultures grown in control and 0.1 M NaCl conditions (A), and in control, 0.2 and 0.3 M NaCl conditions (B, C) (n=3).

In addition, the individual FAME components were analysed by comparing their change over time in terms of their percentage of total biomass. These data are shown in Appendix C, Section 11.1.1. The FAMES that are present (from the 37 FAME mix used as a standard) in lower quantities are C6:0, C8:0, C10:0, C11:0, C12:0, C13:0, C14:0, C14:1, C15:0, C16:1 and C17:1. The FAMES present in higher quantities are C16:0, C17:0, C18:0, C18:1*cis*, C18:2*cis*, and C18:3n3. Occasionally C20:5, C21:0 and C20:3n6 are seen, but not consistently throughout samples. C16:0, C18:3n3 and C18:2*cis* dominate the lipid profile, with C18:1*cis* and C17:0 appearing in smaller quantities, and the rest being minor elements of the profile. Overall, C16, C17 and C18 FAMES dominated – see Appendix C for more details and Figure 4.6 for lipid biosynthesis pathways.

[Image removed for copyright reasons]

Figure 4.6 Lipid biosynthesis processes, image taken from Harwood and Guschina (2009).

#### 4.3.4 Discussion of 0.1, 0.2 and 0.3 M NaCl Salinity Stress Experiments

These experiments showed that *C. reinhardtii* CC-4325 was tolerant of 0.1 M NaCl, but 0.2 and 0.3 M NaCl had a detrimental effect on culture health and 0.3 M NaCl causes cell death. Even 0.2 M NaCl showed some damage to cell structure towards the end of the time course experiment. The FAME profile did not show any large increase in lipid accumulation under the salt stress conditions tested (Figure 4.5).

It was desirable to find out more about what mechanisms *C. reinhardtii* uses to cope with salt stress. For this, the best salt condition to use is one that is high enough to slow the growth of the culture significantly (showing that it is outside the comfortable salinity range for this species), but not so high that it causes cell death. This was desirable because in growth arresting but not toxic environments, such as nitrogen deprivation, *C. reinhardtii* shows increases in lipid production and physiological changes that are useful to algal biofuel research. By studying growth arresting but non-toxic salt conditions, we may see differences from lipid producing conditions that show which parts of the cell mechanisms are simply arresting growth and which parts are linked to the lipid metabolism and accumulation.

Because of this, a second set of experiments looked at a more restricted range of salt conditions, 0.1, 0.15 and 0.2 M NaCl, and is discussed in the following sections.

#### 4.3.5 Effect of 0.1, 0.15 and 0.2 M NaCl on Growth of *C. reinhardtii* CC-4325

As noted above, these further experiments were carried out on *C. reinhardtii*, to establish suitable conditions where the salt concentration significantly decreased the growth of the culture, but did not kill the cells. It was desirable to look for the conditions which normally cause lipid accumulation in microalgae (i.e. the redirection of energy into storage molecules due to retardation of growth of the culture, normally induced by nitrogen deprivation), so that the effects of salt on the cellular mechanisms of *C. reinhardtii* (including effects on lipid metabolism), could be further explored at the proteome level.

The work described in sections 4.2.1 and 4.2.2 showed that the upper limit for salt tolerance of *C. reinhardtii* CC-4325 lies between 0.1 and 0.2 M NaCl. Cultures were therefore grown in a range of concentrations of 0.1, 0.15 and 0.2 M NaCl, as well as a 0 M NaCl control. An issue with the previous experiments was differences in the starting OD, due to the nature of the dilution method employed for those cultures. In the new experiments, the OD was set to be the same for each set of cultures so that growth could be more directly compared. This was set to approximately 0.35 OD<sub>750</sub>. The culture growth, biomass accumulation, lipid content and FAME profile, starch content, chlorophyll content and photosynthesis and respiration rates were then studied at a series of time points over the growth cycle to determine the response of *C. reinhardtii* CC-4325 to these salt conditions. The time points chosen also included multiple sampling points within the first 24 hours, since it is over this period that the control cultures undergo log phase, which was important to study in more detail at different salinities.

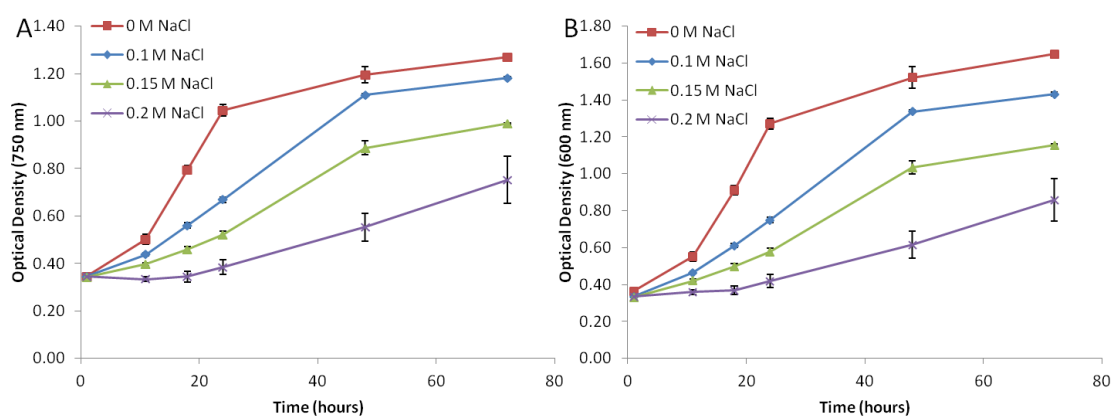


Figure 4.7 Optical density of *C. reinhardtii* grown at 0, 0.1, 0.15 and 0.2 M NaCl TAP media. OD measured at 750 nm (A) and 600 nm (B) (n=3).

Figure 4.7 shows the growth at each salt condition as determined by OD. Both OD<sub>750</sub> and OD<sub>600</sub> are shown but each follows the same pattern. Control conditions (TAP medium with no added salt) demonstrate a standard exponential S-shaped growth curve that begins with a slight lag in growth up until 11 hours, a log phase between 11 hours and 24 hours, and a slowing of growth, approaching stationary phase after 24 hours. As the concentration of NaCl in the media increases, the reduction of the

growth rate is greater. At all three salt concentrations the cultures are able to grow to some extent, with even the 0.2 M NaCl culture showing a slight increase in OD towards the end of the incubation period.

The ability of this culture to grow in 0.2 M NaCl when previous experimentation had indicated that culture growth did not occur at 0.2 M NaCl (Figure 4.1) shows that there is natural biological variation between seeding cultures. The CC-4325 strain was re-obtained from the culture collection a year after the initial experiments were carried out. *C. reinhardtii* has significant genomic and phenotypic variation between strains, and much of this variation has arisen over laboratory culture (Flowers et al., 2015). Amplifications of mutations are common in strains that are isolated from one another and adapting to the laboratory environments they are being cultured in (Flowers et al., 2015). It is therefore possible to have the same strain of *C. reinhardtii* being sub-cultured and kept in a culture collection to show differences over time. In this case, the shift shows a greater resistance to salt stress, allowing cell division at 0.2 M NaCl, when previously this was too high a salinity for culture proliferation. Perrineau et al. (2014) reported growth of *C. reinhardtii* to occur at 0.2 M NaCl, showing that growth at this salinity is consistent with other findings. However, during the time period when the control culture is in log phase, the 0.2 M NaCl culture remains in lag phase, thereby showing the effect of growth retardation that it was desirable to explore.

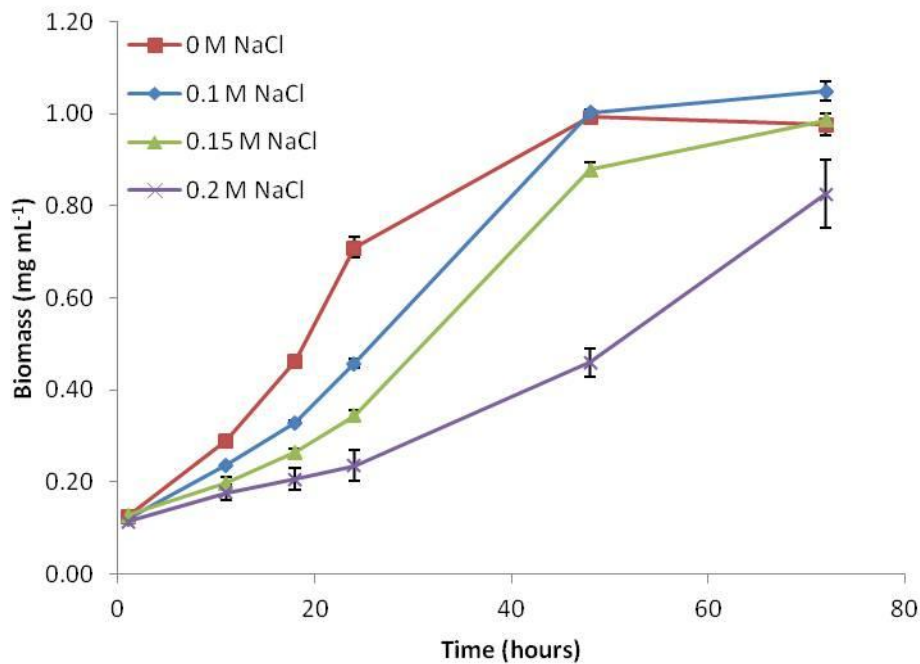


Figure 4.8 Biomass accumulation in *C. reinhardtii* grown in 0, 0.1, 0.15 and 0.2 M NaCl TAP media (n=3).

Figure 4.8 shows the biomass accumulation in the cultures under the different salt conditions. Biomass accumulation does not necessarily follow the same pattern as OD, with the cultures of 0.1 and 0.15 M NaCl showing comparable biomass accumulation to the control cultures towards the end of the time series, and even the 0.2 M NaCl cultures showing increasing biomass accumulation over the time course. The difference in OD and biomass may be due to differences in cell morphology, which are investigated via microscopy of the cells in the following section. It may also be due to differences in chlorophyll content, which is measured and discussed later in this chapter, as salt is known to have detrimental effects on chlorophyll in some algal species (McLachlan, 1961).

Lower final biomass concentrations are also found at stationary phase even in salt adapted strains that are exposed to high salinity (Takouridis et al., 2015). However the improvements in salt tolerance were found to result only in higher growth rates not in improved biomass accumulation.

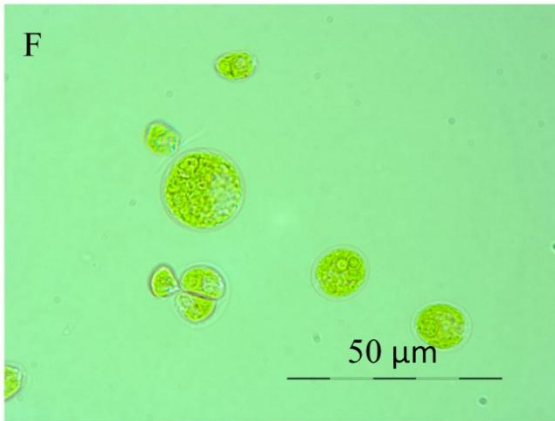
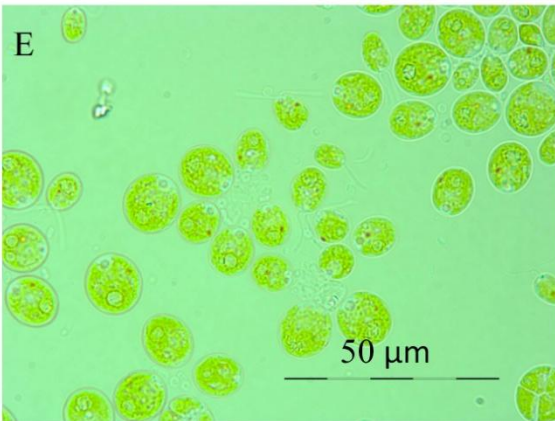
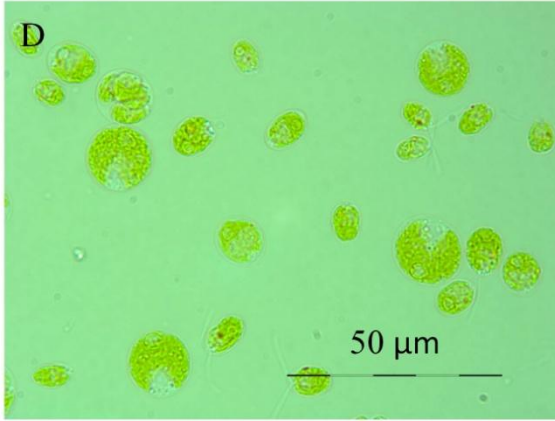
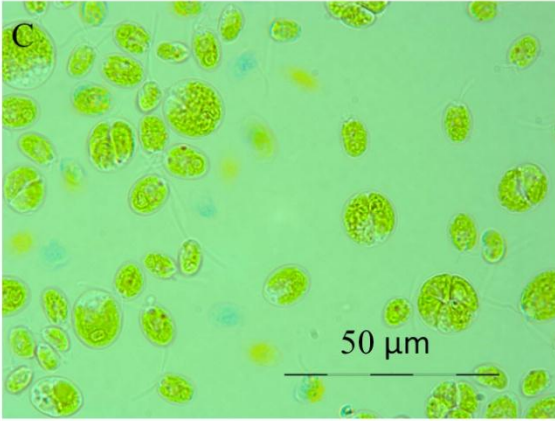
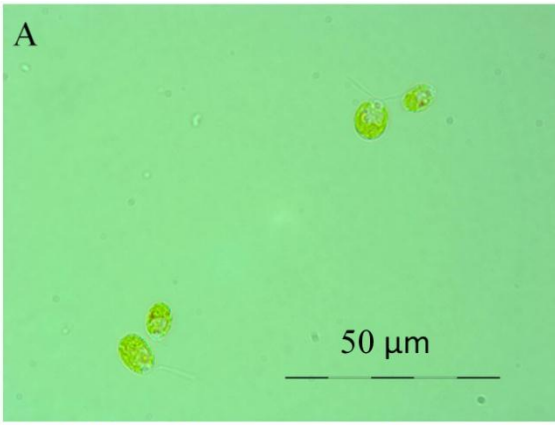
#### 4.3.6 Effect of 0.1, 0.15 and 0.2 M NaCl on Cell Morphology of *C. reinhardtii* CC-4325

Figures 4.9 and 4.10 show the cell morphology of each of the cultures at each time point. Control culture cells remained a similar size and shape throughout the duration of the experiment, with a low number of the observed cells in the process of division even in log phase (Figure 4.9 C and E), whereas those exposed to salt conditions undergo changes to their size and shape, and also appear to be in the dividing part of the growth cycle, and enveloped by a sac. These cells are larger and more irregularly shaped than those in the control cultures, which show the regular oval shape with flagella attached. Those in the salt conditions do not appear to have flagella. Flagella are important in sexual reproduction in *Chlamydomonas*, as they are needed for motility and cell recognition (Hessen et al., 1995), suggesting a reduction in sexual reproduction under the salt conditions. However, normally *Chlamydomonas* enters the sexual cycle under nitrogen stress, and it is thought that this could be an adaptation of allowing trait variation within a population for a higher chance of survival (Goho and Bell, 2000). The non-observing of flagella in this case then may just be due to the clustering of the cells in palmelloids. *C. reinhardtii* shows cell clustering or "multicellularity" under certain conditions (Harris et al., 2009; Ratcliff et al., 2013). For instance palmelloid colonies of four to sixteen cells occur under predation conditions or under calcium ion deficiency when the cells do not break out of their mother sac. The multicellularity is thought to be adaptive by maximising reproduction within the colony under detrimental conditions (Ratcliff et al., 2013). In Section 4.3.2, coenobia were observed as a physiological change under salt stress, and the same structures were found here, reinforcing the conclusion that multicellularity is a response to salt stress.

Takouridis et al. (2015) selectively bred *C. reinhardtii* wild type strain to be able to grow in salt conditions, and were able to reach high levels of 0.7 M NaCl. Their wild type progenitor could also grow at 0.3 M NaCl, a salinity which was found to be toxic to the CC-4325 strain grown here. One of the changes found in salt adapted strains was the formation of palmelloids, which are also observed in salt grown cultures in this experiment. These palmelloids were found to increase in size as salt concentrations increased (Takouridis et al., 2015). They were also dispersed in an overnight period

upon re-introduction to 0 M NaCl conditions. The formation of these groups then appears to be an adaptation to the stress conditions.

It has been shown that cell lines of *C. reinhardtii* undergoing sexual reproduction reach higher levels of salinity tolerance than those undergoing asexual reproduction, as sexual reproduction allows for greater evolutionary adaptation to the selection environment of high salinity stress (Lachapelle and Bell, 2012; Takouridis et al., 2015).



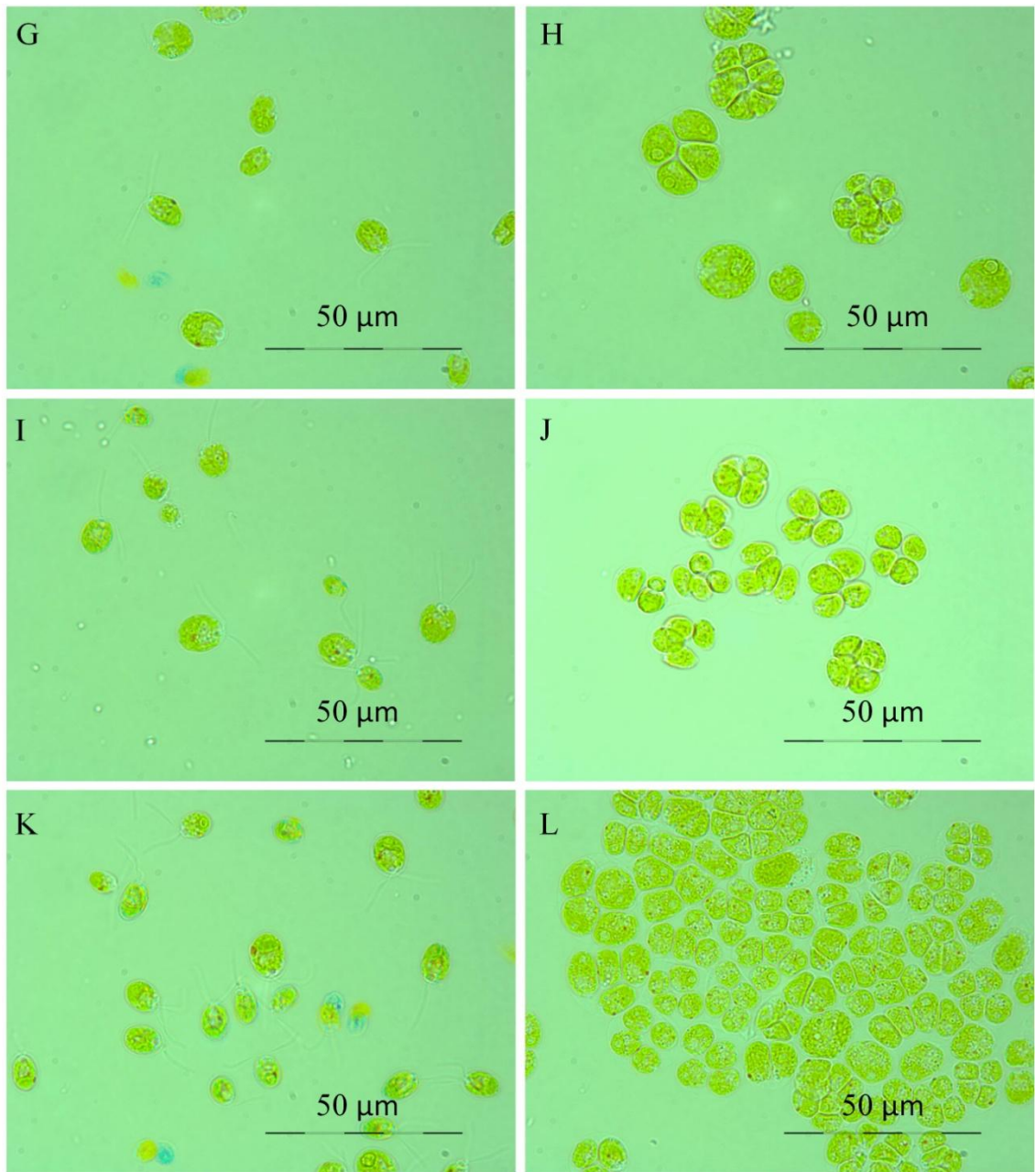
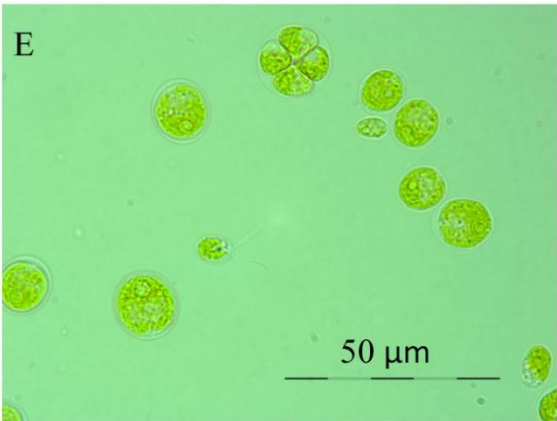
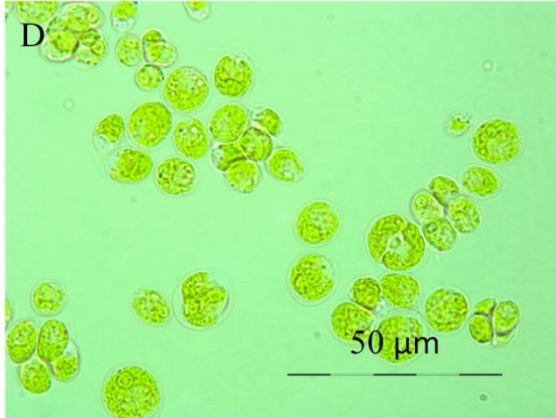
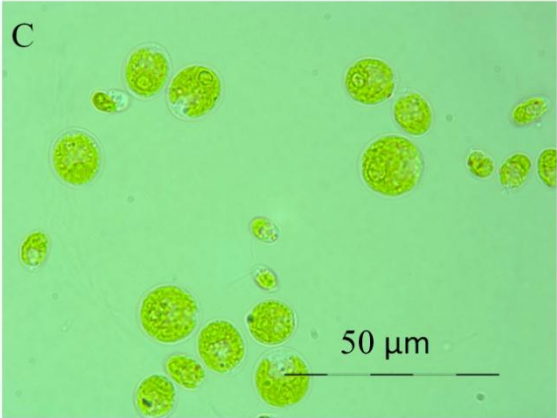
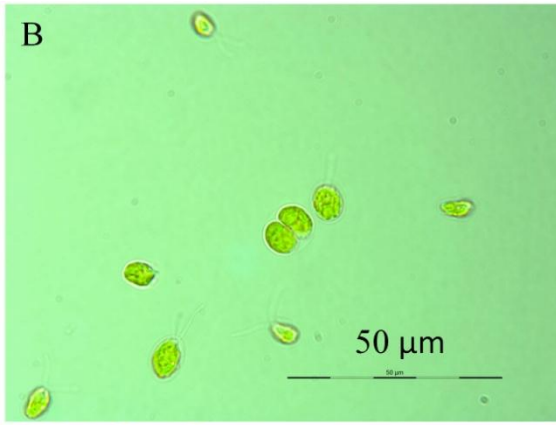
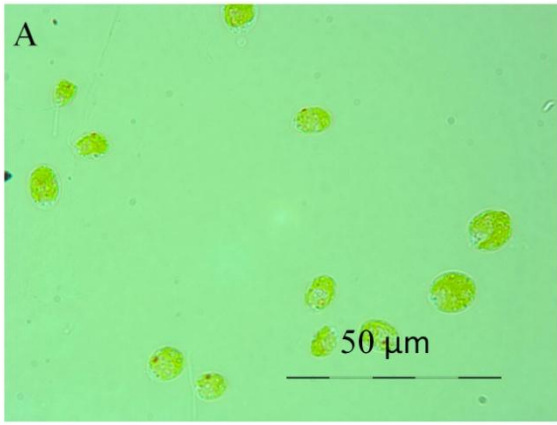


Figure 4.9 Microscopy of 0 M (A, C, E, G, I, K) and 0.1 M NaCl (B, D, F, H, J, L) cultures at 3 hours (A and B), 11 hours (C and D), 18 hours (E and F), 24 hours (G and H), 48 hours (I and J) and 72 hours (K and L). Magnification X1000.



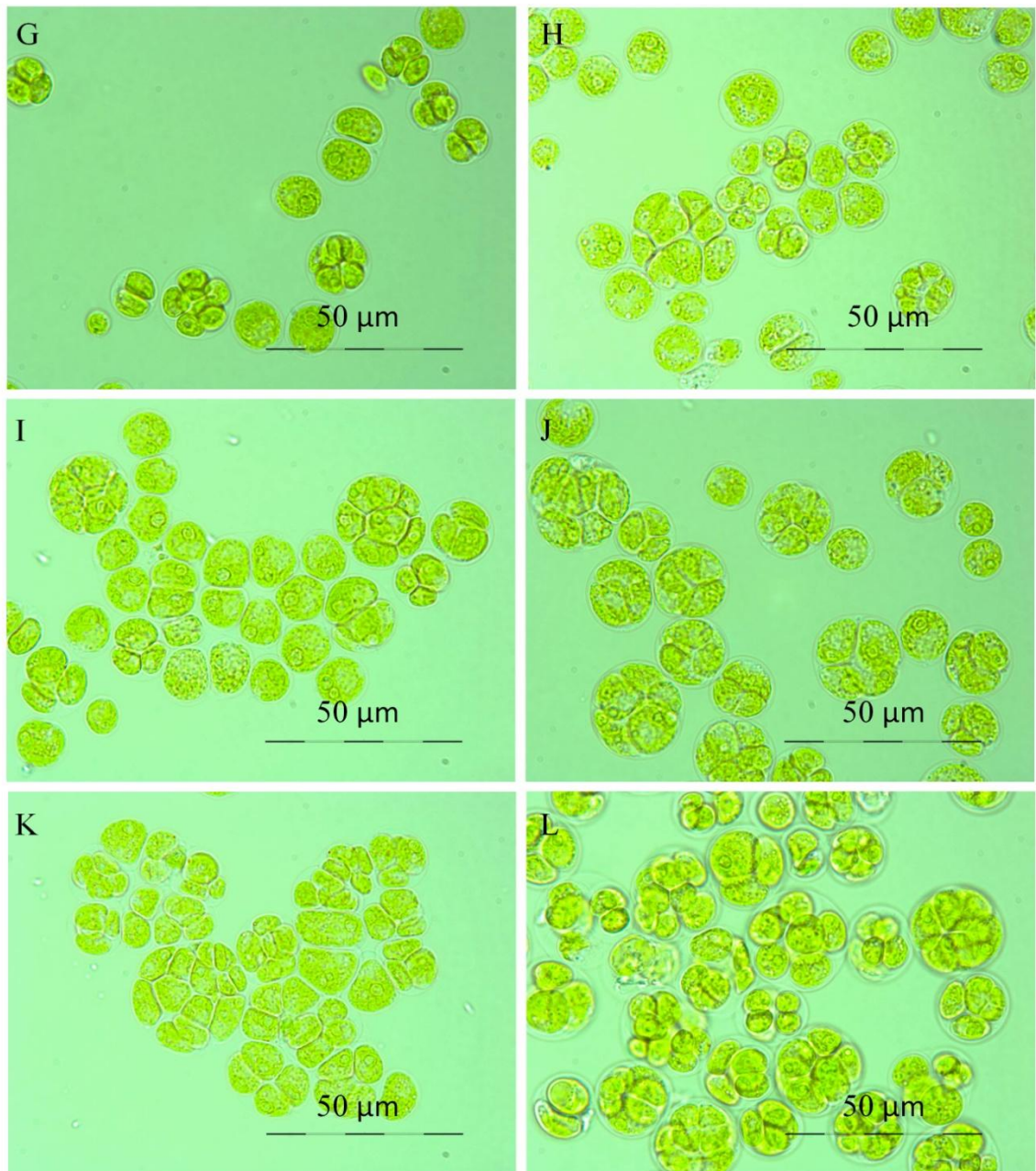


Figure 4.10 Microscopy of 0.15 M (A, C, E, G, I, K) and 0.2 M NaCl (B, D, F, H, J, L) cultures at 3 hours (A and B), 11 hours (C and D), 18 hours (E and F), 24 hours (G and H), 48 hours (I and J) and 72 hours (K and L). Magnification x1000.

#### 4.3.7 Effect of 0.1, 0.15 and 0.2 M NaCl on Neutral Lipid (FAME) Accumulation by *C. reinhardtii* CC-4325

Figure 4.11 shows the total FAME content of cultures grown in 0.1, 0.15 and 0.2 M NaCl TAP medium. Previous data (section 4.2.3) had shown that the salt-induced differences in lipid production were very slight, and the current data confirms this

finding. In this case there is some variation in all cultures FAME content, but the 0.2 M NaCl culture showed consistently lower FAME content than the control. The 0.1 M NaCl culture showed consistently lower FAME content than the control. The 0.1 M NaCl condition remains very stable, with no variation in overall FAME content throughout the time course. The FAME content of the 0.15 M NaCl condition peaks at 24 hours, which is later than the control condition and the 0.2 M NaCl, which both show a peak at 11 hours.

The overall FAME content shown here is higher than in the previous experiments (Figures 4.5 and 4.11), again demonstrating the natural variation that can occur between seeding cultures. Overall, there is no clear pattern in either reduction or increase in FAME content under these salt conditions, but it is possible that FAME profile may vary. The individual FAMES were then investigated to see changes if FAME profile is being used as part of a salt tolerance mechanism.

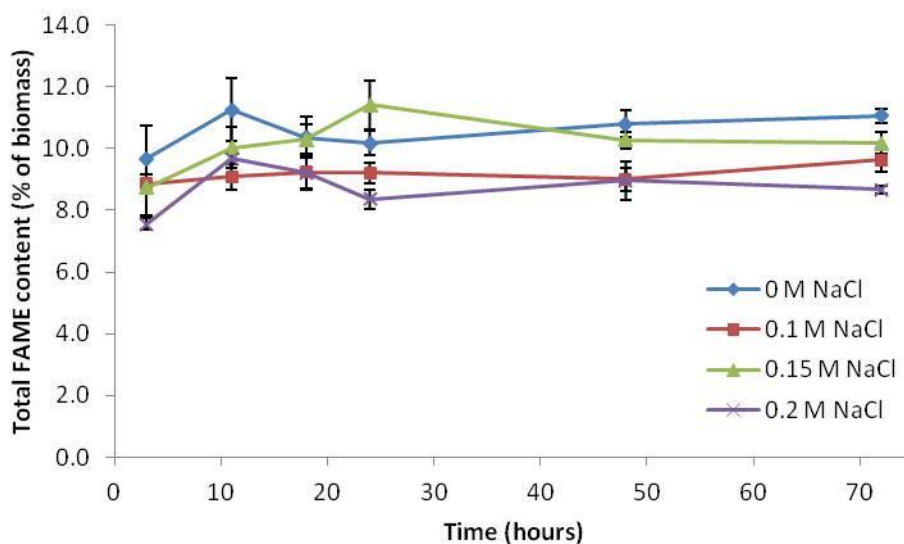


Figure 4.11 Total FAME quantities detected in algal biomass, expressed as a percentage of dry biomass, in 0, 0.1, 0.15 and 0.2 M NaCl (n=3).

The main FAMES of interest are the C16 and C18 fatty acid chains. The majority of algal FAMES comprise these and they are the most suitable for biodiesel production. If grouping the FAMES, they can broadly be divided into monounsaturated fatty acids (MUFAs), polyunsaturated fatty acids (PUFAs), and saturated fatty acids (SFAs). Since the degree of saturation of FAMES affects the quality of biodiesel (Knothe, 2005),

looking at the shift between these main groups is useful to see if salt shifts the composition in a way that impacts biofuel quality. The chain types detected have been grouped into these categories to compare and are displayed in Figure 4.12 as the percentage contribution of these chain types to algal biomass. As with the overall lipid data, there are no great changes in these lipid quantities.

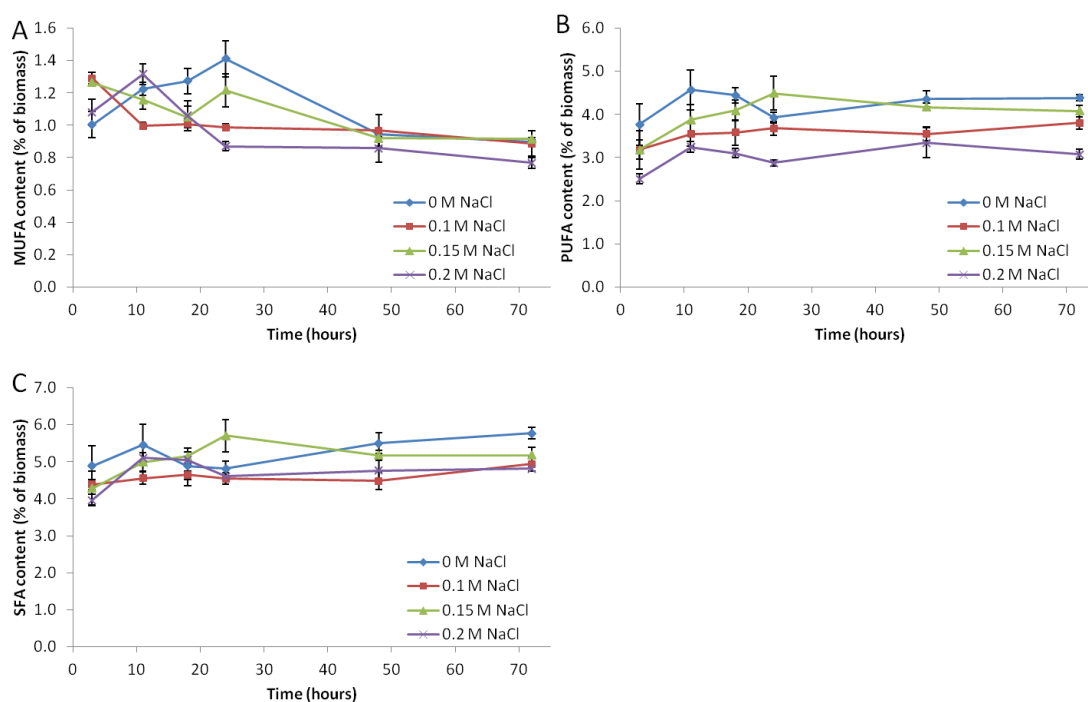


Figure 4.12 MUFA (A), PUFA (B) and SFA (C) content of algal biomass in each culture condition (n=3).

Another way of analysing the degree of unsaturation is to calculate the relative contributions of the chain types to the overall FAME profile (Figure 4.13). The profile of FAMES does not show a large amount of variation over time in terms of degree of unsaturation, in any of the culture conditions. In all the salt conditions, the MUFA content appears to slightly decline over time, but in the control conditions there is a slight peak in MUFA at the 24 point. In all conditions, the SFAs and PUFAs are the biggest contributors to the FAME profile, comprising approximately 40% each of the FAMES present, whilst the MUFAs are less than 20%.

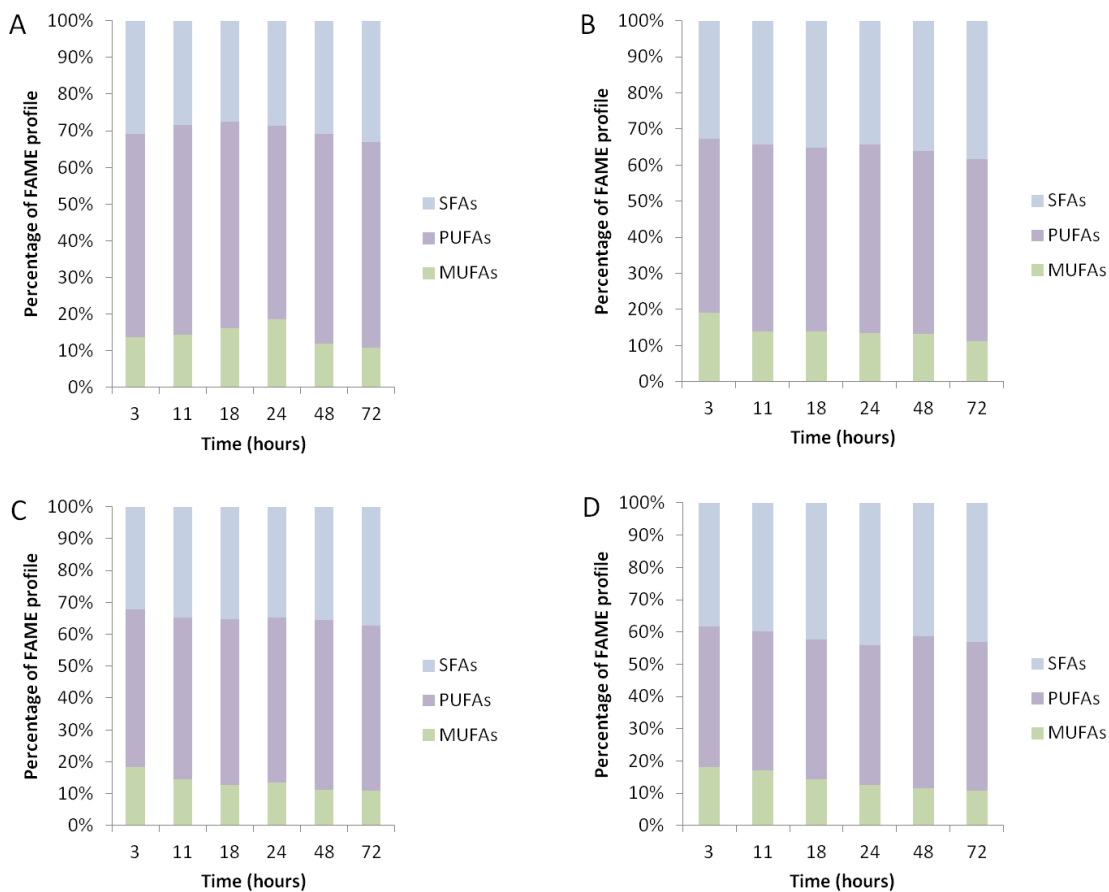


Figure 4.13 Relative percentages of FAME chain types (in terms of degree of unsaturation) in each time course experiment for 0 M NaCl (A), 0.1 M NaCl (B), 0.15 M NaCl (C), 0.2 M NaCl (D) (n=3).

As well as degree of unsaturation, chain length is an important factor when considering algal lipids for biofuel. In Figure 4.14, the FAMEs detected have been grouped into chain length. As C16s, C17s and C18s are those most suitable for biodiesel, these have been displayed as their own groups. Those less than 16 carbon chains long or more than 18 carbons long have been grouped together for simplicity of analysis. There are no discernible shifts in chain lengths, showing that this remains stable in the lipid profile.

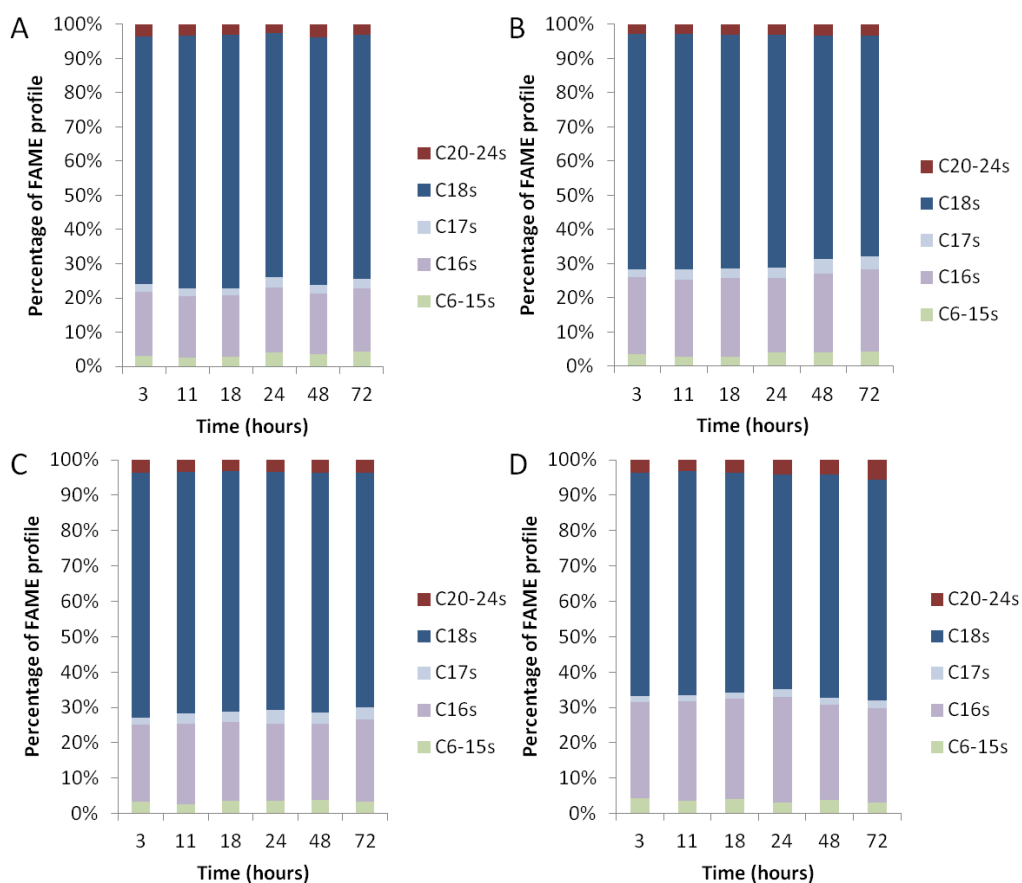


Figure 4.14 Relative contributions of different chain lengths to the total FAME profile of cultures grown under control 0 M NaCl conditions (A), 0.1 M NaCl conditions (B), 0.15 M NaCl conditions (C) and 0.2 M NaCl conditions (D) (n=3).

The largest contributors to the FAME profile were individually analysed and compared between salt conditions. These are represented as percentage content of the algal biomass in Figure 4.15.

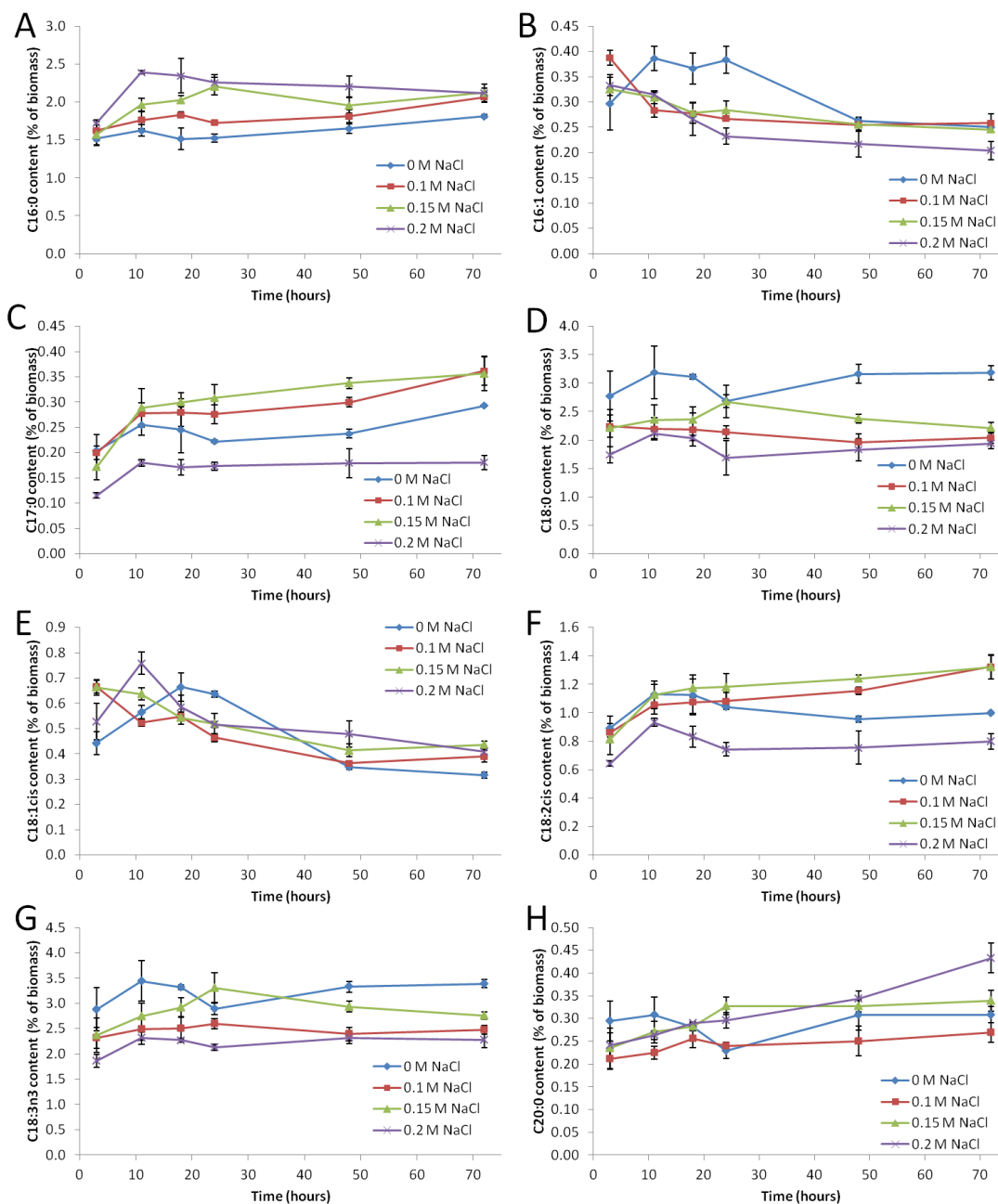


Figure 4.15 Percentage content of main individual FAME types in algal biomass under 0 M (control), 0.1 M, 0.15 M and 0.2 M NaCl. FAMES shown are C16:0 (A), C16:1 (B), C17:0 (C), C18:0 (D), C18:1cis (E), C18:2cis (F), C18:3n3 (G) and C20:0 (H) (n=3).

C16:0 is of great interest as it is one of the biggest contributors to the total FAME profile and a main component in biodiesel (Knothe, 2009). Interestingly, although FAME content overall was not increased in salt conditions in this experiment, C16:0 does appear to slightly increase under salt conditions, further increasing in higher

salinities. This increase is particularly seen between 3 hours and 11 hours in the 0.2 M NaCl grown cells. The fact that this increase is observed and that the C16:0 content under salt conditions remains consistently high indicates that C16:0 is an important FAME in *C. reinhardtii* tolerating high salt conditions. In all other FAMES shown here, 0.2 M NaCl has either a neutral or a detrimental effect on the FAME content, with the exception of C20:0 that shows small increases at 72 hours. The rise in C16:0 in higher salinity does not result in an overall rise in SFA or total FAME because other compounds C18:0, C18:3n3, C18:2cis and C17:0 all show concurrent reductions.

Cells grown in 0.1 and 0.15 M NaCl TAP medium have similar FAME patterns. Small increases in C16:0, C17:0 and C18:2cis are seen compared to the control, but otherwise have either neutral or slightly detrimental effects on the FAME levels.

The main pattern seen here is that none of these FAMES deviates very much from the level found in the controls. Unlike the initial experiments (section 4.2.3), where 0.2 M NaCl caused degradation of some FAMES due to unhealthy cultures, the levels stay relatively stable in these cultures. This shows, along with the growth data discussed earlier, that there is natural variation between seeding cultures.

#### **4.3.8 Effect of 0.1, 0.15 and 0.2 M NaCl on Carbohydrate Content of *C. reinhardtii* CC-4325**

Figure 4.16 shows the carbohydrate content of the biomass under the different salt conditions. In all cases, salt increases the overall percentage of carbohydrate in the biomass. The highest levels were observed in 0.15 and 0.2 M NaCl cultures, indicating a salinity induced increase in carbohydrate for *C. reinhardtii* CC-4325. Possible reasons for the increase are: an increase in starch storage molecules in the cell due to changes in starch metabolism and regulation (possibly unlikely in a starchless mutant, although Ball et al. (1990) stipulate that under certain conditions, even mutants with impaired ADP-glucose pyrophosphorylase activity and starch synthesis can produce low "residual" levels of polysaccharide); changes in polysaccharide content in the cell walls, perhaps thickening to defend against osmotic pressure; or changes to extracellular polysaccharides of the coenobium. It may be changes to the cell wall chemistry that

happens during the onset of sexual reproduction; nitrogen deprivation causes this, and salt may have a similar effect.

A likely reason for the salt induced increase in carbohydrate in *C. reinhardtii* CC-4325 is the formation of palmelloids which are contained within mucilaginous polysaccharide capsules, as described in the Desmid species *Spondylosium panduriforme* (Paulsen and Vieira, 1994).

The comparisons drawn with the literature here are with other species, and formation of extracellular polysaccharide in the form of capsules is species specific (Myklestad, 1995). Phosphate limitation appears to increase the extracellular polysaccharide production, and it also appears to increase in the stationary phase of a culture where N and P are used up, and immediately after nitrate is limited in *Chaetoceros affinis* (Myklestad, 1995). Lombardi et al. (2002) found that mucilaginous capsules had a function of allowing a freshwater alga to cope with toxic environments, in this case excess copper ions, by providing ion retention and metal buffering properties.

The metabolism of carbon in the formation of extracellular polysaccharides in *S. panduriforme* has been studied and it is shown that externally added carbon is incorporated into these extracellular structures very rapidly, just half an hour after addition of  $^{14}\text{C}$  (Vieira et al., 1994). The cultures of *C. reinhardtii* in the current experiment were grown in TAP, which includes acetate as a carbon source, and therefore there is an ample source of carbon to allow the formation of these polysaccharide capsules.

In *Chlamydomonas parvula*, polysaccharides are produced during cell multiplication, but other species such as *Navicula pelliculosa* produce polysaccharides as part of extracellular capsules under conditions where cell division is inhibited by nutrient deficiency, but photosynthesis continues (Lewin, 1956). A similar result of polysaccharides being produced during cell division was found in another *Chlamydomonas* species (species name not specified (Allen, 1956).

Extracellular polysaccharides may also play a chelating role in binding free metal ions in the growth environment as a defence against toxic conditions (Kaplan et al., 1987).

Not all polysaccharide capsules have this ability, however, and more information can be gleaned from studying the chemical structure of the capsules. However, since NaCl dissociates into free metal ions in solution, the presence of Na<sup>+</sup> ions may be triggering the formation of these capsules in *C. reinhardtii*.

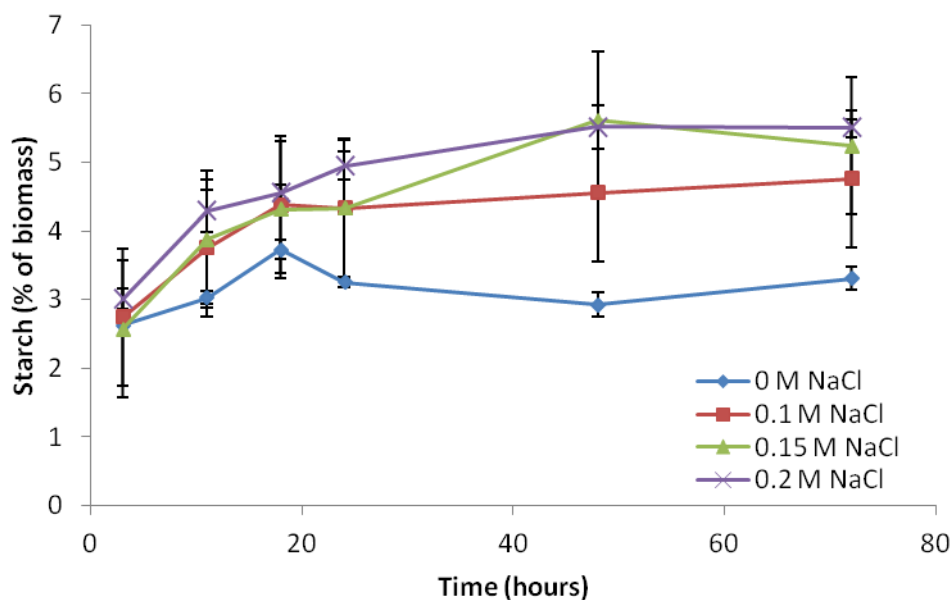


Figure 4.16 Starch content of *C. reinhardtii* cultures grown in 0, 0.1, 0.15 and 0.2 M NaCl, expressed as a percentage of dry biomass (n=3).

#### 4.3.9 Effect of 0.1, 0.15 and 0.2 M NaCl on Chlorophyll and Carotenoid Content of *C. reinhardtii* CC-4325

Figure 4.17 shows the chlorophyll *a*, chlorophyll *b* and carotenoid content of the cultures grown under the different salt conditions. In all cases, the pigments are negatively affected by the presence of salt, showing decreases in overall pigment. The decrease is most markedly seen in the 0.2 M NaCl conditions, with pigments being at lower relative levels. This demonstrates that photosynthetic pigments are detrimentally affected by the presence of salt, even at the relatively low level of 0.1 M NaCl, which in turn will affect the light harvesting complexes in those cultures (Perrine et al., 2012). This decrease in pigment levels may be a possible explanation as to why growth rate slows down with increasing salt concentrations. The effect of salt on photosynthetic capacity has been documented and discussed in the literature

(Allakhverdiev et al., 2000; Neelam and Subramanyam, 2013). To investigate how well the photosynthetic capacity of the strain functions under stress, the photosynthesis and respiration rates of the cultures were measured via an oxygen electrode. Data is presented in the section below.

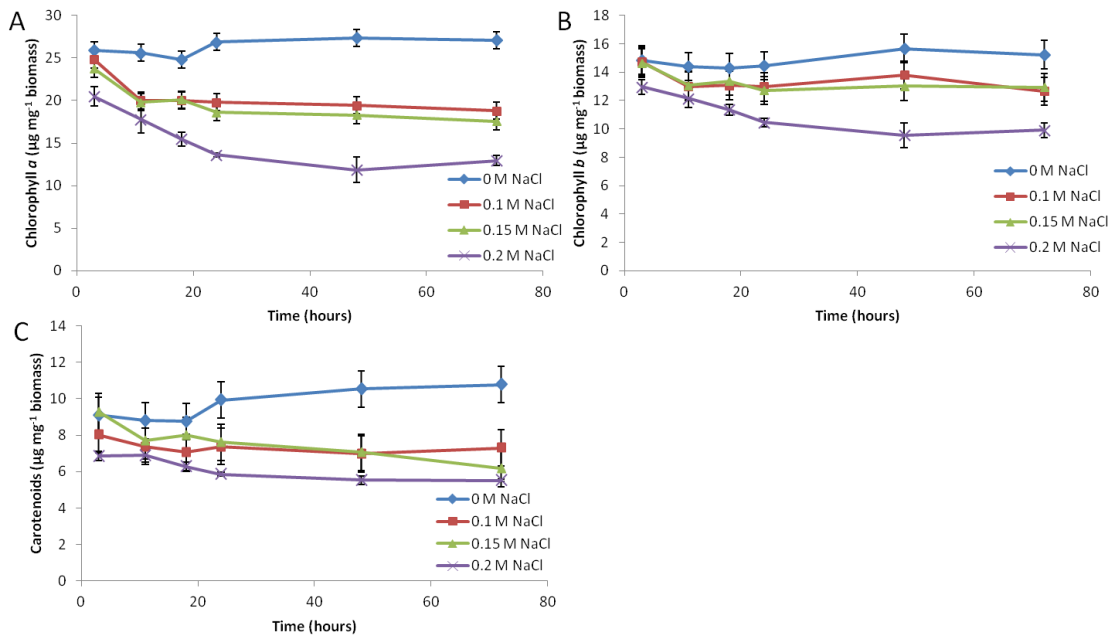


Figure 4.17 Chlorophyll a (A), chlorophyll b (B) and carotenoid (C) content of *C. reinhardtii* cultures grown under 0, 0.1, 0.15 and 0.2 M NaCl (n=3).

In *C. reinhardtii* salt stress causes protein degradation in photosystem II and pigment reduction (Neelam and Subramanyam, 2013). Both photosynthetic activity and chlorophyll contents of cultures are found to decrease in salt stressed cultures of *C. reinhardtii* (Yoshida et al., 2004). Zuo et al. (2014) subjected *C. reinhardtii* to 0.3 M NaCl and found degradation of the photosynthetic pigments within 12 hours of being subjected to salt stress. They did not find a significant decrease in pigments when subjecting them to 0.1 M NaCl, however. Many aspects of photosynthesis activity had been reduced under these conditions, due to an increase in non photochemical dissipation and a corresponding decrease in photochemical quenching, electron transport rate and maximum quantum yield (Zuo et al., 2014).

#### 4.3.10 Effect of 0.1, 0.15 and 0.2 M NaCl on Photosynthesis and Respiration Rates of *C. reinhardtii* CC-4325

Figure 4.18 shows the rates of oxygen evolution and oxygen uptake, as a measure of the photosynthesis and respiration rates (per cell) of the cultures grown under different salt concentrations. The control conditions show the highest rates of photosynthesis during the first 24 hours of growth. At 48 and 72 hours, the photosynthesis rate declines. This may be due to the culture being denser and therefore beginning to self shade (Sutherland et al., 2015). Photosynthesis rates typically decrease in stationary phase (López-Sandoval et al., 2014), this is thought to occur because of nutrient limitation. Similarly, the respiration rates increase in the control culture steadily until 24 hours, and then decrease again.

By contrast, salt has a detrimental effect on the ability of the culture to photosynthesise and respire. The reduction in photosynthesis is more pronounced in cultures with the higher salt concentrations, with this being most aptly demonstrated in the 3 hour and 11 hour time points, where each subsequent increase in salt concentration results in a further reduction in oxygen evolution or uptake. This is consistent with research finding that salt stress can inhibit the activity of photosystems in microalgae (Allakhverdiev et al., 2002; Gilmour et al., 1985; Sudhir and Murthy, 2004). All three cultures exposed to salt conditions are able to photosynthesise to a degree, however, showing that these cultures are tolerant of the 0.1, 0.15 and 0.2 M NaCl conditions even if some functions are impaired (shown by the reduction in photosynthetic pigments, photosynthetic activity, and growth rates).

The presence of NaCl can affect the photosynthesis apparatus. In *Scenedesmus obliquus* salt stress caused significant reduction in the density of photosystem II reaction centres and changes to the size of the antenna (Demetriou et al., 2007). NaCl can have both ionic and osmotic effects on photosynthetic machinery that result in irreversible loss of oxygen evolving activity in photosystem II, and affected electron transport activity in photosystem I (Allakhverdiev et al., 2000). The fact that the inactivation of PSII and PSI is irreversible in some species is a large factor in determining salt tolerance (Yokthongwattana et al., 2001).

Unsaturated fatty acids play a key role in protecting photosynthetic machinery from damage induced by high salinity (Allakhverdiev et al., 2001), and a genetically engineered increase in the unsaturation of fatty acids found in membrane lipids can improve the salinity tolerance of photosystems.

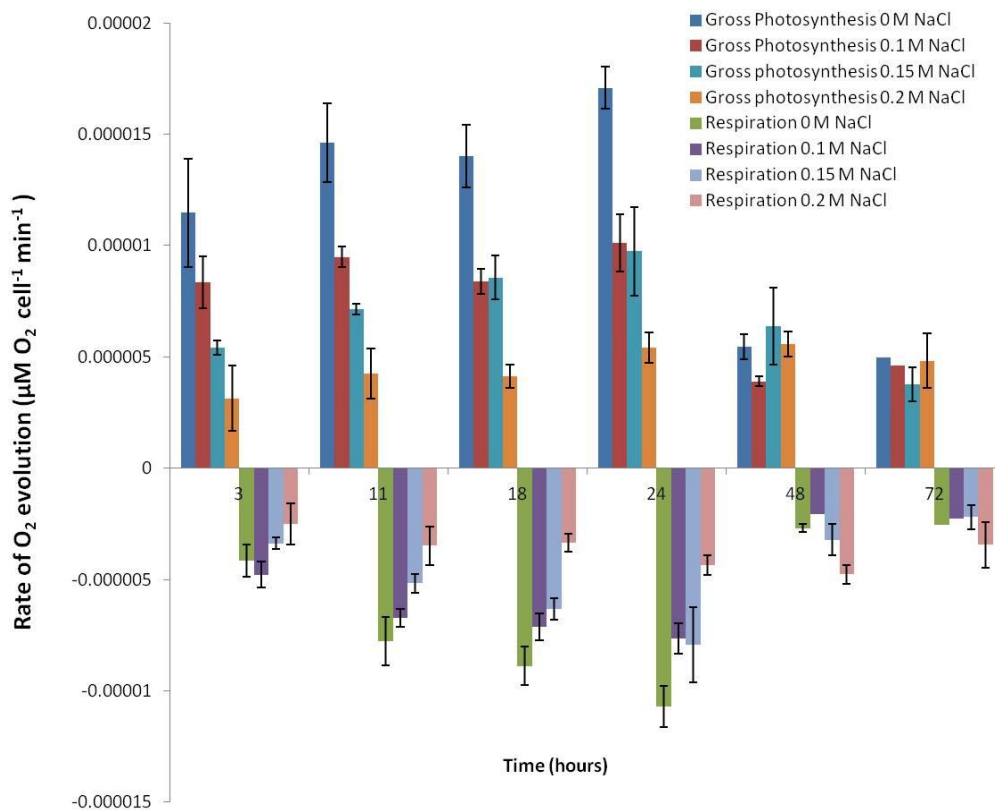


Figure 4.18 Photosynthesis and respiration rates (per cell) of *C. reinhardtii* cultures grown in 0, 0.1, 0.15 and 0.2 M NaCl, measured via oxygen evolution (n=3).

#### 4.3.11 Discussion of metabolomic data

The work described in this chapter shows that the starchless mutant strain (CC-4325) of *C. reinhardtii* has some tolerance to salt stress, and the detrimental effects of salt stress on cellular functions increases as the salt concentration increases. Exposure to higher salinities cause growth reduction, the formation of multi-cell structures, pigment reduction, photosynthesis and respiration reduction, increases in C16:0 and carbohydrate, although there are no large changes in lipid yield.

To gain more insight into how *C. reinhardtii* tolerates salt stress, a proteomic investigation was carried out comparing the 0.2 M NaCl condition at time points 3, 11

and 18 hours, and comparing to time point 18 hours in the control condition. These time points were chosen because there is chance to compare a control condition that is growing in mid log phase with a salt condition where growth has been severely reduced. In the salt condition these time points provide a few interesting changes that the 0.2 M NaCl culture undergoes. Between 3 and 11 hours there are increases in both the starch content of the cultures, and in the C16:0 content of the cultures.

#### 4.4 iTRAQ investigation of the effect of 0.2 M NaCl on the proteome of *C. reinhardtii*

An iTRAQ experiment was carried out on *C. reinhardtii* samples under 0.2 M NaCl conditions, and control conditions of normal TAP medium with no additional NaCl salt, using the second experiment (detailed above in Section 4.3.5) for sampling. iTRAQ allows the comparison of 8 samples in the 8 different channels. In this case, 4 phenotypes were compared in duplicate, using a time course along the salt stressed culture, and a single control time point. The sample conditions and the iTRAQ labelling of samples are described in Table 4.1, with two biological replicates for each sampling point. The time points are chosen according to the equivalent growth phases shown in control conditions i.e. immediately after inoculation (3 hours), an early log phase (11 hours) and a mid to late log phase (18 hours). The aim of this is to show how salt affects the culture during a time course that would normally undergo log phase growth.

**Table 4.1** Samples used for iTRAQ experiment for *C. reinhardtii*.

Sample name	Condition number	Biological replicate	Phenotype conditions	iTRAQ labels
CQD	1	1	3 hour 0.2 M NaCl	113
CQE		2		114
CQK	2	1	11 hour 0.2 M NaCl	115
CGL		2		116
CNL2	3	1	18 hour control (TAP with no additional salt)	117
CNM2		2		118
CQR	4	1	18 hour 0.2 M NaCl	119
CQQ		2		121

Protein samples were obtained as described in the materials and methods chapter (Section 2.6.2). After extraction, acetone precipitation and reconstitution in buffer, the protein samples were quantified using a Bradford Assay and a 15  $\mu\text{L}$  sample was run on an SDS-PAGE gel to check sample quality.

#### 4.4.1 Protein quantification and gel visualisation

The protein concentrations for each condition and biological replicate are shown in Table 4.2.

**Table 4.2 Concentrations of protein from sample extractions.**

Sample name	Condition	Biological replicate	Protein concentration (mg mL <sup>-1</sup> )
CQD	1	1	3.4 $\pm$ 0.043
CQE		2	2.7 $\pm$ 0.050
CQK	2	1	2.7 $\pm$ 0.057
CQL		2	2.8 $\pm$ 0.050
CNL2	3	1	3.7 $\pm$ 0.043
CNM2		2	3.5 $\pm$ 0.079
CQR	4	1	2.0 $\pm$ 0.129
CQQ		2	2.2 $\pm$ 0.043

Figure 4.19 shows the SDS-PAGE of the protein samples (15  $\mu\text{g}$  per lane) and indicate good sample quality, as the distinct and intensely stained separated bands indicate the presence of intact separated proteins in sufficient quantities, with visual consistency between biological replicates, and with well separated marker bands. Since control sample 1 appeared visually different to the other samples, a second gel was run to compare the three available control samples and ensure that the chosen control samples matched each other well (Figure 4.20). Extraction 2 refers to a new aliquot of biomass of the same samples being used. Controls 2 and 3 (extraction 2) were then chosen as the control samples.

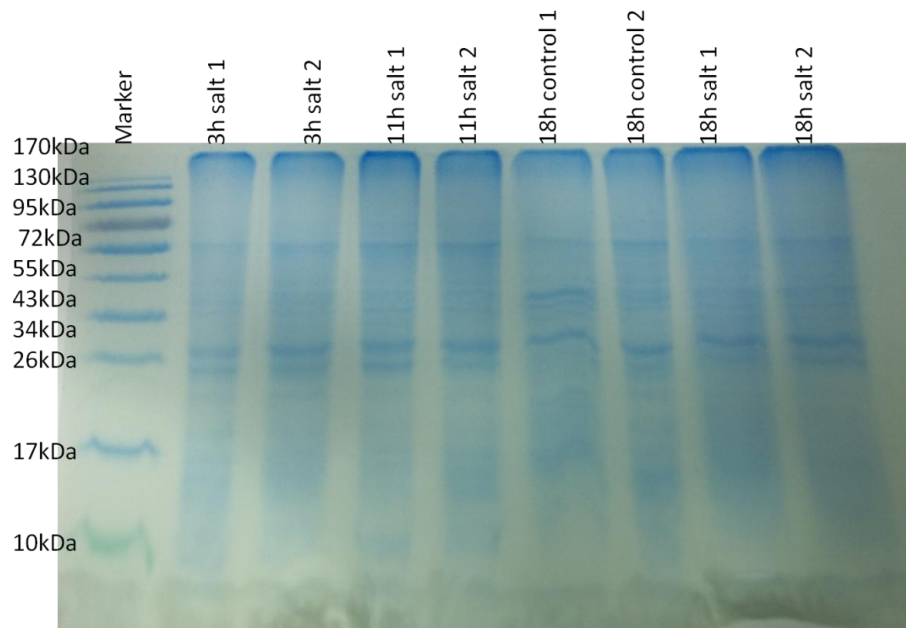


Figure 4.19 SDS PAGE separation of 8 samples for iTRAQ analysis.

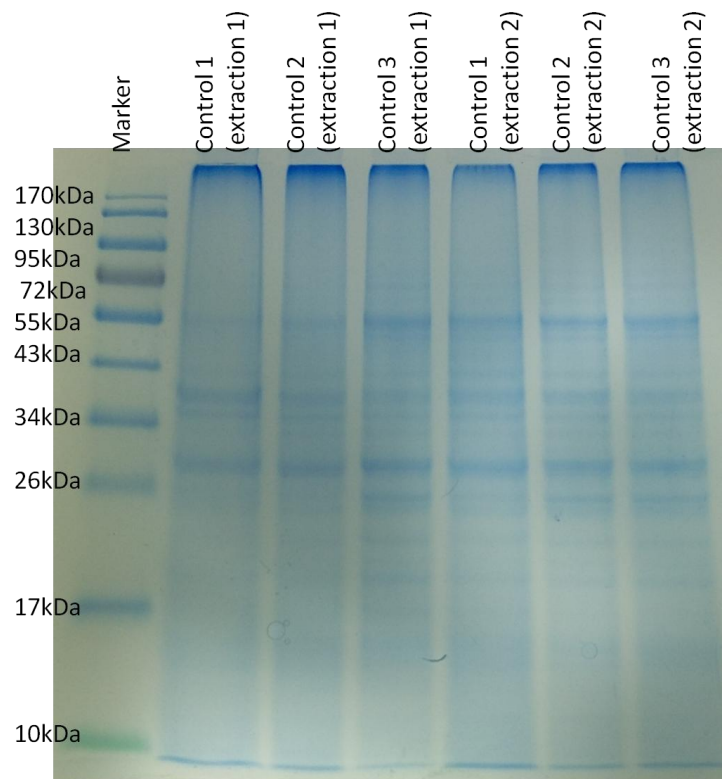


Figure 4.20 SDS PAGE separation of control samples for optimal sample selection.

100 µg of each sample was taken for tryptic digestion, as described in the materials and methods chapter (Section 2.6.7.1). Prior to incubation but after trypsin had been added, 10 µg was removed from each sample and stored at -20 °C. After incubation, another 10 µg was removed from each sample. The 2 aliquots from each sample were run on an SDS-PAGE gel to check if digestion had taken place. The gels should show a clear difference between the pre and post incubation samples, with the former showing banding and the latter having no bands. The gels obtained did not give conclusive results (data not shown), and therefore a small aliquot of one sample was taken to run on AmaZon mass spectrometer, as detailed in the methods chapter. 155 proteins were identified, and 766 of 1020 peptide matches showed zero mis-cleavages. This sample showed the presence of tryptic peptides, indicating complete digestion, and digestion was assumed to be equivalent for all samples.

Samples were labelled with iTRAQ labels and fractionated using Hypercarb™ column (porous graphitic carbon stationary phase) on HPLC (using methods described in Section 2.6.9), causing the peptides to be eluted and separated out over a gradient, based on their polarity. The UV Vis chromatogram (wavelength 214 nm) of the eluted sample is shown in Figure 4.21.

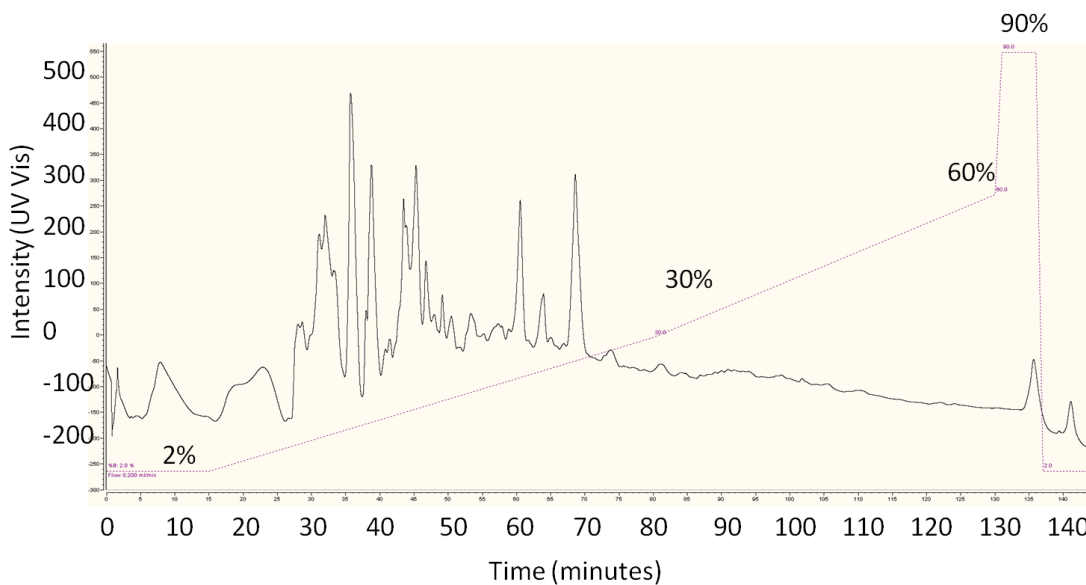


Figure 4.21 UV vis (wavelength 214 nm) chromatogram of digested and labelled peptides in *C. reinhardtii* iTRAQ sample.

#### 4.4.2 Summary of detected peptides and proteins from MS analysis

The six fraction files were processed in data analysis software MaxQuant 1.5.3.8 and PEAKS<sup>®</sup>. MaxQuant is standard software for processing Q Exactive HF MS data (Michalski et al., 2011). PEAKS was also investigated, since in the following chapter, later investigations of *C. nivalis* data rely on the *de novo* sequencing and homology searching capabilities of PEAKS. The data were searched against the *Chlamydomonas reinhardtii* Uniprot proteome database (taxa id: 3055, downloaded 6 May 2016, 15,172 entries). Using the 139,093 MS scans, and 168,249 MS/MS scans, searches were carried out in using both programs with the following settings:

Digestion type: trypsin; Variable modifications: Oxidation (M); fixed modifications: MMTS; MS scan type: MS<sup>2</sup>; PSM FDR 0.01; Protein FDR 0.01; Site FDR 0.01; labelling: iTRAQ 8-plex; MS tolerance 0.2 Da; MS/MS tolerance 0.2 Da; label mass tolerance 0.01 Da; database: Uniprot proteome database for *Chlamydomonas reinhardtii* (taxa id: 3055, downloaded 6 May 2016, 15,172 entries); min peptide length 6; max peptide length 4600; max mis-cleavages 2; maximum charge state 7; min number of unique peptides 1.

Furthermore, FDR 1% was applied to all PSMs and lists of peptides were used to generate relative quantifications of proteins using in-house software uTRAQ. The quantified proteins list was generated using 2 or more unique peptides.

A summary of the results obtained are shown in Table 4.3. This also explores the difference that DB matching only and Spider homology search has on the results.

Table 4.3 Summary of PSMs and proteins identified and quantified from PEAKS and MaxQuant.

Software	Type of search	of PSMs	Proteins
MaxQuant	Database	11595	1926
PEAKS	Database	27275	3276
PEAKS	Homology	27471	2979

PEAKS has the ability to detect peptide mutations, allowing proteins with variations in their peptide sequences to be matched to a database. This is known as spider homology searching, a function in PEAKS that searches for possible variations in the amino acid sequence from a known peptide. Unfortunately, spider homology searching in PEAKS did not improve the dataset compared to just searching the available DB. This is to be expected since *C. reinhardtii* is being matched to its own database. Homology searches were therefore not used in the remainder of this analysis. PEAKS results yield more data than the MaxQuant software. This shows the advantages of using *de novo* sequencing, even on a well sequenced organism. The greater number of PSMs results in higher protein matches of 2 or more unique peptides. The quantified proteins were put through GeneVenn (Figure 4.22) to show how much overlap there was in identifications (<http://genevenn.sourceforge.net/index.htm>).

The manner of reporting proteins is different between PEAKS and MaxQuant, since PEAKS reports quantifications assigned to more than one accession number as separate quantifications, whereas MaxQuant reports proteins grouped together that are essentially the same protein with different accession numbers in one quantification.

Each software also has its own way of matching spectra to peptide identifications, and therefore care must be taken in combining results so that spectra results are not over-reported (Searle et al., 2008). *De novo* sequencing uses MS/MS spectra to derive a peptide's amino acid sequence without using a sequence database, through mass difference of fragment ions in order to determine the mass of each amino acid. The peptides can then be matched to sequenced databases later, or searched for likely amino acid variations and modifications via homology searching. By contrast, MaxQuant uses MS/MS spectra and matches them directly to peptides from a protein database, using the database to find the closest peptide match to a spectrum (Zhang et al., 2012). *De novo* can identify novel peptides as well as known peptides from databases.

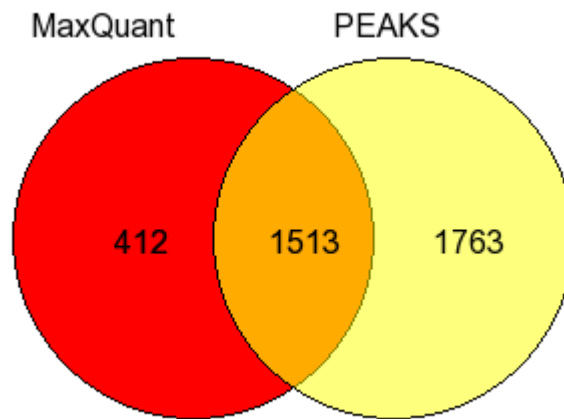


Figure 4.22 Identified and quantified proteins matched by accession number from MaxQuant and PEAKS searches (figure obtained from GeneVenn).

Whilst there is a large number of shared proteins, using both datasets could improve data analysis of changes between phenotypes even further. 3688 protein identifications and quantifications have been identified through combining these lists. However, due to the nature of the software's calculations for quantifications and normalisation, merging of data is not advisable at this stage. Since the use of data from both datasets could result in multiple reporting of spectra, only one dataset was used for analysis of changes between phenotypes. PEAKS reveals a greater number of PSMs and is needed in later study of the genetically un-sequenced organism *C. nivalis* (with a very limited protein database), so it was selected for data acquisition.

Perseus 1.5.2.6 software (data analysis partner software to MaxQuant) was used for data visualisation. Figure 4.23 shows the PCA clustering of data obtained from the protein groups. The points have clustered with biological replicates similar to each other: 3 hour salt conditions (red), 11 hour salt conditions (orange), 18 hour salt conditions (blue) and 18 hour control conditions (green). A dendrogram of the hierarchical clustering is also shown (Figure 4.24). Again it shows good grouping in the biological replicates, showing that the biological replicates are similar enough to gain insights from phenotypic comparisons between groups. It shows that the 3 hour salt and 18 hour control are more proteomically similar than the later 11 and 18 hour salt conditions, which are very similar to each other.

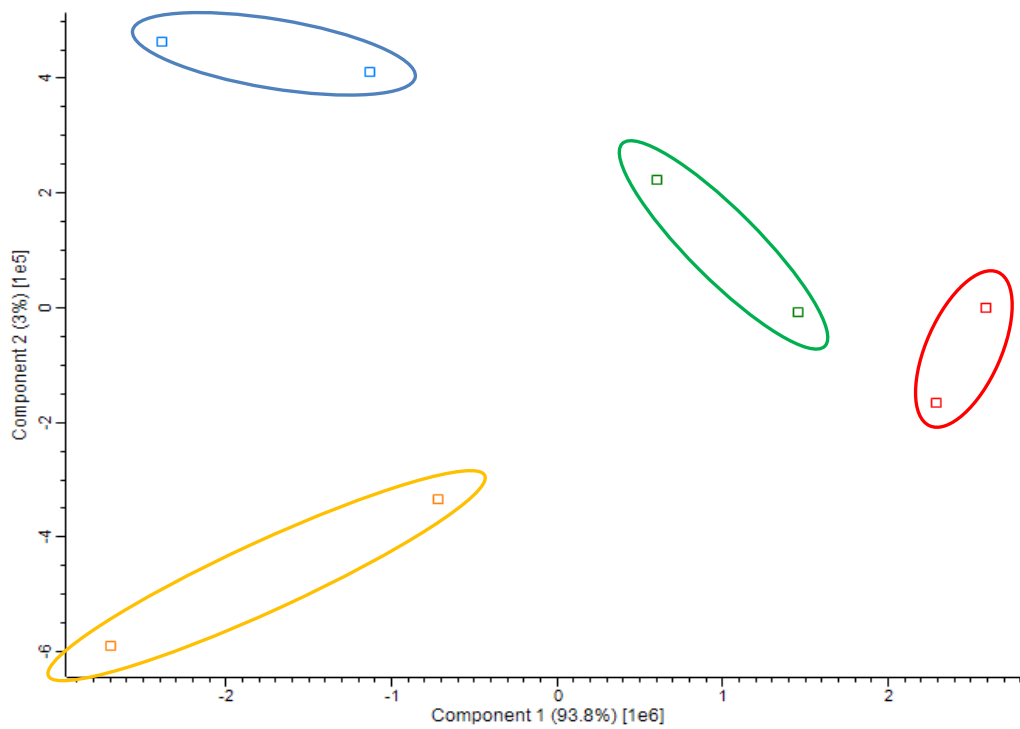


Figure 4.23 PCA plot of the 8 samples, clustered by biological replicates. Clusters show 3 hour salt conditions (red), 11 hour salt conditions (orange), 18 hour salt conditions (blue) and 18 hour control conditions (green).

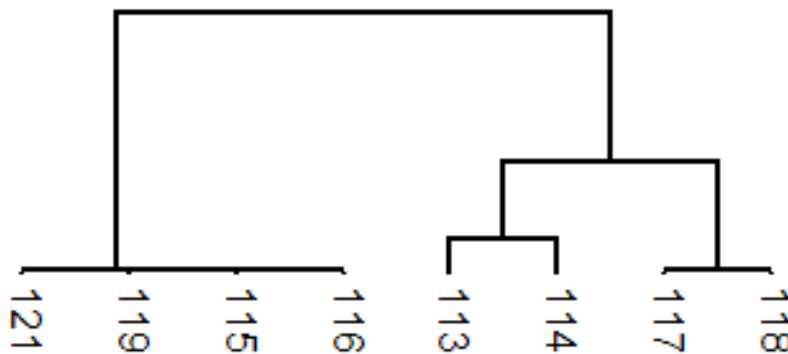


Figure 4.24 Hierarchical clustering of the 8 samples (indicated by iTRAQ label number), showing grouping of replicates.

Table 4.4 Key for dendrogram grouping of labels and phenotypes.

Biological replicate	Phenotype conditions	iTRAQ labels
1	3 hour 0.2 M NaCl	113
2	3 hour 0.2 M NaCl	114
1	11 hour 0.2 M NaCl	115
2	11 hour 0.2 M NaCl	116
1	18 hour control	117
2	18 hour control	118
1	18 hour 0.2 M NaCl	119
2	18 hour 0.2 M NaCl	121

SignifiQuant software was used to calculate significant differences between phenotype groups, using significance threshold 0.05. Peptide lists were converted to uTRAQ format and run through SignifiQuant to obtain differences between phenotype groups. uTRAQ software normalises all data so that each sample has the same amount of peptide reported in it, and then outputs all peptide samples as relative intensities to each other. SignifiQuant calculates the ratios of each of the samples in a comparison (e.g. 113 and 114 against 115 and 116, resulting in 4 difference comparisons) and then uses a t-test to calculate the probability of the difference between sample groups. If a given threshold is 0.05 significance, a protein will only be reported as significantly different if all four comparisons in that group fall below that significance threshold (Pham et al., 2010). In this case, multiple test correction (Bonferroni, 1936) was not applied, to avoid the limitations on data acquisition this can cause, since it leads to such a high level of stringency that the number of changes is drastically reduced (in this case by an order of magnitude), and many important changes could be missed (Datta and DePadilla, 2006).

The comparisons aimed to look at the effect of salt over time on the species, and to compare a salt exposed culture to a non-salt exposed culture at log-stage growth. Full lists of significant changes are detailed in Appendix C in Section 11.3. Summaries of the changes between sample groups are detailed in the following sections, and a broad functional group analysis and metabolic mapping has been carried out to compare each group. Metabolic mapping was carried out using ChlamyCyc, an annotated pathway mapping tool for *C. reinhardtii* onto which changes in enzyme expression can be mapped (<http://pmn.plantcyc.org/CHLAMY/class-tree?object=Pathways>), and assigned enzyme commission (EC) numbers (cataloguing enzyme activity) from the available dataset. Figure 4.25 shows the coverage of the detected proteome on the *Chlamydomonas* metabolic map from 201 EC codes from the full protein list. EC codes were used as these were the most comprehensively covered type of identifier for this metabolic map. There is a large amount of coverage, although it is not comprehensive, showing the limitations of detection and database matching in this type of shotgun proteomic investigation. For example, the lipid and fatty acid metabolism pathways are not well represented in this dataset since not many of the identifiers were

detected, whilst photosynthesis, glycolysis and carbohydrate biosynthesis are all well represented with a large amount of coverage on the metabolic map.

For functional annotation, accession numbers were submitted to DAVID Functional Annotation tool, and annotation categories of biological function were used to group the differentially expressed proteins in terms of the number of up and down regulated proteins. DAVID functional analysis shows the biological process annotation that has been applied to a listed protein in the database, describing its function. These occur at 5 different "levels", with level 1 being the least detailed and level 5 being the most detailed, and the level of specificity increasing along the levels. The most complete annotation with the most useful level of detail is found at levels 3 and 4, since these gave sufficiently detailed information about the protein groups and their biological function, whilst maximising the number of proteins with annotations at that level. Annotation is not complete in the Uniprot database, but this is the most comprehensive database available for study of this organism. The number of proteins that do not have annotation at these levels is stated in the analysis. Proteins can often have more than one annotation grouping, so will appear in more than one category.

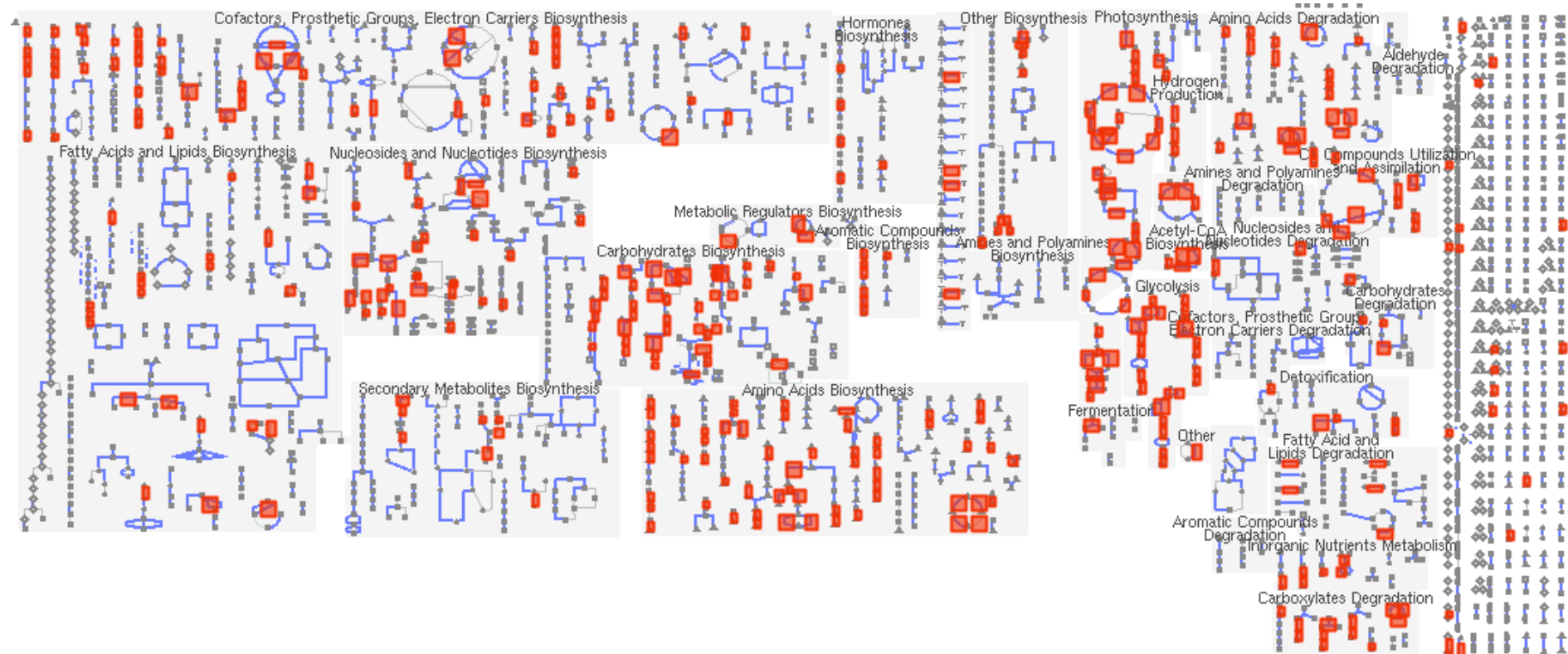


Figure 4.25 Proteins detected in whole quantification data set (201 EC numbers) mapped onto ChlamyCyc metabolic map. Enzymes that were detected are highlighted in red.

Differences were tested along the time course experiment of salt stress of phenotypes 1 (3 hour), 2 (11 hour) and 4 (18 hour). Phenotypes 3 and 4 were also compared to show differences between control and salt conditions at 18 hours. Since there are a large number of changes between groups, the best way to analyse these was via biological function annotation analysis, to give an insight into specific phenotypic changes. Tables of protein changes are listed in Appendix C, and relevant protein changes have been examined in more detail as well as pathway and functional group analysis.

#### **4.4.3 Proteomic changes between early and mid-point stages of exposure to salt (3 against 11 hours salt stress)**

171 proteins were differentially expressed between 3 and 11 hours of exposure to salt stress. 80 of these were down-regulated from 3 to 11 hours, and 91 were up-regulated. Details of these protein changes are listed in Appendix C.

The phenotypic changes between these two time points (which were measured by various techniques as detailed in the methods section) can be summarised as: no increase in OD, an increase in cell size with some clustering, an increase in carbohydrate content, a slight increase in FAMES, a decrease in chlorophyll, and no significant change in photosynthesis or respiration (however these processes take place at low levels compared to the control). This indicates that the cells are in an unhealthy state and unable to proliferate, with a reduced capacity for photosynthesis, with some minor changes in carbohydrate and lipid content.

The majority changes on the ChlamyCyc metabolic map are down-regulations. Only a few changes are seen in lipid and fatty acid biosynthesis, and these are down-regulated proteins. One area of lipid and fatty acid degradation was up-regulated. Carbohydrates biosynthesis shows some up-regulation, which supports the phenotypic change of the rise in carbohydrate content discussed previously, perhaps due to palmelloid formation of clustering of daughter cells into mucilaginous sacs as previously discussed in Section 4.3.6 as a response to salt stress.

Furthermore, photosynthesis was down-regulated, which matches the decrease in photosynthesis found in oxygen electrode data. The other area of up-regulation shown is hormone biosynthesis. The enzymes are involved in jasmonic acid biosynthesis. Jasmonic acid, or jasmonates, are shown to be increased in salt tolerant plants (Pedranzani et al., 2003), suggesting that this pathway was up-regulated as a salt tolerance mechanism. Additionally, the carbohydrate metabolism shows up-regulation of starch biosynthesis, glucose biosynthesis, and UDP- $\alpha$ -D-glucuronate biosynthesis from UDP-glucose, showing that starch metabolism was induced by salt stress.



Figure 4.26 Metabolic mapping of changes between 3 and 11 hours of salt stress, using EC numbers and ChlamyCyc mapping tool. Red highlights indicate up-regulation, blue highlights indicate down-regulation. 46 had EC numbers that were up and down regulated, 44 of which were found.

#### 4.4.3.1 Functional annotation analysis

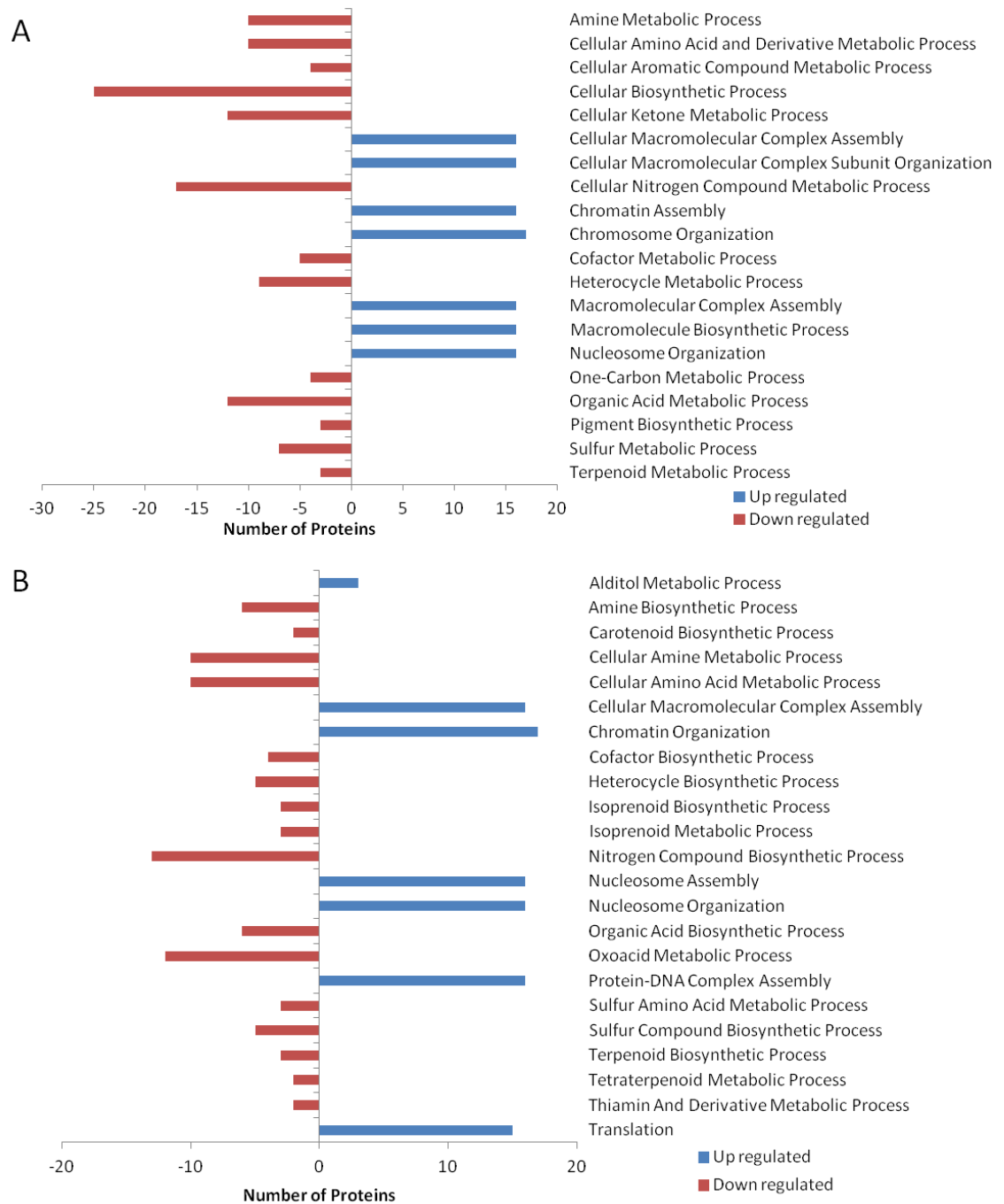


Figure 4.27 Functional annotation grouping for biological process at annotation level 3 (A) and 4 (B) for significant changes between 3 and 11 hours salt exposure. Of the 80 down regulated proteins, 31 weren't found in biological process annotation level 3 (BP3) and 43 were not found in biological processes level 4 (BP4). Of the 91 up-regulated proteins, 50 were not found at BP3 and 48 were not found at BP4.

Functional grouping of biological process labels shows some notable patterns (Figure 4.27). All annotations with metabolic processes were down-regulated. Pigment biosynthesis, namely carotenoid biosynthesis, was also down-regulated. This contrasts

with findings in halotolerant algae, since carotenoid production has been linked to high salt conditions in *Dunaliella* (Borowitzka et al., 1990), and there was no decrease in carotenoids found between the two time points. It seems, however, that carotenoids are not being employed as a salt tolerance mechanism in this species.

The up-regulated proteins were mainly associated with DNA assembly and organisation (chromatin assembly, chromosome organisation and nucleosome organization) or with the biosynthesis and assembly of macromolecules. This suggests that the cells are undergoing cell division processes. Since the cells begin to form palmelloids (groups of daughter cells clustered together in sacs), this shows that this process has been prioritized over the metabolic functions of the cell. It appears that although the culture does not increase in OD (culture density) at this stage, the culture is putting a large amount of resources into replacing and rebuilding damaged cells.

Alditol metabolic processes were also up-regulated. An example of an alditol is glycerol. The protein changes list (Table 11.1 in Appendix C) reveals that glycerol-3-phosphate dehydrogenase is up-regulated. This is a part of the glycerol synthesis pathway and is also involved in maintaining redox potential for glycolysis and one of its products glycerol-3-phosphate can lead to production of TAGs and phospholipids (He et al., 2007; Mráček et al., 2013). Glycerol is a well established compatible solute for algae that helps to regulate the osmotic potential and stress on the cells that is induced by high salt stress conditions (Goyal, 2007). This suggests a rapid adaptation of the cell to the environment, through the production of compatible solute glycerol.

#### **4.4.3.2 Proteomic changes to lipid metabolism**

Lipid metabolism was not shown to be affected in these categories, supporting the evidence from the phenotypes that lipid metabolism in *C. reinhardtii* is not greatly affected by 0.2 M NaCl salt stress, although there are a few individual proteins that can be linked to lipid metabolism, when investigating individual changes. One of these was the up-regulated glycerol-3-phosphate dehydrogenase, responsible for the glycerol metabolism changes discussed above, and shown to be increased in high salinities (Chen et al., 2011a). It is also a major linking protein between the carbohydrate and

lipid metabolism (Yao et al., 2014). Increasing this enzyme in plants can result in a significant increase in oil content (Yu et al., 2011).

Another was the up-regulation of acetyl-CoA acyltransferase, which may be involved in catabolic beta-oxidation of fatty acids (Meurant, 1984), suggesting there may be an increase in the breakdown of lipids for energy release for use in the cell. Overall, there is a slight change in lipid metabolism, but there are no large scale changes in lipid regulation observed at the proteomic level. This correlates with the FAME data (Section 4.3.7) which shows a slight increase over time but no large scale changes.

#### *4.4.3.3 Proteomic changes indicating low growth rates*

Analysis of the individual proteins reflects the salt stress response, low growth rates and decreased photosynthetic ability.

Low-CO<sub>2</sub>-inducible proteins were altered (although one was up-regulated and one was down-regulated), suggesting that the ability to uptake inorganic carbon was affected by salt stress (Ohnishi et al., 2010). Since ribulose biphosphate carboxylase (RuBisCo), carbonic anhydrase (both involved in carbon fixation (Sültemeyer, 1998)), light harvesting protein and chlorophyll a/b binding protein (involved in light harvesting) were also down-regulated, the evidence is that photosynthesis and carbon fixation is negatively affected by salt stress.

Heat shock were proteins up-regulated, indicating stress responses, in addition to a autophagy protein being up-regulated, suggesting that unhealthy cells are undergoing degradation. Autophagy also promotes cell survival by recycling intracellular components, therefore temporarily adapting the culture during stress (Pérez-Pérez et al., 2012). This indicates that the cells are poorly suited to a high salinity environment. With that in mind, certain proteins provide evidence of the cells employing salt stress resistance mechanisms such as the up-regulation of aldehyde-alcohol dehydrogenase. This enzyme has been linked to mitigation of oxidative stress as it acts as an aldehyde scavenger during lipid peroxidation (Singh et al., 2013). Glutamic-gamma-semialdehyde dehydrogenase was also up-regulated, and is an enzyme involved with

the production of proline which has been shown to accumulate under salt stress (Silva-Ortega et al., 2008).

Furthermore, aconitate hydratase was down-regulated, an enzyme involved in the TCA cycle, photorespiration and glycolysis (Ghosh and Xu, 2014). This correlates with respiration being negatively impacted by salt stressed conditions, as shown by oxygen electrode data (although they are at similar levels between the two time points).

Another down-regulated enzyme was ubiquitin-activating enzyme, consistent with findings of oxidative stress in the green alga *H. pluvialis* (Wang et al., 2004). Ubiquitin-proteasome pathway is down-regulated in *C. reinhardtii* under oxidative stress and the accumulation of ROS (Vallentine et al., 2014).

#### **4.4.3.4 Proteomic changes to carbohydrate metabolism**

Individual analysis of expressional changes reveals greater insight into the changes in carbohydrate metabolism. Alpha-1,4 glucan phosphorylase, an enzyme involved in degradation of starch, was up-regulated. UDP-glucose 6-dehydrogenase was also up-regulated, which catalyses degradation of starch into glucose which can then be utilised in the glycolysis pathway, and has been shown to be part of the proteomic response in nitrogen-depletion induced lipid accumulation in *Chlorella* (Li et al., 2014a).

Additionally, starch synthase was down-regulated and although the metabolic map suggests that carbohydrate biosynthesis was up-regulated, analysis of the individual proteins indicates greater starch catabolism and lower starch synthesis. This contradicts the anthrone assay analysis (Section 4.3.8), suggesting there is an increase in carbohydrates between 3 and 11 hours in this species. However, the proteomic analysis suggests it is not due to the formation of intracellular starch. Furthermore, the up-regulation of starch degradation suggests that the salt condition causes utilisation of stored starch for energy, perhaps as a survival mechanism whilst under this osmotic/ionic stress, utilising stored energy to regulate cellular functions. Considering the cellular increase of carbohydrate indicated by the assay, it is possible the cell is storing energy for long term survival in a high salinity. As previously mentioned (Section 4.3.6) it could also be due to increased palmelloids during the cell cycle to

allow for division in a saline stress environment. Unfortunately, the proteomic data is not sufficiently detailed in order to find an explanation for this increase.

#### **4.4.3.5 Individual proteomic changes**

Chloroplast phytoene desaturase and chloroplast phytoene synthase are down-regulated and both are linked to carotenoid accumulation (Toledo-Ortiz et al., 2010), a compound important in helping to protect chlorophyll from excess light. This suggests that carotenoid accumulation is not being employed as a protective mechanism. This may be part of the reason that this strain of *C. reinhardtii* is not more halotolerant.

#### **4.4.3.6 Overall proteomic changes**

Overall the protein changes are indicative of a phenotypic change to a lack of growth or lipid production, which correlates with the measured lipid content, photosynthetic rates and culture density measurements obtained. Several salt stress responses and possible tolerance mechanisms has been highlighted. Some specific changes in carbohydrate and lipid metabolism have been highlighted in the proteome, although this does not always align with the phenotypic data. Metabolic mapping (Figure 4.26) and functional annotation analysis (Figure 4.27) demonstrate proteomic overall changes in down-regulation of photosynthesis, carbon fixation, and many cellular metabolic processes, which is supported by the phenotypic data showing reduced photosynthesis and growth.

#### **4.4.4 Proteomic changes between mid-point and later stages of exposure to salt (11 against 18 hours salt stress)**

Between 11 and 18 hours of salt exposure, 217 proteins were found to be differentially expressed. 123 proteins were down-regulated and 94 proteins were up-regulated.

The previously discussed phenotypic differences between the two sample points can be summarised as: no significant change in photosynthesis or respiration (although this continues to be at a much lower rate than in the control), a further decline in

chlorophyll pigments, a slight increase in carbohydrates (at a lower rate than between time points 3 and 11), a slight decline in FAMES, no notable change in morphology (cells remain bigger than time point 3 hours), and no significant change in OD.

The metabolic map (Figure 4.28) was searched. In comparison to the previous figure showing metabolic map differences between 3 and 11 hours, the changes highlighted in the metabolic map from 11 to 18 hours shows up-regulation in many areas, including photosynthesis, carbohydrates biosynthesis, amino acids biosynthesis, glycolysis, and a few in lipid biosynthesis. Some areas of degradation are also up-regulated, namely in carboxylates, fatty acids and lipids, and amino acids, showing that biosynthesized components are not necessarily accumulating. The majority of processes with changes show up-regulation, indicating that there is an important change in the way that *C. reinhardtii* is responding to salt stress within the time course. After the 18 hour point, the culture later begins to multiply further and appears to gain tolerance to 0.2 M NaCl by being able to multiply in salt conditions which were detrimental at the beginning of the time course experiment. It may be that the metabolic processes taking place in control conditions are simply taking place later in salt stress conditions, but this must be tested by looking at the difference between control and salt conditions at the same time point, which is discussed later. Although growth and photosynthesis data suggests that the culture continues to have impaired photosynthetic ability and ability to proliferate, the change in the proteome suggests that salt tolerance mechanisms are being employed that allow the culture to switch back to its normal metabolic processes between the 11 and 18 hour time points. The proteins discussed that were up-regulated between 3 and 11 hours that have been linked to salt tolerance, such as glycerol production and proline production, may have allowed the cell to adjust to the new environment over time and then revert to putting resources into normal cellular functions for photosynthesis and growth. The fact that the culture remains at a low level of growth and with impaired photosynthetic ability (as reflected by oxygen electrode data) shows that this shift in proteomic mechanisms is still not enough to counter the detrimental effects of salt. However, it does show that the cells are able to adapt to the new condition instead of dying, and to even attempt to carry out their normal cellular functions.



#### *4.4.4.1 Functional annotation analysis*

Functional annotation supports the evidence that metabolism was up-regulated (Figure 4.29).

By contrast to the differences in functional group processes found between 3 and 11 hours, the differences between 11 and 18 hours show decreases in cellular macromolecular complexes and in DNA related processes, both in the BP3 and BP4 levels of annotation. Photosynthesis is down-regulated, and this remains consistent with the findings from oxygen electrode data, that throughout the time course experiment, photosynthesis is reduced by the presence of salt stress. However, it conflicts with information from the metabolic map data that shows both up and down-regulation in photosynthesis. There are limitations to both sets of analysis, in that not all accession numbers have associated EC numbers or DAVID functional annotation, so some of these analyses may produce slightly different results depending on the limitations of Uniprot, ChlamyCyc and DAVID's data annotation.

Many of the metabolic processes previously down-regulated are then up-regulated between 11 and 18 hours of salt stress. Carbohydrate processes are largely up-regulated. Nitrogen compound metabolic processes were up-regulated, as were processes to do with energy generation.

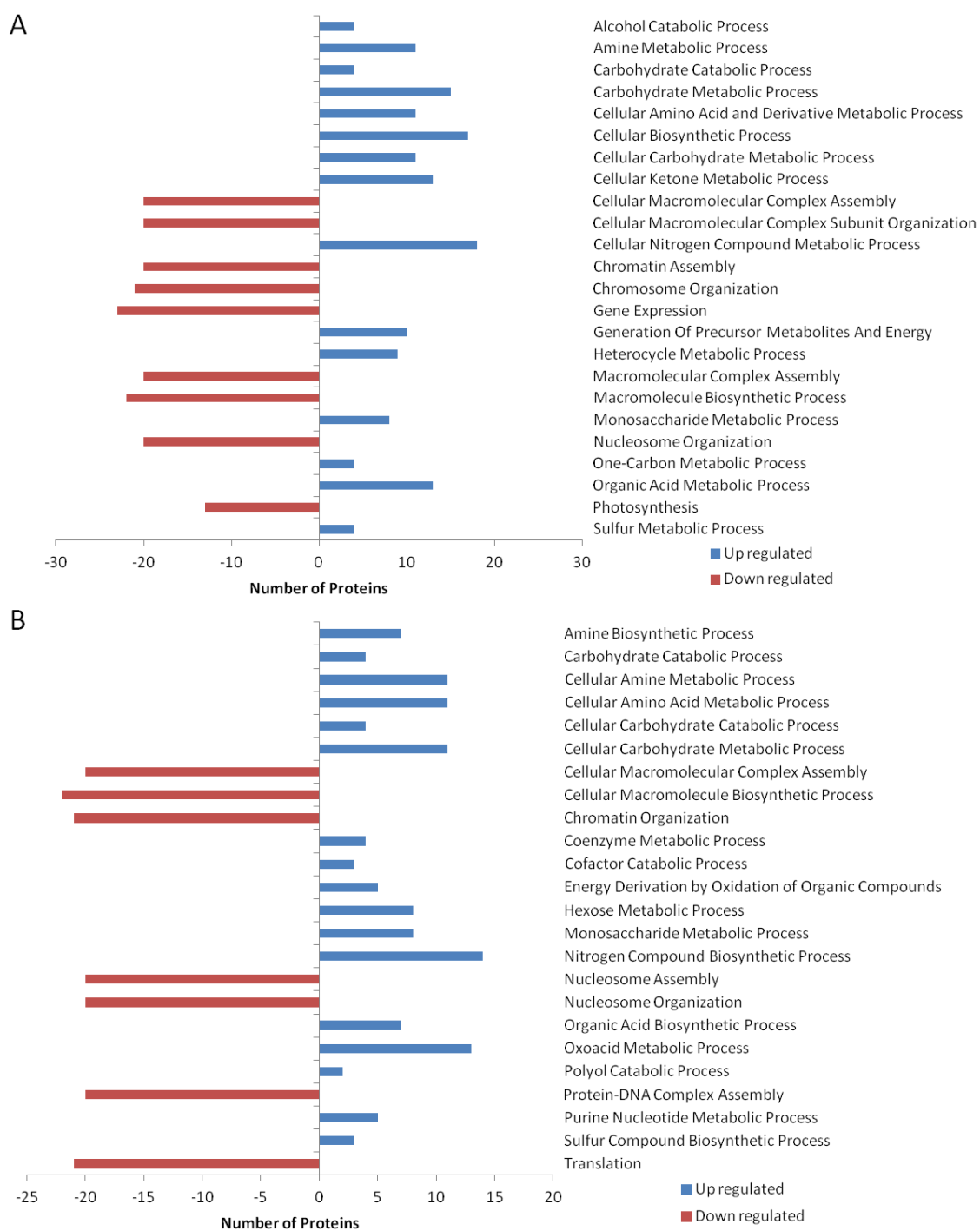


Figure 4.29 Functional annotation of significant differences between 11 and 18 hour salt conditions and BP level 3 (A) and BP level 4 (B). 54 proteins were not found for BP3 down-regulation, and 63 were not found for BP4. For up-regulation, 43 were not found in BP3, and 52 not found in BP4.

#### *4.4.4.2 Proteomic shift between previous time points*

There is clearly a large change in the way salt stress is affecting the proteome over time. The changes shift away from DNA replication, translation and macromolecular processes and towards the metabolic processes that had previously been down-regulated between 3 and 11 hours. This suggests that after the initial diverting of resources towards cell division and palmelloid formation, the culture then remains in this state without further division, but possibly starts to divert resources towards energy generation and storage, and process metabolites within the cell for future growth. This perhaps suggests that the cells are experiencing less salt stress than in the first time points, or are better adapted. Initial reactions to salt stress may have allowed adaptation and rebuilding of damaged cells, and whilst the culture is still clearly not able to grow or photosynthesise as well as in control conditions, the cells are able to re-prioritise metabolic processes. The shift in changes from 3 to 11 and 11 to 18 highlights the nature of this type of investigation - that a sampling point is a snapshot of the proteome from which the temporal changes must be inferred. It is important to interpret such quantitative proteomic investigations with this limitation in mind.

Transcriptomic study of *Arabidopsis* has shown that salinity response involves several factors including osmoprotectants, energy metabolism, detoxification, transport and protein turnover (Jiang and Deyholos, 2006). It is likely that the different processes employed in response to salt take place at different time scales as the culture adapts. These temporal shifts are demonstrated by the changes in the proteome over time.

#### *4.4.4.3 Analysis of individual proteins*

When looking at individual proteins of note, NaCl-inducible protein is down-regulated between 11 and 18 hours. Literature searches and annotation did not reveal information about the function of this protein. It might be expected that prolonged salinity stress would result in up-regulation. However, the down-regulation suggests that the role it plays in salinity response is not employed in the latter stages of salt stress.

A low CO<sub>2</sub> inducible protein is up-regulated. This protein has been shown to increase inorganic carbon uptake (Ohnishi et al., 2010), suggesting that the cell is working to

increase the availability of carbon, probably because the ability to fix carbon via photosynthesis and the carbon fixation pathways has been impaired by salt stress.

Many changes remain consistent with the previous comparison of 3 to 11 hours: photosynthesis, photosystem I and RuBisCo proteins (involved in the Calvin cycle) were down-regulated, since salt continued to have a negative impact on photosynthesis and carbon fixation. UDP-glucose related proteins, including UDP-glucose pyrophosphorylase, continued to be up-regulated, suggesting the continued use of starch degradation to produce glucose for the glycolysis pathway.

In contrast to the previous comparison, translational proteins are down-regulated, suggesting that DNA repair and cell division was decreased between 11 and 18 hours. This is a contrast to the 3 to 11 hours time period comparison, which showed an increase in translation proteins. On top of this, histones were down-regulated, also indicating less cell division. The functional analysis grouping suggests down-regulation of DNA replication and major cellular complex synthesis, so the down regulation of cell division seems consistent. There may be less need for cell division or cell replacement as the culture adapts over time to salt stress and requires less cell replacement. Furthermore, the culture was not undergoing significant cell division and proliferation at the time.

One of the most notable proteins that impacts lipid synthesis is the up-regulation of citrate synthase. The increase in the activity of this enzyme indicates that acetyl CoA is being directed into the TCA cycle and therefore away from fatty acid biosynthesis (Goncalves et al., 2015). Overexpression of this enzyme has been shown to drastically reduce TAG content of algae through this redirection of acetyl CoA, and conversely knocking the gene out results in huge TAG increases (Martin et al., 2014). This enzyme is therefore a key piece of evidence showing that resources are directed away from fatty acid metabolism during salt stress in *C. reinhardtii*, resulting in no TAG accumulation.

Another enzyme of note was that chloroplastic ATP synthase was down-regulated, whilst mitochondrial ATP synthase proteins were up-regulated. It has been shown that

mitochondria in plants may be involved in proline metabolism and in sensing cellular stress and regulating programmed cell death (Pastore et al., 2007), therefore mitochondrial activity may be part of the adaptive process allowing the cells to adjust to the salt stress environment.

An enzyme involved with glycolysis and the production of energy for cellular metabolism, glyceraldehyde-3-phosphate dehydrogenase, was up-regulated. It has also been suggested that this enzyme plays a role in Arabidopsis plants in the mediation of ROS signalling during stresses such as drought or salinity stress, and can aid the plants in adaptation to salinity or other types of stress (Guo et al., 2012).

Interestingly, betaine lipid synthase was down-regulated, a change that was not found between the other comparisons in this iTRAQ experiment. This enzyme is important in the synthesis of DGTS for lipid membranes of *C. reinhardtii* (Riekhof et al., 2005). DGTS is not affected in N-deprivation stress conditions of *C. reinhardtii* (Fan et al., 2011) unlike other lipid types, and is mainly composed of C18:3 FAs. It has been shown in previous research that DGTS decreases in response to salt stress in *C. nivalis*, as this decreases the degree of saturation of fatty acids and permeability of the membrane (Lu et al., 2012c). There is no discussion in the literature, to date, of DGTS reducing in *C. reinhardtii* under salt stress. Whilst no major changes in lipid content were found in this species under salt stress, this proteomic change suggests that between 11 and 18 hours, the cell may be regulating lipid membrane composition to protect against salt stress. However, there is no major change in lipid content of the biomass, and C18:3n3 levels remain unaffected by the salt conditions. Lipid metabolism is shown to have a higher number of significant enzyme changes in ChlamyCyc mapping than in the previous comparison. Glycerol-3-phosphate dehydrogenase was up-regulated, consistent with the previous findings of 3 to 11 hours, due to continued up-regulation of glycerol, suggesting continued production of compatible solutes.

#### **4.4.4.4 Overall proteomic changes**

Overall, the changes indicate increased metabolism in the cell, and lower cell division, especially when comparing the results to the previous 3 to 11 hour comparison. Photosynthesis and some energy producing mechanisms are still impaired by the

presence of salt, showing that the cells are not well adapted, but the evidence suggests that some salt tolerance mechanisms were being induced along the time course experiment. Lipid metabolism mechanisms were affected at the proteome level, but no great shifts in lipid accumulation or degradation are shown to occur from the GC data (Section 4.3.7).

#### **4.4.5 Proteomic changes between early and late stages of exposure to salt (3 against 18 hours salt stress)**

Looking at the overall difference in proteome between 3 and 18 hours may reveal different changes that are only highlighted over a greater time period. 212 proteins were differentially expressed between the early and late salt stress conditions (see Appendix C). 136 proteins were down-regulated and 76 proteins were up-regulated. The majority of changes were down-regulation. Metabolic mapping (Figure 4.30) shows up-regulation in most of the carbohydrate biosynthesis processes, and in glycolysis. Some processes show both up and down-regulation. Fatty acid biosynthesis and photosynthesis were down-regulated. This suggests that overall, salt stress has negative effects of the majority of the processes, with the exception of carbohydrate metabolism.



Figure 4.30 Metabolic map from ChlamyCyc showing significant changes between 3 and 18 hours of salt exposure, using EC numbers. 59 EC numbers were searched on the metabolic map (57 were found).

Between time points 3 and 18 hours, the phenotypic changes can be summarised as: no significant change in OD, a slight increase in cell size and clustering, a slight increase in FAMES overall and in C16:0 particularly, an increase in starch, a decrease in chlorophyll and no significant change in photosynthesis and respiration activity (although these processes remain impaired compared to the control).

#### *4.4.5.1 Functional annotation analysis*

Functional annotation reveals further analysis (Figure 4.31). Cellular biosynthetic processes were greatly down-regulated. Proteins involved in photosynthesis were down-regulated, including pigment biosynthesis, electron transport chain processes and chlorophyll metabolic processes. This is consistent with the data that shows that salt conditions have a detrimental effect on photosynthesis.

Some metabolic processes were down-regulated, as with the 3 to 11 hour comparison, but other metabolic processes were up-regulated, which may be linked to the salt tolerance mechanisms, since these up-regulations include carbohydrates, proline and alditol (glycerol) metabolism. As previously discussed in sections 4.3.8 and 4.4.3, glycerol and carbohydrates (through palmelloid formation) may protect against osmotic damage. Proline is also shown to be a defensive mechanism against the toxic effects of salt stress, especially in preventing lipid peroxidation and membrane integrity (Demiral and Türkan, 2005; Jain et al., 2001).

Lipid metabolic and biosynthetic processes were down-regulated, confirming that lipid induction is not a salt tolerance mechanism in this strain, and that lipid accumulation is also not a side effect of the growth arrest under salt stress. This supports the metabolite data (Section 4.3.7), which does not show any great change in lipid content of biomass, nor profile.

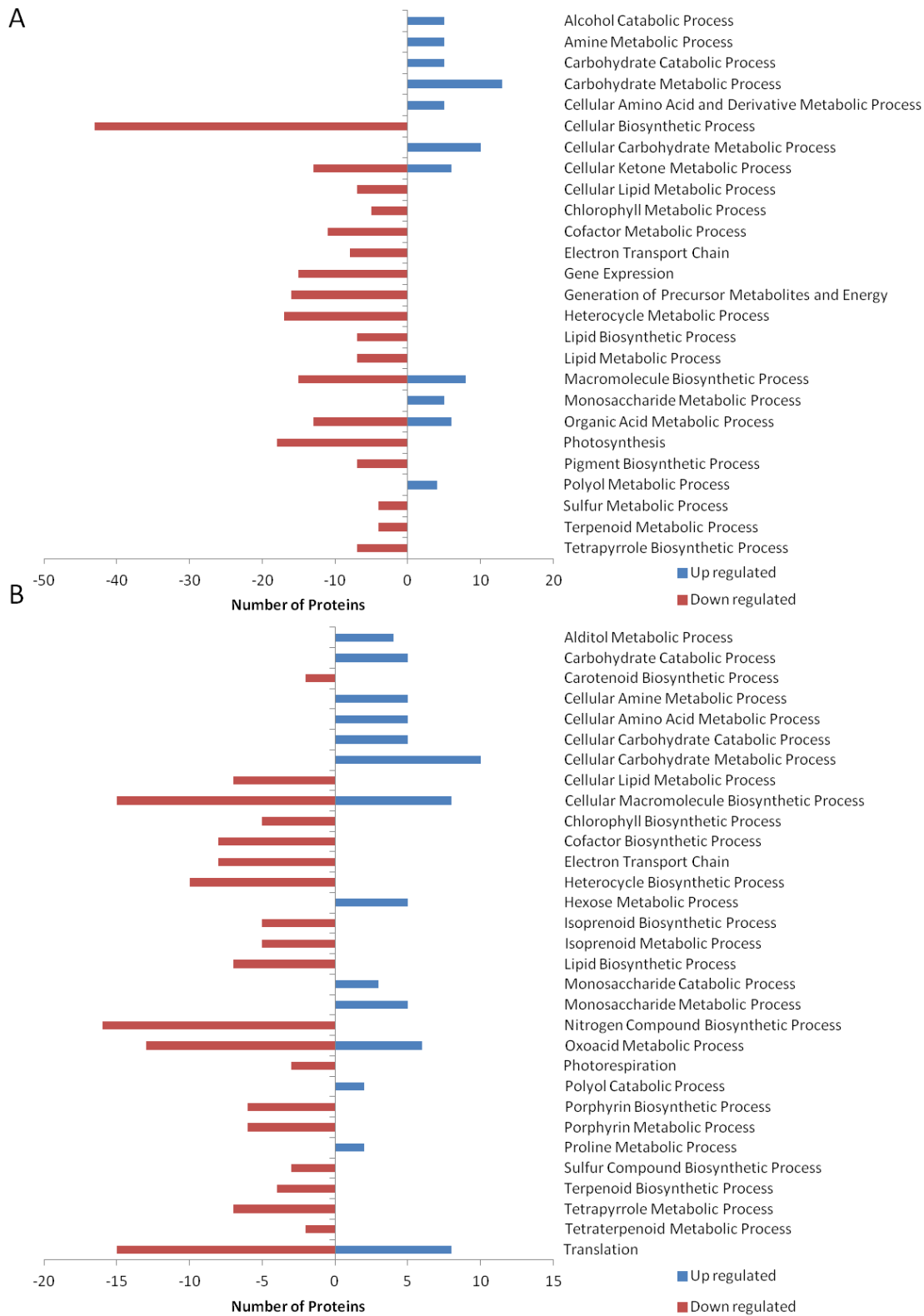


Figure 4.31 Functional analysis grouping for differences between 3 and 18 hours salt exposure for BP level 3 (A) and BP level 4 (B). Of the down-regulated proteins, 54 were not found at BP3 and 62 were not found at BP4. Of the up-regulated proteins, 42 were not found at BP3 and 45 were not found at BP4.

#### *4.4.5.2 Individual protein expressional changes*

Individual proteins reveal more detail. Starch branching enzyme was up-regulated, as in previous comparisons, indicating the formation of starch molecules, despite the strain being a low starch mutant. Pyruvate carboxylase, an enzyme that links carbohydrate and lipid metabolism, was down-regulated. This may be part of a bottleneck that prevents lipid accumulation taking place in these conditions, and may explain the lack of effect of salt on lipid content.

In addition, oxygen evolver proteins of PSII were down-regulated and PSI chlorophyll and reaction centre proteins were down-regulated, indicating a continued impairment of photosynthetic apparatus. As found in previous comparisons, ATP synthase related proteins were down-regulated, indicating limitations on the availability of energy in the cell to carry out processes. This results in reduced culture growth, as supported by a down-regulation of elongation factors and translation proteins. These indicate reduced cell division, mainly due to the later period of salt stress where 11 to 18 hour comparison shows down-regulation of these proteins.

Many of the individual changes have already been discussed in the changes between 3 and 11 and between 11 and 18 time points, and comparing the overall effects of salt stress between 3 and 18 hours shows how these groups are affected over a greater time period. These repeated changes include glycerol-3-phosphate dehydrogenase, citrate synthase and acetyl-CoA acyltransferase up-regulation.

Furthermore, glyeraldehyde-3-phosphate dehydrogenase and glucose-6-phosphate isomerase were up-regulated, indicating an increase in glycolysis and gluconeogenesis. This suggests that the cell is increasing the amount of energy available for culture growth. Since after the 18 hour time point the culture gradually begins to divide and increase, this fits the phenotypic observations.

The changes shown by functional annotation show a mixture of up and down-regulation of metabolic processes, unlike the previous comparisons of 3 to 11 hours and 11 to 18 hours, which show mainly down-regulation followed by mainly up-regulation of the metabolic process groups. This highlights the issues with choosing time points in such an experiment, as choice of time point can suggest a completely

different biological story. Overall, photosynthesis is impaired by 0.2 M NaCl, but carbohydrate metabolism, glycolysis and amino acid biosynthesis were all up-regulated, suggesting an overall increased turnover of proteins and use of carbohydrate metabolism and glycolysis as a salt stress response.

#### **4.4.5.3 Overall proteomic changes**

Overall, lipid metabolism was down-regulated under the salt stress conditions, whilst carbohydrate metabolism was up-regulated. Photosynthesis was down-regulated, matching the phenotypic data that photosynthesis was consistently low in salt stress conditions. The proteins to do with translation and cellular macromolecular biosynthesis showed a mixture of up and down regulation, suggesting that there is a dynamic response in the regulation of formation of major cell components to salt stress. Since the time course experiment goes on to show cell division and increases in culture density later, it appears that the culture was adapting to the conditions by employing certain salt tolerance mechanisms which allowed culture proliferation. The decrease in photosynthetic ability, however, shows that this adaptation is not the most effective, and it appears that the culture has to expend large amount of energy (obtained through glycolysis) in maintaining the basic processes of the cell. This may be why despite the lack of growth, resources were not stored in the cells in the form of lipids, as they were expended on cell maintenance too quickly.

#### **4.4.6 Proteomic changes between late stage exposure to salt and control (18 hour control conditions against 18 salt stress)**

To compare the differences between a mid-log non salt stressed culture and a salt stressed culture at the same time point, control and salt stressed 18 hour sampling points were compared. 337 proteins were differentially expressed: 224 proteins were down-regulated and 113 proteins were up-regulated (Appendix C).

The previously discussed (section 4.3.11), phenotypic differences between the two sample groups are: photosynthesis and respiration are significantly lower in the salt stressed cultures than in control cultures. Pigments are at significantly lower levels, both chlorophylls and carotenoids, in salt stressed cultures than in controls.

Carbohydrates are at slightly higher levels in 0.2 M NaCl compared to control conditions, as both show increases in carbohydrates between 3 and 18 hours but at a greater level in salt conditions. There was no significant difference in FAMES between 18 hour salt and 18 hour control conditions, although control levels are slightly higher than in the salt conditions. The culture density (indicated by OD and biomass accumulation) was much higher in control conditions, and at 18 hours control conditions are mid log phase, undergoing rapid cell division. By contrast, 18 hour salt conditions are a similar OD as they were at time point 3 hours, indicating little cell division.

In metabolic mapping (Figure 4.32), most of the changes were down-regulated, including those in photosynthesis, lipid synthesis and nucleotide biosynthesis, suggesting a general decrease in cell division and photosynthetic ability, consistent with the growth and oxygen electrode data. There is increased turnover of amino acids, with both synthesis and degradation processes being up-regulated. A fatty acid degradation protein is up-regulated.

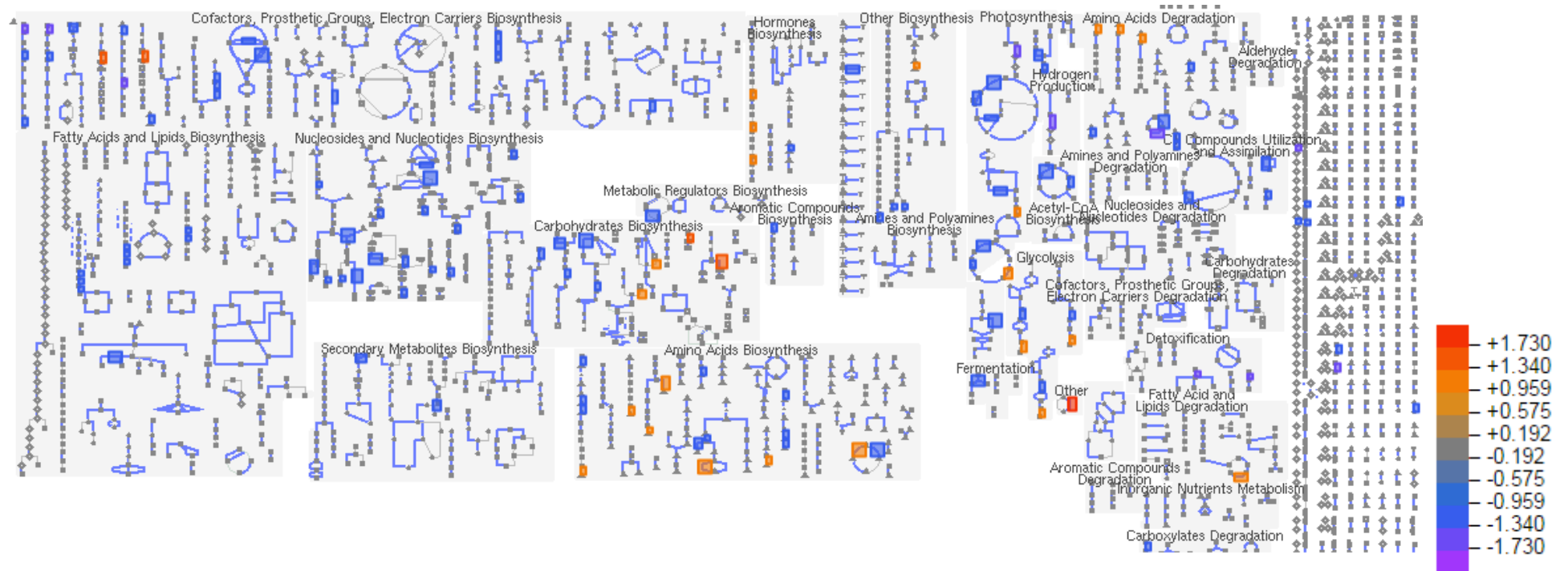


Figure 4.32 ChlamyCyc metabolic map showing differentially expressed proteins between control cultures at 18 hours and salt stressed cultures at 18 hours (EC numbers used). 67 EC numbers were searched, and 66 were found.

#### 4.4.6.1 Functional annotation analysis

Functional annotation analysis shows similar patterns (Figure 4.33). The majority of the biological processes categorised here were down-regulated, or showed a mixture of up and down regulated proteins within the same functional group, but there is some up-regulation in carbohydrate metabolic processes, and in alditol metabolic processes (possible salt stress tolerance mechanisms, as previously discussed). Light harvesting and light reaction processes of photosynthesis were up-regulated, which is a different pattern to the phenotypes, which show a decrease in photosynthesis from control to salt conditions.

Fatty acid and lipid biosynthesis and metabolism processes were down regulated between control and salt conditions. Since there was no increase in the phenotypes in lipid accumulation, it would not be expected to see proteomic changes linked to fatty acid accumulation. However, it is clear that salt has detrimental changes on lipid metabolism in *C. reinhardtii* as resources are diverted away from it, based on both FAME and proteomics evidence. The contrast in the proteome of a culture of *C. reinhardtii* growing well and that of a salt stressed culture with halted growth and reduced photosynthetic ability is a strong one. The fact that the salt stressed species continue to grow and up-regulate certain proteins shows maintenance of their systems under a fairly high salt stress. However, this comes at a cost of reduced growth and reduced photosynthetic ability.

Carbohydrate metabolic processes were up-regulated in salt conditions compared to control conditions. Analysis of the individual proteins shows that this includes starch synthase, suggesting that salt stress cells have a greater need for starch synthesis than control grown cells do. However, starch levels are actually higher in control conditions, and starch increases over time are similar in both conditions. The regulation of starch therefore doesn't necessarily reflect the phenotype, but this may be due to the fact that the strain has a reduced ability to synthesise and store starch. When analysing the carbohydrate synthesis pathways in the mapping, the overall picture suggests down-regulation. These different ways of analysing the data therefore suggest that there

may not be a clear response of carbohydrate metabolism to salt stress, and the response is complex.

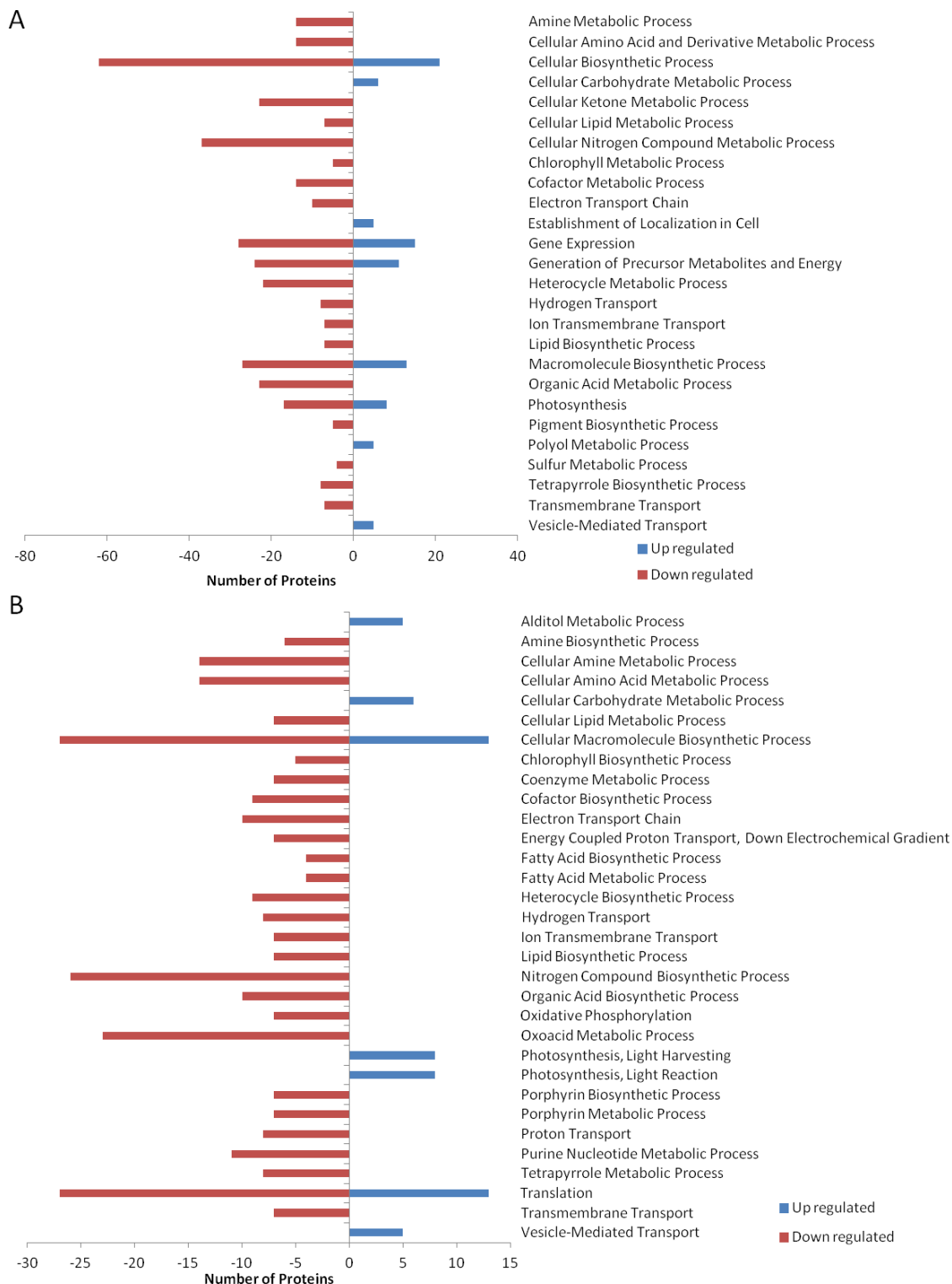


Figure 4.33 Functional annotation grouping analysis for differences between 18 hour control samples and 18 hour salt samples at BP level 3 (A) and BP level 4 (B). Of the down-regulations, 102 were not found in BP3 and 114 were not found in BP4. Of the up-regulations, 61 were not found in BP3 and 72 were not found in BP4.

#### *4.4.6.2 Individual protein expressional changes*

Individual proteins reveal more detail about the effects of salt on the proteome. RuBisCO proteins were down-regulated, as were carbonic anhydrases, showing that salt has a strong effect on carbon fixation from carbon dioxide. Two low CO<sub>2</sub>-inducible proteins were also up-regulated, and a Calvin cycle protein was down-regulated. However, as this species was grown in TAP, there was an alternative carbon source available. As previously discussed, the cells show both down-regulation of carbon fixation but also proteins that can counter the effects of low inorganic carbon.

Stress related proteins were up-regulated, including DNA repair protein, stress-related chlorophyll a/b binding proteins. However the NaCl-inducible protein was down-regulated, which was unexpected. Previous discussion about this protein suggested that down-regulation may be due to temporal changes in salt response. However, a down-regulation from a control condition seems counter to the sample conditions, but without knowing the function of this protein there are limitations to what can be inferred from this.

ATP related proteins were down-regulated such as ATP synthase, indicating that salt conditions limit the availability of ATP that the cells have to carry out their functions.

Several glycerol-3-phosphate dehydrogenase proteins were up-regulated by approximately 2-fold. As previously discussed in the other comparisons, there is no evidence from the GC data that fatty acids were increased, and therefore it unlikely that glycerolipids were being made, however, glycerol may have been induced for compatible solutes as a salt tolerance mechanism, that would not have been needed as much in the control conditions.

Importantly, a subunit of acetyl-CoA carboxylase was down-regulated. This enzyme is the first committing step in the fatty acid biosynthesis pathway, and therefore this proteomic change indicates that salt stressed cells actively reduce the activity of fatty acid synthesis. This is a rate limiting step without which the process cannot take place.

Additionally, acetyl-CoA acyltransferase was up-regulated. This is a protein that may be involved with beta-oxidation of very long chain fatty acids, indicating that fatty acid catabolism was taking place. There is not a great reduction in lipids in the salt stressed cultures, but proteomic analysis suggests that compared to control conditions, salt has a detrimental effect on lipids in the culture.

Of the light-harvesting proteins, many of the changes associated with chlorophyll-binding proteins of LHCII and PSII complexes were up-regulated, whilst those associated with PSI were down-regulated. However, oxygen evolving proteins, especially those of PSII were down-regulated. Photosystem I can be favoured over photosystem II in the case of cyclic photophosphorylation under salt stress in an Antarctic *Chlamydomonas* species (Szyszka-Mroz et al., 2015). However, it is not clear if this is what is taking place here.

## 4.5 Chapter Discussion and Conclusions

### 4.5.1 Summary of phenotypic changes due to salt stress

This data is the first published evidence of the effect of salt stress on the lipid profile of *C. reinhardtii*. Whilst many studies have investigated the effect of salinity stress on this species (Leon and Galvan, 1994; León and Galván, 1999; Neelam and Subramanyam, 2013; Yokthongwattana et al., 2012; Zuo et al., 2012; Zuo et al., 2014), only a single study (Siaut *et al.*, 2011) did so with any information of the effect on lipid content, but this study did not show any information on the lipid profile. Furthermore, their study is limited to 100 mM NaCl stress, and the wild-type strain only. The current study used a starchless mutant and tested a range of salinities to show the effect of increasing salinity on the lipid profile and quantity in *C. reinhardtii*.

It has been shown that many different stresses affect lipid content (Solovchenko, 2012) and other species (such as *Dunaliella salina*) accumulate TAG in response to high salinity. In many species, an increase in unsaturated C18 chains occurs in microalgae in response to salt increases (Azachi et al., 2002; Zhila et al., 2011). In *Botryococcus braunii*, increased salinity caused changes in the FAME profile, with increases in the relative proportion of palmitic acid and oleic acid (Rao et al., 2007).

There is some evidence from the data described in this chapter that lipids are affected by salinity conditions in *C. reinhardtii*, with the level of salinity being key to this response, as shown by the first set of preliminary experiments ("Experiment 1" in Section 4.3.3). In this investigation, the cultures were able to grow and function well at 0.1 M NaCl but reached a tolerance limit between 0.1 and 0.2 M NaCl, and some small increases in FAME levels were observed due to salt conditions.

A second experiment to link metabolomic data with proteomic data was undertaken to explore the effect of salt stress on lipid metabolism and cellular mechanisms in this species. In this second experiment, natural biological variation from the previous experiment was noted, as the salt tolerance of the culture was higher, and the FAME profile was largely unaffected by salt. Each salt concentration tested had a detrimental effect on culture growth and on photosynthetic ability, with increasing salt concentration showing greater impacts on these functions. However, 0.2 M NaCl conditions still allowed small amounts of culture growth, and each culture under salt conditions entered palmelloid formation. The lipid content of these cultures did not show significant overall variations, but C16:0 and starch contents did increase slightly in salt stressed conditions.

Clearly salt stress could not be used as a mechanism for large increases in lipid production in *C. reinhardtii*, as it does not increase lipid concentration like nitrogen stress does.

#### **4.5.2 The effects of salt stress on the cell and salt tolerance mechanisms**

It has been theorized that *C. reinhardtii* copes with salt stress by expressing antioxidant enzymes and suppressing growth (Yoshida *et al.*, 2004; Zuo *et al.*, 2012). Whilst the presence of reactive oxygen species (ROS) or antioxidants was not investigated in this study, the arresting of growth is observed in 0.2 and 0.3 M NaCl cultures of Experiment 1, but not in 0.1 M NaCl cultures. The decreasing of growth is also observed in all salt conditions in Experiment 2, due to the decreasing of photosynthetic ability through the ionic effects of Na<sup>+</sup> ions on the photosystems (Allakhverdiev *et al.*, 2002; Gilmour *et al.*, 1985) and subsequent reduction in energy and resources available for cell division. ROS inhibit RuBisCo activity (Murata *et al.*, 2007) and therefore decrease carbon

fixation. Most strains of *C. reinhardtii* have a poor ability to cope with high ROS levels. However, transgenic lines of *C. reinhardtii* that over-express ferredoxin genes showed enhanced tolerance to both heat and salt stress, reduced ROS levels in the cells, and higher lipid and starch contents under nitrogen stress (Huang et al., 2015). Ferredoxins are electron carrier proteins in the final stage of the photosynthetic pathway. It is suggested that excess electrons are transported more efficiently from the photosystems in these transgenic lines, which prevents photoinhibition. The ferredoxin proteins are also shown to donate electrons to processes that activate ADP glucose pyrophosphorylase and to fatty acid desaturases (Huang et al., 2015). High salt also inactivates ATP-synthase which in turn prevents protein synthesis (Allakhverdiev et al., 2005). ATP and NAD(P)H are also required for fatty acid biosynthesis, so it would inhibit this activity too (Mühlroth et al., 2013).

Salt causes two types of stress: ionic stress and osmotic stress (Allakhverdiev et al., 2000). Green microalgae tolerate osmotic stress using osmoregulation and the formation of a compatible solute, which is often glycerol. The source of carbon for the glycerol can come from starch breakdown, since the high salinity inhibits photosynthesis (Goyal, 2007). In Experiment 1, starch in 0.2 and 0.3 M NaCl cultures is broken down steadily after an initial increase, although this may solely be due to culture death and cell lysis. The reason for the increase in 0.2 M NaCl cultures at 76 hours is not clear. In the 0.1 M NaCl cultures, starch breakdown does not appear to be taking place, which conflicts with the idea of Goyal (2007) on starch breakdown for the production of compatible solutes.

The severe decrease in photosynthetic ability in this study, however shows that salt tolerance mechanisms do not protect sufficiently against the toxic effects of salt stress in this species. Unlike many species that respond to salt stress by changing their lipid profile and accumulating unsaturated fatty acids, especially oleic acid, this strain does not. Although *C. reinhardtii* has the ability to accumulate fatty acids under nitrogen stress, it does not employ this ability as a mechanism against salt stress.

### 4.5.3 Insights of proteomics on metabolic changes due to salt stress

To gain insights into the salt stress responses and how lipid metabolism is affected by salt in *C. reinhardtii*, the metabolic data from Experiment 2 was used as a basis for proteomic investigation using iTRAQ.

There are some common patterns that emerged in the four comparisons made in the iTRAQ experiment, comparing both salt stress in a time course, and salt stress against a non-stressed control in mid log phase. In every case, photosynthesis and carbon fixation were negatively impacted by the exposure to salt stress. In all four cases, aldehyde-alcohol dehydrogenase was up-regulated. This enzyme acts specifically to mitigate oxidative stress to try to prevent lipid peroxidation (Singh et al., 2013). Starch synthase was also up-regulated in every case, and carbohydrate was significantly affected by the presence of salt, suggesting that carbohydrates regulation is important in salt response. The phenotypic changes in starch levels may not be as dramatic as those seen in a wild-type strain, and it is important to remember that this is a low-starch mutant strain.

The regulation and metabolism of acetyl CoA provided the best insights into why lipids were not accumulating in this species. Acetyl-CoA synthetase was down-regulated between 3 and 11 hours salt stress but was unchanged in other comparisons. This is involved in the metabolism of acetate to produce acetyl-CoA, an important compound in fatty acid synthesis and in cellular metabolism, showing that the initial salt response may have detrimental effects on the uptake of carbon from acetate. Additionally, acetyl CoA acyltransferase was up-regulated in every comparison except the 11 to 18 hour comparison, an enzyme involved in fatty acid catabolism and the oxidation of very long chain fatty acids.

The up-regulation of citrate synthase between 11 and 18 hours and between 3 and 18 hours is important, as this indicates the diversion of acetyl CoA into the TCA cycle, resulting in a reduced availability of substrate for fatty acid synthesis (Deng et al., 2013; Martin et al., 2014).

Finally, a acetyl CoA carboxylase subunit was down-regulated between control and salt stressed conditions at 18 hours. This shows down-regulation of a rate limiting step of

fatty acid biosynthesis. Combined with the reduced availability of acetyl CoA suggested from down-regulation of acetyl CoA synthetase and the up-regulation of citrate synthase, this evidence suggests that under salt stress the channeling of acetyl CoA into fatty acid synthesis is severely reduced.

Interestingly, glycerol-3-phosphate dehydrogenase was up-regulated in every comparison, indicating that metabolism of glycerol is a consistent cellular response to salt stress, and that it is likely to be a result of using glycerol formation as a compatible solute that helps mitigate the osmotic effects of salt stress.

Glyceraldehyde-3-phosphate dehydrogenase was up-regulated from 11 to 18 hours and 3 to 18 hours, but not in the other comparisons. Betaine lipid synthase was down-regulated in the 11 to 18 hour comparison, but not in any other comparison.

Other than the effects of salt in reducing growth, the main effects appear to be differences in carbohydrates and their metabolism. Lipids were not greatly affected in the FAME data but a few findings in the proteomic data suggests that lipid metabolism is de-prioritised. The analysis of the proteomic effects of salt have revealed a number of tolerance mechanisms that may aid the culture in survival in such a detrimental growth environment, including glycerol and proline synthesis.

#### 4.5.4 Further investigations

This is the first study to focus on the links between salt stress and lipid metabolism in this species using proteomic data, and there is evidence that lipid metabolism was down-regulated under salt conditions.

To further investigate why changes in lipid abundance were not observed in Experiment 2 (either as a salt tolerance mechanism or for energy storage), proteomic data will be compared to a second iTRAQ study of a salt tolerant, lipid producing *Chlamydomonas* species. This will be used to investigate possible targets for genetic engineering of improved salt tolerance and corresponding lipid accumulation improvements in *Chlamydomonas*. Therefore, the effect of salt stress on lipid metabolism in snow alga *C. nivalis* will be investigated in the following chapter using the same metabolomic and proteomic techniques as in *C. reinhardtii*.

## 5 Chapter 5: The Effect of Salt Stress on Lipid Metabolism of *Chlamydomonas nivalis*

### 5.1 Summary

This chapter explores the effect of salt stress on lipid metabolism in *C. nivalis*, using GC-FID FAME analysis and a proteomic investigation via iTRAQ. 0.2 M NaCl was found to be both inhibitory to cell division and a lipid trigger in *C. nivalis*, which accumulated a high amount of C18:1*cis* compared to a control condition with no additional salt in the medium. Carbohydrates were found to increase under salt stress in the first half of the growth cycle, and then decrease as lipids began to accumulate. Photosynthesis was reduced under salt stress. iTRAQ experimentation revealed down-regulation of many important proteins under salt stress (both in a time course experiment and using a control as a reference), including those involved with carbon fixation, photosynthesis, glycolysis. Important effects on carbohydrate metabolism proteins and lipid metabolism proteins were discussed; the increase in lipid accumulation was not linked to up-regulation of any major lipid pathways, although increased production of acetyl CoA may play an important role. This study is the first to investigate the un-sequenced snow alga *C. nivalis* using proteomic analysis, and its relatedness to *C. reinhardtii* (tested here with genetic analysis) allowed detailed proteomic investigation using a combination of powerful MS/MS machinery, *de novo* sequencing software and protein homology searching.

### 5.2 Introduction

The suitability of the snow algal species *Chlamydomonas nivalis*, as a biofuel producer, especially when cultured under different environmental conditions, has received little attention in the literature. This chapter aims to address this by assessing its suitability by measuring its lipid yield and profile, and biomass accumulation. As *C. nivalis* has a high salt tolerance of 1.2 M NaCl (Lu et al., 2012b), an environmental condition of particular interest is the impact of salt stress upon energy storage molecules within the cells, in particular the lipid profile. Consequently, the impact of a high salt stress condition upon the processes by which *C. nivalis* regulates carbon storage molecules,

pigments, photosynthetic and respiration rates were investigated, in comparison to a control salt-free culture condition. After preliminary investigation using a range of salt conditions, a high salt concentration of 1.4 M NaCl was chosen to investigate this, as the effects of using a salt concentration beyond the tolerance limit of 1.2 M NaCl could show whether *C. nivalis* produces the same sudden effect of FAME accumulation that *C. reinhardtii* does under high salt concentrations beyond its tolerance (0.3 M NaCl, as found in the previous chapter). Preliminary testing of a range of low and high salt concentrations was carried out with one biological replicate; thus all data where n=1 are subsequently referred to as "preliminary data", and those were only used as a guideline to inform subsequent experiments. Subsequent experiments used 0.2 M NaCl, as a follow up to an interesting trend observed in preliminary data. At this low level of salt stress the halotolerant *C. nivalis* species maintains culture growth, but with some interesting effects on its physiology and demonstrates the use of salt as a lipid trigger in this species. These effects were explored using an iTRAQ investigation of conditions associated with lipid triggering in *C. nivalis*.

The experiments were carried out using the growth set up described in section 2.3 in Chapter 2. This growth set up was very different to the conditions used for *C. reinhardtii* due to the requirements for a low specific temperature, and for bubbling with air using CO<sub>2</sub> as the sole carbon source. However, since these species have different growth requirements, growth conditions were set up that allowed control cultures to grow well. Growth medium 3N-BBM-V was used to grow *C. nivalis* as this was the growth medium recommended by the CCAP. It has also been shown that BBM medium allows better growth rates than TAP medium and is the optimal growth medium for *C. nivalis* (Yu-huan et al., 2009). BBM medium was also the medium used by previous studies that examined biomarkers in *C. nivalis* due to salt stress (Lu et al., 2012a; Lu et al., 2013; Lu et al., 2012c).

The limitation in lighting the growth set up for *C. nivalis* meant that the light intensity was lower than that used for *C. reinhardtii*. *C. nivalis* could be grown at a much higher light intensity, since it is highly UV tolerant (Remias et al., 2005), however in this case the light intensity was lower due to restrictions of equipment. Nevertheless, previous

experiments on *C. nivalis* by Lu et al. (2012c) used illumination of 2000 lux, which is approximately 60 microeinsteins/m<sup>2</sup>/second. This shows that relatively low irradiance is suitable for growth of this species. Additionally, growth of *C. nivalis* at a low irradiance helps in assessing the suitability of this species for low light and temperature requirements. Experimental design is detailed in Table 2.1 in Chapter 2.

### 5.3 Preliminary data

#### 5.3.1 Growth

##### 5.3.1.1 Optical Density

Figure 5.1 shows the optical densities (OD) of five different cultures of *C. nivalis* grown in varying salt concentrations. All the tested salt concentrations were observed to have a negative impact upon the optical density of *C. nivalis* cultures, indicative of reduced growth. The 0.2 and 0.5 M NaCl cultures still show signs of optical density increase over time, suggesting that the growth is not completely arrested as it appears to be in 1.0 and 1.5 M NaCl concentration cultures. The high salinity cultures (1.0 and 1.5 M NaCl) have a slightly higher OD after 3 hours, indicating an immediate effect of salt on culture density. These cultures were grown to a high culture density before introducing the salt stress, as it was desirable to have a high quantity of biomass to perform assays on during sampling time points.

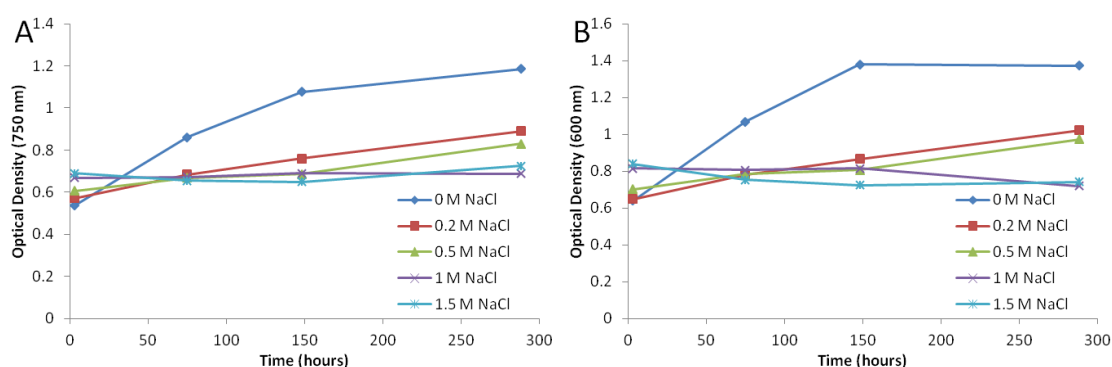


Figure 5.1 Optical density at 750 nm (A) and 600 nm (B) of *C. nivalis* grown under 0, 0.2, 0.5, 1 and 1.5 M NaCl (n=1). Cells were grown in normal 3N-BBM-V medium and then resuspended in the new salinity medium at time zero.

### 5.3.1.2 Dry Cell Weight

Figure 5.2 shows the biomass content of the preliminary *C. nivalis* salt experiments. At a low salt concentration of 0.2 M NaCl, the cultures can still reach a high level of biomass comparable to the control conditions. The cultures at 0.5, 1.0, 1.5 M NaCl remain relatively low in biomass content particularly in the latter stages of the culture, although the first time point for the 0.5 M NaCl culture is very high.

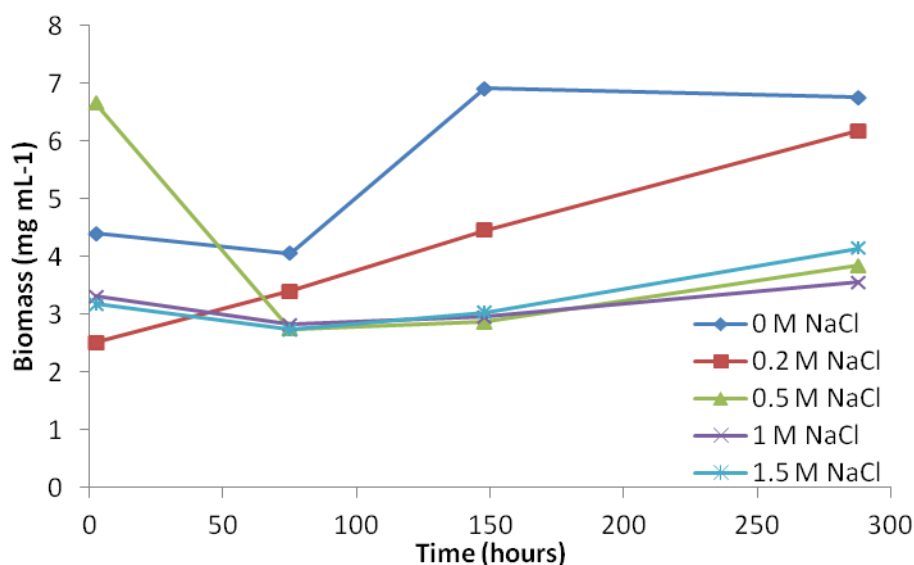


Figure 5.2 Biomass content of *C. nivalis* cultures under 0, 0.2, 0.5, 1 and 1.5 M NaCl (n=1). Cells were grown in normal 3N-BBM-V medium and then resuspended in the new salinity medium at time zero.

### 5.1.2 FAME analysis

Lipid analysis was carried out on the preliminary test *C. nivalis* cultures at various concentrations of salt stress. Figure 5.3 shows the total FAME content over time in each of these conditions. There are no repeats or error bars so these can only be used as a rough guideline for exploring the effect of these salinities on FAME content. The highest lipid concentration was seen in the 0.2 M NaCl culture. The control culture showed an accumulation of lipids in the last sample (t=288 hours) of the time point series. The 0.2, 1.0 and 1.5 M concentrations show an initial increase in the first time point (t=3) above the other conditions. The 0.5 M NaCl culture showed an increase at the second time point, but then decreases in total FAME content. The higher NaCl

concentrations of 1.0 and 1.5 M NaCl cause an overall steady decrease in overall FAME content.

To look at how the FAMES are responding to the different salt concentrations, the main FAMES were analysed in isolation (chain lengths between C16 and C18) over time (Figure 5.4). C16:0 rises over time in the control culture conditions and in 0.2 and 0.5 M NaCl, but stays at a low steady level in the high salt 1.0 M and 1.5 M NaCl conditions (Figure 5.4 A). Similarly C17:0 (Figure 5.4 B) rises over time in the control culture and in the 0.2 M NaCl conditions. The 0.5 M NaCl conditions shows an initial increase in C17:0 at t=75 hours and then a decrease after this point. In contrast, the 1.0 M and 1.5 M NaCl cultures show a steady decrease over the time course, almost to zero (t=288 hours).

Figure 5.4 C shows an initial increase in C18:0 in 0.2 M NaCl at the first time point (t=2.5 hours) but then plateaus followed by a decrease. The control conditions and 0.5 M NaCl conditions show an increase at the second time point only (t=75 hours), followed by a return to the levels similar to those of the first time point (t=2.5 hours). The 1.0 M and 1.5 M NaCl show a decrease in C18:0 overall, to the point that it disappears from the culture towards the end of the time course (t=288).

The 0.2 M NaCl culture shows a very large increase in C18:1*cis* over time (Figure 5.4 D). The control culture shows that C18:1*cis* accumulates a lot in the last time point (t=288 hours) after remaining at a low level. In the higher salt stressed cultures of 0.5 M, 1.0 M and 1.5 M NaCl the levels of C18:1*cis* remain low.

The patterns of C18:2*cis* are quite varied (Figure 5.4 E) and appear to dip to zero in the middle (t=148 hours) of the 0 M and 0.2 M time course experiments. Again as with C16:0, C17:0 and C18:1*cis*, the control conditions and 0.2 M NaCl conditions end in high accumulation of the FAME at the last time point (t=288 hours). The higher salt concentrations (1.0 M and 1.5 M NaCl) show a steady decrease in the abundance of the FAME.

The 1.0 M and 1.5 M NaCl conditions show a steady and marked decrease in the abundance of C18:3*n3*. 0.5 M NaCl shows a spike at the second time point (t=75

hours), followed by a decrease (although more gradual than that seen in higher salt concentrations). The content of C18:3n3 stayed fairly steady in the presence of 0.2 M NaCl with only a slight decrease. The control conditions show a similar pattern to the 0.5 M NaCl conditions, with a spike at the second time point (t=75 hours) (Figure 5.4 F).

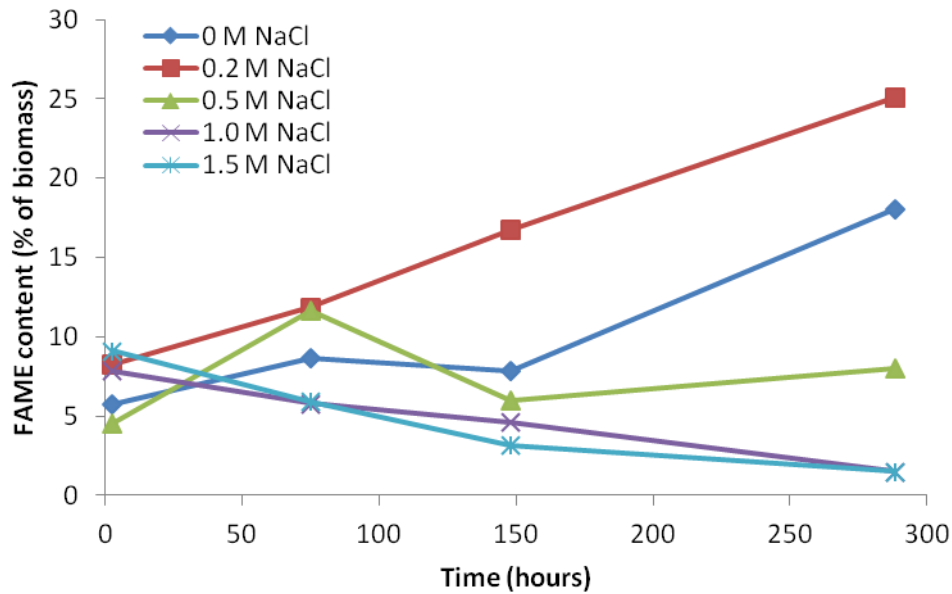


Figure 5.3 Total FAME content in *C. nivalis* cultures under 0, 0.2, 0.5, 1 and 1.5 M NaCl (n=1). Cells were grown in normal 3N-BBM-V medium and then resuspended in the new salinity medium at time zero.

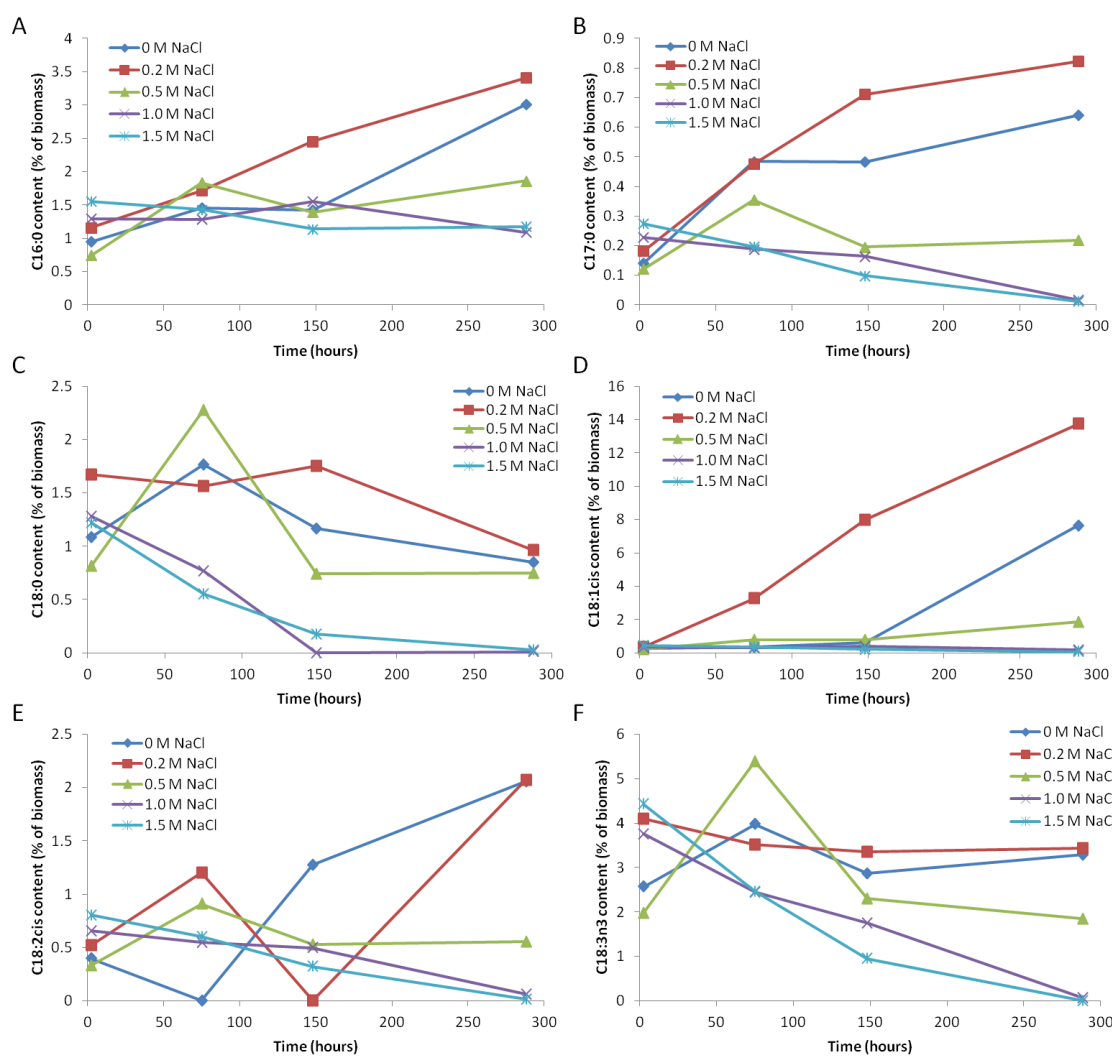


Figure 5.4 Total amounts of individual FAMES present in 0, 0.2, 0.5, 1 and 1.5 M NaCl: C16:0 (A), C17:0 (B), C18:0 (C), C18:1cis (D), C18:2cis (E), C18:3n3 (F) (n=1). Cells were grown in normal 3N-BBM-V medium and then resuspended in the new salinity medium at time zero.

### 5.1.3 Carbohydrate content

Figure 5.5 shows the carbohydrate content of *C. nivalis* under varying salt conditions. The control conditions and the 0.2 M NaCl conditions reached the highest levels of carbohydrate content seen in any of these samples. The control conditions have a slow increase in carbohydrate content up until the third time point (t=148 hours), then this plateaus. The 0.2 M NaCl stressed culture starts with a higher carbohydrate content than the control, peaks at the second time point (t=75 hours), and then gradually decreases. The highest salt concentration, 1.5 M NaCl also starts significantly higher than the control conditions, but then dips slightly (t=75 hours) and stays relatively low

where the control conditions have an increase. A similar pattern of carbohydrate content staying below 3% of total DCW is observed in the 0.5 M and 1.0 M NaCl cultures.

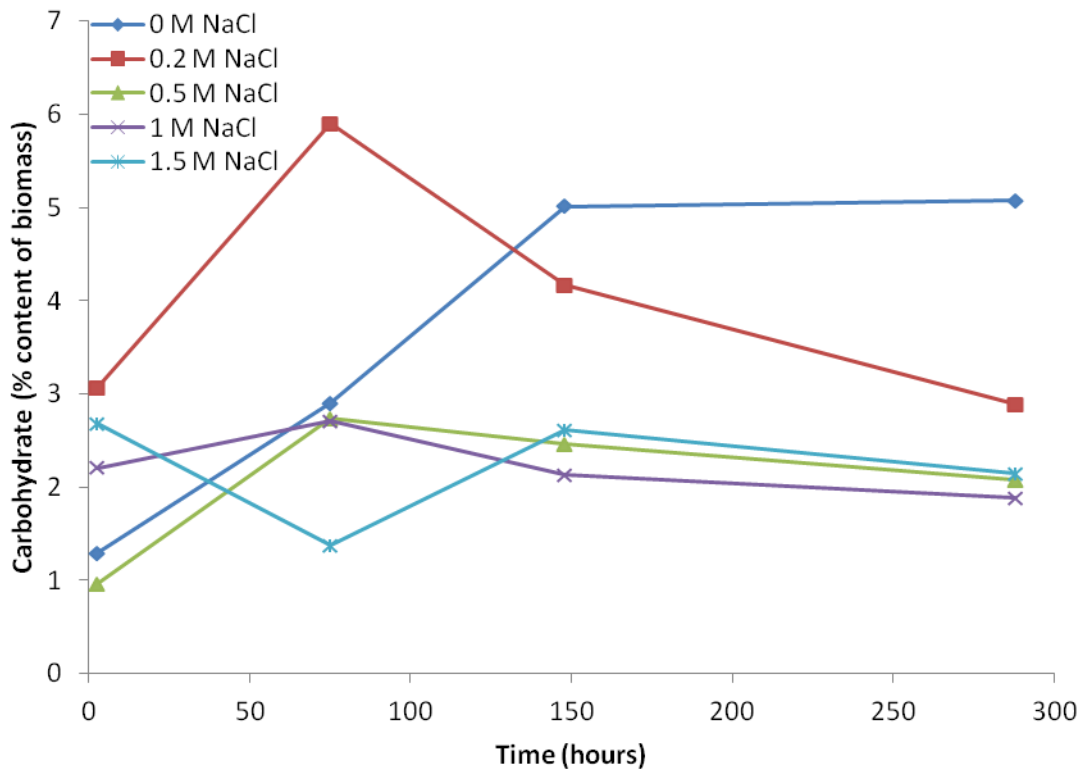


Figure 5.5 Carbohydrate content of *C.nivalis* cultures grown in 0, 0.2, 0.5, 1 and 1.5 M NaCl (n=1). Cells were grown in normal 3N-BBM-V medium and then resuspended in the new salinity medium at time zero.

#### 5.1.4 Chlorophyll content

Figure 5.6 shows the chlorophyll *a*, chlorophyll *b* and carotenoid content of cultures under the different salt concentrations. Carotenoids show a much lower value in the high salt concentrations of 0.5, 1 and 1.5 M NaCl than in the 0 and 0.2 M NaCl. However, chlorophyll *a* and chlorophyll *b* do not show clear patterns of being detrimentally affected by high salt. The data shows some variation between conditions but most conditions follow a similar pattern of peaking at time point 75 hours, and then gradually decreasing, both in the chlorophyll *a* and chlorophyll *b*. The exception to this is the 0.2 M NaCl condition, which shows both these pigments at a very high level after 3 hours, and then gradually decreasing over time. Chlorophyll *b* is highest at

time point 75 hours in the 1 M NaCl, with the next highest being 0.5 and 1.5 M NaCl. Whilst this data has only one biological repeat so strong conclusions cannot be drawn from it, there is some indication that chlorophyll *b* shows increases under high salt conditions in the earlier stages of the culture cycle.

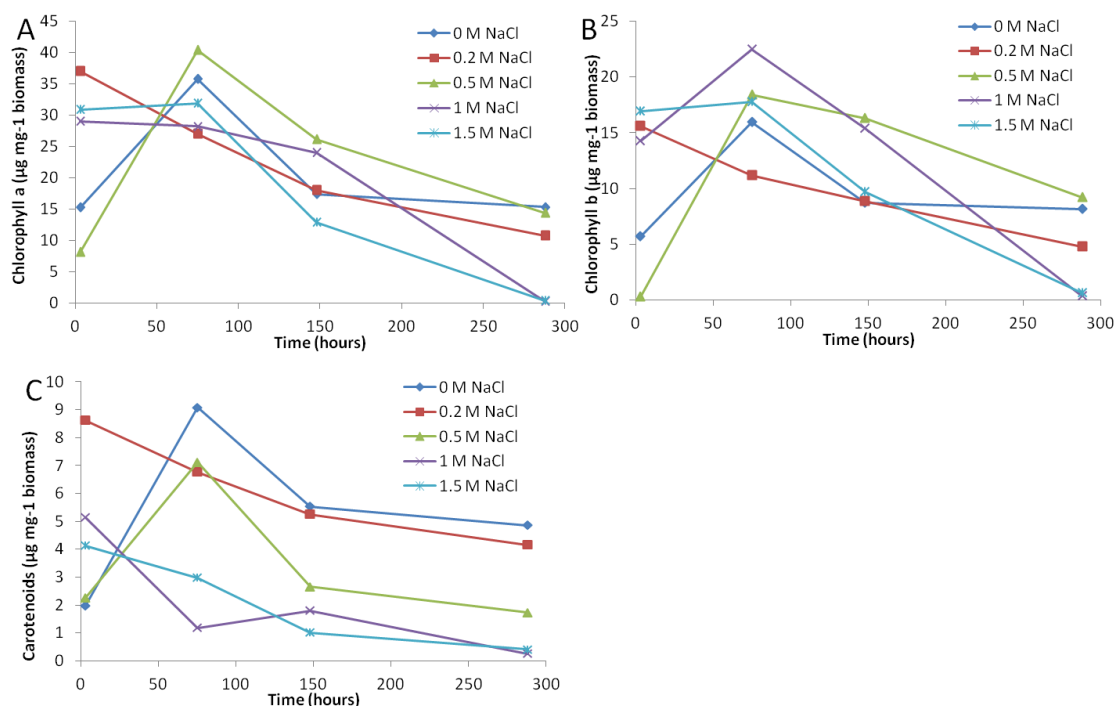


Figure 5.6 Chlorophyll a (A), chlorophyll b (B) and carotenoid (C) content of *C. nivalis* cultures grown in 0, 0.2, 0.5, 1 and 1.5 M NaCl ( $n=1$ ). Cells were grown in normal 3N-BBM-V medium and then resuspended in the new salinity medium at time zero.

### 5.3.2 Conclusions from preliminary data

This data is preliminary in nature, having only 1 biological repeat. It therefore cannot be used to draw scientific conclusions or discussion, but has been reported to show how the subsequent choice of salt conditions was selected for investigation into lipid accumulation and salt tolerance in *C. nivalis*.

From this data, 0.2 M NaCl showed promising results in increasing the total FAME content of the algal cultures. This salt concentration was pursued using full biological repeats as a lipid trigger in *C. nivalis*. The effect of high salt (1.4 M NaCl) beyond the tolerance of *C. nivalis*, was also pursued as a comparison of how toxic levels of salt can affect this species.

## 5.4 Response of *C. nivalis* to high salt (1.4 M NaCl)

### 5.3.1 Effect of high salinity (1.4 M NaCl) stress on optical density

Figure 5.7 shows the optical density of control cultures and 1.4 M NaCl stressed cultures. The growth differs a lot from that seen in *C. reinhardtii* cultures, as the growth curve is shallow and steadily increasing. The photoautotrophic growth of *C. nivalis*, even in the absence of salt, is slower than that seen for *C. reinhardtii* grown in TAP medium which contains acetate. This is because the additional carbon source in TAP medium allows faster growth, and the irradiance is lower in the *C. nivalis* set up. The reasons for this difference in set up were to establish growth conditions suitable for the individual species, as previously discussed. The high salinity of 1.4 M NaCl causes an arresting of the culture growth and a slight decrease over time in optical density. These conditions are therefore clearly detrimental to the functioning of the algal culture.

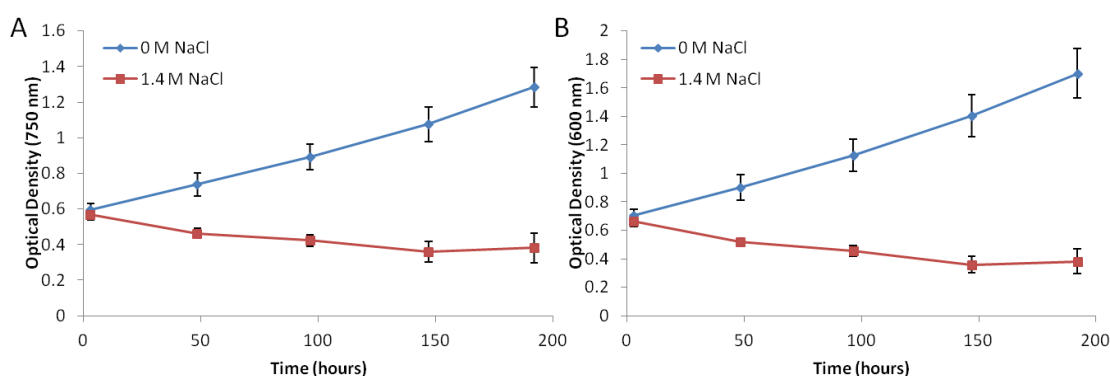


Figure 5.7 Optical density at 750 nm (A) and 600 nm (B) of *C. nivalis* cultures grown in control (0 M NaCl) and 1.4 M NaCl conditions (n=3). Cells were grown in normal 3N-BBM-V medium and then resuspended in the new salinity medium at time zero.

### 5.3.2 Effect of high salinity (1.4 M NaCl) stress on biomass content

Figure 5.8 shows the biomass content of the 1.4 M NaCl and control conditions growth of *C. nivalis*. The 1.4 M NaCl conditions completely arrested the accumulation of biomass, showing that these conditions stop the normal proliferation of the culture

seen in the control conditions. The growth of the culture, even in the absence of salt, is gradual and slow in comparison to the *C. reinhardtii* growth rates.

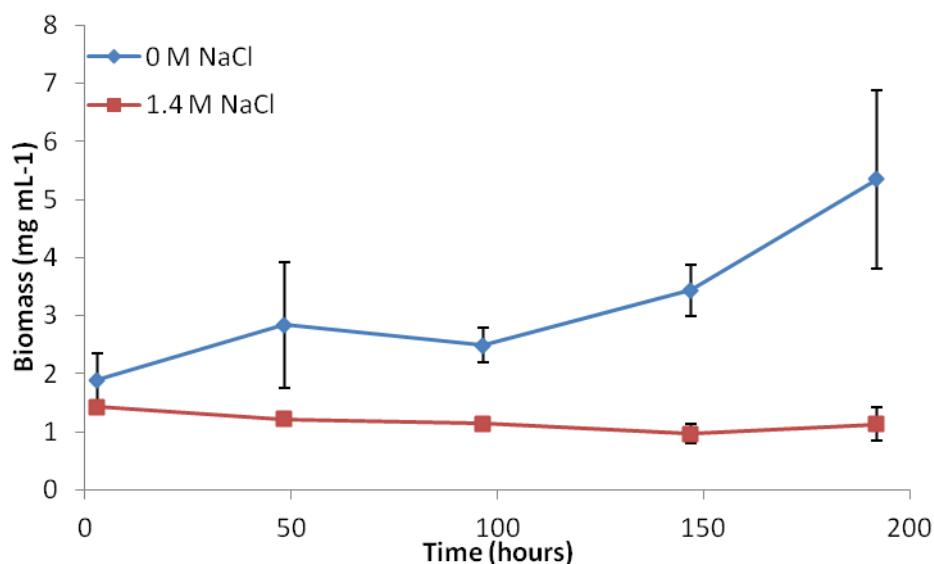


Figure 5.8 Biomass content of *C. nivalis* cultures in 1.4 M NaCl and control (0 M NaCl) conditions (n=3). Cells were grown in normal 3N-BBM-V medium and then resuspended in the new salinity medium at time zero.

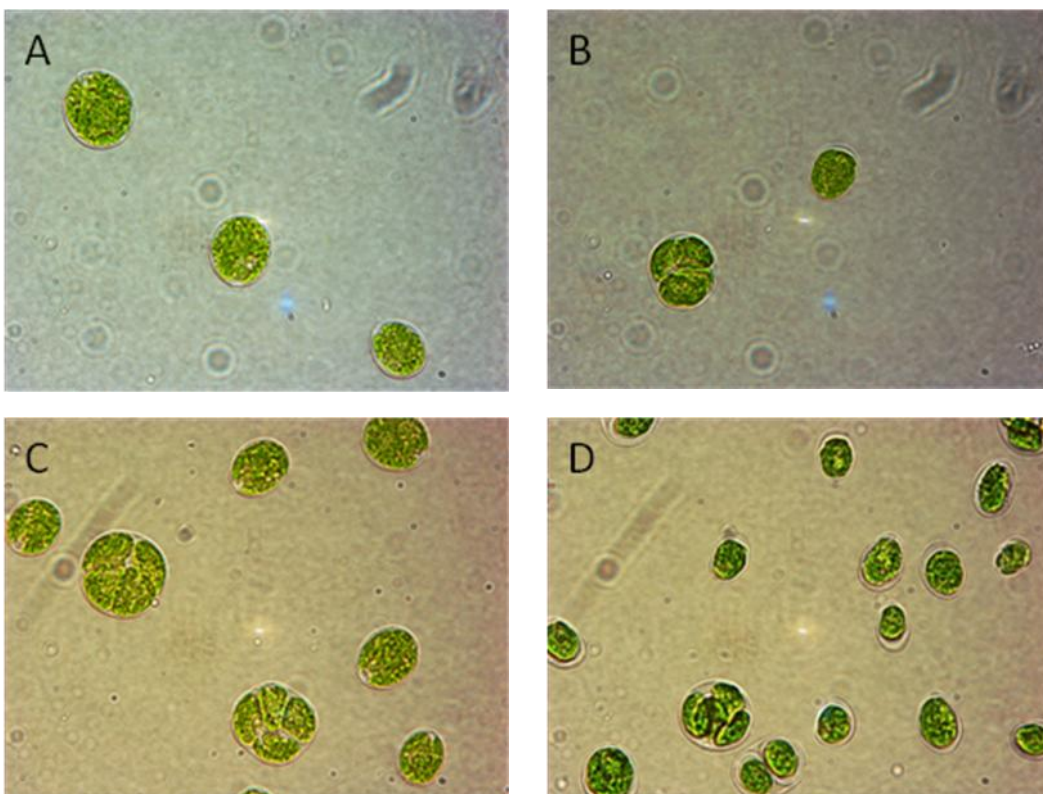
For the experiments that follow concerning FAME content (section 5.3.4) and carbohydrate content (section 5.3.5), biomass was used to standardize results. Experiments were conducted with *C. nivalis* to correlate OD and biomass with cell counts. The data are shown in Appendix D.

### 5.3.3 Effect of High Salt (1.4 M NaCl) on Cell Morphology

Figure 5.9 shows the morphology of *C. nivalis* cells under control conditions and salt stress. The first three time points show that the salt stressed cells retain green pigmentation from chlorophyll up until 96 hours (Figure 5.9 B, D and F) in even this very high salt concentration. The last two time-points (Figure 5.9 H and J) show that later in the culture, the cells lose their pigmentation. The ability of the cells to stay green for many hours after the introduction of high salt stress suggests that this species has good tolerance to salt, and can keep their shape and colour for a relatively long time before succumbing to loss of pigmentation or function. This contrasts with data discussed below which shows that these cells are not photosynthesising under

high salt stress, and therefore it may be expected that toxic salt levels would kill the cells quickly. However, cell degradation appears to be a slower process even if normal biological processes are not taking place. A study by Affenzeller et al. (2009) demonstrated the gradual decline in cell viability in an algal culture subjected to salt stress. The decline was due to programmed cell death, but showed that after 12 hours subjected to detrimental salt stress levels, 80% of cells remain viable. This remains similar until 24 hours and drops to 40% after 48 hours. The cells showed an immediate increase in ROS production at 3 minutes after the introduction of salt stress, but these ROS levels decline dramatically over the course of 3 hours.

Cell viability was not tested here, but it seems likely that due to the presence of intact pigmented cells up until 96 hours, the culture is not completely undergoing cell death (either apoptosis or necrosis) until after this point.



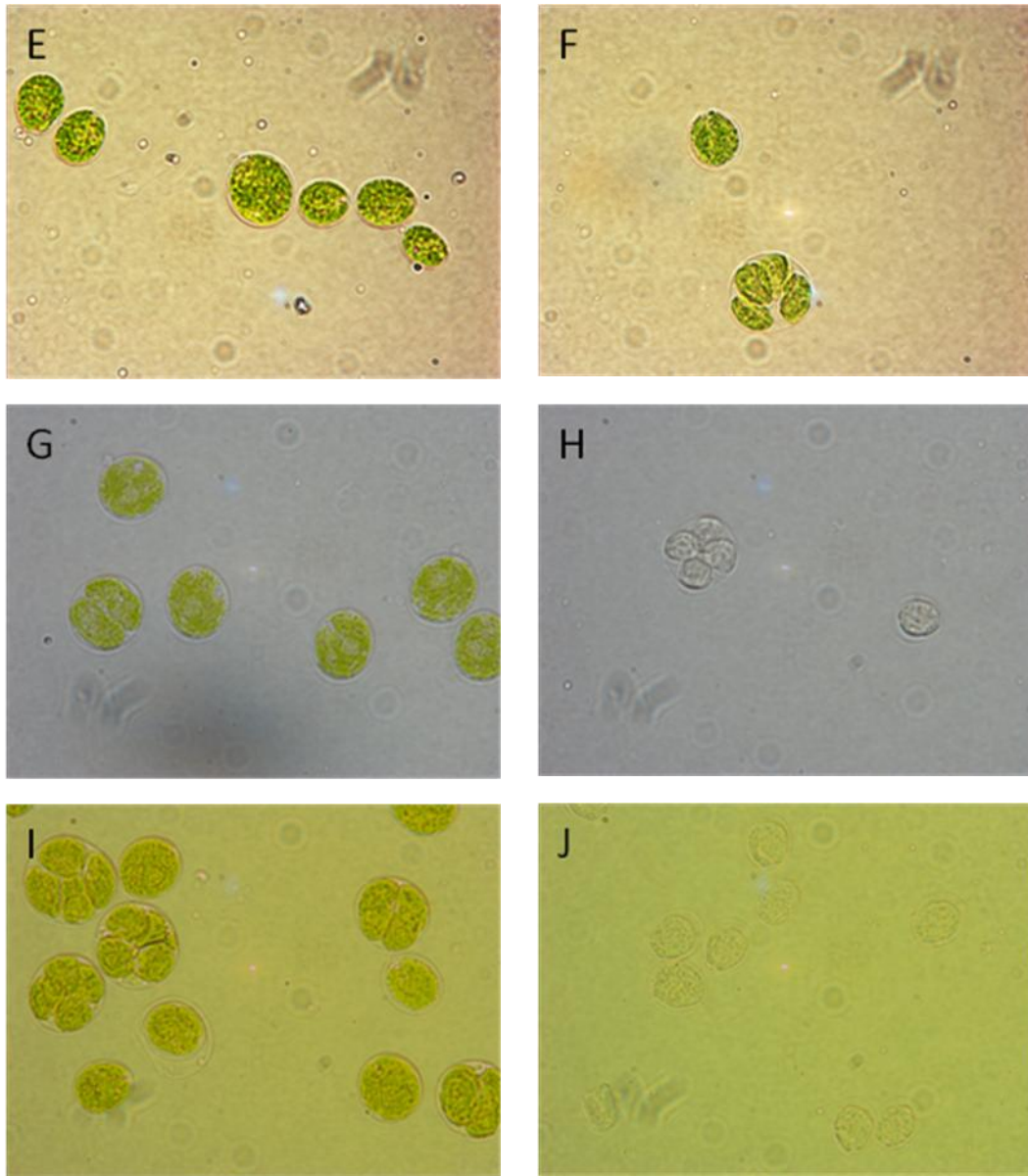


Figure 5.9 Microscopy of *C. nivalis* cells under control conditions (A, C, E, G, I) and 1.4 M salt stress (B, D, F, H, J) at time points 3 (A, B), 48 (C, D), 96 (E, F), 147 (G, H), 192 (I, J) hours (at x1000 magnification).

#### 5.3.4 Effect of Adding 1.4M NaCl on FAME Content of *C. nivalis*

Figure 5.10 shows the total FAME content of *C. nivalis* grown in control conditions (no salt) and high salt stressed conditions of 1.4 M NaCl. The control culture conditions show an increase in total FAME content after 48 hours, which stays at a steady rate. In contrast, the salt stressed cultures show a steady decrease in FAME content from the start of the culture. As the cultures appear to be turning into "ghosts" (from the microscopy seen in Section 5.2.3 towards the end of the time course series, the

degradation of FAMES fits with this. The composition of FAMES was analysed to see how individual FAMES responded to these high salt stress conditions.

Looking at the main FAMES that appear (the C16 to C18 chain lengths) helps to identify how the salt stressed cultures are responding. These individual FAMES are shown in Figure 5.11. In the control (no salt) conditions the C18:3n3 FAME is a large part of the FAME profile throughout the time course, but in the salt stressed conditions, this polyunsaturated FAME disappears towards the end of the time course experiment (t=147 and t=192 hours). C16:0 remains fairly constant in the FAME profile, both in the control and the salt stressed conditions.

In the control conditions, the C18:3n3 decreases at the second time point (t=48 hours) but then rises again. This seems to be a large part of what is contributing to the total FAME increase observed in Figure 5.10. This same pattern is seen in C17:0, C16:0, and C18:0. In contrast the majority of major FAMES decrease drastically under high salt conditions. There is a pattern towards the end of the time course series in the control conditions of some FAMES starting to decrease again, namely C18:3n3, C17:0, C16:0 and C18:0; whilst this is happening certain FAMES increase in abundance towards the end of the time course, namely C18:1*cis* and C18:2*cis*.

The pattern of FAMES in the control conditions is decreasing at the second time point (t=48 hours), and then tending to increase again at the third time point (t=96 hours). This does not appear to match any change in growth rate, so the reason for this is not clear. With the exception of C16:0, the high salinity caused the FAMES to decrease almost to zero in all of the main FAMES analysed here (C16 to C18 chain lengths).

The profiles were analysed by grouping detected FAMES into SFAs, MUFAs and PUFAs (Figure 5.12). Whilst the FAME profile remains fairly consistent in the control conditions, with a slight increase in the proportion of SFAs and MUFAs found at 96 hours onward, salt conditions showed a large shift in the profile of detected FAMES towards SFAs. This is due to the decline in MUFAs and PUFAs observed in Figure 5.11. SFAs appear to be the most resilient FAs during degradation of the FAMES in the dying cultures.

Free radicals, such as ROS induced by salt stress, cause degradation of polyunsaturated fatty acids in membranes (Nagalakshmi and Prasad, 1998). The reduction in PUFAs can therefore be explained by the presence of toxic salt stress. Saturated fatty acids were not reported to undergo the same peroxidation reaction, and the ratio of UFAs to SFAs can decrease due to lipid peroxidation (Blokhina et al., 2003). PUFAs are far more susceptible to peroxidation than SFAs (Kang et al., 2005).

The degradation of PUFAs first has been noted previously in microalgae (Hamm and Rousseau, 2003), causing the relative shift towards higher ratios of saturated fatty acids to unsaturated fatty acids.

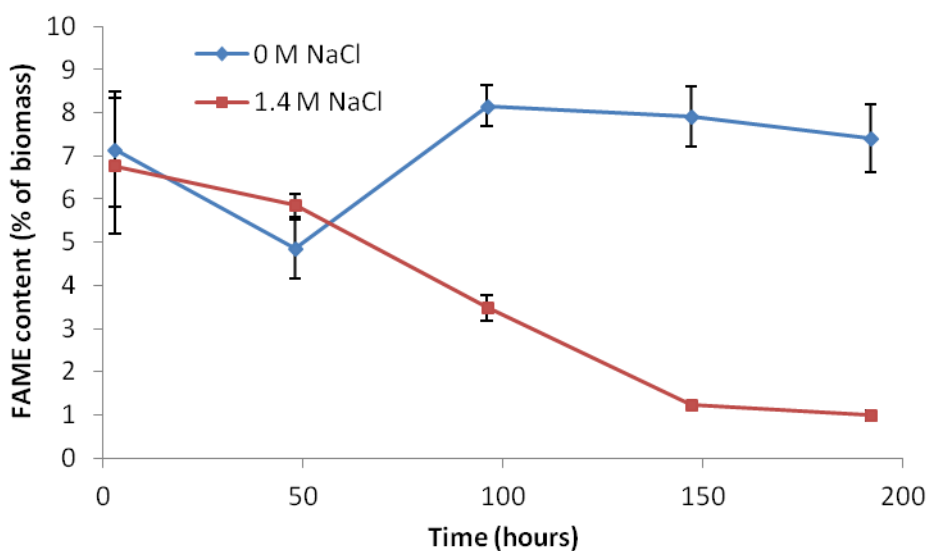


Figure 5.10 Total FAME content of dry algal biomass under control and 1.4 M NaCl conditions (n=3). Cells were grown in normal 3N-BBM-V medium and then resuspended in the new salinity medium at time zero.

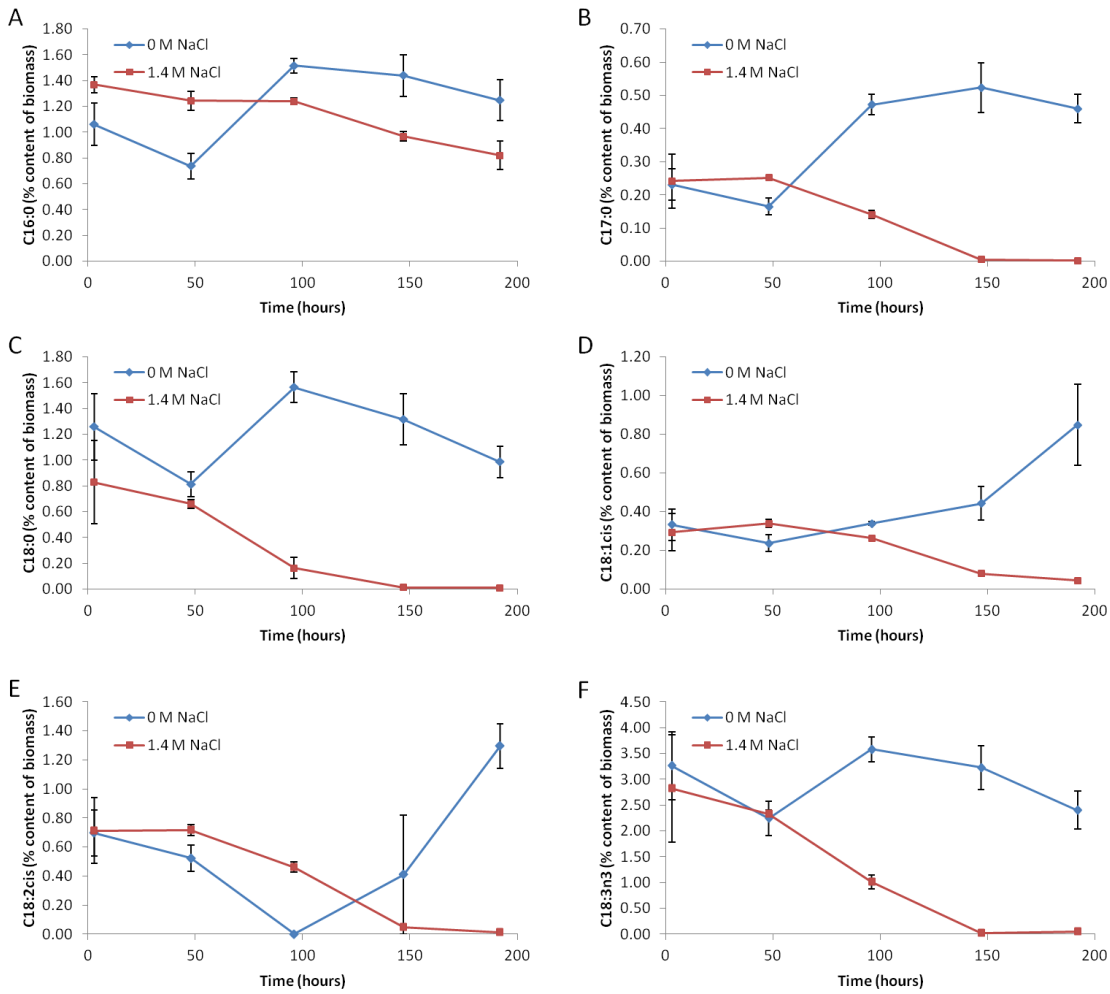


Figure 5.11 Individual FAME contents found in control conditions and 1.4 M NaCl conditions (n=3). Cells were grown in normal 3N-BBM-V medium and then resuspended in the new salinity medium at time zero.

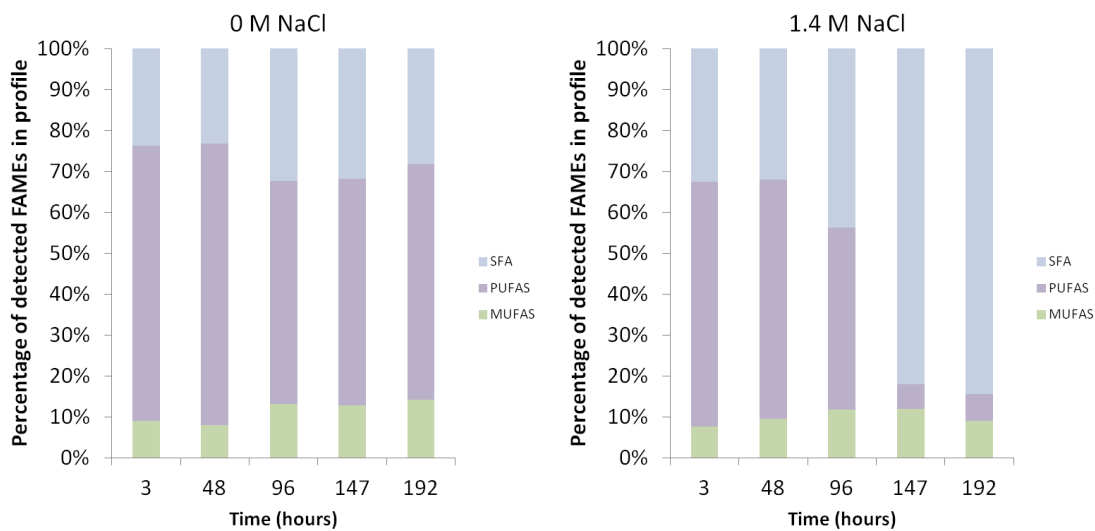


Figure 5.12 Relative percentage of SFAs, MUFAs and PUFAs found in control (0 M NaCl) and 1.4 M NaCl conditions (n=3). Cells were grown in normal 3N-BBM-V medium and then resuspended in the new salinity medium at time zero.

### 5.3.5 Effect of Adding 1.4 M NaCl on Carbohydrate Content

Figure 5.13 shows the carbohydrate content of the control cultures and 1.4 M NaCl stressed cultures. There is a lot of variation at some of these time points, however some clear patterns are shown. The salt stressed cultures start with a significantly higher carbohydrate content than the control (no salt) cultures. This carbohydrate level stays relatively steady in abundance in the biomass. In the control conditions, however, the carbohydrate content starts much lower and rises at the third time point (t=98 hours) to the same level as the salt stress culture. This suggests that carbohydrate synthesis is increased in response to salt stress in a way that is only seen in the latter growth cycle of cells incubated in no salt medium.

Accumulation of carbohydrate is linked to photosynthetic production in excess of protein synthesis requirement (Foy and Smith, 1980). This culture is not showing signs of photosynthetic activity (discussed below), so this would not cause carbohydrate accumulation in this species.

High salt stress in marine algal species caused initial increases in starch content, followed by decreases to a level below that of the lower salinities, which increased towards the end of the time course (Yao et al., 2013). The initial rise in starch content of salt stressed cultures which is only seen in the latter stages of control cultures is similar to that observed here.

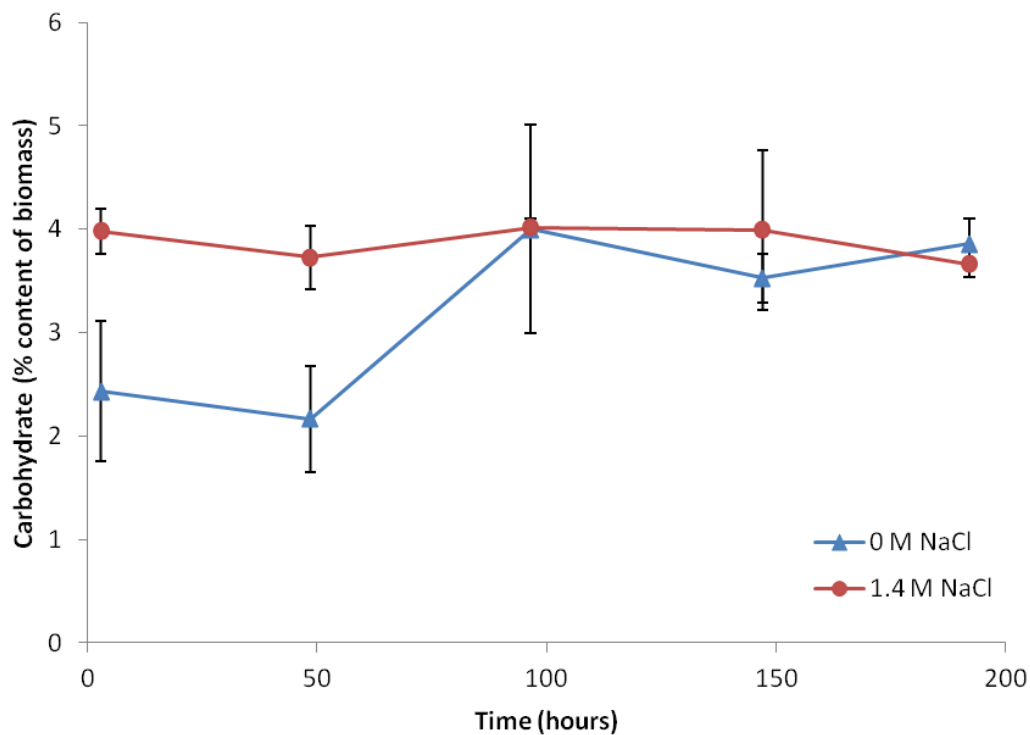


Figure 5.13 Carbohydrate content of *C. nivalis* under control and 1.4 M NaCl conditions (n=3). Cells were grown in normal 3N-BBM-V medium and then resuspended in the new salinity medium at time zero.

Figure 5.14 shows the chlorophyll *a*, chlorophyll *b* and carotenoid content of *C. nivalis* under control conditions and 1.4 M NaCl conditions. Chlorophyll *a* stays relatively level in the control conditions but starts to gradually decrease after 96 hours. In the 1.4 M NaCl conditions, the chlorophyll *a* starts slightly higher at the first time point of 3 hours but then decreases over time. This decrease is gradual at first but then steeply declines after 48 hours to virtually zero. Chlorophyll *b* shows a very similar pattern both in the control and the 1.4 M NaCl conditions to the chlorophyll *a* response. The carotenoids rise slightly in the 1.4 M NaCl condition, before again falling steeply to virtually zero, whilst in the control conditions show a sharp decline at the second time point of 48 hours before rising again at 96 hours and then a slight decrease towards the final time point (t=192 hours).

The level of salinity of 1.4 M clearly has a degrading effect on photosynthetic pigments. During cell death in algae, loss of pigments takes place after the cell membranes have been compromised (Veldhuis et al., 2001). This appears to be what is

taking place here. Since this species has a high salinity tolerance, the membranes may have a greater ability to stay intact than non halotolerant species, allowing this degradation to take place slowly, over time, despite the toxic salinity level.

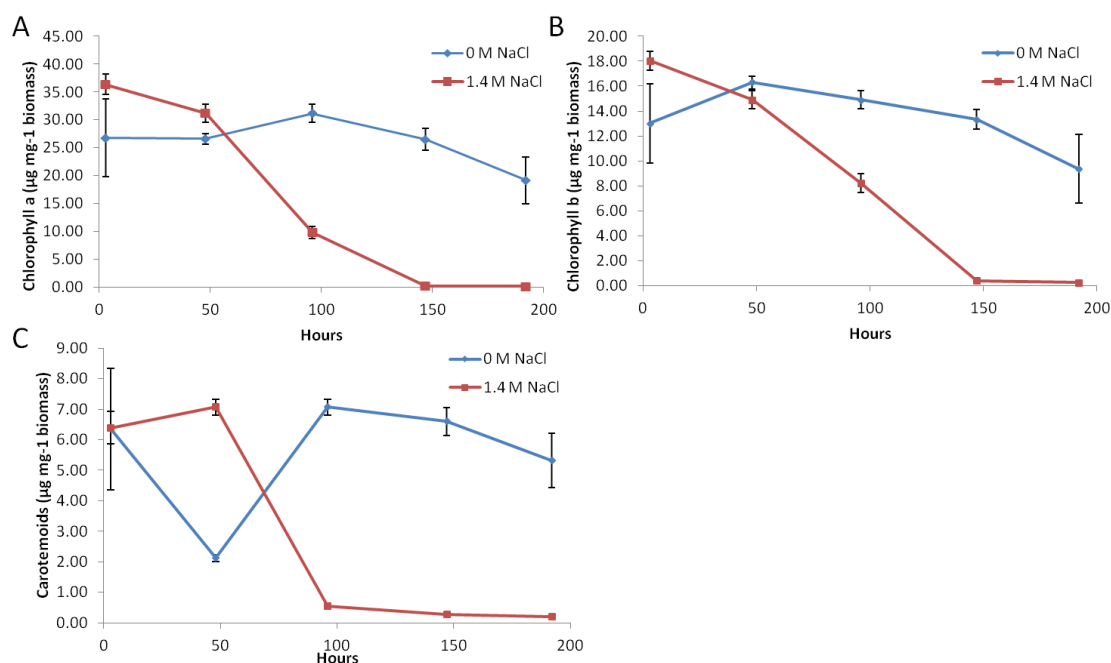


Figure 5.14 Chlorophyll a (A), chlorophyll b (B) and carotenoid (C) content of *C. nivalis* under control and 1.4 M NaCl conditions (n=3).

### 5.3.6 Photosynthesis and respiration activity in *C. nivalis* under 1.4 M NaCl conditions

Figure 5.15 shows the net photosynthesis and respiration for *C. nivalis* under both control (0 M NaCl) conditions and 1.4 M NaCl stress conditions. This is based on the per cell amount calculated from OD taken at the point of sampling and then calculated using the cell count to OD correlation (see Appendix D, section 12.1.1). The salt stressed samples show that even at the first time point of 5.5 hours, the cells cease to photosynthesize under salt stress conditions. In the control conditions, both photosynthesis and respiration are highest at the first time point (t=5.5 hours), and this decreases until t=103.5 hours, after which it plateaus.

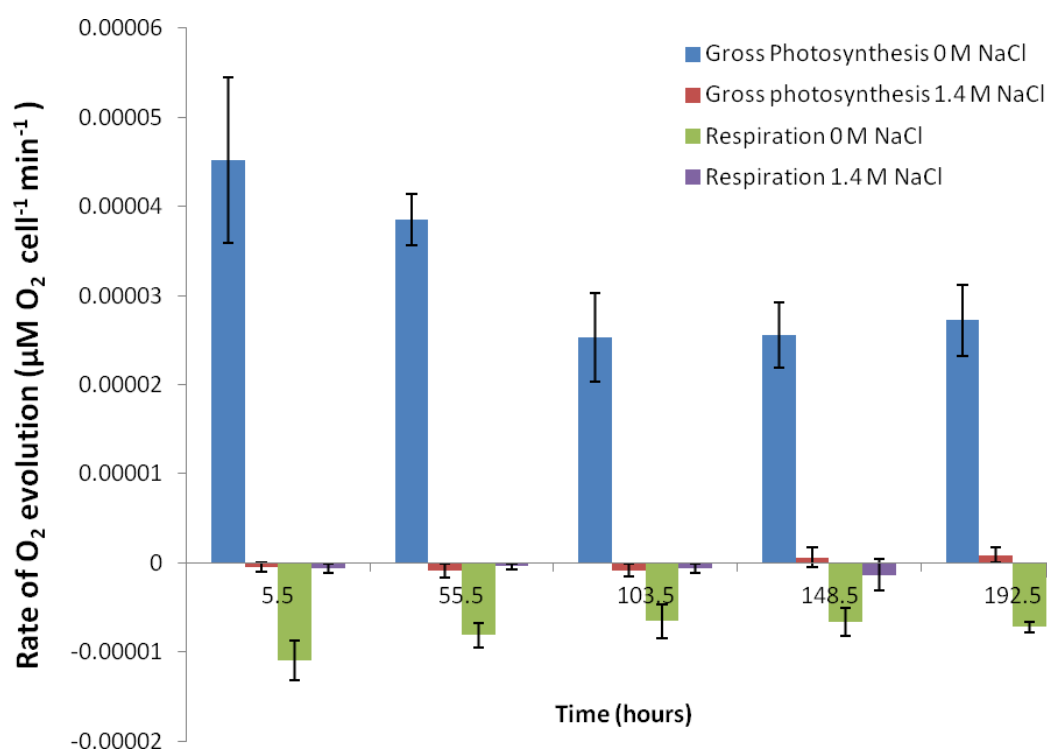


Figure 5.15 Net photosynthesis and respiration data for control (0 M NaCl) and salt stressed (1.4 M NaCl) *C. nivalis* cultures (n=3). Cells were grown in normal 3N-BBM-V medium and then resuspended in the new salinity medium at time zero.

#### 5.4.1 Experiment conclusions

1.4 M NaCl was beyond the tolerance of *C. nivalis*, despite its reported ability to survive in high salinities above 1 M NaCl (Lu et al., 2012a). This is shown by degradation of lipids, loss of photosynthetic pigments, and cessation of photosynthesis. C16:0 and carbohydrates were found to be the most resilient components against salt stress, maintaining constant levels even in dying cultures.

The cells appeared to retain pigment for some time after the introduction of salt stress, showing that the effects are not immediate. This suggests that *C. nivalis* is employing salt tolerance mechanisms, but these mechanisms are halted over time and exposure to these toxic conditions. During salinity induced cell death, Na<sup>+</sup> ions cause membrane depolarisation (Shabala, 2009), which will eventually lead to the breakdown of the cells.

This thesis is investigating the effects of salt stress on the lipid potential of algal cultures for biofuel production. Since salt stress may be a potential way to induce high lipids in an industrial context, it is useful to know how the culture will respond when the salinity is increased too much. This data reveals information particularly about the way the cultures lipid profile and photosynthetic capacity respond to very high salt stress, which is important in understanding the potential downside of using salt as a lipid trigger. However, 1.4 M NaCl is very high and it would require a vast input of saltwater or solid salt to utilize this salinity stress on an industrial scale. It would be useful to fully investigate the range up until 1.4 M NaCl with incremental concentration increases to find out how the algal culture would be affected as salt concentrations gradually increase. In this case, using acclimatized cultures with stepwise salt concentration increases will also be useful, since some increases in salt concentrations may be due to evaporation or salt build up in a culture over time.

Whilst it is useful to note how a species will respond when the toxicity of the salt is beyond its limit, the research then moved on to look at how salt could be useful instead of detrimental to the growth and biofuel production in a culture.

The salinity of 0.2 M NaCl was used, as this was indicated to be a possible lipid trigger by the preliminary data in this chapter (section 5.1.2).

### **5.5 Effect of 0.2 M NaCl on *C. nivalis***

*C. nivalis* was found in the preliminary data to have an interesting response in FAME accumulation to 0.2 M NaCl growth conditions. This condition was therefore chosen as a likely trigger for lipid accumulation in this species and explored.

This experimentation was carried out three times. The first experiment was a full time course experiment with triplicate data to establish trends in FAMEs and other biological parameters of the strains in this condition. The second and third were to identify and take potential time points for proteomic investigation under high lipid production. The second run was carried out at a high starting OD<sub>750</sub> of approximately 0.7 whilst the third run used a lower starting OD<sub>750</sub> of approximately 0.35. This third

run was chosen as the most suitable for proteomic investigation, since it matched the seeding conditions of the first full investigation of growth under 0.2 M NaCl conditions. However, the second run was useful for seeing whether seeding density had a strong effect on the results found. The data for the three experiments are discussed together as all show similar patterns, and show that the trends are repeatable.

#### 5.4.1 Effect of low salinity (0.2 M NaCl) on Optical Density

Figure 5.16 shows the optical density of cultures grown under control and 0.2 M NaCl conditions. At 0.2 M NaCl the salt concentration is high enough to retard growth in the cultures, despite the higher salt tolerance of this species reported in the literature (Lu et al., 2012a). This growth retardation takes place after 24 hours after an initial amount of growth. However, the control cultures steadily increase over the course of 288 hours. The decrease in OD from salt stressed cultures shows that these are not healthy or optimal conditions for growth in *C. nivalis*. It should be noted, therefore, that although this species has a high tolerance for salt stress, even 0.2 M NaCl will arrest cell division. Tolerance is defined as the ability to survive in an environmental conditions, but not necessarily to thrive, hence the distinction between halotolerant and halophilic species (Ginzburg and Ginzburg, 1981). The second set of data (Figure 5.16 C and D) starts at a higher OD and the subsequent OD of both cultures doesn't show the rise in OD at 24 hours observed in A and B. The third experimental run (E and F) matches the patterns results found in A and B, but with a higher OD being reached at the final time point in the control culture. This shows that there can be variability in the productivity of a culture. A number of factors can affect the final productivity of a culture (Jiménez et al., 2003). The key conditions (light, temperature and gas-bubbling) were controlled so that the cultures should have been the same, however small fluctuations in the culture conditions could have caused the effects on the final biomass productivity. The volumes of the culture may have varied between cultures, since the sampling regimes were different between each of the three cultures. Culture concentration can interact with different abiotic factors to affect final culture productivity (Qiang and Richmond, 1996). Having control over the final biomass

content is desirable for predictable productivity of an industrial biotechnology process like biofuels production.

Overall, 0.2 M NaCl stopped growth of *C. nivalis* in these experiments, whilst control cultures were able to gradually increase in cell density. This is seen consistently, showing that 0.2 M NaCl is too high a salt concentration to allow culture density to increase. Comparing this to *C. reinhardtii* cultures, the lack of culture growth is likely due to limitation of the carbon source. *C. reinhardtii* showed vastly reduced photosynthetic capacity under 0.2 M NaCl but due to the availability of carbon in the media and a light regime optimised for high growth rate, the culture was still able to proliferate. In *C. nivalis*, the control growth rates were slower, and the impact of 0.2 M NaCl caused an arrest of culture growth. This may be because limits in the availability of carbon (slightly reduced photosynthesis, no external carbon source) mean that cells cannot divide under this condition. However, lipids are still produced (discussed below), so carbon would appear to be being fixed, and in excess, and diverted into storage molecules. This suggests it is more a difference in the salinity responses of the two species in their respective experimental set ups. In this case, *C. nivalis* responds by halting cell division and culture growth. The differences in responses mechanisms of these two species is of great interest to this research.

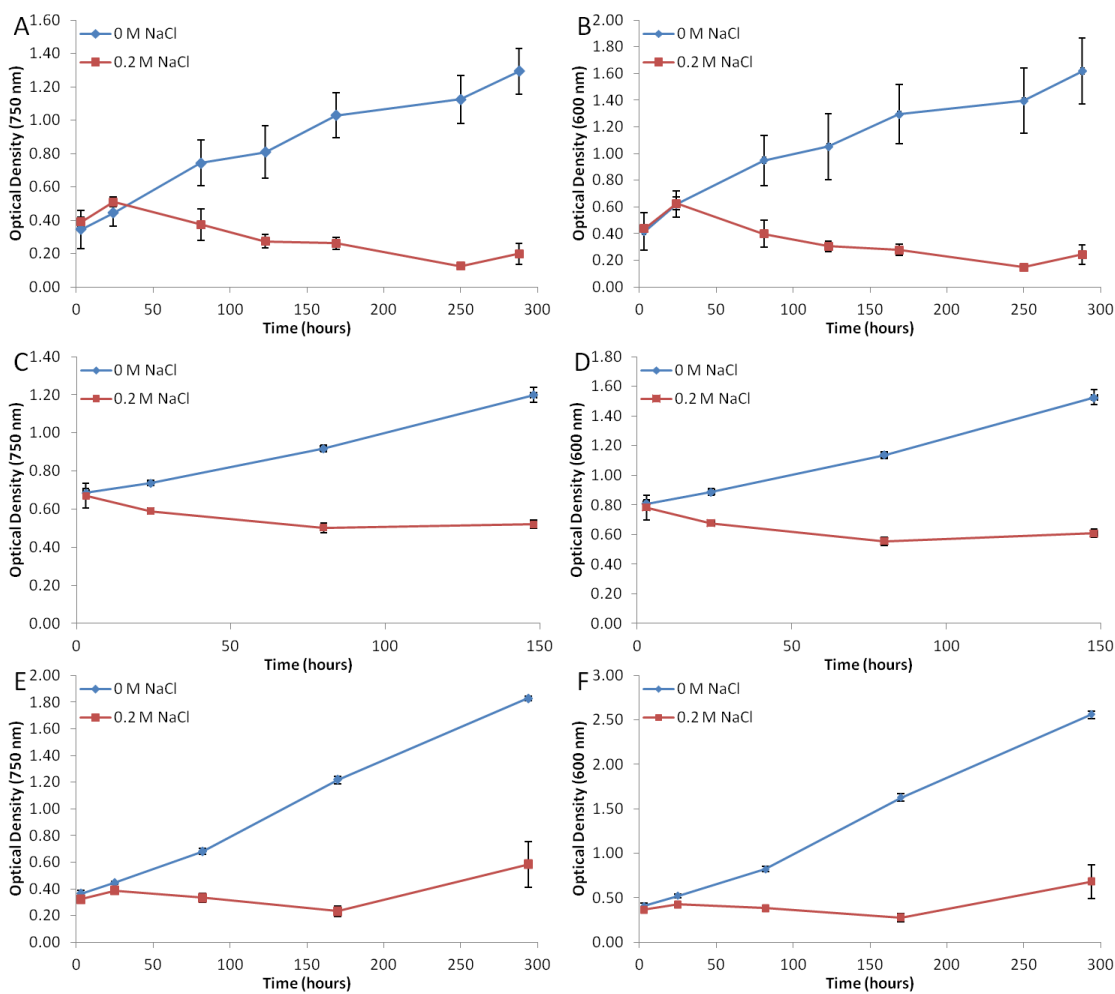


Figure 5.16 Optical density at 750 nm (A, C, E) and 600 nm (B, D, F) of the three experimental runs of *C. nivalis* grown in 0 and 0.2 M NaCl (n=3). Cells were grown in normal 3N-BBM-V medium and then resuspended in the new salinity medium at time zero.

#### 5.4.2 Effect of low salinity (0.2 M NaCl) on Biomass

The patterns found in the optical density data are supported by the results of biomass accumulation in each experiment; biomass increases significantly in the control conditions over time, but the biomass concentration in salt stressed conditions remains low (Figure 5.17). It is clear that cell division and culture growth are greatly reduced under 0.2 M NaCl growth conditions. Biomass accumulation has been shown to be decreased in high salinity conditions, especially those which cause lipid accumulation (Kim et al., 2016b).

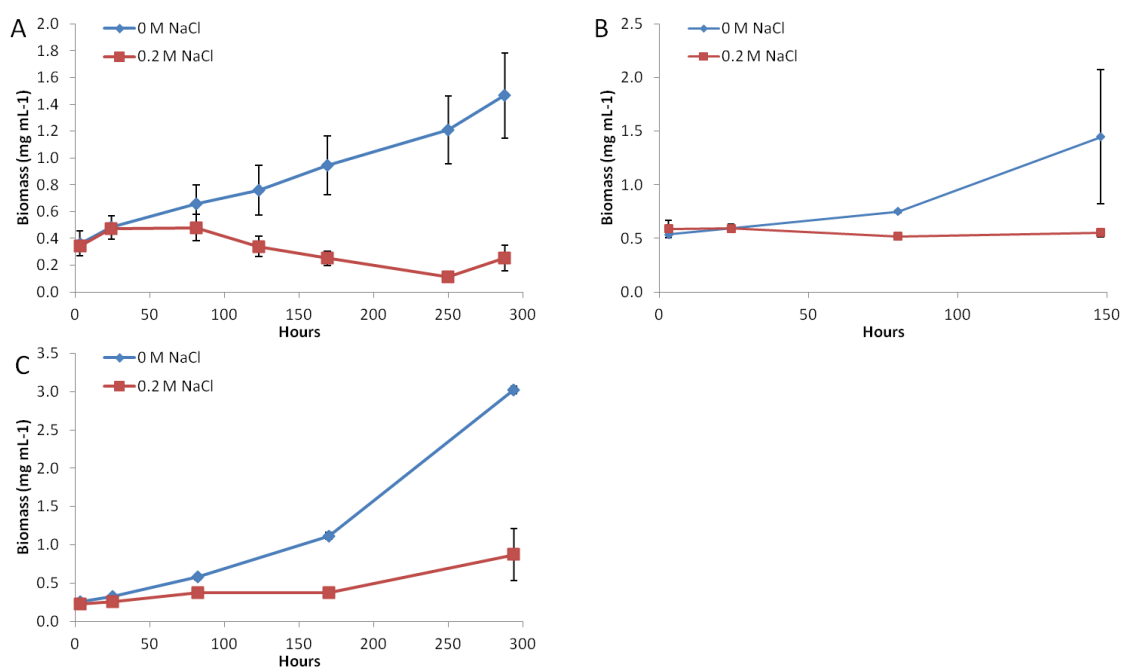
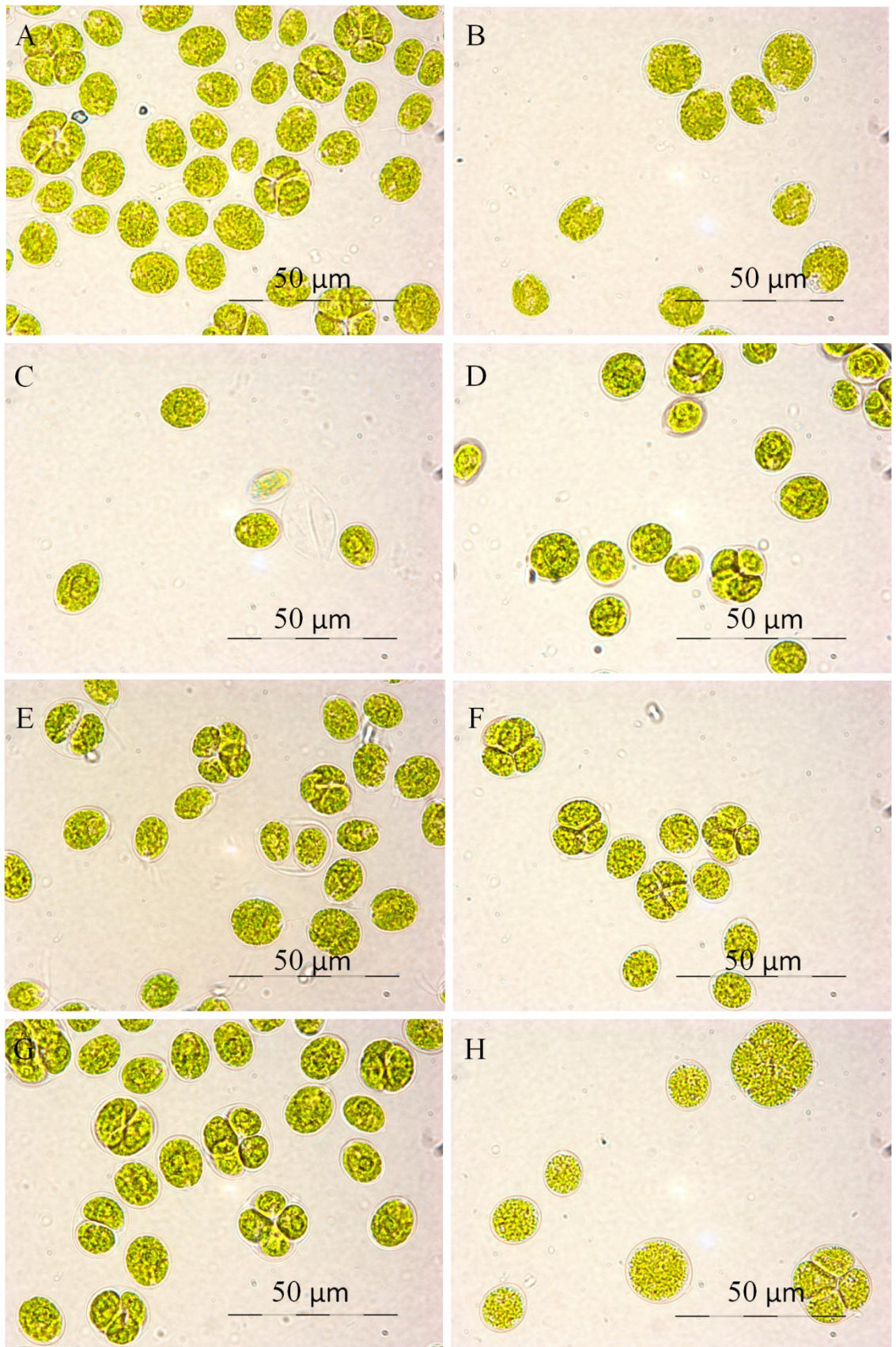


Figure 5.17 Biomass accumulation found in *C. nivalis* grown in 0 and 0.2 M NaCl conditions in the first (A), second (B) and third (C) experimental run (n=3). Cells were grown in normal 3N-BBM-V medium and then resuspended in the new salinity medium at time zero.

#### 5.4.3 Effect of Low Salt (0.2 M NaCl) on Cell Morphology

Photographs of *C. nivalis* were taken during the first and third runs of growth under control and 0.2 M NaCl salt stressed conditions, so that any significant changes in cell morphology could be observed. The main difference in cell morphology that can be noted is in the final two time-points of each experiment, the salt stressed cells are more rounded and swollen than those in the control conditions. Cell division is observed in control conditions, and in D F and H in the first run in 0.2 M NaCl conditions (Figure 5.18). Microscopy could not be obtained during the second run. However in the third run, cell division was not observed at the time of microscopy images being taken in the salt stressed conditions (Figure 5.19). This could be due to timing of cell division not coinciding with microscopy, but it seems likely that cell division was not occurring as much since it was not observed. The control cells appeared to be undergoing cell division in the latter stages of the growth curve, but this was not true of salt stressed cells. High salt stress levels have been shown to reduce cell division in algal cultures (Bartley et al., 2013; Pal et al., 2011; Takagi et al.,

2006). Increases in lag phase has been found with algal species in salinity stress, due to inhibition of DNA synthesis resulting in delayed cell division (Jiang and Chen, 1999).



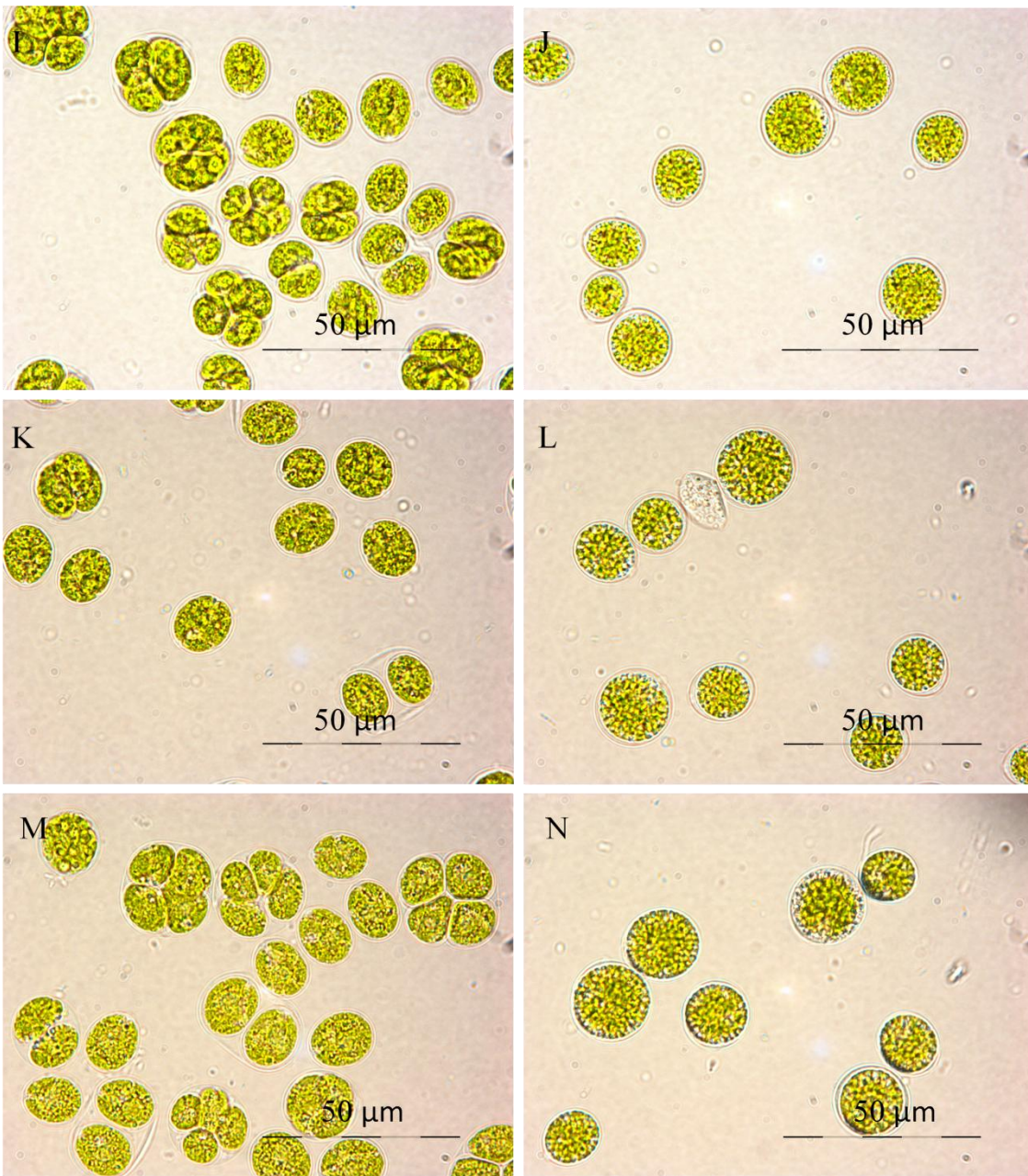
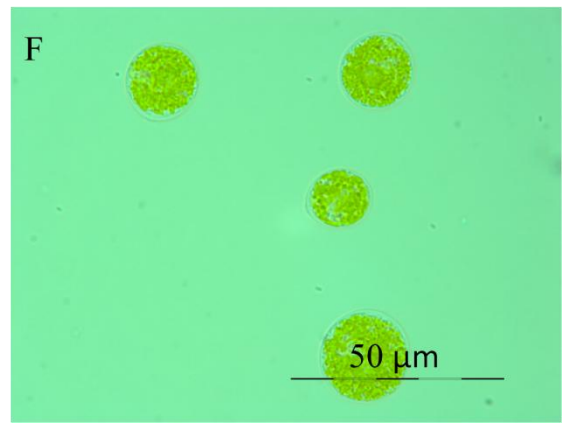
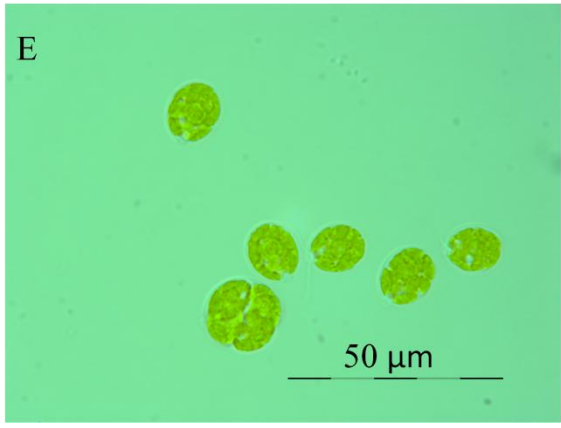
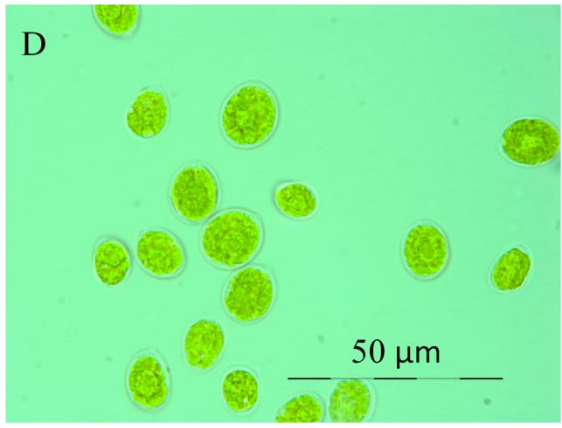
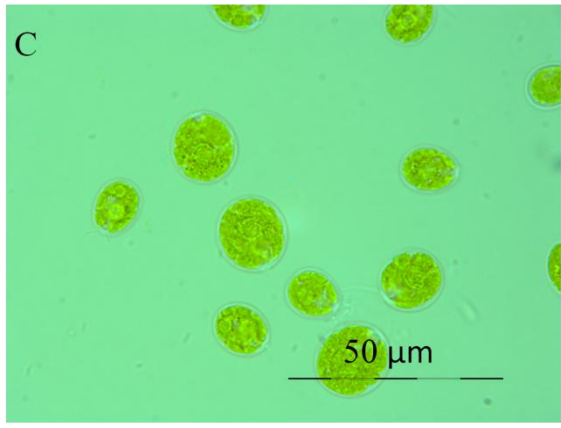
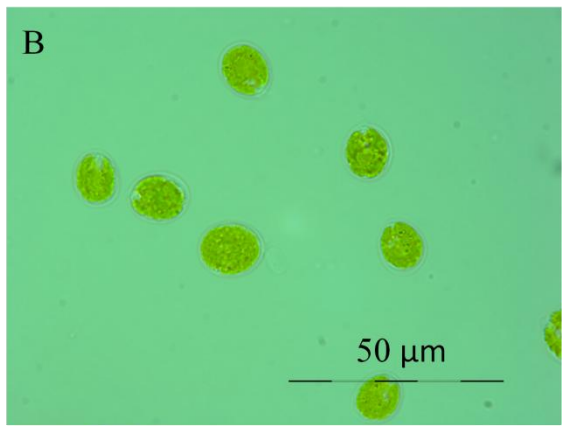
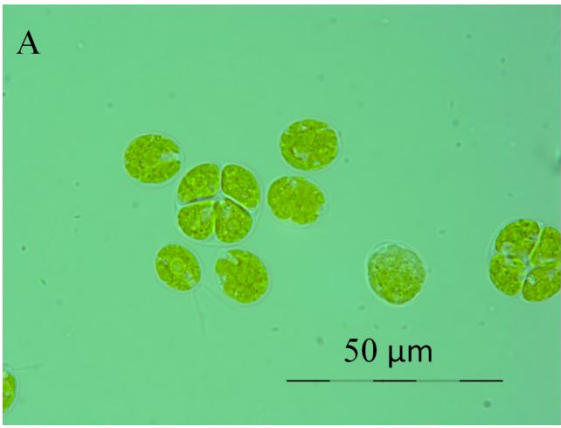


Figure 5.18 First experimental run: microscopy of *C. nivalis* cells under control conditions (A, C, E, G, I, K, M) and 0.2 M salt stress (B, D, F, H, J, L, N) at time points 3 (A, B), 24 (C, D), 81 (E, F), 123 (G, H), 169 (I, J), 250 (K, L), 288 (M, N) hours (at x1000 magnification).



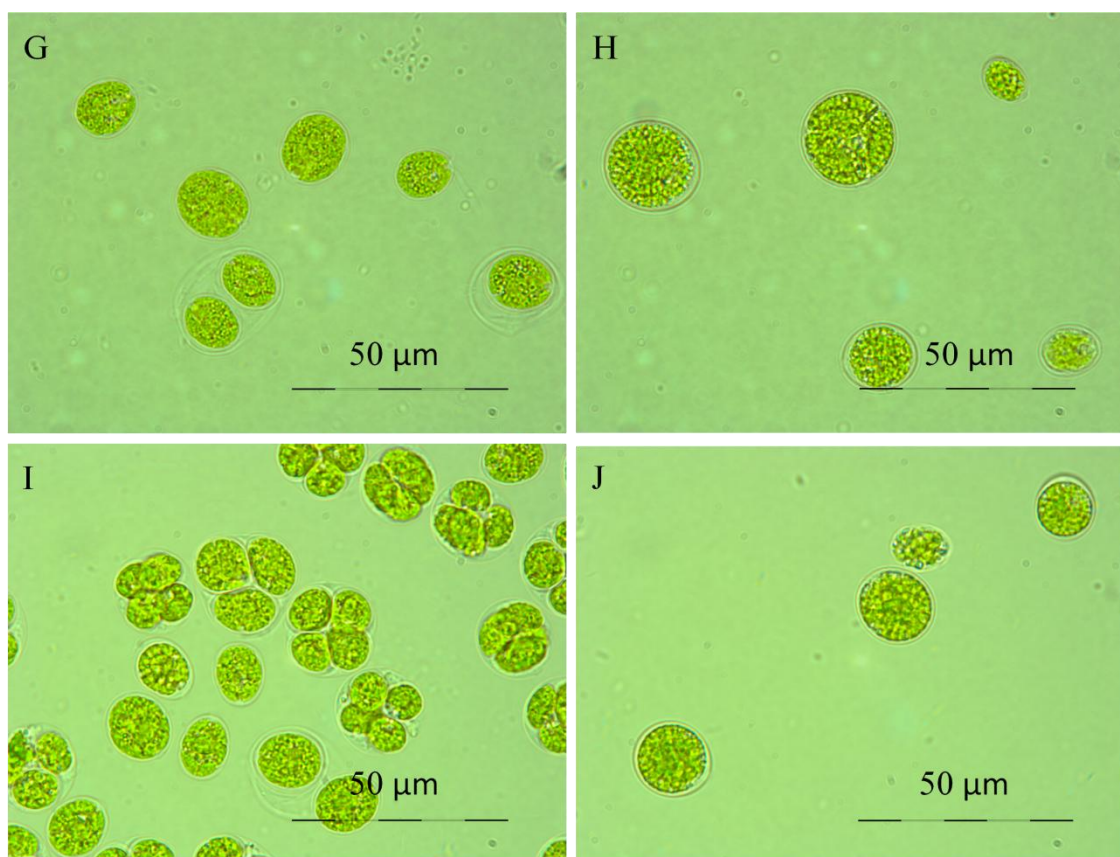


Figure 5.19 Third experimental run: microscopy of *C. nivalis* cells under control conditions (A, C, E, G, I) and 0.2 M salt stress (B, D, F, H, J) at time points 3 (A, B), 25 (C, D), 82 (E, F), 170 (G, H), 294 (I, J) hours (at x1000 magnification).

#### 5.4.4 Effect of low salinity (0.2 M NaCl) on lipid accumulation

The lipid content of each culture was measured using GC-FID analysis and the detected FAMES were expressed as a percentage weight of the biomass, displayed in Figure 5.20. In each experiment, 0.2 M NaCl conditions have a significant effect on the accumulation of FAMES in the culture, with the final time point reaching approximately three times as much total FAME as the control conditions. In *B. braunii*, salt stress (0.085 M) could induce more than twice the control amount of palmitic acid and oleic acid, however this only went from 20% oil in the control to 28% oil content (Rao et al., 2007). Similarly in *Tetraselmis* sp. increasing salinity could increase fatty acid content of biomass, but it still remained at approximately 26% after 8 days of exposure to salinity (Kim et al., 2016b). Marine species *Monoraphidium dybowskii* accumulated lipid at higher rates under salt stress conditions of 0.085, 0.171 and 0.34 M NaCl, but these levels went from approximately 27% in control to 38% in high salt (Yang et al., 2015). The differences seen in the present study seem to show an unusually large

increase in total lipid content. It is hard to make direct comparisons, since all species have different tolerances and different growth regimes, but searching for the maximal amount of lipid per dry weight content found in salinity stressed cultures will be the best way to compare this. One study using an arctic *Chlamydomonas* species used a wide range of salinities (0.12, 0.48 and 0.96 M NaCl), and found the highest lipid content at 0.12 M NaCl (approximately 23% under N replete conditions) (Ahn et al., 2015). However, high lipid levels of over 40% DCW have been induced by salinity stress in freshwater species such as *Monoraphidium dybowskii* (Yang et al., 2014). Also, a marine species of *Chlamydomonas* was reported to produce up to 64.9% of DCW as lipid under high salt stress, however this was combined with nitrogen depletion (Ho et al., 2014).

In the current study, the increase of FAMES above the levels found in control conditions appears to begin at around 80 hours after seeding in the new cultures (Figure 5.20). This happens regardless of whether the seeding density is at OD<sub>750</sub> 0.35 or 0.7, suggesting that the rate of induction of lipids is not necessarily linked to the growth cycle stage of the culture. The reason for this may be nitrogen removal from the culture. Without evidence of the nitrate levels in the culture it is only theorized here, but the reason for the time taken to accumulate lipids could be due to combination salt stress and eventual nitrogen depletion in the medium. This agrees with a report on *C. reinhardtii* grown in phototrophic conditions that showed that nitrogen stress caused fatty acid increase from control conditions after 72 hours, and this then doubles as 6 days or 144 hours is reached, within the first 2 days similar FA levels were seen between stressed and control cultures (Msanne et al., 2012). This pattern is similar to what is seen in the current research.

A study by Kim et al. (2016a) reported growing their strains of freshwater *Chlorella* in BG11 medium until late exponential phase and then transferring them to different salt concentrations. They found high increases in FAMES, especially C16:0, and the increases were identified to come from lipid droplets and TAG accumulation, not membrane lipids. As Kim et al discuss, the response of algae to salt is very variable. They found that the C18:1 and C18:2 decreased under these stress conditions,

however they would expect C18:2, a major constituent of TAGs along with C16:0, to increase.

To better analyse the FAME increase seen in the current study, the data were grouped into monounsaturated FAs, polyunsaturated FAs or saturated FAs. These were shown as both total amounts in the biomass (displayed in Figure 5.21) and as a percentage of the total FAMEs detected, by weight (displayed in Figure 5.22). In salt stress conditions, the FAME profile shifts towards a large proportion of monounsaturated fatty acids. This is caused by a large increase in the amount of MUFAs detected in the biomass. The MUFA content of the biomass is very low in the cultures until the 80 hour time point. There is some increase in MUFA content of the control conditions at the latter stages of the growth curve, but this increase is not nearly as high as those of the salt stressed conditions. By contrast, the PUFA and SFA content of the biomass in the salt conditions is lower than those of the control conditions until the latter stages of the growth cycle. PUFAs and SFAs do not undergo the same dramatic increase that MUFAs do, although some increases in PUFAs and SFAs are seen in the final time points of the salt stressed conditions.

Knothe (2008) suggest that to optimise biodiesel and avoid technical issues of the fuel performance that arise from oxidative stability or cold flow properties for example, it is ideal to maximise one component of the biodiesel and choose one which reduces these technical issues. They suggest oleic acid (C18:1) as such as suitable major component, or alternatively C16:1. The most desirable major component therefore is a MUFA, and the current study of *C. nivalis* has shown a major increase in MUFA.

Lu et al. (2012c), studied lipid biomarkers in *C. nivalis* under salinity stress and found a decrease in the total degree of unsaturation in the lipid biomarkers at 0.13 M NaCl. When studying the shift in relative proportions of the fatty acids present, in the present study there is a decrease in the relative amount of PUFA in relation to MUFA, although SFA stays roughly the same, and therefore this is consistent with what was found in the Lu *et al.* (2012c) study.

Lu et al. (2012b) studied 0.21 M NaCl stress in *C. nivalis* over 15 hours, and used the identification of changes in fatty acid levels as a way to choose biomarkers for their subsequent studies. They found increases in C16:0, C16:1, C18:0, C18:1cis but decreases in C16:2, C16:3 and C18:3. Some of these same increases were found in the current study, but not all the changes were the same, and the time scales of the studies are very different. The full analysis of individual FAME changes in response to 0.2 M NaCl salt stress is shown in Appendix D. The key observation is that one MUFA accounts for much of the increase in FAME induced by 0.2 M NaCl i.e. C18:1cis (oleic acid). Increases in oleic acid were found in nutrient starved cultures of *Nannochloropsis oculata* after 4 days, making this the main fatty acid in the profile. Before this, palmitic acid was the main fatty acid in the profile (Su et al., 2010).

The role of unsaturation of fatty acids in membrane lipids (which contain large amounts of PUFA that are susceptible to oxidative damage) in response to salt is thought to help with salinity stress by changing the membrane fluidity and making algal cells less susceptible to ionic and osmotic stresses of high salt (Singh et al., 2002). However, whilst there is a large increase in unsaturated fatty acids, there is a shift away from PUFAs to MUFAs. PUFAs do decrease in salt conditions at least for the first part of the time course. This suggests that the unsaturation is decreasing, which would go against the logic that unsaturation is a coping mechanism for salt stress. However towards the end of the experiments, the PUFAs increase again (Figure 5.21).

Jayanta et al. (2012) grew a freshwater algal species (*Ankistrodesmus falcatus*) in different salinities and found a slight increase in C18:1 oleic acid and in MUFA overall, as well as a smaller increase in PUFA and a decrease in SFA. However at this salinity of 160 mM, the best growth rate was also found. This increase in fatty acids overall also yielded a higher calorific value, showing that the energy density of the algal biomass can be improved. Salt in algal growth medium has been shown to increase the amount of unsaturated fatty acids whilst decreasing the amount of saturated fatty acids (El-Baky et al., 2004). In that study, it is mainly PUFA that increases, whilst MUFA and SFA decrease. Salt also induced higher C18 to C16 ratios.

A large increase in the MUFA C18:1 (by 430%) was found in an algal species (*Scenedesmus rubescens*-like microalga") under nitrogen deprivation, whilst a decrease in the PUFA C18:3n3 was observed (Li and Lin, 2012). Under nitrogen deprivation it is typically not the membrane lipids that are increased, but the neutral lipids of storage molecules. Therefore observing similar patterns to this algal species suggests a similar mechanism. Rao et al. (2007) found a large increase in C16:0 and C18:1*cis* under increased salinity conditions in *B. braunii*, with the biggest increase found in C18:1*cis*, showing that there are species that response to salt stress in a similar way that *C. nivalis* does.

There is a distinction between changes in fatty acids induced by growth rate alterations and changes in fatty acids induced by salinity (not linked to growth rate) (Renaud and Parry, 1994). To determine the difference, the effects of salt must be investigated on salinities that affect growth rate and those that do not. In the current study it was not possible to separate the effects since the salinity of interest studied also altered the growth rate. Cohen et al. (1988) have linked changes in PUFA due to salinity stress in an algal species as due to the decrease in growth rate.

In the current study, the FAME profile was also studied for differences in amounts of different length FAMES (Figure 5.23). The FAMES detected were grouped into short chain FAs (C6-C15s), C16s, C17s, C18s and long chain FAs C19-24s. C16s, C17s and C18s were not grouped together because these are the main chain lengths of interest for biofuel and because they make up the majority of the FAMES detected. Figure 5.23 shows the relative abundance of these groups in the detected FAME profile. This profile is mainly dominated by C18s in all cultures studied. This abundance in the FAME profile remains relatively consistent throughout the growth curve in both the control and the salt stressed conditions. In control conditions there appears to be a slight increase in the relative amounts of C16 chains over time, but this is not seen in salt stressed conditions, which all show a C16 peak at 24 hours followed by a relative decline compared to the C18 chains, which slightly increase over time in the salt stressed conditions.

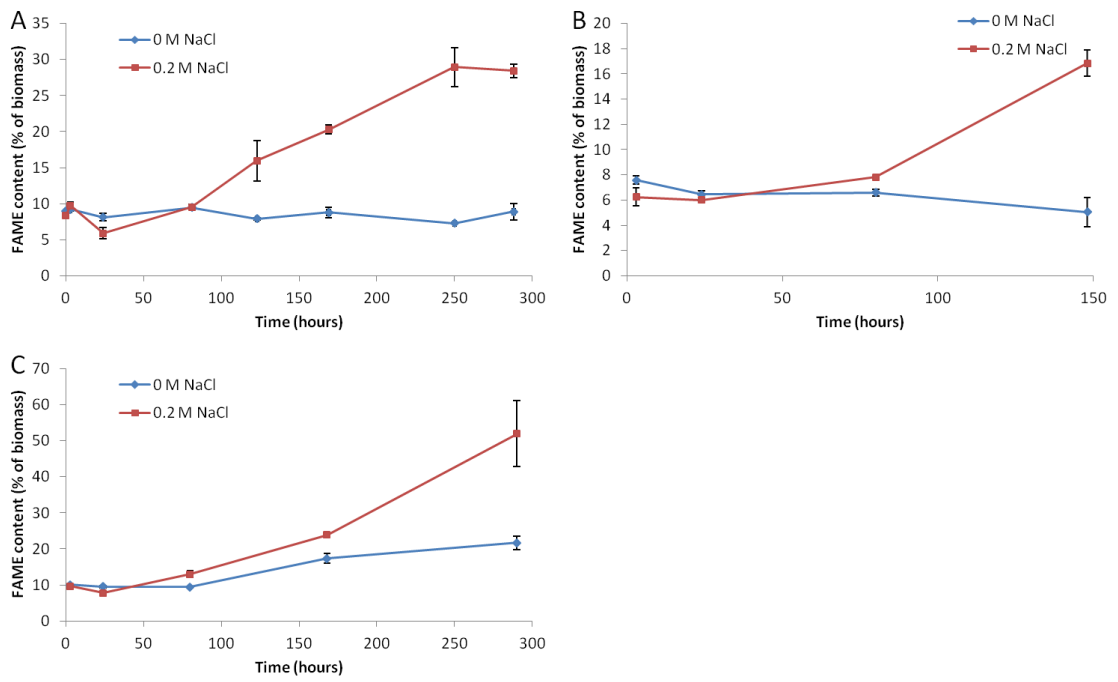


Figure 5.20 Total FAME content of *C. nivalis* cultures grown in 0 and 0.2 M NaCl (n=3). Cells were grown in normal 3N-BBM-V medium and then resuspended in the new salinity medium at time zero.

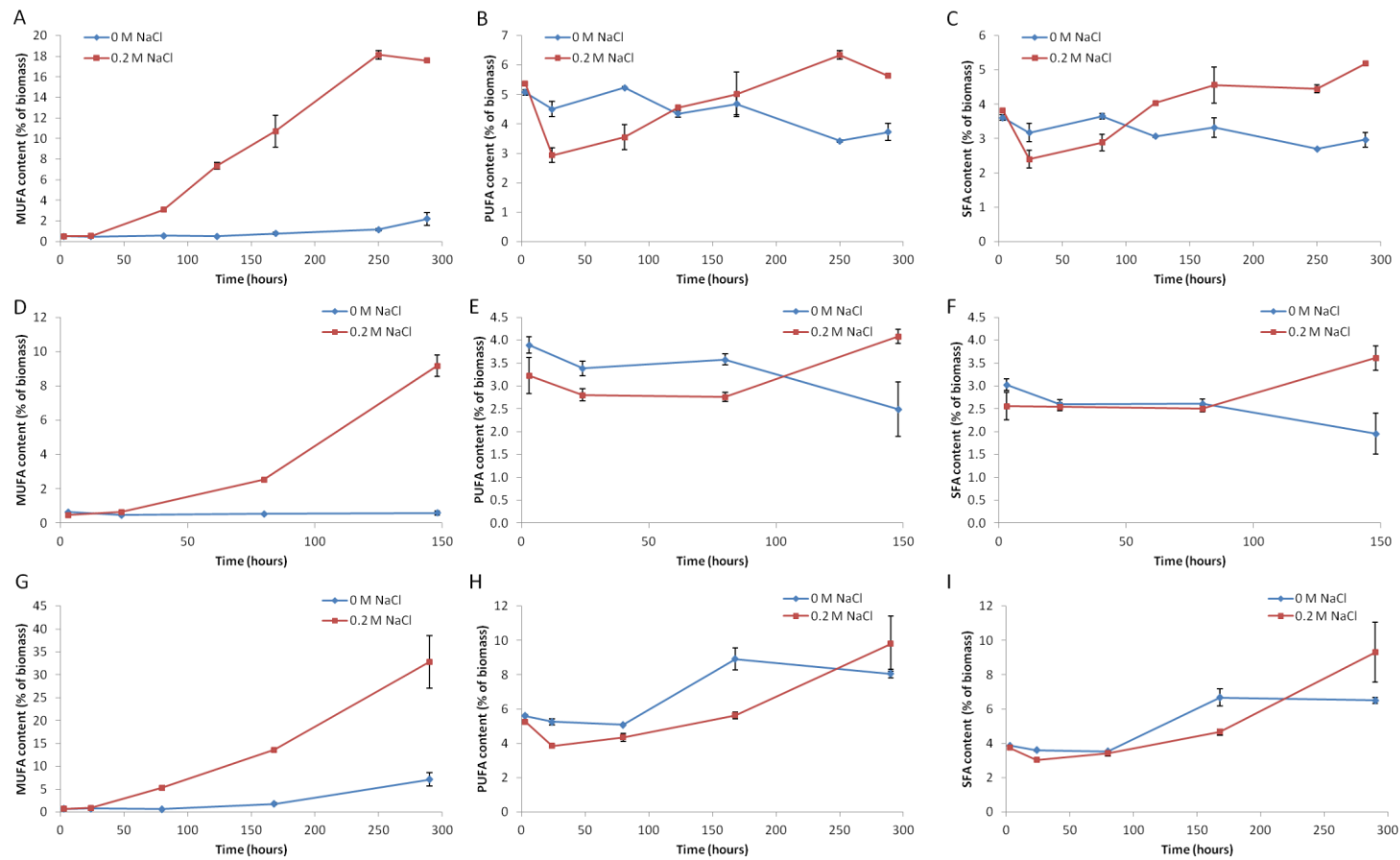


Figure 5.21 MUFA (A, D, G), PUFA (B, E, H) and SFA (C, F, I) content of cultures. First run (A, B, C), second run (D, E, F) and third run (G, H, I) (n=3). In all cases, cells were grown in normal 3N-BBM-V medium and then resuspended in the new salinity medium at time zero. The data are presented as % of total biomass.

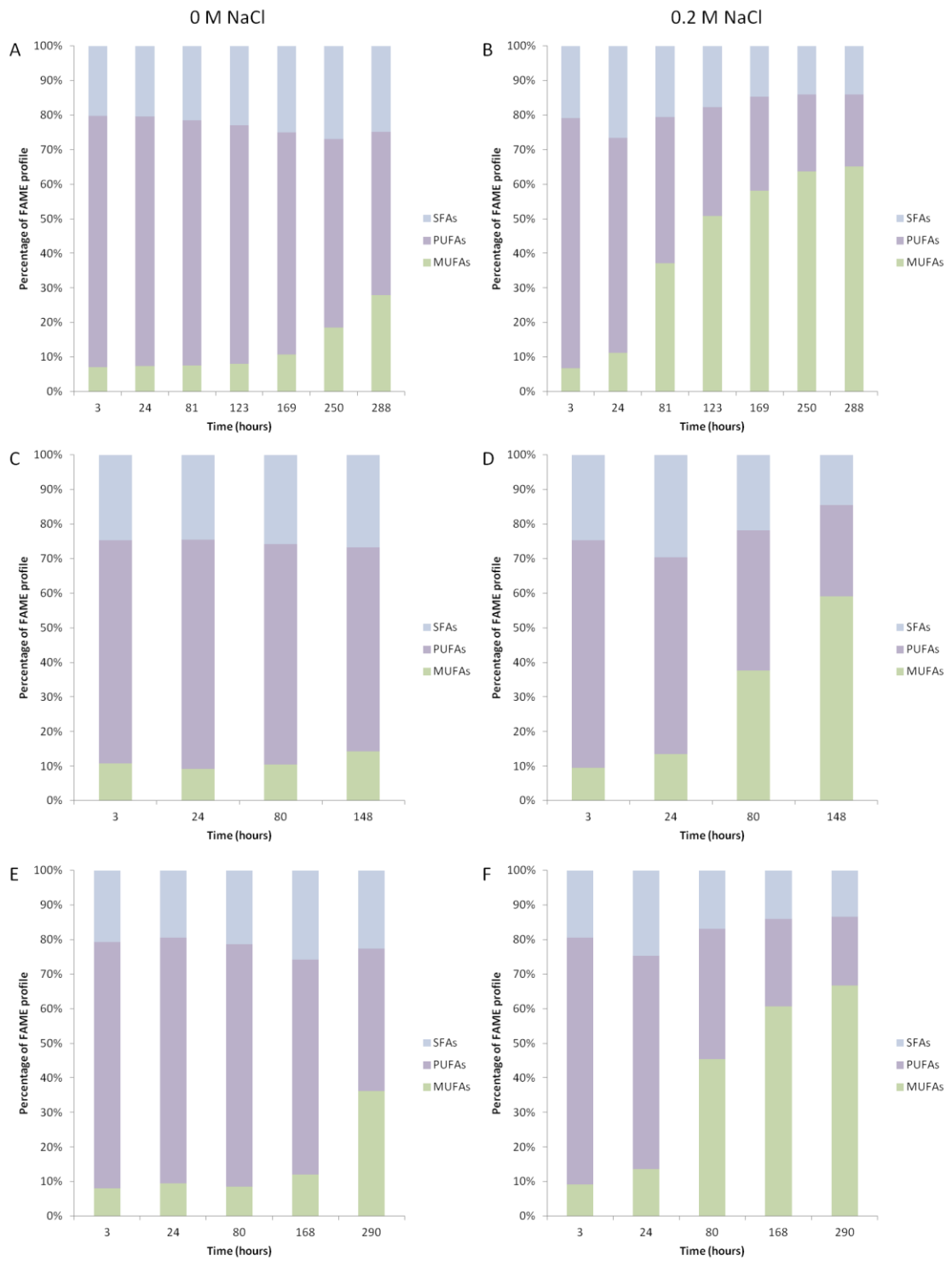


Figure 5.22 Degree of unsaturation of the detected FAME profile (n=3). Cells were grown in normal 3N-BBM-V medium and then resuspended in the new salinity medium at time zero. The data are presented as % of total FAME. Cultures in 0 M NaCl control conditions (A, C, E) and 0.2 M NaCl conditions (B, D, F) are shown for the first (A, B), second (C, D) and third (E, F) experimental runs.

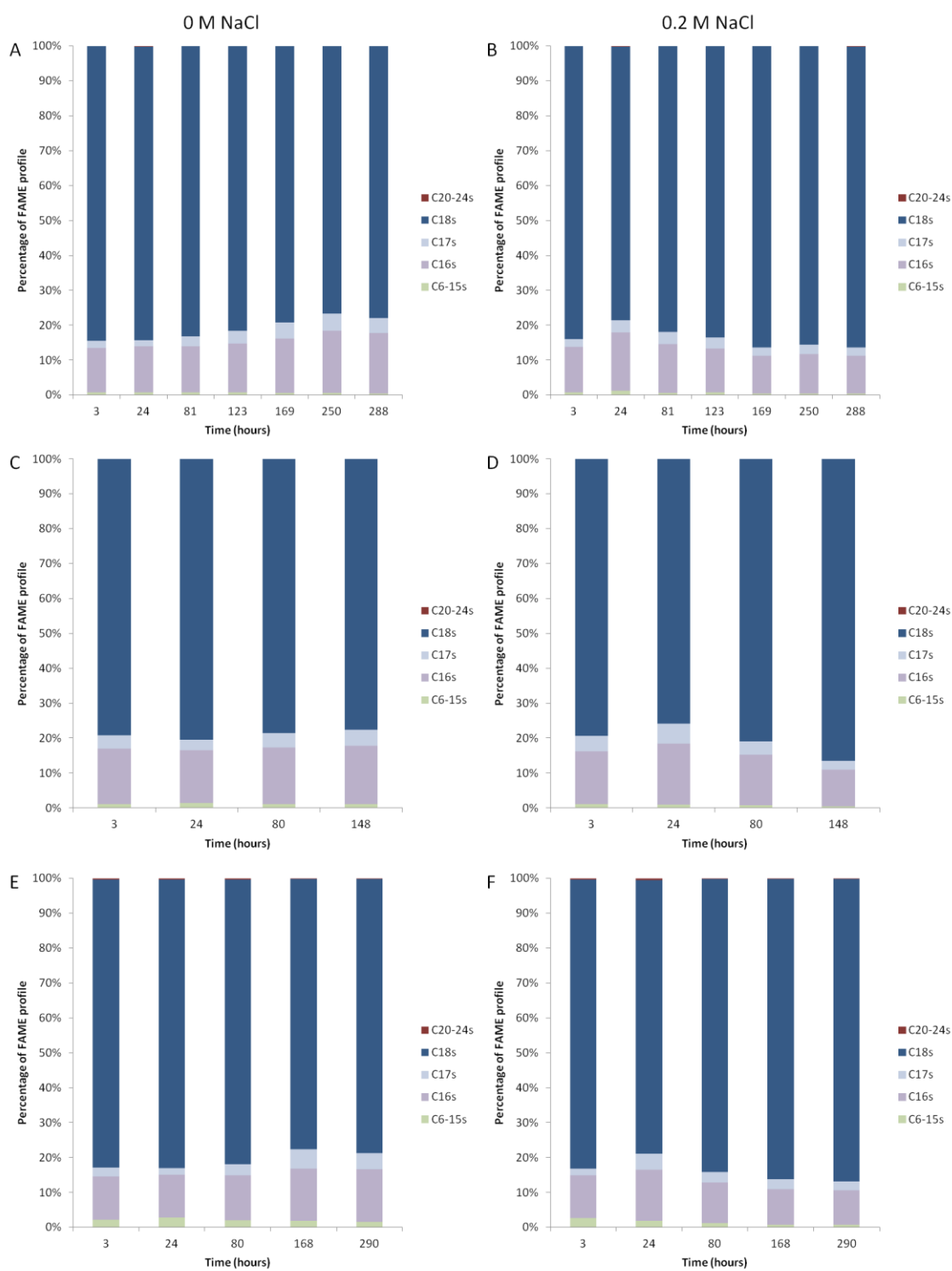


Figure 5.23 Chain lengths of the FAMEs detected (relative abundance by weight), (n=3). Cells were grown in normal 3N-BBM-V medium and then resuspended in the new salinity medium at time zero. Cultures in 0 M NaCl control conditions (A, C, E) and 0.2 M NaCl conditions (B, D, F) are shown for the first (A, B), second (C, D) and third (E, F) experimental runs.

Many of the major FAMES show increases under the salt stress condition, but C18:1*cis* is the biggest contributor to the overall FAME increase in the salt stress conditions (see Figure 5.24 and Appendix D). This is also the reason for the FAME profile shifting towards mainly comprising MUFAs (Figure 5.22). Chloroplasts contain polyunsaturated fatty acids, and a move away from PUFAs to MUFAs and SFAs indicates reduction of these chloroplast lipids, which is found when photosynthesis is reduced, and an increase in storage lipids (Piorreck and Pohl, 1984). Therefore the increases in MUFA and SFA seen here indicate storage molecules. However, towards the end of all the time course experiments, all the FA types increase, including PUFA. And initially SFAs also decrease in the salt stressed conditions. This does not indicate the presence of storage molecules being formed in the cytoplasm, although these rise later in the time course experiment so this storage may not be happening until later in the growth cycle.

It is therefore interesting that only the C18:1*cis* increases at such a large amount whilst other fatty acids do not change as much. This fatty acid is one of the main storage molecules in TAGs (Piorreck and Pohl, 1984) and is shown to increase in *N. oculata* under nutrient starvation (although not salinity stress) (Su et al., 2010). This increase in C18:1*cis* indicates a useful tool for both increasing the lipid content of this algal biomass, and for doing so with a fatty acid suitable for biofuels production. This result therefore shows the practical applications of using this technique for biofuel production, but it would also be useful to know why the cell is responding with lipid increases so that the molecular mechanisms for lipid increase under salt stress can be more fully investigated.

When comparing the FAME profiles of algae grown in photoautotrophic and photoheterotrophic conditions, much higher lipid productivities are found under photoheterotrophic (mixotrophic) conditions. Furthermore the changes in lipid profiles between these two growth regimes are very different, with photoautotrophic conditions leading to more phospholipids and glycolipids in salt stressed conditions, rather than TAGs (Liu et al., 2011). However in the current study, increases in MUFAs (associated with TAGs) are seen with *C. nivalis* under photoautotrophic conditions,

principally a very significant increase in oleic acid. This effect is normally seen in photoheterotrophic cultures but this type of growth condition is less desirable for commercial production because of the need for an organic carbon source, which can increase the cost of culture medium by up to 5 times (Li et al., 2007).

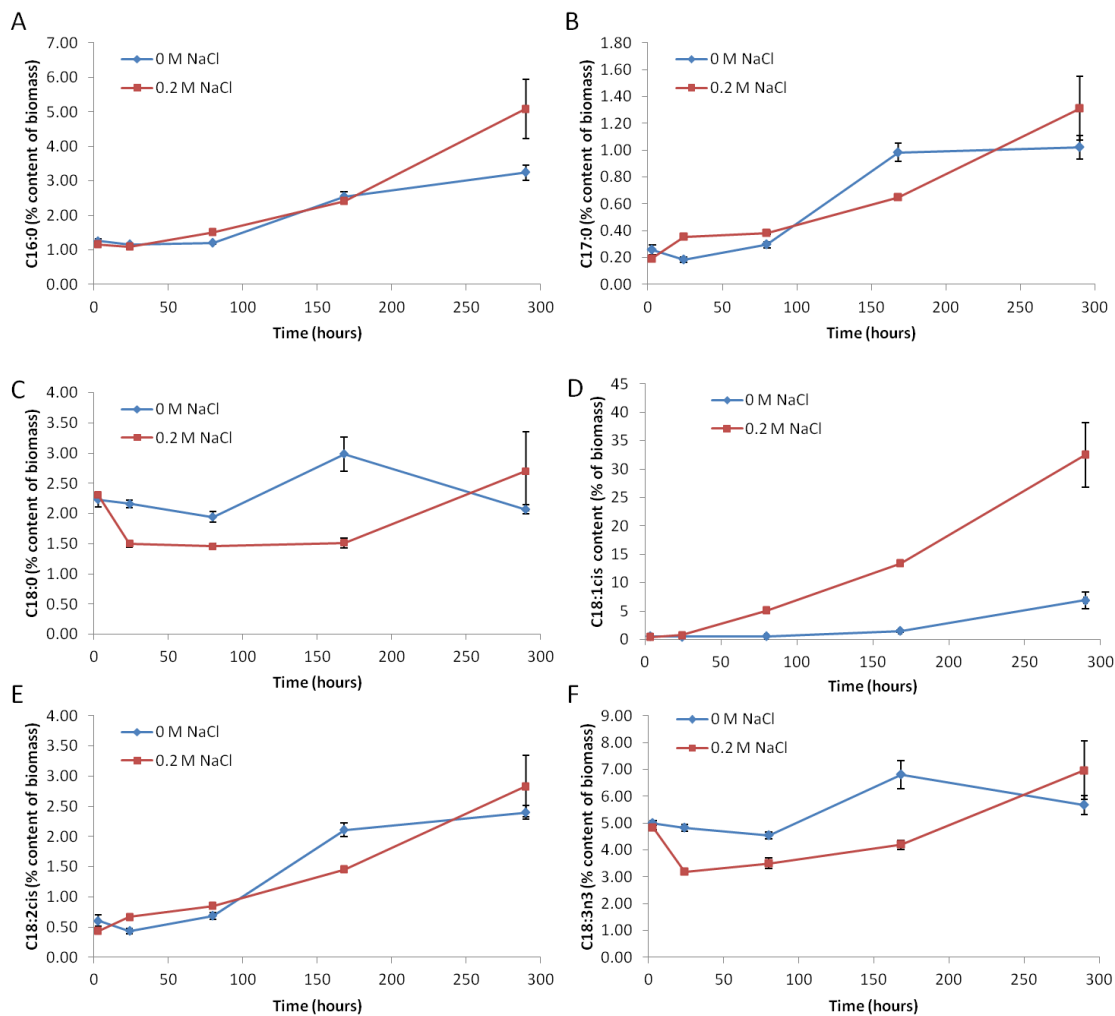


Figure 5.24 Amounts of individual FAMES detected in *C. nivalis* cultures in 0 and 0.2 M NaCl, in the third experimental run (n=3).

#### 5.4.5 Carbohydrate content of *C. nivalis* in 0.2 M NaCl

Carbohydrate content was studied through a colourimetric anthrone assay, which showed that carbohydrate content increased in the salt stressed conditions at an early point in the growth cycle of 24 hours, with a peak at 80 hours. This then declines again at approximately 150 hours. Carbohydrate also increases in the control cultures but at a much later time point of 150 hours. Therefore, carbohydrate accumulation is then

something that happens in the control conditions anyway, but the onset is triggered earlier in the cycle by the presence of salt stress.

The rise in carbohydrate (usually starch) under environmental stress prior to the rise in lipid has been observed in many species (Li et al., 2011; Longworth et al., 2012). It is thought that carbon compounds from carbohydrates such as starch are then converted into neutral lipids (Li et al., 2011). Starch is the primary carbon storage molecule when nitrogen was not limiting, but then when nitrogen becomes limiting the carbon storage molecule is neutral lipid. This is what appears to be taking place in this experiment, but nitrogen is not limiting in the media. Salt is therefore producing the same effect in terms of storage molecules, but it is not caused by the same nutrient limitation. If the effect is the same, it may be that the ability to incorporate nitrogen is affected by the salt stress. Or that there is another common factor linking nitrogen stress and salt stress that causes the same effect in terms of growth and storage molecules.

This response is not always found in algae cultures under salt stress, for instance Kim et al. (2016a) found that carbohydrate content was reduced in *Chlorella* as salt stress increased. However, analysis was only done after 10 days of growth in the medium, meaning that if an early carbohydrate response was shown as it was here, it would not have been observed.

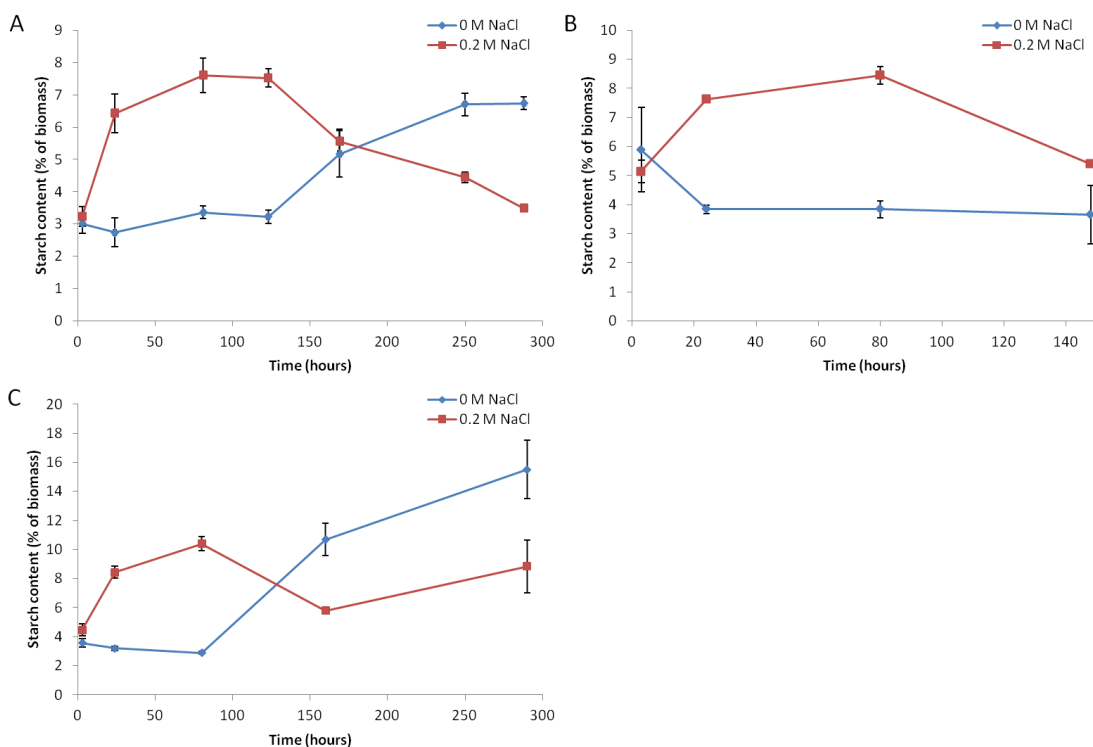


Figure 5.25 Starch content in *C. nivalis* cultures exposed to 0 and 0.2 M NaCl in experimental run 1 (A), 2 (B) and 3 (C) (n=3). Cells were grown in normal 3N-BBM-V medium and then resuspended in the new salinity medium at time zero.

#### 5.4.6 Chlorophyll content in *C. nivalis* grown in 0.2 M NaCl

Chlorophyll content was measured in control and 0.2 M NaCl conditions, and in every culture, chlorophyll content was negatively impacted by the presence of salt (Figure 5.26). The decrease in chlorophyll content was less prominent in the second run experiment, where the culture started off at a higher density before the salt stress was introduced: chlorophyll decreases are not as prominent, but still take place (Figure 5.26 D and E). Since biomass and culture growth is arrested by the presence of salt, it implies that in the existing biomass that has been exposed to salt stress, the chlorophyll is breaking down over time. Detrimental levels of salt affect the light harvesting complexes in algae and cause chlorophyll reduction (Perrine et al., 2012).

A study of *C. nivalis* shows that this species also produces a large amount of non-photosynthetic carotenoid pigments, which are esterified with fatty acids (Remias and Lütz, 2007). These carotenoids are important in protection against UV damage, which

this species is often exposed to due to the high irradiances in its natural habitat. However, no increase in carotenoids were observed in 0.2 M NaCl salt stressed *C. nivalis* cells in the present study (Figure 5.26 C and I) except in the second run (Figure 5.26 F) near the beginning of the salt stress period.

Certain stresses cause a drop in chlorophyll content of green algae. For example in *Haematooccus pluvialis* nitrogen deprivation causes a reduction in chlorophyll, but phosphate deprivation does not (Boussiba et al., 1999). It's suggested that nitrogen deprivation caused cellular damage including to the chloroplast. It may be that this same process is taking place in *C. nivalis* under salt stress. Salt is also shown to negatively impact chlorophyll pigment content in even halotolerant algae, as irradiance remains high but cell division is reduced (Ben-Amotz and Avron, 1983), although carotenoids do not undergo this same reduction because they cause a protecting mechanism against conditions that impair chlorophyll content.

#### **5.5.1 Photosynthesis and respiration rates in *C. nivalis* grown in 0.2 M NaCl**

Photosynthesis and respiration data was also obtained (Figure 5.27). There is a trend in the first and third experimental run of a slightly decreased ability of the salt stressed cultures to photosynthesise, which has been shown to be the case in algae (Perrine et al., 2012; Sudhir and Murthy, 2004), even in halotolerant species (Ben-Amotz and Avron, 1983). Run two showed data with error bars too large to distinguish clear differences between the control and salt stressed cultures, and in this case photosynthesis was not observed to decrease under salt stressed conditions. The difference may be due to the different starting ODs. The greater density of cells in run 2 may mean that detrimental effect of salt on photosynthesis may not be as strong since the salt to chlorophyll ratio is lower. Salt stress is shown to negatively impact photosynthesis by affecting the ion content of the cells and therefore affecting the bioenergetic photosynthesis processes (Sudhir and Murthy, 2004).

This is another advantage to introducing salt at a late stage of culture growth: the ability of the culture to photosynthesise is still high, as is chlorophyll content, but lipid producing conditions are still occurring, so lipids are higher and the culture productivity overall is higher due to greater biomass accumulation.

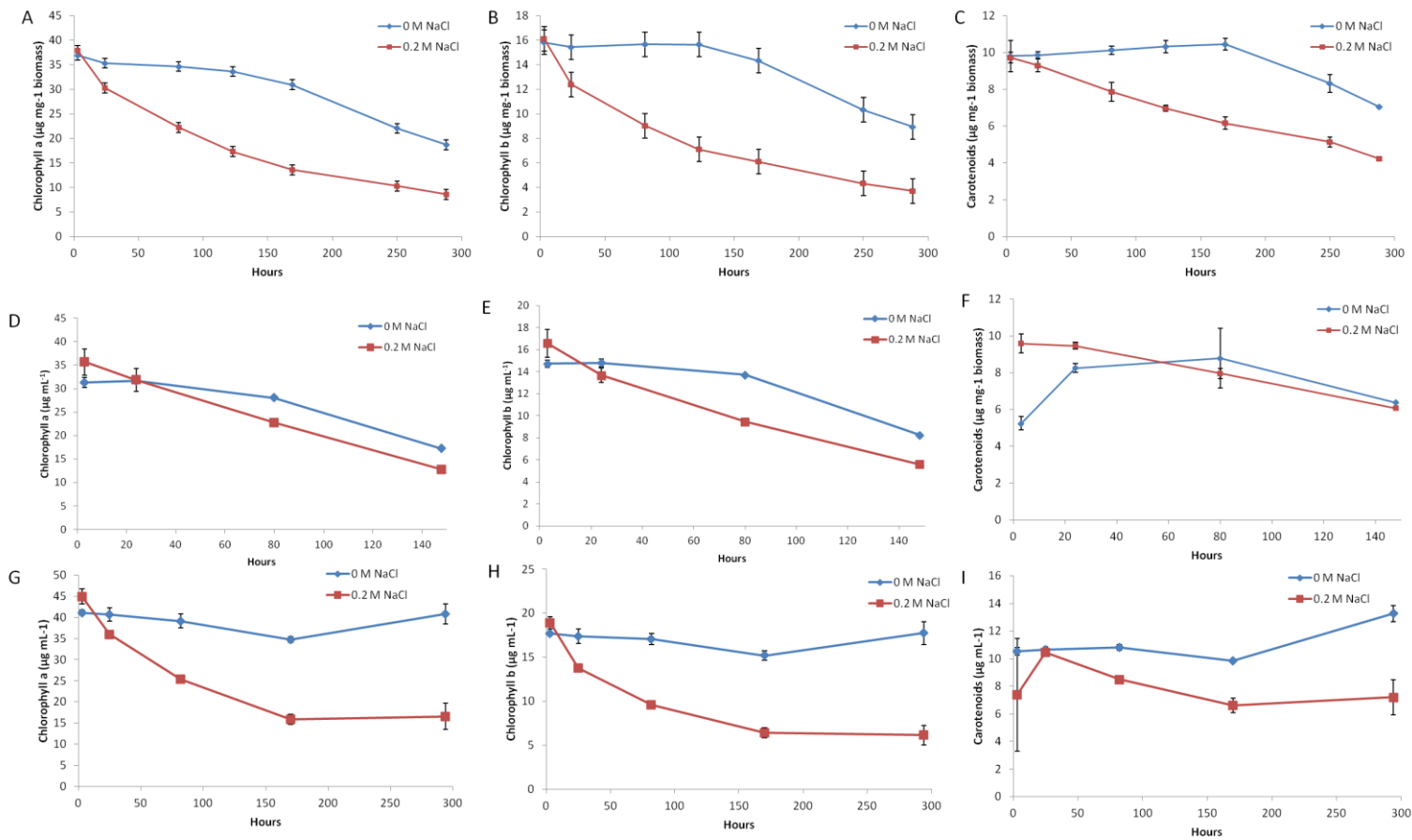


Figure 5.26 Chlorophyll a (A, D, G), chlorophyll b (B, E, H) and carotenoid (C, F, I) content in *C. nivalis* cultures grown in 0 and 0.2 M NaCl, in three experimental runs (n=3). Cells were grown in normal 3N-BBM-V medium and then resuspended in the new salinity medium at time zero.

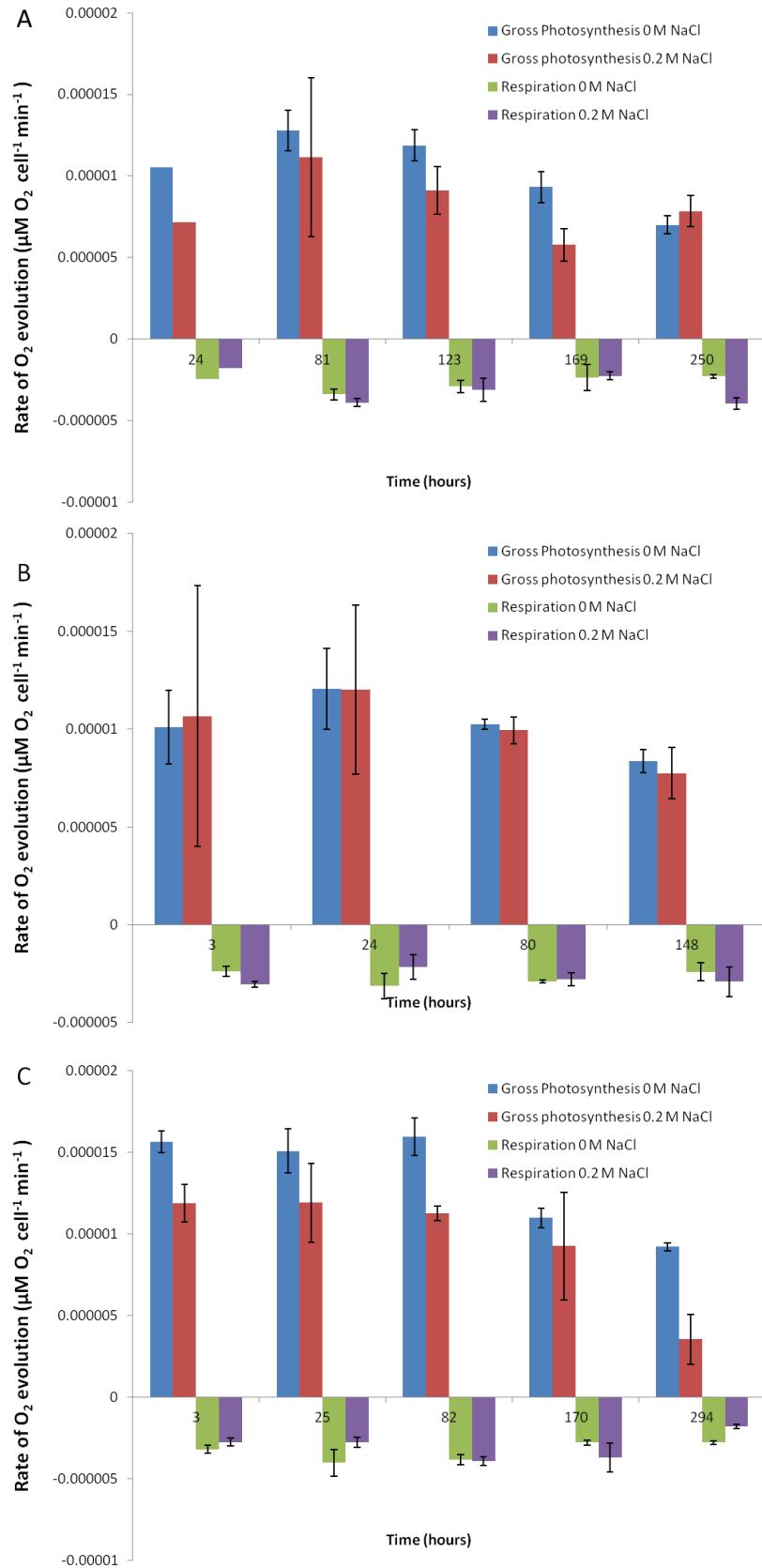


Figure 5.27 Photosynthesis and respiration data in three experimental runs (A, B, C) of *C. nivalis* cultures grown in 0 and 0.2 M NaCl (n=3).

## 5.6 Conclusions from 0.2 M NaCl experiment

The patterns observed in this data were consistent and repeatable across all three runs of this experiment. This level of salt stress (0.2 M NaCl) causes the arresting of the culture growth. Having entered this stationary state, the salt stress clearly induces first carbohydrate increase, followed by a decrease that coincides with lipid increase which is mainly caused by a large increase in C18:1*cis* (oleic acid). Chlorophyll content is reduced in salt stressed cultures and the ability of the culture to photosynthesise is slightly decreased by the presence of salt stress, as is a common response of microalgae to salt stress (Masojídek et al., 2000), although less so in cultures that were grown to 0.7 OD<sub>750</sub> before introducing salt stress. However, *C. nivalis* is still able to photosynthesise in 0.2 M NaCl, showing that the culture is still able to tolerate these conditions although little or no growth is taking place.

The C18:1*cis* is likely to be part of lipid storage molecules (Shen et al., 2016), but the same rise is not seen in C16:0, which is also part of lipid storage molecules, suggesting other possibilities such as involvement in membranes, especially the thylakoid membranes. However, the rise mainly in C18:1 above all other fatty acids has been noted in other species (Rao et al., 2007), in this case oleaginous species *B. braunii*. It has been suggested that the formation of C18:1 chains is a precursor to formation of resistant biopolymers that change the cell membranes and make the algae more resistant to harmful chemical or biological conditions (Laureillard et al., 1988). However these would be elongated to C24-C30 chains, which was not observed in this experiment. Although only certain fatty acids were identified from the standard mix, few peaks were observed in the high end of the chromatograph, and these peaks were very small. To investigate if this were the case, a different FAME standard or GC-MS methods would be employed.

The rise in C18:1*cis*, and of the total FAME levels overall, is of great interest to biofuel research in this species. The desired levels of TAG content in algal cells for biofuels production was 60% (Jorquera et al., 2010), and whilst not all of the salt stress cultures reached this level, one culture reached around 50% from comparatively very low levels, demonstrating that vast increases in lipid contents can be made for this

purpose. Whilst the present research looks only at single chain types and cannot identify the cell location of the fatty acids detected in the samples (nor whether they are derived from polar membrane lipids or from neutral lipid bodies), this work is also the first to assess the biofuel potential of this species via detailed lipid profiling with GC. Previous studies by Lu *et al.* (Lu et al., 2012a; 2012b, c) did not derivatize the fatty acids within a sample to measure its biofuel potential; instead they detect the polar lipid types from extracted crude lipid analysed via mass spectrometry.

Broadly speaking, their findings were that under salt stress: there is a decline in PG, an essential lipid in the light harvesting proteins in photosystem II; an increase in sulfolipid SQDG, which stabilizes proteins in the chloroplast membranes in photosystem II; galactolipids increase, as these maintain membrane stability. The chain types alter under salt stress, for example PE (18:1/18:1) decreased whilst PE (16:0/18:1) increased as it was newly synthesized (Lu et al., 2012a; Lu et al., 2012c). The increase in saturated fatty acids and decrease in unsaturated fatty acids in a phospholipid membrane decreases the permeability of that membrane, as shown with permeability to ethanol in yeast species *Saccharomyces cerevisiae* (Mizoguchi and Hara, 1996); altering cell permeability may be one way a cell under salt stress would act to mitigate osmotic stress. *Chlamydomonas nivalis* was grown at 16°C, a temperature lower than *C. reinhardtii* can comfortably grow. On the other hand, *C. nivalis* would not grow above 20°C in the laboratory during this research. In addition to the different media used and different level of salt stresses, this growth temperature difference must be kept in mind. Photosynthesis and respiration are temperature sensitive, and the damaging effects of low or freezing temperatures include oxidative damage from ROS (Haghjou and Shariati, 2007). *C. nivalis* is adapted to survive in a range of temperatures, particularly low temperatures, and has been described as a cryotolerant mesophile (Lukes et al., 2014).

*Chlamydomonas nivalis* can become red in colour in the wild: this is because of the photoprotective effect of carotenoids, which are employed as a survival mechanism (Lukes et al., 2014). The laboratory strain of *C. nivalis* obtained from the culture collection for the current work is said to have lost its ability to turn red. Many wild type

*Chlamydomonas* snow algae strains still have this ability. Carotenoids have been shown to have antioxidant effects (Sampath-Wiley et al., 2008) and stress tolerance has been associated with elevated metabolism of antioxidants.

A previous study of the effect of temperature on photosynthesis and thylakoid lipids has shown that *C. nivalis* and *C. reinhardtii* show very different lipid compositions of the thylakoid membranes. Although within species there are temperature dependant shifts in lipid composition, these differences between species are observed regardless of the temperatures they are exposed to over a 72 hour period (ranging from 5 to 35°C); in *C. nivalis*, the main lipid in thylakoid membranes is PG whereas in *C. reinhardtii* it is MGDG (Lukes et al., 2014). These two species have very different lipid compositions.

A question arising from the current research, in light of the fact that lipids are produced in salt stress conditions, is in which direction the causal relationship between lipids and salt stress resistance goes. It is possible either for the lipid production to be part of the salt resistance mechanisms, or a consequence of the ability of the strain to continue to function in high salt stress conditions due to other survival mechanisms.

The main conclusion from this section is that salt could be used as lipid trigger in *C. nivalis*, and that this can be done at a variety of culture densities since the effect and timescale is the same. However, the level of salt stress is crucial with 0.2 M NaCl being suitable and 1.4 M NaCl being too high.

## **5.7 Genetic identification in *C. nivalis***

As proteomic investigation was taking place into *C. nivalis* using the *C. reinhardtii* database, DNA was extracted from *C. nivalis* and sequenced using universal 18S primers to find the nearest genetic relations. DNA was extracted from a *C. nivalis* sample using the methodology described in Chapter 2 (Section 2.7).

Three different bead-beating extraction times of 90, 180 and 270 seconds were used. Extracts were visualised on agarose gel via electrophoresis. All three extraction times show some DNA present as shown in Figure 5.28.

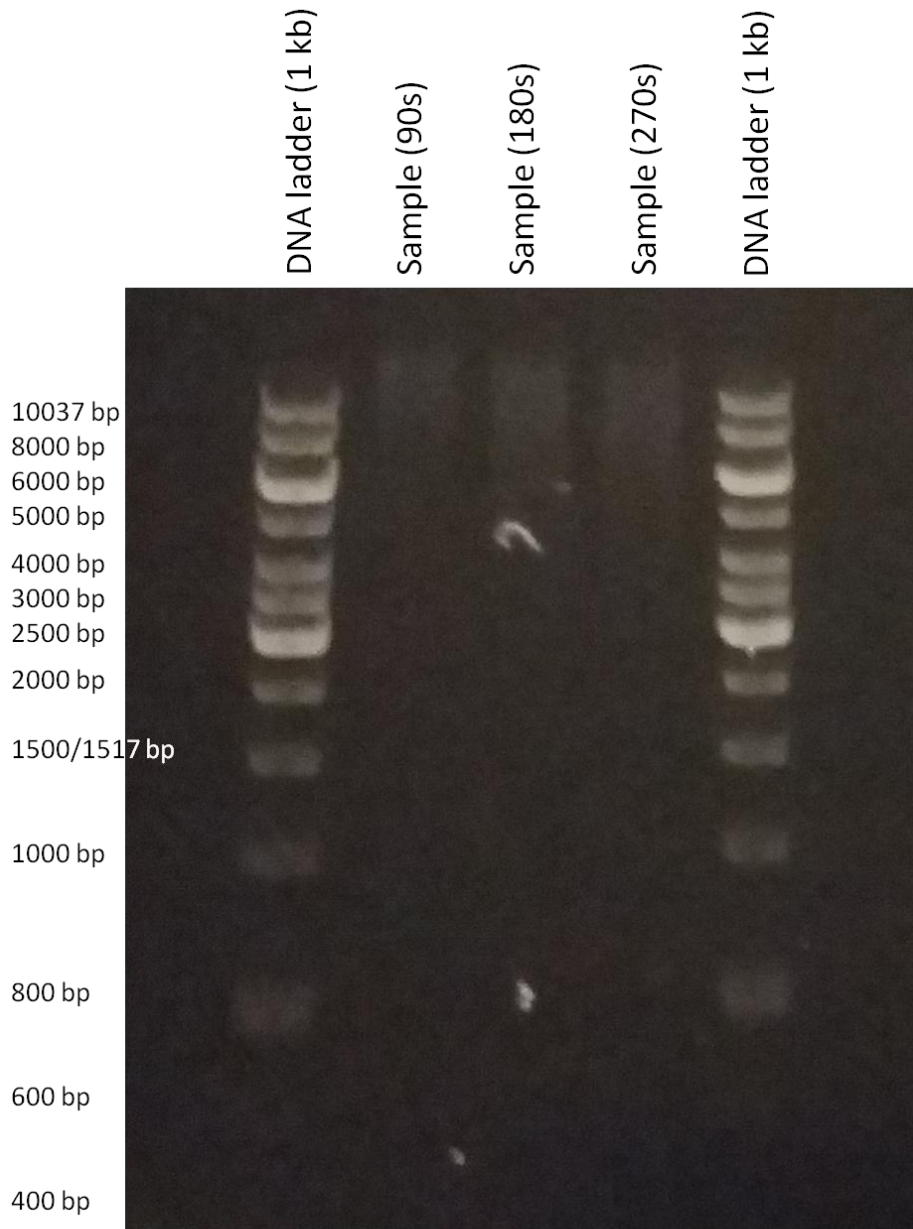


Figure 5.28 Electrophoresis gel of extracted DNA from three different extraction times (90, 180 and 270 seconds), and DNA ladder marker. The genomic DNA bands, although faint, are clearly present.

Two primers were tested, Lim and Sheehan (see section 2.7 for primer details), and following PCR and imaging of the gel, Lim primer was shown to have worked in amplifying the detected DNA whilst Sheehan had not (Figure 5.29). The control showed no DNA present, indicating that the procedure had been carried out correctly (Figure 5.29). Chosen samples were purified as described in section 2.7 and then visualised

again on a gel to check that DNA was still present (Figure 5.30), prior to sending to Eurofins for sequencing.

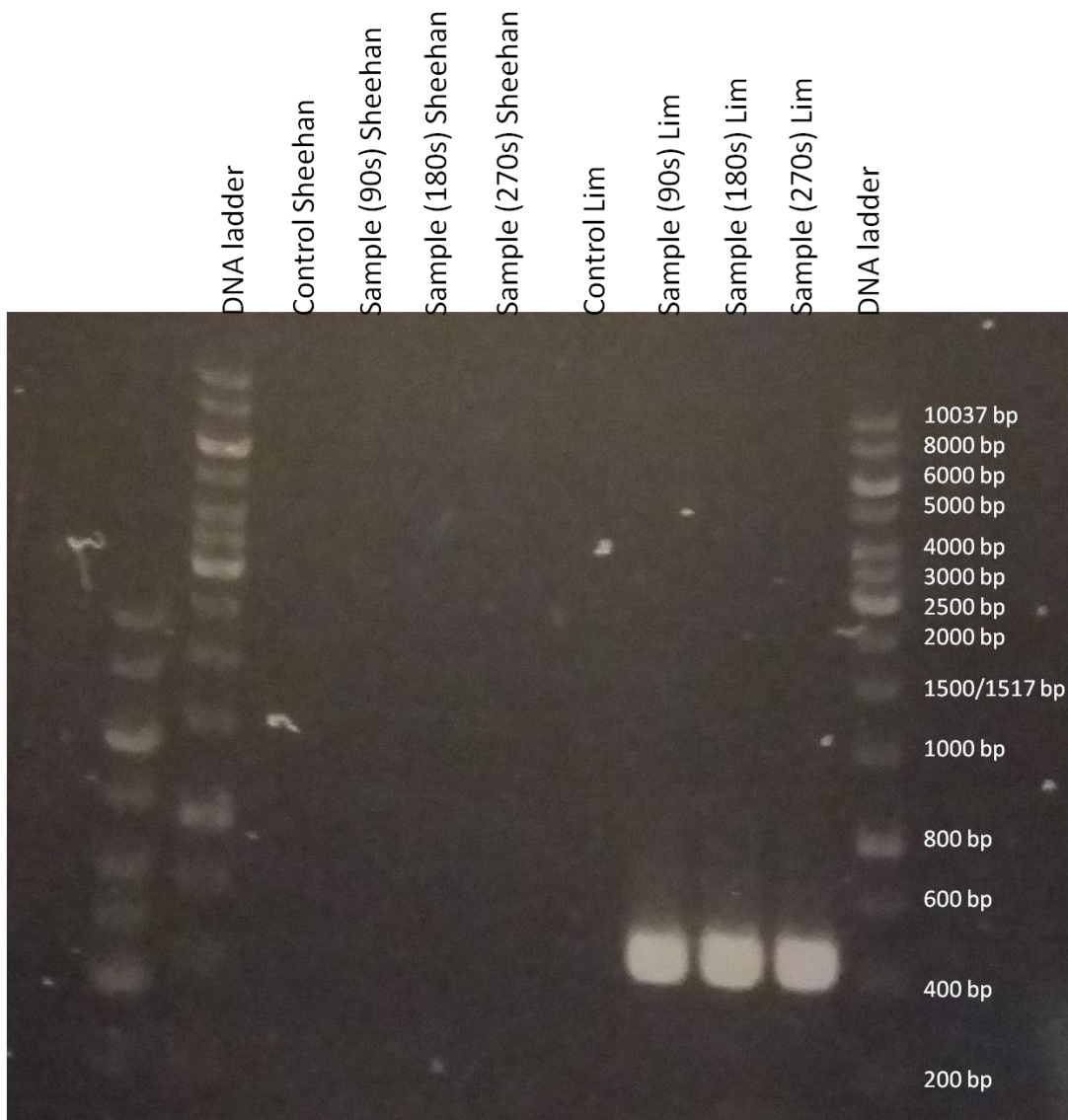


Figure 5.29 Electrophoresis gel of PCR amplified samples using Sheehan and Lim primers. Each extraction time sample, plus a control, was used for each primer.

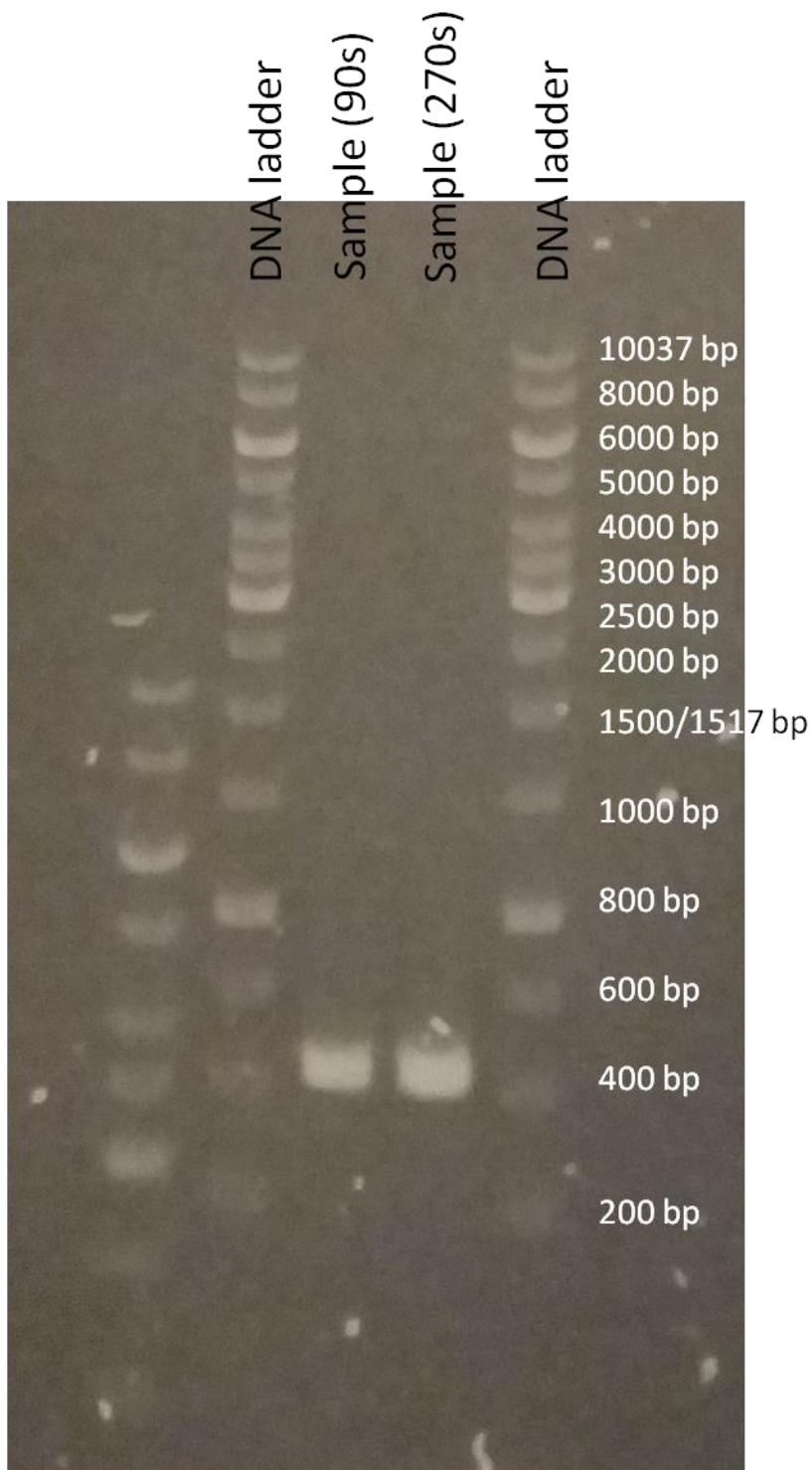


Figure 5.30 PCR amplified and purified DNA samples for 90s and 270s extraction times.

As two samples (from a 90 second and a 270 second extraction time) were sequenced, four sequences were returned: forward and reverse for each of the two sequences.

Sequences obtained are displayed in Table 5.1 below:

Table 5.1 Sequences obtained from Eurofins for *C. nivalis* extracted DNA.

Sample	Sequence
90s For	CGTTAAAGCTCGTAGTTGGATTTGCGGGGGGTCTTAGCGGTCCGGTTCGCTGT GTA CTGC TAGGGCCCTCCTTTCTGCCGGGGACAGGCTCTTGGGCTTCATTGTCTGGGACCT GGAGTC GGCGAGGTTACTTTGAGTAAATTAGAGTGTTCAAAGCAAGCCTACGCTCTGAA TACATTA GCATGGAATAACACGATAGGACTCTGGCCTATCTTGTGGTCTGTAGGACCGG AGTAATG ATTAAGAGGGACAGTCGGGGGCATTCGTATTTTCATTGTCAGAGGTGAAATTCT TGGATTT ATGAAAGACGAACTTCTGCGAAAGCATTGCGCAAGGATGTTTTTATTAATCAAG AACGAA AGTTGGGGGCTCGAAGACGATTAGATACCGTCGTAGTCTCAACCATAAACGAT GCCGACT AGGGATTGGCAGGTGTTCTTTTGATGACCCTGCCAGCACCTTATGAGAAATCA AAGTTTT TGGGTTGCGGGGAAGTT (length = 498 bp)
90s Rev	TCTACGTGCTGGCAGGGTCATCAAAGAACACCTGCCAATCCCTAGTCGGCAT CGTTTAT GGTTGAGACTACGACGGTATCTAATCGTCTTCGAGCCCCCACTTTCGTTCTTG ATTAAT GAAAACATCCTTGGCAAATGCTTTGCGAGAAGTTCGTCTTTCATAAATCCAAGA ATTTCA CCTCTGACAATGAAATACGAATGCCCCGACTGTCCCTCTTAATCATTACTCCG GTCCTA CAGACCAACAAGATAGGCCAGAGTCCTATCGTGTTATTCCATGCTAATGTATT AGAGCG TAGGCTTGCTTTGAACACTCTAATTTACTCAAAGTAACCTCGCCGACTCCAGGT CCCAGA CAATGAAGCCCAAGAGCCTGTCCCCGGCAGAAAGGAGGGCCCTAGCAGTACA CAGCGAAC CGGACCGCTAAGACCCCCCGAAATCCAACACTACGAGCTTTTTAACTGCAACAAC TTAAAT ATACGCTATTGGAGCTGAAATT (length = 502 bp)
270s For	AGTTAAGCTCGTAGTTGGATTTGCGGGGGGTCTTAGCGGTCCGGTTCGCTGTG TACTGCT AGGGCCCTCCTTTCTGCCGGGGACAGGCTCTTGGGCTTCATTGTCTGGGACCT GGAGTCG GCCGAGGTTACTTTGAGTAAATTAGAGTGTTCAAAGCAAGCCTACGCTCTGAAT ACATTAG CATGGAATAACACGATAGGACTCTGGCCTATCTTGTGGTCTGTAGGACCGGA GTAATGA

	<p>TTAAGAGGGACAGTCGGGGGCATTTCGTATTTTCATTGTCAGAGGTGAAATTCTT GGATTTA TGAAAGACGAACTTCTGCGAAAGCATTGCGCAAGGATGTTTTTCATTAATCAAGA ACGAAA GTTGGGGGCTCGAAGACGATTAGATACCGTCGTAGTCTCAACCATAAACGATG CCGACTA GGGATTGGCAGGTGTTCTTTTGATGACCCTGCCAGCACCTTATGAGAAATCAA AGTTTTT GGGTTGCGGGGGGAGTTA (length = 498 bp)</p>
270s Rev	<p>TCTAGGTGCTGGCAGGGTCATCAAAGAACACCTGCCAATCCCTAGTCGGCAT CGTTTAT GGTTGAGACTACGACGGTATCTAATCGTCTTCGAGCCCCAACTTTGTTCTTG ATTAAT GAAAACATCCTTGGCAAATGCTTTCGCAGAAGTTCGTCTTTCATAAATCCAAGA ATTTCA CCTCTGACAATGAAATACGAATGCCCCCGACTGTCCCTCTTAATCATTACTCCG GTCCTA CAGACCAACAAGATAGGCCAGAGTCCTATCGTGTTATTCCATGCTAATGTATTC AGAGCG TAGGCTTGCTTTGAACACTCTAATTTACTCAAAGTAACCTCGCCGACTCCAGGT CCCAGA CAATGAAGCCCAAGAGCCTGTCCCCGGCAGAAAGGAGGGCCCTAGCAGTACA CAGCGAAC CGGACCGCTAAGACCCCCCGAAATCCAACACTACGAGCTTTTTAACTGCAACAAC TTAAAT ATACGCTATTGGAGCTGAATTT (length = 502 bp)</p>

When matching these in BLAST (<http://blast.ncbi.nlm.nih.gov/Blast.cgi>), species names and identity match scores were obtained. For each of the four sequences, the top five species matches are displayed in Table 5.2, plus the sequence coverage match of *C. nivalis* and *C. reinhardtii*.

Sequencing one gene, even the highly conserved 18S rRNA gene, does not always allow an exact species match and a number of closely related strains often show up as very closely related to each other. This is the case here, where the best matches are in the genus *Chlamydomonas* and *Chloromonas*. The relatedness of these species have been displayed in the phylogenetic tree in Figure 5.31. The DNA extracted from *C. nivalis* shows a 95-96% match with *C. reinhardtii* however the results show that there are some differences between the two species since *C. nivalis* is more similar to other species of *Chlamydomonas* and *Chloromonas* than to *C. reinhardtii*. This is a very

important observation in relation to the proteomic experiments involving *C. nivalis* because it suggests that matching the *C. nivalis* proteomic data purely against the *C. reinhardtii* database may limit the number of matches due to genetic differences between the two species. Matching the proteomic data against the *Chlorophyta* database may yield more results.

**Table 5.2 Identity match (%) for sequences obtained from *C. nivalis* extracted DNA.**

<b>Sample</b>	<b>Species name</b>	<b>Identity match (%)</b>
	<i>Chlamydomonas gerloffii</i>	99.594
	<i>Chlamydomonas subtilis</i>	99.594
	<i>Chloromonas typhlos</i>	99.594
	<i>Chlamydomonas sp. A-SIO</i>	99.594
	<i>Chloromonas paraserbinowii</i>	99.594
	<i>Chlamydomonas nivalis</i>	97.972
90s For	<i>Chlamydomonas reinhardtii</i>	95.344
	<i>Chlamydomonas gerloffii</i>	99.799
	<i>Chlamydomonas subtilis</i>	99.799
	<i>Chloromonas typhlos</i>	99.799
	<i>Chlamydomonas sp. A-SIO</i>	99.799
	<i>Chloromonas paraserbinowii</i>	99.799
	<i>Chlamydomonas nivalis</i>	98.189
90s Rev	<i>Chlamydomonas reinhardtii</i>	95.582
	<i>Chlamydomonas gerloffii</i>	99.797
	<i>Chlamydomonas subtilis</i>	99.797
	<i>Chloromonas typhlos</i>	99.797
	<i>Chlamydomonas sp. A-SIO</i>	99.797
	<i>Chloromonas paraserbinowii</i>	99.797
	<i>Chlamydomonas nivalis</i>	98.171
270s For	<i>Chlamydomonas reinhardtii</i>	95.538
	<i>Chlamydomonas gerloffii</i>	99.8
	<i>Chlamydomonas subtilis</i>	99.8
	<i>Chloromonas typhlos</i>	99.8
	<i>Chlamydomonas sp. A-SIO</i>	99.8
	<i>Chloromonas paraserbinowii</i>	99.8
270s	<i>Chlamydomonas nivalis</i>	98.196
Rev	<i>Chlamydomonas reinhardtii</i>	95.6

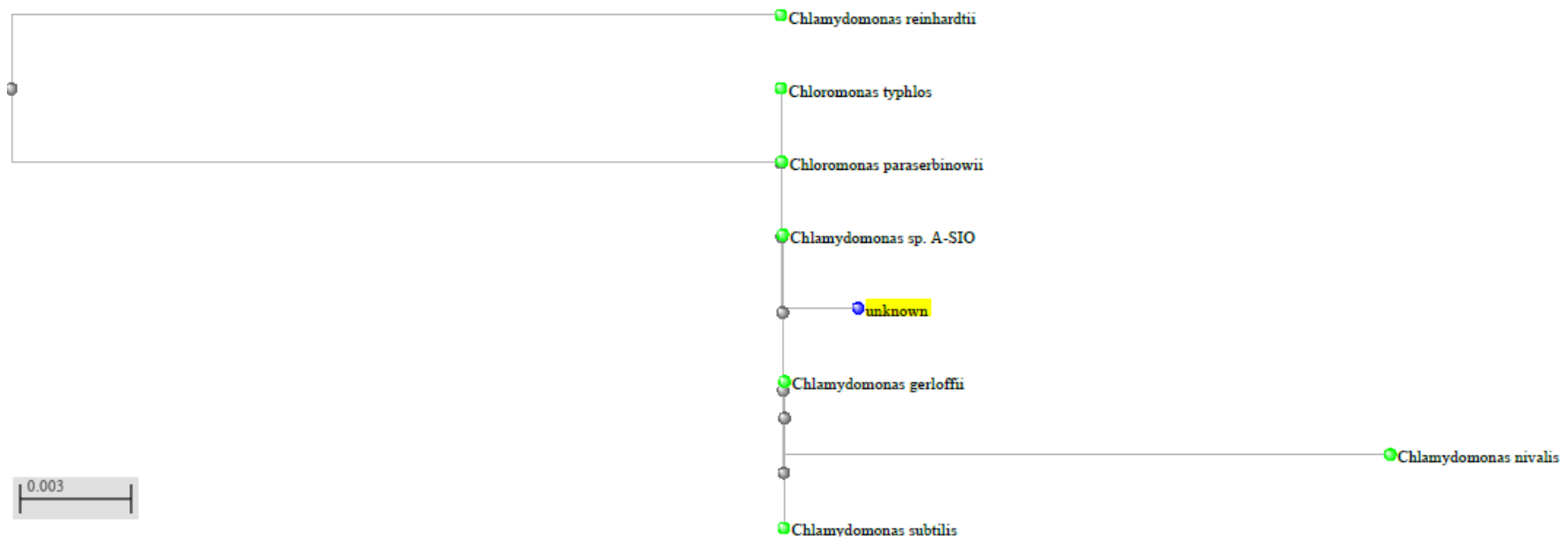


Figure 5.31 Phylogenetic tree of identity matches from rDNA sequencing. Extracted DNA is represented as "unknown" on the tree.

## 5.8 Proteomic investigation of *C. nivalis* under lipid triggering 0.2 M NaCl salt conditions using iTRAQ

Proteomic analysis of *C. nivalis* was carried out in a time course experiment of lipid producing conditions. These were taken from 3 hours, 82 hours and 170 hours of the 0.2 M NaCl condition from the third run of this experimentation, and from 170 hours of the control condition. The aim was to test the effect of salt stress over time on *C. nivalis*, particularly at the points of rises in carbohydrate and lipid, and to compare arrested growth in salt conditions with mid-log growth in control conditions. These conditions were used to construct a 4 way phenotypic comparison between conditions, using the following grouping for iTRAQ labelling:

Table 5.3 Sampling points for iTRAQ comparison.

Condition number	Phenotype conditions	iTRAQ labels
1	3 hour 0.2 M NaCl: low carbohydrates and lipids	113 114
2	82 hour 0.2 M NaCl: High carbohydrates	115 116
3	170 hour control: mid-log growth	117 118
4	170 hour 0.2 M NaCl: high lipids	119 121

Following protein sample extraction and preparation as outlined in the Materials and Methods chapter 2, samples were quantified and analysed by a 1D-SDS-PAGE gel to check the quality of samples prior to digestion, labelling, fractionation and MS analysis. Protein quantifications and 1D-SDS-PAGE gel are shown below.

Table 5.4 Protein concentrations in extracted samples.

Sample name	Condition	Biological replicate	Protein concentration (mg mL <sup>-1</sup> )
CFK	1	1	3.4 ± 0.104
CFL		2	2.0 ± 0.104
CGK	2	1	4.2 ± 0.072
CGL		2	7.8 ± 0.016
CGV	3	1	6.2 ± 0.272
CGW		2	4.8 ± 0
CGX	4	1	4.6 ± 0.144
CGY		2	6.1 ± 0.128

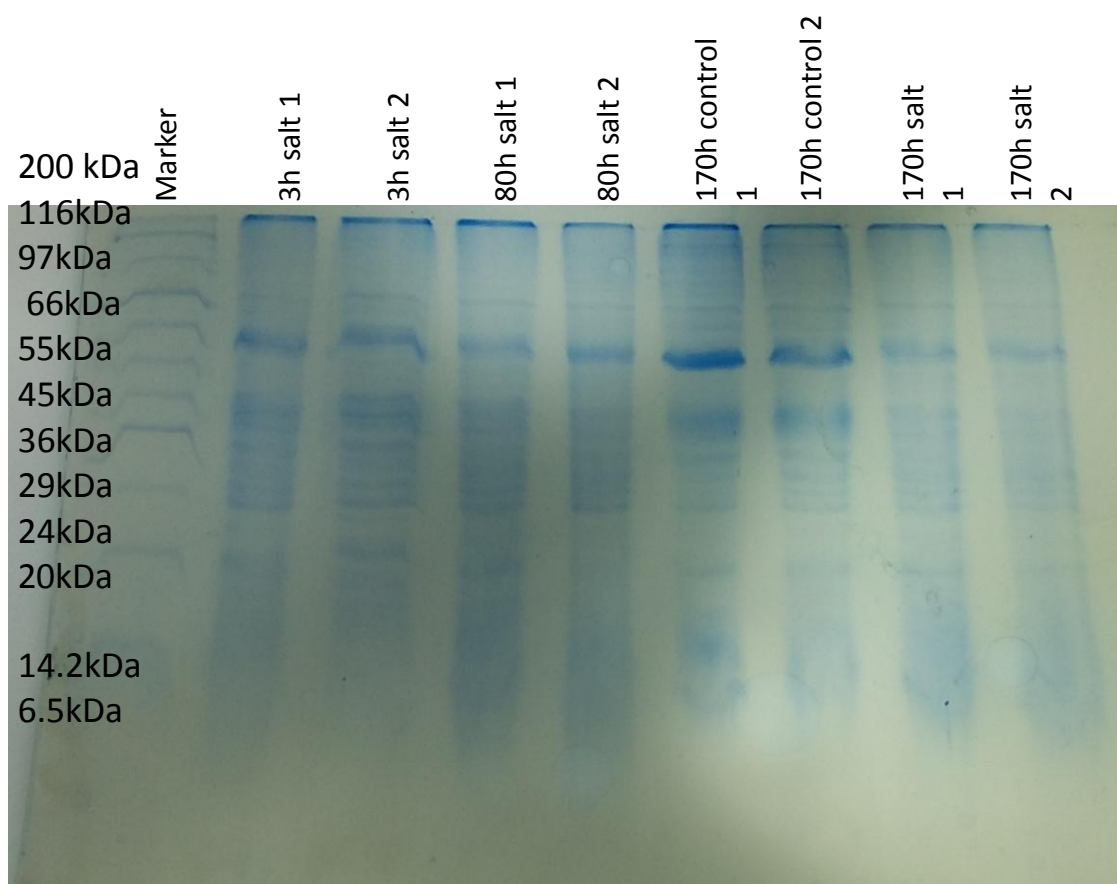


Figure 5.32 SDS PAGE of samples.

Figure 5.32 shows 1D-SDS-PAGE gel of the samples (each lane containing 15 µg) and indicate good sample quality and similarity in biological replicates, since the bands show clear separation of intact proteins through intensely stained and well separated bands, as well as a clear well defined protein marker lane.

Samples were digested and two 10 µg aliquot from each sample (one taken before digestion incubation and one afterwards) were run on gels to check the digestion process had been completed. The results of this gel were not conclusive (data not shown), so a small aliquot of one sample was run on AmaZon MS to check the digestion process. 92 proteins were identified, and the peptide matches showed that the majority of peptides had zero mis-cleavages (179 of 241). Results indicated digestion was complete, and digestion was assumed to be equal between all samples. iTRAQ labelling and HPLC fractionation were then carried out. The UV vis chromatogram, measured at 214 nm) is displayed in Figure 5.33.

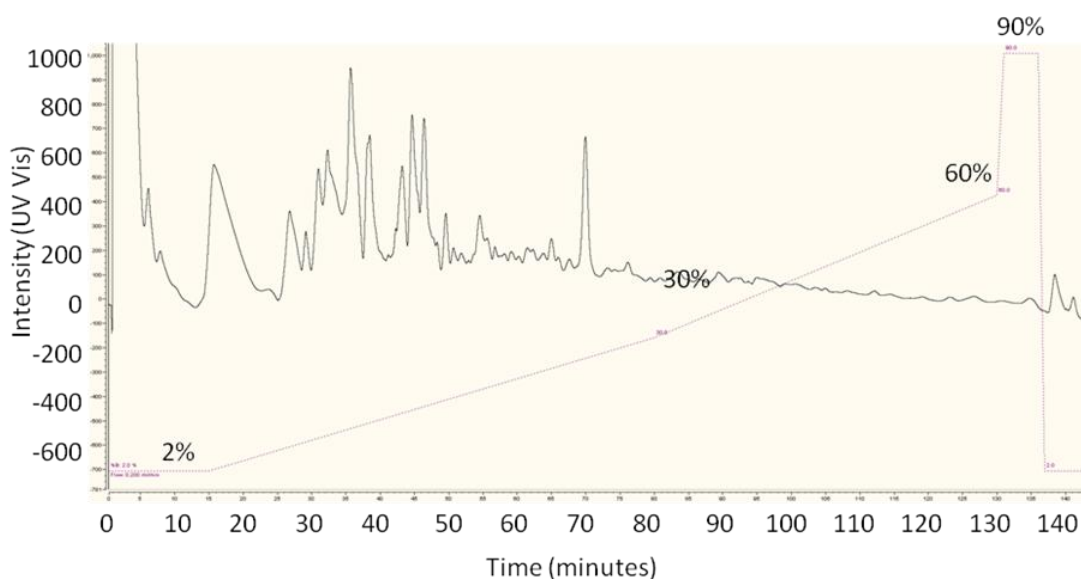


Figure 5.33 UV vis chromatogram of iTRAQ labelled *C. nivalis* samples.

Fractions were separated, dried down, recombined and then were injected into Q Exactive HF MS and run as described in methods Chapter 2, Section 2.6.10.

Two injections of the fractions were carried out, since the first injection gave limited results from Maxquant identifications. Following a second injection to test if CID of iTRAQ labels had been correctly carried out, during which the collision energy was changed from 32 eV to 27 eV, it was concluded that lack of identifications was due to limited database matching, and the second set of injections gave little improvement on the previous PSMs and protein hits.

Because this species is un-sequenced, data analysis is not as straightforward as *C. reinhardtii* proteomic investigations; steps must be taken to maximise the data acquisition. There are two main ways of doing this: using software specialising in *de novo* sequencing and homology searching, and using a variety of organism databases. Maxquant is the standard software used for processing of Q Exactive HF data, and yields good results for sequenced organism *C. reinhardtii*. However, PEAKS has greater scope for identifications through homology searching, which identifies peptides using algorithms that predict amino acid mutations and variations in a peptide sequence. PEAKS and Maxquant have both been used to detect and quantify proteins in this study, however only one could be used for the final dataset. For database searching, the *C. reinhardtii* database is the starting point for identification. Expanding the searches to the *Chlorophyta* taxon database, and to the *Chlamydomonas* genus database may also yield more results. *C. nivalis* does have a small amount of its proteome mapped, with 73 proteins present in the Uniprot database (searched 6th May 2016). This database is too small to carry out meaningful quantitative proteomic investigations, but the *Chlamydomonas* database, consisting of 15,885 entries, may yield greater matches than the *Chlamydomonas reinhardtii* database (15,172 entries). The *Chlorophyta* database contains 167,662 entries. Whilst this may appear to be a good option for searching since it allows for a greater diversity of potential matches, the effect of searching against a larger database on the FDR has negative effects on results yielded (Vensel et al., 2011). Fewer results were obtained when searching against *Chlorophyta* than when searching against *C. reinhardtii* (Table 5.5). Because of this, remaining searches were limited to *Chlamydomonas* genus database and to *C. reinhardtii* database. Searches were carried out using the search criteria described in Section 2.6.10. These searches were carried out on a total of 279,007 MS scans and 264,461 MS/MS scans.

Table 5.5 summarises the number of results yielded for the different searching strategies. All searches used 1% FDR for PSMs, and protein identifications used two or more unique peptides. Use of PEAKS fully utilised the variable PTM and Spider homology searches for maximised identifications and quantifications. These functions search through possible amino acid substitutions in peptides, and PTMs that may not

be specified, to identify peptides with mutations and alterations to the database match, but that are still functionally the same peptide. Peptides were identified by the software (PSM numbers listed in table), then peptide lists (cut off at 1% FDR) were used in uTRAQ to obtain a list of quantified protein identifications (2 or more unique peptides).

Despite the *Chlamydomonas* genus database containing sequences from *C. nivalis* that may be expected to yield more results, the use of this database yields fewer identified and quantified proteins than using the *C. reinhardtii* database. Although *Chlamydomonas* database matches a higher number of PSMs than *C. reinhardtii*, the effects of redundancy in the *Chlamydomonas* database (multiple proteins of the same function from different species) may reduce the number of peptides that can be matched to proteins above the threshold of 2 or more unique peptides. Through exploration of this data, it was therefore concluded that use of the *C. reinhardtii* database through homology matching in PEAKS would give the most complete dataset for comparison of changes between conditions, and later for comparisons to *C. reinhardtii* iTRAQ data. This also allows a greater potential for exploration through functional annotation analysis and metabolic mapping, since these systems have capabilities for model species *C. reinhardtii*, but not necessarily for other species. 1231 proteins were found for PEAKS search of *Chlamydomonas reinhardtii* search, but after removing duplicate accession numbers this is reduced to 1018.

Table 5.5 Summary of search results for *C. nivalis* MS iTRAQ data.

Software	Database	PSMs	Proteins identified/quantified
	<i>Chlamydomonas</i>		
MaxQuant	<i>reinhardtii</i>	799	179
MaxQuant	<i>Chlorophyta</i>	857	43
MaxQuant	<i>Chlamydomonas</i>	858	378
	<i>Chlamydomonas</i>		
PEAKS	<i>reinhardtii</i>	2789	1018
PEAKS	<i>Chlamydomonas</i>	4182	480

PEAKS clearly yields the largest amount of protein identifications and quantifications, due to the nature of the homology search and *de novo* sequencing of peptides. It's therefore a valuable tool in obtaining data for this species by allowing for further insight into its proteome. Whilst MaxQuant is suited to accurate data analysis of the Q Exactive HF obtained data, the limitation to the *C. reinhardtii* database means that without the homology searching, fewer PSMs and proteins were identified, thus PEAKS was used for iTRAQ data analysis of *C. nivalis*.

The detected proteins were compared using Venn diagram analysis via accession number in GeneVenn (found at <http://genevenn.sourceforge.net/>). The majority are found in PEAKS and this is therefore the best tool to use for comparisons between conditions in the iTRAQ, but results from both search engines have been studied here and compared, since there are some identifications that do not overlap. Data from multiple search engines cannot be combined directly as it would require statistical manipulation to stop multiple identifications from the same spectra, since the search engines use different algorithms to create PSMs (Searle et al., 2008). So, PEAKS was selected as the sole search software for identifications.

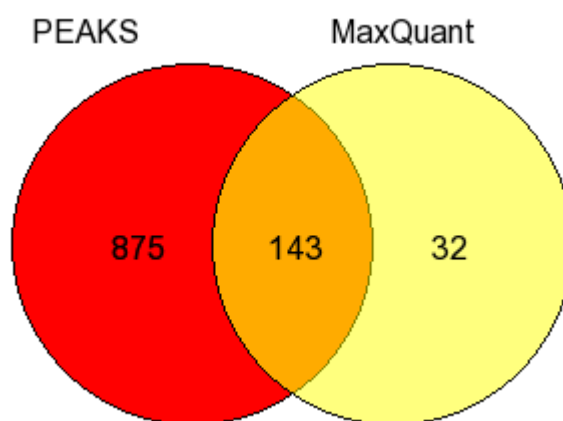


Figure 5.34 GeneVenn diagram showing overlap of accession numbers detected by PEAKS and MaxQuant.

To check the grouping of replicates, data was run through Perseus software for hierarchical clustering and PCA analysis (Figure 5.35 and Figure 5.36). Grouping shows a large difference between control cultures (117 and 118) and the salt grown cultures. 3 hour salt cultures (113 and 114) are distinctly grouped from the later time points of

80 hours (115 and 116) and 170 hours (119 and 121), but these two later time points of salt stress show overlap in the PCA plot and similarity in the hierarchical clustering.

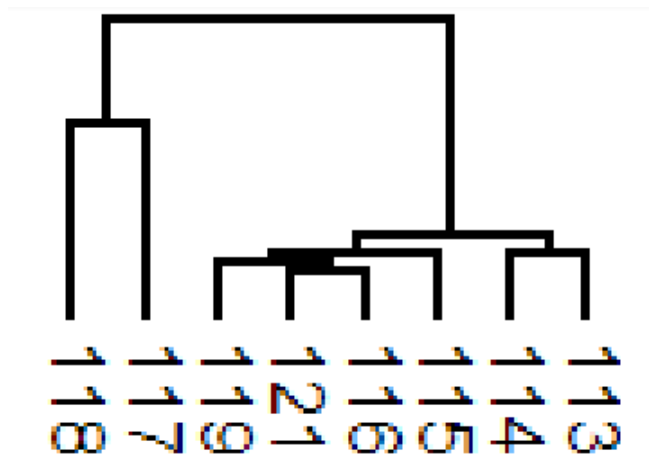


Figure 5.35 Hierarchical clustering analysis of the 8 samples, labelled using the iTRAQ label identifiers.

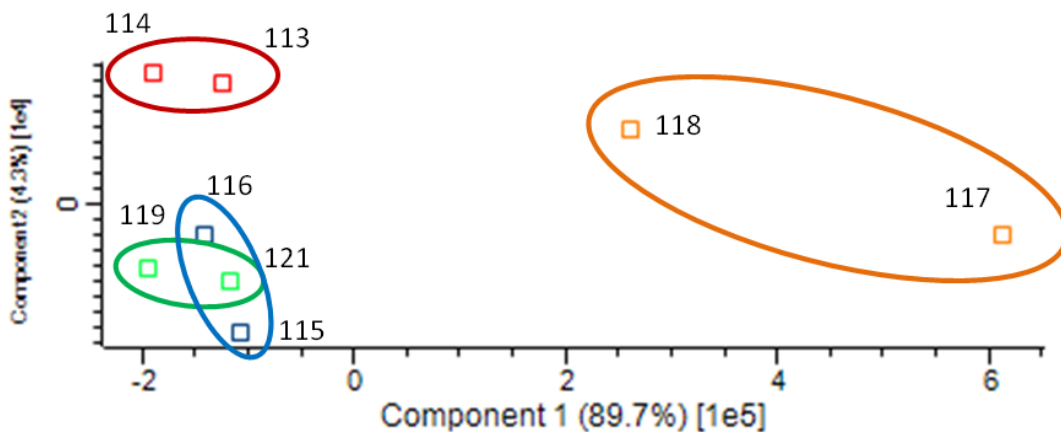


Figure 5.36 PCA analysis showing sample grouping: 3 hour salt (red), 80 hour (blue), 170 hour salt (green) and 170 hour control (orange).

To check the coverage of the detected proteins, EC (Enzyme Commission) numbers were taken from the detected protein list and mapped against ChlamyCyc metabolic map (Figure 5.37), a mapping tool that displays known pathways in *Chlamydomonas reinhardtii*. Of the 1018 detected proteins, 240 had EC numbers. Some proteins have more than one EC number associated with them, so these were separated out to give the full list of 249 EC numbers to ensure full identification, although this contains duplicates so these were removed (without duplicates the list is 159 EC numbers). 17

of these could not be found on the metabolic map. Detected EC numbers are displayed on the map. Although the number of proteins identified and quantified is not as large as may be expected in a similar study on *C. reinhardtii*, a large amount of the proteome and metabolic pathways are still detected using the dataset obtained.



Figure 5.37 Detected pathways identified through ChlamyCyc metabolic mapping and EC numbers from detected proteins in PEAKS dataset for *C. nivalis*. Detected proteins are highlighted red.

To compare the phenotypes, uTRAQ and SignifiQuant were used to quantify proteins and detect differences in proteins of significance  $p < 0.05$ , without multiple test correction applied (since this can limit data drastically and lead to important protein changes being missed (Datta and DePadilla, 2006)). The 3 hour, 82 hour and 170 hour time points were compared along a time course experiment, and the 170 hour time point also had a control to salt stress comparison.

During the time course experiment culture phenotypes were measured (Section 5.5) as described in the methods Chapter 2. The 82 hour salt condition shows a large increase in carbohydrate content. The 170 hour salt condition shows a decrease in carbohydrate content and a significant increase in fatty acid content. The control condition at 170 hours shows a lower fatty acid content and shows a steady rate of growth, compared to the salt condition which did not increase in biomass or cell density along the time course experiment.

### **5.8.1 Differences between 3 hour salt and 82 hour salt (salt induced carbohydrate production)**

Between these sample groups, there were 143 differentially expressed proteins (once duplicate accession numbers have been removed). 115 were down-regulated and 28 were up-regulated. Details of these are shown in Appendix D.

#### ***5.8.1.1 Phenotypic changes between time points***

To link these differences to phenotypic changes, a summary of the changes between 3 and 82 hours follows: there was no increase in OD or biomass accumulation, some increase in cell size and morphology, a slight increase in lipid accumulation, especially due to an increase in C18:1*cis*, a significant increase in carbohydrate accumulation, a significant decrease in chlorophylls but no significant change in carotenoids, no significant change in photosynthesis and a slight increase in respiration (although at a slightly lower level than the control conditions).

### *5.8.1.2 Metabolic map changes between time points*

The functional annotation and metabolic mapping of these changes has been shown in Figure 5.38 and Figure 5.39.

The metabolic map indicates some down-regulation of photosynthesis, which supports oxygen electrode data that photosynthesis was affected by the presence of salt conditions, but there is also some up-regulation, suggesting that photosynthesis was not completely impaired by salt conditions over time. Amino acids biosynthesis was largely up-regulated, as was amino acid degradation, suggesting that there is high turnover of amino acids between the time points. Fatty acid biosynthesis was down-regulated. Carbohydrates showed a mixture of up and down-regulation, but carbohydrate degradation was down-regulated. The decrease in carbohydrate down-regulation may be leading to the accumulation of carbohydrates.

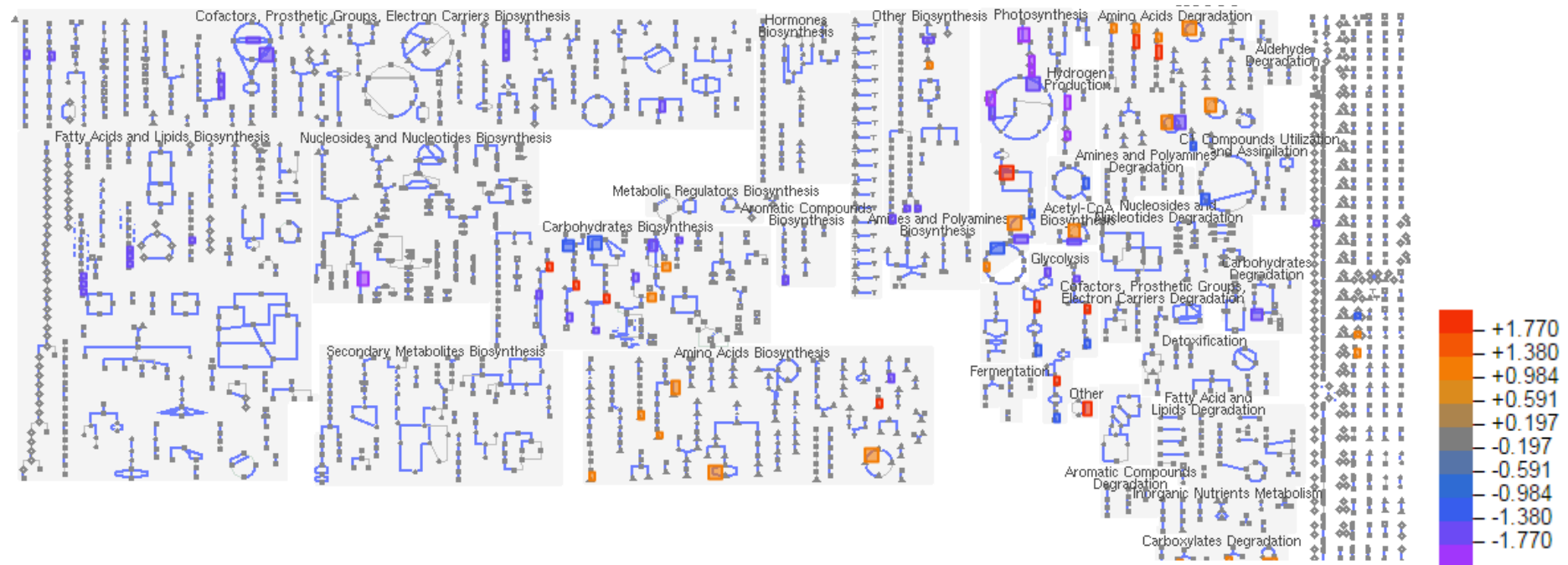


Figure 5.38 Metabolic map from ChlamyCyc indicating up and down-regulation of proteins between 3 and 82 hours. 51 of the changes had EC numbers, 1 of which was not found in the search.

### *5.8.1.3 Functional annotation analysis*

The vast majority of functional annotation (Figure 5.39) indicated down-regulation of protein groups, with the exception of translation which was up-regulated. Carbon fixation was down-regulated, along with photosynthesis and pigment biosynthesis. All metabolic processes were down-regulated, and most processes indicating cell division were also down-regulated, with the exception of translation. Using this analysis does not reveal a lot of information, other than the fact that almost all annotated proteins were down-regulated, showing that many processes were taking place at a decreased rate at 82 hours compared to 3 hours. Such decreases suggest that over time, the salt stressed cells were largely going into stasis and decreasing the rate of most of their main processes. This may explain the cells storing the fixed carbon in carbohydrates and lipids, since metabolism of the cells resources is significantly slowed.

Using solely one type of analysis would give a skewed result, since the functional analysis and the metabolic mapping suggest different things (one showing almost exclusively down-regulation whilst one shows a mixture of up and down-regulation). This indicates the complimentary nature of information from these different type of analysis, and the importance of needing more than one analytical approach.

The optical density data certainly suggests that cell division was completely arrested, and the up-regulation of translation may be due to the need for cellular repair of certain proteins that have been damaged.

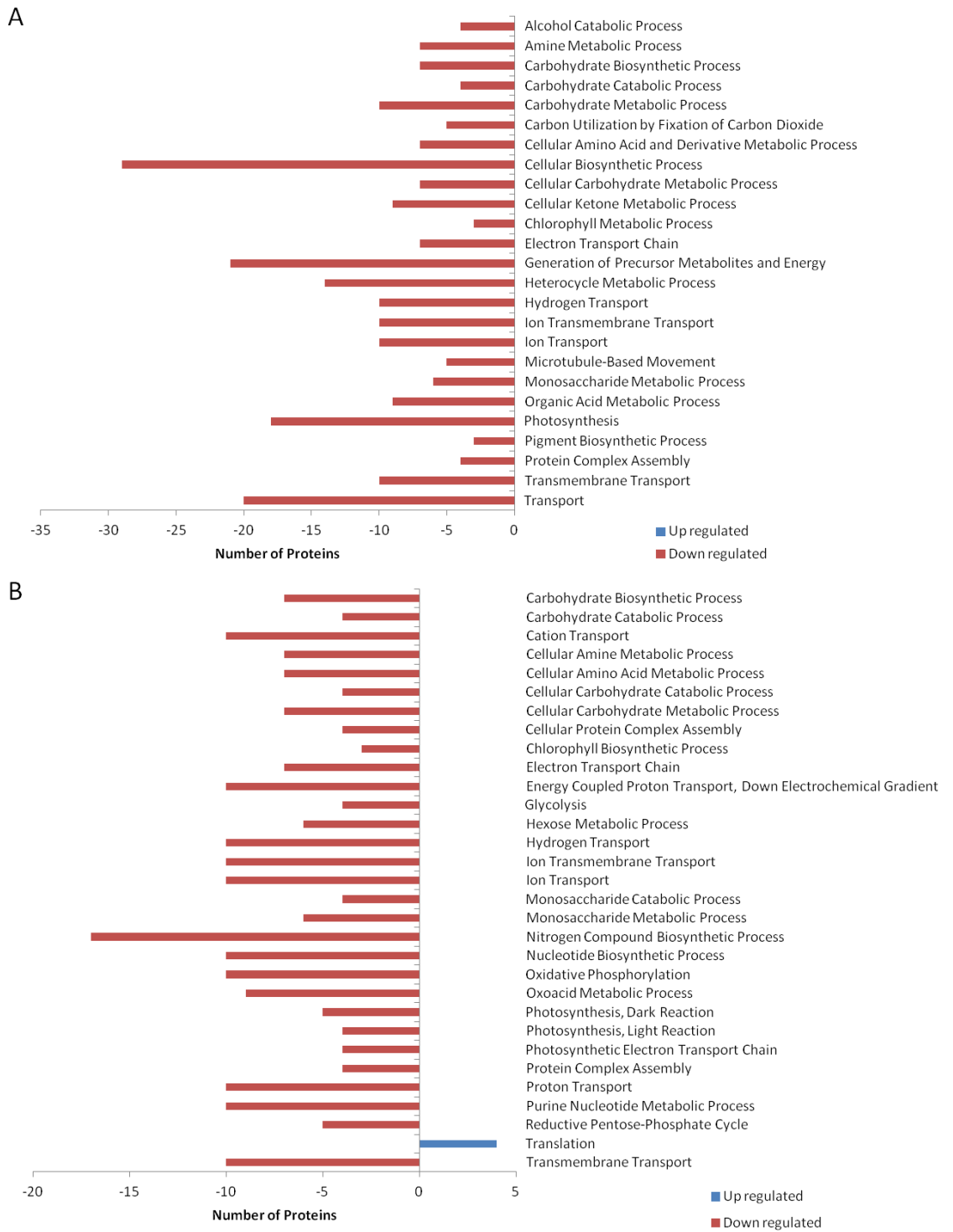


Figure 5.39 Functional annotation analysis of changes between 3 and 82 hour salt stress at BP level 3 (A) and BP level 4 (B). Of 28 down-regulated proteins, none were found in BP3, 21 of the 25 DAVID IDs were not found at BP4. When 115 up-regulated proteins were searched, 91 DAVID IDs were found. 38 of these were not found at BP3, and 54 were not found at BP4.

#### 5.8.1.4 Individual proteomic changes

Analysis of individual proteins reveals more insight, as although no major lipid pathways were affected in the mapping analysis, some individual proteins involved in lipid metabolism were changed. Biotin carboxylase, an essential acetyl-CoA carboxylase (ACC) component, was down-regulated. ACC regulates fatty acid metabolism and biotin carboxylase is involved in FA biosynthesis as well.

Additionally, dihydrolipoamide acetyltransferase was down-regulated, a protein which transfers the acetyl group to coenzyme A (CoA). CoA oxidises pyruvate in the citric acid cycle, but also is important in the oxidation and synthesis of fatty acids. The down-regulation of these enzymes suggests that fatty acid biosynthesis was being reduced, when the phenotypic data suggests the opposite: that fatty acids were beginning to accumulate.

Furthermore, glycerol-3-phosphate dehydrogenase was up-regulated. This is involved in the conversion of carbohydrates to lipids and with glycerol metabolism. Glycerol is essential to TAG production and is also used by many halotolerant algae as a compatible solute to regulate osmotic pressure from salt stress. Therefore, the up-regulation of this protein may be expected for both protection from osmotic damage and as a step in the formation of TAGs. At the later time point, lipid content had already begun to increase.

UDP-sulfoquinovose synthase was down-regulated. This is involved in glycerolipid metabolism, and sulfoquinovosyl diacylglycerol (SQDG) metabolism. SQDG is a major constituent of thylakoid membranes in algae. By contrast, in previous work in *C. nivalis*, NaCl has been shown to trigger the increase of SQDG, and is thought to stabilise membranes and protein complexes in photosystem II (Lu et al., 2012a). SQDG has also been shown to reduce when TAG accumulates under nitrogen deprivation, and it is theorized that FAs are liberated from SQDG for use in TAG synthesis (Martin et al., 2014). Therefore the finding in this study that this protein was down-regulated suggests that TAG was favoured over SQDG, which supports the phenotypic evidence of fatty acid accumulation in this time course experiment.

Overall this resulted in mixed evidence for regulation of fatty acid synthesis pathways; changes in glycerol-3-phosphate dehydrogenase and UDP-sulfoquinovose were consistent with the phenotype change (that lipids had begun to increase), but biotin carboxylase and dihydrolipoamide acetyltransferase regulation did not align with this change.

Although carbohydrates had increased significantly from 3 to 82 hours, some of the individual proteins show down-regulation of carbohydrate synthesis. Glycolate dehydrogenase was down-regulated. This enzyme is involved in the glyoxylate cycle, a function of which is the biosynthesis of carbohydrates from fatty acids. UDP-glucose:protein transglucosylase was also down-regulated. This enzyme is involved in polysaccharide biosynthesis. It may be therefore, that although carbohydrates were higher at 82 hours, the proteins triggering the accumulation were higher at an earlier stage in the time course, and this was not reflected in the proteomic results obtained here.

RuBisCo proteins had been down-regulated, as were the photosynthesis related proteins. Overall, the cultures show lower photosynthetic ability and carbon fixation over long term exposure to salt conditions.

Energy metabolism, however, showed a mixed response over time. Dihydrolipoyl dehydrogenase, an enzyme involved in energy metabolism, was up-regulated. Glyceraldehyde-3-phosphate dehydrogenase showed a mixture of up and down-regulation. This catalyses a step of glycolysis and has been implicated in apoptosis. Pyruvate kinase, the enzyme in the final step of glycolysis, was down-regulated.

Interestingly, succinate dehydrogenase, involved in the TCA cycle and the electron transport chain, was up-regulated (Willeford et al., 1989). The TCA cycle is important in algae for the central metabolism of carbohydrates and the electron transport chain for the generation of ATP. This up-regulation indicates the cell is both attempting to increase photosynthesis or respiration or both. Salt stress has a negative effect on photosynthesis and respiration rates from the phenotypic data, although this does not

change between 3 and 82 hours, therefore the cells could be up-regulating the enzyme in an attempt to increase energy production for cellular maintenance.

Broadly speaking, the phenotypic changes were not always supported by proteomic data, but it is clear that photosynthesis and carbon fixation was impaired, that many central metabolic processes were largely down-regulated (explaining the lack of culture proliferation), and that some proteins in carbohydrate and lipid metabolism were affected by salt stress over time.

### **5.8.2 Differences between 82 and 170 hours salt conditions (decreasing carbohydrates and increasing lipids)**

Between 82 and 170 hours exposure to salt stress, there were 22 proteins differentially expressed (once duplicate accession numbers had been removed). 10 proteins were down-regulated and 12 were up-regulated. These are listed in Appendix D.

#### ***5.8.2.1 Phenotypic changes between time points***

The phenotypic changes between these two groups were: no increase in OD or biomass, no significant changes in photosynthesis or respiration rates (although taking place at slightly lower levels than in control conditions), a significant decrease in chlorophyll a and b but no significant change in carotenoids, a significant decrease in carbohydrates and a significantly higher level of FAMES, especially C18:1*cis*.

#### ***5.8.2.2 Metabolic map changes between time points***

The mapping results (Figure 5.40) show that not many enzymes were significantly changed between the two time points. Despite the phenotypic differences in lipid content of the biomass, no changes were observed in fatty acid biosynthesis or degradation. The main changes shown by the mapping results are the up-regulation of some areas of carbohydrate metabolism. There is a large phenotypic change with the reduction of carbohydrates in biomass so changes in carbohydrate metabolism were expected.

Given the long time period over which this time course experiment takes place, it might be concluded from the small number of proteomic differences between 82 and

170 hour samples that the main changes in the cells salt tolerance mechanisms take place earlier in the time course (so bigger differences were observed between 3 and 82 hours than between 82 and 170 hours). It may also show that large differences in phenotypic changes, such as increases in lipid content, are not always reflected in the proteome.



### 5.8.2.3 Functional annotation analysis

DAVID annotation analysis (Figure 5.41) concurs with the evidence from the metabolic mapping: there are few changes overall and the main difference of note is the up-regulation of carbohydrate metabolism.

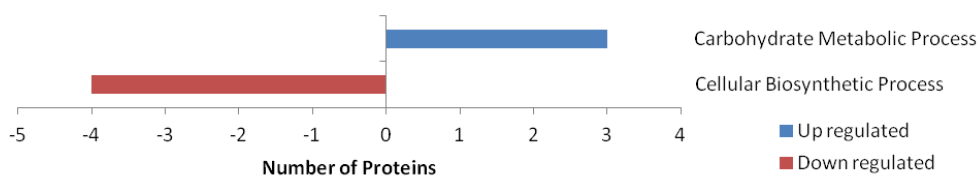


Figure 5.41 DAVID functional annotation of differences between 82 and 170 hours at BP level 3. No annotation information was available at BP level 4. 12 up-regulated proteins resulted in 11 DAVID IDs, 8 of which were not found at BP3, and none of which were found at BP4. 10 down-regulated proteins resulted in 10 DAVID IDs, 6 of which were not found at BP3 and none of which were found at BP4.

### 5.8.2.4 Individual proteomic changes

Analysis of the individual proteins may shed more light, especially on starch metabolism. Alpha-1,4 glucan phosphorylase, a protein causing the degradation of starch, was up-regulated. As carbohydrates decrease between these two phenotypes, this change is consistent with observations. ADP-glucose pyrophosphorylase was up-regulated, an enzyme that catalyses the first committing step in starch synthesis (Ballicora et al., 2004). As starch was decreased between these two time points, it would be expected that only enzymes involved in starch catabolism would be observed as up-regulated, therefore the up-regulation of this enzyme is not consistent with the phenotypic changes observed.

A few proteins indicated stress responses. Glutathione reductase was up-regulated, and acts as an antioxidant removing toxic free-radicals in *C. reinhardtii* (Takeda et al., 1993). This indicates that although *C. nivalis* is more salt stress tolerant than *C. reinhardtii*, the cells still need to employ oxidative stress mitigation mechanisms. Programmed cell death protein 6-interacting protein was also up-regulated, suggesting stress and removal of cells that are not correctly functioning under salt stress. Furthermore, ubiquitin-activating enzyme was up-regulated, an enzyme involved in protein degradation and maintenance, perhaps suggesting that proteins and structures

were being actively maintained or recycled due to damage from the salt stress conditions.

Glycerol-3-phosphate dehydrogenase was up-regulated, which as previously discussed, is involved in glycerol production in algae for compatible solutes during salt stress conditions. Glycerol is also required when making TAGs in the cell, and can be linked to lipid metabolism. In this case, the lipids shown to increase in the phenotypic samples have not been identified from a particular lipid type and it cannot be confirmed whether they are TAGS or another lipid in the cell. However, it is possible that this enzyme is linked both to salt stress tolerance, and to lipid production.

#### ***5.8.2.5 Overall proteomic changes***

Overall few conclusions can be drawn from this comparison, but of the few proteomic changes that occur between the time points, the changes occur more in carbohydrate metabolism than in lipid metabolism. Furthermore, photosynthesis and carbon fixation appear largely unchanged between these conditions indicating stability of these processes in the cultures over long term salt stress. The changes in lipid accumulation were not reflected in the proteome, suggesting either that such control mechanisms could not be detected from this iTRAQ experiment, or that the controlling changes take place at different time points, perhaps earlier in the time course experiment.

#### **5.8.3 Differences between 3 hour and 170 hour salt (low fatty acids to high fatty acids)**

To explore how the proteome matches to the phenotypic differences of low and high fatty acid content, the 3 hour and 170 salt condition samples were compared. From 3 to 170 hours, 155 proteins were differentially expressed (once duplicate accession numbers were removed). 129 of these were down-regulated and 26 were up-regulated. Details are listed in Appendix D.

### ***5.8.3.1 Phenotypic changes between time points***

The phenotypic changes between the groups were: no increase in OD or biomass, an increase in cell size, an increase in FAMES especially C18:1*cis*, a similar level of carbohydrates (though perhaps slightly higher), a significant decrease in chlorophylls a and b, no significant change in carotenoids and no significant change in photosynthesis and respiration (although at lower levels than in the controls).

### ***5.8.3.2 Metabolic map changes between time points***

Mapping the changes in ChlamyCyc (Figure 5.42) shows that overall, photosynthesis was down-regulated, as was fatty acid biosynthesis. Hormone biosynthesis, namely jasmonic acid biosynthesis was up-regulated as found in *C. reinhardtii*, which may be a salt tolerance mechanism as previously discussed in Chapter 4. Carbohydrate biosynthesis showed a mixture of up and down-regulation, as did glycolysis.

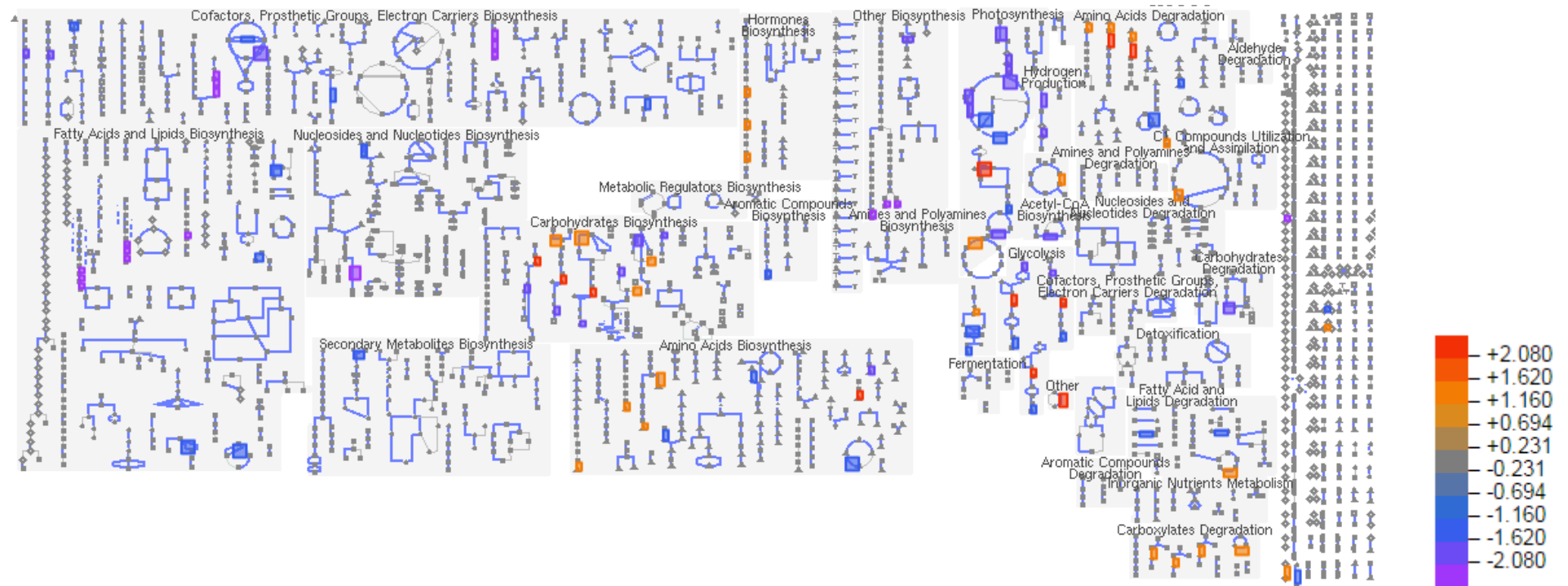


Figure 5.42 ChlamyCyc metabolic mapping of changes between 3 hour and 170 hours 0.2 M NaCl conditions. Up-regulation in red, down-regulation in blue. Of the 155 changes, 61 had EC numbers and 56 were found on the map.

### 5.8.3.3 Functional annotation analysis

When analysing DAVID annotation (Figure 5.43), almost all processes were down-regulated, except for carbohydrate metabolism, and some up-regulation in photosynthesis, although overall this process shows down-regulation. Lipid metabolism was not detected in this analysis. Like the 3 to 82 hour comparison, most processes appear to be down-regulated.

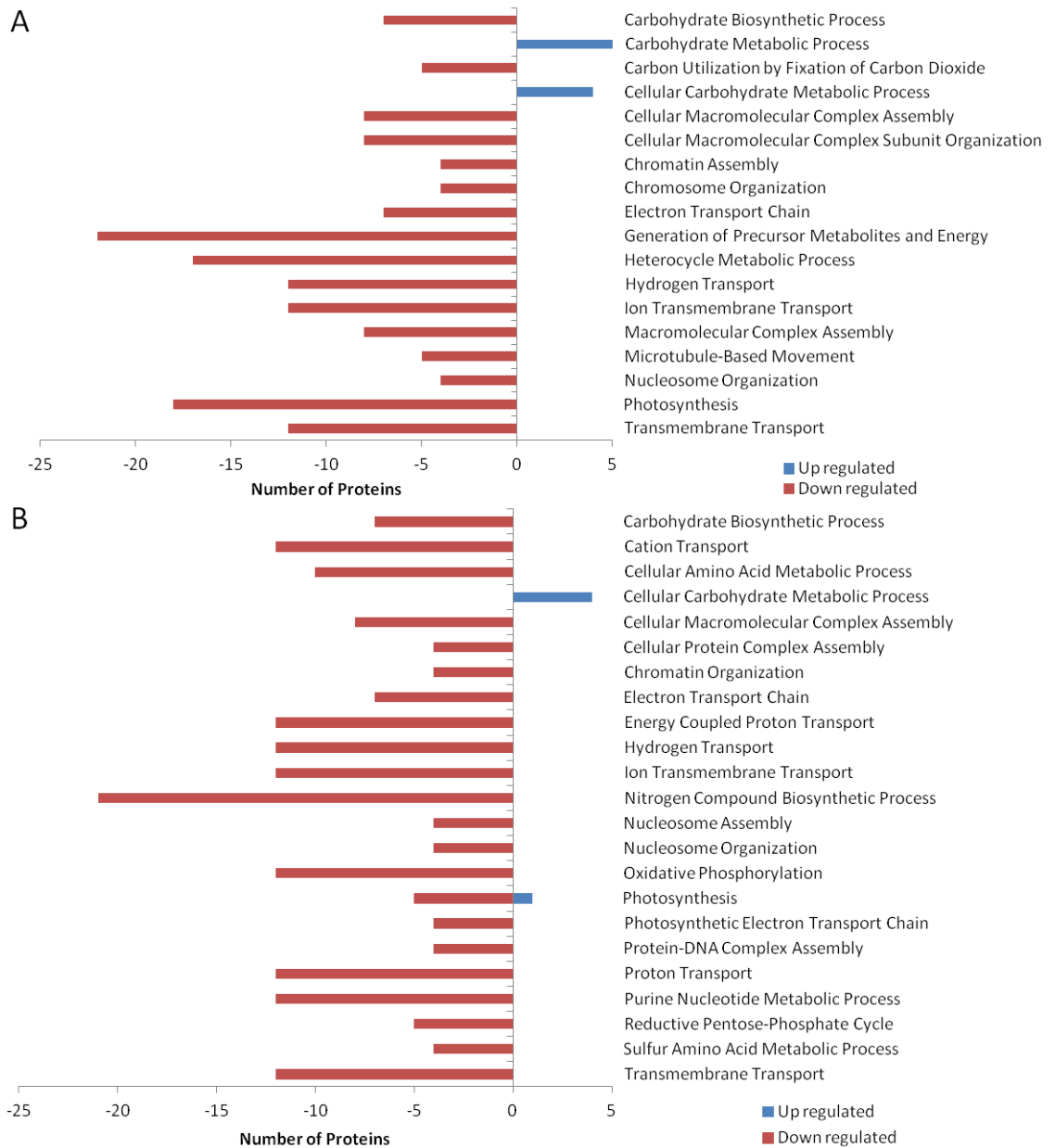


Figure 5.43 Functional annotation analysis of up and down-regulated proteins, using DAVID annotation at level 3 (A) and level 4 (B). There were 24 DAVID IDs of up-regulated proteins. 20 were not found at BP3 and 19 were not found at BP4. 132 DAVID IDs of down-regulated proteins were found, but 63 were not found at BP3 and 62 were not found at BP4.

#### 5.8.3.4 Individual proteomic changes

Individual protein analysis reveals more information, particularly about lipid metabolism. Acetyl CoA-acyltransferase was up-regulated, a change that was not detected in the previous comparisons, but was found to be up-regulated in *C. reinhardtii* salt stress comparisons. As previously discussed in the *C. reinhardtii* chapter (Chapter 4), this enzyme is linked to beta-oxidation and catabolism of fatty acids. As lipids were accumulating between 3 and 170 hours, the up-regulation of this enzyme does not match the metabolomic data. Glycerol-3-phosphate dehydrogenase was up-regulated and biotin carboxylase was down-regulated, consistent with previous findings. In addition, UDP-sulfoquinovose synthase was down-regulated, as found in the 3 to 82 hour comparison. This shows that even over the greater time period and with further changes in lipid accumulation observed, the enzyme involved with SQDG and glycerolipid metabolism was adversely affected by salt stress, explaining the continued trend in accumulation of lipid storage molecules as a result of TAG being favoured over SQDG (Martin et al., 2014). Dihydrolipoamide acetyltransferase was down-regulated, as in the 3 to 82 hour comparison.

Generally, ATP, RuBisCo and photosynthesis related proteins were all down-regulated, showing that salt stress showed a negative impact on these processes in *C. nivalis*.

Some proteins that suggested stress response mechanisms were up-regulated, such as aldehyde dehydrogenase. This has been linked to stress tolerance in Arabidopsis (Sunkar et al., 2003). Betaine aldehyde dehydrogenase has been linked to salinity and drought tolerance in some species. An autophagy-related protein was also up-regulated, suggesting programmed cell death due to salt stress, but also as discussed in the previous *C. reinhardtii* proteomic data (section 4.4), it can cause the degradation and recycling of cell components to improve the health of the culture, in an attempt to promote cell survival under stress (Pérez-Pérez et al., 2012).

In addition, a stress-related chlorophyll a/b binding protein was also up-regulated, showing the mechanisms of the cell to try to maintain chlorophyll function under salt stress. Ubiquitin-activating enzyme was up-regulated, suggesting as previously

discussed, that under salt conditions, proteins required active degradation/recycling and maintenance due to damage.

Alpha-1,4 glucan phosphorylase was up-regulated, as found in the 82 to 169 hour comparison, since degradation of accumulated starch was active at this time, shown by the time course experiment anthrone assay. UDP-glucose:protein transglucosylase was down-regulated, as in the 3 to 82 hour comparison, suggesting polysaccharide synthesis was down-regulated. This matches observed patterns in carbohydrates since they were decreasing from previous accumulation over the course of the experiment.

Furthermore, glyceraldehyde-3-phosphate dehydrogenase, has a mixture of up and down-regulation, as found in the 3 to 82 comparison, suggesting that the effects on glycolysis are constant after the initial effects. The same is true for the down-regulation of pyruvate kinase, which was down-regulated between 3 and 82 hours.

Up-regulation of phosphoribosylaminoimidazole carboxylase, which is involved in nucleotide biosynthesis, shows that DNA replication was still taking place at this time and that the culture, although down-regulating many of its processes, was actively maintaining cells and DNA.

#### *5.8.3.5 Overall proteomic changes*

Overall, in this comparison, there is mixed evidence for the alignment of proteomic data with the lipid accumulation occurring between 3 and 170 hours of salt stress; the up-regulation of glycerol-3-phosphate hydrogenase and the down-regulation of UDP-sulfoquinovose synthase may explain the lipid accumulation, but the changes in acetyl CoA-acyltransferase and biotin carboxylase do not align with the metabolomic data. There are also many changes in carbohydrate metabolism that may be causing the changes in starch levels over time, although these don't always align with the observations. Generally, salt causes arrest of cell division, likely due to the decrease in photosynthetic abilities and carbon fixation, even though this species is reported to be salt tolerant at this level of salinity.

#### **5.8.4 Differences between 170 hour control conditions (mid log growth) and 170 hour salt condition (non-growth and high lipid)**

To compare the proteomic differences between a healthily growing culture and a salt stressed culture accumulating fatty acids, control cultures and salt grown cultures were compared at 170 hours. Between the two conditions, there were 231 differentially changed proteins (once duplicate accession numbers were removed). 188 proteins were down-regulated and 43 proteins were up-regulated. A list of these changes is displayed in Appendix D.

##### ***5.8.4.1 Phenotypic changes between time points***

The phenotypic changes between the two groups were: no significant change between control and salt conditions in photosynthesis and respiration activity (since the control conditions photosynthesis decreased from the previous time point), significantly higher levels of all photosynthetic pigments in control conditions, higher levels of carbohydrates in control conditions than in salt conditions (since salt conditions show a decrease in carbohydrates whilst control conditions are increasing). Higher levels of FAMES (especially C18:1cis), although FAMES are increasing in both conditions from the previous time point, and this change is bigger in salt conditions. The OD and biomass are at a much higher level in the control conditions compared to the salt conditions, and the control conditions were still in the middle of their growth cycle (mid log phase), whilst the salt conditions remained in an arrested state without significant cell division.

##### ***5.8.4.2 Metabolic map changes between time points***

The changes were mapped onto the ChlamyCyc metabolic map (Figure 5.44). Mapping analysis shows that the majority of processes were down-regulated in salt stressed cultures in comparison to a control culture in mid-log growth. Hormone biosynthesis was up-regulated in salt stressed cultures, as were some areas of acetyl CoA biosynthesis, carbohydrate biosynthesis and amino acid metabolism.

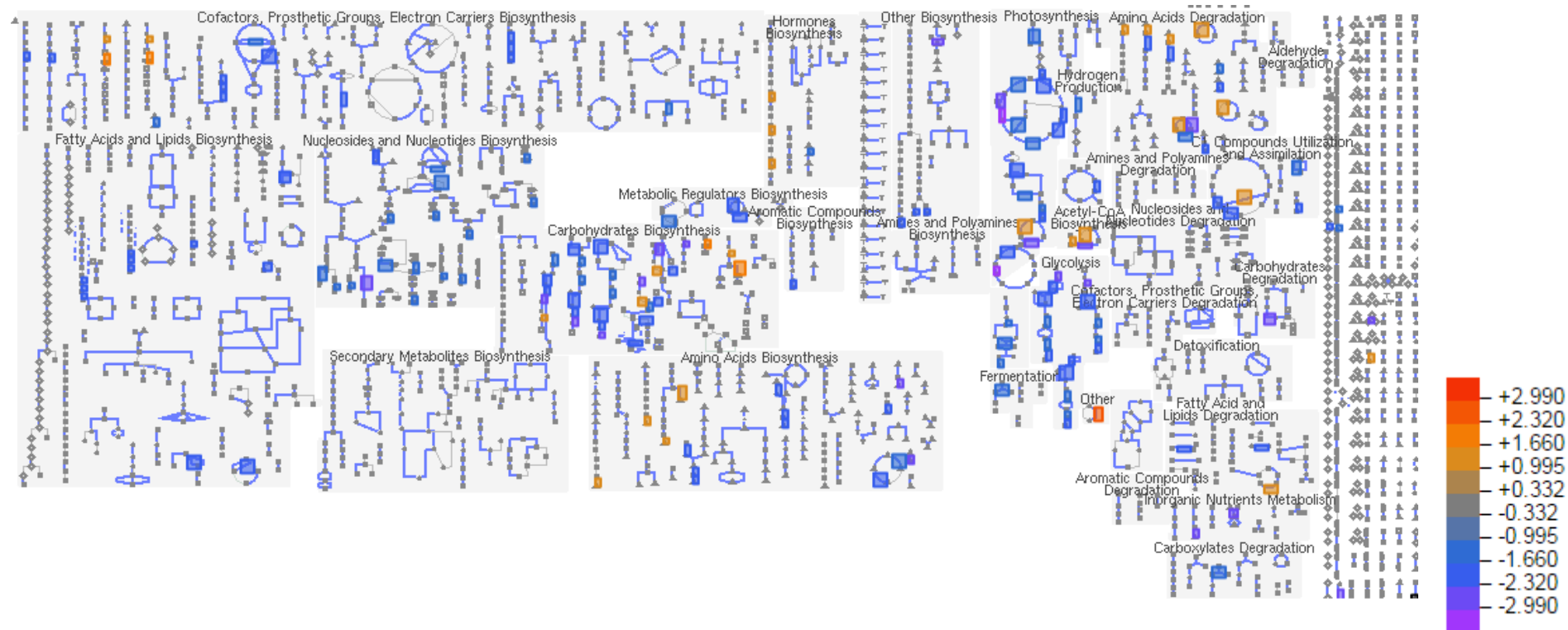


Figure 5.44 ChlamyCyc metabolic mapping of up-regulation (red) and down-regulation (blue) between control conditions at 170 hours and 0.2 M NaCl salt conditions at 170 hours. From 231 protein changes, 91 had EC numbers, 81 of which were found.

#### *5.8.4.3 Functional annotation analysis*

Changes were also grouped using DAVID functional annotation analysis (Figure 5.45). Like previous comparisons, many processes were largely down-regulated. Carbohydrate metabolism showed a mixture of up and down-regulation. Gene expression, translation, and cellular biosynthetic processes were all up-regulated in salt stress cultures compared to control conditions. Lipid metabolism was not detected as changed in this analysis.

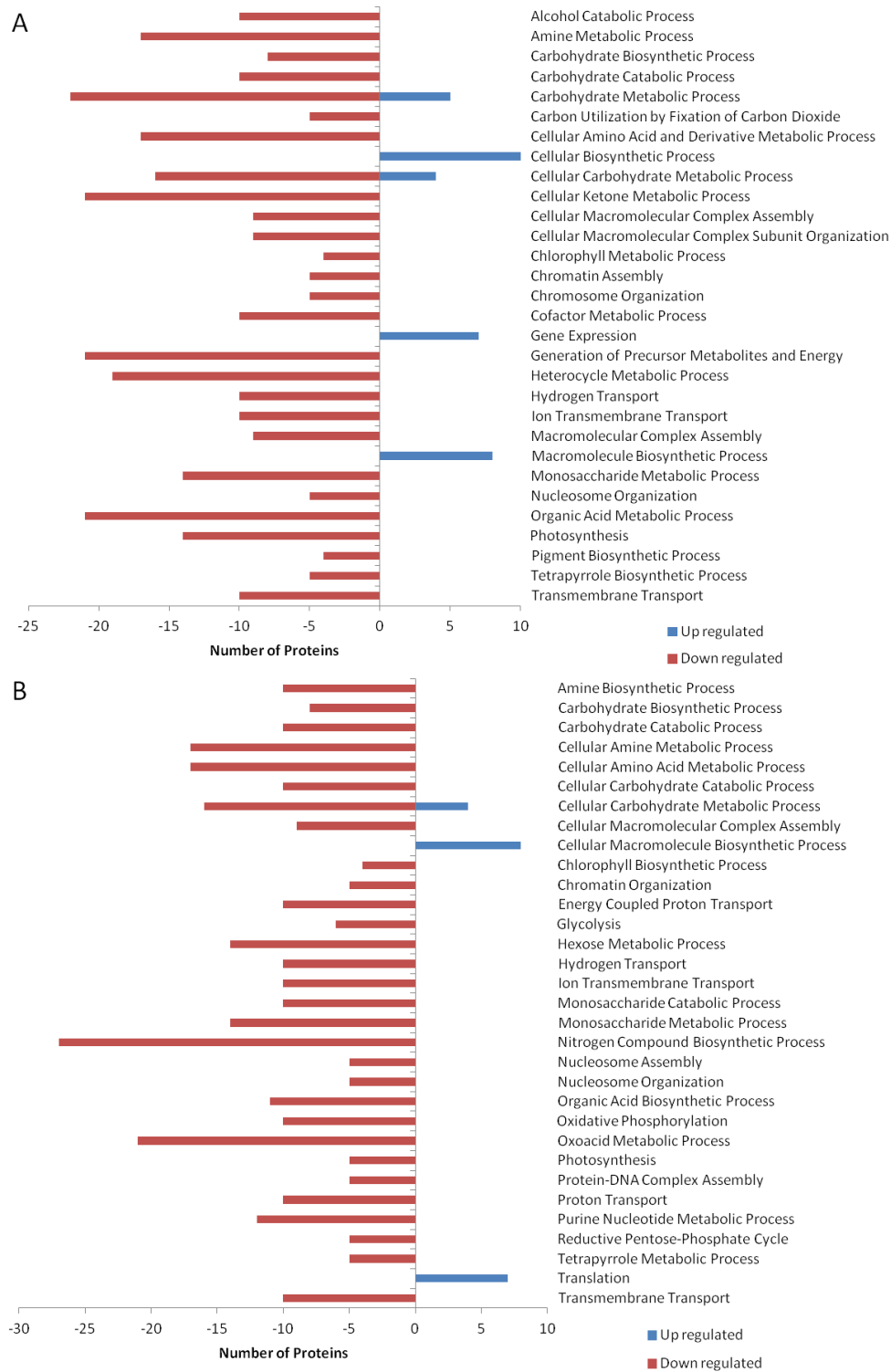


Figure 5.45 DAVID functional annotation analysis at level 3 (A) and level 4 (B). Of the up-regulated proteins, 41 DAVID IDs were found. 27 of these were not found at BP3 and 30 were not found at BP4. Of the down-regulated proteins, 176 DAVID IDs were found. 82 were not found at BP3, and 91 were not found at BP4.

#### 5.8.4.4 Individual proteomic changes

Many of the changes are consistent with those found between 3 and 170 hours of salt exposure, and have been discussed previously in this chapter: acetyl-CoA acyltransferase was up-regulated and biotin-carboxylase was down-regulated. ATP synthase proteins, RuBisCo and photosynthesis related proteins were down-regulated. Glycerol-3-phosphate dehydrogenase was up-regulated.

An important protein of note was the down-regulation of citrate synthase. This enzyme, as discussed in Chapter 4 with reference to *C. reinhardtii*, utilises acetyl CoA for the citrate cycle, and directly competes with fatty acid biosynthesis (Deng et al., 2013; Martin et al., 2014). The down-regulation of this protein therefore shows that under a lipid accumulating salt stressed culture, the cells direct resources away from the TCA cycle, which allows acetyl CoA to be utilised in fatty acid synthesis.

Alpha-1,4 glucan phosphorylase was down-regulated which differs from the previous comparisons. The difference between the two samples in carbohydrate metabolism was very stark, with one condition showing accumulation (control) whilst the other condition showed breakdown of carbohydrates (salt conditions). ADP-glucose pyrophosphorylase showed one up and one down-regulated protein, with different accession numbers. This protein is an important committing step in starch synthesis (Ballicora et al., 2004). It is not clear from this which direction the proteomic change is going in, therefore it is not possible to link this effectively with the phenotype.

In alignment with the phenotype observed, starch branching enzyme was down-regulated. A change in this enzyme was not found between the other comparisons. Since carbohydrates were decreasing in salt conditions at this point, and increasing in control conditions, the down-regulation of this enzyme fits with the phenotypic data observed. Conversely, soluble starch synthase was up-regulated, a change that was also not seen in other comparisons. This enzyme is also active in the forming and storage of starch, so the up-regulation of this enzyme is contrary to the observations. However, it's possible its

effect is overridden by the conversion of carbohydrates to lipids in the salt stressed condition, which is shown by a gradual decrease in carbohydrates and increase in lipids over the course of the salt stressed time course experiment. This conversion of carbohydrates to lipids is further corroborated by a decrease in glyceraldehyde-3-phosphate dehydrogenase, discussed below.

UDP-glucose 6-dehydrogenase was up-regulated, an enzyme that catalyses starch into glucose for use in glycolysis (Li et al., 2014a), which matches the phenotypes observed since starch was being decreased in salt conditions but rising in control conditions at the compared time-points. UDP-glucose:protein transglucosylase was down-regulated, as in previous comparisons, which may be expected since polysaccharide biosynthesis was taking place at a higher rate in control conditions than in salt stress conditions.

Furthermore, glyceraldehyde-3-phosphate (G-3-P) dehydrogenase, a part of the glycolysis pathway, was down-regulated. This has been found to be decreased when photosynthesis is impaired (Li et al., 2012). Where previously this showed a mixture of up and down-regulation, in this comparison the enzyme was down-regulated. In potatoes, the gene for this protein has been linked to salt tolerance (Jeong et al., 2001). G-3-P is an immediate product of the Calvin cycle, and when it is limited by impaired photosynthesis, an increase in lipids is mainly attributed to production via carbohydrate metabolism (Li et al., 2012). In this experiment, photosynthetic rates were also reduced through salt stress, and an increase in lipids coincided with a decrease in carbohydrates, likely due to the decrease in G-3-P available from the Calvin cycle, which would then result in a reduced need for glyceraldehyde-3-phosphate dehydrogenase.

Other enzymes involved in glycolysis were down-regulated, such as glucose-6-phosphate isomerase, phosphoglycerate kinase, phosphoglycerate mutase and phosphoglyceromutase, fructose bisphosphatase, and fructose bisphosphate aldolase. Glucose-6-phosphate isomerase is also involved in gluconeogenesis. Dihydrolypoamide acetyltransferase was down-regulated, a protein which transfers an acetyl group to

coenzyme A (CoA) and is involved in pyruvate decarboxylation, linking glycolysis to the TCA cycle. Pyruvate kinase showed a mixture of up and down-regulation. Down-regulation of glycolysis overall suggests that glucose may be cyclically reused, or not broken down, and thus reducing the availability of energy and pyruvic acid for the cell to carry out other functions. Since the salt stressed cultures were not dividing compared to log phase growing control cultures, this may be partly explained by the down-regulation of glycolysis, since energy was not available for growth.

However, dihydrolipoyl dehydrogenase, an enzyme involved in energy metabolism, was up-regulated. This enzyme was shown to be up-regulated in nitrogen starved algae *Micractinium pusillum*, and they note that this enzyme plays a key role in the production of acetyl CoA from pyruvate, and is a member of the pyruvate dehydrogenase complex (Li et al., 2012). Acetyl CoA is important for fatty acid biosynthesis. This is significant because it helps explain the phenotypic change of an increased level of fatty acids in the salt stressed culture.

A protein involved in chlorophyll and porphyrin metabolism, 3,8-divinyl chlorophyllide *a* 8-vinyl-reductase, was down-regulated. Phosphoenolpyruvate carboxylase was also down-regulated, an enzyme involved in C4 photosynthesis. The general down-regulation of photosynthesis shown from both these and from oxygen evolver proteins in photosystem 2 show that photosynthesis is negatively impacted by salt stress. Although photosynthesis rates are not significantly higher in the control than the salt stress at this time point, the photosynthesis rates decrease in the next time point, indicating this may be an onset of reduction in photosynthesis in salt stressed cells.

Another down-regulation was glutamate dehydrogenase. This enzyme has also been found to decrease in N-starved *C. reinhardtii* cells (Muñoz-Blanco and Cardenas, 1989), however it is primarily connected with carbon metabolism, and serves to try to maintain glutamate levels. Drops in this enzyme were accompanied by pyruvate kinase decreases (Muñoz-Blanco and Cardenas, 1989), suggesting an interdependent relationship.

Furthermore, glutamine synthetase was down-regulated, an enzyme that metabolises and assimilates nitrogen (Temple et al., 1998). This suggests therefore that salt stress decreases the ability of the cells to assimilate nitrogen for proteins, which corroborates the lack of cell division, and in fact the patterns of carbohydrate and lipid accumulation that are similar to those found in nitrogen starved cultures.

The enzyme peptidyl-prolyl cis-trans isomerase was up-regulated. This is an enzyme that has been linked to low CO<sub>2</sub> conditions (Somanchi and Moroney, 1999) and may help to concentrate CO<sub>2</sub>. This may be one of the mechanisms that is employed in salt stressed conditions and helps to obtain carbon for storage molecules, ready for when the cell enters a healthy state again. It has also been linked to salt stress tolerance in *Anabaena* (Rai et al., 2014)

Again as with the other comparisons, UDP-sulfoquinovose synthase was down-regulated, showing that both over time, and in comparison to a control culture in mid-log phase, the metabolism of SQDG was decreased. This contrasts to what has been observed in previous studies on the effect of salt in *C. nivalis*, which show increases in SQDG (Lu et al., 2012a). However, as discussed in sections 5.8.1.4 and 5.8.2.4, it may be that this lipid component is reduced during salt stress in favour of alternative lipids including TAGs, and therefore it is down-regulated to prioritise other lipid types.

#### **5.8.4.5 Overall proteomic changes**

Overall, most protein groups show down-regulation. There is strong evidence of salt stress causing decreases in photosynthesis and carbon fixation, as well as many basic metabolic processes, as with previous comparisons. However, there are some differences in starch synthesis that may play a key role in the storage of carbon in the form of starch and lipids in response to salt stress.

Another factor to bear in mind is that in both control and salt stressed phenotypes, lipids were accumulating, albeit at a lower level in the control conditions, as a healthily growing culture would in the latter stages of its growth curve.

## 5.9 Chapter Discussion and Conclusions

### 5.9.1 Summary of phenotypic changes

This chapter has explored, for the first time, the proteomic differences between control conditions, salt stressed carbohydrate induction and salt stressed lipid induction in the snow alga *C. nivalis*. Preliminary experimentation led to two main salt concentrations being explored: 1.4 M and 0.2 M NaCl. The former was found to be much too high for *C. nivalis* and causes complete halting of photosynthesis and growth, ultimately resulting in cell death. 0.2 M NaCl caused arresting of culture growth, but only caused a small reduction in the ability of the culture to photosynthesise. These cultures had a rise in carbohydrates followed by a rise in FAME content as the carbohydrates started to decrease. The main cause for the rise in FAMES was a large increase in C18:1*cis*, which caused a shift in FAME profile towards a greater proportion of MUFAs and therefore makes the lipid content of *C. nivalis* more suitable for biofuel.

The triggering of lipid accumulation has been repeatedly demonstrated regardless of the culture starting density. Unlike the model strain, *C. reinhardtii*, which doesn't show the accumulation of lipids under salt stress conditions, *C. nivalis* responds to salt stress by remaining in a non-dividing state and by accumulating carbon storage molecules.

### 5.9.2 Genetic relatedness of *C. nivalis* to *C. reinhardtii*

18S sequencing was carried out to find the relatedness of this strain to *C. reinhardtii*. The results showed a high level of relatedness, but also that *C. nivalis* is more closely related to some *Chloromonas* strains than to *C. reinhardtii*.

The similarity of the species allowed a high quality proteomic dataset for *C. nivalis* to be obtained for the first time, using the *C. reinhardtii* database. A combination of powerful MS/MS techniques with *de novo* sequencing software and homology searching tools allowed a high number of proteins to be identified and quantified.

### 5.9.3 Summary of proteomic data

iTRAQ experimentation compared salt stressed cultures along a time course at the starting point of salt stress application (3 hours) to the points of high carbohydrate accumulation (82 hours) and the point of high lipid accumulation (170 hours), as well as comparing the high lipid culture to a log phase control culture at the same time point (170 hours).

The most notable changes overall in the proteome of this species is that the majority of processes were down-regulated under salt stress, and that both from the growth data and from the proteomic evidence, the cells appear to be going into a stasis mode.

Predictably, salt had a detrimental effect on photosynthesis and carbon fixation, and on glycolysis. However, it might be expected that salt had less of an effect on these processes than in *C. reinhardtii*, which showed lower photosynthetic rates under 0.2 M NaCl stress.

Few changes were found between 82 and 170 hours, showing that the large difference in phenotype was not reflected by the proteome at this time points. The main changes between these points were in carbohydrate metabolism, and there is some proteomic evidence for the breakdown of carbohydrates that coincides with lipid increases.

Changes to lipid metabolism were of particular interest and these have been discussed in the most detail. Certain protein changes do not align with the accumulation of fatty acids. For example, in all cases except the 82 versus 170 hour salt condition, biotin carboxylase was down-regulated. This enzyme is a component of acetyl CoA carboxylase, the committing step of fatty acid biosynthesis, and yet the decrease in this protein does not seem to have caused limitation to the synthesis of fatty acids. Acetyl CoA acyltransferase was up-regulated, suggesting catabolism of fatty acids. However these do not cause a reduction in fatty acids, and other key proteins are implicated in allowing fatty acids to accumulate. The down-regulation of UDP-sulfoquinovose synthase suggests that SQDG is down-regulated, leading to greater FA accumulation in TAGs. Citrate synthase was down-regulated, which is an important step in directing acetyl CoA away from the TCA cycle and making it available for fatty acid synthesis. The down-regulation of dihydrolipoamide

acetyltransferase and glyceraldehyde-3-phosphate dehydrogenase indicate further that glycolysis and the TCA cycle were deprioritised. Additionally, dihydrolipoyl dehydrogenase catalyses the production of acetyl CoA and therefore its up-regulation provided additional substrate for fatty acid synthesis. The regulation of these key enzymes suggests that acetyl CoA is more readily available in the cell under salt stress for use in fatty acid biosynthesis, and in combination with the down-regulation of competing processes, this substrate is directed towards TAG synthesis instead. These enzymes could provide interesting targets for genetic engineering for increase fatty acid synthesis in the cell.

#### 5.9.4 Further investigations

This data is valuable for studying how *C. nivalis* controls its cellular processes to accumulate lipids, especially as this species is such a promising candidate for biofuels research. It is also valuable for comparing to the non-halotolerant species *C. reinhardtii*, which did not accumulate lipids under salt stress. Both species were able to survive in 0.2 M NaCl, but both showed severely reduced growth. The following chapter takes both iTRAQ studies on the effect of salt stress on the proteomes of *C. reinhardtii* and *C. nivalis* and compares them to help answer the question of why salt triggers lipid accumulation in one species whilst it does not in the other.

## 6 Chapter 6: Comparison of *C. nivalis* data and *C. reinhardtii* proteomic data and discussion

### 6.1 Summary

This chapter compares the datasets obtained from the iTRAQ experiments from *Chlamydomonas reinhardtii* and *C. nivalis* under salt stress, and analyses the molecular mechanisms that cause *C. nivalis*, but not *C. reinhardtii*, to have salt stress as a lipid producing and accumulating trigger. Key findings include the differences in the response of lipid metabolism to salt stress in the two species, especially the down-regulation in *C. reinhardtii* of the enzyme acetyl CoA carboxylase (ACCase), which catalyses the first committed reaction in fatty acid biosynthesis and is a rate-limiting step in lipid biosynthesis. A number of proteins linked to acetyl CoA and fatty acid synthesis were identified that explain the lipid metabolism differences between the species. Implications of the findings for biofuels research are also discussed.

### 6.2 Introduction

The experiments presented in this thesis have provided significant novel findings on growth, compositional analysis and proteomic data on both the model species *Chlamydomonas reinhardtii* and the snow alga *C. nivalis* when under salt stress. These algae show very different responses to 0.2 M NaCl, both are able to survive in this condition but have their growth negatively impacted by the salt stress, due to the damaging effects of osmotic and ionic stress on the cells.

To summarise the findings on growth, metabolomic lipid data, and compositional analysis of carbohydrates, pigments and photosynthetic activity under 0.2 M NaCl from the previous chapters, there is a substantially large difference in the accumulation of lipids between the two species. Metabolomic data from Chapter 4 was consistent in suggesting that salt stress did not cause increases in total lipid content in *C. reinhardtii*, whereas experiments on *C. nivalis* (Chapter 5) have repeatedly shown that lipids can be

accumulated under this salt condition. Both species show an increase in carbohydrate in response to salt stress, but the increase is larger in *C. nivalis* and is shown to increase far above that of the control, unlike *C. reinhardtii*. Growth was negatively impacted in both species, with growth being completely halted in *C. nivalis*, and significantly reduced in *C. reinhardtii*. Chlorophyll pigment concentration was decreased by salt stress in both species. Photosynthesis was negatively impacted in both species compared to control conditions, as measured by the rates of oxygen evolution used to measure photosynthesis and respiration rates in Chapters 4 and 5, but the reduction in photosynthetic rate is much greater in *C. reinhardtii*.

Comparing quantitative proteomic data from the two iTRAQ experiments described in Chapters 4 and 5 may give insights into why each species behaves differently in response to salt stress, particularly when it comes to the accumulation of fatty acids for biofuels research. These insights may provide information on how to engineer the two species for an improved biofuel producing alga, since proteomics can reveal targets for potential genetic engineering (Guarnieri et al., 2013).

#### **6.2.1.1 Limitations of the experiment and their implications**

There are some differences between the two sets of experimental culture conditions for *C. reinhardtii* and *C. nivalis* that may explain some of the contrasting results obtained, but parallels can be drawn between the two species by comparing equivalent places on the growth curve. Using the same proteomic database of *C. reinhardtii* to detect quantitative changes in the two species is advantageous in terms of directly comparing their responses to salt stress. There are limitations to the approach of comparing two separate iTRAQ experiments, for several reasons. The first is that the two species revealed different numbers of identifications from the iTRAQ experiments, because one is un-sequenced and one is sequenced; the *de novo* sequencing allowed a large number of proteins and peptides to be identified, but some in *C. nivalis* may be too far removed from the model species to be a match, even through homology searching. Another limitation is that by comparing any two iTRAQ experiments, there is a risk of false interpretations when a

protein is not observed to have significantly changed, since this does not necessarily mean it has not changed. In particular, iTRAQ has issues with under-reporting changes and with compressing the ratios of changes towards 1, as discussed in the introductory chapter. The degree of this under-reporting may vary between the two experiments, since the degree of compression will depend on the ratios and total peptides detected for each experiment, however, this must be accepted and noted as a limitation to this approach of quantitative proteomics. The third is that because the growth conditions of the two species are different according to their growth requirements (most notably, different growth media and different growth temperatures), the chosen sampling time points were chosen based on the relative positions in their growth cycles, i.e. mid log phase, which occurred at a different number of hours after inoculation for each species. Parallels can be drawn between the two species by comparing equivalent places on the growth curve and by using a control culture as a reference point in each experiment, however, it is difficult to determine if these sampling points are directly equivalent.

#### ***6.2.1.2 Potential for lipid production***

*Chlamydomonas reinhardtii* has the potential to produce much larger amounts of fatty acids than observed in these experiments, especially the low starch mutant strain (CC-4325) used in this case which produces elevated fatty acid levels (James et al., 2011). *Chlamydomonas reinhardtii* can show lipid induction rapidly after nitrogen deprivation, with lipid accumulation showing significant increases between 32 and 40 hours (Longworth et al., 2012). Therefore, if salt was a lipid trigger in this species we would expect to see it within the time frame of 72 hours (the minimum amount of time that *C. reinhardtii* cultures in the current work were exposed to salt stress), although without carrying out a nitrogen deprivation experiment in this investigation this cannot be confirmed for certain. With that in mind and the data presented here, there is an apparent key difference between these two species in the relationship between response to salt stress, and lipid metabolism and accumulation.

Comparisons were made using up and down-regulation of functional annotation groups and using mapping analysis of up and down-regulation.

### 6.3 Results and Discussion

The proteins identified in both iTRAQ datasets were compared using GeneVenn, using accession numbers as unique protein identifiers, to determine differences in the amount of the proteome that had been detected, as shown in Figure 6.1.

885 proteins were detected and quantified in both iTRAQ experiments (i.e. in both species), using PSM FDR 1% and two or more unique peptides. *Chlamydomonas reinhardtii* data gives a large number of detected proteins due to the much larger dataset obtained, but there were also 133 proteins found in *C. nivalis* that were not detected in *C. reinhardtii*. The large overlap shows that there is a good basis for comparing the two datasets directly, even though one dataset has more information than the other.

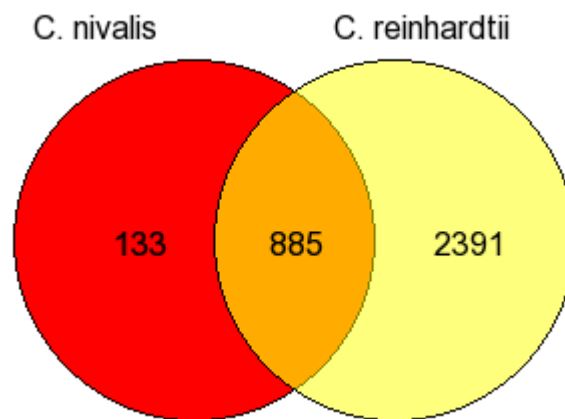


Figure 6.1 Numbers of proteins detected in *C. nivalis* and *C. reinhardtii* using *C. reinhardtii* database (diagram from GeneVenn).

### 6.3.1 Analysis of the differences in iTRAQ datasets: effect of salt stress causing arrest of culture growth compared to a control at mid-log phase

To directly compare the two iTRAQ experiments, analysis of up and down regulation in biological functional groups was analysed. DAVID functional annotation tool was used as in chapters 4 and 5, and the changes in each functional group in biological processes level 3 were summarised in Table 6.1, and level 4 in Table 6.2. As previously discussed in Chapters 4 and 5, levels 3 and 4 biological process annotation optimise the amount of information gained and was chosen as the best basis for comparison. Red boxes show where all detected proteins in a group were down-regulated, green where they were all up-regulated, and yellow where there a mix of up and down-regulation in a group.

#### 6.3.1.1 DAVID functional annotation analysis

In both cases the phenotypes of the salt stressed cultures showed arrested growth in comparison to the controls, which were at mid-log growth for both species. Photosynthesis activity was vastly reduced in *C. reinhardtii* but only slightly reduced in *C. nivalis* during salt stress. *Chlamydomonas reinhardtii* did not show significant differences in lipids in comparison to control, but *C. nivalis* had much higher lipids accumulating in the salt conditions than the control. Additionally, carbohydrate levels were higher in the control than in salt stress for *C. nivalis*, but higher in the salt stressed than control for *C. reinhardtii*. Proteins involved in photosynthesis are up-regulated (or showed a mixture of up and down-regulation) in *C. reinhardtii*, but not in *C. nivalis*, suggesting that *C. reinhardtii* had a greater need to maintain photosynthetic apparatus, due to increased salt damage.

Table 6.1 Changes in regulation of functional annotation groups BP3 for both species.

Functional group	<i>C. reinhardtii</i>	<i>C. nivalis</i>
Alcohol Catabolic Process		-10
Amine Metabolic Process	-14	-17
Carbohydrate Biosynthetic Process		-8
Carbohydrate Catabolic Process		-10
Carbohydrate Metabolic Process		5/-22
Carbon Utilization by Fixation of Carbon Dioxide		-5

Cellular Amino Acid and Derivative Metabolic Process	-14	-17
Cellular Biosynthetic Process	21/-62	10
Cellular Carbohydrate Metabolic Process	6	4/-16
Cellular Ketone Metabolic Process	-23	-21
Cellular Lipid Metabolic Process	-7	
Cellular Macromolecular Complex Assembly		-9
Cellular Macromolecular Complex Subunit Organization		-9
Cellular Nitrogen Compound Metabolic Process	-37	
Chlorophyll Metabolic Process	-5	-4
Chromatin Assembly		-5
Chromosome Organization		-5
Cofactor Metabolic Process	-14	-10
Electron Transport Chain	-10	
Establishment of Localization in Cell	5	
Gene Expression	15/-28	7
Generation of Precursor Metabolites and Energy	11/-24	-21
Heterocycle Metabolic Process	-22	-19
Hydrogen Transport	-8	-10
Ion Transmembrane Transport	-7	-10
Lipid Biosynthetic Process	-7	
Macromolecular Complex Assembly		-9
Macromolecule Biosynthetic Process	13/-27	8
Monosaccharide Metabolic Process		-14
Nucleosome Organization		-5
Organic Acid Metabolic Process	-23	-21
Photosynthesis	8/-17	-14
Pigment Biosynthetic Process	-5	-4
Polyol Metabolic Process	5	
Sulfur Metabolic Process	-4	
Tetrapyrrole Biosynthetic Process	-8	-5
Transmembrane Transport	-7	-10
Vesicle-Mediated Transport	5	

Table 6.2 Changes in regulation of function annotation groups at BP4 for both species.

Functional Group	<i>C. reinhardtii</i>	<i>C. nivalis</i>
Alditol Metabolic Process	5	
Amine Biosynthetic Process	-6	-10
Carbohydrate Biosynthetic Process		-8

Carbohydrate Catabolic Process		-10
Cellular Amine Metabolic Process	-14	-17
Cellular Amino Acid Metabolic Process	-14	-17
Cellular Carbohydrate Catabolic Process		-10
Cellular Carbohydrate Metabolic Process	6	4/-16
Cellular Lipid Metabolic Process	-7	
Cellular Macromolecular Complex Assembly		-9
Cellular Macromolecule Biosynthetic Process	13/-27	8
Chlorophyll Biosynthetic Process	-5	-4
Chromatin Organization		-5
Coenzyme Metabolic Process	-7	
Cofactor Biosynthetic Process	-9	
Electron Transport Chain	-10	
Energy Coupled Proton Transport		-10
Energy Coupled Proton Transport, Down Electrochemical Gradient	-7	
Fatty Acid Biosynthetic Process	-4	
Fatty Acid Metabolic Process	-4	
Glycolysis		-6
Heterocycle Biosynthetic Process	-9	
Hexose Metabolic Process		-14
Hydrogen Transport	-8	-10
Ion Transmembrane Transport	-7	-10
Lipid Biosynthetic Process	-7	
Monosaccharide Catabolic Process		-10
Monosaccharide Metabolic Process		-14
Nitrogen Compound Biosynthetic Process	-26	-27
Nucleosome Assembly		-5
Nucleosome Organization		-5
Organic Acid Biosynthetic Process	-10	-11
Oxidative Phosphorylation	-7	-10
Oxoacid Metabolic Process	-23	-21
Photosynthesis		-5
Photosynthesis, Light Harvesting	8	
Photosynthesis, Light Reaction	8	
Porphyrin Biosynthetic Process	-7	
Porphyrin Metabolic Process	-7	
Protein-DNA Complex Assembly		-5
Proton Transport	-8	-10
Purine Nucleotide Metabolic Process	-11	-12
Reductive Pentose-Phosphate Cycle		-5
Tetrapyrrole Metabolic Process	-8	-5

Translation	13/-27	7
Transmembrane Transport	-7	-10
Vesicle-Mediated Transport	5	

This comparison of the changes in regulation of functional groups demonstrates that the two species have some common proteomics responses to salt stress, but also some differences, compared to a healthy growing culture.

Similarities include the down-regulation of amino acids and amine metabolism, hydrogen transport, ion transmembrane transport, organic acid metabolism, and pigment biosynthesis. Salt stress clearly causes down-regulation of many cellular processes in both species, since it prevents normal log-phase growth.

There were also many notable differences in the responses, where a group was either regulated in different directions in the two species, or where a change was found in a group for one species but not for the other.

Most notably, lipid biosynthesis is down-regulated in *C. reinhardtii*, but is not detected to have changed in *C. nivalis*. The 7 proteins down-regulated in lipid biosynthesis were searched for their presence in the *C. nivalis* dataset: 2 were not detected and 5 were detected, but had not been down-regulated in the *C. nivalis* experiment. This suggests that this is a genuine proteomic difference between the responses of the species. *Chlamydomonas reinhardtii* not only slows growth in response to salt stress, but also down-regulates lipid and fatty acid biosynthesis. The tables also demonstrate other differences between the species responses. For example, photosynthesis groups appear to be down-regulated more in *C. nivalis* than in *C. reinhardtii*, which even shows some up-regulation of some proteins involved in photosynthesis. Carbon fixation was also down-regulated in *C. nivalis* but not in *C. reinhardtii*, as was glycolysis. The regulation of carbon fixation is important, because Miller et al. (2010) found that newly synthesized fatty acids required the fixation of carbon. In the case of *C. nivalis*, down-regulation of carbon fixation has not impaired the ability to make fatty acids, but ideally carbon fixation

abilities would be maintained when using a lipid trigger to increase lipid accumulation. Carbohydrate associated proteins also show more down-regulation in *C. nivalis* than they do in *C. reinhardtii*. Also the electron transfer chain was down-regulated in *C. reinhardtii* but not in *C. nivalis*. However, gene expression and macromolecular biosynthetic processes were up-regulated more in *C. nivalis*.

Lipid biosynthesis and metabolism were of particular interest, since lipid accumulation was so different between the species. KEGG mapping indicates key differences in the up and down-regulation (Figure 6.2) and as can be seen from the fatty acid biosynthesis area (a), *C. reinhardtii* appears to have down-regulated fatty acid biosynthesis whilst *C. nivalis* does not. Carbohydrate metabolism was up-regulated in *C. reinhardtii* but down-regulated in *C. nivalis* (b), as was amino acid metabolism (c).

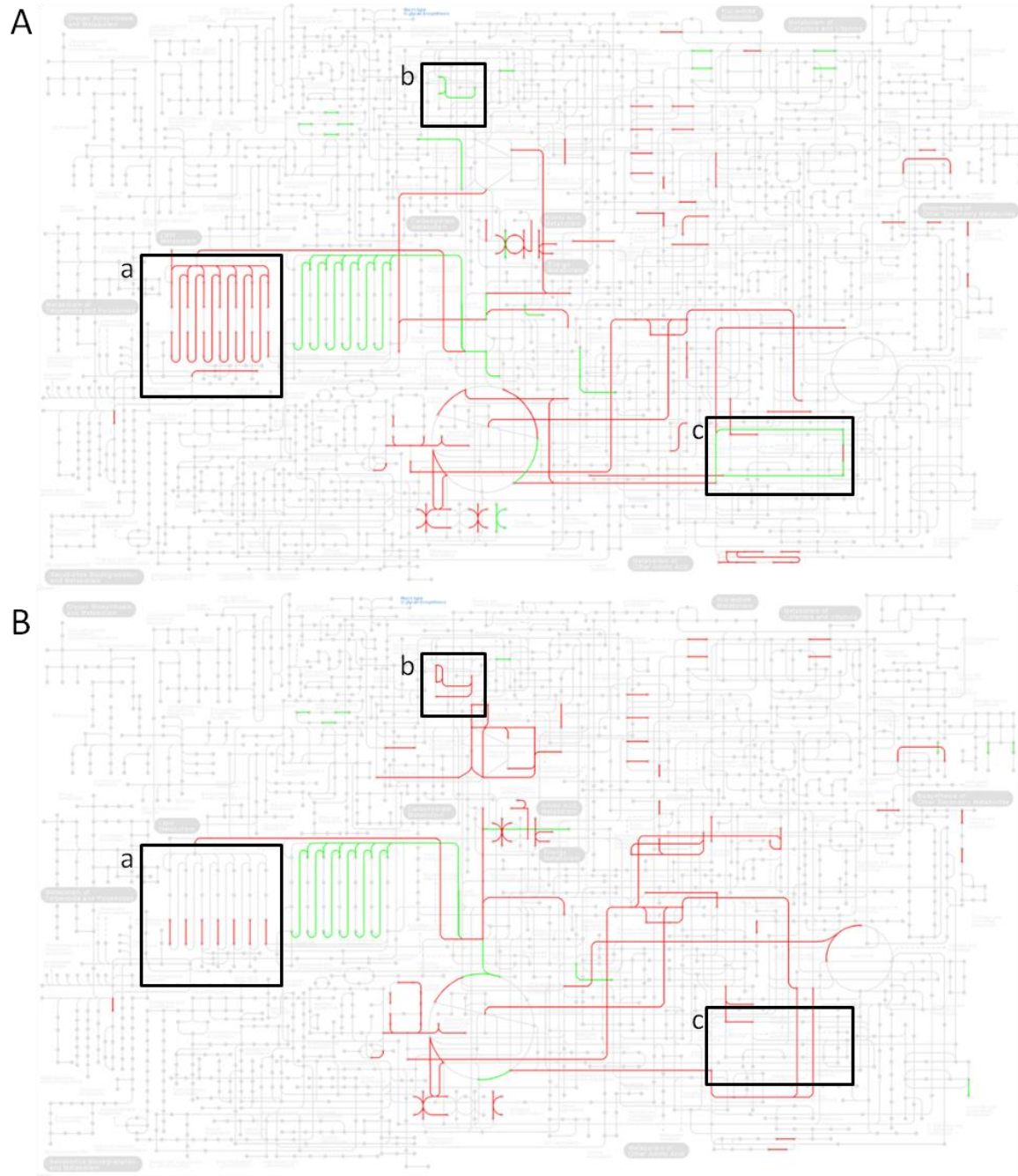


Figure 6.2 KEGG mapping of *C. reinhardtii* (A) and *C. nivalis* (B) showing significant changes in down-regulation (red) and up-regulation (green) from control conditions to salt stress conditions. Highlighted boxes show the differences between the two species in lipid metabolism (a), carbohydrate metabolism (b) and amino acid metabolism (c).

### 6.3.1.2 Proteomic changes to individual proteins of relevance

Some individual proteins of relevance to this investigation have been identified. Acetyl-CoA carboxylase was down regulated by salt conditions in *C. reinhardtii*, but this effect was not seen in salt stressed *C. nivalis*. Acetyl CoA-carboxylase is the committing step in fatty acid synthesis, which produces malonyl CoA as the fatty acid building block (Sukenik and Livne, 1991). The down-regulation of this enzyme shows a rate limiting step in *C. reinhardtii* that prevents the accumulation of fatty acids under salt stress conditions, whilst this step was not limited in *C. nivalis*. This protein therefore provides some evidence of what is causing the differences in lipid response of the two species, although it must be considered in context with other parts of lipid metabolism and with the proteomic changes as a whole.

It has already been shown that up-regulating this enzyme alone is not enough to increase lipid production in algal species (Sheehan et al., 1998). Furthermore, the model species down-regulates this enzyme for a reason during salt stress, likely a survival mechanism to channel as much energy into maintaining the basic cell functions as possible. With the model species being less halotolerant, more active resources appear to be channelled into maintaining culture health as opposed to simply going into a resting state and gathering resources for when conditions are more favourable, as happens with the snow algae species, *C. nivalis*.

Biotin carboxylase is also an important part of the pathway for lipid biosynthesis, since it is a sub-unit of acetyl CoA carboxylase, the catalysing enzyme for the reaction of carboxylating acetyl CoA into malonyl CoA. This enzyme was down-regulated between control and salt 18 hour conditions in *C. reinhardtii*, and was down-regulated in all comparisons except the 82 and 170 hour salt conditions in *C. nivalis*. This shows that there are similarities in the lipid pathway responses to salt stress when compared to a control, but suggests that biotin carboxylase down-regulation is not a rate-limiting step, since it did not cause restriction of lipid production in *C. nivalis*, as observed using the GC data. A previous study by Longworth et al. (2012) also showed down-regulation of biotin

carboxylase during nitrogen depletion triggered lipid accumulation. This confirms that decreased biotin carboxylase occurs during lipid accumulating conditions and does not limit lipid biosynthesis.

Glycerol-3-phosphate dehydrogenase was up-regulated in both species under salt stress, and as discussed in chapters 4 and 5 is important in the production of glycerol both as a compatible solute to protect against osmotic stress, and as the supplier of the glycerol backbone for TAG synthesis. However, it only led to lipid increase in *C. nivalis*, suggesting that in both species the primary function was osmotic stress protection.

Carbohydrates undergo significant changes in both species in response to salt, and changes in carbohydrate associated proteins are also observed in the proteome of both species. *C. nivalis* has lower carbohydrate levels in the salt stressed cultures than the control conditions, so the down-regulation of carbohydrate related proteins in *C. nivalis* is consistent with carbohydrate content data, whilst the up-regulation in *C. reinhardtii* is also consistent with the observed carbohydrate data.

### **6.3.2 Comparison of changes between initial exposure (3 hour) and final salt stress time point (18 or 170 hours respectively)**

The differences between the initial exposure to salt stress and the last proteomic time point (chosen because this represents the mid-log phase in the equivalent control condition) were compared between the two species. This was explored in addition to the previous comparison to see if further information could be yielded on the salt response mechanisms of the two species. A limitation of these data is that for these final time points, although taken at equivalent times when accounting for the speed of cell division, being over different time scales will have an impact on the ability to directly compare them. However, these points were chosen as the most comparable examples of the species response to salt stress over time, especially given the need to study lipid accumulation in *C. nivalis*.

The species showed difference responses in the phenotypic growth, GC, carbohydrate and photosynthesis data. In both species, the culture experienced an arrest of culture growth. Photosynthesis rates were affected in both species, but more so in *C. reinhardtii* than in *C. nivalis*. Carbohydrates had increased and then decreased in *C. nivalis* cultures but had simply increased steadily in *C. reinhardtii*. Lipids had increased significantly in *C. nivalis* but not in *C. reinhardtii*.

#### **6.3.2.1 DAVID functional annotation analysis**

Table 6.3 shows the changes annotated in both species at biological process level 3, and Table 6.4 shows changes at BP level 4. Again, *C. nivalis* tended to show a down-regulation of most functional groups over time, whilst *C. reinhardtii* shows a mixture of up and down-regulation over time. The common area of up-regulation in both was carbohydrate metabolism, whilst common areas of down-regulation were photosynthesis, the electron transfer chain, nitrogen compound biosynthesis, heterocycle metabolic processes, and precursor metabolite and energy generation.

The two levels of annotations show different stories in some cases, since the changes in photosynthesis grouping were not completely consistent between the two annotation levels. However, this is why the two annotation levels were analysed in this discussion, since it helps to give a more comprehensive analysis in case one level does not provide enough information.

Pigment biosynthesis was down-regulated in *C. reinhardtii*, but not *C. nivalis*, suggesting the ability of *C. reinhardtii* to make chlorophyll was detrimentally affected over time. Amino acids metabolic processes were up-regulated in *C. reinhardtii*, but down-regulated in *C. nivalis*. This suggests over time that *C. reinhardtii* has a higher turnover of amino acids than *C. nivalis* under salt exposure, perhaps due to increased damage to the cell/proteins in *C. reinhardtii*, as it is not as tolerant to salt as *C. nivalis*.

Carbon fixation was down-regulated in *C. nivalis*, but not in *C. reinhardtii*. As photosynthetic abilities were higher in *C. nivalis* salt stressed cultures than in *C. reinhardtii* cultures, this result was unexpected, however perhaps the greater length of time of salt exposure in *C. nivalis* can help account for this. Proline metabolism was up-regulated in *C. reinhardtii* but not in *C. nivalis*. Proline accumulation is associated with salt stress conditions, as previously discussed. This may be a tolerance mechanism or salt stress response present in *C. reinhardtii* but not in *C. nivalis*.

The tables of proteomic changes show that over increased exposure time to salt stress, *C. reinhardtii* down-regulates lipid metabolism, but these changes were not shown in *C. nivalis*. Lipid metabolism was not shown to be significantly up-regulated at the proteome level in *C. nivalis*, showing that the rise in lipids was not due to up-regulation of lipid biosynthetic pathways. However, as with the previous comparison, the lack of down-regulation in *C. nivalis* may be just as relevant to the phenotypic differences observed.

Carbohydrate metabolism also showed different proteomic responses over time. Carbohydrate catabolism was up-regulated in *C. reinhardtii*, suggesting active breakdown of starch under salt stress. The same was not found in *C. nivalis*, although carbohydrate biosynthesis was down-regulated, which matches with the observed phenotype.

**Table 6.3** Changes found at functional annotation biological process level 3 between the 3 and 18 hour time points for *C. reinhardtii*, compared to the differences between 3 and 170 hours for *C. nivalis*.

Process	<i>C. reinhardtii</i>	<i>C. nivalis</i>
Alcohol Catabolic Process	5	
Amine Metabolic Process	5	
Carbohydrate Biosynthetic Process		-7
Carbohydrate Catabolic Process	5	
Carbohydrate Metabolic Process	13	5
Carbon Utilization by Fixation of Carbon Dioxide		-5
Cellular Amino Acid and Derivative Metabolic Process	5	
Cellular Biosynthetic Process	-43	
Cellular Carbohydrate Metabolic Process	10	4

Cellular Ketone Metabolic Process	6/-13	
Cellular Lipid Metabolic Process	-7	
Cellular Macromolecular Complex Assembly		-8
Cellular Macromolecular Complex Subunit Organization		-8
Chlorophyll Metabolic Process	-5	
Chromatin Assembly		-4
Chromosome Organization		-4
Cofactor Metabolic Process	-11	
Electron Transport Chain	-8	-7
Gene Expression	-15	
Generation of Precursor Metabolites and Energy	-16	-22
Heterocycle Metabolic Process	-17	-17
Hydrogen Transport		-12
Ion Transmembrane Transport		-12
Lipid Biosynthetic Process	-7	
Lipid Metabolic Process	-7	
Macromolecular Complex Assembly		-8
Macromolecule Biosynthetic Process	8/-15	
Microtubule-Based Movement		-5
Monosaccharide Metabolic Process	5	
Nucleosome Organization		-4
Organic Acid Metabolic Process	6/-13	
Photosynthesis	-18	-18
Pigment Biosynthetic Process	-7	
Polyol Metabolic Process	4	
Sulfur Metabolic Process	-4	
Terpenoid Metabolic Process	-4	
Tetrapyrrole Biosynthetic Process	-7	
Transmembrane Transport		-12

Table 6.4 Changes found at functional annotation biological process level 4 between the 3 and 18 hour time points for *C. reinhardtii*, compared to the differences between 3 and 170 hours for *C. nivalis*.

Process	<i>C. reinhardtii</i>	<i>C. nivalis</i>
Alditol Metabolic Process	4	
Carbohydrate Biosynthetic Process		-7
Carbohydrate Catabolic Process	5	
Carotenoid Biosynthetic Process	-2	
Cation Transport		-12
Cellular Amine Metabolic Process	5	
Cellular Amino Acid Metabolic Process	5	-10

Cellular Carbohydrate Catabolic Process	5	
Cellular Carbohydrate Metabolic Process	10	4
Cellular Lipid Metabolic Process	-7	
Cellular Macromolecular Complex Assembly		-8
Cellular Macromolecule Biosynthetic Process	8/-15	
Cellular Protein Complex Assembly		-4
Chlorophyll Biosynthetic Process	-5	
Chromatin Organization		-4
Cofactor Biosynthetic Process	-8	
Electron Transport Chain	-8	-7
Energy Coupled Proton Transport		-12
Heterocycle Biosynthetic Process	-10	
Hexose Metabolic Process	5	
Hydrogen Transport		-12
Ion Transmembrane Transport		-12
Isoprenoid Biosynthetic Process	-5	
Isoprenoid Metabolic Process	-5	
Lipid Biosynthetic Process	-7	
Monosaccharide Catabolic Process	3	
Monosaccharide Metabolic Process	5	
Nitrogen Compound Biosynthetic Process	-16	-21
Nucleosome Assembly		-4
Nucleosome Organization		-4
Oxidative Phosphorylation		-12
Oxoacid Metabolic Process	6/-13	
Photorespiration	-3	
Photosynthesis		1/-5
Photosynthetic Electron Transport Chain		-4
Polyol Catabolic Process	2	
Porphyrin Biosynthetic Process	-6	
Porphyrin Metabolic Process	-6	
Proline Metabolic Process	2	
Protein-DNA Complex Assembly		-4
Proton Transport		-12
Purine Nucleotide Metabolic Process		-12
Reductive Pentose-Phosphate Cycle		-5
Sulfur Amino Acid Metabolic Process		-4
Sulfur Compound Biosynthetic Process	-3	
Terpenoid Biosynthetic Process	-4	
Tetrapyrrole Metabolic Process	-7	
Tetraterpenoid Metabolic Process	-2	
Translation	8/-15	

The KEGG metabolic map shows some differences between the two species exposed to salt stress over time (Figure 6.3). *Chlamydomonas reinhardtii* showed down-regulation in fatty acid biosynthesis (a) and the citrate or TCA cycle (b) where *C. nivalis* did not. *Chlamydomonas reinhardtii* showed up-regulation of amino acid metabolism where *C. nivalis* did not (c). In the literature, inhibition of the TCA cycle can cause a decrease in the oxidation of fatty acids and therefore increase the available pool of acetyl CoA for fatty acid synthesis (Sheehan et al., 1998), however in this case down-regulation of the TCA cycle in *C. reinhardtii* did not result in an increase in lipid biosynthesis.

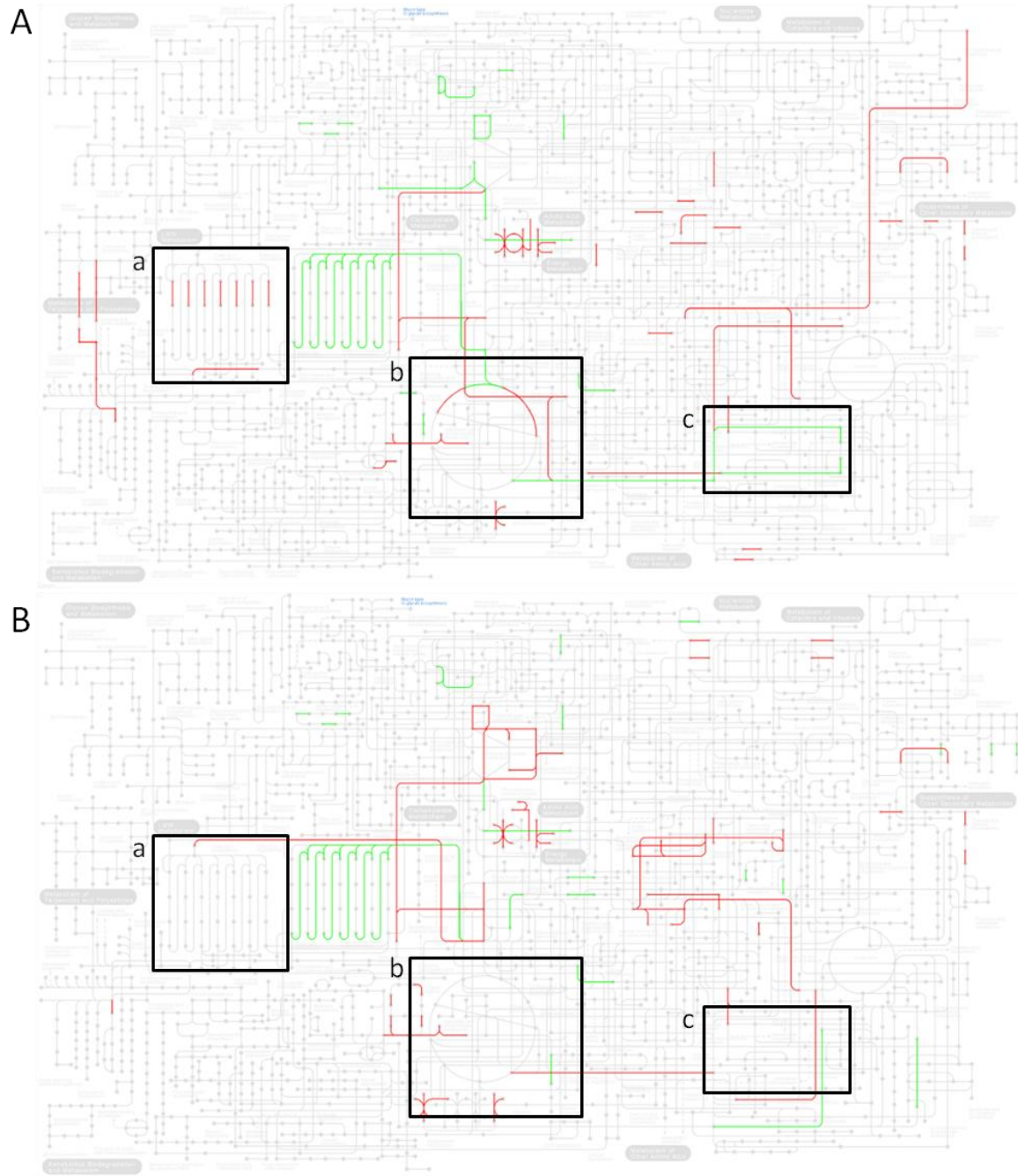


Figure 6.3 KEGG mapping of *C. reinhardtii* (A) and *C. nivalis* (B) showing significant changes in down-regulation (red) and up-regulation (green) between the first and last sample point in salt stress conditions. Highlighted boxes show the differences between the two species in lipid metabolism (a), TCA cycle (b) and amino acid metabolism (c).

## 6.4 Discussion of important lipid metabolism proteins

In terms of the different lipid accumulation and metabolism in these species, the evidence suggests that the salt stressed non-halotolerant species (*C. reinhardtii*) down-regulate lipid biosynthesis over time whilst the halotolerant species (*C. nivalis*) did not. This may explain why lipid accumulation is observed in *C. nivalis* over time but not in *C. reinhardtii*.

Key proteins noted during the iTRAQ investigations in Chapters 4 and 5 have helped elucidate the specific lipid metabolism responses of each species to salt stress.

UDP-sulfoquinovose synthase was down-regulated in *C. nivalis* subjected to salt stress, both over a time course experiment and with reference to a control. This indicates that in salt stressed *C. nivalis*, SQDG lipid production was reduced and FAs were instead used in TAG synthesis (Martin et al., 2014). However, this change was not noted in *C. reinhardtii*. SQDG is utilised in thylakoids, and as *C. reinhardtii* suffers greater salinity damage to photosynthetic equipment than *C. nivalis* does, it may be necessary for *C. reinhardtii* to put more resources, including FAs, into maintaining this part of the cell, thus the FAs cannot be utilised for TAG synthesis.

The regulation of citrate synthase was another important contrast between the two species, since it was down-regulated in *C. nivalis* but up-regulated in *C. reinhardtii*. Knocking out citrate synthase can significantly increase TAG synthesis and accumulation (Deng et al., 2013), and likewise overexpression causes decreases in TAG. This enzyme competes directly with fatty acid synthesis by incorporating acetyl CoA into the citric acid cycle instead of into fatty acid synthesis (Goncalves et al., 2015). Therefore under salt stress, *C. reinhardtii* appears to favour the TCA cycle over fatty acid synthesis whilst the opposite is true in *C. nivalis*.

There is evidence that *C. nivalis* has a higher availability of acetyl CoA under salt stress, since it shows up-regulation of dihydrolipoyl dehydrogenase, which is involved in the production of acetyl CoA, but this protein was unaffected in *C. reinhardtii*. This therefore suggests a greater availability of the substrate for fatty acid synthesis in *C. nivalis*. The

increase in this has been shown to increase TAG accumulation in algae in a previous study (Avidan et al., 2015).

During the initial 3 to 11 hour salt stress in *C. reinhardtii*, acetyl CoA synthetase was down-regulated, presumably causing a decreased supply of acetyl CoA for subsequent reactions. Acetyl CoA production may thus be the rate limiting step that is better targeted for increasing lipid production in algae. Acetyl-CoA carboxylase subunit was also down-regulated in *C. reinhardtii* but not in *C. nivalis*, suggesting that the use of acetyl CoA was directed away from fatty acid synthesis in *C. reinhardtii*.

A combination of an increase in acetyl CoA availability, and no down-regulation of the rate-limiting step of fatty acid synthesis via the enzyme ACCase, appears to contribute towards the ability of *C. nivalis* to accumulate lipids under salt stress whilst in *C. reinhardtii* this does not occur.

Acetyl-CoA acyltransferase is up-regulated at salt stress condition 170 hours (from both 3 hour salt and 170 hour control) *C. nivalis* but not at 82 hours. The same protein was up-regulated between 3 and 11 hours, 3 and 18 hours, and between control and salt 18 hour conditions for *C. reinhardtii*. Fatty acid degradation was therefore up-regulated at a much earlier point in the growth cycle in salt stressed *C. reinhardtii* than in salt stressed *C. nivalis*. This suggests that for *C. nivalis*, fatty acid degradation only happens later in the growth cycle, perhaps once resources become more limited due to a decrease in photosynthesis. The early degradation of fatty acids in *C. reinhardtii* cultures could be one of the key reasons that they did not accumulate in the model species.

Glycerol-3-phosphate dehydrogenase was up-regulated in both species in response to salt stress. This has been shown in other species to be a response to salinity stress. It has also been shown that up-regulating this enzyme causes glycerol and neutral lipid accumulation (mostly from a large increase in MUFAs) the model diatom species (Yao et al., 2014). However, this phenotypic effect was only seen in *C. nivalis*, showing that this alone was

not enough to trigger lipid production. Another study showed that this enzyme was essential for growth under osmotic stress in yeast (Albertyn et al., 1994).

## 6.5 Conclusions

This chapter has shown that the regulatory responses of the two species, studied here by comparing two iTRAQ experiments to quantify proteomic changes in salt stressed cultures, show some key differences. Whilst some regulatory responses are common, other areas of regulation show important differences between the two species which help to elucidate what causes salt stress to be a lipid trigger for one species but not for the other.

Broadly speaking, the differences between the two species in proteomic responses show a greater proportion of the changes in *C. nivalis* being down-regulation. This suggests that *C. nivalis* is going into a stasis state and this may be part of the reason for the accumulation of carbohydrates and lipids. *C. reinhardtii*, by comparison, slows in growth (although then goes on later in the experiment to proliferate), and suffers reduction in photosynthesis, yet shows up-regulation of key processes in cell division and metabolism at different points along the time course experiment. *C. reinhardtii* may then be continuing to use the available energy and resources to maintain cell functions under increased intracellular ionic or osmotic stress. Part of the reason that *C. reinhardtii* may not have produced carbon storage molecules was that growth was arrested for a certain period, but then resumed at a slow pace later in the growth cycle. This was unexpected since *C. nivalis* is reported to be more halotolerant than *C. reinhardtii*, but perhaps *C. nivalis* is more likely to be triggered into a resting state.

The difference in growth set up, with *C. reinhardtii* grown mixotrophically and *C. nivalis* growth photoautotrophically, may account for some of the differences in the response of the species. If *C. nivalis* had a fixed carbon source in the medium, it would rely less on photosynthesis to provide carbon and energy, and the growth of the culture may be higher. However, the reduction in oxygen evolution in photosynthesis experiments was

smaller in *C. nivalis*, indicating that the cells are more robust to the harmful ionic or osmotic effects of salt stress, especially on photosynthesis, and therefore still fix carbon. Additionally, *C. reinhardtii* was more able to rely on the acetate carbon source in the medium, and therefore may have had less need for photosynthesis in the stressed environment. However, studies using nitrogen deprivation in mixotrophic conditions show that the availability of acetate for *C. reinhardtii* was a carbon source for lipid accumulation (Longworth et al., 2012). Therefore neither under photoautotrophic or mixotrophic growth conditions did carbon availability appear to be limited, meaning that the difference in carbon source is unlikely to account for the difference in lipid accumulation.

The most significant finding from this comparison is the difference in how lipid metabolism and carbohydrate metabolism are affected by salt stress, and many of phenotypic changes observed can be explained through these regulatory changes. The down-regulation of fatty acid biosynthesis in *C. reinhardtii* might be attributed to not having effective salt tolerance mechanisms. Due to the fact that *C. reinhardtii* has a greater detrimental response to salt, shown through the large decrease in photosynthetic activity, it is likely that the cell is directing a greater amount of resources into survival, and that lipid accumulation is being shut down as an unnecessary part of metabolism. Changes in lipid production are not used as a survival mechanism, in this case.

The maintenance of photosynthetic capacity is important, as this study searched for an alternative lipid trigger to nitrogen deprivation - a trigger that caused photosynthetic capacity to be lost (Johnson and Alric, 2013). Part of salt tolerance is the ability to maintain photosynthetic apparatus and repair damage to photosystems, and therefore salt tolerance plays an important role in an effective salt-triggered lipid producer.

The question may therefore remain of what causes the difference in halotolerance between the two species. The main mechanisms of halotolerance are ways of maintaining a suitable ion and water balance within the cell. If *C. reinhardtii* were better able to adapt to saline conditions through control of ionic and osmotic balances, it might be possible to

use salt as a lipid trigger in this species as well. However, *C. nivalis* seems a better candidate in this case for biofuel research and potential large scale culture, having higher lipid producing capabilities, and lower optimum temperature requirements than *C. reinhardtii*. Using a robust species like *C. nivalis* is important to ensure that cultures in industrial settings do not suffer population crashes under unfavourable conditions, particularly in an open pond setting.

Additionally, using the results from this comparison chapter, it may be possible to identify some of the key enzymatic steps that control accumulation of lipids in microalgae, and to maximise biofuel production, using genetic engineering techniques in suitable species.

## 7 Chapter 7: Thesis discussion, conclusions and future work

### 7.1 Overview

The work in this thesis has explored the effect of salt stress on the lipid producing capabilities of two *Chlamydomonas* green algal species, through complimentary GC and quantitative proteomics analysis using iTRAQ. These investigations are the first of their kind in the literature, since the effects of salt stress on *C. reinhardtii* lipid profile have not been previously investigated, and part of this novel work has been published in a study of salt effects on *C. reinhardtii* lipid profile by Hounslow et al. (2016a) during the writing of this thesis. Proteomic investigation of *C. nivalis* was also novel, as this un-sequenced organism had not previously been used in such as experiment. Use of closely related species shows the potential for cross-species experimentation, particularly using *de novo* sequencing and homology searching tools in PEAKS software, demonstrating the advantages of such an approach to widening the potential candidates for proteomic analysis. This final chapter explores the implications of the novel findings of this thesis for algal biofuels research, and presents possibilities for how research should be directed in the future. The work presented in this thesis is of significance because exploration of the molecular mechanisms, elucidated by proteomic data, adds to the understanding of lipid triggers in microalgae.

### 7.2 Data summary

After initial exploratory investigations of the effects of varying levels of salt detailed in Chapters 4 and 5, 0.2 M NaCl salinity levels were chosen to explore because this presented a moderate level of salt stress at which both species could survive but that significantly impacted their ability to grow.

Both species suffered severely reduced growth. Whilst *C. reinhardtii* is able to survive in these conditions, the photosynthesis activity is hugely reduced compared to that of

control conditions. By contrast, *C. nivalis* does show some reduction in photosynthesis and respiration activity under 0.2 M NaCl compared to a control, but this reduction is much smaller. Lipids, particularly MUFAs, were induced in *C. nivalis* but not in *C. reinhardtii*. Proteomic investigation suggests that the salt tolerance mechanisms of *C. nivalis* allow it to maintain many lipid biosynthetic processes under salt stress, whilst *C. reinhardtii* down-regulated lipid metabolism, perhaps as a survival mechanism for redirecting resources towards vital cell maintenance functions and combating ionic or osmotic damage.

### 7.3 Discussion of thesis aims

To review if the results had answered the questions raised by this thesis, the aims of the project were revisited. The overall aim was to find ways to increase the useful output from microalgae for biofuels research through biological manipulation of cultures, and the project focused on environmental manipulation and the use of proteomics to study biosynthetic pathways to find ways of creating a high lipid producing algal species. More specifically, the questions this thesis addressed was firstly whether salt stress could be used as a lipid accumulating trigger in the chosen species, and secondly how the molecular mechanisms of the cell controlled the production of lipids under salt stress conditions in each species. The chapters in this thesis aimed to address these questions, and the ability of the thesis to answer these questions has been reviewed below.

#### 7.3.1 Aim 1: Salt stress influence on lipid abundance and profile in *C. reinhardtii*

The first aim was to establish whether salt stress was a lipid trigger in *Chlamydomonas reinhardtii* and how this influenced the lipid profile of the species. The tolerance of the strain was found to be different between two main sets of experimentation, indicating that biological variation in a strain can play a role in tolerance.

Overall, although salt can have a significant effect on the lipid profile of the *C. reinhardtii* strains investigated, and cause some short term increases using 0.3 M NaCl as observed in Chapter 4 and in Appendix C, FAMES were not observed to greatly increase and

accumulate in the salt stressed cultures. The salt tolerance of this strain is less than 0.3 M NaCl, since cultures were killed by this level of salt. At increasing salinities from 0.1 to 0.2 M NaCl, photosynthesis was increasingly negatively impacted, showing that salt stress causes significant impairment to photosynthetic apparatus. Growth was not completely halted by salt stress, rather growth curves showed a lower doubling time, and 0.2 M NaCl arrested growth for the first 24 hours (the period over which the control condition goes through log phase). Changes in cell division were noted, with cells frequently being observed in clusters of daughter cells, a response to salt stress that has previously been found in *C. reinhardtii* (Takouridis et al., 2015).

Compared to the percentages of lipid content seen in *C. reinhardtii*, especially starch-less mutant BAFJ5, under nitrogen starvation, these results did not reveal a high lipid content under the culture conditions studied. Salt stress therefore would not be recommended as a way to obtain high lipid content in the biomass of this *C. reinhardtii* strain, in contrast to nitrogen stress which is a proven lipid trigger (James et al., 2011; James et al., 2013).

### **7.3.2 Aim 2: Detection of changes in the proteome, especially related to lipid metabolism, in *C. reinhardtii* under salt stress**

The second aim was to identify changes in the regulation of proteins associated with lipid metabolism under salt stress. A high number of proteins were relatively quantified using iTRAQ analysis, providing a good quality dataset to explore the effects of salt stress both over a time course experiment, and with reference to a control culture in mid log phase. A large number of proteomic changes were found between the compared phenotypes. Photosynthesis and carbon fixation were down-regulated, with many aspects of central metabolism being impacted by the detrimental effects of salt stress. Salt stress induced some coping and tolerance mechanisms, including up-regulation of proteins linked to proline and to glycerol production. Carbohydrate related proteins were significantly changed by salt stress. Lipid metabolism showed some significant changes under salt

stress. In particular, acetyl-CoA carboxylase was shown to be down-regulated between the control and the salt stressed conditions. This enzyme has been shown to be an important rate limiting step in fatty acid biosynthesis and the down-regulation of this protein may explain why under non-dividing conditions, lipids were not accumulated.

### **7.3.3 Aim 3: Salt stress influence on lipid abundance and profile in *C. nivalis***

The third aim was to investigate the snow alga *C. nivalis* for suitability as a biofuels producer and to investigate the effect of salt on the lipid profile of the cultures.

This basic biology of this species is as yet little studied, and not at all for its biofuel producing potential. After preliminary investigation, 0.2 M NaCl was found to be a lipid trigger in this species, in particular large increases in C18:1*cis* were found. This trend was confirmed, showing a repeatable trend that salt induces first carbohydrate then lipid accumulation in *C. nivalis*. This effect was found both when the salt stress was introduced to a lower density culture (OD<sub>750</sub> of 0.35) and a high density culture (OD<sub>750</sub> of 0.7). This shifted the profile of fatty acids towards a higher proportion of MUFAs, which are highly suited to use in biofuel production. Furthermore, the lipid percentage content of the biomass reached as high as 52% in one experiment (Section 5.4.4), although the initial experiment indicated the highest lipid content was approximately 30%, demonstrating some natural variation between experimental cultures. As discussed in Chapter 1, for algal biofuels to be economically viable, the lipid content of biomass should be 60% (Jorquera et al., 2010), so these salt stressed cultures approached this target lipid content, and tripling the lipid content found in the other experiments (Section 5.4.4).

There may be a few reasons for this lipid induction. One is changes to the lipid membrane composition for better control of osmotic pressure. The other is that the halting of growth due to increased salinity causes an excess of carbon that is stored in carbohydrates and lipids for future utilization during resumed growth.

#### 7.3.4 Aim 4: Detection of changes in the proteome, especially related to lipid metabolism, in *C. nivalis* under salt stress

An additional aim was to use *C. nivalis* as a homologue to *C. reinhardtii*, ultimately to investigate the effect of salt stress on the proteome of *C. nivalis*, particularly with reference to lipid metabolism, by observing proteomic changes in both species during salt stress.

A large number of proteins were identified, using a combination of high resolution mass spectrometry, and PEAKS software that employs *de novo* sequencing and homology searching using a related model species database for *C. reinhardtii*. This study is the first to investigate the proteome of this snow algae species, and a large number of phenotypic and proteomic changes were observed between samples along a salt stressed time course experiment (including significant rises in carbohydrate and lipid carbon storage molecules) and with relation to a control log phase culture. This iTRAQ study revealed information on how *C. nivalis* responds to salt stress, and how lipid metabolism is affected by salt stress conditions. Genetic investigation showed a 95% similarity between this species and the model alga, and the relatedness of this species with *C. reinhardtii* allowed comparisons to be drawn in the proteomic responses and regulation of lipid metabolism between the two species using the two iTRAQ experiments. These comparisons help to elucidate the differences between the mechanisms controlled purely as a salt stress response, and those that are employed as a salt stress response resulting in lipid accumulation - thereby pinpointing areas that should be targeted for genetic engineering to increase lipid production.

One species accumulated lipids under salt stress whilst the other did not. A key rate-limiting enzyme in fatty acid metabolism (ACCase) was found to be down-regulated in *C. reinhardtii* during salt stress, whilst it was not down-regulated in *C. nivalis*. Furthermore, functional annotation analysis indicated that *C. reinhardtii* showed down-regulation in lipid metabolism generally, whilst *C. nivalis* did not show those same down-regulations. Further analysis revealed several important enzymes that indicated that there was greater

channelling of acetyl CoA into fatty acid synthesis in *C. nivalis* than in *C. reinhardtii*. It was postulated that lipid metabolism was down-regulated in salt stressed *C. reinhardtii* because resources were directed instead to maintaining cell function during high osmotic or ionic stress. *C. nivalis*, which has higher salt tolerance, may not experience the same levels of stress and damage to the internal mechanisms that *C. reinhardtii* does, and instead enters a non-dividing state during salt stress, and diverts resources towards storage molecules in carbohydrate and lipid form, for when the cell re-enters ideal growth conditions.

#### **7.4 How iTRAQ has helped to address the question of which mechanisms are controlling lipid production under salt stress**

iTRAQ is a powerful tool for analysing the molecular mechanisms of cells and for studying how relative changes in proteomes can explain the phenomena observed in experiments. In conjunction with powerful MS/MS analysis, it can be used to gain quantitative information on a large number of protein identifications, and correlate them to the changes in growth, lipid levels, carbohydrate levels and photosynthetic activity observed in these species in response to salt. iTRAQ has limitations to its quantification abilities, as discussed in Chapter 1, and therefore some changes in regulation of proteins may have been underestimated and not detected as significantly changed. The 8-plex design has allowed duplicate comparisons of four different sample types in each experiment and therefore supplied a large amount of data in comparing both salt stress at three points along a time course experiment, and compared to a control log phase culture. In this case, iTRAQ quantification of proteomic samples has helped to analyse the mechanisms behind the salt lipid trigger in *C. nivalis* and how these differ to the salt responses in *C. reinhardtii*. Linking genes, proteins and metabolic pathways to the conditions that trigger lipid synthesis is an important part of algal lipid research for biofuels purposes (Guschina and Harwood, 2006; Harwood and Guschina, 2009).

## 7.5 Discussion of the use of lipid measurement methods

Throughout the course of this PhD project, lipid measurement methods have played a central role in establishing the lipid producing conditions for biofuels research. Although the majority of the results obtained and discussed here used GC lipid measurement, several methods were undertaken for measuring the lipid production in *C. reinhardtii* in this project, namely: Bligh and Dyer gravimetric, microcolorimetric, Nile Red and transesterification with GC. The preliminary work was conducted using these different techniques, and some of these experiments highlighted the possibilities of false positives in research, or of inaccuracies of a technique in assessing the lipid contents of microalgal biomass. A thorough literature investigation of the available techniques was carried out, as a guide for researchers to choose a suitable technique for their research, and is now available as a published review by Hounslow et al. (2016b). It can be referred to in Appendix B. This literature review and published guide was a valuable part of the work undertaken, since large amounts of time can be wasted when researchers use unsuitable techniques.

This investigation was carried out as a result of the experimental problems in lipid assays, partially as a way of identifying the most suitable technique for the current work, but also as a way of informing future researchers on the pitfalls involved in these lipid measurement techniques. Reliance on the Nile Red technique - classically used for screening purposes - can lead to false positives and mislead research. Finally, GC was identified as the best tool for measuring lipids, as it provided detailed lipid profile data, and therefore provides information on not only the quantity but also the quality of lipids in a sample suitable for biofuel production. It also requires little enough sample to be able to take multiple time points from a laboratory scale culture.

## 7.6 Implications of salt stress for biofuels production generally and in temperate Europe

When assessing the suitability of the fatty acid profile to biodiesel production, the results must be put into context of the requirements for fatty acid composition of a suitable

biofuel (Islam *et al.*, 2013). Stansell *et al.* (2012) discuss the required characteristics of biodiesel, highlighting that cetane number, cold-flow characteristics, viscosity, and oxidative stability are all important, and are affected by the length and degree of saturation of the fatty acids. According to their analysis, the ideal biodiesel feedstock would entirely comprise C16:1 and C18:1 chains, as monounsaturated fatty acids (MUFAs) are desirable for biodiesel, although one must consider the composition of the FA profile as a whole. To summarise the characteristics of desired biodiesel: higher cetane number is better and this increases in higher chain length and lower unsaturation; unsaturated FAMES have better cold flow characteristics; high viscosity causes problems in fuel properties, and this increases with longer chain lengths and higher unsaturation; high oxidation rate is undesirable and increases with a higher number of double bonds in a FAME; the desirable properties of cold-flow characteristics and cetane number are conflicting and therefore need to be balanced (Stansell *et al.*, 2012). Microalgae change their FA compositions in response to environmental change such as temperature and nutrient response. The relationships between FA compositions, environmental variables and species are complex and need further investigation, as altering the FA composition can lead to a more suitable biofuel (Knothe, 2009; Stansell *et al.*, 2012).

The desired shift towards MUFAs is not found in the lipid profiles of *C. reinhardtii* under salt stress, so it is not a suitable lipid trigger for improving biodiesel quality. Although C16:0 was increased in both *C. reinhardtii* experiments, in the second experiment C18:0 was decreased, causing no overall increase in SFAs. If overall an increase in SFAs occur via the increase in C16:0 under 0.3 M NaCl, it would affect the biodiesel by increasing the energy content and decreasing the oxidation rate.

Lipid induction can be triggered using salt on a *C. nivalis* culture, at various points in its growth cycle, and this increase is ideal for biofuels since it is mainly the MUFAs that increase, which are the best fatty acids for biodiesel (Knothe, 2008). This shows that the use of salt in algal cultures could be of great relevance to industrial production of biofuels. Use of brackish water, or other saline water sources could be incorporated into this

industrial process. This would have to be used as a lipid inducer after the culture reached a high productivity, since despite the reported salinity tolerance of *C. nivalis* in literature, 0.2 M NaCl still causes enough of a detrimental effect that the culture ceases cell division. It would also be important for the salinity level to be relatively controlled, as too high a salinity may not trigger lipid production. Salinity may also be a good way to prevent invading species to an industrial culture, since fewer species can thrive in high salinity conditions.

Chapter 1 discussed the need for a biofuel-producing algal species with low energy input requirements. *Chlamydomonas nivalis* is a species showing great potential to produce a large proportion of algal biomass as lipids, which grows optimally between 5 and 15°C (Lukes et al., 2014), and therefore would require much lower heating in cool climates, such as temperate Europe, than *C. reinhardtii* and other species which require a 25°C growth condition. *C. nivalis* was grown photoautotrophically, showing that lipids can be accumulated as a high percentage of biomass, utilising CO<sub>2</sub> as the sole carbon source; the robustness of the cells to salt stress means that photosynthesis and carbon fixation mechanisms remain largely undamaged (although temporarily down-regulated). Furthermore, *C. nivalis* can grow over a wide range of light intensities - the current research used a relatively low light intensity for growth of *C. nivalis* yet yielded a high percentage of lipid accumulation. In areas where light intensity was highly variable, like temperate Europe, this adaptability is very useful.

Salt as a lipid trigger does not, however, increase the lipid productivity of the culture as a whole. The aim at the beginning of this thesis was to find ways to increase the output of microalgae for use in biofuels, potentially by finding targets for engineering that could increase lipid content whilst also maintaining culture growth in non-stressed conditions. This study has not demonstrated a concurrent increase in lipid content whilst also maintaining culture growth, due to arrest of cell division and the down-regulation in salt stressed cultures of vital processes including photosynthesis and carbon fixation. However, the study has provided more information on the molecular mechanisms behind

salt as a lipid trigger, and reinforced the need for the supply of acetyl CoA and for non-limitation of ACCase in order for cells to produce lipids. Targeting the important enzymes controlling these processes for genetic manipulation could lead to greater biofuel production from these species in the future.

### **7.7 Limitations of the research**

In this case, the comparison between the two iTRAQ experiments was not directly equivalent since the two species had different optimal culture conditions. One species was grown with a fixed carbon source and one was not. Large differences can be found between the photosynthetic ability in algae of phototrophic, mixotrophic and heterotrophic cultures (Smith et al., 2015), and therefore it is possible that this photosynthetic ability affected the responses of these species to salt stress. By using a control culture in each case, this should be accounted for. However, future work should work to eliminate these variations.

It is important to distinguish that although TAG is often discussed as the desired product of algae for biofuels production, the increases in fatty acids observed in this research cannot necessarily be attributed to TAG, since the source of the fatty acids was not investigated. Regardless of the source of the FAMES and whether they can be attributed to TAG or whether they are due to changes in membrane lipids, an increase in FAs in the cells is valuable since they can still be converted to FAMES.

### **7.8 Questions raised by the research**

In this case, part of the mechanism that caused lipid accumulation in *C. nivalis* was the fact that growth was arrested, and therefore resources were redirected to storage molecules. To engineer algae to produce biofuels, it is desirable to maintain culture growth as well as improve lipid content, and find ways that algae increase their lipid content other than simply arresting their growth. A salt trigger was not able to achieve this in these experiments, however perhaps further experimentation in this research area will find a condition that allows both.

The effect of lipid induction took place after the same number of hours (onset between 80 and 150) after salt application in *C. nivalis*, regardless of culture density. This raises the question of why that period of time is needed for lipids to be induced. This may be down to the rate of carbon fixation. It would be interesting to note if this time period was reduced by manipulation of the growth conditions, for example by using higher light intensity.

## 7.9 Conclusions

Whilst *C. reinhardtii* is a model species for microalgae and is therefore highly suited to proteomic investigation and genetic manipulation, *C. nivalis* has a greater capacity for variable salt growth conditions (Lu et al., 2012c) and shows greater potential which makes it an interesting candidate for looking at stress induced lipid production.

Economically and energetically feasible biofuel from algae remains in the conceptual stages and a big part of making it a reality will be in improving lipid yields from algal biomass. Being able to accurately measure these yields is an integral part of the research and the analysis of methods in this thesis will help guide researchers to choose their methods appropriately.

The data obtained in the results chapters has informed the research on biofuels by providing detailed fatty acid profiling of two microalgal species under salt stress, with quantitative proteomic data to support the phenotypic data collected. This information is completely new as the biofuel producing capabilities of both species under salt stress has not previously been investigated to this level of detail.

The interplay between salt stress and lipid metabolism is complex and species specific. The two species reacted differently to the selected salt stress level, with *C. nivalis* showing a large increase in lipids and *C. reinhardtii* showing much smaller or no lipid increases. The mechanisms for the increase of lipid in salt stressed cultures still need to be elucidated, but it is likely that changes in membrane lipids are playing a large role, as well as changes in carbon storage molecules.

Differences in the lipid metabolism of the two species in response to salt provide important considerations for the culturing of algae under lipid triggering conditions. The model species, *C. reinhardtii*, showed an early response of up-regulation of lipid degradation under salt conditions, showing that even though a certain condition may trigger lipid accumulation in one species, the toxic effects of salt can cause resources to be used before they can be accumulated in fatty acids.

Alternatively, resources may be directed into glycerol production as a compatible solute, but not converted to TAGs because the key committing step of Acetyl-CoA carboxylase has been down-regulated in the model species, but not in the snow algae species.

The reason for the "lipid trigger" phenomenon occurring, first documented by Sheehan *et al.* (1998), was suggested to be due to nitrogen deprivation decreasing some key processes including cell division but not affecting lipid production, so lipids accumulate. However, more recently it has been suggested that oxidative stress is linked to lipid production in microalgae (Yilancioglu *et al.*, 2014), and applying oxidative stress leads to increases in lipid content. Since salt can induce oxidative stress, it follows that salt may cause a lipid increase. The occurrence of lipid accumulation under salt stress observed in this study may support the theory that it is oxidative stress that causes lipid accumulation, rather than an excess of ATP:AMP ratio as theorized by Botham and Ratledge (1979).

In practice, salt culture conditions could be a way of utilising brackish water or saline culturing environments that would otherwise be deemed "waste" resources. However, to utilise salt to induce lipid changes in terms of biological engineering, a greater understanding of how salt may cause lipid accumulation and proteomic profiling is needed. As with nitrogen stress or any other lipid trigger, the exact cellular mechanisms employed in this response are not well known. The original problem with lipid accumulation is that high lipid content and high cell division are often not achievable at the same time. In this case, lipid accumulation and culture growth were not achieved concurrently, even using the halotolerant species *C. nivalis*.

As part of obtaining the ideal biofuel candidate and its culturing conditions is to choose a suitable strain, to this end screening of new and promising species is vital to meeting this aim. Profiling an uncharacterised species which has potentially low energy inputs due to its low growth temperature and potentially high lipid outputs provides a good candidate to help meet this need. *C. nivalis* has demonstrated its suitability as a temperate Northern European species that can grow in low temperatures, thus having a reduced energy input via heating requirements; it is also a species that can be manipulated via salt stress for increased lipid content. Since biological engineering is also needed to maximise the biofuel output from microalgae, understanding all mechanisms that lead to increases in lipids is desirable, and salt as a potential lipid trigger can provide a more complete picture of these in both species, particularly by comparing differences in response to salt stress. Proteomic analysis revealed insights into how salt acts as a lipid trigger in *C. nivalis* but not in *C. reinhardtii*. This could be used in future to reveal and engineer pathways that could improve the ability of these species to produce biofuels.

Since improving lipid productivity in an algal culture is vital to make algal biofuels more economically and energetically feasible, using this method of biological manipulation is a step towards making this a more viable biofuel option.

Understanding the processes that control lipid metabolism could ultimately lead to breakthroughs in biofuel research; now more than ever, these are needed to reach our continually increasing need for renewable energy sources.

## 7.10 Future work

There were many avenues of research which, had the time and scope of the project allowed, this PhD project would have addressed. Instead it is suggested that certain parts of this research would be ideal for future projects.

*Chlamydomonas nivalis* is an interesting algal species that has had little lipidomic and no proteomic research carried out on it until now, yet is a promising biofuel candidate. The low temperature requirements of *C. nivalis* mean that it could be grown outdoors in cool

countries without the need for heating, but the effect of temperature on the lipid profile would be important for judging the suitability of such culture conditions for biofuels production. This study took place at 16°C; the growth rates and lipid profiling of the strain under higher and lower temperatures, as well as the effect of temperature fluctuations part way through culturing, would be very valuable to determine the suitability of this strain for biofuel production, particularly in a variable open pond culturing environment.

A more complete dataset could be obtained for *C. nivalis* if the DNA sequence and proteomic databases were available. Therefore, future investigations on this species should first focus on sequencing the genome and building a proteomic database.

For further comparisons between the two species, using comparative nitrogen stress to explore the lipid responses in each species may be interesting. Furthermore, the study had limitations in the growth set ups being different, therefore carrying out studies with closer experimental set ups would be advantageous, to rule out these effects on the results obtained.

A further study on the effects of salt stress on each species could test their ability to recover by returning salt stressed cultures to control media. This may yield information on the ability of a culture to recover if detrimental salt conditions are reached, which may be relevant for industrial production of algal biomass in which salt is used as either a lipid trigger or as a way of limiting invading species to a culture.

The levels of light used in the current *C. nivalis* investigations were relatively low, due to the limitations in experimental equipment set up, but this species has a great capacity for withstanding high light levels. With this in mind the effects of ultraviolet light stress could be interesting, since this species has a large tolerance for high light levels in its natural snowy habitat, which is likely to experience high intensity ultraviolet light. Also combinations of variables of light level, carbon source and salt level would be interesting to explore, as this may allow for even greater lipid productivity in a culture.

Although *C. reinhardtii* does not appear to be as promising a biofuels producer as *C. nivalis* in terms of overall FAME content, investigating the effects of salt stress on the growth and lipid profile of different strains could be advantageous. The low starch mutant strain I7 was used in this case, but strain BAFJ5 has shown higher lipid accumulation than I7 in another study (James et al., 2011), and therefore using this alternative strain under the differing salt stress conditions may reveal bigger increases in lipid accumulation than were observed in this study. The wild type strain would also be useful to investigate. In this case a low starch mutant was selected so that potential changes in lipid profile could be maximised, but wild type strains may behave differently.

This study has highlighted potential mechanisms of lipid accumulation in salt conditions, and these can be targeted for engineering in the chosen species. Targeting genes involved in salt tolerance in *C. nivalis* for up-regulation in *C. reinhardtii* may improve the model species growth and lipid production under salt conditions. However, the more promising candidate *C. nivalis*, could potentially be engineered by up-regulating the production of acetyl CoA. This pathway was shown to be differentially expressed in *C. nivalis* but not in *C. reinhardtii*, and increasing the availability may help to boost lipid production in this species without the need to arrest growth. Future experiments should focus on potential gene targets and produce knock-out or over-expression of target genes for enhanced growth and lipid production.

## 8 References

- . U.S. Energy Information Administration.
- Abis, K.L., and Mara, D.D. (2005). Primary facultative ponds in the UK: the effect of operational parameters on performance and algal populations. *Water Science and Technology* *51*, 61-67.
- Adams, C., Godfrey, V., Wahlen, B., Seefeldt, L., and Bugbee, B. (2013). Understanding precision nitrogen stress to optimize the growth and lipid content tradeoff in oleaginous green microalgae. *Bioresource Technology* *131*, 188-194.
- Affenzeller, M.J., Darehshouri, A., Andosch, A., Lütz, C., and Lütz-Meindl, U. (2009). Salt stress-induced cell death in the unicellular green alga *Micrasterias denticulata*. *Journal of Experimental Botany* *60*, 939-954.
- Aggarwal, K., Choe, L.H., and Lee, K.H. (2006). Shotgun proteomics using the iTRAQ isobaric tags. *Briefings in Functional Genomics & Proteomics* *5*, 112-120.
- Ahn, J.W., Hwangbo, K., Yin, C.J., Lim, J.M., Choi, H.G., Park, Y.I., and Jeong, W.J. (2015). Salinity-dependent changes in growth and fatty acid composition of new Arctic *Chlamydomonas* species, ArM0029A. *Plant Cell Tissue Organ Cult* *120*, 1015-1021.
- Albertyn, J., Hohmann, S., Thevelein, J.M., and Prior, B.A. (1994). GPD1, which encodes glycerol-3-phosphate dehydrogenase, is essential for growth under osmotic stress in *Saccharomyces cerevisiae*, and its expression is regulated by the high-osmolarity glycerol response pathway. *Meth Cell Biol* *14*.
- Allakhverdiev, S.I., Kinoshita, M., Inaba, M., Suzuki, I., and Murata, N. (2001). Unsaturated Fatty Acids in Membrane Lipids Protect the Photosynthetic Machinery against Salt-Induced Damage in *Synechococcus*. *Plant Physiology* *125*, 1842-1853.
- Allakhverdiev, S.I., Nishiyama, Y., Miyairi, S., Yamamoto, H., Inagaki, N., Kanesaki, Y., and Murata, N. (2002). Salt Stress Inhibits the Repair of Photodamaged Photosystem II by Suppressing the Transcription and Translation of psbA Genes in *Synechocystis*. *Plant Physiology* *130*, 1443-1453.
- Allakhverdiev, S.I., Nishiyama, Y., Takahashi, S., Miyairi, S., Suzuki, I., and Murata, N. (2005). Systematic analysis of the relation of electron transport and ATP synthesis to the photodamage and repair of photosystem II in *Synechocystis*. *Plant Physiology* *137*, 263-273.
- Allakhverdiev, S.I., Sakamoto, A., Nishiyama, Y., Inaba, M., and Murata, N. (2000). Ionic and Osmotic Effects of NaCl-Induced Inactivation of Photosystems I and II in *Synechococcus* sp. *Plant Physiology* *123*, 1047-1056.

Allen, M.B. (1956). Excretion of Organic Compounds by *Chlamydomonas*. *Archiv Fur Mikrobiologie* 24, 163-168.

An, M., Mou, S., Zhang, X., Zheng, Z., Ye, N., Wang, D., Zhang, W., and Miao, J. (2013). Expression of fatty acid desaturase genes and fatty acid accumulation in *Chlamydomonas* sp. ICE-L under salt stress. *Bioresource Technology* 149, 77-83.

Avidan, O., Brandis, A., Rogachev, I., and Pick, U. (2015). Enhanced acetyl-CoA production is associated with increased triglyceride accumulation in the green alga *Chlorella desiccata*. *Journal of Experimental Botany* 66, 3725-3735.

Azachi, M., Sadka, A., Fisher, M., Goldshlag, P., Gokhman, I., and Zamir, A. (2002). Salt induction of fatty acid elongase and membrane lipid modifications in the extreme halotolerant alga *Dunaliella salina*. *Plant Physiology* 129, 1320-1329.

Baliga, R., and Powers, S.E. (2010). Sustainable algae biodiesel production in cold climates. *International Journal of Chemical Engineering*.

Ball, S.G., Dirick, L., Decq, A., Martiat, J.-C., and Matagne, R. (1990). Physiology of starch storage in the monocellular alga *Chlamydomonas reinhardtii*. *Plant Science* 66, 1-9.

Ballicora, M.A., Iglesias, A.A., and Preiss, J. (2004). ADP-glucose pyrophosphorylase: a regulatory enzyme for plant starch synthesis. *Photosynthesis Research* 79, 1-24.

Bantscheff, M., Schirle, M., Sweetman, G., Rick, J., and Kuster, B. (2007). Quantitative mass spectrometry in proteomics: a critical review. *Analytical and Bioanalytical Chemistry* 389, 1017-1031.

Bartley, M.L., Boeing, W.J., Corcoran, A.A., Holguin, F.O., and Schaub, T. (2013). Effects of salinity on growth and lipid accumulation of biofuel microalga *Nannochloropsis salina* and invading organisms. *Biomass and Bioenergy* 54, 83-88.

Barupal, D., Kind, T., Kothari, S., Lee, D., and Fiehn, O. (2010). Hydrocarbon phenotyping of algal species using pyrolysis-gas chromatography mass spectrometry. *BMC Biotechnology* 10, 40.

Batterto, J.C., and Vanbaale, C. (1971). Growth responses of blue-green algae to sodium chloride concentration. *Archiv Fur Mikrobiologie* 76, 151-&.

Beal, C., Smith, C., Webber, M., Ruoff, R., and Hebner, R. (2011). A Framework to Report the Production of Renewable Diesel from Algae. *Bioenergy Research* 4, 36-60.

Beal, C.M., Webber, M.E., Ruoff, R.S., and Hebner, R.E. (2010). Lipid analysis of *Neochloris oleoabundans* by liquid state NMR. *Biotechnology and Bioengineering* 106, 573-583.

Beckmann, J., Lehr, F., Finazzi, G., Hankamer, B., Posten, C., Wobbe, L., and Kruse, O. (2009). Improvement of light to biomass conversion by de-regulation of light-harvesting protein translation in *Chlamydomonas reinhardtii*. *Journal of Biotechnology* 142, 70-77.

Ben-Amotz, A., and Avron, M. (1983). On the Factors Which Determine Massive  $\beta$ -Carotene Accumulation in the Halotolerant Alga *Dunaliella bardawil*. *Plant Physiology* 72, 593-597.

Benemann, J.R. (1993). Utilization of carbon dioxide from fossil fuel-burning power plants with biological systems. *Energy Conversion and Management* 34, 999-1004.

Beynon, R.J., and Pratt, J.M. (2005). Metabolic Labeling of Proteins for Proteomics. *Molecular & Cellular Proteomics* 4, 857-872.

Bhatnagar, A., Chinnasamy, S., Singh, M., and Das, K.C. (2011). Renewable biomass production by mixotrophic algae in the presence of various carbon sources and wastewaters. *Applied Energy* 88, 3425-3431.

Bišová, K., and Zachleder, V. (2014). Cell-cycle regulation in green algae dividing by multiple fission. *Journal of Experimental Botany*.

Blatti, J.L., Michaud, J., and Burkart, M.D. (2013). Engineering fatty acid biosynthesis in microalgae for sustainable biodiesel. *Current Opinion in Chemical Biology* 17, 496-505.

Bligh, E.G., and Dyer, W.J. (1959). A rapid method of total lipid extraction and purification. *Canadian Journal of Biochemistry and Physiology* 37, 911-917.

Blokhina, O., Virolainen, E., and Fagerstedt, K.V. (2003). Antioxidants, Oxidative Damage and Oxygen Deprivation Stress: a Review. *Annals of Botany* 91, 179-194.

Bonferroni, C.E. (1936). *Teoria statistica delle classi e calcolo delle probabilita* (Libreria internazionale Seeber).

Borowitzka, M.A., Borowitzka, L.J., and Kessly, D. (1990). Effects of salinity increase on carotenoid accumulation in the green alga *Dunaliella salina*. *Journal of Applied Phycology* 2, 111-119.

Botham, P.A., and Ratledge, C. (1979). A biochemical explanation for lipid accumulation in *Candida* 107 and other oleaginous micro-organisms. *Journal of General Microbiology* 114, 361-375.

Boussiba, S., Bing, W., Yuan, J.-P., Zarka, A., and Chen, F. (1999). Changes in pigments profile in the green alga *Haematococcus pluvialis* exposed to environmental stresses. *Biotechnology Letters* *21*, 601-604.

Brennan, L., and Owende, P. (2010). Biofuels from microalgae-A review of technologies for production, processing, and extractions of biofuels and co-products. *Renewable & Sustainable Energy Reviews* *14*, 557-577.

Brönstrup, M. (2004). Absolute quantification strategies in proteomics based on mass spectrometry. *Expert Review of Proteomics* *1*, 503-512.

Buhr, H.O., and Miller, S.B. (1983). A dynamic model of the high-rate algal-bacterial wastewater treatment pond. *Water Research* *17*, 29-37.

Cai, G., Jin, B., Saint, C., and Monis, P. (2011). Genetic manipulation of butyrate formation pathways in *Clostridium butyricum*. *J Biotechnol* *155*, 269-274.

Cakmak, T., Angun, P., Demiray, Y.E., Ozkan, A.D., Elibol, Z., and Tekinay, T. (2012). Differential effects of nitrogen and sulfur deprivation on growth and biodiesel feedstock production of *Chlamydomonas reinhardtii*. *Biotechnology and Bioengineering* *109*, 1947-1957.

Chen, H., Lao, Y.-M., and Jiang, J.-G. (2011a). Effects of salinities on the gene expression of a (NAD<sup>+</sup>)-dependent glycerol-3-phosphate dehydrogenase in *Dunaliella salina*. *Science of the Total Environment* *409*, 1291-1297.

Chen, L., Wu, L.N., Zhu, Y., Song, Z.D., Wang, J.X., and Zhang, W.W. (2014). An orphan two-component response regulator Slr1588 involves salt tolerance by directly regulating synthesis of compatible solutes in photosynthetic *Synechocystis* sp PCC 6803. *Molecular Biosystems* *10*, 1765-1774.

Chen, M., Tang, H., Ma, H., Holland, T.C., Ng, K.Y.S., and Salley, S.O. (2011b). Effect of nutrients on growth and lipid accumulation in the green algae *Dunaliella tertiolecta*. *Bioresource Technology* *102*, 1649-1655.

Chen, S., Chen, X., Peng, Y., and Peng, K. (2009a). A mathematical model of the effect of nitrogen and phosphorus on the growth of blue-green algae population. *Applied Mathematical Modelling* *33*, 1097-1106.

Chen, W., Zhang, C., Song, L., Sommerfeld, M., and Hu, Q. (2009b). A high throughput Nile red method for quantitative measurement of neutral lipids in microalgae. *Journal of Microbiological Methods* *77*, 41-47.

Chen, Y., and Vaidyanathan, S. (2012). A simple, reproducible and sensitive spectrophotometric method to estimate microalgal lipids. *Analytica Chimica Acta* 724, 67-72.

Cheng, Y.S., Zheng, Y., and VanderGheynst, J.S. (2011). Rapid Quantitative Analysis of Lipids Using a Colorimetric Method in a Microplate Format. *Lipids* 46, 95-103.

Cherif, A., Dubacq, J., Mache, R., Oursel, A., and Tremolieres, A. (1975). Biosynthesis of  $\alpha$ -linolenic acid by desaturation of oleic and linoleic acids in several organs of higher and lower plants and in algae. *Phytochemistry* 14, 703-706.

Chisti, Y. (2007). Biodiesel from microalgae. *Biotechnology Advances* 25, 294-306.

Chisti, Y. (2008). Biodiesel from microalgae beats bioethanol. *Trends in Biotechnology* 26, 126-131.

Chisti, Y. (2013). Constraints to commercialization of algal fuels. *Journal of Biotechnology* 167, 201-214.

Chiu, S.Y., Kao, C.Y., Tsai, M.T., Ong, S.C., Chen, C.H., and Lin, C.S. (2009). Lipid accumulation and CO<sub>2</sub> utilization of *Nannochloropsis oculata* in response to CO<sub>2</sub> aeration. *Bioresource Technology* 100, 833-838.

Choi, Y.E., Hwang, H., Kim, H.S., Ahn, J.W., Jeong, W.J., and Yang, J.W. (2013). Comparative proteomics using lipid over-producing or less-producing mutants unravels lipid metabolisms in *Chlamydomonas reinhardtii*. *Bioresource Technology* 145, 108-115.

Chong, P.K., Gan, C.S., Pham, T.K., and Wright, P.C. (2006). Isobaric Tags for Relative and Absolute Quantitation (iTRAQ) Reproducibility: Implication of Multiple Injections. *Journal of Proteome Research* 5, 1232-1240.

Cirulis, J.T., Strasser, B.C., Scott, J.A., and Ross, G.M. (2012). Optimization of staining conditions for microalgae with three lipophilic dyes to reduce precipitation and fluorescence variability. *Cytometry Part A* 81A, 618-626.

Cohen, Z., Vonshak, A., and Richmond, A. (1988). Effect of environmental conditions on fatty acid composition of the red alga *Porphyridium cruentum*: Correlation to growth rate. *Journal of Phycology* 24, 328-332.

Courchesne, N.M.D., Parisien, A., Wang, B., and Lan, C.Q. (2009). Enhancement of lipid production using biochemical, genetic and transcription factor engineering approaches. *Journal of Biotechnology* 141, 31-41.

Cox, J., and Mann, M. (2011). Quantitative, High-Resolution Proteomics for Data-Driven Systems Biology. In *Annual Review of Biochemistry*, Vol 80, R.D. Kornberg, C.R.H. Raetz, J.E. Rothman, and J.W. Thorner, eds., pp. 273-299.

Datta, S., and DePadilla, L.M. (2006). Feature selection and machine learning with mass spectrometry data for distinguishing cancer and non-cancer samples. *Statistical Methodology* 3, 79-92.

Davis, R., Aden, A., and Pienkos, P.T. (2011). Techno-economic analysis of autotrophic microalgae for fuel production. *Applied Energy* 88, 3524-3531.

De Bhowmick, G., Koduru, L., and Sen, R. (2015). Metabolic pathway engineering towards enhancing microalgal lipid biosynthesis for biofuel application—A review. *Renewable and Sustainable Energy Reviews* 50, 1239-1253.

Dean, A.P., Sigee, D.C., Estrada, B., and Pittman, J.K. (2010). Using FTIR spectroscopy for rapid determination of lipid accumulation in response to nitrogen limitation in freshwater microalgae. *Bioresource Technology* 101, 4499-4507.

Demetriou, G., Neonaki, C., Navakoudis, E., and Kotzabasis, K. (2007). Salt stress impact on the molecular structure and function of the photosynthetic apparatus—The protective role of polyamines. *Biochimica et Biophysica Acta (BBA) - Bioenergetics* 1767, 272-280.

Demiral, T., and Türkan, İ. (2005). Comparative lipid peroxidation, antioxidant defense systems and proline content in roots of two rice cultivars differing in salt tolerance. *Environmental and Experimental Botany* 53, 247-257.

Devos, N., Ingouff, M., Loppes, R., and Matagne, R.F. (1998). Rubisco adaptation to low temperatures: A comparative study in psychrophilic and mesophilic unicellular algae. *Journal of Phycology* 34, 655-660.

Dismukes, G.C., Carrieri, D., Bennette, N., Ananyev, G.M., and Posewitz, M.C. (2008). Aquatic phototrophs: efficient alternatives to land-based crops for biofuels. *Current Opinion in Biotechnology* 19, 235-240.

Domon, B., and Aebersold, R. (2006). Review - Mass spectrometry and protein analysis. *Science* 312, 212-217.

Domon, B., and Aebersold, R. (2010). Options and considerations when selecting a quantitative proteomics strategy. *Nat Biotech* 28, 710-721.

Drubin, D.A., Way, J.C., and Silver, P.A. (2007). Designing biological systems. *Genes & Development* 21, 242-254.

Du, C., Liang, J.-R., Chen, D.-D., Xu, B., Zhuo, W.-H., Gao, Y.-H., Chen, C.-P., Bowler, C., and Zhang, W. (2014). iTRAQ-Based Proteomic Analysis of the Metabolism Mechanism Associated with Silicon Response in the Marine Diatom *Thalassiosira pseudonana*. *Journal of Proteome Research* 13, 720-734.

Dubini, A. (2011). Green Energy from Green Algae. *The Biochemical Society*, 20-23.

Dubinsky, Z., and Berman-Frank, I. (2001). Uncoupling primary production from population growth in photosynthesizing organisms in aquatic ecosystems. *Aquatic Sciences* 63, 4-17.

Eckardt, N.A. (2014). Nitrogen-Sparing Mechanisms in *Chlamydomonas*: Reduce, Reuse, Recycle, and Reallocate. *Plant Cell* 26, 1379-1379.

El-Baky, H.H.A., El-Baz, F.K., and El-Baroty, G.S. (2004). Production of lipids rich in omega 3 fatty acids from the halotolerant alga *Dunaliella salina*. *Biotechnology* 3, 102-108.

Elliott, M.H., Smith, D.S., Parker, C.E., and Borchers, C. (2009). Current trends in quantitative proteomics. *Journal of Mass Spectrometry* 44, 1637-1660.

Eroglu, E., and Melis, A. (2009). "Density Equilibrium" Method for the Quantitative and Rapid In Situ Determination of Lipid, Hydrocarbon, or Biopolymer Content in Microorganisms. *Biotechnology and Bioengineering* 102, 1406-1415.

Evans, C., Noirel, J., Ow, S.Y., Salim, M., Pereira-Medrano, A.G., Couto, N., Pandhal, J., Smith, D., Pham, T.K., Karunakaran, E., *et al.* (2012). An insight into iTRAQ: where do we stand now? *Analytical and Bioanalytical Chemistry* 404, 1011-1027.

Fan, J., Andre, C., and Xu, C. (2011). A chloroplast pathway for the de novo biosynthesis of triacylglycerol in *Chlamydomonas reinhardtii*. *Febs Letters* 585, 1985-1991.

Fidalgo, J.P., Cid, A., Torres, E., Sukenik, A., and Herrero, C. (1998). Effects of nitrogen source and growth phase on proximate biochemical composition, lipid classes and fatty acid profile of the marine microalga *Isochrysis galbana*. *Aquaculture* 166, 105-116.

Fjerbaek, L., Christensen, K.V., and Norddahl, B. (2009). A review of the current state of biodiesel production using enzymatic transesterification. *Biotechnology and Bioengineering* 102, 1298-1315.

Flowers, J.M., Hazzouri, K.M., Pham, G.M., Rosas, U., Bahmani, T., Khraiwesh, B., Nelson, D.R., Jijakli, K., Abdrabu, R., Harris, E.H., *et al.* (2015). Whole-Genome Resequencing Reveals Extensive Natural Variation in the Model Green Alga *Chlamydomonas reinhardtii*. *The Plant Cell* 27, 2353-2369.

Foy, R.H., and Smith, R.V. (1980). The role of carbohydrate accumulation in the growth of planktonic *Oscillatoria* species. *British Phycological Journal* 15, 139-150.

Fu, X.-h., Gao, Y.-f., Hao, S.-j., Zhang, B.-s., and Ren, D.-m. (2007). Knockout of *aroL* gene in *Escherichia coli* Top10F' and its effects on the shikimic acid biosynthesis. *Fudan Xuebao Ziranxueban* 46, 366-370.

Fuller, H., and Morris, G. (2012). Quantitative proteomics using iTRAQ labeling and mass spectrometry. *Integrative Proteomics Croatia: InTech*, 347-362.

Gallagher, B.J. (2011). The economics of producing biodiesel from algae. *Renewable Energy* 36, 158-162.

Gan, C.S., Chong, P.K., Pham, T.K., and Wright, P.C. (2007). Technical, experimental, and biological variations in isobaric tags for relative and absolute quantitation (iTRAQ). *Journal of Proteome Research* 6, 821-827.

Gao, C., Xiong, W., Zhang, Y., Yuan, W., and Wu, Q. (2008). Rapid quantitation of lipid in microalgae by time-domain nuclear magnetic resonance. *Journal of Microbiological Methods* 75, 437-440.

Gao, Y., Lim, T.K., Lin, Q., and Li, S.F.Y. (in press). Identification of cypermethrin induced protein changes in green algae by iTRAQ quantitative proteomics. *Journal of Proteomics*.

Ghosh, D., and Xu, J. (2014). Abiotic stress responses in plant roots: a proteomics perspective. *Frontiers in Plant Science* 5, 6.

Gilmour, D.J., Hipkins, M.F., Webber, A.N., Baker, N.R., and Boney, A.D. (1985). The Effect of Ionic Stress on Photosynthesis in *Dunaliella tertiolecta* - Chlorophyll Fluorescence Kinetics and Spectral Characteristics. *Planta* 163, 250-256.

Ginzburg, M., and Ginzburg, B.Z. (1981). Interrelationships of light, temperature, sodium chloride and carbon source in growth of halotolerant and halophilic strains of *Dunaliella*. *British Phycological Journal* 16, 313-324.

Giroud, C., Gerber, A., and Eichenberger, W. (1988). Lipids of *Chlamydomonas reinhardtii*. Analysis of Molecular Species and Intracellular Site(s) of Biosynthesis. *Plant and Cell Physiology* 29, 587-595.

Go, S., Lee, S.-J., Jeong, G.-T., and Kim, S.-K. (2012). Factors affecting the growth and the oil accumulation of marine microalgae, *Tetraselmis suecica*. *Bioprocess and Biosystems Engineering* 35, 145-150.

Goho, S., and Bell, G. (2000). Mild environmental stress elicits mutations affecting fitness in *Chlamydomonas*. *Proceedings of the Royal Society B: Biological Sciences* 267, 123-129.

Goldemberg, J. (2007). Ethanol for a sustainable energy future. *Science* 315, 808-810.

Goldman, J.C. (1977). Temperature effects on phytoplankton growth in continuous culture. *Limnology and Oceanography* 22, 932-936.

Gouveia, L., and Oliveira, A.C. (2009). Microalgae as a raw material for biofuels production. *Journal of Industrial Microbiology & Biotechnology* 36, 269-274.

Goyal, A. (2007). Osmoregulation in *Dunaliella*, Part II: Photosynthesis and starch contribute carbon for glycerol synthesis during a salt stress in *Dunaliella tertiolecta*. *Plant Physiology and Biochemistry* 45, 705-710.

Griffin, N.M., Yu, J., Long, F., Oh, P., Shore, S., Li, Y., Koziol, J.A., and Schnitzer, J.E. (2010). Label-free, normalized quantification of complex mass spectrometry data for proteomic analysis. *Nat Biotech* 28, 83-89.

Griffiths, M.J., Garcin, C., van Hille, R.P., and Harrison, S.T.L. (2011). Interference by pigment in the estimation of microalgal biomass concentration by optical density. *Journal of Microbiological Methods* 85, 119-123.

Griffiths, M.J., and Harrison, S.T.L. (2009). Lipid productivity as a key characteristic for choosing algal species for biodiesel production. *Journal of Applied Phycology* 21, 493-507.

Grossman, A.R., Harris, E.E., Hauser, C., Lefebvre, P.A., Martinez, D., Rokhsar, D., Shrager, J., Silflow, C.D., Stern, D., Vallon, O., *et al.* (2003). *Chlamydomonas reinhardtii* at the crossroads of genomics. *Eukaryot Cell* 2, 1137-1150.

Gu, Q., David, F., Lynen, F., Vanormelingen, P., Vyverman, W., Rumpel, K., Xu, G., and Sandra, P. (2011). Evaluation of ionic liquid stationary phases for one dimensional gas chromatography–mass spectrometry and comprehensive two dimensional gas chromatographic analyses of fatty acids in marine biota. *Journal of Chromatography A* 1218, 3056-3063.

Guarnieri, M.T., Nag, A., Smolinski, S.L., Darzins, A., Seibert, M., and Pienkos, P.T. (2011). Examination of Triacylglycerol Biosynthetic Pathways via De Novo Transcriptomic and Proteomic Analyses in an Unsequenced Microalga. *PLoS ONE* 6.

Guarnieri, M.T., Nag, A., Yang, S., and Pienkos, P.T. (2013). Proteomic analysis of *Chlorella vulgaris*: Potential targets for enhanced lipid accumulation. *Journal of Proteomics* 93, 245-253.

Guo, L., Devaiah, S.P., Narasimhan, R., Pan, X., Zhang, Y., Zhang, W., and Wang, X. (2012). Cytosolic Glyceraldehyde-3-Phosphate Dehydrogenases Interact with Phospholipase D $\delta$  to Transduce Hydrogen Peroxide Signals in the Arabidopsis Response to Stress. *The Plant Cell* *24*, 2200-2212.

Guschina, I.A., and Harwood, J.L. (2006). Lipids and lipid metabolism in eukaryotic algae. *Progress in Lipid Research* *45*, 160-186.

Haghjou, M.M., and Shariati, M. (2007). Photosynthesis and Respiration under Low Temperature Stress in Two *Dunaliella* Strains. *World Applied Sciences Journal* *2*, 276-282.

Hamm, C.E., and Rousseau, V. (2003). Composition, assimilation and degradation of *Phaeocystis globosa*-derived fatty acids in the North Sea. *Journal of Sea Research* *50*, 271-283.

Harris, E.H. (2001). *Chlamydomonas* as a model organism. *Annual Review of Plant Physiology and Plant Molecular Biology* *52*, 363-406.

Harris, E.H., Stern, D.B., and Witman, G.B. (2009). *The Chlamydomonas Sourcebook* (Second Edition) (Academic Press).

Harris, R.V., and James, A.T. (1965). Linoleic ,  $\alpha$ -linolenic acid biosynthesis in plant leaves and a green alga. *Biochimica et Biophysica Acta (BBA) - Lipids and Lipid Metabolism* *106*, 456-464.

Harwood, J.L., and Guschina, I.A. (2009). The versatility of algae and their lipid metabolism. *Biochimie* *91*, 679-684.

He, Q., Qiao, D., Bai, L., Zhang, Q., Yang, W., Li, Q., and Cao, Y. (2007). Cloning and characterization of a plastidic glycerol 3-phosphate dehydrogenase cDNA from *Dunaliella salina*. *J Plant Physiol* *164*.

Hessen, D.O., Van Donk, E., and Andersen, T. (1995). Growth responses, P-uptake and loss of flagellae in *Chlamydomonas reinhardtii* exposed to UV-B. *Journal of Plankton Research* *17*, 17-27.

Himmel, M.E., Ding, S.Y., Johnson, D.K., Adney, W.S., Nimlos, M.R., Brady, J.W., and Foust, T.D. (2007). Biomass recalcitrance: Engineering plants and enzymes for biofuels production. *Science* *315*, 804-807.

Ho, S.H., Nakanishi, A., Ye, X.T., Chang, J.S., Hara, K., Hasunuma, T., and Kondo, A. (2014). Optimizing biodiesel production in marine *Chlamydomonas* sp JSC4 through metabolic profiling and an innovative salinity-gradient strategy. *Biotechnology for Biofuels* *7*.

Hoham, R.W. (1975). Optimum temperatures and temperature ranges for growth of snow algae. *Arctic and Alpine Research* 7, 13-24.

Hohner, R., Barth, J., Magneschi, L., Jaeger, D., Niehues, A., Bald, T., Grossman, A., Fufezan, C., and Hippler, M. (2013). The Metabolic Status Drives Acclimation of Iron Deficiency Responses in *Chlamydomonas reinhardtii* as Revealed by Proteomics Based Hierarchical Clustering and Reverse Genetics. *Molecular & Cellular Proteomics* 12, 2774-2790.

Hounslow, E., Kapoore, R.V., Vaidyanathan, S., Gilmour, D.J., and Wright, P.C. (2016a). The Search for a Lipid Trigger: The Effect of Salt Stress on the Lipid Profile of the Model Microalgal Species *Chlamydomonas reinhardtii* for Biofuels Production. *Current Biotechnology* 5, 1-9.

Hounslow, E., Noirel, J., Gilmour, D.J., and Wright, P.C. (2016b). Lipid quantification techniques for screening oleaginous species of microalgae for biofuel production. *European Journal of Lipid Science and Technology*, n/a-n/a.

Hsieh, S.I., Castruita, M., Malasarn, D., Urzica, E., Erde, J., Page, M.D., Yamasaki, H., Casero, D., Pellegrini, M., Merchant, S.S., *et al.* (2013). The Proteome of Copper, Iron, Zinc, and Manganese Micronutrient Deficiency in *Chlamydomonas reinhardtii*. *Molecular & Cellular Proteomics* 12, 65-86.

Hu, J., Jin, L., Wang, X., Cai, W., Liu, Y., and Wang, G. (2014). Response of photosynthetic systems to salinity stress in the desert cyanobacterium *Scytonema javanicum*. *Advances in Space Research* 53, 30-36.

Hu, Q., Sommerfeld, M., Jarvis, E., Ghirardi, M., Posewitz, M., Seibert, M., and Darzins, A. (2008). Microalgal triacylglycerols as feedstocks for biofuel production: perspectives and advances. *Plant Journal* 54, 621-639.

Huang, L.-F., Lin, J.-Y., Pan, K.-Y., Huang, C.-K., and Chu, Y.-K. (2015). Overexpressing Ferredoxins in *Chlamydomonas reinhardtii* Increase Starch and Oil Yields and Enhance Electric Power Production in a Photo Microbial Fuel Cell. *International Journal of Molecular Sciences* 16, 19308-19325.

Inouye, L.S., and Lotufo, G.R. (2006). Comparison of macro-gravimetric and micro-colorimetric lipid determination methods. *Talanta* 70, 584-587.

Islam, M.A., Ayoko, G.A., Brown, R., Stuart, D., and Heimann, K. (2013). Influence of Fatty Acid Structure on Fuel Properties of Algae Derived Biodiesel. *Procedia Engineering* 56, 591-596.

Jain, M., Mathur, G., Koul, S., and Sarin, N. (2001). Ameliorative effects of proline on salt stress-induced lipid peroxidation in cell lines of groundnut (*Arachis hypogaea* L.). *Plant Cell Reports* 20, 463-468.

James, G.O., Hocart, C.H., Hillier, W., Chen, H.C., Kordbacheh, F., Price, G.D., and Djordjevic, M.A. (2011). Fatty acid profiling of *Chlamydomonas reinhardtii* under nitrogen deprivation. *Bioresource Technology* 102, 3343-3351.

James, G.O., Hocart, C.H., Hillier, W., Price, G.D., and Djordjevic, M.A. (2013). Temperature modulation of fatty acid profiles for biofuel production in nitrogen deprived *Chlamydomonas reinhardtii*. *Bioresource Technology* 127, 441-447.

Jayanta, T., Chandra, K.M., and Chandra, G.B. (2012). Growth, total lipid content and fatty acid profile of a native strain of the freshwater oleaginous microalgae *Ankistrodesmus falcatus* (Ralf) grown under salt stress condition. *International Research Journal of Biological Sciences* 1, 27-35.

Jeong, M.-J., Park, S.-C., and Byun, M.-O. (2001). Improvement of salt tolerance in transgenic potato plants by glyceraldehyde-3 phosphate dehydrogenase gene transfer. *Molecules & Cells* 12.

Jiang, Y., and Chen, F. (1999). Effects of salinity on cell growth and docosahexaenoic acid content of the heterotrophic marine microalga *Cryptocodinium cohnii*. *Journal of Industrial Microbiology & Biotechnology* 23, 508-513.

Jiang, Y., and Deyholos, M.K. (2006). Comprehensive transcriptional profiling of NaCl-stressed *Arabidopsis* roots reveals novel classes of responsive genes. *BMC Plant Biology* 6, 1-20.

Jiménez, C., Cossi, amp, x, o, B.R., and Niell, F.X. (2003). Relationship between physicochemical variables and productivity in open ponds for the production of *Spirulina*: a predictive model of algal yield. *Aquaculture* 221, 331-345.

Johnson, X., and Alric, J. (2013). Central Carbon Metabolism and Electron Transport in *Chlamydomonas reinhardtii*: Metabolic Constraints for Carbon Partitioning between Oil and Starch. *Eukaryotic Cell* 12, 776-793.

Jorquera, O., Kiperstok, A., Sales, E.A., Embirucu, M., and Ghirardi, M.L. (2010). Comparative energy life-cycle analyses of microalgal biomass production in open ponds and photobioreactors. *Bioresource Technology* 101, 1406-1413.

Kan, G.-F., Miao, J.-L., Shi, C.-J., and Li, G.-Y. (2006). Proteomic Alterations of Antarctic Ice Microalga *Chlamydomonas* sp. Under Low-Temperature Stress. *Journal of Integrative Plant Biology* 48, 965-970.

Kang, M.J., Shin, M.S., Park, J.N., and Lee, S.S. (2005). The effects of polyunsaturated:saturated fatty acids ratios and peroxidisability index values of dietary fats on serum lipid profiles and hepatic enzyme activities in rats. *British Journal of Nutrition* 94, 526-532.

Kaplan, D., Christiaen, D., and Arad, S.M. (1987). Chelating Properties of Extracellular Polysaccharides from *Chlorella* Spp. *Applied and Environmental Microbiology* *53*, 2953-2956.

Karp, N.A., Huber, W., Sadowski, P.G., Charles, P.D., Hester, S.V., and Lilley, K.S. (2010). Addressing Accuracy and Precision Issues in iTRAQ Quantitation. *Molecular & Cellular Proteomics* *9*, 1885-1897.

Khozin-Goldberg, I., and Cohen, Z. (2006). The effect of phosphate starvation on the lipid and fatty acid composition of the fresh water eustigmatophyte *Monodus subterraneus*. *Phytochemistry* *67*, 696-701.

Kim, B.-H., Ramanan, R., Kang, Z., Cho, D.-H., Oh, H.-M., and Kim, H.-S. (2016a). *Chlorella sorokiniana* HS1, a novel freshwater green algal strain, grows and hyperaccumulates lipid droplets in seawater salinity. *Biomass and Bioenergy* *85*, 300-305.

Kim, G., Lee, C.H., and Lee, K. (2016b). Enhancement of lipid production in marine microalga *Tetraselmis* sp through salinity variation. *Korean Journal of Chemical Engineering* *33*, 230-237.

Kim, M.D., Han, K.C., Kang, H.A., Rhee, S.K., and Seo, J.H. (2003). Coexpression of BiP increased antithrombotic hirudin production in recombinant *Sacchdromyces cerevisiae*. *J Biotechnol* *101*, 81-87.

Kitano, H. (2002). *Systems Biology: A Brief Overview*. *Science* *295*, 1662-1664.

Klok, A.J., Martens, D.E., Wijffels, R.H., and Lamers, P.P. (2013). Simultaneous growth and neutral lipid accumulation in microalgae. *Bioresource Technology* *134*, 233-243.

Knothe, G. (2005). Dependence of biodiesel fuel properties on the structure of fatty acid alkyl esters. *Fuel Processing Technology* *86*, 1059-1070.

Knothe, G. (2008). "Designer" biodiesel: Optimizing fatty ester (composition to improve fuel properties. *Energy & Fuels* *22*, 1358-1364.

Knothe, G. (2009). Improving biodiesel fuel properties by modifying fatty ester composition. *Energy & Environmental Science* *2*, 759-766.

Kong, Q.-x., Li, L., Martinez, B., Chen, P., and Ruan, R. (2010). Culture of Microalgae *Chlamydomonas reinhardtii* in Wastewater for Biomass Feedstock Production. *Applied Biochemistry and Biotechnology* *160*, 9-18.

Kovacevic, V., and Wesseler, J. (2010). Cost-effectiveness analysis of algae energy production in the EU. *Energy Policy* *38*, 5749-5757.

Kumari, P., Reddy, C.R.K., and Jha, B. (2011). Comparative evaluation and selection of a method for lipid and fatty acid extraction from macroalgae. *Analytical Biochemistry* *415*, 134-144.

Lachapelle, J., and Bell, G. (2012). Evolutionary Rescue of Sexual and Asexual Populations in a Deteriorating Environment. *Evolution* *66*, 3508-3518.

Laureillard, J., Largeau, C., and Casadevall, E. (1988). Oleic acid in the biosynthesis of the resistant biopolymers of *Botryococcus braunii*. *Phytochemistry* *27*, 2095-2098.

Laurens, L., Quinn, M., Van Wychen, S., Templeton, D., and Wolfrum, E. (2012). Accurate and reliable quantification of total microalgal fuel potential as fatty acid methyl esters by *in situ* transesterification. *Analytical and Bioanalytical Chemistry* *403*, 167-178.

Lee, B., Choi, G.G., Choi, Y.E., Sung, M., Park, M.S., and Yang, J.W. (2014). Enhancement of lipid productivity by ethyl methane sulfonate-mediated random mutagenesis and proteomic analysis in *Chlamydomonas reinhardtii*. *Korean Journal of Chemical Engineering* *31*, 1036-1042.

Lee, D.Y., Park, J.J., Barupal, D.K., and Fiehn, O. (2012). System Response of Metabolic Networks in *Chlamydomonas reinhardtii* to Total Available Ammonium. *Molecular & Cellular Proteomics* *11*, 973-988.

Lee, Y.-K., Tan, H.-M., and Low, C.-S. (1989). Effect of salinity of medium on cellular fatty acid composition of marine alga *Porphyridium cruentum* (Rhodophyceae). *Journal of Applied Phycology* *1*, 19-23.

Leite, G.B., Abdelaziz, A.E.M., and Hallenbeck, P.C. (2013). Algal biofuels: Challenges and opportunities. *Bioresource Technology* *145*, 134-141.

Leon-Banares, R., Gonzalez-Ballester, D., Galvan, A., and Fernandez, E. (2004). Transgenic microalgae as green cell-factories. *Trends in Biotechnology* *22*, 45-52.

Leon, R., and Galvan, F. (1994). Halotolerance studies on *Chlamydomonas reinhardtii* glycerol excretion by free and immobilized cells. *Journal of Applied Phycology* *6*, 13-20.

León, R., and Galván, F. (1999). Interaction between saline stress and photoinhibition of photosynthesis in the freshwater green algae *Chlamydomonas reinhardtii*. Implications for glycerol photoproduction. *Plant Physiology and Biochemistry* *37*, 623-628.

Lewin, R.A. (1956). Extracellular Polysaccharides of Green Algae. *Canadian Journal of Microbiology* *2*, 665-672.

Li, P., and Lin, J. (2012). Effect of ultraviolet radiation on photosynthesis, biomass, and fatty acid content and profile of a *Scenedesmus rubescens*-like microalga. *Bioresource Technology* *111*, 316-322.

Li, X., Xu, H., and Wu, Q. (2007). Large-scale biodiesel production from microalga *Chlorella protothecoides* through heterotrophic cultivation in bioreactors. *Biotechnology and Bioengineering* *98*, 764-771.

Li, Y., Fei, X., and Deng, X. (2012). Novel molecular insights into nitrogen starvation-induced triacylglycerols accumulation revealed by differential gene expression analysis in green algae *Micractinium pusillum*. *Biomass and Bioenergy* *42*, 199-211.

Li, Y., Han, D., Sommerfeld, M., and Hu, Q. (2011). Photosynthetic carbon partitioning and lipid production in the oleaginous microalga *Pseudochlorococum* sp. (Chlorophyceae) under nitrogen-limited conditions. *Bioresource Technology* *102*, 123-129.

Li, Y., Han, F., Xu, H., Mu, J., Chen, D., Feng, B., and Zeng, H. (2014). Potential lipid accumulation and growth characteristic of the green alga *Chlorella* with combination cultivation mode of nitrogen (N) and phosphorus (P). *Bioresource Technology* *174*, 24-32.

Li, Y., Horsman, M., Wang, B., Wu, N., and Lan, C. (2008a). Effects of nitrogen sources on cell growth and lipid accumulation of green alga *Neochloris oleoabundans*. *Applied Microbiology and Biotechnology* *81*, 629-636.

Li, Y., Horsman, M., Wu, N., Lan, C.Q., and Dubois-Calero, N. (2008b). Biofuels from microalgae. *Biotechnology Progress* *24*, 815-820.

Li, Y.T., Han, D.X., Hu, G.R., Dauvillee, D., Sommerfeld, M., Ball, S., and Hua, Q. (2010a). *Chlamydomonas* starchless mutant defective in ADP-glucose pyrophosphorylase hyper-accumulates triacylglycerol. *Metabolic Engineering* *12*, 387-391.

Li, Y.T., Han, D.X., Hu, G.R., Sommerfeld, M., and Hu, Q.A. (2010b). Inhibition of Starch Synthesis Results in Overproduction of Lipids in *Chlamydomonas reinhardtii*. *Biotechnology and Bioengineering* *107*, 258-268.

Liang, Y., Sarkany, N., and Cui, Y. (2009). Biomass and lipid productivities of *Chlorella vulgaris* under autotrophic, heterotrophic and mixotrophic growth conditions. *Biotechnology Letters* *31*, 1043-1049.

Liska, A.J., Shevchenko, A., Pick, U., and Katz, A. (2004). Enhanced photosynthesis and redox energy production contribute to salinity tolerance in *Dunaliella* as revealed by homology-based proteomics. *Plant Physiology* *136*, 2806-2817.

Liu, J., Huang, J., Sun, Z., Zhong, Y., Jiang, Y., and Chen, F. (2011). Differential lipid and fatty acid profiles of photoautotrophic and heterotrophic *Chlorella zofingiensis*: Assessment of algal oils for biodiesel production. *Bioresource Technology* *102*, 106-110.

Lombardi, A.T., Vieira, A.A.H., and Sartori, L.A. (2002). Mucilaginous capsule adsorption and intracellular uptake of copper by *Kirchneriella aperta* (Chlorococcales). *Journal of Phycology* *38*, 332-337.

Longworth, J., Noirel, J., Pandhal, J., Wright, P.C., and Vaidyanathan, S. (2012). HILIC- and SCX-Based Quantitative Proteomics of *Chlamydomonas reinhardtii* during Nitrogen Starvation Induced Lipid and Carbohydrate Accumulation. *Journal of Proteome Research* *11*, 5959-5971.

López-Sandoval, D.C., Rodríguez-Ramos, T., Cermeño, P., Sobrino, C., and Marañón, E. (2014). Photosynthesis and respiration in marine phytoplankton: Relationship with cell size, taxonomic affiliation, and growth phase. *Journal of Experimental Marine Biology and Ecology* *457*, 151-159.

Lu, N., Wei, D., Chen, F., and Yang, S.-T. (2012a). Lipidomic profiling and discovery of lipid biomarkers in snow alga *Chlamydomonas nivalis* under salt stress. *European Journal of Lipid Science and Technology* *114*, 253-265.

Lu, N., Wei, D., Chen, F., and Yang, S.T. (2013). Lipidomic profiling reveals lipid regulation in the snow alga *Chlamydomonas nivalis* in response to nitrate or phosphate deprivation. *Process Biochemistry* *48*, 605-613.

Lu, N., Wei, D., Jiang, X.-L., Chen, F., and Yang, S.-T. (2012b). Fatty acids profiling and biomarker identification in snow alga *Chlamydomonas nivalis* by NaCl stress using GC/MS and multivariate statistical analysis. *Analytical Letters* *45*, 1172-1183.

Lu, N., Wei, D., Jiang, X.-L., Chen, F., and Yang, S.-T. (2012c). Regulation of lipid metabolism in the snow alga *Chlamydomonas nivalis* in response to NaCl stress: An integrated analysis by cytomic and lipidomic approaches. *Process Biochemistry* *47*, 1163-1170.

Lukes, M., Prochazkova, L., Shmidt, V., Nedbalova, L., and Kaftan, D. (2014). Temperature dependence of photosynthesis and thylakoid lipid composition in the red snow alga *Chlamydomonas cf. nivalis* (Chlorophyceae). *Fems Microbiology Ecology* *89*, 303-315.

Lv, H., Qu, G., Qi, X., Lu, L., Tian, C., and Ma, Y. (2013). Transcriptome analysis of *Chlamydomonas reinhardtii* during the process of lipid accumulation. *Genomics* *101*, 229-237.

Lv, J.-M., Cheng, L.-H., Xu, X.-H., Zhang, L., and Chen, H.-L. (2010). Enhanced lipid production of *Chlorella vulgaris* by adjustment of cultivation conditions. *Bioresource Technology* *101*, 6797-6804.

Macedougall, K.M., McNichol, J., McGinn, P.J., O'Leary, S.J., and Melanson, J.E. (2011). Triacylglycerol profiling of microalgae strains for biofuel feedstock by liquid chromatography-high-resolution mass spectrometry. *Analytical and Bioanalytical Chemistry*.

MacKinney, G. (1941). Absorption of light by chlorophyll solutions. *Journal of Biological Chemistry* *140*, 315-322.

Masojídek, J., Torzillo, G., Kopecký, J., Koblížek, M., Nidiaci, L., Komenda, J., Lukavská, A., and Sacchi, A. (2000). Changes in chlorophyll fluorescence quenching and pigment composition in the green alga *Chlorococcum* sp. grown under nitrogen deficiency and salinity stress. *Journal of Applied Phycology* *12*, 417-426.

Mastrobuoni, G., Irgang, S., Pietzke, M., ASZmus, H., Wenzel, M., Schulze, W., and Kempa, S. (2012). Proteome dynamics and early salt stress response of the photosynthetic organism *Chlamydomonas reinhardtii*. *BMC Genomics* *13*, 215.

McLachlan, J. (1961). The Effect of Salinity on Growth and Chlorophyll Content in Representative Classes of Unicellular Marine Algae. *Canadian Journal of Microbiology* *7*, 399-406.

Merchant, S.S., Kropat, J., Liu, B., Shaw, J., and Warakanont, J. (2012). TAG, You're it! *Chlamydomonas* as a reference organism for understanding algal triacylglycerol accumulation. *Current Opinion in Biotechnology* *23*, 352-363.

Meurant, G. (1984). *Fatty Acid Metabolism and its Regulation* (Elsevier Science).

Michalski, A., Damoc, E., Hauschild, J.-P., Lange, O., Wiegand, A., Makarov, A., Nagaraj, N., Cox, J., Mann, M., and Horning, S. (2011). Mass Spectrometry-based Proteomics Using Q Exactive, a High-performance Benchtop Quadrupole Orbitrap Mass Spectrometer. *Molecular & cellular proteomics : MCP* *10*, M111.011015.

Miller, R., Wu, G., Deshpande, R.R., Vieler, A., Gaertner, K., Li, X., Moellering, E.R., Zaeuner, S., Cornish, A.J., Liu, B., *et al.* (2010). Changes in Transcript Abundance in *Chlamydomonas reinhardtii* following Nitrogen Deprivation Predict Diversion of Metabolism. *Plant Physiology* *154*, 1737-1752.

Mizoguchi, H., and Hara, S. (1996). Effect of fatty acid saturation in membrane lipid bilayers on simple diffusion in the presence of ethanol at high concentrations. *Journal of Fermentation and Bioengineering* *81*, 406-411.

Moellering, E.R., and Benning, C. (2010). RNA Interference Silencing of a Major Lipid Droplet Protein Affects Lipid Droplet Size in *Chlamydomonas reinhardtii*. *Eukaryotic Cell* *9*, 97-106.

Mohammed, S., and Heck, A.J.R. (2011). Strong cation exchange (SCX) based analytical methods for the targeted analysis of protein post-translational modifications. *Current Opinion in Biotechnology* 22, 9-16.

Moheimani, N.R., and Borowitzka, M.A. (2007). Limits to productivity of the alga *Pleurochrysis carterae* (Haptophyta) grown in outdoor raceway ponds. *Biotechnology and Bioengineering* 96, 27-36.

Mohr, A., and Raman, S. (2013). Lessons from first generation biofuels and implications for the sustainability appraisal of second generation biofuels. *Energy Policy* 63, 114-122.

Moon, M., Kim, C.W., Park, W.-K., Yoo, G., Choi, Y.-E., and Yang, J.-W. (2013). Mixotrophic growth with acetate or volatile fatty acids maximizes growth and lipid production in *Chlamydomonas reinhardtii*. *Algal Research* 2, 352-357.

Mráček, T., Drahota, Z., and Houštěk, J. (2013). The function and the role of the mitochondrial glycerol-3-phosphate dehydrogenase in mammalian tissues. *Biochimica et Biophysica Acta (BBA)-Bioenergetics* 1827, 401-410.

Msanne, J., Xu, D., Konda, A.R., Casas-Mollano, J.A., Awada, T., Cahoon, E.B., and Cerutti, H. (2012). Metabolic and gene expression changes triggered by nitrogen deprivation in the photoautotrophically grown microalgae *Chlamydomonas reinhardtii* and *Coccomyxa* sp. C-169. *Phytochemistry* 75.

Muhlhaus, T., Weiss, J., Hemme, D., Sommer, F., and Schroda, M. (2011). Quantitative shotgun proteomics using a uniform <sup>5</sup>N-labeled standard to monitor proteome dynamics in time course experiments reveals new insights into the heat stress response of *Chlamydomonas reinhardtii*. *Molecular & cellular proteomics : MCP* 10, M110.004739-M004110.004739.

Mühlroth, A., Li, K., Røkke, G., Winge, P., Olsen, Y., Hohmann-Marriott, M.F., Vadstein, O., and Bones, A.M. (2013). Pathways of Lipid Metabolism in Marine Algae, Co-Expression Network, Bottlenecks and Candidate Genes for Enhanced Production of EPA and DHA in Species of Chromista. *Marine Drugs* 11, 4662-4697.

Muñoz-Blanco, J., and Cardenas, J. (1989). Changes in glutamate dehydrogenase activity of *Chlamydomonas reinhardtii* under different trophic and stress conditions. *Plant, Cell & Environment* 12, 173-182.

Murata, N., Takahashi, S., Nishiyama, Y., and Allakhverdiev, S.I. (2007). Photoinhibition of photosystem II under environmental stress. *Biochimica et Biophysica Acta (BBA) - Bioenergetics* 1767, 414-421.

Myklestad, S.M. (1995). Release of Extracellular Products by Phytoplankton with Special Emphasis on Polysaccharides. *Science of the Total Environment* 165, 155-164.

Nagalakshmi, N., and Prasad, M.N.V. (1998). Copper-induced oxidative stress in *Scenedesmus bijugatus*: Protective role of free radical scavengers. *Bulletin of Environmental Contamination and Toxicology* 61, 623-628.

Ndimba, B.K., Ndimba, R.J., Johnson, T.S., Waditee-Sirisattha, R., Baba, M., Sirisattha, S., Shiraiwa, Y., Agrawal, G.K., and Rakwal, R. (2013). Biofuels as a sustainable energy source: An update of the applications of proteomics in bioenergy crops and algae. *Journal of Proteomics* 93, 234-244.

Neale, P.J., and Melis, A. (1989). Salinity-stress Enhances Photoinhibition of Photosynthesis in *Chlamydomonas reinhardtii*. *J Plant Physiol* 134, 619-622.

Neelam, S., and Subramanyam, R. (2013). Alteration of photochemistry and protein degradation of photosystem II from *Chlamydomonas reinhardtii* under high salt grown cells. *Journal of Photochemistry and Photobiology B: Biology* 124, 63-70.

Nguyen, H.M., Baudet, M., Cuine, S., Adriano, J.-M., Barthe, D., Billon, E., Bruley, C., Beisson, F., Peltier, G., Ferro, M., *et al.* (2011). Proteomic profiling of oil bodies isolated from the unicellular green microalga *Chlamydomonas reinhardtii*: With focus on proteins involved in lipid metabolism. *Proteomics* 11, 4266-4273.

Nogueira, F.C.S., Palmisano, G., Schwammle, V., Campos, F.A.P., Larsen, M.R., Domont, G.B., and Roepstorff, P. (2012). Performance of Isobaric and Isotopic Labeling in Quantitative Plant Proteomics. *Journal of Proteome Research* 11, 3046-3052.

Ohnishi, N., Mukherjee, B., Tsujikawa, T., Yanase, M., Nakano, H., Moroney, J.V., and Fukuzawa, H. (2010). Expression of a Low CO<sub>2</sub>-Inducible Protein, LCI1, Increases Inorganic Carbon Uptake in the Green Alga *Chlamydomonas reinhardtii*. *The Plant Cell* 22, 3105-3117.

Olsen, J.V., Ong, S.E., and Mann, M. (2004). Trypsin cleaves exclusively C-terminal to arginine and lysine residues. *Molecular & Cellular Proteomics* 3, 608-614.

Oncel, S.S. (2013). Microalgae for a macroenergy world. *Renewable & Sustainable Energy Reviews* 26, 241-264.

Ong, S.-E., Blagoev, B., Kratchmarova, I., Kristensen, D.B., Steen, H., Pandey, A., and Mann, M. (2002). Stable Isotope Labeling by Amino Acids in Cell Culture, SILAC, as a Simple and Accurate Approach to Expression Proteomics. *Molecular & Cellular Proteomics* 1, 376-386.

Ong, S.-E., and Mann, M. (2005). Mass spectrometry–based proteomics turns quantitative. *Nature chemical biology* *1*, 252-262.

Ow, S.Y., Salim, M., Noirel, J., Evans, C., Rehman, I., and Wright, P.C. (2009). iTRAQ Underestimation in Simple and Complex Mixtures: "The Good, the Bad and the Ugly". *Journal of Proteome Research* *8*, 5347-5355.

Ow, S.Y., Salim, M., Noirel, J., Evans, C., and Wright, P.C. (2011). Minimising iTRAQ ratio compression through understanding LC-MS elution dependence and high-resolution HILIC fractionation. *Proteomics* *11*, 2341-2346.

Pal, D., Khozin-Goldberg, I., Cohen, Z., and Boussiba, S. (2011). The effect of light, salinity, and nitrogen availability on lipid production by *Nannochloropsis* sp. *Applied Microbiology and Biotechnology* *90*, 1429-1441.

Palmisano, A.C., and Sullivan, C.W. (1982). PHYSIOLOGY OF SEA ICE DIATOMS .1. RESPONSE OF 3 POLAR DIATOMS TO A SIMULATED SUMMER-WINTER TRANSITION. *Journal of Phycology* *18*, 489-498.

Pandhal, J., Snijders, A.P.L., Wright, P.C., and Biggs, C.A. (2008). A cross-species quantitative proteomic study of salt adaptation in a halotolerant environmental isolate using (15)N metabolic labelling. *Proteomics* *8*, 2266-2284.

Pastore, D., Trono, D., Laus, M.N., Di Fonzo, N., and Flagella, Z. (2007). Possible plant mitochondria involvement in cell adaptation to drought stress: A case study: durum wheat mitochondria. *Journal of Experimental Botany* *58*, 195-210.

Paulsen, B.S., and Vieira, A.A.H. (1994). Structure of the Capsular and Extracellular Polysaccharides Produced by the Desmid *Spondylosium panduriforma* (Chlorophyta). *Journal of Phycology* *30*, 638-641.

Pedranzani, H., Racagni, G., Alemano, S., Miersch, O., Ramírez, I., Peña-Cortés, H., Taleisnik, E., Machado-Domenech, E., and Abdala, G. (2003). Salt tolerant tomato plants show increased levels of jasmonic acid. *Plant Growth Regulation* *41*, 149-158.

Pereira-Medrano, A.G., Margesin, R., and Wright, P.C. (2012). Proteome characterization of the unsequenced psychrophile *Pedobacter cryoconitis* using 15N metabolic labeling, tandem mass spectrometry, and a new bioinformatic workflow. *Proteomics* *12*, 775-789.

Pérez-Pérez, M.E., Lemaire, S.D., and Crespo, J.L. (2012). Reactive oxygen species and autophagy in plants and algae. *Plant Physiol* *160*.

Perrine, Z., Negi, S., and Sayre, R.T. (2012). Optimization of photosynthetic light energy utilization by microalgae. *Algal Research* *1*, 134-142.

Perrineau, M.M., Zelzion, E., Gross, J., Price, D.C., Boyd, J., and Bhattacharya, D. (2014). Evolution of salt tolerance in a laboratory reared population of *Chlamydomonas reinhardtii*. *Environ Microbiol* *16*, 1755-1766.

Pfromm, P.H., Amanor-Boadu, V., and Nelson, R. (2011). Sustainability of algae derived biodiesel: A mass balance approach. *Bioresource Technology* *102*, 1185-1193.

Pham, T.K., Roy, S., Noirel, J., Douglas, I., Wright, P.C., and Stafford, G.P. (2010). A quantitative proteomic analysis of biofilm adaptation by the periodontal pathogen *Tannerella forsythia*. *Proteomics* *10*, 3130-3141.

Pichler, P., Köcher, T., Holzmann, J., Mazanek, M., Taus, T., Ammerer, G., and Mechtler, K. (2010). Peptide Labeling with Isobaric Tags Yields Higher Identification Rates Using iTRAQ 4-Plex Compared to TMT 6-Plex and iTRAQ 8-Plex on LTQ Orbitrap. *Analytical Chemistry* *82*, 6549-6558.

Pick, U., and Rachutin-Zalagin, T. (2012). Kinetic anomalies in the interactions of Nile red with microalgae. *Journal of Microbiological Methods* *88*, 189-196.

Piorreck, M., and Pohl, P. (1984). Formation of biomass, total protein, chlorophylls, lipids and fatty acids in green and blue-green algae during one growth phase. *Phytochemistry* *23*, 217-223.

Pittman, J.K., Dean, A.P., and Osundeko, O. (2011). The potential of sustainable algal biofuel production using wastewater resources. *Bioresource Technology* *102*, 17-25.

Pottiez, G., Wiederin, J., Fox, H.S., and Ciborowski, P. (2012). Comparison of 4-plex to 8-plex iTRAQ Quantitative Measurements of Proteins in Human Plasma Samples. *Journal of Proteome Research* *11*, 3774-3781.

Qiang, H., and Richmond, A. (1996). Productivity and photosynthetic efficiency of *Spirulina platensis* as affected by light intensity, algal density and rate of mixing in a flat plate photobioreactor. *Journal of Applied Phycology* *8*, 139-145.

Radakovits, R., Jinkerson, R.E., Darzins, A., and Posewitz, M.C. (2010). Genetic Engineering of Algae for Enhanced Biofuel Production. *Eukaryotic Cell* *9*, 486-501.

Radmer, R., and Kok, B. (1977). Photosynthesis - Limited Yields, Unlimited Dreams. *Bioscience* *27*, 599-605.

Rai, S., Agrawal, C., Shrivastava, A.K., Singh, P.K., and Rai, L.C. (2014). Comparative proteomics unveils cross species variations in *Anabaena* under salt stress. *Journal of Proteomics* *98*, 254-270.

Rao, A.R., Dayananda, C., Sarada, R., Shamala, T.R., and Ravishankar, G.A. (2007). Effect of salinity on growth of green alga *Botryococcus braunii* and its constituents. *Bioresource Technology* *98*, 560-564.

Rasala, B.A., Chao, S.S., Pier, M., Barrera, D.J., and Mayfield, S.P. (2014). Enhanced Genetic Tools for Engineering Multigene Traits into Green Algae. *PLoS ONE* *9*.

Ratcliff, W.C., Herron, M.D., Howell, K., Pentz, J.T., Rosenzweig, F., and Travisano, M. (2013). Experimental evolution of an alternating uni- and multicellular life cycle in *Chlamydomonas reinhardtii*. *Nat Commun* *4*.

Remias, D., Albert, A., and Lütz, C. (2010). Effects of realistically simulated, elevated UV irradiation on photosynthesis and pigment composition of the alpine snow alga *Chlamydomonas nivalis* and the arctic soil alga *Tetracystis* sp (Chlorophyceae). *Photosynthetica* *48*, 269-277.

Remias, D., Lütz-Meindl, U., and Lütz, C. (2005). Photosynthesis, pigments and ultrastructure of the alpine snow alga *Chlamydomonas nivalis*. *European Journal of Phycology* *40*, 259-268.

Remias, D., and Lütz, C. (2007). Characterisation of esterified secondary carotenoids and of their isomers in green algae: a HPLC approach. *Algological Studies* *124*, 85-94.

Renaud, S.M., and Parry, D.L. (1994). Microalgae for use in tropical aquaculture II: Effect of salinity on growth, gross chemical composition and fatty acid composition of three species of marine microalgae. *Journal of Applied Phycology* *6*, 347-356.

Richmond, A. (2004). *Handbook of microalgal culture: biotechnology and applied phycology* (Oxford, UK: Blackwell Science Ltd).

Riekhof, W.R., Sears, B.B., and Benning, C. (2005). Annotation of genes involved in glycerolipid biosynthesis in *Chlamydomonas reinhardtii*: Discovery of the betaine lipid synthase BTA1(Cr). *Eukaryotic Cell* *4*, 242-252.

Rolland, N., Atteia, A., Decottignies, P., Garin, J., Hippler, M., Kreimer, G., Lemaire, S.D., Mittag, M., and Wagner, V. (2009). *Chlamydomonas* proteomics. *Current Opinion in Microbiology* *12*, 285-291.

Ross, P.L., Huang, Y.L.N., Marchese, J.N., Williamson, B., Parker, K., Hattan, S., Khainovski, N., Pillai, S., Dey, S., Daniels, S., *et al.* (2004). Multiplexed protein quantitation in *Saccharomyces cerevisiae* using amine-reactive isobaric tagging reagents. *Molecular & Cellular Proteomics* *3*, 1154-1169.

Rupprecht, J. (2009). From systems biology to fuel-*Chlamydomonas reinhardtii* as a model for a systems biology approach to improve biohydrogen production. *Journal of Biotechnology* *142*, 10-20.

Sadowski, P.G., Dunkley, T.P.J., Shadforth, I.P., Dupree, P., Bessant, C., Griffin, J.L., and Lilley, K.S. (2006). Quantitative proteomic approach to study subcellular localization of membrane proteins. *Nature Protocols* *1*, 1778-1789.

Sakamoto, T., and Murata, N. (2002). Regulation of the desaturation of fatty acids and its role in tolerance to cold and salt stress. *Current Opinion in Microbiology* *5*, 206-210.

Salama, E.-S., Kim, H.-C., Abou-Shanab, R.I., Ji, M.-K., Oh, Y.-K., Kim, S.-H., and Jeon, B.-H. (2013). Biomass, lipid content, and fatty acid composition of freshwater *Chlamydomonas mexicana* and *Scenedesmus obliquus* grown under salt stress. *Bioprocess and Biosystems Engineering* *36*, 827-833.

Samek, O., Jonas, A., Pilat, Z., Zemanek, P., Nedbal, L., Triska, J., Kotas, P., and Trtilek, M. (2010). Raman Microspectroscopy of Individual Algal Cells: Sensing Unsaturation of Storage Lipids in vivo. *Sensors* *10*, 8635-8651.

Sampath-Wiley, P., Neefus, C.D., and Jahnke, L.S. (2008). Seasonal effects of sun exposure and emersion on intertidal seaweed physiology: Fluctuations in antioxidant contents, photosynthetic pigments and photosynthetic efficiency in the red alga *Porphyra umbilicalis* Kützting (Rhodophyta, Bangiales). *Journal of Experimental Marine Biology and Ecology* *361*, 83-91.

Scaife, M.A., Burja, A.M., and Wright, P.C. (2009). Characterization of Cyanobacterial beta-Carotene Ketolase and Hydroxylase Genes in *Escherichia coli*, and Their Application for Astaxanthin Biosynthesis. *Biotechnology and Bioengineering* *103*, 944-955.

Schmollinger, S., Muehlhaus, T., Boyle, N.R., Blaby, I.K., Casero, D., Mettler, T., Moseley, J.L., Kropat, J., Sommer, F., Strenkert, D., *et al.* (2014). Nitrogen-Sparing Mechanisms in *Chlamydomonas* Affect the Transcriptome, the Proteome, and Photosynthetic Metabolism. *Plant Cell* *26*, 1410-1435.

Schwille, P. (2011). Bottom-Up Synthetic Biology: Engineering in a Tinkerer's World. *Science* *333*, 1252-1254.

Scott, S.A., Davey, M.P., Dennis, J.S., Horst, I., Howe, C.J., Lea-Smith, D.J., and Smith, A.G. (2010). Biodiesel from algae: challenges and prospects. *Current Opinion in Biotechnology* *21*, 277-286.

Searle, B.C., Turner, M., and Nesvizhskii, A.I. (2008). Improving Sensitivity by Probabilistically Combining Results from Multiple MS/MS Search Methodologies. *Journal of Proteome Research* 7, 245-253.

Shabala, S. (2009). Salinity and programmed cell death: unravelling mechanisms for ion specific signalling. *Journal of Experimental Botany* 60, 709-712.

Sharma, K.K., Schuhmann, H., and Schenk, P.M. (2012). High Lipid Induction in Microalgae for Biodiesel Production. *Energies* 5, 1532-1553.

Sheehan, J., Dunahay, T., Benemann, J., and Roessler, P. (1998). A look back at the U.S. Department of Energy's Aquatic Species Program: Biodiesel from Algae, N.R.E. Laboratory, ed. (Golden, Colorado).

Shen, P.-L., Wang, H.-T., Pan, Y.-F., Meng, Y.-Y., Wu, P.-C., and Xue, S. (2016). Identification of Characteristic Fatty Acids to Quantify Triacylglycerols in Microalgae. *Frontiers in Plant Science* 7, 162.

Siaut, M., Cuine, S., Cagnon, C., Fessler, B., Nguyen, M., Carrier, P., Beyly, A., Beisson, F., Triantaphylides, C., Li-Beisson, Y.H., *et al.* (2011). Oil accumulation in the model green alga *Chlamydomonas reinhardtii*: characterization, variability between common laboratory strains and relationship with starch reserves. *Bmc Biotechnology* 11.

Silva-Ortega, C.O., Ochoa-Alfaro, A.E., Reyes-Agüero, J.A., Aguado-Santacruz, G.A., and Jiménez-Bremont, J.F. (2008). Salt stress increases the expression of p5cs gene and induces proline accumulation in cactus pear. *Plant Physiology and Biochemistry* 46, 82-92.

Singh, S., Brocker, C., Koppaka, V., Ying, C., Jackson, B., Matsumoto, A., Thompson, D.C., and Vasiliou, V. (2013). Aldehyde Dehydrogenases in Cellular Responses to Oxidative/electrophilic Stress. *Free radical biology & medicine* 56, 89-101.

Singh, S.C., Sinha, R.P., and Hader, D.P. (2002). Role of lipids and fatty acids in stress tolerance in cyanobacteria. *Acta Protozoologica* 41, 297-308.

Slade, R., and Bauen, A. (2013). Micro-algae cultivation for biofuels: Cost, energy balance, environmental impacts and future prospects. *Biomass & Bioenergy* 53, 29-38.

Smith, R., Bangert, K., Wilkinson, S., and Gilmour, D.J. (in press). Symbiotic interactions between organic and inorganic carbon metabolism in a fast growing mixotrophic freshwater microalgal species *Micractinium inermum*. *Biomass and Bioenergy*.

Smith, R.T., Bangert, K., Wilkinson, S.J., and Gilmour, D.J. (2015). Synergistic carbon metabolism in a fast growing mixotrophic freshwater microalgal species *Micractinium inermum*. *Biomass and Bioenergy* 82, 73-86.

Smith, V.H. (1986). Light and Nutrient Effects on the Relative Biomass of Blue-Green Algae in Lake Phytoplankton. *Canadian Journal of Fisheries and Aquatic Sciences* 43, 148-153.

Smolke, Christina D., and Silver, Pamela A. (2011). Informing Biological Design by Integration of Systems and Synthetic Biology. *Cell* 144, 855-859.

Snijders, A.P.L., de Koning, B., and Wright, P.C. (2007). Relative quantification of proteins across the species boundary through the use of shared peptides. *Journal of Proteome Research* 6, 97-104.

Sogaard, D.H., Hansen, P.J., Rysgaard, S., and Glud, R.N. (2011). Growth limitation of three Arctic sea ice algal species: effects of salinity, pH, and inorganic carbon availability. *Polar Biology* 34, 1157-1165.

Solovchenko, A.E. (2012). Physiological Role of Neutral Lipid Accumulation in Eukaryotic Microalgae under Stresses. *Russian Journal of Plant Physiology* 59, 167-176.

Somanchi, A., and Moroney, J.V. (1999). As *Chlamydomonas reinhardtii* acclimates to low-CO<sub>2</sub> conditions there is an increase in cyclophilin expression. *Plant Molecular Biology* 40, 1055-1062.

Stansell, G.R., Gray, V.M., and Sym, S.D. (2012). Microalgal fatty acid composition: implications for biodiesel quality. *Journal of Applied Phycology* 24, 791-801.

Stauber, E.J., and Hippler, M. (2004). *Chlamydomonas reinhardtii* proteomics. *Plant Physiology and Biochemistry* 42, 989-1001.

Steen, H., and Mann, M. (2004). The abc's (and xyz's) of peptide sequencing. *Nat Rev Mol Cell Biol* 5, 699-711.

Stehfest, K., Toepel, J., and Wilhelm, C. (2005). The application of micro-FTIR spectroscopy to analyze nutrient stress-related changes in biomass composition of phytoplankton algae. *Plant Physiology and Biochemistry* 43, 717-726.

Stephanopoulos, G. (1999). Metabolic Fluxes and Metabolic Engineering. *Metab Eng* 1, 1-11.

Su, C.-H., Chien, L.-J., Gomes, J., Lin, Y.-S., Yu, Y.-K., Liou, J.-S., and Syu, R.-J. (2010). Factors affecting lipid accumulation by *Nannochloropsis oculata* in a two-stage cultivation process. *Journal of Applied Phycology* 23, 903-908.

Su, C.H., Chien, L.J., Gomes, J., Lin, Y.S., Yu, Y.K., Liou, J.S., and Syu, R.J. (2011). Factors affecting lipid accumulation by *Nannochloropsis oculata* in a two-stage cultivation process. *Journal of Applied Phycology* 23, 903-908.

Subramanyam, R., Jolley, C., Thangaraj, B., Nellaepalli, S., Webber, A.N., and Fromme, P. (2010). Structural and functional changes of PSI-LHCI supercomplexes of *Chlamydomonas reinhardtii* cells grown under high salt conditions. *Planta* 231, 913-922.

Sudhir, P., and Murthy, S.D.S. (2004). Effects of salt stress on basic processes of photosynthesis. *Photosynthetica* 42, 481-486.

Sukenik, A., and Livne, A. (1991). Variations in Lipid and Fatty Acid Content in Relation to Acetyl CoA Carboxylase in the Marine Prymnesiophyte *Isochrysis galbana*. *Plant and Cell Physiology* 32, 371-378.

Sültemeyer, D. (1998). Carbonic anhydrase in eukaryotic algae: characterization, regulation, and possible function during photosynthesis. *Canadian Journal of Botany* 76, 962-972.

Sunkar, R., Bartels, D., and Kirch, H.-H. (2003). Overexpression of a stress-inducible aldehyde dehydrogenase gene from *Arabidopsis thaliana* in transgenic plants improves stress tolerance. *The Plant Journal* 35, 452-464.

Sutherland, D.L., Montemezzani, V., Howard-Williams, C., Turnbull, M.H., Broady, P.A., and Craggs, R.J. (2015). Modifying the high rate algal pond light environment and its effects on light absorption and photosynthesis. *Water Research* 70, 86-96.

Szyszk-Mroz, B., Pittock, P., Ivanov, A.G., Lajoie, G., and Hüner, N.P.A. (2015). The Antarctic Psychrophile *Chlamydomonas* sp. UWO 241 Preferentially Phosphorylates a Photosystem I-Cytochrome b6/f Supercomplex. *Plant Physiology* 169, 717-736.

Takagi, M., Karseno, and Yoshida, T. (2006). Effect of salt concentration on intracellular accumulation of lipids and triacylglyceride in marine microalgae *Dunaliella* cells. *Journal of Bioscience and Bioengineering* 101, 223-226.

Takeda, T., Ishikawa, T., Shigeoka, S., Hirayama, O., and Mitsunaga, T. (1993). Purification and characterization of glutathione reductase from *Chlamydomonas reinhardtii*. *Microbiology* 139, 2233-2238.

Takouridis, S.J., Tribe, D.E., Gras, S.L., and Martin, G.J.O. (2015). The selective breeding of the freshwater microalga *Chlamydomonas reinhardtii* for growth in salinity. *Bioresource Technology* 184, 18-22.

Temple, S.J., Vance, C.P., and Stephen Gantt, J. (1998). Glutamate synthase and nitrogen assimilation. *Trends in Plant Science* 3, 51-56.

Titman, D. (1976). Ecological Competition Between Algae: Experimental Confirmation of Resource-Based Competition Theory. *Science* 192, 463-465.

Toledo-Ortiz, G., Huq, E., and Rodríguez-Concepción, M. (2010). Direct regulation of phytoene synthase gene expression and carotenoid biosynthesis by phytochrome-interacting factors. *Proceedings of the National Academy of Sciences* 107, 11626-11631.

Unwin, R.D. (2010). Quantification of Proteins by iTRAQ. In *Lc-MS/MS in Proteomics: Methods and Applications*, P.R. Cutillas, and J.F. Timms, eds., pp. 205-215.

Vallentine, P., Hung, C.-Y., Xie, J., and Van Hoewyk, D. (2014). The ubiquitin–proteasome pathway protects *Chlamydomonas reinhardtii* against selenite toxicity, but is impaired as reactive oxygen species accumulate. *AoB Plants* 6.

Van Wagenen, J., Miller, T.W., Hobbs, S., Hook, P., Crowe, B., and Huesemann, M. (2012). Effects of Light and Temperature on Fatty Acid Production in *Nannochloropsis Salina*. *Energies* 5, 731-740.

Vasudevan, P., and Briggs, M. (2008). Biodiesel production—current state of the art and challenges. *Journal of Industrial Microbiology & Biotechnology* 35, 421-430.

Vaughn, C.P., Crockett, D.K., Lim, M.S., and Elenitoba-Johnson, K.S.J. (2006). Analytical Characteristics of Cleavable Isotope-Coded Affinity Tag-LC-Tandem Mass Spectrometry for Quantitative Proteomic Studies. *The Journal of Molecular Diagnostics* 8, 513-520.

Veldhuis, M.J.W., Kraay, G.W., and Timmermans, K.R. (2001). Cell death in phytoplankton: correlation between changes in membrane permeability, photosynthetic activity, pigmentation and growth. *European Journal of Phycology* 36, 167-177.

Velmurugan, N., Sung, M.J., Yim, S.S., Park, M.S., Yang, J.W., and Jeong, K.J. (2014). Systematically programmed adaptive evolution reveals potential role of carbon and nitrogen pathways during lipid accumulation in *Chlamydomonas reinhardtii*. *Biotechnology for Biofuels* 7.

Venkata Mohan, S., and Devi, M.P. (2014). Salinity stress induced lipid synthesis to harness biodiesel during dual mode cultivation of mixotrophic microalgae. *Bioresource Technology* 165, 288-294.

Vensel, W.H., Dupont, F.M., Sloane, S., and Altenbach, S.B. (2011). Effect of cleavage enzyme, search algorithm and decoy database on mass spectrometric identification of wheat gluten proteins. *Phytochemistry* 72, 1154-1161.

Vieira, A.A.H., Nascimento, O.R., and Sartori, A.L. (1994). Release of Extracellular Polysaccharide by *Spondylosium panduriforme* (Desmidiaceae). *Revista De Microbiologia* 25, 6-10.

Vítová, M., Bišová, K., Umysová, D., Hlavová, M., Kawano, S., Zachleder, V., and Čížková, M. (2010). *Chlamydomonas reinhardtii*: duration of its cell cycle and phases at growth rates affected by light intensity. *Planta* 233, 75-86.

Wagner, V., Gessner, G., Heiland, I., Kaminski, M., Hawat, S., Scheffler, K., and Mittag, M. (2006). Analysis of the phosphoproteome of *Chlamydomonas reinhardtii* provides new insights into various cellular pathways. *Eukaryot Cell* 5, 457-468.

Walker, D.A. (2009). Biofuels, facts, fantasy, and feasibility. *Journal of Applied Phycology* 21, 509-517.

Wang, H., Alvarez, S., and Hicks, L.M. (2012). Comprehensive Comparison of iTRAQ and Label-free LC-Based Quantitative Proteomics Approaches Using Two *Chlamydomonas reinhardtii* Strains of Interest for Biofuels Engineering. *Journal of Proteome Research* 11, 487-501.

Wang, S.-B., Chen, F., Sommerfeld, M., and Hu, Q. (2004). Proteomic analysis of molecular response to oxidative stress by the green alga *Haematococcus pluvialis* (Chlorophyceae). *Planta* 220, 17-29.

Wang, Z.T., Ullrich, N., Joo, S., Waffenschmidt, S., and Goodenough, U. (2009). Algal Lipid Bodies: Stress Induction, Purification, and Biochemical Characterization in Wild-Type and Starchless *Chlamydomonas reinhardtii*. *Eukaryotic Cell* 8, 1856-1868.

Wase, N., Black, P.N., Stanley, B.A., and DiRusso, C.C. (2014). Integrated Quantitative Analysis of Nitrogen Stress Response in *Chlamydomonas reinhardtii* Using Metabolite and Protein Profiling. *Journal of Proteome Research* 13, 1373-1396.

Wawrik, B., and Harriman, B.H. (2010). Rapid, colorimetric quantification of lipid from algal cultures. *Journal of Microbiological Methods* 80, 262-266.

Weast, R.C., Editor (1976-77). *Handbook of Chemistry and Physics*, 57th Edition (Cleveland, Ohio: CRC Press).

Wellburn, A.R. (1994). THE SPECTRAL DETERMINATION OF CHLOROPHYLL-A AND CHLOROPHYLL-B, AS WELL AS TOTAL CAROTENOIDS, USING VARIOUS SOLVENTS WITH SPECTROPHOTOMETERS OF DIFFERENT RESOLUTION. *J Plant Physiol* 144, 307-313.

Weyer, K.M., Bush, D.R., Darzins, A., and Willson, B.D. (2010). Theoretical Maximum Algal Oil Production. *Bioenerg Res* 3, 204-213.

Wiese, S., Reidegeld, K.A., Meyer, H.E., and Warscheid, B. (2007). Protein labeling by iTRAQ: A new tool for quantitative mass spectrometry in proteome research. *Proteomics* 7, 340-350.

Willeford, K.O., Gombos, Z., and Gibbs, M. (1989). Evidence for Chloroplastic Succinate Dehydrogenase Participating in the Chloroplastic Respiratory and Photosynthetic Electron Transport Chains of *Chlamydomonas reinhardtii*. *Plant Physiology* 90, 1084-1087.

Williams, P.J.L., and Laurens, L.M.L. (2010). Microalgae as biodiesel & biomass feedstocks: Review & analysis of the biochemistry, energetics & economics. *Energy & Environmental Science* 3, 554-590.

Wood, A.M., Everroad, R.C., and Wingard, L.M. (2005). Measuring Growth Rates in Microalgal Cultures. In *Algal Culturing Techniques*, R.A. Anderson, ed. (Elsevier Academic Press).

Work, V.H., Radakovits, R., Jinkerson, R.E., Meuser, J.E., Elliott, L.G., Vinyard, D.J., Laurens, L.M.L., Dismukes, G.C., and Posewitz, M.C. (2010). Increased Lipid Accumulation in the *Chlamydomonas reinhardtii* sta7-10 Starchless Isoamylase Mutant and Increased Carbohydrate Synthesis in Complemented Strains. *Eukaryotic Cell* 9, 1251-1261.

World Meteorological Organization (2014). WMO Greenhouse Gas Bulletin: The State of Greenhouse Gases in the Atmosphere Based on Global Observations through 2013.

Wright, J.C., Beynon, R.J., and Hubbard, S.J. (2010). Cross Species Proteomics. In *Proteome Bioinformatics*, S.J. Hubbard, and A.R. Jones, eds. (Humana Press), pp. 123-135.

Wu, C.C., and MacCoss, M.J. (2002). Shotgun proteomics: tools for the analysis of complex biological systems. *Curr Opin Mol Ther* 4, 242-250.

Wu, H., Volponi, J.V., Oliver, A.E., Parikh, A.N., Simmons, B.A., and Singh, S. (2011). In vivo lipidomics using single-cell Raman spectroscopy. *Proceedings of the National Academy of Sciences* 108, 3809-3814.

Wu, W.W., Wang, G., Baek, S.J., and Shen, R.-F. (2006). Comparative Study of Three Proteomic Quantitative Methods, DIGE, cICAT, and iTRAQ, Using 2D Gel- or LC-MALDI TOF/TOF. *Journal of Proteome Research* 5, 651-658.

Xia, L., Rong, J.F., Yang, H.J., He, Q.N., Zhang, D.L., and Hu, C.X. (2014). NaCl as an effective inducer for lipid accumulation in freshwater microalgae *Desmodesmus abundans*. *Bioresource Technology* 161, 402-409.

Yang, H., He, Q., and Hu, C. (2015). Lipid accumulation by NaCl induction at different growth stages and concentrations in photoautotrophic two-step cultivation of *Monoraphidium dybowskii* LB50. *Bioresource Technology* 187, 221-227.

Yang, H., He, Q., Rong, J., Xia, L., and Hu, C. (2014). Rapid neutral lipid accumulation of the alkali-resistant oleaginous *Monoraphidium dybowskii* LB50 by NaCl induction. *Bioresource Technology* 172, 131-137.

Yao, C.-H., Ai, J.-N., Cao, X.-P., and Xue, S. (2013). Salinity manipulation as an effective method for enhanced starch production in the marine microalga *Tetraselmis subcordiformis*. *Bioresource Technology* 146, 663-671.

Yao, Y., Lu, Y., Peng, K.-T., Huang, T., Niu, Y.-F., Xie, W.-H., Yang, W.-D., Liu, J.-S., and Li, H.-Y. (2014). Glycerol and neutral lipid production in the oleaginous marine diatom *Phaeodactylum tricornutum* promoted by overexpression of glycerol-3-phosphate dehydrogenase. *Biotechnology for Biofuels* 7, 1-9.

Yilancioglu, K., Cokol, M., Pastirmaci, I., Erman, B., and Cetiner, S. (2014). Oxidative Stress Is a Mediator for Increased Lipid Accumulation in a Newly Isolated *Dunaliella salina* Strain. *PLoS ONE* 9, e91957.

Yokthongwattana, C., Mahong, B., Roytrakul, S., Phaonaklop, N., Narangajavana, J., and Yokthongwattana, K. (2012). Proteomic analysis of salinity-stressed *Chlamydomonas reinhardtii* revealed differential suppression and induction of a large number of important housekeeping proteins. *Planta* 235, 649-659.

Yokthongwattana, K., Chrost, B., Behrman, S., Casper-Lindley, C., and Melis, A. (2001). Photosystem II Damage and Repair Cycle in the Green Alga *Dunaliella salina*: Involvement of a Chloroplast-Localized HSP70. *Plant and Cell Physiology* 42, 1389-1397.

Yoshida, K., Igarashi, E., Wakatsuki, E., Miyamoto, K., and Hirata, K. (2004). Mitigation of osmotic and salt stresses by abscisic acid through reduction of stress-derived oxidative damage in *Chlamydomonas reinhardtii*. *Plant Science* 167, 1335-1341.

Yu-huan, G., Lin, L., and Dong, W. (2009). Growth and Production of Astaxanthin in *Chlamydomonas nivalis* Cultured in Various Media. *Natural Product Research & Development* 21, 641-644.

Yu, W.-L., Ansari, W., Schoepp, N.G., Hannon, M.J., Mayfield, S.P., and Burkart, M.D. (2011). Modifications of the metabolic pathways of lipid and triacylglycerol production in microalgae. *Microbial Cell Factories* 10.

Yuzawa, Y., Shimojima, M., Sato, R., Mizusawa, N., Ikeda, K., Suzuki, M., Iwai, M., Hori, K., Wada, H., Masuda, S., *et al.* (2014). Cyanobacterial monogalactosyldiacylglycerol-synthesis pathway is involved in normal unsaturation of galactolipids and low-temperature adaptation of *Synechocystis* sp. PCC 6803. *Biochimica et Biophysica Acta (BBA) - Molecular and Cell Biology of Lipids* 1841, 475-483.

Zachleder, V., and Vandenende, H. (1992). Cell Cycle Events in the Green Alga *Chlamydomonas eugametic* and their Control by Environmental Factors. *Journal of Cell Science* *102*, 469-474.

Zhang, J., Xin, L., Shan, B., Chen, W., Xie, M., Yuen, D., Zhang, W., Zhang, Z., Lajoie, G.A., and Ma, B. (2012). PEAKS DB: De Novo Sequencing Assisted Database Search for Sensitive and Accurate Peptide Identification. *Molecular and Cellular Proteomics* *11*, M111.010587.

Zhang, T., Gong, H., Wen, X., and Lu, C. (2010). Salt stress induces a decrease in excitation energy transfer from phycobilisomes to photosystem II but an increase to photosystem I in the cyanobacterium *Spirulina platensis*. *J Plant Physiol* *167*, 951-958.

Zhila, N.O., Kalacheva, G.S., and Volova, T.G. (2011). Effect of salinity on the biochemical composition of the alga *Botryococcus braunii* Kutz IPPAS H-252. *Journal of Applied Phycology* *23*, 47-52.

Zuo, Z.-J., Zhu, Y.-R., Bai, Y.-L., and Wang, Y. (2012). Volatile communication between *Chlamydomonas reinhardtii* cells under salt stress. *Biochemical Systematics and Ecology* *40*, 19-24.

Zuo, Z., Chen, Z., Zhu, Y., Bai, Y., and Wang, Y. (2014). Effects of NaCl and Na<sub>2</sub>CO<sub>3</sub> stresses on photosynthetic ability of *Chlamydomonas reinhardtii*. *Biologia* *69*, 1314-1322.

## 9 Appendix A: protocols

### 9.1 Growth media protocols

#### 9.1.1 TAP medium

Compound	Quantity	Solution protocol
Tris	2.42 g	
Solution #1 (TAP salts)	25 mL	NH <sub>4</sub> Cl 15.0 g MgSO <sub>4</sub> ·7H <sub>2</sub> O 4.0 g CaCl <sub>2</sub> ·2H <sub>2</sub> O 2.0 g Water to 1 L
Solution #2 (Phosphate solution)	0.375 mL	K <sub>2</sub> HPO <sub>4</sub> 28.8 g KH <sub>2</sub> PO <sub>4</sub> 14.4 g Water to 100 mL
Solution #3 (Hutner's trace elements)	1 mL	(See table below)
Glacial acetic acid	1 mL	
dH <sub>2</sub> O	To 1 L	

#### 9.1.2 Hutner's trace elements

Compound	Amount (g)	Water (mL)
EDTA disodium salt	50.0	250

ZnSO <sub>4</sub> ·7H <sub>2</sub> O	22.0	100
H <sub>3</sub> BO <sub>3</sub>	11.4	200
MnCl <sub>2</sub> ·4H <sub>2</sub> O	5.06	50
CoCl <sub>2</sub> ·6H <sub>2</sub> O	1.61	50
CuSO <sub>4</sub> ·5H <sub>2</sub> O	1.57	50
(NH <sub>4</sub> ) <sub>6</sub> Mo <sub>7</sub> O <sub>24</sub> ·4H <sub>2</sub> O	1.10	50
FeSO <sub>4</sub> ·7H <sub>2</sub> O	4.99	50

### 9.1.3 3N+BBM+V

Make up to 1 L with distilled water. Autoclave.

Component	Stock solution (g·L <sup>-1</sup> dH <sub>2</sub> O)	Quantity used (mL)
NaNO <sub>3</sub>	25.0	30.0
CaCl <sub>2</sub> ·H <sub>2</sub> O	2.5	10.0
MgSO <sub>4</sub> ·7H <sub>2</sub> O	7.5	10.0
K <sub>2</sub> HPO <sub>4</sub> ·3H <sub>2</sub> O	7.5	10.0
KH <sub>2</sub> PO <sub>4</sub>	17.5	10.0
NaCl	2.5	10.0
<i>Trace Element Solution</i>		6.0
FeCl <sub>3</sub> ·6H <sub>2</sub> O	0.097	

MnCl <sub>2</sub> .4H <sub>2</sub> O	0.041	
ZnCl <sub>2</sub> .6H <sub>2</sub> O	0.005	
CoCl <sub>2</sub> .6H <sub>2</sub> O	0.002	
Na <sub>2</sub> MoO <sub>4</sub> .2H <sub>2</sub> O	0.004	
<i>Vitamin B<sub>1</sub></i>		1.0
Thiaminhydrochloride in 100 mL distilled water. Filter sterile.	0.12	
<i>Vitamin B<sub>12</sub></i>		1.0
0.1 g Cyanocobalamin in 100 mL distilled water, take 1ml of this solution and add 99 mL distilled water. Filter sterile.		

## 9.2 PBS 1x Buffer solution protocol

All components are dissolved together in 800 mL dH<sub>2</sub>O. The pH is adjusted to 7.4 using HCl. Volume is made up to 1 L with dH<sub>2</sub>O, and sterilized by autoclaving.

Component	Mass (g)
NaCl	8
KCl	0.2
Na <sub>2</sub> HPO <sub>4</sub>	1.44
KH <sub>2</sub> PO <sub>4</sub>	0.24

## 10 Appendix B: Lipid quantification techniques for screening oleaginous species of microalgae for biofuel production

Emily Hounslow<sup>1, 2</sup>, Josselin Noirel<sup>3</sup>, D. James Gilmour<sup>2</sup>, Phillip C. Wright<sup>1</sup>

ChELSI Institute, Department of Chemical and Biological Engineering<sup>1</sup> and Department of Molecular Biology and Biotechnology<sup>2</sup>, The University of Sheffield, UK. Chaire de bioinformatique, LGBA, Conservatoire national des arts et métiers, 75003 Paris, France<sup>3</sup>

### 10.1 Abstract

This review examines the available literature on quantifying lipids in microalgae suitable for biofuels research. It discusses their advantages and disadvantages, their prevalence in the literature, and draws conclusions about the best way to approach choosing a suitable lipid measurement technique for microalgal biofuels research. We conclude that the method must be chosen based on the following key criteria: (1) the level of detail required in the results, and (2) the amount of biomass that can be spared for the assay. This review establishes that no method can be used as a “golden standard” for all microalgae. However, we present a systematic decision chart to choose the best measurement method or combination of methods to provide a guide to those wishing to understand the differences between the myriad of lipid measurement techniques.

**Practical Applications** This review will allow researchers new to the field to choose the most appropriate techniques for quantifying lipids in the microalgal species under study. The review is also intended to act as a gateway to the wider literature and will enable researchers to look in depth at a particular technique before carrying out experimental work.

### Keywords

Microalgae, Biofuels, Lipid, Triacylglycerides, Measurement, Quantification, Oil, Assay

## 10.2 Introduction

Fossil fuels are finite and cause a large number of environmental problems (Dresselhaus and Thomas, 2001). The economic production and uptake of biofuels, particularly those from microalgae, shows great promise in helping to mitigate these problems (Demirbas, 2011). Microalgae are a group of organisms that is highly efficient at converting sunlight into useful products for biofuels (Schenk et al., 2008). Most notably, they can produce triacylglycerides (TAGs) in abundance under certain conditions; this is highly desirable because TAGs can be converted by transesterification to biodiesel (Fjerbaek et al., 2009). If algae are to be used as a fuel source, an appropriate species must be chosen based on their fuel precursor producing capabilities, which greatly varies between species (Gouveia and Oliveira, 2009).

The extent of microalgal biodiversity has only been fully appreciated in the last 10 years or so as molecular sequencing techniques have become routine in aiding the identification of algal species (Adl et al., 2012). This huge biodiversity provides a wide range of species that can potentially be exploited for biodiesel production, but it also means that there are a large number of different cell morphologies (unicellular versus filamentous) and cell wall types (cellulose, silica) of varying thickness (Mutanda et al., 2011). Clearly methods of harvesting and lysing cells to get access to the lipids will vary depending on the algal type involved. Another source of variability is the growth conditions used and the time of harvest, both of which will affect the reproducibility of the results (Lv et al., 2010; Ruangsomboon, 2012).

However, the ability to accurately and reliably measure the lipid content, and especially TAG content, of microalgal cell samples is vital for assessing and comparing the suitability of microalgal strains for biofuels production. The current lack of standardisation is problematic, as it makes comparison between species that have been assessed with different quantification methods difficult. It also suggests that there may be inaccuracies in the predictions of algal biofuel yields based on calculations of their productivity, as the

oil content of the cells is such a key factor, and must be accurate. Ideally there would be a single standardised method for assessing algal lipid content, allowing both accurate quantification and realistic comparison. However, as we argue below, each method has problems associated with it. Different techniques can even give conflicting results on lipid yields, as demonstrated by data produced during this study and detailed in Appendix 1.

When the US Department of Energy (US DoE) Aquatic Species Program started their screening procedure in 1983, there was no standardized lipid analysis protocol (Sheehan et al., 1998). In the Technical Review part of "A look back at the Aquatic Species Programme..." (Sheehan et al., 1998), the authors identify Nile Red as a rapid screening process for algal lipids, but also point out that Nile Red staining is species specific, and therefore not suitable to compare species. Like Nile Red, each method introduced hitherto comes with its own set of advantages and disadvantages. Thus several different methods may need to be used to quantify lipids in a single algal species. The variety of these methods is very large, as demonstrated by our literature analysis.

To date, there is only one review of microalgal lipid measurement methods published, by Han et al. (2011). Many other papers compare a limited number of methods, such as Cheng et al. (2011b), who compared microcolorimetric methods with macro-gravimetric, or Cirulis et al., who carried out a comparison of different lipid staining methods (Cirulis et al., 2012).

The review by Han et al (2011) gives a "brief overview of the most recent strategies used to analyze microalgal lipid content". Whilst they give a description of the main methods, it doesn't critically assess their abilities to distinguish the composition and types of lipids in a sample as well as the lipid quantities. These aspects are important to bear in mind when designing experiments; and, we cover them here.

Han et al. (2011) state that the gravimetric method is the most accurate way to measure lipid content, presumably because it is a direct measurement of the lipid weight, but they do not address the issues of accuracy with gravimetric methods (discussed in this review).

However, as gravimetric analysis doesn't allow for compositional analysis unless coupled with mass spectrometry, and because it requires large amounts of biomass (limited by the weighing accuracy of a fine balance, so lowest detection level is typically in the order of 10 µg dry lipid), it is not the best method for all experiments. Han et al. (2011) rank each method in a characteristics matrix, and conclude that there is no method fit for all purposes, but that a method can always be chosen that is fit for the research. However, whilst the matrix can help to compare these methods, we find this review lacking in specific detail about the limitations of the methods, for example how much culture each method needs and how much information about the lipid composition can be gained. We propose decision trees to assess the methods for suitability, which takes into account the requirements of the test being carried out. We also critically assess all methods to highlight potential problems with them and discuss how methods vary with modifications.

We aim to comprehensively review all of the available methods in the literature and assess their suitability to screen algal species for potential biofuels production. As well as accuracy, key elements include reproducibility between species, and practical issues such as the amount of sample required. We also investigate the prevalence of these methods within existing literature and assess which are currently the most widely used methods.

The methods under examination are summarised in Table 1. Broadly speaking, these are gravimetric, fluorescence, colorimetric, chromatographic and mass spectrometry techniques. These methods are already reviewed in Han *et al.* (2011), but they fail to address the additional "miscellaneous" methods used, such as density equilibrium, and provide only a brief overview of these methods. Table 1 provides a comprehensive overview of all methods, and an assessment of their qualities. A discussion of the techniques follows. One of the main differences between groups of methods are that some methods, for example gravimetric and chromatography, rely on extraction of the oils from the algal biomass, whereas some are in situ; extraction protocols will therefore also be important in this discussion.

When analysing the suitability of a method to measure lipids, it is important to take into account exactly which lipids are needed for biofuels, and therefore to what degree of detail we need to be able to analyse lipids from microalgae. Indeed, the size distribution and degree of unsaturation of the fatty acids in TAGs are important for biofuel properties (Hoekman et al., 2012). Therefore, it is important to know not just the level of TAGs in an algal species, but this more detailed chemical information.

As a consequence, when considering these methods, we need to set out certain questions to ascertain whether the method is suitable. These questions can be summarised as:

1. What level of detail about the lipid composition do you want to gain from the test? For example, total lipids/lipid classes/position of double bonds in hydrocarbons.
2. Do you want absolute or relative lipid quantification?
3. How much culture can you spare for the test? For example, 100 mL/2 mL/ a few cells.
4. Do you want the cells to be alive at the end of the test?

It should be noted that the term "lipids" is ambiguous, as discussed by Laurens et al. (2012a): the term "lipids" could be used to describe any biochemical compounds insoluble in water but soluble in organic solvents. Laurens et al. (2012a) use lipids to describe fatty acids and their derivatives and describe "fuel potential" as the fraction of lipids that is composed of fatty acids that are amenable to transesterification. In all methods, the term "lipids" must be clearly defined, we take care to clarify this point for each method reviewed here. This is especially important for all algal lipid investigations that have a focus on biofuels production. Certain standards must be met for biofuels for transport, as they must be compatible with engines of aeroplanes or other vehicles. The European Commission sets out the guidelines for biofuels standards, known as EN14214 (Biofuel Systems Group Ltd; Costenoble et al., 2008; Hamelinck et al., 2007), and these must be complied with. The equivalent standards in the USA and Canada are ASTM D6751 (ASTM International). The standards specify the required physical and chemical properties

needed for biodiesel, which means information about the chemical structure and composition of the lipids obtained from algae is required. We take this into account here.

### 10.3 Table 1 Summary of lipid quantification techniques in microalgae

Technique type	Technique variation	Sensitivity	Lipid detection type	In situ or extraction	Qualitative/quantitative	Advantages	Disadvantages/ problems	References
<b>Gravimetric</b> Use of cell lysis and a solvent to extract lipids from biomass, followed by drying and weighing lipid extract	Bligh and Dyer: 1:2 chloroform methanol	500 mg wet biomass	"Crude" lipid	E	N	Direct measurement	Extracts other compounds than lipids Requires large amounts of culture Solvent type favours certain lipid types	(Bligh and Dyer, 1959; Kumari et al., 2011)
	Folch: 2:1 chloroform methanol	500 mg wet biomass*	"Crude" lipid	E	N	Direct measurement	Solvent type favours certain lipid types	(Kumari et al., 2011)
	Soxhlet: Hexane and use of Soxhlet extractor	1 g dry biomass	"Crude" lipid	E	N	Direct measurement	Solvent type favours certain lipid types	(Go et al., 2012; Li et al., 2008a)
	Cequier-Sánchez: Dichloromethane instead of chloroform	500 mg wet biomass*	"Crude" lipid	E	N	Less toxic solvents used	Solvent type favours certain lipid types	(Kumari et al., 2011)
<b>Fluorescent lipid dye</b> Dye is applied to whole cells to penetrate in and bind to lipids. Excitation and emission filters are used to read dye fluorescence as a relative measure of lipids.	Nile Red: binds to neutral lipids.	0.2 to 1 x 10 <sup>6</sup> cells mL <sup>-1</sup> ; 5 µL for microplate method	Neutral lipids	I	L, S	In situ Relatively fast procedure Can process many samples at once	Varies between species as penetration of cell wall and concentration of dye must be optimized. Doesn't distinguish between neutral lipid types Relative measure unless using standards	(Chen et al., 2009b; Cirulis et al., 2012)
	BODIPY: Binds to a range of lipids and fluoresces when excited at 488nm	0.2 to 1 x 10 <sup>6</sup> cells mL <sup>-1</sup>	Fatty acids, phospholipids, ceramides, cholesterol and cholesteryl ethers	I	L	In situ Relatively fast procedure Can process many samples at once Has no chlorophyll interference	Shows lower quantification correlation with other methods compared to Nile Red	(Cirulis et al., 2012)
	DiO: Binds to phospholipids.	0.2 to 1 x 10 <sup>6</sup> cells mL <sup>-1</sup>	Phospholipids	I	L	In situ Relatively fast procedure Can process many samples at once	Suitable for phospholipids only	(Cirulis et al., 2012)

<b>Colorimetric</b> Extraction of lipids and reaction with a colour developer. Degree of colour change is proportional to lipid concentration.	Phospho-vanillin (SPV)	5-120 µg dried lipid	Fatty acids	E	S	Can be done on small volumes	Relies on extraction Signal decreases with chain length of less than 12 carbons so hard to detect smaller chains No structural information gained.	(Cheng et al., 2011b)
	TFA-Cu salts: Triethanolamine and copper	2 mL at OD <sub>680</sub> 0.06-1.2	Fatty acids	E	S		No structural information gained.	(Chen and Vaidyanathan, 2012b)
	TFA-metal	1-2 mL (OD not stated)	Fatty acids	E	S		No structural information gained.	(Wawrik and Harriman, 2010)
<b>Raman microscopy</b> Lasers alter the vibrational state of a sample and the shift in energy is specific to chemical bonds and structures, yielding information about the sample content.	N/A	1 cell	Lipid type and degree of unsaturation	I	H	Small samples needed In situ and non destructive Detailed information of lipid properties	Photosynthetic pigments can interfere with signal Components in low abundance can't be detected.	(Samek et al., 2010; Wu et al., 2011)
<b>Density equilibrium</b> Samples are centrifuged in a 10-80% (w/v) sucrose gradient to find in vivo buoyant densities. An equation is used to convert the density values to lipid content values.	N/A	2 mL sample or 5 mg dry biomass	Lipid, hydro-carbon or biopolymer	I	N	Rapid, In situ	Indirect, relies on the relationship between density and lipid content being constant between all samples	(Eroglu and Melis, 2009)
<b>Direct transesterification/ In situ esterification</b> Direct conversion of lipids in biomass to FAMES using a solvent and catalyst and measurement with GC	Lepage and Roy: Acetyl chloride/methanol reagent	500 mg wet biomass	FAME	E	N	Measures true potential of algal biomass to be converted to FAME		(Kumari et al., 2011)
	Garcia: Toluene and 5% methanolic HCl reagent	500 mg wet biomass	FAME	E	N	Detailed information on molecular structure of lipids		(Kumari et al., 2011)
	In situ esterification	4-7 mg wet biomass	FAME	I	N	Detailed information on molecular structure of lipids		(Laurens et al., 2012a)
<b>NMR</b> Applying magnetic field to sample and measuring the resonant frequency emitted to provide spectra of chemical shifts and information about molecule structure.	Time domain: This method is based on relaxation time of lipids' hydrogen nuclei in different phases of the samples.	1 g dried biomass	Specific targeted lipid compounds and molecular structure	I or E	S	Detailed information on molecular structure of lipids	Can be interference from other compounds, which is not consistent between samples. Water can interfere so to exclude this samples must be freeze-dried.	(Gao et al., 2008)
	Liquid state	1 g wet biomass	Specific targeted lipid	I	S	Detailed information on molecular structure of lipids	Can be interference from other compounds, which is not consistent between samples.	(Beal et al., 2010)

			compounds and molecular structure					
<b>Mass Spectrometry</b> Fatty acid extraction, derivitazation, separation via chromatography, electron ionization, and measurement of the mass to charge ratio of the compound in a mass spectrometer.	GCMS	5 mg dry biomass	Lipid classes and chain types	E	N	Lipid classes obtained as well as quantitation	Relies on the assumption that derivatized fatty acids can correctly identify all the lipid portions in the correct proportions. Assumes that all lipid types will ionize at the same rate.	(Barupal et al., 2010; Gu et al., 2011b)
	LCMS	500 mg dry biomass	Lipid classes and chain types	E	N	Detailed identification of lipid composition	Detection of lipids is dependent on lipid type.	(Macdougall et al., 2011)
<b>FTIR</b> Measurements of infrared absorption and molecular vibrational modes are used to identify and quantify ester groups at wavelength $1740\text{cm}^{-1}$ in dried cells. Relative lipid content is determined by calculating the ratio of the lipid band ( $1740\text{cm}^{-1}$ ) to the amide I band.	N/A	0.15-2 mL culture (OD not specified)	Ester groups	I	L	No extraction needed	Not specific to TAGs or lipids	(Dean et al., 2010; Stehfest et al., 2005)

Table 1 | in situ=I. extraction=E. N=quantitative, L=qualitative, S=quantitative with standards, H=semi quantitative. \*Tested on macroalgal biomass.

## 10.4 Prevalence of lipid techniques in literature

To assess the frequency of use of algal lipid techniques within the academic community, we used a search in Web of Science, on 10<sup>th</sup> July 2015, using search terms "TOPIC: ((\*alga OR \*algae OR \*algal OR (microorganism\* AND photosynth\*))) AND; TOPIC: ((lipid OR lipids OR TAG OR TAGs)) AND; TOPIC: ((oil OR biofuel\* OR biodiesel)); NOT TOPIC: ((fish\* OR meat OR chicken OR egg OR nutrition OR cyanobacteri\* OR biogas OR biomethane OR methane OR diet\* OR sediment\*)); Databases: ( WOS OR MEDLINE ) AND; LANGUAGES: ( ENGLISH ); Timespan: All years; Search language=Auto" we find a list of all the available literature on lipids in algae for biofuels production, excluding those for nutritional uses. This search excludes a number of non-relevant Web of Science Categories, and excludes the Arts and Humanities Citation Database. The resulting list contains 2266 publications.

Figure 10.1 displays the number of publications that meet these criteria over time. The number of publications has dramatically increased since 2008, as this field gains momentum in research. This growth is likely due to the renewed need for alternative energy research and increased funding in this area of research.

Figure 10.2 displays the percentage of these publications that contain key words in the abstract relevant to lipid quantification techniques. Although the abstract does not necessarily contain the level of technical detail needed, the percentages are still believed to reflect the prevalence of the techniques. "GC" (22%) and "MS" (approximately 20%) are very prevalent, as GC-MS is often used to characterise extracted lipids once they have been quantified. Colorimetric is low in occurrence, whilst Nile Red (12%) and gravimetric (5%) are reasonably high. "Esterification" (53%) is the highest, but this may be because esterification is often mentioned as the method for converting algal lipids to biofuels rather than an actual experimental step. Of the gravimetric techniques, Bligh and Dyer and Soxhlet are the most prevalent. Nile Red is by far the highest fluorescent lipid probe technique and one of the most prevalent techniques overall. This may be because Nile Red is a well-established technique, made well-known by Cooksey et al. (1987), and is

often used as a screening technique for lipid suitability. Since this was the method adopted by the Aquatic Species Program (Sheehan et al., 1998), many algae researchers may have followed this lead by using it, but subsequent discussion demonstrates that as a screening technique and analytical technique, this method may not be the best available. It may be that the sheer momentum of researchers using this technique has caused its continued use, rather than its suitability to purpose.

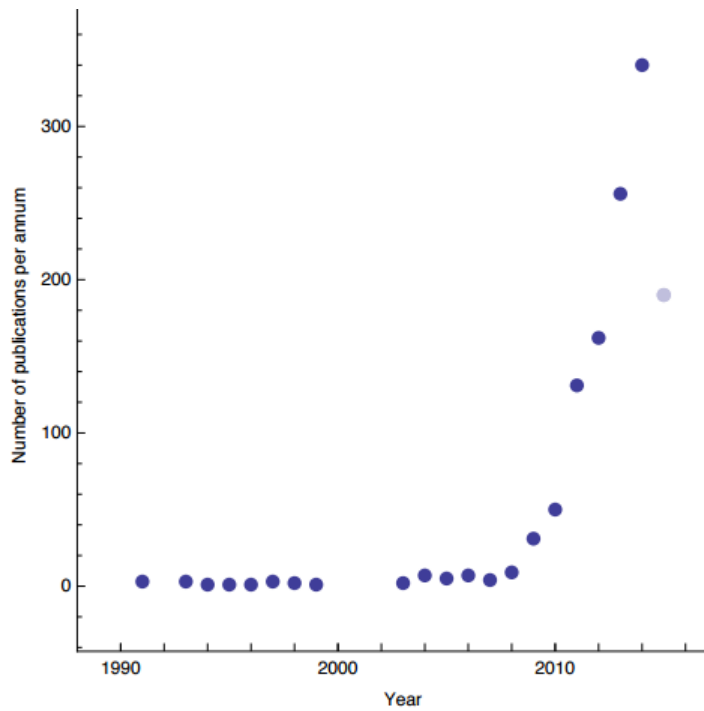


Figure 10.1 Publication numbers about lipid analysis in algae for biofuels, per year. The final dot represents 2015 up to 10<sup>th</sup> July.

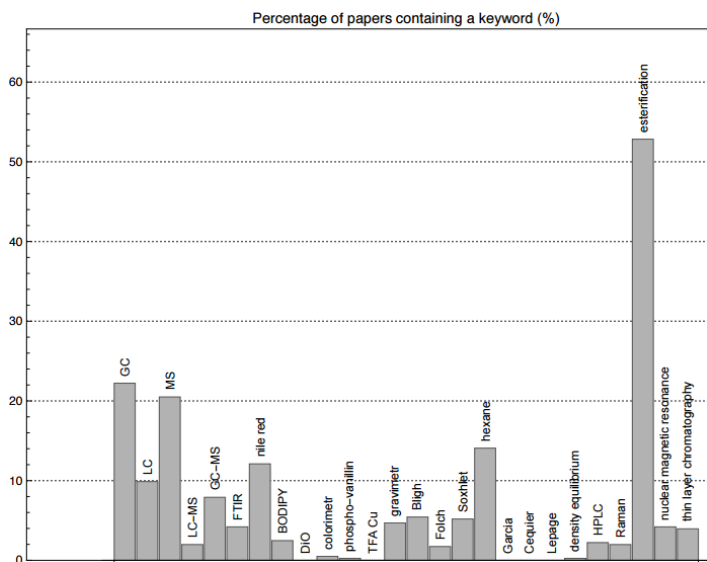


Figure 10.2 Key words of algal lipid measurement techniques and their occurrence in the literature (percentage).

It is clear that some methods are far more commonly used than others in the literature. Methods may be well established not only in the wider scientific community as a whole, but also within laboratories or research groups - especially when specialised equipment has been obtained for lipid analysis, such as a gas chromatograph or plate reader. Researchers will turn to what is available if they do not have other options in their research environment. Without detailed knowledge of the techniques it is easy to use the established "go-to" methods in the research community, rather than the most suitable. The aim of the next section is to help researchers choose their techniques in an informed but simple way.

## 10.5 Choosing a suitable lipid measurement technique

Given there are at least 9 main options (without going into the variations within those techniques) for lipid measurement tools and techniques, we have devised decision trees for choosing appropriate methods for the research question an algal researcher wishes to answer.

Returning to the questions in the introduction, Figure 10.3 shows decision trees for these questions.

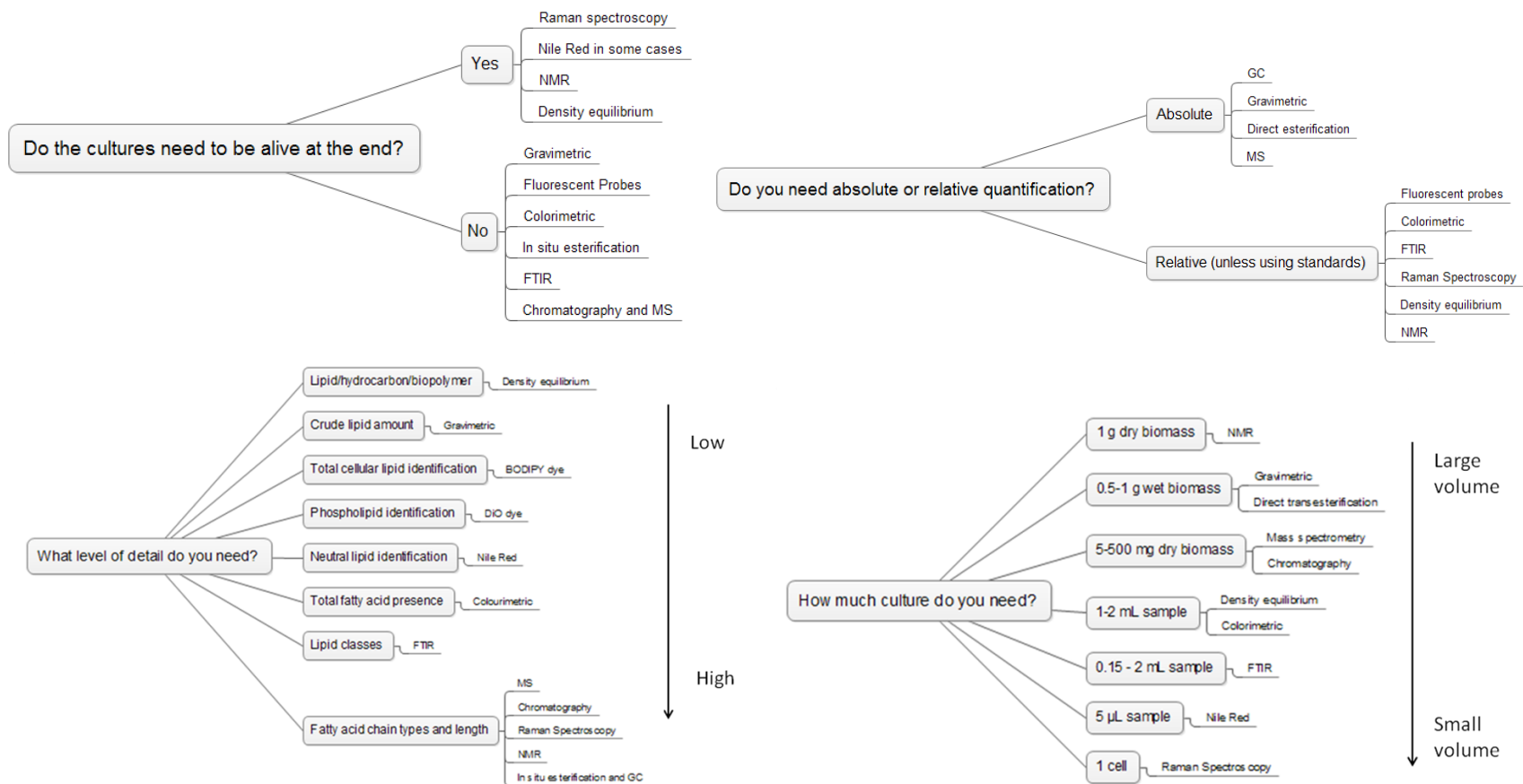


Figure 10.3 Decision trees for deciding how to choose a method based on the limitations of the experiment. Note that there are usually multiple answers to the questions, which means that more than one technique may be applied.

Using these decision trees it is easier to narrow down the possibilities from the available methods. The most important factor should be the level of detail needed in the investigation, but other factors such as needing the culture alive afterwards or having limited amount of culture to spare may cause more practical limitations.

## 10.6 *Characteristics of lipid quantification techniques*

The techniques summarised in Table 1 vary in their specificity in terms of: the level of information about lipids they reveal (e.g. gravimetric showing total lipids versus Nile Red showing the presence of neutral lipids versus GC-MS identifying the chain length of fatty acids identified); the type of lipids they are suited to detecting (e.g. some solvents in gravimetric methods favour certain classes of lipids over others or Nile Red only shows neutral lipids); and the accuracy of the results. Even within types of methods, there is diversity in how the protocols are performed and how suited they are to different algal species.

With all methods, there is a need for consistency of sample testing and normalisation of data, especially when comparing between different species or conditions. When assessing the lipid content of a sample, that sample must be normalized by measuring the algae cell population or using a proxy for this such as biomass or optical density (Wood et al., 2005). Cell number is the most accurate way to do this but it is time consuming and thus proxy methods may be chosen instead. The normalization of data depends partly on the method being used, and this will be explored in more detail in individual methods. In cases where a relative quantification between two treatments is all that's needed, lipid values could be expressed as a ratio of the control samples.

Furthermore, with all methods there must be adequate quality control measures. The problem with any comparison between different analyses is that variation in methodology and instrumentation will cause differences in results, as shown by Laurens *et al.* (Laurens et al., 2012b), who compared results between different laboratories and different researchers carrying out the same analysis. They found that there was little difference between researchers in the same laboratory, but big differences between researchers in different laboratories.

It is recommended to run standards for each experimental run of a procedure or piece of equipment. For example, Nile Red fluorescence could be affected by the brightness of a lamp which will reduce over time due to aging, or simply due to day to day variations (De la Hoz Siegler et al., 2012), so standards should be run with every plate. By using standards, it is possible to account for the variation that occurs between instruments or equipment as well as procedure.

A key difference between methods is whether or not the protocol requires lipid extraction. Gravimetric and chromatographic methods rely on extraction of the oils from the algal biomass, whilst fluorescence methods take place in situ. The effectiveness of extraction is thus important. Extraction techniques can vary greatly, for example the number of extractions performed on the biomass, the technique and length of time used for cell lysis. This has implications for how the efficiency of the extraction process varies between methods. It is interesting to note that certain techniques have become more prevalent than others; for example, Bligh and Dyer is the most commonly used gravimetric technique. Likewise Nile Red has become the most popular dye used for in situ analysis of lipids over other dyes such as BODIPY. The following subsections examine the techniques in detail and assess the reasons for popularity (or not).

### ***10.7 Fluorescent lipid probes***

Lipid probes are dyes which bind to lipids and the level of their relative fluorescence is used as a measure of the lipid abundance in the cells. The dyes are used by permeating the cells in situ and then measuring the fluorescence when the dyes bind to lipids. This measurement is used as a relative measure, or it can be quantified. There is some debate as to whether these techniques can be used for time course experiments; Brennan et al. (2012) state that an advantage of lipophilic probes such as Nile Red and BODIPY is that they can be used to measure the lipid content of individual cells and therefore measure their lipid content over time, which can be useful for checking the homogeneity of cell cultures. It would also be useful for measuring lipid changes over time at the cellular level and for strain selection. However, Pick and Rachutin-Zalugin (2012) suggest that although Nile Red staining is in situ, it kills the cells, so they cannot

be kept alive for time course experiments. The nature of Nile Red dye permeating the cells suggests that even if the cells are not killed (for example when reducing the Nile Red and solvent concentrations to be non-lethal), they will be significantly altered by the process, and therefore Nile Red cannot be thought to be a completely non-destructive assay.

### **10.7.1 Nile Red**

Nile Red is a dye that binds to neutral lipids and fluoresces yellow or red when excited, and the wavelength range used can vary between protocols. It is used with microalgae by permeating the cells to allow the dye to bind with the intracellular lipid droplets. Nile Red workflows must be optimised for every single species and strain, since every strain responds differently to Nile Red fluorescence (Rumin et al., 2015). There are two main considerations with Nile Red: one is the ability of the Nile Red to effectively permeate the cells, depending on the type of cell and the conditions of the protocol, and for the fluorescence to be expressed. The second is the quantification of the fluorescence response rather than a simple qualitative one.

Nile Red must be used with an organic solvent, as it is quenched in water (Greenspan et al., 1985). For a detailed discussion of how Nile Red interacts with lipid droplets and different solvents, although not with reference to microalgae, see Greenspan et al. (1985). The hydrophobicity of the solvent will dictate the choice of excitation and emission wavelengths, which may vary by up to 60 nm. These wavelengths are important for accurate lipid detection. At excitation wavelengths less than 570 nm, Nile Red selects for neutral lipids, and at less than 590 nm it is a general lipid dye. At higher wavelengths than 590 nm it loses its selectivity for lipid droplets (Greenspan et al., 1985). In algal species, emission 575 nm and excitation 530 nm wavelengths are used for neutral lipid determination; if studying total lipid, the wavelengths can range between 470 to 549 nm for excitation and 540 to 628 nm for emission, depending on the organism tested and its respective lipid content composition (Chen et al., 2009b). Alternatively, an argon laser can be used, but this emits at 488 nm; this means the polar lipid excitation wavelength is slightly further from its optima than neutral lipid is, which impacts on the calculation of neutral to polar lipid ratios used in some methods

(de la Jara et al., 2003). It is also important that unstained samples are run so that background fluorescence can be taken into account, and washing cells to remove residual Nile Red may be necessary (Chen et al., 2009b).

This method can be made high throughput by using a microplate format (Higgins et al., 2014) such as a 96 well plate (Storms et al., 2014) to measure many samples at once.

#### *10.7.1.1 How penetration varies*

It is important to make sure the dye penetrates the cells fully so that the subsequent fluorescence accurately reflects the lipid content. The thickness and permeability of the cell wall will be a defining factor of how easily the Nile Red can enter the cells, therefore methods must be optimised using penetration techniques. These include hand grinding samples (Damiani et al., 2010), microwave irradiation (reported to increase penetration whilst avoiding fluorescence quenching) (Chen et al., 2011c), grinding in liquid nitrogen, heating to 80°C for 10 minutes, 20% methanol, 20% DMSO, 20% acetone, 20% isopropanol and ethanol (Chen et al., 2009b; Storms et al., 2014).

Once a permeation method is chosen, several parameters need to be optimized: Nile Red concentration, solvent concentration, stain time, temperature and algal cell concentration (Chen et al., 2009b; Rumin et al., 2015). The effectiveness of solvents in facilitating Nile Red staining is species dependant and recalcitrance of the cell wall has a large effect on the ability of the solvent to permeate (Natunen et al., 2015).

DMSO has been reported as achieving the highest fluorescence in a comparison of penetration methods and has subsequently been investigated for protocol optimisation, including staining temperature and DMSO concentration (Chen et al., 2009b). The concentration of DMSO is important, as it can also cause fluorescence quenching of Nile Red dye above the optimum concentration, but below the optimum concentration DMSO is not effective at facilitating Nile Red staining of the neutral lipids (Chen et al., 2011c). Nile Red fluorescence quenching is time dependent and the rate and extent of fluorescence decay are species specific (Pick and Rachutin-Zalagin, 2012).

### 10.7.1.2 How quantification varies

Since Nile Red fluorescence is a relative measure of lipid content, quantification requires either standards or imaging software. Triolein has been demonstrated in *Skeletonema marinoi*, *Chaetoceros socialis* and *Alexandrium minutum* as a potentially useful standard for a range of 0.12 to 12 µg lipid per mL sample (Bertozzini et al., 2011). Unfortunately, Bertozzini et al. (2011) show that the concentration curves are species specific and suggest the use of a standard addition concentration curve method which involves adding different amounts of triolein to samples containing algal cells.

White et al (2011) used Laser Scanning Confocal Microscopy to image the Nile Red stained cells in 3D, and then lipid to cell ratios were calculated using Cell Profiler software, in which a brightness threshold of pixels was set to distinguish between lipids and non-lipid parts of the cell. The numbers of the lipid and non-lipid pixels were then used to calculate a percentage lipid content of the cell. This method appears to be a good way to quantify the Nile Red method, since instead of a relative "fluorescence" measurement, it can actually measure a percentage lipid content using the dye as an indicator of presence/absence within the cell.

In cases where this single cell imaging technique is not used and instead data is expressed as a relative fluorescence value of a sample, quantification relies on using a normalization technique for the samples. To compare the fluorescence of two samples, either the same cell density must be used, or the same amount of biomass. This is especially important since the effect of Nile Red can vary with cell concentration (Chen et al., 2009b).

As already mentioned, background fluorescence must be taken into account, and this can help to set a baseline to account for variability between samples or between sample runs (e.g. between one 96-well plate and the next) (Chen et al., 2009b). In as many cases as possible, direct comparisons should be made between samples on the same plate to reduce error due to variability in sample processing.

### **10.7.1.3 Use of Nile Red with flow cytometry for strain selection**

Absolute measurements may not always be necessary and instead a researcher may just want to select cells above a certain lipid threshold. Nile Red is commonly used for strain selection using flow cytometry for rapid, and automated selection of desired lipid production levels (da Silva et al., 2009) and in vivo quantification (de la Jara et al., 2003), using fluorescence-activated cell sorting techniques or FACS (Cabanelas et al., 2015; Terashima et al., 2015). This can use previously calculated correlations of Nile Red fluorescence with gravimetric techniques, thin layer chromatography and GC to set fluorescence level to the desired amount. The advantages of this method are that subpopulations can be characterised and separated (de la Jara et al., 2003), and also that the fluorescence is measured per cell so cell concentration does not need to be taken into account (Cirulis et al., 2012). As previously discussed, the toxicity of the Nile Red and solvent solution may prevent survival of viable cells that can be selected and cultured later. It may be possible to find lower, non-toxic concentrations of Nile Red solutions, but it is not known if this would allow full permeation of Nile Red into the cell (de la Jara et al., 2003).

### **10.7.1.4 How conditions like salt or DMSO affect Nile Red**

In addition to strain and protocol variation, other substances can affect Nile Red fluorescence. Pick and Rachutin-Zalogin (2012) investigated the kinetic interactions of Nile Red in algae. NaCl has been shown to retard the interactions of Nile Red with lipid globules in the algae cells. Studies with *Dunaliella salina* show that high NaCl medium concentrations significantly affect the emission spectrum and the kinetics of Nile Red fluorescence (Pick and Rachutin-Zalogin, 2012). Therefore, care must be taken to remove substances that could interfere, like salt, particulates, precipitates or cell fragments (Cirulis et al., 2012), using isotonic wash buffers (Pick and Rachutin-Zalogin, 2012) or flow cytometry for "gating" off these substances (Cirulis et al., 2012).

## **10.7.2 BODIPY**

BODIPY (boron-dipyrromethene) is a lipophilic neutral fluorophore which binds to a wide range of lipids including fatty acids, phospholipids, ceramides, cholesterol and cholesteryl esters (Govender et al., 2012). It has good photostability and is not affected

by the presence of chlorophyll (Govender et al., 2012), giving it an advantage over Nile Red (Cirulis et al., 2012). It has been shown that fluorescing lipids in BODIPY-stained cells were distinct from chlorophyll, which has some fluorescence under Nile Red (Govender et al., 2012). The reason for this is that BODIPY is excited with a blue 488 nm laser, whilst the maximum emission on the green spectrum is 515 nm (Brennan et al., 2012). BODIPY can be used in conjunction with confocal imaging or for high content screening of algae for valuable products (Brennan et al., 2012). The dye reaches maximum fluorescence in less than a minute, when monitored over a 25 minute period. BODIPY can be used in confocal time lapse measurements (Brennan et al., 2012).

Like Nile Red, BODIPY staining requires optimization of dye concentration and staining time, but after optimization can achieve high correlation ( $R^2 = 0.93$ ) to gravimetric analysis in terms of quantified lipid, and it has the advantage of easily crossing cell membranes and organelle membranes (Xu et al., 2013).

#### *10.7.2.1 Need for pre-treatment*

There is no consensus in the literature as to whether BODIPY staining requires pre-treatment, for example between Govender et al. (2012), who state that it is not necessary, and Brennan et al. (2012) who demonstrate that species with thick cell walls do not allow full dye permeation. Brennan et al.'s (2012) study compared four species and show that for full permeation, pre-treatment is needed. Furthermore, staining temperature, BODIPY concentration, and algal cell concentration are also important in achieving maximal dye permeation and fluorescence - in this case the optimal DMSO concentration was 0.06 g/mL and the temperature optimum was 25°C, with the optimal stain concentration at 1.12 µg/mL. The cell concentration must be below  $10^6$  cells/mL. By optimising these three parameters, specimen fluorescence was increased by 798 times using glycerol pre-treatment and by 845 times using DMSO pre-treatment, over the baseline autofluorescence, showing DMSO as the more effective of the two treatments. By comparison, the dye with neither pre-treatment reached only 35 times more than the baseline autofluorescence. The drawbacks of this

are that pre-treatments will potentially inhibit cell growth, and also render any high throughput screening "non stop flow" systems unsuitable (Brennan et al., 2012).

#### ***10.7.2.2 Quantification***

Fluorescence imaging coupled with software analysis can be used to quantify intensity distributions across cells. Averaging such data has been demonstrated (Holcomb et al., 2011) and coupled with laser scanning confocal microscopy to show the locations as well as the volumes of the lipids in the cells (Wong and Franz, 2013; Xu et al., 2013). The lipid storage locations can be analysed for better understanding how and where in the cells the lipids are stored, which is information not normally given in most quantification protocols.

#### **10.7.3 4.1.3 DiO**

DiO-C<sub>18</sub> is an amphiphilic compound that binds to phospholipid. It has been proposed as a potential lipid probe (Cirulis et al., 2012), but has been shown to be poor for lipid quantification as we discuss more broadly below.

#### **10.7.4 Considerations for lipid probes**

For a detailed discussion on lipophilic dyes Nile Red, BODIPY and DiO, refer to Cirulis et al. and Rumin et al (2012; Rumin et al., 2015). The parameters that affect the usefulness of the dye, as a measure of lipid content in the cells, include dye concentration, organic solvent concentration, staining duration and cell concentration, as well as the presence of non-cellular events (meaning cell fragments, salts, precipitates of the dye, and other debris). When applying the dyes, the concentrations must be sufficient to saturate the cells, but not be any higher due to precipitate forming and causing interference. Issues were raised with all three dyes. DiO shows no relationship between lipid quantity and fluorescence intensity, therefore it has been rejected as a tool for lipid quantification. BODIPY shows a correlation, but small changes in dye and solvent concentration cause large variability in the fluorescence and there is not a range of dye concentration where the fluorescence is stable, making the reproducibility of this correlation questionable (Cirulis et al., 2012). Nile Red is the favourite dye to use for this purpose since, under optimised conditions (Nile Red concentration and acetone concentration) there is a high correlation with lipid

quantity ( $R^2 = 0.9912$ ) which is robust to cell concentration. When the conditions are not optimised, however, the correlation is poor (Cirulis et al., 2012).

Organic solvents generally cause problems with the protocols since they extract lipids and chlorophyll from the cells, therefore they should be kept to a minimum. Nile Red has been found to be the most suitable dye of the three options, so long as the Nile Red working concentration and solvent concentration have been optimised (Cirulis et al., 2012; Rumin et al., 2015).

### **10.8 Gravimetry**

Gravimetric techniques employ cell disruption and solvents to extract total or "crude" lipid from the biomass, and then weigh it. There are many gravimetric methods, differing in the types of solvents used, the number of extractions, and the application of rupturing methods (e.g. sonication or bead beating). The methods include, but are not limited to, Bligh and Dyer, Soxhlet (Go et al., 2012; Li et al., 2008a), Folch and Cequier-Sánchez, so named for their solvent combinations. Several papers discuss these differences and we discuss workflow below. To truly compare methods, ideally the biomass must be standardized, since variations in the biomass humidity, ash content and harvesting method can cause variations downstream (Ríos et al., 2013). Additionally, moisture contents above 5% can reduce the lipid extraction efficiency and alter the lipid profile obtained (Balasubramanian et al., 2013). Since the lipid contents are expressed as a percentage of dry weight, these methods are normalized as standard by biomass. However, other normalization methods such as taking a sample of identical cell count could be another way to normalize this data.

When comparing methods, it is important to remember that all algae respond differently to these methods, dependant on their lipid profile and their cell wall thickness. One study that noted the issue of variable results using different gravimetric techniques used a Thermogravimetry Analyzer to estimate lipid content after correlating it with a number of extraction methods coupled with FAME analysis (Li et al., 2014b).

### 10.8.1 Type of solvent

Successful gravimetric analysis requires penetration of the solvent into algal cells followed by extraction. The solvent polarity influences the types of lipids and materials extracted, and therefore the overall "crude lipid" yield and composition (Cheng et al., 2011a). It is clear from the literature that a careful match between lipids and solvent chemistry is required to fully remove the desired lipids from the other cell constituents (Kumari et al., 2011).

Making sure that all of the lipid is extracted is vital for accurate quantification, therefore methods aim for the highest possible lipid yield. Accordingly, Bligh and Dyer (BD), which consistently shows high lipid extraction yields from microalgae, is often favoured over other methods (see section 2). However, mis-matching the solvent to the algal lipids will extract the wrong lipid and cell components, including non-lipid materials such as alcohol-containing groups from phospholipids, glycerol, polyphenols, phosphate, pigments and cholesterol (Kumari et al., 2011), and will overestimate yields. Therefore, unless the extracted crude lipid has been analysed with GC to confirm that it does not contain other substances, extraction yields alone are not enough to confirm that a method is the most suitable to the sample. Indeed, Kumari et al. (2011) consistently found higher crude lipid extraction yields from gravimetric methods than from total fatty acid values from the conventional and direct transesterification (DT) methods due to co-extraction of those substances, demonstrating the importance of knowing what is contributing to the total lipid measurement both in terms of lipid composition and other components.

Microalgal lipids for biodiesel are non-polar and therefore a solvent with low polarity (such as hexane/methanol mix) should be more selective in extracting desired lipids and fewer impurities than a more polar solvent like toluene, ethyl acetate (Cheng et al., 2011a), or 1:2 chloroform methanol in BD (Kumari et al., 2011). However, less polar solvents ethanol, iso-propanol, butanol, hexane and acetic ester are not as effective as chloroform and methanol at extracting lipids and they extract more non-lipid compounds (Sheng et al., 2011). Hexane, especially, has high non-lipid material extraction and low lipid yields (Araujo et al., 2013; Balasubramanian et al., 2013; Sheng

et al., 2011). The Soxhlet method uses hexane, and is a slow process with low lipid yields, mainly reliant on diffusion of lipids through the cell membrane (Araujo et al., 2013).

Chloroform and methanol systems (Folch and BD) dissolve lipids across the entire polarity range, and can help to break up membranes, denature lipo-proteins (Kumari et al., 2011) and interact strongly with hydrogen bonds (Sheng et al., 2011), so these systems give higher lipid recoveries in comparison to others (Balasubramanian et al., 2013). Folch systems have been shown to recover higher total lipid (TL) and FA amounts than BD (Kumari et al., 2011). Griffiths et al (2010) concur, finding Folch system more effective than BD, with Askland and Smedes method in the middle. Combining a polar and a non-polar solvent also widens the range of neutral and polar lipids that can be recovered (Balasubramanian et al., 2013; Khozin-Goldberg and Cohen, 2006). Although chloroform and methanol are good solvents, their toxicity to people makes them unsuitable for large-scale extractions in a laboratory working environment. Toxic chloroform can be replaced with methyl tert-butyl ether (MTBE) (Sheng et al., 2011) or dichloromethane (as in Cequier-Sánchez method) (Kumari et al., 2011) to give slightly lower and significantly lower extraction rates, respectively.

For further discussion of different solvent systems see Balasubramanian et al. (2013), Kumari et al. (2011), Araujo et al. (2013) and Sheng et al. (2011).

#### 10.8.2 Type of cell disruption method

There are many cell disruption methods, including grinding dried biomass (Yu et al., 2012), using DMSO pre-treatment (Khozin-Goldberg and Cohen, 2006), free nitrous acid pre-treatment (Bai et al., 2014), osmotic shock using NaCl or sorbitol (Yoo et al., 2012), sonication, bead beating, autoclaving, microwave heating (Prabakaran and Ravindran, 2011), ultrasound, powdered silica (Araujo et al., 2013), high-pressure homogenisation (Halim et al., 2013), and supercritical fluid extraction with ultrasonic shaking (Cheng et al., 2011a). No one disruption method is "best", since it is species specific (Prabakaran and Ravindran, 2011) and also because there is a significant interaction between solvent system and disruption method, in terms of extraction

efficiency (Balasubramanian et al., 2013). For example, sonication has been identified as the best disruption method in one study (Prabakaran and Ravindran, 2011), and yet has no improvement on lipid yield in another using the same solvent system (Ríos et al., 2013).

Many papers test and directly compare the effects of different cell disruption methods, and depending on the study, the method being identified as giving the highest yield is microwave heating (Lee et al., 2010), bead beating (Cheng et al., 2011a), sonication (Prabakaran and Ravindran, 2011), or ultrasound (Araujo et al., 2013).

Surprisingly, one technique, powdered silica, has been shown to reduce lipid yield in all tested methods (Araujo et al., 2013). Other techniques have been identified as potentially damaging to the lipid extract, such as lipid degradation caused by high pressure homogenisation (Halim et al., 2013), or conformational changes of lipids from the induced heat of prolonged sonication (Kumari et al., 2011). Therefore, for this method, an optimum sonication time was required to strike a balance between cell wall breakdown and degradation of lipids, and again this varied depending on the solvent system (Kumari et al., 2011). However, it has been shown that elevated temperature and pressure and optimised extraction time enhance lipid recovery (Laurens et al., 2012a). It has also been shown that multiple extractions enhance yield (Herrera-Valencia et al., 2011; Widjaja et al., 2009), as does combining multiple disruption methods (Pernet and Tremblay, 2003). As well as the lipid yield, the lipid profile may be affected. The drying treatment of algal biomass can affect the lipid profile, although not lipid yield (Balasubramanian et al., 2013).

Use of a buffer achieves higher TL and FA recoveries, as it prevents ionic adsorption effects in samples containing high amounts of inorganic salts. These ionic adsorption effects cause ionized phospholipids to be retained in the aqueous phase during separation and therefore not measured in the organic phase that is recovered and measured gravimetrically. Using a buffer allows the recovery of these phospholipids (Kumari et al., 2011). Other parameters can affect the efficiency of the cell disruption

method. Halim et al. (2013) found that cell concentration was a key factor in the disruption rate.

Pernet and Tremblay (2003) investigated the effects of sample storage and sample volume on TAG level in cells. They found that combining ultrasonication and grinding led to higher free FA and TL levels if the sample was 6 months old, but not if it was three days or one month old. When the samples are tested within one month, the combination of lysis methods can decrease TAG recovery. What is clear is that the cell disruption method can actually influence the determination of the lipid classes (Pernet and Tremblay, 2003). It has also been shown that whether the extract is washed before weighing affects the yield (Laurens et al., 2012a).

### 10.8.3 Suitability of gravimetric methods to purpose

Often it is a combination of the above factors that can affect the suitability of a method for lipid quantification. A factorial categorical design experiment by Kumari et al. (2011), comparing three types of gravimetric analysis (BD, FM and CS) on three species of macroalgae, showed that the "best" gravimetric technique varied according to the algal species. This is because their lipid profiles will be drastically different, so choosing a method which favours the extraction of particular lipid classes will skew the results. In their matrix of determining factors, solvent system, algal species and buffer were all vital determinants and interacted with each other, making different systems the most suitable for different algae (Kumari et al., 2011). The effectiveness of the methods are highly dependent on experimental parameters (Laurens et al., 2012b).

Since impurities are co-extracted with lipids, gravimetric methods cannot truly represent the lipid content (Cheng et al., 2011a), hence the disparity between GC-derived FAME analysis and gravimetric results. For chlorophyll a contamination, this can be potentially mitigated by estimating the chlorophyll a concentration using fluorometry, as described by White et al. (2011). Gravimetric samples can be assayed using GC analysis (Yu et al., 2012). However, gravimetric methods are often used because they are relatively rapid and do not require advanced instrumentation. They are therefore suitable for a large number of laboratories (Laurens et al., 2012b).

Gravimetric methods require careful optimisation and cannot show information about lipid classes, so GC is often needed both to correct overestimation of lipids due to the inclusion of other substances, and to gain this information (McNichol et al., 2012). Subsequent GC can show that the "crude lipid" can be up to 7 times greater than the FA content of the gravimetric extract (McNichol et al., 2012).

### **10.9 Direct (In-situ) transesterification**

Direct transesterification (DT), also known as in situ transesterification, is the conversion of lipids to FAMES or fatty acid acyl esters (FAAEs) (Wahlen et al., 2011). The method converts the saponifiable lipids from microalgae directly into FAMES with no pre-extraction step (Griffiths et al., 2010; Pflaster et al., 2014). This can be done using either an acid or a base catalyst and an alcohol. If the alcohol is methanol, the result will be FAMES (Wahlen et al., 2011). The method uses around 1 mg dry biomass (McNichol et al., 2012).

An advantage of this method is that pre-extraction is not needed (Laurens et al., 2012a), and direct transesterification methods can yield similar results to two-step transesterification (Cavonius et al., 2014). Comparisons of DT method with esterification of pre-extracted crude lipid (using gravimetric or Soxhlet extraction) show that DT is much more accurate and consistent than the two-step process, due to the relationship between solvents and lipid profiles discussed in the gravimetry section (Laurens et al., 2012a; McNichol et al., 2012).

DT can give a reliable upper limit to the yield of biodiesel that can be produced from algal biomass, since it uses all saponifiable lipid, including those in membrane lipids (McNichol et al., 2012), i.e. it shows the amount of biomass that can be converted to FAME. Therefore, species with a high percentage of convertible biomass will be the most suitable for biofuels production (McNichol et al., 2012). However, a two-step (extraction followed by conversion) process can also be employed (Hidalgo et al., 2013).

### 10.9.1 Variations in DT

The critical factors in DT are alcohol type, catalyst type, temperature, co-solvents and, most importantly, moisture content (Hidalgo et al., 2013), since high water content in biomass reduces extraction efficiency. DT efficiency is sensitive to both water and catalyst combination (Griffiths et al., 2010). Cell lysis and sample preparation can also vary. It is also important to minimize oxidation and degradation of FA to be able to give an accurate profile of the FA content (Laurens et al., 2012a).

The choice of catalyst can affect the FAME yield. Base catalysts result in potential partial saponification and soap formation. Acid catalysts result in consistently higher yields, as they can esterify all fatty acids, whether free or linked (Laurens et al., 2012a). Acid hydrolysis is shown in studies to give a greater recovery of FA (McNichol et al., 2012). Sequential addition of basic and acid catalyst improves the efficiency of DT, as opposed to using a single catalyst (Griffiths et al., 2010). Hidalgo et al. (2013) fully discuss the advantages and disadvantages of different catalyst types. Penetration of the catalyst through the cell walls is essential for an effectively working catalyst, and this could vary as nutrient depleted algal cells are thought to be more recalcitrant than replete ones (Laurens et al., 2012a). The presence of free fatty acids could lower the efficiency of the base catalyst as well (Laurens et al., 2012a).

Catalysts include NaOMe,  $\text{BF}_3$  and HCl. NaOMe alone is not effective as a catalyst, but is when used with  $\text{BF}_3$ . However,  $\text{BF}_3$  is a highly corrosive and dangerous chemical; using HCl is a safer and effective alternative (Laurens et al., 2012a). Using concentrated HCl in methanol is also a way to simplify the original Lepage and Roy procedure (Laurens et al., 2012a; Lepage and Roy, 1986). To improve and accelerate cell disruption and lipid release, microwave technology and ultrasonic technology can be applied. Microwave-assisted transesterification may even not need a catalyst (Griffiths et al., 2010).

The type of alcohol has some effect on the lipids extracted (Wahlen et al., 2011), but using 1.8%  $\text{H}_2\text{SO}_4$  can negate the effect that the type of alcohol used has on the TAG and FAME extracted. An excess of methanol is needed for the most efficient conversion, and it can reduce the negative impact that high water content has on

FAME yield (Wahlen et al., 2011). Using a co-solvent can also improve DT yields (Griffiths et al., 2010). It is important that the catalyst has good access to the substrate, and the solubility of non-polar lipids in a highly polar medium like acidic methanol could compromise the reaction efficiency (Laurens et al., 2012a).

The biomass to solvent ratio can affect the FAME yield and must be optimised. Too high a biomass to solvent ratio will lead to diffusion problems which reduces the reaction rate in the mix (Ríos et al., 2013). Moisture content in the samples can be up to 80% without affecting the recovery of fatty acids (Laurens et al., 2012a), but this could also dilute the catalyst, which is a problem if there's a relatively high concentration of non-polar lipids. To reduce the effect of water in the reaction, water scavengers can be used at the point of catalyst addition, such as 2,2-dimethoxypropane (Godswill et al., 2014). The addition of water scavengers can improve the yield of FAMEs following the transesterification reaction (Melero et al., 2015).

#### 10.9.2 Discussion of limitations of DT

The success of DT as a lipid measurement method relies on the ability to convert the lipids to FAME equally, therefore the catalyst must be chosen according to its ability to convert lipids.

By converting all lipids into FAME, one cannot separate them into their separate classes (Griffiths et al., 2010), and it is not possible to determine the original source of the FAME (McNichol et al., 2012). However, this is a simple way to evaluate the potential biodiesel yield from microalgae without pre-extraction, since transesterification is the method for converting lipids to biodiesel (Griffiths et al., 2010). A possible drawback to DT is the varying ability of lipids to be converted to FAME. Triglyceride lipids convert to 100% FAME (Laurens et al., 2012a) but not all lipids do this, therefore only the weight of pure triglycerides can be recovered as FAME.

### 10.9.3 Comparison of DT to gravimetric

Kumari et al (2011) found that DT methods were better than conventional extraction methods for obtaining optimum FA recoveries, regardless of species. Therefore, if FA information is the desired outcome, DT methods are the best. However, if information about the lipid classes is needed, gravimetric or Soxhlet methods are better since DT does not separate the lipid fractions (Kumari et al., 2011; McNichol et al., 2012).

Wahlen et al (2011) found that DT methods showed higher FAME output than gravimetric methods coupled to GC, because other sources of fatty acids such as membrane phospholipids can contribute to the DT yield, but they are not extracted in gravimetric processes. It can be argued that since biodiesel is formed from transesterification, a DT method shows the true potential of microalgae to release biodiesel, as opposed to gravimetric methods that have been found to misrepresent lipid content.

As with gravimetric methods, a good way to normalize these data is by taking the same amount of biomass for each sample so that they can be directly compared.

### 10.10 Raman spectroscopy

Raman spectroscopy uses a laser which alters the vibrational state of a molecule resulting in an energy shift that yields information on the vibrational modes, specific to the chemical bonds and structure of the molecule. It can therefore yield information about which specific molecules are present in a sample. The method is based on Beer's law, which shows that spontaneous Raman scattering is linearly dependent on analyte concentration. However, in practice, there are some limitations to the applicability of this law (Wu et al., 2011). The method can be quantitative however, using diagnostic markers and ratiometric analyses (Wu et al., 2011). The level of information yielded is the degree of unsaturation of lipids, and their transition temperatures, which is important information for determining the suitability of algal lipids for engine compatibility and performance metrics of the fuel (Samek et al., 2010; Wu et al., 2011). The ability of Raman spectroscopy to accurately detect FA chain length has been confirmed by GC testing (Wu et al., 2011).

Quantification requires calibration, using standards (Fu et al., 2012) or iodine values (Samek et al., 2010) to identify the lipids from the spectral peaks, and it remains a semi-quantitative measure of lipid content and saturation degree. The peaks correspond to the saturated and unsaturated carbon-carbon bonds (Samek et al., 2010). A new imaging method using a laser scanning microscope can be calibrated to certain channels, and using more channels allows the measurement of several lipid species. However, there is a trade off; the more channels, the larger the spectral bandwidth, the better the selectivity of the method, but this could come at a cost to the laser power at each individual band (Fu et al., 2012).

The method relies on the contribution of each component to the spectra depending on the detection sensitivity and relative abundance of that component (Huang et al., 2010). Calibration spectra can be created using pure fatty acid samples (Samek et al., 2010). Using an assembled Raman spectral library of model microalgal lipids, one can guide analyses and obtain quantitative or semi-quantitative information about the presence and concentration of lipid types, as well as the degree of unsaturation, lipid chain length, and melting temperature of the fatty acids (Wu et al., 2011). However, this method has been described as "qualitative" by another study (Huang et al., 2010).

#### 10.10.1 Advantages

Raman spectrometry can be applied to single algal cells (Wu et al., 2011). These may be immobilised in an agarose gel (Samek et al., 2010), but this technique is not always used. The cells require no pre-treatment and analysis is done *in vivo*, which has the advantage that it is possible to track oil production over time and measure a live cell during its growth cycle (Wu et al., 2011), and that it is non-invasive (Samek et al., 2010). The method has low sensitivity to water, which makes it suitable for live biological samples (Huang et al., 2010). The location, as well as the identification, of the compounds within the scanned region can be determined, as seen with the study of TAGs within algal cells (Huang et al., 2010), and from imaging techniques that display the location of lipid droplets within the cell (Fu et al., 2012). This means that all comparisons between samples happen on a per-cell basis.

The method can be filtered to the wavelengths of the characteristic peaks that correspond to the compounds of interest (e.g. lipids), so the analysis can be targeted to some extent (Huang et al., 2010).

#### 10.10.2 Limitations

Photosynthetic organisms can be difficult to analyse using this method, since the autofluorescence of photosynthetic pigments can obscure the Raman spectral features (Samek et al., 2010), and therefore this limits the applicability to those species that do not have strong autofluorescence, or to spectral peaks from lipids that don't have significant interference or overlapping signals from other cellular components. It has been shown that, in particular, beta carotene can interfere with some of the lipid bands in the compositional analysis (Samek et al., 2010). It is possible to subtract the experimentally measured peak height of beta carotene to negate this. It is important to make sure the excitation laser does not photo-damage the cells and also that background fluorescence is minimized, and for that reason Samek et al. (2010) used a near-infrared spectral region of 785 nm. Another way to avoid interfering fluorescence is to use coherent anti-Stokes Raman scattering (CARS) spectroscopy, which detects a blue-shifted signal instead of the red-shifted signal of normal Raman spectroscopy (Cavonius et al., 2015).

Huang et al. (2010) claim that the position of carbon-carbon double bonds do not alter the spectrum to a large extent, which implies that the exact structure of the chain will not be detected by this method. However, this may not be important if these different chain types always produce biodiesel that complies with the ASTM biodiesel standards (Huang et al., 2010). Another limitation of this method is that the diameter of the focal region can limit resolution, which may not allow the detection of targeted components, such as TAG, in low abundance (Huang et al., 2010).

The analysis of a single cell means that it is suitable for cell sorting of strains, but it is not suitable for determining the lipid content of an entire culture, since there will be a

large amount of cell-to-cell variability due to differences in growth phases or slight variations of cultivation conditions in the sample (Samek et al., 2010).

### 10.11 *Chromatography and Mass Spectrometry*

Chromatography methods and mass spectrometry (MS) are often used in conjunction, so here they will be discussed together. Chromatography is used to separate lipids based on their size and therefore their elution time, and identify them using standards.

Mass spectrometric techniques are used for detailed identification of lipid composition. They are used to identify lipids based on their mass to charge ratio when ionized and fragmented in a mass spectrometer. Using mass spectrometers to quantify lipids is also known as "lipidomics" (Taleb et al., 2015).

The methods can be used in a number of combinations and the equipment that is connected directly is reflected in the names or acronyms used. For example LC-MS uses a liquid chromatograph connected directly to a mass spectrometer. However if the named methods are not hyphenated (or separated by a slash), they will be carried out on two different items of equipment, such as using HPLC separation followed by injection into MS/MS (tandem mass spectrometry that uses two steps of selection and fragmentation).

Mass spectrometry and chromatography techniques have many possibilities for variation, and as a result, although lipidomics has great power for identification and measurement of lipids, there are a great many challenges and pitfalls to the area too. The subject of MS and chromatography of lipids is a very extensive and this review can only summarise the main points of consideration when choosing this method for algal biofuel measurement. A review by Bou Khalil et al. (2010) describes variations in lipidomics in detail, highlighting that the main challenge is a lack of consistency in the techniques and analysis, or no "uniform analytical platform". Another challenge is the great diversity of lipids, for which accurate identification and quantification relies on the availability of standards, but these are not universally available for lipidomics. Lipid databases are not universal since the structure of lipids varies between species or tissues (Bou Khalil et al., 2010).

### 10.11.1 Variations in chromatography

The main chromatography techniques are gas chromatography (GC), liquid chromatography (LC) and thin layer chromatography (TLC). These include high performance liquid chromatography (HPLC) and comprehensive two-dimensional gas chromatography (GCxGC). GC is often used as a way of measuring transmethylated (Recht et al., 2012) or transesterified fatty acids (Khotimchenko and Yakovleva, 2005). Chromatographic techniques are useful for both clear identification of different lipid classes, and quantification of these classes by using standards and appropriate analytical software. When using these techniques, a greater resolving power prevents different lipids classes eluting at the same time, which can solve the problem of some lipids not being identified (Gu et al., 2011a).

Chromatography can give a certain amount of information, but MS is used when more detail is needed, such as the contribution of acyl residues to individual lipid fractions (Vieler et al., 2007). Therefore methods such as LC-MS/MS are employed (Taleb et al., 2015).

### 10.11.2 Variations in sample processing

The main variations in chromatography and MS techniques are: how the sample is prepared for analysis, whether chromatography is used alone or in conjunction with MS, which MS platform is used, whether one lipid or a group of lipids are selected, whether there is a full range scan, and whether it is for identity or quantification. The ionisation techniques, MS platforms, capillary columns and temperature can affect the outcome of results.

It is important in the sample processing to take into account sample normalization - i.e. if absolute quantification of lipid samples is the aim, the lipid samples being processed must be taken from a set culture density or set amount of biomass.

Prior to putting algal samples through MS or chromatography, it is usually necessary to extract the lipids from the biomass and prepare them via a time consuming process.

Separating lipids from the rest of the biomass can be done using a suitable solvent such as MTBE (Sheng et al., 2011). Prior to MS, lipid samples are often separated or fractionated, either via a connected process such as with LC-MS/MS, or by a separate chromatography method, although this is not always the case and some methods use direct infusion via ESI (electrospray ionisation) (Christensen et al., 2015).. Automated analysis which is available with many systems makes data analysis simpler and easier (Yamada et al., 2013), which is of great benefit to the researcher. Using a non-automated system may be due to equipment limitations or the requirement for manual separation and targeting. Many methods use non automated systems, such as Liu et al (2011) who used Folch extraction followed by 1D TLC, for separation and identification of lipid classes using pure standards, and acid transesterification followed by capillary GC with flame ionization detection (FID). This is of course a large amount of sample preparation and will be subject to the issues associated with extraction of lipids from microalgae, as discussed in the gravimetry section. This can lead to variation in data from the problems associated with extraction efficiency, as well as being able to process fewer samples in a set period of time. Avoiding lengthy or multiple-step sample preparation procedures is therefore preferable if possible. It is not always necessary to transesterify FA into FAME, as several types of lipids can be analysed using GC-MS (Guan et al., 2011). Supercritical CO<sub>2</sub> extraction can be carried out on dry biomass to obtain lipids from algae (Aresta et al., 2005). However, this still then requires transesterification.

Barupal et al. (2010) used pyrolysis GC-MS to resolve this issue. Pyrolysis automatically produces volatile compounds for the GC-MS to characterize, allowing up to 36 automated samples per day. There is however the potential for information to be lost, and the pyrolysis process needs to be carefully managed. This study found the optimal temperature was 600°C, for 12 seconds. Above this temperature, there was a decline in intact high molecular weight pyrolysis products; below, there were lower pyrogram ion intensities observed, as there is likely to be insufficient breakdown of the lipid constituents (Barupal et al., 2010). Therefore, this is a way for information to

potentially be lost. The main attraction of this method is the preparation is minimal as so much of it is automated.

In many methods, extraction is required (Vieler et al., 2007). To remove the need for this, direct thermal desorption is a way to make components of a solid matrix more volatile so that they can be separated without an extraction or alternative preparation step (Akoto et al., 2008). However, in studies which are targeted towards analysing specific compounds, for example for biofuels, extraction is useful for targeting the desired lipids (Guan et al., 2011). One such targeting and separation extraction method is solid-phase extraction, which can separate lipids into TAG and free fatty acids (Paik et al., 2009). This employed a sorbent, such as sodium carbonate and 20% dichloromethane, as well as an extraction solvent, in this case n-hexane. The TAG fraction can then be targeted for analysis, as can the FFA.

#### 10.11.3 Variation in quantification techniques

Quantification can be done using internal standard methods (Guan et al., 2011). GC can use an internal standard at the point of lipid extraction and this can compensate for incomplete extraction efficiency or dilution variability, as well as a way to quantify GC analysis (Laurens et al., 2012a). The GC quantification of FAME is based on the peak area of each FAME relative to that of the internal standard used, as well as the molecular mass of each FAME (Lim et al., 2012; Paik et al., 2009). Identifications of the FAME use mass spectral profiles, standards, and projected retention times from the particular method and equipment used (Lim et al., 2012). Additionally to internal standards, multi-standard solutions are used as calibrating references for equipment to then calculate sample lipids based on peak area ratios (Paik et al., 2009).

GC can be used in conjunction with flame ionisation detection (FID) to measure the concentration of chemical species within a sample (Adam et al., 2012; Yeh and Chang, 2011). This works on the basis that the frequency of the ionisation detection is proportional to the concentration of the chemical species in the gas stream. GC can also be used in conjunction with MS; in GC-MS, quantification can be carried out by assuming that the mass spectrometry response factors between compounds of the

same chemical class is similar, and therefore signal intensity can be used to compare abundance (Barupal et al., 2010).

Using data analysis software, it is possible to enhance the detection of analytes that are present in low amounts in the analyte complex matrix. To detect both high and low abundance species, two exploratory sample analyses can be run with normal and increased sample concentrations (Akoto et al., 2008).

Chromatography methods rely on the use of response factors of each compound (calculated as the peak area generated divided by the concentration of the compound), and studies have shown that the response factors between different TAG standards can vary significantly (Liu et al., 2013), as much as up to 50% (Macdougall et al., 2011), therefore accurately quantifying different TAGs in parallel is not possible. If standards are used this is not a problem, however, not all compounds have commercially available standards and some techniques may rely on these response factors. Lipid libraries can be used, and there are a number of database resources that catalogue different lipid compounds for MS identification (Navas-Iglesias et al., 2009). However, many of the lipids in these libraries are based on human lipids and not algal lipids, and may not have the information for algal lipid research (Christensen et al., 2015).

#### **10.11.4** Variation in equipment used

The main variations with the equipment used are: the choice of chromatography or MS system and whether they are used in combination.

Although a very popular method, as seen in our literature data, traditional 1D GC still has problems of co-eluting FAME of different carbon chain lengths and degree of unsaturation, even with selective sample clean up procedures (Akoto et al., 2008). Chromatography methods can be carried out in a 2-D space to give greater resolving power than a 1-D space, as shown with 2-D GC (Akoto et al., 2008; Gu et al., 2011b) and TLC (Khozin-Goldberg and Cohen, 2006). It is important to have complete resolution of FAME for unambiguous peak identification. The second dimension allows group-type separation of fatty acids with different carbon numbers and double bonds,

whereas many compounds would not be detected and identified as they would co-elute in 1D space (Gu et al., 2011b), or be in low abundance and masked by other analytes (Akoto et al., 2008). In the second dimension, FAME types are separated according to the degree of unsaturation: Saturated FAME are eluted first, and then those which have an increasing degree of unsaturation (Akoto et al., 2008). One important factor in GC is column choice. Polar columns are better for separation than non-polar columns for C16-C18 FAMEs (Woo et al., 2012).

Combining chromatography methods with MS results in improved profiling of microalgal lipid samples (Akoto et al., 2008; Olmstead et al., 2013), since there is both good separation and identification. Both are needed for good and reliable spectra of pure compounds (Akoto et al., 2008). In particular, combining with ToF-MS is said to be an especially fast and effective way to achieve this high quality level of data (Akoto et al., 2008; Herrero et al., 2007). Depending on the required level of detail, it is possible to use MS platforms in conjunction (Kind et al., 2012). However, when it comes to choosing MS equipment, the technical limitations must be considered for their effect on lipid identifications (Vieler et al., 2007). For example, electron ionisation MS (EI-MS) have a similar fragmentation profile for polyunsaturated fatty acids, and do not give molecular ion information (Gu et al., 2011a). It is difficult to gain specific information about fatty acids this way, such as the carbon number and the position and geometry of double bonds, or even of the identity of specific fatty acids (Gu et al., 2011a). To overcome this, derivatization and soft ionisation can be used to detect molecular ion and specific fragments (Gu et al., 2011a).

It has been shown that the choice of capillary column and selected stationary phases can greatly affect the differentiation of fatty acids; using a polar capillary column coated with polyethylene glycol or bis(cyanopropyl)siloxane allows differentiation of the carbon numbers, numbers of double bonds, location and geometry of the fatty acids (Gu et al., 2011a). It is important to make sure elution times are correct and not affected by the equipment and gradient used, for example the effect of response variation caused by elution gradients in HPLC (McNichol et al., 2012). It is also important to know the limit of detection and the precision of the equipment and

methods used, since temperature programmes, capillary columns and sample concentration can affect these parameters (Guan et al., 2011).

Following the processing and identification of certain lipids via GC analysis, it may be advantageous to target a desired lipid for analysis using TLC (Vieler et al., 2007), such as with nutritional studies on algal lipids (Tsai and Sun Pan, 2012). However, this may have limited utility for biofuels, because several lipids from a sample will be of interest.

#### 10.11.5 Advantages

The advantages in chromatography and MS are the level of detailed data obtained, both about the identification and abundance of different lipid classes and compounds, as discussed above. They are also sensitive methods, making them useful for analysis of species such as *C. reinhardtii* which has TAG present in low abundance (at 9% FAME content) (Barupal et al., 2010; James et al., 2011).

MS methods coupled with chromatography are powerful because they can target specific compounds and achieve a very high level of detail; not only lipid group types, but also the carbon chain length and structure can be identified and quantified. For biofuels research, it is important to know the structure and properties of the fuel for its compatibility to ICEs, and therefore these techniques are highly suited to obtaining this information. Furthermore, GC-MS allows for individual fatty acid quantification. Profiling the lipids can also help to identify suitable extraction solvents for an industrial process (Olmstead et al., 2013).

#### 10.11.6 Limitations

Many of the methods listed above have problems resolving and identifying lipid compounds. There may be several reasons why peaks are not detected. The problems of incomplete resolution have been discussed above. Incomplete resolution or overlap with unknown impurities can cause problems (Paik et al., 2009). Lipids with higher detection sensitivity can suppress and compromise the detection of those with lower sensitivity in MS (Vieler et al., 2007). Chlorophyll dominates the positive ion spectra in MS and can mask lipid detection; it is better to remove the chlorophyll prior to MS, or

to use negative ion spectra where lipids have a higher detection level (Vieler et al., 2007).

If chromatographic run times are shortened, the resolution of compounds is compromised (Barupal et al., 2010), and in pyrolysis GC-MS, there is risk of cross-contamination of samples with high boiling constituents starting to overlap. Thermal degradation can also fragment some of the compounds (Barupal et al., 2010).

Even when peaks are detected, there may be problems with identifications: since not all peaks may be identified, it is important to report all peaks and not just the known identifications in the analysis, to set data in its proper context and to account for the whole sample

(Barupal et al., 2010). Standards can be used for identification and quantification, but not all algal lipids are commercially available and therefore their spectra may not be identified (Vieler et al., 2007). Some methods will be targeted to specific groups of compounds, therefore it is good for quantifying desired compounds but not for giving an overview of what is present (Guan et al., 2011).

Some methods use derivatization or transesterification prior to GC or MS analysis and some use the original lipid samples (Guan et al., 2011). Clearly a major issue with this group of techniques is the amount of time and preparation that goes into sample processing; each sample will be run individually on MS or GC so running many samples could take days, whilst some methods like Nile Red can be done in a batch using 96 well plates and a plate reader in a single 6 hour (or less) run. This group of methods therefore seems unsuited to screening techniques. However, the quality of information obtained is very high, and necessary for ensuring the lipids are of good biofuel quality; choosing a method that is this information-rich is better if time and resources allow. Many methods discussed above are amenable to automation or simplification. The variation and potential for information loss due to poor separation techniques demonstrates that all programs must be optimized to ensure correct

identifications, since many parameters can affect the outcome. However, detailed and reliable information is possible if this optimization is carried out.

## 10.12 *Colorimetric techniques*

Colorimetric techniques use the reaction of fatty acids with another compound to effect a colorimetric change. The degree of the colour change is then used as a measure of the lipid content in the sample. To reduce the effect of variation between samples, background absorbance is taken into account (Cheng et al., 2011b).

### 10.12.1 Variations

Wawrik and Harriman (2010) used a colorimetric assay based on hydrolysis of lipids to fatty acids and extraction of their copper salts into chloroform, followed by a colour developing reagent (diethyldithiocarbamate) to form a yellow colour and measurement of optical density at 440 nm. Chen and Vaidyanathan (2012b) adapted this method so that it did not require a colour developer and also to ensure that triethanolamine was added in sufficient quantities to promote dissolution of copper ions in the organic phase. They also separated the extraction and complexing of FA, therefore avoiding the need for neutralisation after saponification. The pH of the copper and FA reaction is important and must be between 8 and 10, otherwise a film of FA is formed between the aqueous and organic phases. They also adapted the method to be done at room temperature, unlike the Wawrik and Harriman (2010) method which required 60°C. The method uses cell lysis, saponification of lipids and reaction with triethanolamine-copper salts (TEA-Cu) and the TEA-Cu-FA complex was detected at 260 nm. Lipid concentrations from as little as 1 mL of culture, using standards (shikimic acid, sodium decanoate, sodium dodecanoate, sodium palmitate and linoleic acid) are possible (Chen and Vaidyanathan, 2012b).

Cheng et al. (2011b) used a microplate sulfo-phospho-vanillin (SPV) colorimetric method, adapted from the original SPV method developed by Chabrol et al (1937) and used corn oil as a standard. The sample size required is less than 100  $\mu$ L and it is ideal for standards and samples that contain 5-120  $\mu$ g lipids. The method requires extraction so the previous issues of lipid extraction efficiency apply (see section 4.2), and data are normalized by lipid content of biomass. However, extraction can minimize the

interference of other cell components with the assay. After pre-treatment the assay takes less than one hour. The sample volume must be less than 100  $\mu$ L otherwise the reaction with the sulfuric acid cannot go to completion (Cheng et al., 2011b). An obvious advantage is that the optical spectra and reaction conditions do not have to be adapted for each sample source.

#### 10.12.2 Advantages

This group of methods operates on small volumes of 1-2 mL of algal culture. Using a micro-centrifuge format, 24 to 30 samples can be run at a time with the procedure taking less than two hours (Wawrik and Harriman, 2010). A big advantage is that nmol concentrations of FA can be quantified with recovery values above 95% and good reproducibility (Chen and Vaidyanathan, 2012b). There is an excellent linear relationship between absorbance and concentration for all fatty acid standards, with the exception of shikimic acid (Chen and Vaidyanathan, 2012b). The potential issue of protein co-extraction is minimized by the saponification reaction.

#### 10.12.3 Limitations

For these methods, lipids need to be saponified by heating so that membrane lipids are included. No structural information (chain length or degrees of unsaturation) is gained from this assay. Furthermore, direct mass quantitation is not possible, as the molar concentration of chloroform-extractable carboxyl groups, complexed with copper ions, is measured. An assumption of the average fatty acid chain length can convert the detected signal into a quantity of fatty acid in terms of mass, but due to this assumption it will be an estimation (Wawrik and Harriman, 2010). Importantly, short chain fatty acids are not measured, as the signal quickly decreases for chains less than twelve carbons long; similarly, cholesterol and lactic acid will not interfere with detection. Detergents cannot be used for cell lysis since they interfere with the assay. Instead glass beads can be used (Wawrik and Harriman, 2010). Finally, for the FA-copper method, copper contamination interferes with the assay measurement (Chen and Vaidyanathan, 2012b). Since colorimetric measurement is a multistep process, the potential for error is higher.

### 10.13 NMR

Liquid state NMR (nuclear magnetic resonance) spectroscopy is a non-destructive method which applies magnetic fields to nuclei of atoms in a sample and measures the resonant frequency emitted from the sample. This information can be used to create spectra of chemical shifts, which in turn provide information about the structure of a molecule. By measuring spectral peaks of desired molecules against either a standard or against another sample, information can be obtained on the levels of the molecule present in the sample.

The nuclei of specific element isotopes are targeted and measured in NMR. For example, Beal et al. (2010), used liquid state  $^{13}\text{C}$  and  $^{31}\text{P}$  NMR to identify lipids in intact algae cells, using glyceryl trioleate as a reference compound for indicating the presence of triglycerides in the samples. Specifically, the methylene peak is used as an indicator of lipid content. In another example, Gao et al. used time-domain NMR (2008) in a method based on relaxation time of the hydrogen nuclei of lipids in different phases of the analysed samples and of standards from pure lipid extract from the alga. Sarpal et al. (2015) used  $^1\text{H}$  and  $^{13}\text{C}$  spectra.

NMR can either be performed on whole cells or on extracted and esterified algal lipids using an internal standard to quantify the FAME (Boyle-Roden et al., 2003).

#### 10.13.1 Advantages

A significant advantage of NMR is that it is non-invasive, so the sample can be used for other tests (Gao et al., 2008). The movement of  $^{13}\text{C}$  in lipids and other compounds can be measured by NMR, so this is a tool not just for identifying chemical structure, but also the source of carbon assimilated (Boyle-Roden et al., 2003). Since chlorophyll and carotenoids do not contribute significant signals, they do not interfere (Beal et al., 2010).

If the test is non-invasive, the data cannot be expressed on a dry weight basis and instead must be normalized with cell numbers.

### 10.13.2 Limitations

There is a possibility of interference, as other compounds can contribute to the characteristic peaks for triglyceride (Beal et al., 2010). These compounds are those with long hydrocarbon chains — mainly, monoglycerides, diglycerides and phospholipids. Beal et al. (2010) showed that it is important to exclude the contributions of phospholipids to spectral peaks as they are less useful for biodiesel production.

The interference from other compounds may also be sample dependant, especially when comparing healthy and stressed cultures; indeed, healthy cultures tend to have higher proportions of mono- and diglycerides, which contribute to the apparent triglyceride peak (Beal et al., 2010). However, as these compounds are useful for biodiesel production, these peaks can still give useful information on the suitability of algal samples to biodiesel production (Beal et al., 2010).

Gao et al. (2008) showed that water can interfere with the measurement of lipids using TD-NMR, since the relaxation properties of lipids and free water are similar, making high water content in the sample a problem. In order to eliminate this, the sample can be freeze-dried (Gao et al., 2008).

### 10.14 FTIR

FTIR uses measurements of infrared absorption and molecular vibrational modes to identify and quantify macromolecules (Dean et al., 2010). This can be done on live cells (Wagner et al., 2010) or on dried algal samples (Stehfest et al., 2005).

The identification of lipids and fatty acids is by the assignment of wave number  $1740\text{ cm}^{-1}$  to C=O of ester groups, which are primarily from lipids and fatty acids (Stehfest et al., 2005). Levels are expressed in terms of ratios with other molecules, such as amides (Stehfest et al., 2005). In order to make it a quantitative procedure, the functional group needs to be quantified using a calibration curve of reference substances specific to the lipid classes (Wagner et al., 2010). Triolein is an example standard (Miglio et al., 2013). Spectra of reference substances and algal cells are used to calculate the relative contribution of these substances to the cell spectrum (Wagner et al., 2010). Since it is

possible to measure the CH<sub>2</sub>/CH<sub>3</sub> ratio, quantification of chain-type differences between samples is achievable (Miglio et al., 2013). Variation in spectra can be assumed to arise from variation in lipid type (i.e. chain length and molecular structure) (Wagner et al., 2010). A similar technique is near-infrared spectroscopy which measures absorption and vibration in the near-infrared spectrum (Liu et al., 2015).

#### 10.14.1 Advantages

The advantage of FTIR is that it can be used on intact cells, it can get information at the cellular level, and it can simultaneously be used to study other macromolecules as well as lipids (Dean et al., 2010). Using a wide range of standards, many lipid classes can be studied, and the cellular content data can be determined without cell preparation (Wagner et al., 2010). A small number of cells can be used for analysis (Wagner et al., 2010) - as little as a single cell (Stehfest et al., 2005) - and FTIR can be used over a period of several hours and therefore give information on cellular macromolecular compositional changes (Wagner et al., 2010). The data is therefore expressed on a per cell basis. It has been suggested that the method is able to identify greater lipid changes than Nile Red staining (Dean et al., 2010).

#### 10.14.2 Limitations

FTIR band shifts in relation to nutrient deprivation are species specific, and therefore in common with the majority of lipid methods, this method cannot be used to detect changes in mixed algal cultures (Stehfest et al., 2005). There is debate about the limitations of the Beer-Lambert law in analysing the chosen analyte in whole cells via absorbance measurements. As there is limitation in the absorption range, the cell concentrations in the sample must be restricted so that the Beer-Lambert law applies (Wagner et al., 2010).

It seems possible that contributions from other molecules with C=O in ester groups will interfere with lipid readings, although there is no evidence of this in the literature reviewed here. FTIR can provide a high degree of information with a small sample size

and minimal sample preparation, making it a very useful tool for analysing lipid types in algae cells.

### **10.15 *Miscellaneous techniques***

In this section less popular techniques, that do not fit into any of the previous categories, are briefly discussed.

Elemental analysis, whereby the lipid is calculated by subtracting the carbohydrate, protein and ash content of the biomass (Torzillo et al., 1991), has the obvious downside that there are no definitive direct measurements of the lipid content. Whilst some assumptions can be made about the biomass composition, this technique can yield no useful information to answer the questions of interest about algal lipid content.

Eroglu and Melis (2009) used gradient centrifugation of a sample within a gradient of either sucrose, Percoll<sup>®</sup> or CsCl as a measurement of sample density. The density of biomass was compared to that of pure target products, such as extracellular hydrocarbons or lipids. These densities are then used to calculate the percentage of target product in a sample. The advantages of this method lie in it being a fast and easy method to use, however, it relies heavily on estimation of the density and would suffer from accuracy issues.

One method (Solovchenko et al., 2011) used prepared correlation curves of Car/Chl ratio and TFA percentage (measured by GC) and then used spectrophotometric measurements to estimate the TFA content subsequently in a non-destructive assay. Therefore this method is only applicable to the tested species and relies on the relationship between the Car/Chl ratio and TFA staying consistent in all subsequent experiments, but it can show stress induced lipid changes without repeating the lipid measurement procedure. This is advantageous in cases where all the desired information is about one strain.

## 10.16 *Conclusions*

As previously discussed, methods for lipid analysis of algae must be selected according to their suitability to the species and to the type of information required from the assay. To obtain detailed information about the type of lipid classes in a sample, chromatography methods such as GC must be used. For fast screening of species for their overall lipid content, a high throughput method such as Nile Red is often used for comparative analysis, but in practice is rarely truly comparable between species. Instead, methods must be optimised to the species and information required and researchers must look beyond the commonly accepted methods to those most suitable to their needs. The decision trees we have constructed here will help researchers in choosing a suitable technique for lipid measurement for microalgae. We have demonstrated that one size does not fit all in terms of measurement of algal lipids. Nile Red staining, which was previously identified by another review as the most suitable method on average (Han et al., 2011), has been shown to have many limitations in terms of confounding factors and no differentiation of lipid types. Similarly, the gravimetric method, which Han et al. state to be the most accurate method (2011), has issues relating to its accuracy that have been discussed in detail in this review.

Methods must mainly be chosen according to the amount of culture available and the information required from the study. Perhaps the most suitable method for direct comparison between species is direct esterification, since this shows the potential of algal biomass to be converted to lipids. However, this method like all others is subject to variation in its execution, so it is only truly comparable if the method is standardised. This area of research continues to be very problematic, but by analysing the potential advantages and problems associated with each technique, we hope to come closer to solving the issue of how to choose between the myriad of algal lipid measurement techniques available. Ultimately the choice of methods will also be influenced by the availability of equipment and resources in a researcher's laboratory, but where possible we must strive to shift the adoption of methods towards those that are the most scientifically suitable.

## 10.17 Acknowledgements

Many thanks to the EPSRC (EP/E036252/1) and the Energy Futures DTC and to Fondation pour la Recherche Médicale (FRM, grant code: ING20140129444) (funding body of Josselin Noirel).

## 10.18 References

. U.S. Energy Information Administration.

Abis, K.L., and Mara, D.D. (2005). Primary facultative ponds in the UK: the effect of operational parameters on performance and algal populations. *Water Science and Technology* *51*, 61-67.

Adam, F., Abert-Vian, M., Peltier, G., and Chemat, F. (2012). "Solvent-free" ultrasound-assisted extraction of lipids from fresh microalgae cells: A green, clean and scalable process. *Bioresource Technology* *114*, 457-465.

Adams, C., Godfrey, V., Wahlen, B., Seefeldt, L., and Bugbee, B. (2013). Understanding precision nitrogen stress to optimize the growth and lipid content tradeoff in oleaginous green microalgae. *Bioresource Technology* *131*, 188-194.

Adl, S.M., Simpson, A.G.B., Lane, C.E., Lukes, J., Bass, D., Bowser, S.S., Brown, M.W., Burki, F., Dunthorn, M., Hampl, V., *et al.* (2012). The Revised Classification of Eukaryotes. *Journal of Eukaryotic Microbiology* *59*, 429-493.

Affenzeller, M.J., Darehshouri, A., Andosch, A., Lütz, C., and Lütz-Meindl, U. (2009). Salt stress-induced cell death in the unicellular green alga *Micrasterias denticulata*. *Journal of Experimental Botany* *60*, 939-954.

Aggarwal, K., Choe, L.H., and Lee, K.H. (2006). Shotgun proteomics using the iTRAQ isobaric tags. *Briefings in Functional Genomics & Proteomics* *5*, 112-120.

Ahn, J.W., Hwangbo, K., Yin, C.J., Lim, J.M., Choi, H.G., Park, Y.I., and Jeong, W.J. (2015). Salinity-dependent changes in growth and fatty acid composition of new Arctic *Chlamydomonas* species, ArM0029A. *Plant Cell Tissue Organ Cult* *120*, 1015-1021.

Akoto, L., Stellaard, F., Irth, H., Vreuls, R.J.J., and Pel, R. (2008). Improved fatty acid detection in micro-algae and aquatic meiofauna species using a direct thermal desorption interface combined with comprehensive gas chromatography–time-of-flight mass spectrometry. *Journal of Chromatography A* *1186*, 254-261.

Albertyn, J., Hohmann, S., Thevelein, J.M., and Prior, B.A. (1994). GPD1, which encodes glycerol-3-phosphate dehydrogenase, is essential for growth under osmotic stress in

*Saccharomyces cerevisiae*, and its expression is regulated by the high-osmolarity glycerol response pathway. *Meth Cell Biol* **14**.

Allakhverdiev, S.I., Kinoshita, M., Inaba, M., Suzuki, I., and Murata, N. (2001). Unsaturated Fatty Acids in Membrane Lipids Protect the Photosynthetic Machinery against Salt-Induced Damage in *Synechococcus*. *Plant Physiology* **125**, 1842-1853.

Allakhverdiev, S.I., Nishiyama, Y., Miyairi, S., Yamamoto, H., Inagaki, N., Kanesaki, Y., and Murata, N. (2002). Salt Stress Inhibits the Repair of Photodamaged Photosystem II by Suppressing the Transcription and Translation of *psbA* Genes in *Synechocystis*. *Plant Physiology* **130**, 1443-1453.

Allakhverdiev, S.I., Nishiyama, Y., Takahashi, S., Miyairi, S., Suzuki, I., and Murata, N. (2005). Systematic analysis of the relation of electron transport and ATP synthesis to the photodamage and repair of photosystem II in *Synechocystis*. *Plant Physiology* **137**, 263-273.

Allakhverdiev, S.I., Sakamoto, A., Nishiyama, Y., Inaba, M., and Murata, N. (2000). Ionic and Osmotic Effects of NaCl-Induced Inactivation of Photosystems I and II in *Synechococcus* sp. *Plant Physiology* **123**, 1047-1056.

Allen, M.B. (1956). Excretion of Organic Compounds by *Chlamydomonas*. *Archiv Fur Mikrobiologie* **24**, 163-168.

An, M., Mou, S., Zhang, X., Zheng, Z., Ye, N., Wang, D., Zhang, W., and Miao, J. (2013). Expression of fatty acid desaturase genes and fatty acid accumulation in *Chlamydomonas* sp. ICE-L under salt stress. *Bioresource Technology* **149**, 77-83.

Araujo, G.S., Matos, L.J.B.L., Fernandes, J.O., Cartaxo, S.J.M., Gonçalves, L.R.B., Fernandes, F.A.N., and Farias, W.R.L. (2013). Extraction of lipids from microalgae by ultrasound application: Prospection of the optimal extraction method. *Ultrasonics Sonochemistry*.

Aresta, M., Dibenedetto, A., Carone, M., Colonna, T., and Fragale, C. (2005). Production of biodiesel from macroalgae by supercritical CO<sub>2</sub> extraction and thermochemical liquefaction. *Environmental Chemistry Letters* **3**, 136-139.

ASTM International. ASTM D6751 - 12: Standard Specification for Biodiesel Fuel Blend Stock (B100) for Middle Distillate Fuels.

Avidan, O., Brandis, A., Rogachev, I., and Pick, U. (2015). Enhanced acetyl-CoA production is associated with increased triglyceride accumulation in the green alga *Chlorella desiccata*. *Journal of Experimental Botany* **66**, 3725-3735.

Azachi, M., Sadka, A., Fisher, M., Goldshlag, P., Gokhman, I., and Zamir, A. (2002). Salt induction of fatty acid elongase and membrane lipid modifications in the extreme halotolerant alga *Dunaliella salina*. *Plant Physiology* **129**, 1320-1329.

Bai, X., Ghasemi Naghdi, F., Ye, L., Lant, P., and Pratt, S. (2014). Enhanced lipid extraction from algae using free nitrous acid pretreatment. *Bioresource Technology* 159, 36-40.

Balasubramanian, R.K., Thi Thai Yen, D., and Obbard, J.P. (2013). Factors affecting cellular lipid extraction from marine microalgae. *Chemical Engineering Journal* 215, 929-936.

Baliga, R., and Powers, S.E. (2010). Sustainable algae biodiesel production in cold climates. *International Journal of Chemical Engineering*.

Ball, S.G., Dirick, L., Decq, A., Martiat, J.-C., and Matagne, R. (1990). Physiology of starch storage in the monocellular alga *Chlamydomonas reinhardtii*. *Plant Science* 66, 1-9.

Ballicora, M.A., Iglesias, A.A., and Preiss, J. (2004). ADP-glucose pyrophosphorylase: a regulatory enzyme for plant starch synthesis. *Photosynthesis Research* 79, 1-24.

Bantscheff, M., Schirle, M., Sweetman, G., Rick, J., and Kuster, B. (2007). Quantitative mass spectrometry in proteomics: a critical review. *Analytical and Bioanalytical Chemistry* 389, 1017-1031.

Bartley, M.L., Boeing, W.J., Corcoran, A.A., Holguin, F.O., and Schaub, T. (2013). Effects of salinity on growth and lipid accumulation of biofuel microalga *Nannochloropsis salina* and invading organisms. *Biomass and Bioenergy* 54, 83-88.

Barupal, D., Kind, T., Kothari, S., Lee, D., and Fiehn, O. (2010). Hydrocarbon phenotyping of algal species using pyrolysis-gas chromatography mass spectrometry. *BMC Biotechnology* 10, 40.

Batterto, J.C., and Vanbaale, C. (1971). Growth responses of blue-green algae to sodium chloride concentration. *Archiv Fur Mikrobiologie* 76, 151-&.

Beal, C., Smith, C., Webber, M., Ruoff, R., and Hebner, R. (2011). A Framework to Report the Production of Renewable Diesel from Algae. *Bioenergy Research* 4, 36-60.

Beal, C.M., Webber, M.E., Ruoff, R.S., and Hebner, R.E. (2010). Lipid analysis of *Neochloris oleoabundans* by liquid state NMR. *Biotechnology and Bioengineering* 106, 573-583.

Beckmann, J., Lehr, F., Finazzi, G., Hankamer, B., Posten, C., Wobbe, L., and Kruse, O. (2009). Improvement of light to biomass conversion by de-regulation of light-harvesting protein translation in *Chlamydomonas reinhardtii*. *Journal of Biotechnology* 142, 70-77.

Ben-Amotz, A., and Avron, M. (1983). On the Factors Which Determine Massive  $\beta$ -Carotene Accumulation in the Halotolerant Alga *Dunaliella bardawil*. *Plant Physiology* 72, 593-597.

Benemann, J.R. (1993). Utilization of carbon dioxide from fossil fuel-burning power plants with biological systems. *Energy Conversion and Management* 34, 999-1004.

Bertozzini, E., Galluzzi, L., Penna, A., and Magnani, M. (2011). Application of the standard addition method for the absolute quantification of neutral lipids in microalgae using Nile red. *Journal of Microbiological Methods* *87*, 17-23.

Beynon, R.J., and Pratt, J.M. (2005). Metabolic Labeling of Proteins for Proteomics. *Molecular & Cellular Proteomics* *4*, 857-872.

Bhatnagar, A., Chinnasamy, S., Singh, M., and Das, K.C. (2011). Renewable biomass production by mixotrophic algae in the presence of various carbon sources and wastewaters. *Applied Energy* *88*, 3425-3431.

Biofuel Systems Group Ltd. Biodiesel Standards.

Bišová, K., and Zachleder, V. (2014). Cell-cycle regulation in green algae dividing by multiple fission. *Journal of Experimental Botany*.

Blatti, J.L., Michaud, J., and Burkart, M.D. (2013). Engineering fatty acid biosynthesis in microalgae for sustainable biodiesel. *Current Opinion in Chemical Biology* *17*, 496-505.

Bligh, E.G., and Dyer, W.J. (1959). A rapid method of total lipid extraction and purification. *Canadian Journal of Biochemistry and Physiology* *37*, 911-917.

Blokhina, O., Virolainen, E., and Fagerstedt, K.V. (2003). Antioxidants, Oxidative Damage and Oxygen Deprivation Stress: a Review. *Annals of Botany* *91*, 179-194.

Bonferroni, C.E. (1936). *Teoria statistica delle classi e calcolo delle probabilita* (Libreria internazionale Seeber).

Borowitzka, M.A., Borowitzka, L.J., and Kessly, D. (1990). Effects of salinity increase on carotenoid accumulation in the green alga *Dunaliella salina*. *Journal of Applied Phycology* *2*, 111-119.

Botham, P.A., and Ratledge, C. (1979). A biochemical explanation for lipid accumulation in *Candida* 107 and other oleaginous micro-organisms. *Journal of General Microbiology* *114*, 361-375.

Bou Khalil, M., Hou, W., Zhou, H., Elisma, F., Swayne, L.A., Blanchard, A.P., Yao, Z., Bennett, S.A.L., and Figeys, D. (2010). Lipidomics era: Accomplishments and challenges. *Mass Spectrometry Reviews* *29*, 877-929.

Boussiba, S., Bing, W., Yuan, J.-P., Zarka, A., and Chen, F. (1999). Changes in pigments profile in the green alga *Haematoctococcus pluvialis* exposed to environmental stresses. *Biotechnology Letters* *21*, 601-604.

Boyle-Roden, E., German, J.B., and Wood, B.J.B. (2003). The production of lipids alternately labelled with carbon-13. *Biomolecular Engineering* *20*, 285-289.

Brennan, L., Blanco Fernández, A., Mostaert, A.S., and Owende, P. (2012). Enhancement of BODIPY505/515 lipid fluorescence method for applications in biofuel-directed microalgae production. *Journal of Microbiological Methods* *90*, 137-143.

Brennan, L., and Owende, P. (2010). Biofuels from microalgae-A review of technologies for production, processing, and extractions of biofuels and co-products. *Renewable & Sustainable Energy Reviews* *14*, 557-577.

Brönstrup, M. (2004). Absolute quantification strategies in proteomics based on mass spectrometry. *Expert Review of Proteomics* *1*, 503-512.

Buhr, H.O., and Miller, S.B. (1983). A dynamic model of the high-rate algal-bacterial wastewater treatment pond. *Water Research* *17*, 29-37.

Cabanelas, I.T.D., van der Zwart, M., Kleinegris, D.M.M., Barbosa, M.J., and Wijffels, R.H. (2015). Rapid method to screen and sort lipid accumulating microalgae. *Bioresource Technology* *184*, 47-52.

Cai, G., Jin, B., Saint, C., and Monis, P. (2011). Genetic manipulation of butyrate formation pathways in *Clostridium butyricum*. *J Biotechnol* *155*, 269-274.

Cakmak, T., Angun, P., Demiray, Y.E., Ozkan, A.D., Elibol, Z., and Tekinay, T. (2012). Differential effects of nitrogen and sulfur deprivation on growth and biodiesel feedstock production of *Chlamydomonas reinhardtii*. *Biotechnology and Bioengineering* *109*, 1947-1957.

Cavonius, L., Fink, H., Kiskis, J., Albers, E., Undeland, I., and Enejder, A. (2015). Imaging of Lipids in Microalgae with Coherent Anti-Stokes Raman Scattering Microscopy. *Plant Physiology* *167*, 603-616.

Cavonius, L.R., Carlsson, N.-G., and Undeland, I. (2014). Quantification of total fatty acids in microalgae: comparison of extraction and transesterification methods. *Analytical and Bioanalytical Chemistry* *406*, 7313-7322.

Chen, H., Lao, Y.-M., and Jiang, J.-G. (2011a). Effects of salinities on the gene expression of a (NAD<sup>+</sup>)-dependent glycerol-3-phosphate dehydrogenase in *Dunaliella salina*. *Science of the Total Environment* *409*, 1291-1297.

Chen, L., Wu, L.N., Zhu, Y., Song, Z.D., Wang, J.X., and Zhang, W.W. (2014). An orphan two-component response regulator Slr1588 involves salt tolerance by directly regulating synthesis of compatible solutes in photosynthetic *Synechocystis* sp PCC 6803. *Molecular Biosystems* *10*, 1765-1774.

Chen, M., Tang, H., Ma, H., Holland, T.C., Ng, K.Y.S., and Salley, S.O. (2011b). Effect of nutrients on growth and lipid accumulation in the green algae *Dunaliella tertiolecta*. *Bioresource Technology* *102*, 1649-1655.

Chen, S., Chen, X., Peng, Y., and Peng, K. (2009a). A mathematical model of the effect of nitrogen and phosphorus on the growth of blue-green algae population. *Applied Mathematical Modelling* 33, 1097-1106.

Chen, W., Sommerfeld, M., and Hu, Q. (2011c). Microwave-assisted Nile red method for in vivo quantification of neutral lipids in microalgae. *Bioresource Technology* 102, 135-141.

Chen, W., Zhang, C., Song, L., Sommerfeld, M., and Hu, Q. (2009b). A high throughput Nile red method for quantitative measurement of neutral lipids in microalgae. *Journal of Microbiological Methods* 77, 41-47.

Chen, Y., and Vaidyanathan, S. (2012a). A simple, reproducible and sensitive spectrophotometric method to estimate microalgal lipids. *Analytica Chimica Acta* 724, 67-72.

Chen, Y., and Vaidyanathan, S. (2012b). A simple, reproducible and sensitive spectrophotometric method to estimate microalgal lipids. *Analytica Chimica Acta* 724, 67-72.

Cheng, C.-H., Du, T.-B., Pi, H.-C., Jang, S.-M., Lin, Y.-H., and Lee, H.-T. (2011a). Comparative study of lipid extraction from microalgae by organic solvent and supercritical CO<sub>2</sub>. *Bioresource Technology* 102, 10151-10153.

Cheng, Y.S., Zheng, Y., and VanderGheynst, J.S. (2011b). Rapid Quantitative Analysis of Lipids Using a Colorimetric Method in a Microplate Format. *Lipids* 46, 95-103.

Cherif, A., Dubacq, J., Mache, R., Oursel, A., and Tremolieres, A. (1975). Biosynthesis of  $\alpha$ -linolenic acid by desaturation of oleic and linoleic acids in several organs of higher and lower plants and in algae. *Phytochemistry* 14, 703-706.

Chisti, Y. (2007). Biodiesel from microalgae. *Biotechnology Advances* 25, 294-306.

Chisti, Y. (2008). Biodiesel from microalgae beats bioethanol. *Trends in Biotechnology* 26, 126-131.

Chisti, Y. (2013). Constraints to commercialization of algal fuels. *Journal of Biotechnology* 167, 201-214.

Chiu, S.Y., Kao, C.Y., Tsai, M.T., Ong, S.C., Chen, C.H., and Lin, C.S. (2009). Lipid accumulation and CO<sub>2</sub> utilization of *Nannochloropsis oculata* in response to CO<sub>2</sub> aeration. *Bioresource Technology* 100, 833-838.

Choi, Y.E., Hwang, H., Kim, H.S., Ahn, J.W., Jeong, W.J., and Yang, J.W. (2013). Comparative proteomics using lipid over-producing or less-producing mutants unravels lipid metabolisms in *Chlamydomonas reinhardtii*. *Bioresource Technology* 145, 108-115.

Chong, P.K., Gan, C.S., Pham, T.K., and Wright, P.C. (2006). Isobaric Tags for Relative and Absolute Quantitation (iTRAQ) Reproducibility: Implication of Multiple Injections. *Journal of Proteome Research* 5, 1232-1240.

Christensen, E., Sudasinghe, N., Dandamudi, K.P.R., Sebag, R., Schaub, T., and Laurens, L.M.L. (2015). Rapid Analysis of Microalgal Triacylglycerols with Direct-Infusion Mass Spectrometry. *Energy & Fuels* 29, 6443-6449.

Cirulis, J.T., Strasser, B.C., Scott, J.A., and Ross, G.M. (2012). Optimization of staining conditions for microalgae with three lipophilic dyes to reduce precipitation and fluorescence variability. *Cytometry Part A* 81A, 618-626.

Cohen, Z., Vonshak, A., and Richmond, A. (1988). Effect of environmental conditions on fatty acid composition of the red alga *Porphyridium cruentum*: Correlation to growth rate. *Journal of Phycology* 24, 328-332.

Cooksey, K.E., Guckert, J.B., Williams, S.A., and Callis, P.R. (1987). Fluorometric determination of the neutral lipid content of microalgal cells using Nile Red. *Journal of Microbiological Methods* 6, 333-345.

Costenoble, O., Mittelbach, M., Schober, S., Fischer, J., and Haupt, J. (2008). Improvements needed for the biodiesel standard EN 14214: Final report for Lot 1 of the Bioscopes project

Courchesne, N.M.D., Parisien, A., Wang, B., and Lan, C.Q. (2009). Enhancement of lipid production using biochemical, genetic and transcription factor engineering approaches. *Journal of Biotechnology* 141, 31-41.

Cox, J., and Mann, M. (2011). Quantitative, High-Resolution Proteomics for Data-Driven Systems Biology. In *Annual Review of Biochemistry*, Vol 80, R.D. Kornberg, C.R.H. Raetz, J.E. Rothman, and J.W. Thorner, eds., pp. 273-299.

da Silva, T., Reis, A., Medeiros, R., Oliveira, A., and Gouveia, L. (2009). Oil Production Towards Biofuel from Autotrophic Microalgae Semicontinuous Cultivations Monitorized by Flow Cytometry. *Applied Biochemistry and Biotechnology* 159, 568-578.

Damiani, M.C., Popovich, C.A., Constenla, D., and Leonardi, P.I. (2010). Lipid analysis in *Haematococcus pluvialis* to assess its potential use as a biodiesel feedstock. *Bioresource Technology* 101, 3801-3807.

Datta, S., and DePadilla, L.M. (2006). Feature selection and machine learning with mass spectrometry data for distinguishing cancer and non-cancer samples. *Statistical Methodology* 3, 79-92.

Davis, R., Aden, A., and Pienkos, P.T. (2011). Techno-economic analysis of autotrophic microalgae for fuel production. *Applied Energy* 88, 3524-3531.

De Bhowmick, G., Koduru, L., and Sen, R. (2015). Metabolic pathway engineering towards enhancing microalgal lipid biosynthesis for biofuel application—A review. *Renewable and Sustainable Energy Reviews* *50*, 1239-1253.

De la Hoz Siegler, H., Ayidzoe, W., Ben-Zvi, A., Burrell, R.E., and McCaffrey, W.C. (2012). Improving the reliability of fluorescence-based neutral lipid content measurements in microalgal cultures. *Algal Research* *1*, 176-184.

de la Jara, A., Mendoza, H., Martel, A., Molina, C., Nordstron, L., de la Rosa, V., and Diaz, R. (2003). Flow cytometric determination of lipid content in a marine dinoflagellate, *Cryptothecodinium cohnii*. *Journal of Applied Phycology* *15*, 433-438.

Dean, A.P., Sigee, D.C., Estrada, B., and Pittman, J.K. (2010). Using FTIR spectroscopy for rapid determination of lipid accumulation in response to nitrogen limitation in freshwater microalgae. *Bioresource Technology* *101*, 4499-4507.

Demetriou, G., Neonaki, C., Navakoudis, E., and Kotzabasis, K. (2007). Salt stress impact on the molecular structure and function of the photosynthetic apparatus—The protective role of polyamines. *Biochimica et Biophysica Acta (BBA) - Bioenergetics* *1767*, 272-280.

Demiral, T., and Türkan, İ. (2005). Comparative lipid peroxidation, antioxidant defense systems and proline content in roots of two rice cultivars differing in salt tolerance. *Environmental and Experimental Botany* *53*, 247-257.

Demirbas, A. (2011). Biodiesel from oilgae, biofixation of carbon dioxide by microalgae: A solution to pollution problems. *Applied Energy* *88*, 3541-3547.

Deng, X., Cai, J., and Fei, X. (2013). Effect of the expression and knockdown of citrate synthase gene on carbon flux during triacylglycerol biosynthesis by green algae *Chlamydomonas reinhardtii*. *BMC Biochemistry* *14*, 38-38.

Devos, N., Ingouff, M., Loppes, R., and Matagne, R.F. (1998). Rubisco adaptation to low temperatures: A comparative study in psychrophilic and mesophilic unicellular algae. *Journal of Phycology* *34*, 655-660.

Dismukes, G.C., Carrieri, D., Bennette, N., Ananyev, G.M., and Posewitz, M.C. (2008). Aquatic phototrophs: efficient alternatives to land-based crops for biofuels. *Current Opinion in Biotechnology* *19*, 235-240.

Domon, B., and Aebersold, R. (2006). Review - Mass spectrometry and protein analysis. *Science* *312*, 212-217.

Domon, B., and Aebersold, R. (2010). Options and considerations when selecting a quantitative proteomics strategy. *Nat Biotech* *28*, 710-721.

Dresselhaus, M.S., and Thomas, I.L. (2001). Alternative energy technologies. *Nature* 414, 332-337.

Drubin, D.A., Way, J.C., and Silver, P.A. (2007). Designing biological systems. *Genes & Development* 21, 242-254.

Du, C., Liang, J.-R., Chen, D.-D., Xu, B., Zhuo, W.-H., Gao, Y.-H., Chen, C.-P., Bowler, C., and Zhang, W. (2014). iTRAQ-Based Proteomic Analysis of the Metabolism Mechanism Associated with Silicon Response in the Marine Diatom *Thalassiosira pseudonana*. *Journal of Proteome Research* 13, 720-734.

Dubini, A. (2011). Green Energy from Green Algae. *The Biochemical Society*, 20-23.

Dubinsky, Z., and Berman-Frank, I. (2001). Uncoupling primary production from population growth in photosynthesizing organisms in aquatic ecosystems. *Aquatic Sciences* 63, 4-17.

Eckardt, N.A. (2014). Nitrogen-Sparing Mechanisms in *Chlamydomonas*: Reduce, Reuse, Recycle, and Reallocate. *Plant Cell* 26, 1379-1379.

El-Baky, H.H.A., El-Baz, F.K., and El-Baroty, G.S. (2004). Production of lipids rich in omega 3 fatty acids from the halotolerant alga *Dunaliella salina*. *Biotechnology* 3, 102-108.

Elliott, M.H., Smith, D.S., Parker, C.E., and Borchers, C. (2009). Current trends in quantitative proteomics. *Journal of Mass Spectrometry* 44, 1637-1660.

Eroglu, E., and Melis, A. (2009). "Density Equilibrium" Method for the Quantitative and Rapid In Situ Determination of Lipid, Hydrocarbon, or Biopolymer Content in Microorganisms. *Biotechnology and Bioengineering* 102, 1406-1415.

Evans, C., Noirel, J., Ow, S.Y., Salim, M., Pereira-Medrano, A.G., Couto, N., Pandhal, J., Smith, D., Pham, T.K., Karunakaran, E., *et al.* (2012). An insight into iTRAQ: where do we stand now? *Analytical and Bioanalytical Chemistry* 404, 1011-1027.

Fan, J., Andre, C., and Xu, C. (2011). A chloroplast pathway for the de novo biosynthesis of triacylglycerol in *Chlamydomonas reinhardtii*. *Febs Letters* 585, 1985-1991.

Fidalgo, J.P., Cid, A., Torres, E., Sukenik, A., and Herrero, C. (1998). Effects of nitrogen source and growth phase on proximate biochemical composition, lipid classes and fatty acid profile of the marine microalga *Isochrysis galbana*. *Aquaculture* 166, 105-116.

Fjerbaek, L., Christensen, K.V., and Norddahl, B. (2009). A review of the current state of biodiesel production using enzymatic transesterification. *Biotechnology and Bioengineering* 102, 1298-1315.

Flowers, J.M., Hazzouri, K.M., Pham, G.M., Rosas, U., Bahmani, T., Khraiwesh, B., Nelson, D.R., Jijakli, K., Abdrabu, R., Harris, E.H., *et al.* (2015). Whole-Genome Resequencing Reveals

Extensive Natural Variation in the Model Green Alga *Chlamydomonas reinhardtii*. *The Plant Cell* 27, 2353-2369.

Foy, R.H., and Smith, R.V. (1980). The role of carbohydrate accumulation in the growth of planktonic *Oscillatoria* species. *British Phycological Journal* 15, 139-150.

Fu, D., Lu, F.-K., Zhang, X., Freudiger, C., Pernik, D.R., Holtom, G., and Xie, X.S. (2012). Quantitative Chemical Imaging with Multiplex Stimulated Raman Scattering Microscopy. *Journal of the American Chemical Society* 134, 3623-3626.

Fu, X.-h., Gao, Y.-f., Hao, S.-j., Zhang, B.-s., and Ren, D.-m. (2007). Knockout of *aroL* gene in *Escherichia coli* Top10F' and its effects on the shikimic acid biosynthesis. *Fudan Xuebao Ziranxueban* 46, 366-370.

Fuller, H., and Morris, G. (2012). Quantitative proteomics using iTRAQ labeling and mass spectrometry. *Integrative Proteomics Croatia: InTech*, 347-362.

Gallagher, B.J. (2011). The economics of producing biodiesel from algae. *Renewable Energy* 36, 158-162.

Gan, C.S., Chong, P.K., Pham, T.K., and Wright, P.C. (2007). Technical, experimental, and biological variations in isobaric tags for relative and absolute quantitation (iTRAQ). *Journal of Proteome Research* 6, 821-827.

Gao, C., Xiong, W., Zhang, Y., Yuan, W., and Wu, Q. (2008). Rapid quantitation of lipid in microalgae by time-domain nuclear magnetic resonance. *Journal of Microbiological Methods* 75, 437-440.

Gao, Y., Lim, T.K., Lin, Q., and Li, S.F.Y. (in press). Identification of cypermethrin induced protein changes in green algae by iTRAQ quantitative proteomics. *Journal of Proteomics*.

Ghosh, D., and Xu, J. (2014). Abiotic stress responses in plant roots: a proteomics perspective. *Frontiers in Plant Science* 5, 6.

Gilmour, D.J., Hipkins, M.F., Webber, A.N., Baker, N.R., and Boney, A.D. (1985). The Effect of Ionic Stress on Photosynthesis in *Dunaliella tertiolecta* - Chlorophyll Fluorescence Kinetics and Spectral Characteristics. *Planta* 163, 250-256.

Ginzburg, M., and Ginzburg, B.Z. (1981). Interrelationships of light, temperature, sodium chloride and carbon source in growth of halotolerant and halophilic strains of *Dunaliella*. *British Phycological Journal* 16, 313-324.

Giroud, C., Gerber, A., and Eichenberger, W. (1988). Lipids of *Chlamydomonas reinhardtii*. Analysis of Molecular Species and Intracellular Site(s) of Biosynthesis. *Plant and Cell Physiology* 29, 587-595.

Go, S., Lee, S.-J., Jeong, G.-T., and Kim, S.-K. (2012). Factors affecting the growth and the oil accumulation of marine microalgae, *Tetraselmis suecica*. *Bioprocess and Biosystems Engineering* 35, 145-150.

Godswill, N.-N., Frank, N.-E.G., Edson, M.-Y.J., Emmanue, Y., Martin, B.J., Hermine, N.-B., Kingsley, T.-M., Constant, L.-L.-N.B., and Armand, N.-M. (2014). GC-FID Method Development and Validation Parameters for Analysis of Palm Oil (*Elaeis guineensis* Jacq.) Fatty Acids Composition. *Research in Plant Sciences* 2, 53-66.

Goho, S., and Bell, G. (2000). Mild environmental stress elicits mutations affecting fitness in *Chlamydomonas*. *Proceedings of the Royal Society B: Biological Sciences* 267, 123-129.

Goldemberg, J. (2007). Ethanol for a sustainable energy future. *Science* 315, 808-810.

Goldman, J.C. (1977). Temperature effects on phytoplankton growth in continuous culture. *Limnology and Oceanography* 22, 932-936.

Goncalves, E.C., Wilkie, A.C., Kirst, M., and Rathinasabapathi, B. (2015). Metabolic regulation of triacylglycerol accumulation in the green algae: identification of potential targets for engineering to improve oil yield. *Plant Biotechnology Journal*, n/a-n/a.

Gouveia, L., and Oliveira, A.C. (2009). Microalgae as a raw material for biofuels production. *Journal of Industrial Microbiology & Biotechnology* 36, 269-274.

Govender, T., Ramanna, L., Rawat, I., and Bux, F. (2012). BODIPY staining, an alternative to the Nile Red fluorescence method for the evaluation of intracellular lipids in microalgae. *Bioresource Technology* 114, 507-511.

Goyal, A. (2007). Osmoregulation in *Dunaliella*, Part II: Photosynthesis and starch contribute carbon for glycerol synthesis during a salt stress in *Dunaliella tertiolecta*. *Plant Physiology and Biochemistry* 45, 705-710.

Greenspan, P., Mayer, E.P., and Fowler, S.D. (1985). NILE RED - A SELECTIVE FLUORESCENT STAIN FOR INTRACELLULAR LIPID DROPLETS. *Journal of Cell Biology* 100, 965-973.

Griffin, N.M., Yu, J., Long, F., Oh, P., Shore, S., Li, Y., Koziol, J.A., and Schnitzer, J.E. (2010). Label-free, normalized quantification of complex mass spectrometry data for proteomic analysis. *Nat Biotech* 28, 83-89.

Griffiths, M.J., Garcin, C., van Hille, R.P., and Harrison, S.T.L. (2011). Interference by pigment in the estimation of microalgal biomass concentration by optical density. *Journal of Microbiological Methods* 85, 119-123.

Griffiths, M.J., and Harrison, S.T.L. (2009). Lipid productivity as a key characteristic for choosing algal species for biodiesel production. *Journal of Applied Phycology* 21, 493-507.

Griffiths, M.J., van Hille, R.P., and Harrison, S.T.L. (2010). Selection of Direct Transesterification as the Preferred Method for Assay of Fatty Acid Content of Microalgae. *Lipids* 45, 1053-1060.

Grossman, A.R., Harris, E.E., Hauser, C., Lefebvre, P.A., Martinez, D., Rokhsar, D., Shrager, J., Silflow, C.D., Stern, D., Vallon, O., *et al.* (2003). *Chlamydomonas reinhardtii* at the crossroads of genomics. *Eukaryot Cell* 2, 1137-1150.

Gu, Q., David, F., Lynen, F., Vanormelingen, P., Vyverman, W., Rumpel, K., Xu, G., and Sandra, P. (2011a). Evaluation of ionic liquid stationary phases for one dimensional gas chromatography-mass spectrometry and comprehensive two dimensional gas chromatographic analyses of fatty acids in marine biota. *Journal of Chromatography A* 1218, 3056-3063.

Gu, Q., David, F., Lynen, F., Vanormelingen, P., Vyverman, W., Rumpel, K., Xu, G., and Sandra, P. (2011b). Evaluation of ionic liquid stationary phases for one dimensional gas chromatography-mass spectrometry and comprehensive two dimensional gas chromatographic analyses of fatty acids in marine biota. *Journal of Chromatography A* 1218, 3056-3063.

Guan, W., Zhao, H., Lu, X., Wang, C., Yang, M., and Bai, F. (2011). Quantitative analysis of fatty-acid-based biofuels produced by wild-type and genetically engineered cyanobacteria by gas chromatography-mass spectrometry. *Journal of Chromatography A* 1218, 8289-8293.

Guarnieri, M.T., Nag, A., Smolinski, S.L., Darzins, A., Seibert, M., and Pienkos, P.T. (2011). Examination of Triacylglycerol Biosynthetic Pathways via De Novo Transcriptomic and Proteomic Analyses in an Unsequenced Microalga. *PLoS ONE* 6.

Guarnieri, M.T., Nag, A., Yang, S., and Pienkos, P.T. (2013). Proteomic analysis of *Chlorella vulgaris*: Potential targets for enhanced lipid accumulation. *Journal of Proteomics* 93, 245-253.

Guo, L., Devaiah, S.P., Narasimhan, R., Pan, X., Zhang, Y., Zhang, W., and Wang, X. (2012). Cytosolic Glyceraldehyde-3-Phosphate Dehydrogenases Interact with Phospholipase D $\delta$  to Transduce Hydrogen Peroxide Signals in the Arabidopsis Response to Stress. *The Plant Cell* 24, 2200-2212.

Guschina, I.A., and Harwood, J.L. (2006). Lipids and lipid metabolism in eukaryotic algae. *Progress in Lipid Research* 45, 160-186.

Haghjou, M.M., and Shariati, M. (2007). Photosynthesis and Respiration under Low Temperature Stress in Two *Dunaliella* Strains. *World Applied Sciences Journal* 2, 276-282.

Halim, R., Rupasinghe, T.W.T., Tull, D.L., and Webley, P.A. (2013). Mechanical cell disruption for lipid extraction from microalgal biomass. *Bioresource Technology* 140, 53-63.

Hamelinck, C., Schober, S., Mittelbach, M., Verolet, J., and Dehue, B. (2007). Fatty acid ethyl esters: Final report for Lot 3a of the Bioscopes project

Hamm, C.E., and Rousseau, V. (2003). Composition, assimilation and degradation of *Phaeocystis globosa*-derived fatty acids in the North Sea. *Journal of Sea Research* 50, 271-283.

Han, Y., Wen, Q., Chen, Z., and Li, P. (2011). Review of Methods Used for Microalgal Lipid-Content Analysis. *Energy Procedia* 12, 944-950.

Harris, E.H. (2001). *Chlamydomonas* as a model organism. *Annual Review of Plant Physiology and Plant Molecular Biology* 52, 363-406.

Harris, E.H., Stern, D.B., and Witman, G.B. (2009). *The Chlamydomonas Sourcebook* (Second Edition) (Academic Press).

Harris, R.V., and James, A.T. (1965). Linoleic ,  $\alpha$ -linolenic acid biosynthesis in plant leaves and a green alga. *Biochimica et Biophysica Acta (BBA) - Lipids and Lipid Metabolism* 106, 456-464.

Harwood, J.L., and Guschina, I.A. (2009). The versatility of algae and their lipid metabolism. *Biochimie* 91, 679-684.

He, Q., Qiao, D., Bai, L., Zhang, Q., Yang, W., Li, Q., and Cao, Y. (2007). Cloning and characterization of a plastidic glycerol 3-phosphate dehydrogenase cDNA from *Dunaliella salina*. *J Plant Physiol* 164.

Herrera-Valencia, V., Contreras-Pool, P., López-Adrián, S., Peraza-Echeverría, S., and Barahona-Pérez, L. (2011). The Green Microalga *Chlorella saccharophila* as a Suitable Source of Oil for Biodiesel Production. *Current Microbiology* 63, 151-157.

Herrero, M., Vicente, M.J., Cifuentes, A., and Ibáñez, E. (2007). Characterization by high-performance liquid chromatography/electrospray ionization quadrupole time-of-flight mass spectrometry of the lipid fraction of *Spirulina platensis* pressurized ethanol extract. *Rapid Communications in Mass Spectrometry* 21, 1729-1738.

Hessen, D.O., Van Donk, E., and Andersen, T. (1995). Growth responses, P-uptake and loss of flagellae in *Chlamydomonas reinhardtii* exposed to UV-B. *Journal of Plankton Research* 17, 17-27.

Hidalgo, P., Toro, C., Ciudad, G., and Navia, R. (2013). Advances in direct transesterification of microalgal biomass for biodiesel production. *Reviews in Environmental Science and Bio-Technology* 12, 179-199.

Higgins, B.T., Thornton-Dunwoody, A., Labavitch, J.M., and VanderGheynst, J.S. (2014). Microplate assay for quantitation of neutral lipids in extracts from microalgae. *Analytical Biochemistry* 465, 81-89.

Himmel, M.E., Ding, S.Y., Johnson, D.K., Adney, W.S., Nimlos, M.R., Brady, J.W., and Foust, T.D. (2007). Biomass recalcitrance: Engineering plants and enzymes for biofuels production. *Science* 315, 804-807.

Ho, S.H., Nakanishi, A., Ye, X.T., Chang, J.S., Hara, K., Hasunuma, T., and Kondo, A. (2014). Optimizing biodiesel production in marine *Chlamydomonas* sp JSC4 through metabolic profiling and an innovative salinity-gradient strategy. *Biotechnology for Biofuels* 7.

Hoekman, S.K., Broch, A., Robbins, C., Cenicerros, E., and Natarajan, M. (2012). Review of biodiesel composition, properties, and specifications. *Renewable and Sustainable Energy Reviews* 16, 143-169.

Hoham, R.W. (1975). Optimum temperatures and temperature ranges for growth of snow algae. *Arctic and Alpine Research* 7, 13-24.

Hohner, R., Barth, J., Magneschi, L., Jaeger, D., Niehues, A., Bald, T., Grossman, A., Fufezan, C., and Hippler, M. (2013). The Metabolic Status Drives Acclimation of Iron Deficiency Responses in *Chlamydomonas reinhardtii* as Revealed by Proteomics Based Hierarchical Clustering and Reverse Genetics. *Molecular & Cellular Proteomics* 12, 2774-2790.

Holcomb, R., Mason, L., Reardon, K., Crokek, D., and Henry, C. (2011). Culturing and investigation of stress-induced lipid accumulation in microalgae using a microfluidic device. *Analytical and Bioanalytical Chemistry* 400, 245-253.

Hounslow, E., Kapoore, R.V., Vaidyanathan, S., Gilmour, D.J., and Wright, P.C. (2016a). The Search for a Lipid Trigger: The Effect of Salt Stress on the Lipid Profile of the Model Microalgal Species *Chlamydomonas reinhardtii* for Biofuels Production. *Current Biotechnology* 5, 1-9.

Hounslow, E., Noirel, J., Gilmour, D.J., and Wright, P.C. (2016b). Lipid quantification techniques for screening oleaginous species of microalgae for biofuel production. *European Journal of Lipid Science and Technology*, n/a-n/a.

Hsieh, S.I., Castruita, M., Malasarn, D., Urzica, E., Erde, J., Page, M.D., Yamasaki, H., Casero, D., Pellegrini, M., Merchant, S.S., *et al.* (2013). The Proteome of Copper, Iron, Zinc, and Manganese Micronutrient Deficiency in *Chlamydomonas reinhardtii*. *Molecular & Cellular Proteomics* 12, 65-86.

Hu, J., Jin, L., Wang, X., Cai, W., Liu, Y., and Wang, G. (2014). Response of photosynthetic systems to salinity stress in the desert cyanobacterium *Scytonema javanicum*. *Advances in Space Research* 53, 30-36.

Hu, Q., Sommerfeld, M., Jarvis, E., Ghirardi, M., Posewitz, M., Seibert, M., and Darzins, A. (2008). Microalgal triacylglycerols as feedstocks for biofuel production: perspectives and advances. *Plant Journal* 54, 621-639.

Huang, L.-F., Lin, J.-Y., Pan, K.-Y., Huang, C.-K., and Chu, Y.-K. (2015). Overexpressing Ferredoxins in *Chlamydomonas reinhardtii* Increase Starch and Oil Yields and Enhance Electric Power Production in a Photo Microbial Fuel Cell. *International Journal of Molecular Sciences* *16*, 19308-19325.

Huang, Y.Y., Beal, C.M., Cai, W.W., Ruoff, R.S., and Terentjev, E.M. (2010). Micro-Raman spectroscopy of algae: Composition analysis and fluorescence background behavior. *Biotechnology and Bioengineering* *105*, 889-898.

Inouye, L.S., and Lotufo, G.R. (2006). Comparison of macro-gravimetric and micro-colorimetric lipid determination methods. *Talanta* *70*, 584-587.

Islam, M.A., Ayoko, G.A., Brown, R., Stuart, D., and Heimann, K. (2013). Influence of Fatty Acid Structure on Fuel Properties of Algae Derived Biodiesel. *Procedia Engineering* *56*, 591-596.

Jain, M., Mathur, G., Koul, S., and Sarin, N. (2001). Ameliorative effects of proline on salt stress-induced lipid peroxidation in cell lines of groundnut (*Arachis hypogaea* L.). *Plant Cell Reports* *20*, 463-468.

James, G.O., Hocart, C.H., Hillier, W., Chen, H.C., Kordbacheh, F., Price, G.D., and Djordjevic, M.A. (2011). Fatty acid profiling of *Chlamydomonas reinhardtii* under nitrogen deprivation. *Bioresource Technology* *102*, 3343-3351.

James, G.O., Hocart, C.H., Hillier, W., Price, G.D., and Djordjevic, M.A. (2013). Temperature modulation of fatty acid profiles for biofuel production in nitrogen deprived *Chlamydomonas reinhardtii*. *Bioresource Technology* *127*, 441-447.

Jayanta, T., Chandra, K.M., and Chandra, G.B. (2012). Growth, total lipid content and fatty acid profile of a native strain of the freshwater oleaginous microalgae *Ankistrodesmus falcatus* (Ralf) grown under salt stress condition. *International Research Journal of Biological Sciences* *1*, 27-35.

Jeong, M.-J., Park, S.-C., and Byun, M.-O. (2001). Improvement of salt tolerance in transgenic potato plants by glyceraldehyde-3 phosphate dehydrogenase gene transfer. *Molecules & Cells* *12*.

Jiang, Y., and Chen, F. (1999). Effects of salinity on cell growth and docosahexaenoic acid content of the heterotrophic marine microalga *Cryptocodinium cohnii*. *Journal of Industrial Microbiology & Biotechnology* *23*, 508-513.

Jiang, Y., and Deyholos, M.K. (2006). Comprehensive transcriptional profiling of NaCl-stressed *Arabidopsis* roots reveals novel classes of responsive genes. *BMC Plant Biology* *6*, 1-20.

Jiménez, C., Cossi, amp, x, o, B.R., and Niell, F.X. (2003). Relationship between physicochemical variables and productivity in open ponds for the production of *Spirulina*: a predictive model of algal yield. *Aquaculture* *221*, 331-345.

Johnson, X., and Alric, J. (2013). Central Carbon Metabolism and Electron Transport in *Chlamydomonas reinhardtii*: Metabolic Constraints for Carbon Partitioning between Oil and Starch. *Eukaryotic Cell* *12*, 776-793.

Jorquera, O., Kiperstok, A., Sales, E.A., Embirucu, M., and Ghirardi, M.L. (2010). Comparative energy life-cycle analyses of microalgal biomass production in open ponds and photobioreactors. *Bioresource Technology* *101*, 1406-1413.

Kan, G.-F., Miao, J.-L., Shi, C.-J., and Li, G.-Y. (2006). Proteomic Alterations of Antarctic Ice Microalga *Chlamydomonas* sp. Under Low-Temperature Stress. *Journal of Integrative Plant Biology* *48*, 965-970.

Kang, M.J., Shin, M.S., Park, J.N., and Lee, S.S. (2005). The effects of polyunsaturated:saturated fatty acids ratios and peroxidisability index values of dietary fats on serum lipid profiles and hepatic enzyme activities in rats. *British Journal of Nutrition* *94*, 526-532.

Kaplan, D., Christiaen, D., and Arad, S.M. (1987). Chelating Properties of Extracellular Polysaccharides from *Chlorella* Spp. *Applied and Environmental Microbiology* *53*, 2953-2956.

Karp, N.A., Huber, W., Sadowski, P.G., Charles, P.D., Hester, S.V., and Lilley, K.S. (2010). Addressing Accuracy and Precision Issues in iTRAQ Quantitation. *Molecular & Cellular Proteomics* *9*, 1885-1897.

Khotimchenko, S.V., and Yakovleva, I.M. (2005). Lipid composition of the red alga *Tichocarpus crinitus* exposed to different levels of photon irradiance. *Phytochemistry* *66*, 73-79.

Khozin-Goldberg, I., and Cohen, Z. (2006). The effect of phosphate starvation on the lipid and fatty acid composition of the fresh water eustigmatophyte *Monodus subterraneus*. *Phytochemistry* *67*, 696-701.

Kim, B.-H., Ramanan, R., Kang, Z., Cho, D.-H., Oh, H.-M., and Kim, H.-S. (2016a). *Chlorella sorokiniana* HS1, a novel freshwater green algal strain, grows and hyperaccumulates lipid droplets in seawater salinity. *Biomass and Bioenergy* *85*, 300-305.

Kim, G., Lee, C.H., and Lee, K. (2016b). Enhancement of lipid production in marine microalga *Tetraselmis* sp through salinity variation. *Korean Journal of Chemical Engineering* *33*, 230-237.

Kim, M.D., Han, K.C., Kang, H.A., Rhee, S.K., and Seo, J.H. (2003). Coexpression of BiP increased antithrombotic hirudin production in recombinant *Sacchdromyces cerevisiae*. *J Biotechnol* *101*, 81-87.

Kind, T., Meissen, J.K., Yang, D., Nocito, F., Vaniya, A., Cheng, Y.-S., VanderGheynst, J.S., and Fiehn, O. (2012). Qualitative analysis of algal secretions with multiple mass spectrometric platforms. *Journal of Chromatography A* *1244*, 139-147.

Kitano, H. (2002). Systems Biology: A Brief Overview. *Science* *295*, 1662-1664.

Klok, A.J., Martens, D.E., Wijffels, R.H., and Lamers, P.P. (2013). Simultaneous growth and neutral lipid accumulation in microalgae. *Bioresource Technology* *134*, 233-243.

Knothe, G. (2005). Dependence of biodiesel fuel properties on the structure of fatty acid alkyl esters. *Fuel Processing Technology* *86*, 1059-1070.

Knothe, G. (2008). "Designer" biodiesel: Optimizing fatty ester (composition to improve fuel properties. *Energy & Fuels* *22*, 1358-1364.

Knothe, G. (2009). Improving biodiesel fuel properties by modifying fatty ester composition. *Energy & Environmental Science* *2*, 759-766.

Kong, Q.-x., Li, L., Martinez, B., Chen, P., and Ruan, R. (2010). Culture of Microalgae *Chlamydomonas reinhardtii* in Wastewater for Biomass Feedstock Production. *Applied Biochemistry and Biotechnology* *160*, 9-18.

Kovacevic, V., and Wesseler, J. (2010). Cost-effectiveness analysis of algae energy production in the EU. *Energy Policy* *38*, 5749-5757.

Kumari, P., Reddy, C.R.K., and Jha, B. (2011). Comparative evaluation and selection of a method for lipid and fatty acid extraction from macroalgae. *Analytical Biochemistry* *415*, 134-144.

Lachapelle, J., and Bell, G. (2012). Evolutionary Rescue of Sexual and Asexual Populations in a Deteriorating Environment. *Evolution* *66*, 3508-3518.

Laureillard, J., Largeau, C., and Casadevall, E. (1988). Oleic acid in the biosynthesis of the resistant biopolymers of *Botryococcus braunii*. *Phytochemistry* *27*, 2095-2098.

Laurens, L., Quinn, M., Van Wycken, S., Templeton, D., and Wolfrum, E. (2012a). Accurate and reliable quantification of total microalgal fuel potential as fatty acid methyl esters by *in situ* transesterification. *Analytical and Bioanalytical Chemistry* *403*, 167-178.

Laurens, L.M.L., Dempster, T.A., Jones, H.D.T., Wolfrum, E.J., Van Wycken, S., McAllister, J.S.P., Rencenberger, M., Parchert, K.J., and Gloe, L.M. (2012b). Algal Biomass Constituent Analysis: Method Uncertainties and Investigation of the Underlying Measuring Chemistries. *Analytical Chemistry* *84*, 1879-1887.

Lee, B., Choi, G.G., Choi, Y.E., Sung, M., Park, M.S., and Yang, J.W. (2014). Enhancement of lipid productivity by ethyl methane sulfonate-mediated random mutagenesis and proteomic analysis in *Chlamydomonas reinhardtii*. *Korean Journal of Chemical Engineering* *31*, 1036-1042.

Lee, D.Y., Park, J.J., Barupal, D.K., and Fiehn, O. (2012). System Response of Metabolic Networks in *Chlamydomonas reinhardtii* to Total Available Ammonium. *Molecular & Cellular Proteomics* *11*, 973-988.

Lee, J.-Y., Yoo, C., Jun, S.-Y., Ahn, C.-Y., and Oh, H.-M. (2010). Comparison of several methods for effective lipid extraction from microalgae. *Bioresource Technology* *101*, S75-S77.

Leite, G.B., Abdelaziz, A.E.M., and Hallenbeck, P.C. (2013). Algal biofuels: Challenges and opportunities. *Bioresource Technology* *145*, 134-141.

Leon-Banares, R., Gonzalez-Ballester, D., Galvan, A., and Fernandez, E. (2004). Transgenic microalgae as green cell-factories. *Trends in Biotechnology* *22*, 45-52.

Leon, R., and Galvan, F. (1994). Halotolerance studies on *Chlamydomonas reinhardtii* glycerol excretion by free and immobilized cells. *Journal of Applied Phycology* *6*, 13-20.

León, R., and Galván, F. (1999). Interaction between saline stress and photoinhibition of photosynthesis in the freshwater green algae *Chlamydomonas reinhardtii*. Implications for glycerol photoproduction. *Plant Physiology and Biochemistry* *37*, 623-628.

Lepage, G., and Roy, C.C. (1986). Direct transesterification of all classes of lipids in a one-step reaction. *Journal of Lipid Research* *27*, 114-120.

Lewin, R.A. (1956). Extracellular Polysaccharides of Green Algae. *Canadian Journal of Microbiology* *2*, 665-672.

Li, P., and Lin, J. (2012). Effect of ultraviolet radiation on photosynthesis, biomass, and fatty acid content and profile of a *Scenedesmus rubescens*-like microalga. *Bioresource Technology* *111*, 316-322.

Li, X., Xu, H., and Wu, Q. (2007). Large-scale biodiesel production from microalga *Chlorella protothecoides* through heterotrophic cultivation in bioreactors. *Biotechnology and Bioengineering* *98*, 764-771.

Li, Y., Fei, X., and Deng, X. (2012). Novel molecular insights into nitrogen starvation-induced triacylglycerols accumulation revealed by differential gene expression analysis in green algae *Micractinium pusillum*. *Biomass and Bioenergy* *42*, 199-211.

Li, Y., Han, D., Sommerfeld, M., and Hu, Q. (2011). Photosynthetic carbon partitioning and lipid production in the oleaginous microalga *Pseudochlorococcum* sp. (Chlorophyceae) under nitrogen-limited conditions. *Bioresource Technology* *102*, 123-129.

Li, Y., Han, F., Xu, H., Mu, J., Chen, D., Feng, B., and Zeng, H. (2014a). Potential lipid accumulation and growth characteristic of the green alga *Chlorella* with combination cultivation mode of nitrogen (N) and phosphorus (P). *Bioresource Technology* *174*, 24-32.

Li, Y., Horsman, M., Wang, B., Wu, N., and Lan, C. (2008a). Effects of nitrogen sources on cell growth and lipid accumulation of green alga *Neochloris oleoabundans*. *Applied Microbiology and Biotechnology* *81*, 629-636.

Li, Y., Horsman, M., Wu, N., Lan, C.Q., and Dubois-Calero, N. (2008b). Biofuels from microalgae. *Biotechnology Progress* *24*, 815-820.

Li, Y., Naghdi, F.G., Garg, S., Adarme-Vega, T.C., Thurecht, K.J., Ghafor, W.A., Tannock, S., and Schenk, P.M. (2014b). A comparative study: the impact of different lipid extraction methods on current microalgal lipid research. *Microbial Cell Factories* *13*.

Li, Y.T., Han, D.X., Hu, G.R., Dauvillee, D., Sommerfeld, M., Ball, S., and Hua, Q. (2010a). *Chlamydomonas* starchless mutant defective in ADP-glucose pyrophosphorylase hyper-accumulates triacylglycerol. *Metabolic Engineering* *12*, 387-391.

Li, Y.T., Han, D.X., Hu, G.R., Sommerfeld, M., and Hu, Q.A. (2010b). Inhibition of Starch Synthesis Results in Overproduction of Lipids in *Chlamydomonas reinhardtii*. *Biotechnology and Bioengineering* *107*, 258-268.

Liang, Y., Sarkany, N., and Cui, Y. (2009). Biomass and lipid productivities of *Chlorella vulgaris* under autotrophic, heterotrophic and mixotrophic growth conditions. *Biotechnology Letters* *31*, 1043-1049.

Lim, D.K.Y., Garg, S., Timmins, M., Zhang, E.S.B., Thomas-Hall, S.R., Schuhmann, H., Li, Y., and Schenk, P.M. (2012). Isolation and Evaluation of Oil-Producing Microalgae from Subtropical Coastal and Brackish Waters. *PLoS ONE* *7*, e40751.

Liska, A.J., Shevchenko, A., Pick, U., and Katz, A. (2004). Enhanced photosynthesis and redox energy production contribute to salinity tolerance in *Dunaliella* as revealed by homology-based proteomics. *Plant Physiology* *136*, 2806-2817.

Liu, B., Liu, J., Chen, T., Yang, B., Jiang, Y., Wei, D., and Chen, F. (2015). Rapid Characterization of Fatty Acids in Oleaginous Microalgae by Near-Infrared Spectroscopy. *International Journal of Molecular Sciences* *16*, 7045-7056.

Liu, B., Vieler, A., Li, C., Daniel Jones, A., and Benning, C. (2013). Triacylglycerol profiling of microalgae *Chlamydomonas reinhardtii* and *Nannochloropsis oceanica*. *Bioresource Technology* *146*, 310-316.

Liu, J., Huang, J., Sun, Z., Zhong, Y., Jiang, Y., and Chen, F. (2011). Differential lipid and fatty acid profiles of photoautotrophic and heterotrophic *Chlorella zofingiensis*: Assessment of algal oils for biodiesel production. *Bioresource Technology* *102*, 106-110.

Lombardi, A.T., Vieira, A.A.H., and Sartori, L.A. (2002). Mucilaginous capsule adsorption and intracellular uptake of copper by *Kirchneriella aperta* (Chlorococcales). *Journal of Phycology* *38*, 332-337.

Longworth, J., Noirel, J., Pandhal, J., Wright, P.C., and Vaidyanathan, S. (2012). HILIC- and SCX-Based Quantitative Proteomics of *Chlamydomonas reinhardtii* during Nitrogen Starvation Induced Lipid and Carbohydrate Accumulation. *Journal of Proteome Research* *11*, 5959-5971.

López-Sandoval, D.C., Rodríguez-Ramos, T., Cermeño, P., Sobrino, C., and Marañón, E. (2014). Photosynthesis and respiration in marine phytoplankton: Relationship with cell size, taxonomic affiliation, and growth phase. *Journal of Experimental Marine Biology and Ecology* *457*, 151-159.

Lu, N., Wei, D., Chen, F., and Yang, S.-T. (2012a). Lipidomic profiling and discovery of lipid biomarkers in snow alga *Chlamydomonas nivalis* under salt stress. *European Journal of Lipid Science and Technology* *114*, 253-265.

Lu, N., Wei, D., Chen, F., and Yang, S.T. (2013). Lipidomic profiling reveals lipid regulation in the snow alga *Chlamydomonas nivalis* in response to nitrate or phosphate deprivation. *Process Biochemistry* *48*, 605-613.

Lu, N., Wei, D., Jiang, X.-L., Chen, F., and Yang, S.-T. (2012b). Fatty acids profiling and biomarker identification in snow alga *Chlamydomonas nivalis* by NaCl stress using GC/MS and multivariate statistical analysis. *Analytical Letters* *45*, 1172-1183.

Lu, N., Wei, D., Jiang, X.-L., Chen, F., and Yang, S.-T. (2012c). Regulation of lipid metabolism in the snow alga *Chlamydomonas nivalis* in response to NaCl stress: An integrated analysis by cytomic and lipidomic approaches. *Process Biochemistry* *47*, 1163-1170.

Lukes, M., Prochazkova, L., Shmidt, V., Nedbalova, L., and Kaftan, D. (2014). Temperature dependence of photosynthesis and thylakoid lipid composition in the red snow alga *Chlamydomonas cf. nivalis* (Chlorophyceae). *Fems Microbiology Ecology* *89*, 303-315.

Lv, H., Qu, G., Qi, X., Lu, L., Tian, C., and Ma, Y. (2013). Transcriptome analysis of *Chlamydomonas reinhardtii* during the process of lipid accumulation. *Genomics* *101*, 229-237.

Lv, J.-M., Cheng, L.-H., Xu, X.-H., Zhang, L., and Chen, H.-L. (2010). Enhanced lipid production of *Chlorella vulgaris* by adjustment of cultivation conditions. *Bioresource Technology* *101*, 6797-6804.

Macdougall, K.M., McNichol, J., McGinn, P.J., O'Leary, S.J., and Melanson, J.E. (2011). Triacylglycerol profiling of microalgae strains for biofuel feedstock by liquid chromatography-high-resolution mass spectrometry. *Analytical and Bioanalytical Chemistry*.

MacKinney, G. (1941). Absorption of light by chlorophyll solutions. *Journal of Biological Chemistry* *140*, 315-322.

Martin, G.J.O., Hill, D.R.A., Olmstead, I.L.D., Bergamin, A., Shears, M.J., Dias, D.A., Kentish, S.E., Scales, P.J., Botté, C.Y., and Callahan, D.L. (2014). Lipid Profile Remodeling in Response to Nitrogen Deprivation in the Microalgae *Chlorella* sp. (Trebouxiophyceae) and *Nannochloropsis* sp. (Eustigmatophyceae). *PLoS ONE* 9, e103389.

Masojídek, J., Torzillo, G., Kopecký, J., Koblížek, M., Nidiaci, L., Komenda, J., Lukavská, A., and Sacchi, A. (2000). Changes in chlorophyll fluorescence quenching and pigment composition in the green alga *Chlorococcum* sp. grown under nitrogen deficiency and salinity stress. *Journal of Applied Phycology* 12, 417-426.

Mastrobuoni, G., Irgang, S., Pietzke, M., ASZmus, H., Wenzel, M., Schulze, W., and Kempa, S. (2012). Proteome dynamics and early salt stress response of the photosynthetic organism *Chlamydomonas reinhardtii*. *BMC Genomics* 13, 215.

McLachlan, J. (1961). The Effect of Salinity on Growth and Chlorophyll Content in Representative Classes of Unicellular Marine Algae. *Canadian Journal of Microbiology* 7, 399-406.

McNichol, J., MacDougall, K., Melanson, J., and McGinn, P. (2012). Suitability of Soxhlet Extraction to Quantify Microalgal Fatty Acids as Determined by Comparison with In Situ Transesterification. *Lipids* 47, 195-207.

Melero, J.A., Bautista, L.F., Morales, G., Iglesias, J., and Sánchez-Vázquez, R. (2015). Acid-catalyzed production of biodiesel over arenesulfonic SBA-15: Insights into the role of water in the reaction network. *Renewable Energy* 75, 425-432.

Merchant, S.S., Kropat, J., Liu, B., Shaw, J., and Warakanont, J. (2012). TAG, You're it! *Chlamydomonas* as a reference organism for understanding algal triacylglycerol accumulation. *Current Opinion in Biotechnology* 23, 352-363.

Meurant, G. (1984). *Fatty Acid Metabolism and its Regulation* (Elsevier Science).

Michalski, A., Damoc, E., Hauschild, J.-P., Lange, O., Wieghaus, A., Makarov, A., Nagaraj, N., Cox, J., Mann, M., and Horning, S. (2011). Mass Spectrometry-based Proteomics Using Q Exactive, a High-performance Benchtop Quadrupole Orbitrap Mass Spectrometer. *Molecular & cellular proteomics : MCP* 10, M111.011015.

Miglio, R., Palmery, S., Salvalaggio, M., Carnelli, L., Capuano, F., and Borrelli, R. (2013). Microalgae triacylglycerols content by FT-IR spectroscopy. *Journal of Applied Phycology*.

Miller, R., Wu, G., Deshpande, R.R., Vieler, A., Gaertner, K., Li, X., Moellering, E.R., Zaeuner, S., Cornish, A.J., Liu, B., *et al.* (2010). Changes in Transcript Abundance in *Chlamydomonas reinhardtii* following Nitrogen Deprivation Predict Diversion of Metabolism. *Plant Physiology* 154, 1737-1752.

Mizoguchi, H., and Hara, S. (1996). Effect of fatty acid saturation in membrane lipid bilayers on simple diffusion in the presence of ethanol at high concentrations. *Journal of Fermentation and Bioengineering* 81, 406-411.

Moellering, E.R., and Benning, C. (2010). RNA Interference Silencing of a Major Lipid Droplet Protein Affects Lipid Droplet Size in *Chlamydomonas reinhardtii*. *Eukaryotic Cell* 9, 97-106.

Mohammed, S., and Heck, A.J.R. (2011). Strong cation exchange (SCX) based analytical methods for the targeted analysis of protein post-translational modifications. *Current Opinion in Biotechnology* 22, 9-16.

Moheimani, N.R., and Borowitzka, M.A. (2007). Limits to productivity of the alga *Pleurochrysis carterae* (Haptophyta) grown in outdoor raceway ponds. *Biotechnology and Bioengineering* 96, 27-36.

Mohr, A., and Raman, S. (2013). Lessons from first generation biofuels and implications for the sustainability appraisal of second generation biofuels. *Energy Policy* 63, 114-122.

Moon, M., Kim, C.W., Park, W.-K., Yoo, G., Choi, Y.-E., and Yang, J.-W. (2013). Mixotrophic growth with acetate or volatile fatty acids maximizes growth and lipid production in *Chlamydomonas reinhardtii*. *Algal Research* 2, 352-357.

Mráček, T., Drahotka, Z., and Houštěk, J. (2013). The function and the role of the mitochondrial glycerol-3-phosphate dehydrogenase in mammalian tissues. *Biochimica et Biophysica Acta (BBA)-Bioenergetics* 1827, 401-410.

Msanne, J., Xu, D., Konda, A.R., Casas-Mollano, J.A., Awada, T., Cahoon, E.B., and Cerutti, H. (2012). Metabolic and gene expression changes triggered by nitrogen deprivation in the photoautotrophically grown microalgae *Chlamydomonas reinhardtii* and *Coccomyxa* sp. C-169. *Phytochemistry* 75.

Muhlhaus, T., Weiss, J., Hemme, D., Sommer, F., and Schroda, M. (2011). Quantitative shotgun proteomics using a uniform <sup>5</sup>N-labeled standard to monitor proteome dynamics in time course experiments reveals new insights into the heat stress response of *Chlamydomonas reinhardtii*. *Molecular & cellular proteomics : MCP* 10, M110.004739-M004110.004739.

Mühlroth, A., Li, K., Røkke, G., Winge, P., Olsen, Y., Hohmann-Marriott, M.F., Vadstein, O., and Bones, A.M. (2013). Pathways of Lipid Metabolism in Marine Algae, Co-Expression Network, Bottlenecks and Candidate Genes for Enhanced Production of EPA and DHA in Species of Chromista. *Marine Drugs* 11, 4662-4697.

Muñoz-Blanco, J., and Cardenas, J. (1989). Changes in glutamate dehydrogenase activity of *Chlamydomonas reinhardtii* under different trophic and stress conditions. *Plant, Cell & Environment* 12, 173-182.

Murata, N., Takahashi, S., Nishiyama, Y., and Allakhverdiev, S.I. (2007). Photoinhibition of photosystem II under environmental stress. *Biochimica et Biophysica Acta (BBA) - Bioenergetics* 1767, 414-421.

Mutanda, T., Ramesh, D., Karthikeyan, S., Kumari, S., Anandraj, A., and Bux, F. (2011). Bioprospecting for hyper-lipid producing microalgal strains for sustainable biofuel production. *Bioresour Technol* 102, 57-70.

Myklestad, S.M. (1995). Release of Extracellular Products by Phytoplankton with Special Emphasis on Polysaccharides. *Science of the Total Environment* 165, 155-164.

Nagalakshmi, N., and Prasad, M.N.V. (1998). Copper-induced oxidative stress in *Scenedesmus bijugatus*: Protective role of free radical scavengers. *Bulletin of Environmental Contamination and Toxicology* 61, 623-628.

Natunen, K., Seppala, J., Schwenk, D., Rischer, H., Spilling, K., and Tamminen, T. (2015). Nile Red staining of phytoplankton neutral lipids: species-specific fluorescence kinetics in various solvents. *Journal of Applied Phycology* 27, 1161-1168.

Navas-Iglesias, N., Carrasco-Pancorbo, A., and Cuadros-Rodríguez, L. (2009). From lipids analysis towards lipidomics, a new challenge for the analytical chemistry of the 21st century. Part II: Analytical lipidomics. *TrAC Trends in Analytical Chemistry* 28, 393-403.

Ndimba, B.K., Ndimba, R.J., Johnson, T.S., Waditee-Sirisattha, R., Baba, M., Sirisattha, S., Shiraiwa, Y., Agrawal, G.K., and Rakwal, R. (2013). Biofuels as a sustainable energy source: An update of the applications of proteomics in bioenergy crops and algae. *Journal of Proteomics* 93, 234-244.

Neale, P.J., and Melis, A. (1989). Salinity-stress Enhances Photoinhibition of Photosynthesis in *Chlamydomonas reinhardtii*. *J Plant Physiol* 134, 619-622.

Neelam, S., and Subramanyam, R. (2013). Alteration of photochemistry and protein degradation of photosystem II from *Chlamydomonas reinhardtii* under high salt grown cells. *Journal of Photochemistry and Photobiology B: Biology* 124, 63-70.

Nguyen, H.M., Baudet, M., Cuine, S., Adriano, J.-M., Barthe, D., Billon, E., Bruley, C., Beisson, F., Peltier, G., Ferro, M., *et al.* (2011). Proteomic profiling of oil bodies isolated from the unicellular green microalga *Chlamydomonas reinhardtii*: With focus on proteins involved in lipid metabolism. *Proteomics* 11, 4266-4273.

Nogueira, F.C.S., Palmisano, G., Schwammle, V., Campos, F.A.P., Larsen, M.R., Domont, G.B., and Roepstorff, P. (2012). Performance of Isobaric and Isotopic Labeling in Quantitative Plant Proteomics. *Journal of Proteome Research* 11, 3046-3052.

Ohnishi, N., Mukherjee, B., Tsujikawa, T., Yanase, M., Nakano, H., Moroney, J.V., and Fukuzawa, H. (2010). Expression of a Low CO<sub>2</sub>-Inducible Protein, LCI1, Increases Inorganic Carbon Uptake in the Green Alga *Chlamydomonas reinhardtii*. *The Plant Cell* **22**, 3105-3117.

Olmstead, I.L.D., Hill, D.R.A., Dias, D.A., Jayasinghe, N.S., Callahan, D.L., Kentish, S.E., Scales, P.J., and Martin, G.J.O. (2013). A quantitative analysis of microalgal lipids for optimization of biodiesel and omega-3 production. *Biotechnology and Bioengineering* **110**, 2096-2104.

Olsen, J.V., Ong, S.E., and Mann, M. (2004). Trypsin cleaves exclusively C-terminal to arginine and lysine residues. *Molecular & Cellular Proteomics* **3**, 608-614.

Oncel, S.S. (2013). Microalgae for a macroenergy world. *Renewable & Sustainable Energy Reviews* **26**, 241-264.

Ong, S.-E., Blagoev, B., Kratchmarova, I., Kristensen, D.B., Steen, H., Pandey, A., and Mann, M. (2002). Stable Isotope Labeling by Amino Acids in Cell Culture, SILAC, as a Simple and Accurate Approach to Expression Proteomics. *Molecular & Cellular Proteomics* **1**, 376-386.

Ong, S.-E., and Mann, M. (2005). Mass spectrometry-based proteomics turns quantitative. *Nature chemical biology* **1**, 252-262.

Ow, S.Y., Salim, M., Noirel, J., Evans, C., Rehman, I., and Wright, P.C. (2009). iTRAQ Underestimation in Simple and Complex Mixtures: "The Good, the Bad and the Ugly". *Journal of Proteome Research* **8**, 5347-5355.

Ow, S.Y., Salim, M., Noirel, J., Evans, C., and Wright, P.C. (2011). Minimising iTRAQ ratio compression through understanding LC-MS elution dependence and high-resolution HILIC fractionation. *Proteomics* **11**, 2341-2346.

Paik, M.-J., Kim, H., Lee, J., Brand, J., and Kim, K.-R. (2009). Separation of triacylglycerols and free fatty acids in microalgal lipids by solid-phase extraction for separate fatty acid profiling analysis by gas chromatography. *Journal of Chromatography A* **1216**, 5917-5923.

Pal, D., Khozin-Goldberg, I., Cohen, Z., and Boussiba, S. (2011). The effect of light, salinity, and nitrogen availability on lipid production by *Nannochloropsis* sp. *Applied Microbiology and Biotechnology* **90**, 1429-1441.

Palmisano, A.C., and Sullivan, C.W. (1982). PHYSIOLOGY OF SEA ICE DIATOMS .1. RESPONSE OF 3 POLAR DIATOMS TO A SIMULATED SUMMER-WINTER TRANSITION. *Journal of Phycology* **18**, 489-498.

Pandhal, J., Snijders, A.P.L., Wright, P.C., and Biggs, C.A. (2008). A cross-species quantitative proteomic study of salt adaptation in a halotolerant environmental isolate using (15)N metabolic labelling. *Proteomics* **8**, 2266-2284.

Pastore, D., Trono, D., Laus, M.N., Di Fonzo, N., and Flagella, Z. (2007). Possible plant mitochondria involvement in cell adaptation to drought stress: A case study: durum wheat mitochondria. *Journal of Experimental Botany* *58*, 195-210.

Paulsen, B.S., and Vieira, A.A.H. (1994). Structure of the Capsular and Extracellular Polysaccharides Produced by the Desmid *Spondylosium panduriforma* (Chlorophyta). *Journal of Phycology* *30*, 638-641.

Pedranzani, H., Racagni, G., Alemano, S., Miersch, O., Ramírez, I., Peña-Cortés, H., Taleisnik, E., Machado-Domenech, E., and Abdala, G. (2003). Salt tolerant tomato plants show increased levels of jasmonic acid. *Plant Growth Regulation* *41*, 149-158.

Pereira-Medrano, A.G., Margesin, R., and Wright, P.C. (2012). Proteome characterization of the unsequenced psychrophile *Pedobacter cryoconitis* using <sup>15</sup>N metabolic labeling, tandem mass spectrometry, and a new bioinformatic workflow. *Proteomics* *12*, 775-789.

Pérez-Pérez, M.E., Lemaire, S.D., and Crespo, J.L. (2012). Reactive oxygen species and autophagy in plants and algae. *Plant Physiol* *160*.

Pernet, F., and Tremblay, R. (2003). Effect of ultrasonication and grinding on the determination of lipid class content of microalgae harvested on filters. *Lipids* *38*, 1191-1195.

Perrine, Z., Negi, S., and Sayre, R.T. (2012). Optimization of photosynthetic light energy utilization by microalgae. *Algal Research* *1*, 134-142.

Perrineau, M.M., Zelzion, E., Gross, J., Price, D.C., Boyd, J., and Bhattacharya, D. (2014). Evolution of salt tolerance in a laboratory reared population of *Chlamydomonas reinhardtii*. *Environ Microbiol* *16*, 1755-1766.

Pflaster, E.L., Schwabe, M.J., Becker, J., Wilkinson, M.S., Parmer, A., Clemente, T.E., Cahoon, E.B., and Riekhof, W.R. (2014). A High-Throughput Fatty Acid Profiling Screen Reveals Novel Variations in Fatty Acid Biosynthesis in *Chlamydomonas reinhardtii* and Related Algae. *Eukaryotic Cell* *13*, 1431-1438.

Pfromm, P.H., Amanor-Boadu, V., and Nelson, R. (2011). Sustainability of algae derived biodiesel: A mass balance approach. *Bioresource Technology* *102*, 1185-1193.

Pham, T.K., Roy, S., Noirel, J., Douglas, I., Wright, P.C., and Stafford, G.P. (2010). A quantitative proteomic analysis of biofilm adaptation by the periodontal pathogen *Tannerella forsythia*. *Proteomics* *10*, 3130-3141.

Pichler, P., Köcher, T., Holzmann, J., Mazanek, M., Taus, T., Ammerer, G., and Mechtler, K. (2010). Peptide Labeling with Isobaric Tags Yields Higher Identification Rates Using iTRAQ 4-Plex Compared to TMT 6-Plex and iTRAQ 8-Plex on LTQ Orbitrap. *Analytical Chemistry* *82*, 6549-6558.

Pick, U., and Rachutin-Zalogin, T. (2012). Kinetic anomalies in the interactions of Nile red with microalgae. *Journal of Microbiological Methods* 88, 189-196.

Piorreck, M., and Pohl, P. (1984). Formation of biomass, total protein, chlorophylls, lipids and fatty acids in green and blue-green algae during one growth phase. *Phytochemistry* 23, 217-223.

Pittman, J.K., Dean, A.P., and Osundeko, O. (2011). The potential of sustainable algal biofuel production using wastewater resources. *Bioresource Technology* 102, 17-25.

Pottiez, G., Wiederin, J., Fox, H.S., and Ciborowski, P. (2012). Comparison of 4-plex to 8-plex iTRAQ Quantitative Measurements of Proteins in Human Plasma Samples. *Journal of Proteome Research* 11, 3774-3781.

Prabakaran, P., and Ravindran, A.D. (2011). A comparative study on effective cell disruption methods for lipid extraction from microalgae. *Letters in Applied Microbiology* 53, 150-154.

Qiang, H., and Richmond, A. (1996). Productivity and photosynthetic efficiency of *Spirulina platensis* as affected by light intensity, algal density and rate of mixing in a flat plate photobioreactor. *Journal of Applied Phycology* 8, 139-145.

Radakovits, R., Jinkerson, R.E., Darzins, A., and Posewitz, M.C. (2010). Genetic Engineering of Algae for Enhanced Biofuel Production. *Eukaryotic Cell* 9, 486-501.

Radmer, R., and Kok, B. (1977). Photosynthesis - Limited Yields, Unlimited Dreams. *Bioscience* 27, 599-605.

Rai, S., Agrawal, C., Shrivastava, A.K., Singh, P.K., and Rai, L.C. (2014). Comparative proteomics unveils cross species variations in *Anabaena* under salt stress. *Journal of Proteomics* 98, 254-270.

Rao, A.R., Dayananda, C., Sarada, R., Shamala, T.R., and Ravishankar, G.A. (2007). Effect of salinity on growth of green alga *Botryococcus braunii* and its constituents. *Bioresource Technology* 98, 560-564.

Rasala, B.A., Chao, S.S., Pier, M., Barrera, D.J., and Mayfield, S.P. (2014). Enhanced Genetic Tools for Engineering Multigene Traits into Green Algae. *PLoS ONE* 9.

Ratcliff, W.C., Herron, M.D., Howell, K., Pentz, J.T., Rosenzweig, F., and Travisano, M. (2013). Experimental evolution of an alternating uni- and multicellular life cycle in *Chlamydomonas reinhardtii*. *Nat Commun* 4.

Recht, L., Zarka, A., and Boussiba, S. (2012). Patterns of carbohydrate and fatty acid changes under nitrogen starvation in the microalgae <i>Haematococcus pluvialis</i> and <i>Nannochloropsis</i> sp. *Applied Microbiology and Biotechnology* 94, 1495-1503.

Remias, D., Albert, A., and Lutz, C. (2010). Effects of realistically simulated, elevated UV irradiation on photosynthesis and pigment composition of the alpine snow alga *Chlamydomonas nivalis* and the arctic soil alga *Tetracystis* sp (Chlorophyceae). *Photosynthetica* 48, 269-277.

Remias, D., Lütz-Meindl, U., and Lütz, C. (2005). Photosynthesis, pigments and ultrastructure of the alpine snow alga *Chlamydomonas nivalis*. *European Journal of Phycology* 40, 259-268.

Remias, D., and Lütz, C. (2007). Characterisation of esterified secondary carotenoids and of their isomers in green algae: a HPLC approach. *Algological Studies* 124, 85-94.

Renaud, S.M., and Parry, D.L. (1994). Microalgae for use in tropical aquaculture II: Effect of salinity on growth, gross chemical composition and fatty acid composition of three species of marine microalgae. *Journal of Applied Phycology* 6, 347-356.

Richmond, A. (2004). *Handbook of microalgal culture: biotechnology and applied phycology* (Oxford, UK: Blackwell Science Ltd).

Riekhof, W.R., Sears, B.B., and Benning, C. (2005). Annotation of genes involved in glycerolipid biosynthesis in *Chlamydomonas reinhardtii*: Discovery of the betaine lipid synthase BTA1(Cr). *Eukaryotic Cell* 4, 242-252.

Ríos, S.D., Castaneda, J., Torras, C., Farriol, X., and Salvado, J. (2013). Lipid extraction methods from microalgal biomass harvested by two different paths: Screening studies toward biodiesel production. *Bioresource Technology* 133, 378-388.

Rolland, N., Atteia, A., Decottignies, P., Garin, J., Hippler, M., Kreimer, G., Lemaire, S.D., Mittag, M., and Wagner, V. (2009). *Chlamydomonas* proteomics. *Current Opinion in Microbiology* 12, 285-291.

Ross, P.L., Huang, Y.L.N., Marchese, J.N., Williamson, B., Parker, K., Hattan, S., Khainovski, N., Pillai, S., Dey, S., Daniels, S., *et al.* (2004). Multiplexed protein quantitation in *Saccharomyces cerevisiae* using amine-reactive isobaric tagging reagents. *Molecular & Cellular Proteomics* 3, 1154-1169.

Ruangsomboon, S. (2012). Effect of light, nutrient, cultivation time and salinity on lipid production of newly isolated strain of the green microalga, *Botryococcus braunii* KMITL 2. *Bioresource Technology* 109, 261-265.

Rumin, J., Bonnefond, H., Saint-Jean, B., Rouxel, C., Sciandra, A., Bernard, O., Cadoret, J.-P., and Bougaran, G. (2015). The use of fluorescent Nile red and BODIPY for lipid measurement in microalgae. *Biotechnology for Biofuels* 8.

Rupprecht, J. (2009). From systems biology to fuel-*Chlamydomonas reinhardtii* as a model for a systems biology approach to improve biohydrogen production. *Journal of Biotechnology* 142, 10-20.

Sadowski, P.G., Dunkley, T.P.J., Shadforth, I.P., Dupree, P., Bessant, C., Griffin, J.L., and Lilley, K.S. (2006). Quantitative proteomic approach to study subcellular localization of membrane proteins. *Nature Protocols* 1, 1778-1789.

Sakamoto, T., and Murata, N. (2002). Regulation of the desaturation of fatty acids and its role in tolerance to cold and salt stress. *Current Opinion in Microbiology* 5, 206-210.

Salama, E.-S., Kim, H.-C., Abou-Shanab, R.I., Ji, M.-K., Oh, Y.-K., Kim, S.-H., and Jeon, B.-H. (2013). Biomass, lipid content, and fatty acid composition of freshwater *Chlamydomonas mexicana* and *Scenedesmus obliquus* grown under salt stress. *Bioprocess and Biosystems Engineering* 36, 827-833.

Samek, O., Jonas, A., Pilat, Z., Zemanek, P., Nedbal, L., Triska, J., Kotas, P., and Trtilek, M. (2010). Raman Microspectroscopy of Individual Algal Cells: Sensing Unsaturation of Storage Lipids in vivo. *Sensors* 10, 8635-8651.

Sampath-Wiley, P., Neefus, C.D., and Jahnke, L.S. (2008). Seasonal effects of sun exposure and emersion on intertidal seaweed physiology: Fluctuations in antioxidant contents, photosynthetic pigments and photosynthetic efficiency in the red alga *Porphyra umbilicalis* Kützting (Rhodophyta, Bangiales). *Journal of Experimental Marine Biology and Ecology* 361, 83-91.

Sarpal, A.S., Teixeira, C.M.L.L., Silva, P.R.M., Lima, G.M., Silva, S.R., Monteiro, T.V., Cunha, V.S., and Daroda, R.J. (2015). Determination of lipid content of oleaginous microalgal biomass by NMR spectroscopic and GC-MS techniques. *Analytical and Bioanalytical Chemistry* 407, 3799-3816.

Scaife, M.A., Burja, A.M., and Wright, P.C. (2009). Characterization of Cyanobacterial beta-Carotene Ketolase and Hydroxylase Genes in *Escherichia coli*, and Their Application for Astaxanthin Biosynthesis. *Biotechnology and Bioengineering* 103, 944-955.

Schenk, P., Thomas-Hall, S., Stephens, E., Marx, U., Mussnug, J., Posten, C., Kruse, O., and Hankamer, B. (2008). Second Generation Biofuels: High-Efficiency Microalgae for Biodiesel Production. *Bioenerg Res* 1, 20-43.

Schmollinger, S., Muehlhaus, T., Boyle, N.R., Blaby, I.K., Casero, D., Mettler, T., Moseley, J.L., Kropat, J., Sommer, F., Strenkert, D., *et al.* (2014). Nitrogen-Sparing Mechanisms in *Chlamydomonas* Affect the Transcriptome, the Proteome, and Photosynthetic Metabolism. *Plant Cell* 26, 1410-1435.

Schwille, P. (2011). Bottom-Up Synthetic Biology: Engineering in a Tinkerer's World. *Science* 333, 1252-1254.

Scott, S.A., Davey, M.P., Dennis, J.S., Horst, I., Howe, C.J., Lea-Smith, D.J., and Smith, A.G. (2010). Biodiesel from algae: challenges and prospects. *Current Opinion in Biotechnology* 21, 277-286.

Searle, B.C., Turner, M., and Nesvizhskii, A.I. (2008). Improving Sensitivity by Probabilistically Combining Results from Multiple MS/MS Search Methodologies. *Journal of Proteome Research* 7, 245-253.

Shabala, S. (2009). Salinity and programmed cell death: unravelling mechanisms for ion specific signalling. *Journal of Experimental Botany* 60, 709-712.

Sharma, K.K., Schuhmann, H., and Schenk, P.M. (2012). High Lipid Induction in Microalgae for Biodiesel Production. *Energies* 5, 1532-1553.

Sheehan, J., Dunahay, T., Benemann, J., and Roessler, P. (1998). A look back at the U.S. Department of Energy's Aquatic Species Program: Biodiesel from Algae, N.R.E. Laboratory, ed. (Golden, Colorado).

Shen, P.-L., Wang, H.-T., Pan, Y.-F., Meng, Y.-Y., Wu, P.-C., and Xue, S. (2016). Identification of Characteristic Fatty Acids to Quantify Triacylglycerols in Microalgae. *Frontiers in Plant Science* 7, 162.

Sheng, J., Vannela, R., and Rittmann, B.E. (2011). Evaluation of methods to extract and quantify lipids from *Synechocystis* PCC 6803. *Bioresource Technology* 102, 1697-1703.

Siaut, M., Cuine, S., Cagnon, C., Fessler, B., Nguyen, M., Carrier, P., Beyly, A., Beisson, F., Triantaphylides, C., Li-Beisson, Y.H., *et al.* (2011). Oil accumulation in the model green alga *Chlamydomonas reinhardtii*: characterization, variability between common laboratory strains and relationship with starch reserves. *Bmc Biotechnology* 11.

Silva-Ortega, C.O., Ochoa-Alfaro, A.E., Reyes-Agüero, J.A., Aguado-Santacruz, G.A., and Jiménez-Bremont, J.F. (2008). Salt stress increases the expression of p5cs gene and induces proline accumulation in cactus pear. *Plant Physiology and Biochemistry* 46, 82-92.

Singh, S., Brocker, C., Koppaka, V., Ying, C., Jackson, B., Matsumoto, A., Thompson, D.C., and Vasiliou, V. (2013). Aldehyde Dehydrogenases in Cellular Responses to Oxidative/electrophilic Stress. *Free radical biology & medicine* 56, 89-101.

Singh, S.C., Sinha, R.P., and Hader, D.P. (2002). Role of lipids and fatty acids in stress tolerance in cyanobacteria. *Acta Protozoologica* 41, 297-308.

Slade, R., and Bauen, A. (2013). Micro-algae cultivation for biofuels: Cost, energy balance, environmental impacts and future prospects. *Biomass & Bioenergy* 53, 29-38.

Smith, R., Bangert, K., Wilkinson, S., and Gilmour, D.J. (in press). Symbiotic interactions between organic and inorganic carbon metabolism in a fast growing mixotrophic freshwater microalgal species *Micractinium inermum*. *Biomass and Bioenergy*.

Smith, R.T., Bangert, K., Wilkinson, S.J., and Gilmour, D.J. (2015). Synergistic carbon metabolism in a fast growing mixotrophic freshwater microalgal species *Micractinium inermum*. *Biomass and Bioenergy* *82*, 73-86.

Smith, V.H. (1986). Light and Nutrient Effects on the Relative Biomass of Blue-Green Algae in Lake Phytoplankton. *Canadian Journal of Fisheries and Aquatic Sciences* *43*, 148-153.

Smolke, Christina D., and Silver, Pamela A. (2011). Informing Biological Design by Integration of Systems and Synthetic Biology. *Cell* *144*, 855-859.

Snijders, A.P.L., de Koning, B., and Wright, P.C. (2007). Relative quantification of proteins across the species boundary through the use of shared peptides. *Journal of Proteome Research* *6*, 97-104.

Sogaard, D.H., Hansen, P.J., Rysgaard, S., and Glud, R.N. (2011). Growth limitation of three Arctic sea ice algal species: effects of salinity, pH, and inorganic carbon availability. *Polar Biology* *34*, 1157-1165.

Solovchenko, A., Khozin-Goldberg, I., Recht, L., and Boussiba, S. (2011). Stress-Induced Changes in Optical Properties, Pigment and Fatty Acid Content of *Nannochloropsis* sp.: Implications for Non-destructive Assay of Total Fatty Acids. *Marine Biotechnology* *13*, 527-535.

Solovchenko, A.E. (2012). Physiological Role of Neutral Lipid Accumulation in Eukaryotic Microalgae under Stresses. *Russian Journal of Plant Physiology* *59*, 167-176.

Somanchi, A., and Moroney, J.V. (1999). As *Chlamydomonas reinhardtii* acclimates to low-CO<sub>2</sub> conditions there is an increase in cyclophilin expression. *Plant Molecular Biology* *40*, 1055-1062.

Stansell, G.R., Gray, V.M., and Sym, S.D. (2012). Microalgal fatty acid composition: implications for biodiesel quality. *Journal of Applied Phycology* *24*, 791-801.

Stauber, E.J., and Hippler, M. (2004). *Chlamydomonas reinhardtii* proteomics. *Plant Physiology and Biochemistry* *42*, 989-1001.

Steen, H., and Mann, M. (2004). The abc's (and xyz's) of peptide sequencing. *Nat Rev Mol Cell Biol* *5*, 699-711.

Stehfest, K., Toepel, J., and Wilhelm, C. (2005). The application of micro-FTIR spectroscopy to analyze nutrient stress-related changes in biomass composition of phytoplankton algae. *Plant Physiology and Biochemistry* *43*, 717-726.

Stephanopoulos, G. (1999). Metabolic Fluxes and Metabolic Engineering. *Metab Eng* 1, 1-11.

Storms, Z.J., Cameron, E., Siegler, H.d.I.H., and McCaffrey, W.C. (2014). A Simple and Rapid Protocol for Measuring Neutral Lipids in Algal Cells Using Fluorescence. *Jove-Journal of Visualized Experiments*.

Su, C.-H., Chien, L.-J., Gomes, J., Lin, Y.-S., Yu, Y.-K., Liou, J.-S., and Syu, R.-J. (2010). Factors affecting lipid accumulation by *Nannochloropsis oculata* in a two-stage cultivation process. *Journal of Applied Phycology* 23, 903-908.

Su, C.H., Chien, L.J., Gomes, J., Lin, Y.S., Yu, Y.K., Liou, J.S., and Syu, R.J. (2011). Factors affecting lipid accumulation by *Nannochloropsis oculata* in a two-stage cultivation process. *Journal of Applied Phycology* 23, 903-908.

Subramanyam, R., Jolley, C., Thangaraj, B., Nellaepalli, S., Webber, A.N., and Fromme, P. (2010). Structural and functional changes of PSI-LHCI supercomplexes of *Chlamydomonas reinhardtii* cells grown under high salt conditions. *Planta* 231, 913-922.

Sudhir, P., and Murthy, S.D.S. (2004). Effects of salt stress on basic processes of photosynthesis. *Photosynthetica* 42, 481-486.

Sukenik, A., and Livne, A. (1991). Variations in Lipid and Fatty Acid Content in Relation to Acetyl CoA Carboxylase in the Marine Prymnesiophyte *Isochrysis galbana*. *Plant and Cell Physiology* 32, 371-378.

Sültemeyer, D. (1998). Carbonic anhydrase in eukaryotic algae: characterization, regulation, and possible function during photosynthesis. *Canadian Journal of Botany* 76, 962-972.

Sunkar, R., Bartels, D., and Kirch, H.-H. (2003). Overexpression of a stress-inducible aldehyde dehydrogenase gene from *Arabidopsis thaliana* in transgenic plants improves stress tolerance. *The Plant Journal* 35, 452-464.

Sutherland, D.L., Montemezzani, V., Howard-Williams, C., Turnbull, M.H., Broady, P.A., and Craggs, R.J. (2015). Modifying the high rate algal pond light environment and its effects on light absorption and photosynthesis. *Water Research* 70, 86-96.

Szyszk-Mroz, B., Pittock, P., Ivanov, A.G., Lajoie, G., and Hüner, N.P.A. (2015). The Antarctic Psychrophile *Chlamydomonas* sp. UWO 241 Preferentially Phosphorylates a Photosystem I-Cytochrome b6/f Supercomplex. *Plant Physiology* 169, 717-736.

Takagi, M., Karseno, and Yoshida, T. (2006). Effect of salt concentration on intracellular accumulation of lipids and triacylglyceride in marine microalgae *Dunaliella* cells. *Journal of Bioscience and Bioengineering* 101, 223-226.

Takeda, T., Ishikawa, T., Shigeoka, S., Hirayama, O., and Mitsunaga, T. (1993). Purification and characterization of glutathione reductase from *Chlamydomonas reinhardtii*. *Microbiology* *139*, 2233-2238.

Takouridis, S.J., Tribe, D.E., Gras, S.L., and Martin, G.J.O. (2015). The selective breeding of the freshwater microalga *Chlamydomonas reinhardtii* for growth in salinity. *Bioresource Technology* *184*, 18-22.

Taleb, A., Pruvost, J., Legrand, J., Marec, H., Le-Gouic, B., Mirabella, B., Legeret, B., Bouvet, S., Peltier, G., Li-Beisson, Y., *et al.* (2015). Development and validation of a screening procedure of microalgae for biodiesel production: Application to the genus of marine microalgae *Nannochloropsis*. *Bioresource Technology* *177*, 224-232.

Temple, S.J., Vance, C.P., and Stephen Gantt, J. (1998). Glutamate synthase and nitrogen assimilation. *Trends in Plant Science* *3*, 51-56.

Terashima, M., Freeman, E.S., Jinkerson, R.E., and Jonikas, M.C. (2015). A fluorescence-activated cell sorting-based strategy for rapid isolation of high-lipid *Chlamydomonas* mutants. *Plant Journal* *81*, 147-159.

Titman, D. (1976). Ecological Competition Between Algae: Experimental Confirmation of Resource-Based Competition Theory. *Science* *192*, 463-465.

Toledo-Ortiz, G., Huq, E., and Rodríguez-Concepción, M. (2010). Direct regulation of phytoene synthase gene expression and carotenoid biosynthesis by phytochrome-interacting factors. *Proceedings of the National Academy of Sciences* *107*, 11626-11631.

Torzillo, G., Sacchi, A., and Materassi, R. (1991). Temperature as an important factor affecting productivity and night biomass loss in *Spirulina platensis* grown outdoors in tubular photobioreactors. *Bioresource Technology* *38*, 95-100.

Tsai, C.-J., and Sun Pan, B. (2012). Identification of Sulfoglycolipid Bioactivities and Characteristic Fatty Acids of Marine Macroalgae. *Journal of Agricultural and Food Chemistry*.

Unwin, R.D. (2010). Quantification of Proteins by iTRAQ. In *Lc-MS/MS in Proteomics: Methods and Applications*, P.R. Cutillas, and J.F. Timms, eds., pp. 205-215.

Vallentine, P., Hung, C.-Y., Xie, J., and Van Hoewyk, D. (2014). The ubiquitin–proteasome pathway protects *Chlamydomonas reinhardtii* against selenite toxicity, but is impaired as reactive oxygen species accumulate. *AoB Plants* *6*.

Van Wagenen, J., Miller, T.W., Hobbs, S., Hook, P., Crowe, B., and Huesemann, M. (2012). Effects of Light and Temperature on Fatty Acid Production in *Nannochloropsis Salina*. *Energies* *5*, 731-740.

Vasudevan, P., and Briggs, M. (2008). Biodiesel production—current state of the art and challenges. *Journal of Industrial Microbiology & Biotechnology* 35, 421-430.

Vaughn, C.P., Crockett, D.K., Lim, M.S., and Elenitoba-Johnson, K.S.J. (2006). Analytical Characteristics of Cleavable Isotope-Coded Affinity Tag-LC-Tandem Mass Spectrometry for Quantitative Proteomic Studies. *The Journal of Molecular Diagnostics* 8, 513-520.

Veldhuis, M.J.W., Kraay, G.W., and Timmermans, K.R. (2001). Cell death in phytoplankton: correlation between changes in membrane permeability, photosynthetic activity, pigmentation and growth. *European Journal of Phycology* 36, 167-177.

Velmurugan, N., Sung, M.J., Yim, S.S., Park, M.S., Yang, J.W., and Jeong, K.J. (2014). Systematically programmed adaptive evolution reveals potential role of carbon and nitrogen pathways during lipid accumulation in *Chlamydomonas reinhardtii*. *Biotechnology for Biofuels* 7.

Venkata Mohan, S., and Devi, M.P. (2014). Salinity stress induced lipid synthesis to harness biodiesel during dual mode cultivation of mixotrophic microalgae. *Bioresource Technology* 165, 288-294.

Vensel, W.H., Dupont, F.M., Sloane, S., and Altenbach, S.B. (2011). Effect of cleavage enzyme, search algorithm and decoy database on mass spectrometric identification of wheat gluten proteins. *Phytochemistry* 72, 1154-1161.

Vieira, A.A.H., Nascimento, O.R., and Sartori, A.L. (1994). Release of Extracellular Polysaccharide by *Spondylosium panduriforme* (Desmidiaceae). *Revista De Microbiologia* 25, 6-10.

Vieler, A., Wilhelm, C., Goss, R., Süß, R., and Schiller, J. (2007). The lipid composition of the unicellular green alga *Chlamydomonas reinhardtii* and the diatom *Cyclotella meneghiniana* investigated by MALDI-TOF MS and TLC. *Chemistry and Physics of Lipids* 150, 143-155.

Vítová, M., Bišová, K., Umysová, D., Hlavová, M., Kawano, S., Zachleder, V., and Čížková, M. (2010). *Chlamydomonas reinhardtii*: duration of its cell cycle and phases at growth rates affected by light intensity. *Planta* 233, 75-86.

Wagner, H., Liu, Z., Langner, U., Stehfest, K., and Wilhelm, C. (2010). The use of FTIR spectroscopy to assess quantitative changes in the biochemical composition of microalgae. *Journal of Biophotonics* 3, 557-566.

Wagner, V., Gessner, G., Heiland, I., Kaminski, M., Hawat, S., Scheffler, K., and Mittag, M. (2006). Analysis of the phosphoproteome of *Chlamydomonas reinhardtii* provides new insights into various cellular pathways. *Eukaryot Cell* 5, 457-468.

Wahlen, B.D., Willis, R.M., and Seefeldt, L.C. (2011). Biodiesel production by simultaneous extraction and conversion of total lipids from microalgae, cyanobacteria, and wild mixed-cultures. *Bioresource Technology* *102*, 2724-2730.

Walker, D.A. (2009). Biofuels, facts, fantasy, and feasibility. *Journal of Applied Phycology* *21*, 509-517.

Wang, H., Alvarez, S., and Hicks, L.M. (2012). Comprehensive Comparison of iTRAQ and Label-free LC-Based Quantitative Proteomics Approaches Using Two *Chlamydomonas reinhardtii* Strains of Interest for Biofuels Engineering. *Journal of Proteome Research* *11*, 487-501.

Wang, S.-B., Chen, F., Sommerfeld, M., and Hu, Q. (2004). Proteomic analysis of molecular response to oxidative stress by the green alga *Haematococcus pluvialis* (Chlorophyceae). *Planta* *220*, 17-29.

Wang, Z.T., Ullrich, N., Joo, S., Waffenschmidt, S., and Goodenough, U. (2009). Algal Lipid Bodies: Stress Induction, Purification, and Biochemical Characterization in Wild-Type and Starchless *Chlamydomonas reinhardtii*. *Eukaryotic Cell* *8*, 1856-1868.

Wase, N., Black, P.N., Stanley, B.A., and DiRusso, C.C. (2014). Integrated Quantitative Analysis of Nitrogen Stress Response in *Chlamydomonas reinhardtii* Using Metabolite and Protein Profiling. *Journal of Proteome Research* *13*, 1373-1396.

Wawrik, B., and Harriman, B.H. (2010). Rapid, colorimetric quantification of lipid from algal cultures. *Journal of Microbiological Methods* *80*, 262-266.

Weast, R.C., Editor (1976-77). *Handbook of Chemistry and Physics*, 57th Edition (Cleveland, Ohio: CRC Press).

Wellburn, A.R. (1994). THE SPECTRAL DETERMINATION OF CHLOROPHYLL-A AND CHLOROPHYLL-B, AS WELL AS TOTAL CAROTENOIDS, USING VARIOUS SOLVENTS WITH SPECTROPHOTOMETERS OF DIFFERENT RESOLUTION. *J Plant Physiol* *144*, 307-313.

Weyer, K.M., Bush, D.R., Darzins, A., and Willson, B.D. (2010). Theoretical Maximum Algal Oil Production. *Bioenerg Res* *3*, 204-213.

White, S., Anandraj, A., and Bux, F. (2011). PAM fluorometry as a tool to assess microalgal nutrient stress and monitor cellular neutral lipids. *Bioresource Technology* *102*, 1675-1682.

Widjaja, A., Chien, C.-C., and Ju, Y.-H. (2009). Study of increasing lipid production from fresh water microalgae *Chlorella vulgaris*. *Journal of the Taiwan Institute of Chemical Engineers* *40*, 13-20.

Wiese, S., Reidegeld, K.A., Meyer, H.E., and Warscheid, B. (2007). Protein labeling by iTRAQ: A new tool for quantitative mass spectrometry in proteome research. *Proteomics* *7*, 340-350.

Willeford, K.O., Gombos, Z., and Gibbs, M. (1989). Evidence for Chloroplastic Succinate Dehydrogenase Participating in the Chloroplastic Respiratory and Photosynthetic Electron Transport Chains of *Chlamydomonas reinhardtii*. *Plant Physiology* 90, 1084-1087.

Williams, P.J.L., and Laurens, L.M.L. (2010). Microalgae as biodiesel & biomass feedstocks: Review & analysis of the biochemistry, energetics & economics. *Energy & Environmental Science* 3, 554-590.

Wong, D.M., and Franz, A.K. (2013). A comparison of lipid storage in *Phaeodactylum tricornutum* and *Tetraselmis suecica* using laser scanning confocal microscopy. *Journal of Microbiological Methods* 95, 122-128.

Woo, S.-G., Yoo, K., Lee, J., Bang, S., Lee, M., On, K., and Park, J. (2012). Comparison of fatty acid analysis methods for assessing biorefinery applicability of wastewater cultivated microalgae. *Talanta* 97, 103-110.

Wood, A.M., Everroad, R.C., and Wingard, L.M. (2005). Measuring Growth Rates in Microalgal Cultures. In *Algal Culturing Techniques*, R.A. Anderson, ed. (Elsevier Academic Press).

Work, V.H., Radakovits, R., Jinkerson, R.E., Meuser, J.E., Elliott, L.G., Vinyard, D.J., Laurens, L.M.L., Dismukes, G.C., and Posewitz, M.C. (2010). Increased Lipid Accumulation in the *Chlamydomonas reinhardtii* sta7-10 Starchless Isoamylase Mutant and Increased Carbohydrate Synthesis in Complemented Strains. *Eukaryotic Cell* 9, 1251-1261.

World Meteorological Organization (2014). WMO Greenhouse Gas Bulletin: The State of Greenhouse Gases in the Atmosphere Based on Global Observations through 2013.

Wright, J.C., Beynon, R.J., and Hubbard, S.J. (2010). Cross Species Proteomics. In *Proteome Bioinformatics*, S.J. Hubbard, and A.R. Jones, eds. (Humana Press), pp. 123-135.

Wu, C.C., and MacCoss, M.J. (2002). Shotgun proteomics: tools for the analysis of complex biological systems. *Curr Opin Mol Ther* 4, 242-250.

Wu, H., Volponi, J.V., Oliver, A.E., Parikh, A.N., Simmons, B.A., and Singh, S. (2011). In vivo lipidomics using single-cell Raman spectroscopy. *Proceedings of the National Academy of Sciences* 108, 3809-3814.

Wu, W.W., Wang, G., Baek, S.J., and Shen, R.-F. (2006). Comparative Study of Three Proteomic Quantitative Methods, DIGE, cICAT, and iTRAQ, Using 2D Gel- or LC-MALDI TOF/TOF. *Journal of Proteome Research* 5, 651-658.

Xia, L., Rong, J.F., Yang, H.J., He, Q.N., Zhang, D.L., and Hu, C.X. (2014). NaCl as an effective inducer for lipid accumulation in freshwater microalgae *Desmodesmus abundans*. *Bioresource Technology* 161, 402-409.

Xu, D., Gao, Z.Q., Li, F., Fan, X., Zhang, X.W., Ye, N.H., Mou, S.L., Liang, C.W., and Li, D.M. (2013). Detection and quantitation of lipid in the microalga *Tetraselmis subcordiformis* (Wille) Butcher with BODIPY 505/515 staining. *Bioresource Technology* 127, 386-390.

Yamada, T., Uchikata, T., Sakamoto, S., Yokoi, Y., Fukusaki, E., and Bamba, T. (2013). Development of a lipid profiling system using reverse-phase liquid chromatography coupled to high-resolution mass spectrometry with rapid polarity switching and an automated lipid identification software. *Journal of Chromatography A* 1292, 211-218.

Yang, H., He, Q., and Hu, C. (2015). Lipid accumulation by NaCl induction at different growth stages and concentrations in photoautotrophic two-step cultivation of *Monoraphidium dybowskii* LB50. *Bioresource Technology* 187, 221-227.

Yang, H., He, Q., Rong, J., Xia, L., and Hu, C. (2014). Rapid neutral lipid accumulation of the alkali-resistant oleaginous *Monoraphidium dybowskii* LB50 by NaCl induction. *Bioresource Technology* 172, 131-137.

Yao, C.-H., Ai, J.-N., Cao, X.-P., and Xue, S. (2013). Salinity manipulation as an effective method for enhanced starch production in the marine microalga *Tetraselmis subcordiformis*. *Bioresource Technology* 146, 663-671.

Yao, Y., Lu, Y., Peng, K.-T., Huang, T., Niu, Y.-F., Xie, W.-H., Yang, W.-D., Liu, J.-S., and Li, H.-Y. (2014). Glycerol and neutral lipid production in the oleaginous marine diatom *Phaeodactylum tricorutum* promoted by overexpression of glycerol-3-phosphate dehydrogenase. *Biotechnology for Biofuels* 7, 1-9.

Yeh, K.-L., and Chang, J.-S. (2011). Nitrogen starvation strategies and photobioreactor design for enhancing lipid content and lipid production of a newly isolated microalga *Chlorella vulgaris* ESP-31: Implications for biofuels. *Biotechnology Journal* 6, 1358-1366.

Yilancioglu, K., Cokol, M., Pastirmaci, I., Erman, B., and Cetiner, S. (2014). Oxidative Stress Is a Mediator for Increased Lipid Accumulation in a Newly Isolated *Dunaliella salina* Strain. *PLoS ONE* 9, e91957.

Yokthongwattana, C., Mahong, B., Roytrakul, S., Phaonaklop, N., Narangajavana, J., and Yokthongwattana, K. (2012). Proteomic analysis of salinity-stressed *Chlamydomonas reinhardtii* revealed differential suppression and induction of a large number of important housekeeping proteins. *Planta* 235, 649-659.

Yokthongwattana, K., Chrost, B., Behrman, S., Casper-Lindley, C., and Melis, A. (2001). Photosystem II Damage and Repair Cycle in the Green Alga *Dunaliella salina*: Involvement of a Chloroplast-Localized HSP70. *Plant and Cell Physiology* 42, 1389-1397.

Yoo, G., Park, W.-K., Kim, C.W., Choi, Y.-E., and Yang, J.-W. (2012). Direct lipid extraction from wet *Chlamydomonas reinhardtii* biomass using osmotic shock. *Bioresource Technology*.

Yoshida, K., Igarashi, E., Wakatsuki, E., Miyamoto, K., and Hirata, K. (2004). Mitigation of osmotic and salt stresses by abscisic acid through reduction of stress-derived oxidative damage in *Chlamydomonas reinhardtii*. *Plant Science* 167, 1335-1341.

Yu-huan, G., Lin, L., and Dong, W. (2009). Growth and Production of Astaxanthin in *Chlamydomonas nivalis* Cultured in Various Media. *Natural Product Research & Development* 21, 641-644.

Yu, W.-L., Ansari, W., Schoepp, N.G., Hannon, M.J., Mayfield, S.P., and Burkart, M.D. (2011). Modifications of the metabolic pathways of lipid and triacylglycerol production in microalgae. *Microbial Cell Factories* 10.

Yu, X., Zhao, P., He, C., Li, J., Tang, X., Zhou, J., and Huang, Z. (2012). Isolation of a novel strain of *Monoraphidium* sp. and characterization of its potential application as biodiesel feedstock. *Bioresource Technology* 121, 256-262.

Yuzawa, Y., Shimojima, M., Sato, R., Mizusawa, N., Ikeda, K., Suzuki, M., Iwai, M., Hori, K., Wada, H., Masuda, S., *et al.* (2014). Cyanobacterial monogalactosyldiacylglycerol-synthesis pathway is involved in normal unsaturation of galactolipids and low-temperature adaptation of *Synechocystis* sp. PCC 6803. *Biochimica et Biophysica Acta (BBA) - Molecular and Cell Biology of Lipids* 1841, 475-483.

Zachleder, V., and Vandenende, H. (1992). Cell Cycle Events in the Green Alga *Chlamydomonas eugametic* and their Control by Environmental Factors. *Journal of Cell Science* 102, 469-474.

Zhang, J., Xin, L., Shan, B., Chen, W., Xie, M., Yuen, D., Zhang, W., Zhang, Z., Lajoie, G.A., and Ma, B. (2012). PEAKS DB: De Novo Sequencing Assisted Database Search for Sensitive and Accurate Peptide Identification. *Molecular and Cellular Proteomics* 11, M111.010587.

Zhang, T., Gong, H., Wen, X., and Lu, C. (2010). Salt stress induces a decrease in excitation energy transfer from phycobilisomes to photosystem II but an increase to photosystem I in the cyanobacterium *Spirulina platensis*. *J Plant Physiol* 167, 951-958.

Zhila, N.O., Kalacheva, G.S., and Volova, T.G. (2011). Effect of salinity on the biochemical composition of the alga *Botryococcus braunii* Kutz IPPAS H-252. *Journal of Applied Phycology* 23, 47-52.

Zuo, Z.-J., Zhu, Y.-R., Bai, Y.-L., and Wang, Y. (2012). Volatile communication between *Chlamydomonas reinhardtii* cells under salt stress. *Biochemical Systematics and Ecology* 40, 19-24.

Zuo, Z., Chen, Z., Zhu, Y., Bai, Y., and Wang, Y. (2014). Effects of NaCl and Na<sub>2</sub>CO<sub>3</sub> stresses on photosynthetic ability of *Chlamydomonas reinhardtii*. *Biologia* 69, 1314-1322.

## 10.19 Appendix 1

During the course of this study, a selection of the lipid measurement techniques were employed on some algal samples grown under varying salt conditions.

Figures A and B show the contrasting results obtained from using one set of samples using esterification with GC (Figure A), and Nile Red staining and fluorescence measurement (Figure B). The Nile Red method indicates a high accumulation of lipids over time in 0.3 M salt conditions, using fluorescence as an arbitrary unit of measurement. However, the GC method indicates the opposite pattern of decreasing FAME content over time in these conditions. This is likely due to cell breakage in the samples that allows the membrane lipids to be fully exposed to Nile Red dye and gives a high reading that cannot be compared to intact cells with lipid droplets. These two vastly contrasting results indicate the problem of accuracy in lipid measurement techniques, and how it is possible to obtain false readings.

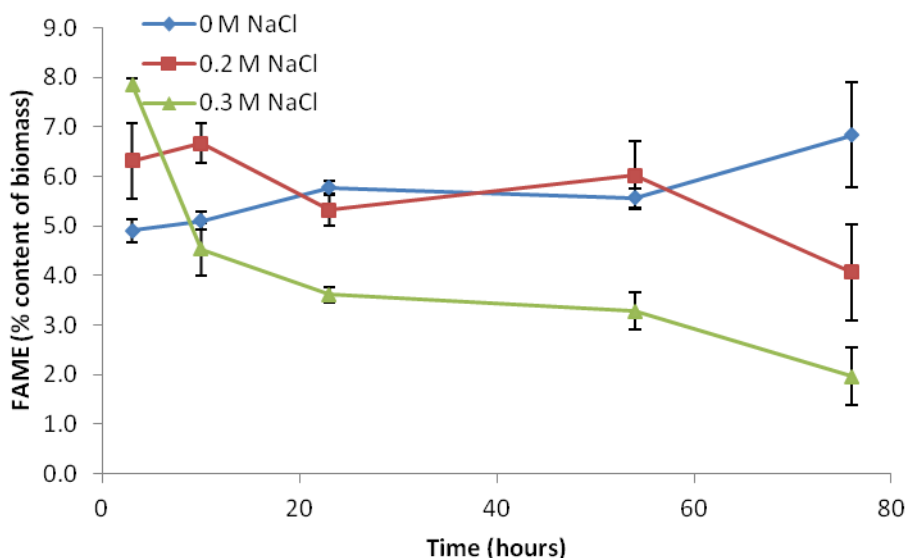


Figure A: Overall FAME content of biomass in *C. reinhardtii* under 0, 0.2 and 0.3 M conditions (n=3).

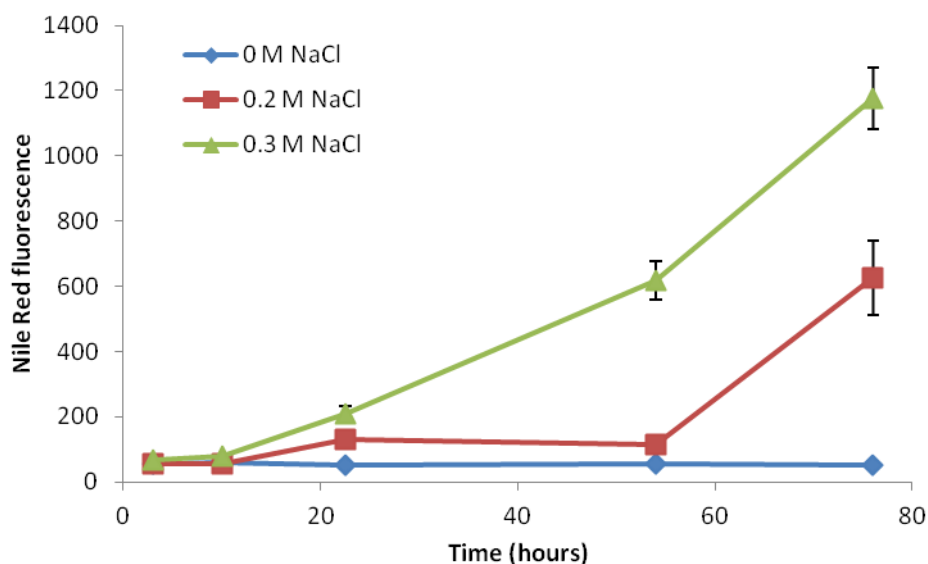


Figure B: Nile Red fluorescence of 0, 0.2 and 0.3 M NaCl *C. reinhardtii* cultures (n=3).

Figure C shows calibration curves for colorimetric (SPV) method using two different standards, and Table A shows the estimations of lipid content in samples that have been tested with these two different calibration curves and a variety of sample concentrations. These samples were also tested using the Bligh and Dyer gravimetric method, as detailed in Table A. As this data indicates, results vary between the colorimetric and the gravimetric methods, but also within the colorimetric method, depending on the standards used and sample size used.

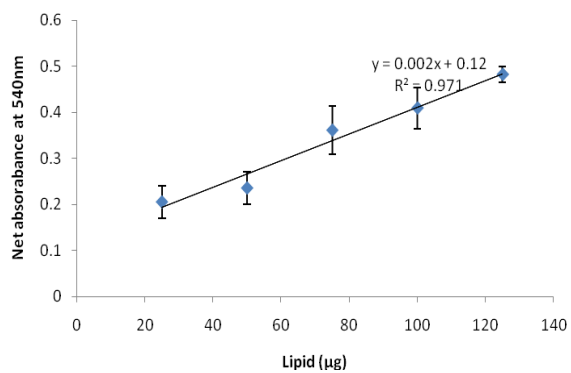
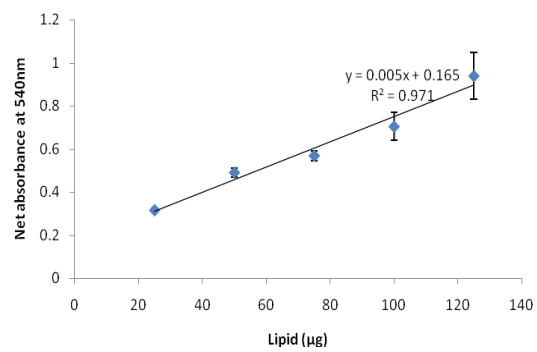


Figure C: Net absorbance curves for standard quantities of vegetable oil (left) and corn oil (right), measured using the microcolorimetric microplate format.

**Table A: Lipid measurements obtained from microcolorimetric method, with comparison to values obtained from gravimetric method. Two sets of values were calculated, based on calibration curves obtained from the corn oil and vegetable oil.**

Media	Solvent	Gravimetric result lipid content (µg/ml)	Corn oil equation			Vegetable oil equation		
			Lipid content µg/ml (25µl aliquot)	Lipid content µg/ml (50µl aliquot)	Lipid content µg/ml (100µl aliquot)	Lipid content µg/ml (25µl aliquot)	Lipid content µg/ml (50µl aliquot)	Lipid content µg/ml (100µl aliquot)
Standard TAP	1:2 Chloroform: Methanol	195.6	915.1	694.8	Overflow	375.7	282.7	Overflow
Standard TAP	Chloroform	195.6	214.1	179.2	143.5	95.3	76.5	Overflow
TAP 0.05M NaCl	1:2 Chloroform: Methanol	283.3	1165.3	Overflow	Overflow	475.7	Overflow	Overflow
TAP 0.05M NaCl	Chloroform	283.3	475.4	250.5	178.6	199.8	105.0	73.8
TAP 0.1M NaCl	1:2 Chloroform: Methanol	246.7	1049.0	791.8	Overflow	429.2	321.5	Overflow
TAP 0.1M NaCl	Chloroform	246.7	453.4	211.1	139.0	191.0	89.2	58.0
TAP 0.15M NaCl	1:2 Chloroform: Methanol	221.7	721.6	668.1	Overflow	298.3	272.0	Overflow
TAP 0.15M NaCl	Chloroform	221.7	358.5	197.3	162.3	153.0	83.7	67.3
TAP 0.05M NaCl	2:1 Chloroform: Methanol	266.7	1177.8	Overflow	Overflow	352.1	155.3	146.7
TAP 0.2M NaCl	2:1 Chloroform: Methanol	80.0	595.3	Overflow	Overflow	200.0	169.6	120.1

## 11 Appendix C: Supplementary material from Chapter 4

### 11.1 *C. reinhardtii* Experiment 1 data

#### 11.1.1 FAME Data

To more fully analyse the GC results, the individual components of the FAME data were analysed. The individual FAME components of the algal biomass components can be analysed in several ways. In this research, a 1 mg sample was analysed to compare the total amounts of FAME detected therein. The relative percentage contributions towards the biomass, or the relative make up of the FAMES in the total FAME, could also be examined. In this case, the percentage of the biomass that was FAME was calculated and compared, since this was a good way to compare the patterns of the different fatty acids.

Under 0.1 M NaCl stress, the levels of C16:0 in the 0.1 M NaCl cultures continue to rise beyond the range of the control cultures, and appear to be a major contributor to the overall rise in FAMES observed. This happens after stationary phase has been reached. Similar patterns are seen in C18:0 (stearic acid), C18:1*cis* (oleic acid) and C18:2*cis*; in all these major FAME elements, the 0.1 M salt stressed cultures had higher quantities of the FAME element in stationary phase than the cultures grown in normal TAP medium. Only C18:2*cis* and C17:0 showed higher quantities in salt stressed cells throughout the sampling points. C18:3n3 decreased in the 0.1 M salt stress cultures, although by the last sampling point the quantities were at similar levels again. This suggests a move away from C18:3n3 (alpha-linolenic acid) towards the other main FAME groups in response to 0.1 M salt stress.

C18:2*cis* is linoleic acid, and this is the other biggest contributor (with C16:0) to the FAMES that also shows an increase quantity under 0.1 M salt stress. Linoleic acid is part of the two-stage desaturation process of oleic acid to linolenic acid (Cherif *et al.*, 1975). Linolenic acid and the oleic and linoleic acid precursors are found in the photosynthetic tissue of the chloroplast, and linolenic and linoleic acids are the major

unsaturated fatty acids in photosynthetic tissue (Harris and James, 1965). This suggests that there are some changes taking place in photosynthetic activity under salt stress.

C16:0, or palmitic acid, is commonly found as an ester in triglycerides. It is also the first fatty acid formed during fatty acid synthesis (see Figure 1.6) (Harwood and Guschina, 2009). An increase in this fatty acid suggests that new fatty acids may be being synthesized after the salt stressed culture reaches stationary phase, whilst they are not in the control culture. An alternative hypothesis is that they are being synthesized in both cultures but not used in the salt stressed culture, and that the control culture utilizes these fatty acids in the stationary phase and converts them to other fatty acids. However, if this were the case, we would expect to see the rise of other fatty acids in the later stages of the control cultures as the C16:0 chains are converted. No such effect was observed.

In the 0.2 and 0.3 M NaCl experiments, the C16:0 content was increased at the three hour time point in the 0.3 M NaCl culture relative to the control, and then fluctuated. This initial increase is a large part of the overall increase in total FAME content. Since C16:0 is one of the first fatty acids made in fatty acid synthesis, this data suggests that fatty acids are being synthesized at the 3 hour 0.3 M NaCl data point. This may be a response of the cell to salinity stress for which additional lipids are required for compatible solutes or for maintaining membrane function, or it may be a stress response similar to that seen during nitrogen deprivation where fatty acids start to accumulate because growth is halted. The 0.2 M NaCl culture shows an overall higher level of C16:0, showing higher accumulation without the degradation. Similar patterns are seen in C18:2*cis*, C18:3n3 and C17:0 to the C16:0; there is an initial spike in the 0.3 M NaCl stressed culture above that of control conditions, and then a sharp decline as the culture starts to die off and the fatty acids degrade or are otherwise lost from the samples.

In the full time course experiment, C18:0 rises over time with 0.2 and 0.3 M salt stress, after starting at a similar level to the control conditions. Stearic acid (C18:0) is a saturated fatty acid, from which unsaturated fatty acids can be derived within the

algae cell. Since this coincides with the decline of many of the unsaturated C18 chains, it suggests that the conversion from saturated to unsaturated is halted, but that the C18:0 fatty acids are still being made in the cells despite the decaying culture. In the 2nd 0.2 and 0.3 M NaCl experiment, the C18:0 increases under control conditions but not in saline conditions, which is the opposite pattern to that seen in the previous 0.2 M and 0.3 M NaCl experiment. As this data is so conflicting, it suggests that something differed between these two experiments either in the measuring of this particular fatty acid, or that biologically it has genuinely behaved completely differently between the two experiments. There are large error bars on the control conditions (t=50), meaning this data point is unreliable to draw conclusions from.

C18:1*cis* does not show the same response in both the salt conditions. High salt at 0.3 M NaCl causes an overall decline resulting in almost complete degradation of this fatty acid. 0.2 M NaCl salt shows a sharp increase in C18:1*cis* level after the first time point and continues to be higher than the control culture. It is clear from the growth data that this level of salt halts culture growth, but the microscopy suggests that the cells are still alive throughout this experiment. C18:1*cis*, therefore, may play a role in salt tolerance and surviving these high salinity conditions. However, the latter 0.2 and 0.3 M NaCl data showed a different response that conflicted with this data. The second 0.2 and 0.3 M NaCl experiment shows that C18:3n3 behaves differently to the data of the first 0.2 and 0.3 M NaCl experiment; the initial FAME increase in the 0.3 M NaCl conditions of the first experiment is not present in the experiment using internal standards. The FAME then decreases under salt stress in the same pattern in the later time point, although much more markedly in the 0.3 M NaCl than in the 0.2 M.

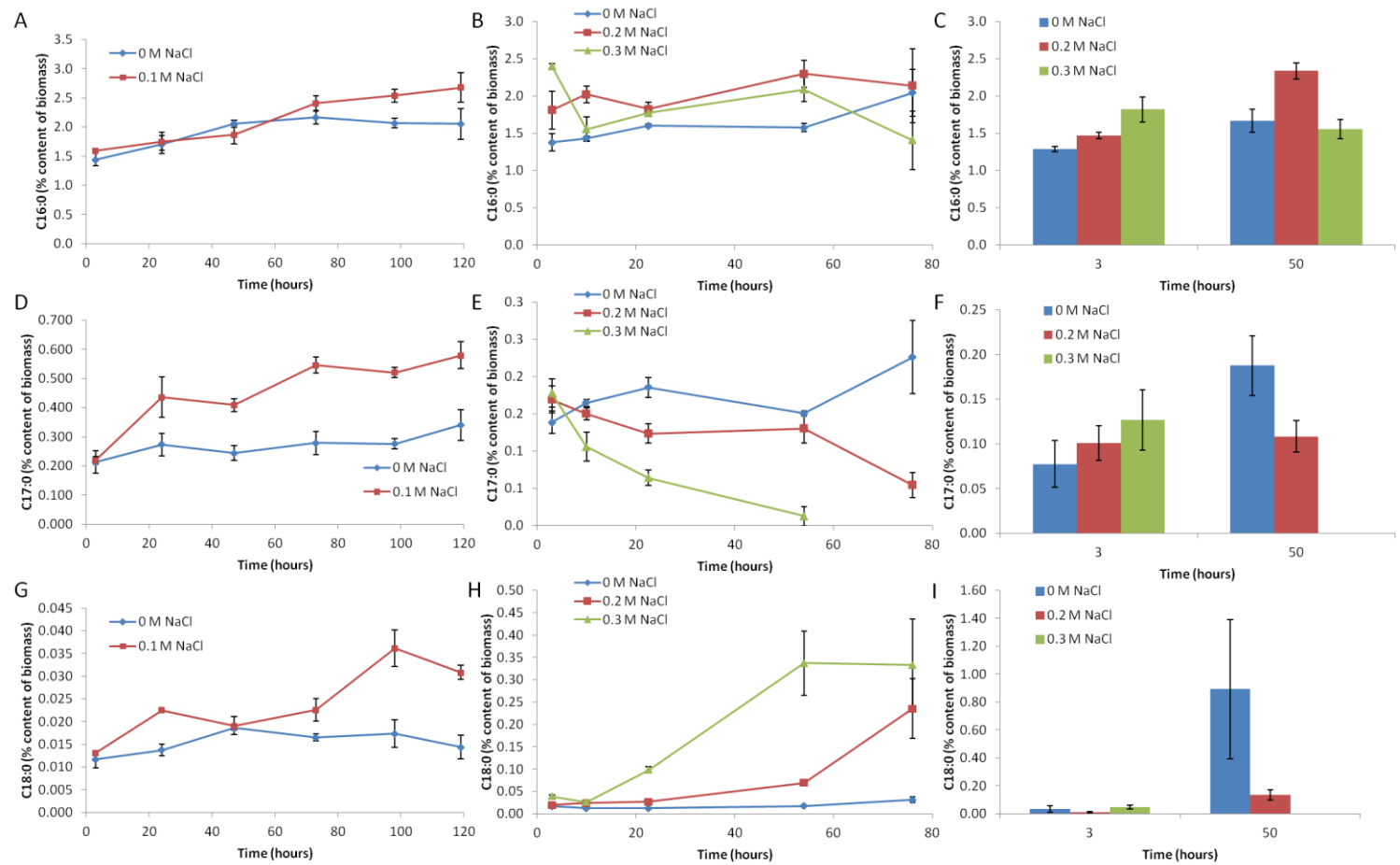


Figure 11.1 Percentage content of biomass of C16:0, C17:0 and C18:0 under control and 0.1 M NaCl (A, D, G), control with 0.2 and 0.3 M NaCl (B, C, E, F, H, I) (n=3).

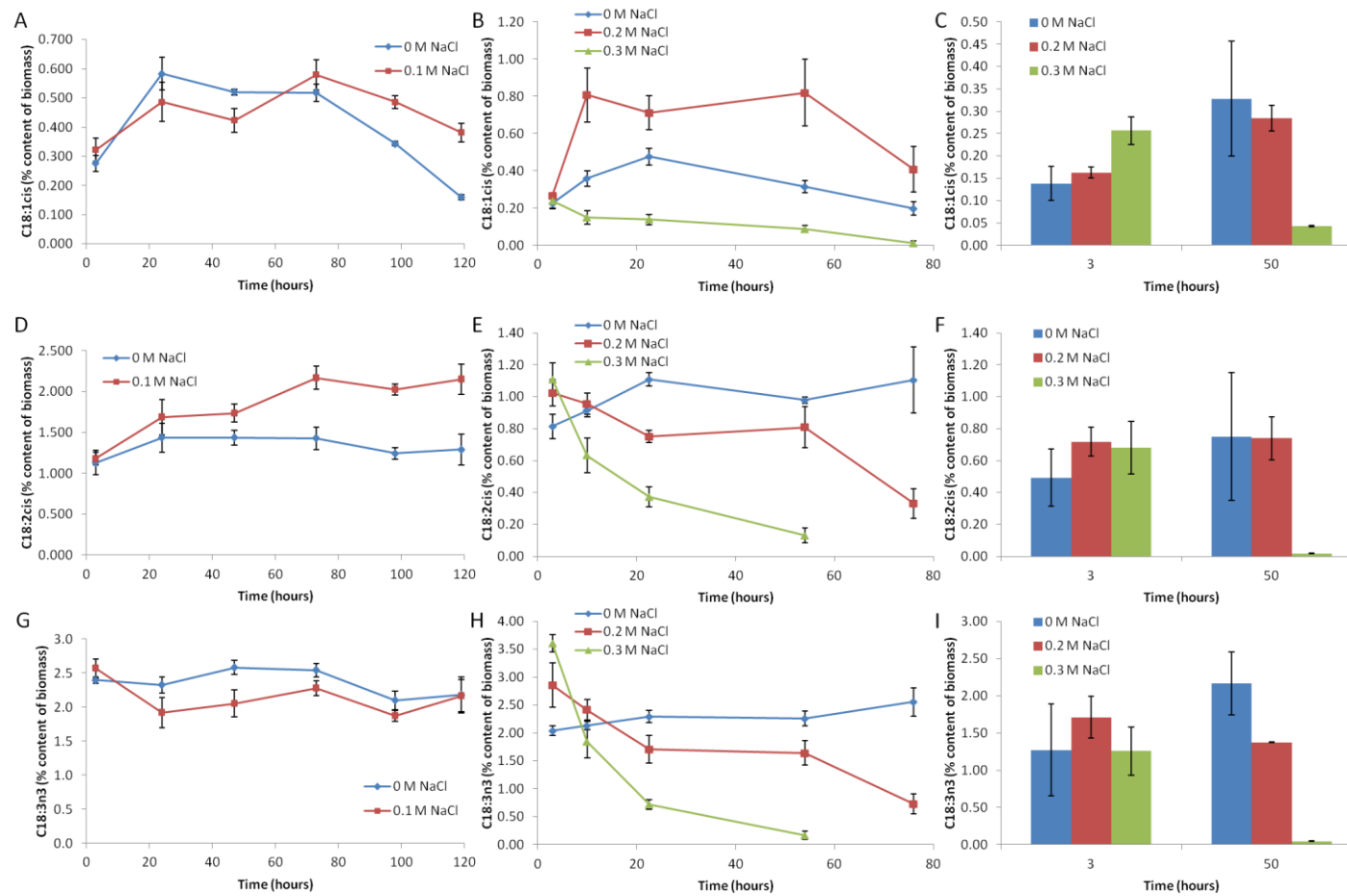


Figure 11.2 Percentage content of biomass of C18:1cis, C18:2cis and C18:3n3 under control and 0.1 M NaCl (A, D, G), control with 0.2 and 0.3 M NaCl (B, C, E, F, H, I) (n=3).

### 11.1.2 Starch content of algal biomass

Figure 11.3 shows the carbohydrate content of biomass under control, 0.1 M, 0.2 and 0.3 M NaCl conditions. The control TAP conditions show a steady increase in carbohydrate content followed by a shallow decline. In 0.1 M NaCl, the carbohydrate contents are the same as the control until 24 hours, and after this point the two conditions diverge slightly in relative levels, although the pattern over time is very similar for the two. Both cultures show a slight decline in carbohydrate level as the culture growth plateaus, suggesting that some carbohydrates are being utilised or converted during this period. The 0.1 M salt culture having a higher carbohydrate level suggests that more is being stored and less is being utilised than in the normal TAP conditions.

At the initial time point, 0.2 and 0.3 M NaCl salt concentrations induce an increase in carbohydrate content in comparison to the control conditions. When comparing this with the growth curves, the increase in carbohydrate occurs at the same time as the increase in biomass and OD. This suggests that carbohydrates start at a low level in a culture but increase as the culture reaches its stationary phase. This supports the idea that carbohydrates are storage molecules and therefore not usually accumulating until the cells have stopped dividing. The slight decrease in carbohydrate after this point suggests some of this storage molecule is being used up as time goes on. The 0.2 and 0.3 M salt conditions show a decline in carbohydrate content after the initially high carbohydrate level, suggesting that carbohydrates are being used up or converted under these conditions. These stay low until the last time point, when the 0.2 M NaCl cultures show an increase in carbohydrate levels.

In the second 0.2 and 0.3 M NaCl experiment, the 0.2 M salt cultures behaved slightly differently to the previous experimental run. The initial carbohydrate increase is not present in 0.2 M salt but is found in 0.3 M salt cultures. The 0.2 M salt also shows a large increase in carbohydrate concentration, but at a much earlier time point than the previous experiment. However, this data point shows a large amount of variation, making it unreliable to draw conclusions on. It is clear, however, that salt has a large effect on carbohydrate metabolism of the *C. reinhardtii* cells, even in this starchless

mutant. This is of interest since carbohydrates are the alternative carbon storage molecule of microalgae (Ball et al., 1990), and increases in carbohydrate also represent a partitioning of carbon resources under stress, although not towards the desired lipid product.

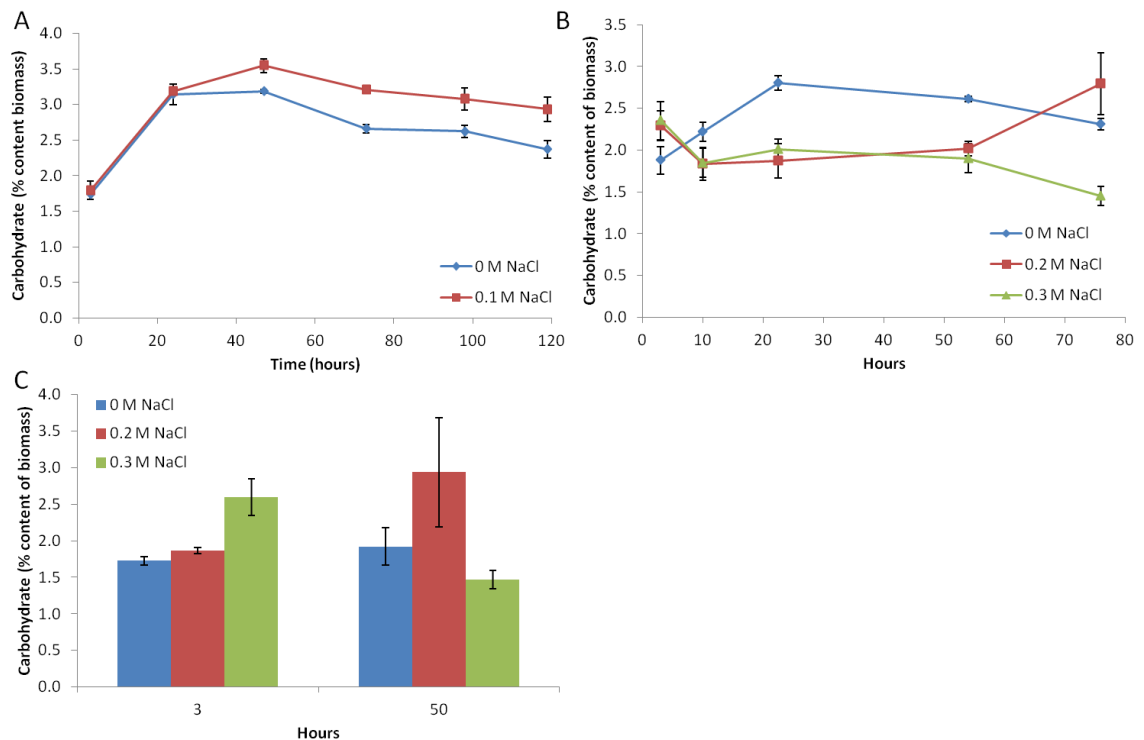


Figure 11.3 Carbohydrate content of *C. reinhardtii* cultures growth under control with 0.1 M NaCl conditions (A) and in control with 0.2 and 0.3 M NaCl conditions (B, C) (n=3).

### 11.1.3 Chlorophyll data

Some species of algae have their chlorophyll contents affected by salinity, whilst others show little chlorophyll variation under different salinities (McLachlan, 1961). Figure 11.4 shows the pigment content of the biomass obtained in cultures grown in control and salt conditions. Whilst there are slight fluctuations, the 0.1 M NaCl condition does not deviate far from the control conditions. This suggests that 0.1 M NaCl does not have any detrimental effect on the pigmentation of *C. reinhardtii*, nor does it alter it in any significant way. This adds to the body of evidence amassed in this chapter showing that *C. reinhardtii* can function comfortable under a 0.1 M NaCl concentration.

0.2 and 0.3 M NaCl have a severe detrimental effect on the photosynthetic pigments, with chlorophyll *a*, chlorophyll *b* and carotenoids all showing lower concentrations in 0.2 M NaCl conditions and the lowest concentrations in 0.3 M NaCl conditions. The steady decrease in these concentrations over time in the salt stressed cultures support the evidence that 0.2 and 0.3 M NaCl are lethal to these cells and prevent their normal biological function.

Batterto and Vanbaale (1971) describe how salt stress leads to a loss of pigmentation in green algae. This is what has been observed here in 0.2 and 0.3 M NaCl cultures, but not in 0.1 M NaCl cultures. This supports the evidence that *C. reinhardtii* is tolerant of salinity 0.1 M NaCl as neither photosynthetic pigments nor growth are negatively affected.

In *C. reinhardtii*, salinity stress lowers the rates of light saturated photosynthesis as salinity reduces the repair of cells from photodamage, and increases photoinhibition (Neale and Melis, 1989).

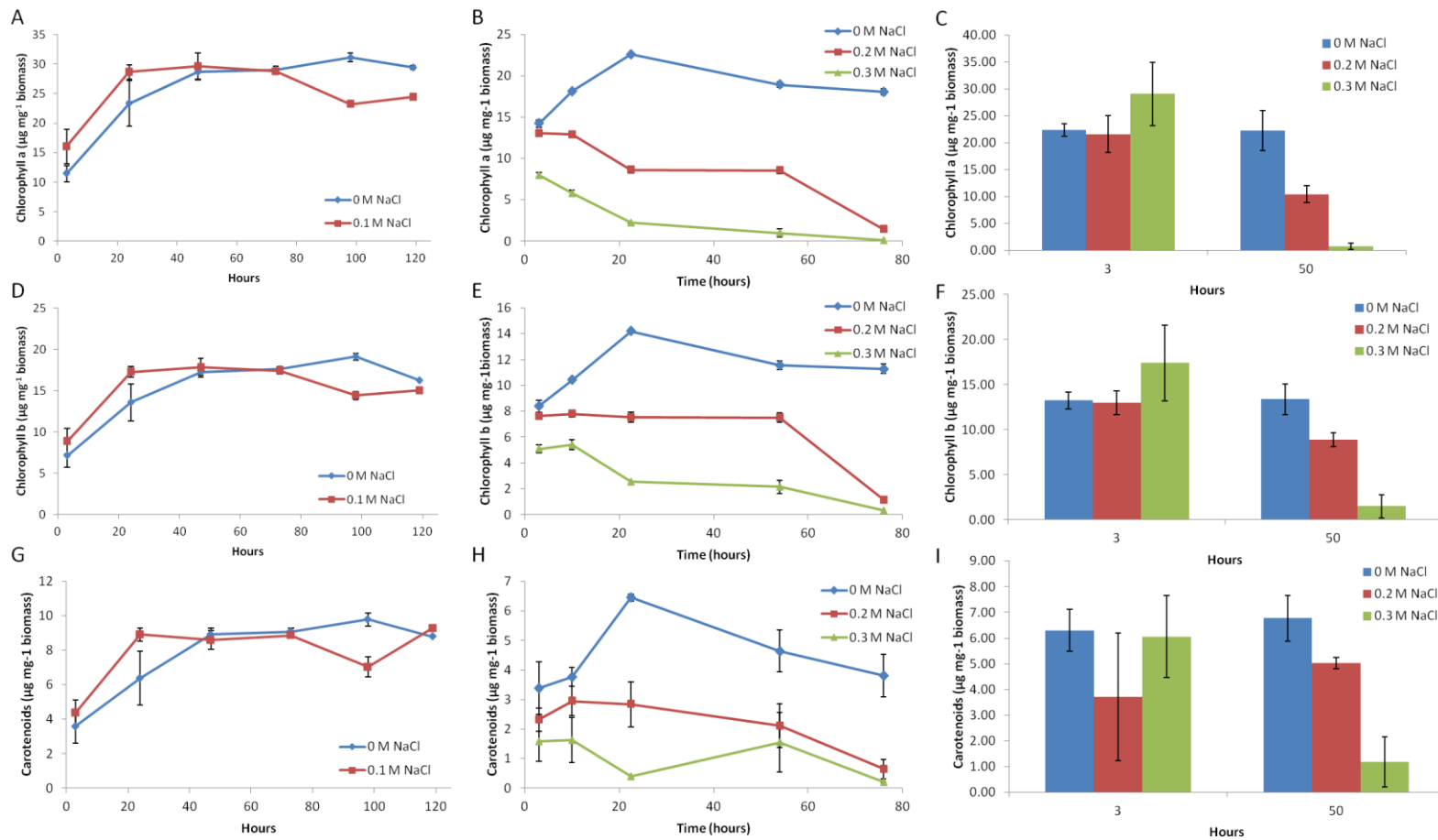


Figure 11.4 Chlorophyll a (A, B, C), chlorophyll b (D, E, F) and carotenoid (G, H, I) content of algal biomass under 0.1 M NaCl (A, D, G) and under 0.2 and 0.3 M NaCl (B, C, E, F, H, I) (n=3).

## 11.2 Bradford protein quantification

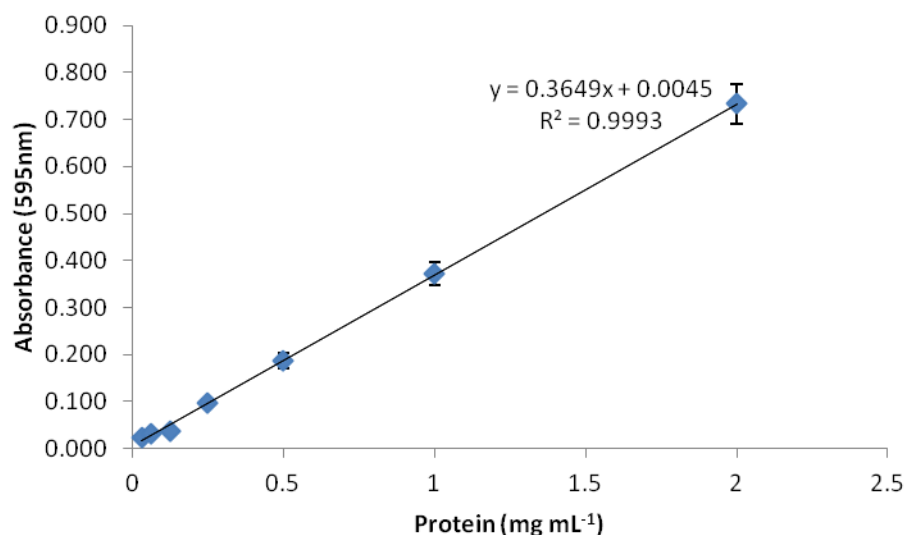


Figure 11.5 Bradford calibration curve for protein quantification.

## 11.3 Protein changes between phenotypes in iTRAQ experiment

Table 11.1 Protein changes between 3 hour 0.2 M NaCl and 11 hour 0.2 M NaCl cultures in *C. reinhardtii*.

Accession number	Protein name	No. unique peptides	Fold change	P value
A8JFW4	1-deoxy-D-xylulose 5-phosphate synthase (EC 2.2.1.7) (Fragment)	18	-1.203	0.005
P46295	40S ribosomal protein S14	15	1.246	0.005
A8HS48	40S ribosomal protein S3a	19	1.323	0.000
A8IMP6	40S ribosomal protein S4	26	1.122	0.026
A8J1G8	40S ribosomal protein S6	24	1.342	0.000
A8IUV7	60S ribosomal protein L13	20	1.178	0.009
A8JCQ8	Acetyl CoA synthetase (EC 6.2.1.1)	8	-1.166	0.006
A8J6J6	Acetyl-CoA acyltransferase (EC 2.3.1.16)	23	1.162	0.005
A8HMQ1	Aconitate hydratase, mitochondrial (Aconitase) (EC 4.2.1.-)	53	-1.181	0.000
A8J6A7	Adenylylphosphosulfate reductase	10	-1.325	0.000
A8J3Y6	AIR synthase-related protein	26	-1.221	0.014
A8HZZ4	Alanine aminotransferase (EC 2.6.1.2)	22	-1.222	0.000
A8JFJ2	Alanine-glyoxylate transaminase	20	-1.100	0.021
Q1RS84	Aldehyde-alcohol dehydrogenase	51	1.134	0.001
A8IYK1	Alpha-1,4 glucan phosphorylase (EC 2.4.1.1)	34	1.098	0.009
Q2VA41	Alpha-1,4 glucan phosphorylase (EC 2.4.1.1)	34	1.098	0.009

Q2VA40	Alpha-1,4 glucan phosphorylase (EC 2.4.1.1)	34	1.123	0.001
A8HT91	Aminotransferase	9	-1.134	0.013
A8I263	Aspartate aminotransferase (EC 2.6.1.1)	11	-1.283	0.005
A8HXW8	Aspartate aminotransferase (EC 2.6.1.1)	8	-1.253	0.005
A8J173	Aspartate semialdehyde dehydrogenase	10	-1.165	0.013
Q39595	ATP sulfurylase Ats1	14	-1.207	0.002
A8IXF1	ATP-sulfurylase	13	-1.189	0.007
A8JB85	Autophagy-related protein	5	1.385	0.017
A8J1S7	Bifunctional aspartate kinase/homoserine dehydrogenase (EC 2.7.2.4)	25	-1.102	0.004
Q75T33	Calcium sensing receptor	37	1.106	0.019
A8IT01	Carbonic anhydrase (EC 4.2.1.1)	28	-1.254	0.001
P20507	Carbonic anhydrase 1 (EC 4.2.1.1) (Carbonate dehydratase 1) (CA1) [Cleaved into: Carbonic anhydrase 1 large chain; Carbonic anhydrase 1 small chain]	28	-1.254	0.001
A8IF48	Centriole proteome protein (Fragment)	11	1.138	0.032
A8J094	Chitinase-related protein	12	1.142	0.002
Q8S567	Chlorophyll a/b-binding protein	13	-1.190	0.014
Q539Y4	Chloroplast lycopene epsilon-cyclase (Fragment)	5	-1.238	0.006
Q6J213	Chloroplast phytoene desaturase (Phytoene desaturase) (EC 1.3.-.-) (EC 1.3.99.-)	28	-1.115	0.001
Q6J216	Chloroplast phytoene synthase (Fragment)	8	-1.183	0.012
Q6J214	Chloroplast phytoene synthase (Phytoene synthase) (EC 2.5.1.32)	8	-1.183	0.012
A8IDJ7	Chromodomain-helicase-DNA-binding protein	7	1.195	0.009
A8ILK1	Cilia- and flagella-associated protein 52	7	-1.175	0.030
A8I972	CipB chaperone, Hsp100 family	33	1.152	0.000
A8HYR2	Cobalamin-dependent methionine synthase (EC 2.1.1.13)	23	-1.121	0.010
A8JJT1	Cobalamin-dependent methionine synthase (Fragment)	18	-1.131	0.015
Q84X74	CR057 protein (Mitochondrial phosphate carrier 1)	19	1.158	0.008
A8J355	Cystathionine gamma-synthase	16	-1.120	0.014
A8J5W8	DNA replication factor C complex subunit 1 (Fragment)	6	1.338	0.025
A8JI07	Dual function alcohol dehydrogenase / acetaldehyde dehydrogenase	51	1.134	0.001
A8J637	Elongation factor Ts	47	-1.126	0.004
Q5QEB2	Elongation factor Ts	47	-1.126	0.004
A8IIK8	ER-located HSP110/SSE-like protein	23	1.234	0.014
A8HX38	Eukaryotic translation elongation factor 1 alpha 1 (EC 3.6.5.3) (Eukaryotic translation elongation factor 1 alpha 2)	76	1.108	0.008
Q9LD42	Fe-assimilating protein 1 (High-CO2 inducible, periplasmic protein)	5	-1.248	0.017
A8IYA1	Fe-assimilating protein 2	16	-1.439	0.000
Q8LL91	Ferroxidase-like protein (Multicopper ferroxidase)	18	-1.250	0.002
A8JG73	Flagellar associated protein	16	-1.308	0.000
A8J9R3	Flagellar associated protein	5	1.252	0.016
A8IZV9	Flagellar associated protein (Fragment)	37	1.170	0.000
A8JGD1	Glutamate dehydrogenase	14	1.220	0.002
A8J2W0	Glutamic-gamma-semialdehyde dehydrogenase	9	1.186	0.022
A8HXA6	Glutathione reductase	8	-1.195	0.006
A8JEB2	Glutathione S-transferase (EC 2.5.1.18)	3	-1.294	0.018
A0A0B5KTL4	Glycerol-3-phosphate dehydrogenase [NAD(+)] (EC 1.1.1.8)	33	1.675	0.000
A8HNN4	Glycerol-3-phosphate dehydrogenase [NAD(+)] (EC 1.1.1.8)	33	1.675	0.000
A0A0B5KYA7	Glycerol-3-phosphate dehydrogenase [NAD(+)] (EC 1.1.1.8)	29	1.719	0.000
A8HNN6	Glycerol-3-phosphate dehydrogenase [NAD(+)] (EC 1.1.1.8) (Fragment)	27	1.744	0.000
A8IZS5	Glycine-rich RNA-binding protein	22	1.223	0.012

Q945T2	GrpE protein homolog	16	-1.223	0.000
A8HYV3	Heat shock protein 70B	62	1.073	0.003
Q39603	Heat shock protein 70B	62	1.073	0.003
A8HN65	High light-induced nuclease	14	1.128	0.011
A8HXE1	High mobility group protein	8	1.164	0.024
A8IR79	Histone H2B	15	1.246	0.005
A8JDC0	Histone H2B	15	1.257	0.003
A8HWX1	Histone H2B	15	1.262	0.003
A8HSB2	Histone H2B	15	1.266	0.003
A8HV98	Histone H2B	15	1.270	0.002
A8HWX5	Histone H2B	15	1.270	0.002
A8IR69	Histone H2B	15	1.270	0.002
A8IW75	Histone H2B	15	1.331	0.002
A8IW84	Histone H2B	15	1.331	0.002
P54346	Histone H2B.3 (H2B-III)	15	1.270	0.002
P54347	Histone H2B.4 (H2B-IV)	15	1.270	0.002
A8HSA7	Histone H3	11	1.149	0.017
A8J9M0	Histone H3	11	1.149	0.017
A8HWY2	Histone H3 (Fragment)	11	1.149	0.017
A8IK09	Histone H3 (Fragment)	11	1.149	0.017
Q6LCW8	Histone H3 type 2	11	1.149	0.017
P50564	Histone H3 type 3	11	1.149	0.017
A8I3J7	Homoserine dehydrogenase (HDH) (EC 1.1.1.3)	4	-1.242	0.020
A8J841	Hydroxymethylpyrimidine phosphate synthase	14	-1.244	0.008
A8I4F6	Imidazoleglycerol-phosphate dehydratase (EC 4.2.1.19)	3	-1.124	0.031
A8ICC8	Inorganic pyrophosphatase	11	-1.215	0.002
Q39577	Isocitrate lyase	24	-1.138	0.003
A8J244	Isocitrate lyase (EC 4.1.3.1)	26	-1.162	0.002
Q75VY7	Light-harvesting chlorophyll-a/b protein of photosystem I (Light-harvesting protein of photosystem I)	9	-1.240	0.014
A8ITV3	Light-harvesting protein of photosystem I	13	-1.190	0.014
A8JOB1	Low-CO2-inducible protein	12	-1.161	0.013
A8J225	Low-CO2-inducible protein (Fragment)	14	1.285	0.016
A8HWI0	Lycopene epsilon cyclase (EC 1.14.-.-)	5	-1.238	0.006
Q93WE2	Magnesium chelatase H subunit (Magnesium chelatase H-subunit)	33	-1.161	0.001
A8I7P5	Magnesium chelatase subunit H	33	-1.161	0.001
A8IJ34	Methyltransferase (EC 2.1.1.-)	18	1.146	0.007
I2FKQ9	Mitochondrial chaperonin 60	36	1.072	0.013
A8IEH0	Mitochondrial phosphate carrier 1, minor isoform	19	1.158	0.008
A8IZT9	Multicopper ferroxidase	18	-1.250	0.002
A2PZD2	NAD-dependent epimerase/dehydratase (Predicted protein)	10	1.363	0.005
A8IA86	Nucleolar protein, component of C/D snoRNPs	16	1.158	0.019
A8IRU6	Peptidyl-prolyl cis-trans isomerase, cyclophilin-type	32	1.092	0.012
Q3HTK2	Pherophorin-C5 protein	4	-1.986	0.008
A8IFK0	Plasma membrane ATPase (EC 3.6.3.6)	17	-1.122	0.021
Q93Z22	Plasma membrane ATPase (EC 3.6.3.6)	23	1.102	0.020
A8HVP7	Plastid ribosomal protein L10	13	-1.186	0.016
A8JAL6	Plastid ribosomal protein L15	15	1.100	0.024
A8HTY0	Plastid ribosomal protein L7/L12	27	-1.163	0.003
Q70DX8	Plastid ribosomal protein S1 (Ribosomal protein S1 homologue)	15	-1.243	0.000

A8J8M5	Plastid ribosomal protein S5	27	-1.117	0.004
A8J5Y7	Plastid ribosomal protein S6	5	-1.316	0.017
A8J8B2	Plastid-specific ribosomal protein 1	17	1.232	0.002
A8I8A3	Plastid-specific ribosomal protein 3	10	-1.227	0.003
A8JH68	Plastocyanin	11	-1.272	0.012
P18068	Plastocyanin, chloroplastic (PC6-2)	11	-1.272	0.012
A8HPE9	Predicted protein	9	-1.280	0.001
A8JC37	Predicted protein	3	-1.259	0.020
A8JGL0	Predicted protein	4	-1.252	0.016
A8JHB7	Predicted protein	26	-1.127	0.001
A8J8V6	Predicted protein	28	-1.099	0.007
A8IWL3	Predicted protein	26	1.126	0.000
A8ITU2	Predicted protein	24	1.131	0.006
A8J5N1	Predicted protein	12	1.156	0.030
A8J2L0	Predicted protein	21	1.229	0.014
A8I804	Predicted protein	4	1.351	0.014
A8JCP3	Predicted protein	13	1.373	0.002
A8J135	Predicted protein	5	1.530	0.017
A8ISG3	Predicted protein (Fragment)	21	1.108	0.003
A8JCE1	Predicted protein (Fragment)	13	1.140	0.020
A8JK31	Predicted protein (Fragment)	4	1.240	0.017
A8IBM2	Predicted protein of CLR family	6	1.273	0.010
A8I8V6	Prohibitin	9	1.170	0.007
A8HQT1	Protein disulfide isomerase	14	1.278	0.000
O48949	Protein disulfide-isomerase (EC 5.3.4.1)	32	1.194	0.000
A8J214	Pyruvate kinase (EC 2.7.1.40)	11	-1.108	0.016
A8I6T5	R1 protein, alpha-glucan water dikinase	28	1.144	0.001
A8JGM1	Rhodanese-like Ca-sensing receptor	37	1.106	0.019
A8IZW6	Ribose-phosphate pyrophosphokinase	7	-1.184	0.019
A8J239	Ribosomal protein L23a	13	1.247	0.008
A8J1A3	Ribosomal protein L24	7	1.280	0.003
A8HMG7	Ribosomal protein L26	15	1.180	0.019
A8JF05	Ribosomal protein L28	7	1.288	0.017
A8J0I0	Ribosomal protein L4	34	1.128	0.019
A8JHC3	Ribosomal protein S11	11	1.206	0.009
A8IGY1	Ribosomal protein S13	12	1.213	0.005
A8J768	Ribosomal protein S14	15	1.246	0.005
A8IZ36	Ribosomal protein S25	8	1.353	0.003
A8I4P5	Ribosomal protein S3	20	1.186	0.002
Q7Y258	Ribosomal protein S5	27	-1.117	0.004
A8JGP9	Ribulose biphosphate carboxylase small chain (EC 4.1.1.39)	23	-1.213	0.012
P00873	Ribulose biphosphate carboxylase small chain 1, chloroplastic (RuBisCO small subunit 1) (EC 4.1.1.39)	23	-1.213	0.012
P08475	Ribulose biphosphate carboxylase small chain 2, chloroplastic (RuBisCO small subunit 2) (EC 4.1.1.39)	23	-1.219	0.012
A8HYU5	S-adenosylmethionine synthase (AdoMet synthase) (EC 2.5.1.6) (Methionine adenosyltransferase) (MAT)	21	-1.180	0.017
A8J4R9	Serine hydroxymethyltransferase (EC 2.1.2.1)	17	-1.191	0.003
Q93Y52	Soluble inorganic pyrophosphatase 1, chloroplastic (EC 3.6.1.1) (Pyrophosphate phospho-hydrolase 1) (PPase 1)	11	-1.215	0.002
O64927	Starch synthase, chloroplastic/amyloplastic (EC 2.4.1.-)	6	-1.115	0.012

A8HX04	Succinate dehydrogenase [ubiquinone] iron-sulfur subunit, mitochondrial (EC 1.3.5.1)	12	1.147	0.002
A8IGH1	Superoxide dismutase (EC 1.15.1.1)	9	-1.201	0.013
A8I5N5	Tetrapyrrole-binding protein	6	-1.280	0.007
A8J9T5	Thiamine thiazole synthase, chloroplastic (Thiazole biosynthetic enzyme)	30	-1.306	0.000
A8I9R1	Threonine dehydratase (EC 4.3.1.19) (Threonine deaminase)	7	-1.197	0.007
A8J724	Transcriptional coactivator-like protein	16	1.091	0.026
A8JI60	Type-II calcium-dependent NADH dehydrogenase	14	-1.122	0.022
A8J1C1	Ubiquitin-activating enzyme E1 (EC 6.3.2.19)	24	-1.088	0.023
A8J9S9	UDP-glucose 4-epimerase	10	-1.204	0.004
A8J9I4	UDP-glucose 6-dehydrogenase (EC 1.1.1.22)	15	1.263	0.001
A2PZC3	UDP-glucose 6-dehydrogenase (EC 1.1.1.22)	14	1.298	0.000
A8JC21	Uroporphyrinogen decarboxylase (EC 4.1.1.37)	12	-1.240	0.000

**Table 11.2 Protein changes between 11 hour 0.2 M NaCl cultures and 18 hour 0.2 M NaCl cultures in *C. reinhardtii*.**

Accession number	Protein name	No. unique peptides	Fold Change	P value
A8HRS5	10-formyltetrahydrofolate synthetase	5	1.128	0.015
A8JGV6	14-3-3 protein (EC 3.1.1.4)	26	1.123	0.003
Q7X7A7	14-3-3 protein (EC 3.1.1.4) (14-3-3-like protein)	24	1.120	0.002
P52908	14-3-3-like protein	26	1.123	0.003
A8J8V5	26S proteasome regulatory subunit	5	1.101	0.015
O47027	30S ribosomal protein S2, chloroplastic	22	-1.099	0.004
Q08365	30S ribosomal protein S3, chloroplastic (ORF 712)	38	-1.082	0.002
Q6EMK7	38 kDa RNA-binding protein (Chloroplast-targeted RNA-binding protein) (RNA-binding protein RB38)	7	-1.195	0.020
A8HVQ1	40S ribosomal protein S8	13	-1.091	0.015
P11094	50S ribosomal protein L14, chloroplastic	8	-1.151	0.001
Q8HTL2	50S ribosomal protein L2, chloroplastic	16	-1.159	0.009
Q8HTL1	50S ribosomal protein L5, chloroplastic	15	-1.109	0.007
A8IQC1	60S ribosomal protein L27	10	-1.115	0.014
A8IAT4	Acetohydroxy acid isomeroeductase (EC 1.1.1.86)	18	1.104	0.011
A8IX80	Acetohydroxyacid dehydratase	25	1.077	0.012
A8HMQ1	Aconitate hydratase, mitochondrial (Aconitase) (EC 4.2.1.-)	53	1.075	0.005
A8IXE0	Adenosylhomocysteinase (EC 3.3.1.1)	47	1.244	0.000
A2PZC1	Adrenodoxin reductase (Predicted protein)	17	1.176	0.009
A8J3Y6	AIR synthase-related protein	26	1.181	0.000
A8HZZ4	Alanine aminotransferase (EC 2.6.1.2)	22	1.135	0.001
A8J5Z8	Aldehyde dehydrogenase	7	1.180	0.009
Q2VA40	Alpha-1,4 glucan phosphorylase (EC 2.4.1.1)	34	1.105	0.001
A8IWI3	Aminomethyltransferase (EC 2.1.2.10)	13	-1.255	0.000
Q9M6D7	Apospory-associated protein C	6	1.151	0.010
A8JAG8	Argonaute-like protein	18	1.065	0.029
O49822	Ascorbate peroxidase (EC 1.11.1.11)	9	-1.133	0.015
A8J129	Aspartate aminotransferase (EC 2.6.1.1)	20	-1.078	0.012
Q39595	ATP sulfurylase Ats1	14	1.241	0.002
Q42687	ATP synthase delta chain, chloroplastic (F-ATPase delta chain)	18	-1.131	0.008

A8J785	ATP synthase subunit b', chloroplastic (ATP synthase F(0) sector subunit b') (ATPase subunit II)	15	-1.252	0.000
A8IQU3	ATP synthase subunit beta (EC 3.6.3.14)	100	1.052	0.024
P38482	ATP synthase subunit beta, mitochondrial (EC 3.6.3.14)	100	1.052	0.024
A8IXF1	ATP-sulfurylase	13	1.239	0.003
P31178	Autolysin (EC 3.4.24.38) (Gamete lytic enzyme) (GLE) (Gametolysin)	8	-1.164	0.003
Q6DN05	Betaine lipid synthase (Diacylglyceryl-N,N,N-trimethylhomoserine synthesis protein)	11	-1.093	0.023
A8J1S7	Bifunctional aspartate kinase/homoserine dehydrogenase (EC 2.7.2.4)	25	1.124	0.000
A8I9N4	Cell wall protein pherophorin-C21	5	1.136	0.019
A8JIB7	Chaperonin 60A	32	-1.105	0.014
Q9FEH5	Chlamyopsis 2	15	-1.199	0.001
A8JF15	Chloroplast ATP synthase delta chain	18	-1.131	0.008
A2BCY1	Chloroplast nucleosome assembly protein-like (Nucleosome assembly protein) (Fragment)	15	-1.090	0.012
Q5S7Y5	Chloroplast triosephosphate isomerase (Triose phosphate isomerase)	9	1.180	0.007
A8JHC9	Citrate synthase	7	1.167	0.004
A8JH37	Cobalamin-independent methionine synthase (EC 2.1.1.14)	62	1.123	0.000
Q84X75	CR051 protein (Predicted protein)	8	-1.242	0.003
A8J355	Cystathionine gamma-synthase	16	1.155	0.002
A8J9Y1	Cytochrome b6-f complex iron-sulfur subunit (EC 1.10.9.1)	18	-1.161	0.021
P49728	Cytochrome b6-f complex iron-sulfur subunit, chloroplastic (EC 1.10.9.1) (Plastohydroquinone:plastocyanin oxidoreductase iron-sulfur protein) (Rieske iron-sulfur protein) (ISP) (RISP)	18	-1.161	0.021
P15451	Cytochrome c	12	-1.583	0.000
P23577	Cytochrome f	26	-1.278	0.001
C5HJ53	Cytochrome f	26	-1.278	0.001
Q7PCJ6	DNA-directed RNA polymerase subunit beta" (EC 2.7.7.6) (PEP) (Plastid-encoded RNA polymerase subunit beta") (RNA polymerase subunit beta")	8	-1.152	0.039
A8JHX9	Elongation factor 2 (EC 3.6.5.3)	74	-1.063	0.004
A8ISZ1	Elongation factor EF-3	52	-1.119	0.007
A8J637	Elongation factor Ts	47	-1.083	0.004
Q5QEB2	Elongation factor Ts	47	-1.083	0.004
P17746	Elongation factor Tu, chloroplastic (EF-Tu)	57	-1.144	0.001
A8JH98	Enolase (EC 4.2.1.11)	34	1.097	0.007
A8JBN7	Eukaryotic initiation factor	13	-1.063	0.018
A8HX38	Eukaryotic translation elongation factor 1 alpha 1 (EC 3.6.5.3) (Eukaryotic translation elongation factor 1 alpha 2)	76	-1.239	0.000
A8JDR9	Fasciclin-like protein	8	1.299	0.003
A8JC09	Flagellar associated protein	11	-1.077	0.010
A8I7W0	Flagellar associated protein	17	-1.110	0.009
A8JG73	Flagellar associated protein	16	1.205	0.001
A8IXD1	Flagellar associated protein, adenosine kinase-like protein	7	1.350	0.003
A8I3Q0	Flagellar associated protein, transcriptional coactivator-like protein	7	-1.496	0.002
A8JCY4	Fructose-bisphosphate aldolase (EC 4.1.2.13)	12	1.273	0.000
A8HYA9	Fumarate hydratase	10	1.127	0.023
A8HVE0	Gamma-glutamyl hydrolase	8	1.114	0.017
A8HNE8	Geranylgeranyl reductase (EC 1.3.1.-)	29	-1.113	0.000
A8JHE3	Global transcription factor (Fragment)	10	1.093	0.008
Q9LLL6	Glucose-1-phosphate adenylyltransferase (EC 2.7.7.27) (ADP-glucose pyrophosphorylase)	20	1.114	0.018
A8HS14	Glucose-1-phosphate adenylyltransferase (EC 2.7.7.27) (ADP-glucose pyrophosphorylase)	17	1.132	0.002

A8IWA6	Glutamate synthase, NADH-dependent (EC 1.4.1.14)	47	1.074	0.009
A8HXA6	Glutathione reductase	8	1.201	0.011
A8JHR9	Glyceraldehyde-3-phosphate dehydrogenase (EC 1.2.1.-)	18	1.155	0.001
A8JHS0	Glyceraldehyde-3-phosphate dehydrogenase (EC 1.2.1.-)	18	1.155	0.001
P49644	Glyceraldehyde-3-phosphate dehydrogenase, cytosolic (EC 1.2.1.12)	18	1.155	0.001
A0A0B5KTL4	Glycerol-3-phosphate dehydrogenase [NAD(+)] (EC 1.1.1.8)	33	1.169	0.000
A8HNN4	Glycerol-3-phosphate dehydrogenase [NAD(+)] (EC 1.1.1.8)	33	1.169	0.000
A0A0B5KYA7	Glycerol-3-phosphate dehydrogenase [NAD(+)] (EC 1.1.1.8)	29	1.179	0.000
A8HNN6	Glycerol-3-phosphate dehydrogenase [NAD(+)] (EC 1.1.1.8) (Fragment)	27	1.189	0.000
A8IRW5	Glycoside-hydrolase-like protein	12	1.151	0.012
A8ICF4	Heme oxygenase (EC 1.14.99.3)	8	-1.401	0.004
A8HN65	High light-induced nuclease	14	-1.267	0.000
A8HXE1	High mobility group protein	8	-1.366	0.001
A8J3F0	High mobility group protein	8	-1.166	0.014
Q39576	Histone H1	3	-1.425	0.025
A8HWF6	Histone H2A	6	-1.309	0.010
A8HWM8	Histone H2A	6	-1.309	0.010
A8HSB2	Histone H2B	15	-1.250	0.006
A8HWX1	Histone H2B	15	-1.249	0.005
A8HV98	Histone H2B	15	-1.249	0.006
A8HWX5	Histone H2B	15	-1.249	0.006
A8IR69	Histone H2B	15	-1.249	0.006
A8JDC0	Histone H2B	15	-1.245	0.005
A8IR79	Histone H2B	15	-1.234	0.007
A8IW75	Histone H2B	15	-1.204	0.013
A8IW84	Histone H2B	15	-1.204	0.013
P54346	Histone H2B.3 (H2B-III)	15	-1.249	0.006
P54347	Histone H2B.4 (H2B-IV)	15	-1.249	0.006
A8HSA7	Histone H3	11	-1.197	0.005
A8J9M0	Histone H3	11	-1.197	0.005
A8HWY2	Histone H3 (Fragment)	11	-1.197	0.005
A8IK09	Histone H3 (Fragment)	11	-1.197	0.005
Q6LCW8	Histone H3 type 2	11	-1.197	0.005
P50564	Histone H3 type 3	11	-1.197	0.005
A8I3J7	Homoserine dehydrogenase (HDH) (EC 1.1.1.3)	4	1.190	0.025
A8ICC8	Inorganic pyrophosphatase	11	1.117	0.006
A8JAP7	Inosine-5'-monophosphate dehydrogenase (EC 1.1.1.205)	16	1.077	0.017
A8J0R7	Isocitrate dehydrogenase [NAD] subunit, mitochondrial (EC 1.1.1.41)	16	1.177	0.006
A8J244	Isocitrate lyase (EC 4.1.3.1)	26	1.069	0.025
A8JG56	L-ascorbate peroxidase	11	-1.130	0.012
Q75VY4	Light-harvesting chlorophyll-a/b protein of photosystem I	7	-1.239	0.023
A8IW39	LL-diaminopimelate aminotransferase	11	1.126	0.018
Q75NZ1	Low-CO2 inducible protein (Low-CO2 inducible protein LCIC)	48	1.067	0.002
A8JHU0	Malate dehydrogenase (EC 1.1.1.37)	33	-1.259	0.000
Q42686	Malate dehydrogenase, mitochondrial (EC 1.1.1.37)	33	-1.259	0.000
A8JII3	Matrix metalloproteinase	8	-1.164	0.003
A8J5T0	Mitochondrial cytochrome c	12	-1.583	0.000
A8HRZ4	Mitochondrial cytochrome c oxidase subunit 4, 13 kD	4	-1.186	0.023
A8JGD2	Mitochondrial NADH dehydrogenase	8	-1.116	0.014

A8J9F6	Mitochondrial transcription termination factor	8	-1.161	0.003
A8JGR1	NaCl-inducible protein	4	-1.201	0.011
A8I893	NAD-dependent epimerase/dehydratase	16	1.455	0.000
A8I629	Non-discriminatory gln-glu-trna synthetase (EC 6.1.1.17)	9	-1.164	0.005
A8IA86	Nucleolar protein, component of C/D snoRNPs	16	-1.179	0.013
A8J9H8	Nucleoside diphosphate kinase (EC 2.7.4.6)	14	1.181	0.003
A8JBF2	Organellar elongation factor P	4	-1.291	0.016
A8JEV1	Oxygen evolving enhancer protein 3	39	-1.150	0.001
A8J0E4	Oxygen-evolving enhancer protein 1 of photosystem II	69	-1.094	0.001
P12852	Oxygen-evolving enhancer protein 3, chloroplastic (OEE3)	39	-1.150	0.001
A8IW09	Peptidyl-prolyl cis-trans isomerase	5	-1.312	0.002
A8IRU6	Peptidyl-prolyl cis-trans isomerase, cyclophilin-type	32	-1.210	0.000
A8JHN8	Peptidyl-prolyl cis-trans isomerase, cyclophilin-type	6	-1.152	0.009
A8JC04	Phosphoglycerate kinase (EC 2.7.2.3)	36	-1.180	0.000
A8ICV4	Photosystem I 8.1 kDa reaction center subunit IV	8	-1.139	0.016
Q5NKW4	Photosystem I reaction center subunit II, 20 kDa (Photosystem I subunit)	22	-1.177	0.001
Q39615	Photosystem I reaction center subunit II, chloroplastic (Photosystem I 20 kDa subunit) (PSI-D)	22	-1.177	0.001
A8J4S1	Photosystem I reaction center subunit III	14	-1.255	0.004
P12356	Photosystem I reaction center subunit III, chloroplastic (Light-harvesting complex I 17 kDa protein) (P21 protein) (PSI-F)	14	-1.255	0.004
P12352	Photosystem I reaction center subunit IV, chloroplastic (PSI-E) (P30 protein) (Photosystem I 8.1 kDa protein)	8	-1.139	0.016
A8IXU7	Phototropin	21	-1.069	0.014
A8JAL6	Plastid ribosomal protein L15	15	-1.191	0.000
A8HWS8	Plastid ribosomal protein L28	6	-1.143	0.008
A8J503	Plastid ribosomal protein L6	13	-1.155	0.000
A8JDP6	Plastid ribosomal protein S13	8	-1.310	0.001
A8JGS2	Plastid ribosomal protein S17	10	-1.114	0.002
A8JDN4	Plastid ribosomal protein S20	7	-1.191	0.025
A8J5Y7	Plastid ribosomal protein S6	5	-1.229	0.031
A8I282	Predicted protein	4	-1.287	0.000
A8J3Q5	Predicted protein	6	1.151	0.010
A8JAW4	Predicted protein	23	-1.108	0.002
A8JH83	Predicted protein	2	-1.179	0.025
A8JBW0	Predicted protein	5	1.235	0.017
A8IMV0	Predicted protein	8	-1.218	0.002
A8JH97	Predicted protein	14	-1.163	0.000
A8ILP2	Predicted protein	6	-1.152	0.011
A8IBF4	Predicted protein	14	-1.129	0.008
A8IVX4	Predicted protein	3	1.059	0.014
A8HX52	Predicted protein	14	1.105	0.003
A8HX54	Predicted protein	20	1.107	0.003
A8IGN6	Predicted protein	6	1.154	0.008
A8IYK3	Predicted protein	3	1.161	0.026
A8J4Y6	Predicted protein	15	1.188	0.009
A8JCP3	Predicted protein	13	1.196	0.002
A8HX50	Predicted protein	17	1.207	0.001
A8J3E5	Predicted protein	3	1.234	0.016
A8J6Y3	Predicted protein	10	1.237	0.003

A8I193	Predicted protein	5	1.245	0.016
A8J7J5	Predicted protein (Fragment)	11	-1.171	0.023
A8I751	Predicted protein (Fragment)	7	-1.247	0.006
A8IG58	Predicted protein (Fragment)	9	1.175	0.002
A8HQT5	Predicted protein (Fragment)	4	1.222	0.022
A8ISG3	Predicted protein (Fragment)	21	-1.107	0.002
A8JHG2	Predicted protein (Fragment)	3	1.230	0.026
A8J8A7	Predicted protein (Fragment)	3	1.234	0.012
A8JGK4	Predicted protein (Fragment)	3	1.274	0.007
A8JHP2	Predicted protein (Fragment)	4	1.282	0.012
A8HPV3	Presequence protease	6	1.173	0.026
A8IS98	PRLI-interacting factor L	9	-1.135	0.004
A8JGX5	Protein arginine N-methyltransferase	9	1.181	0.006
A8HQT1	Protein disulfide isomerase	14	-1.135	0.004
Q8LPD9	Putative blue light receptor	21	-1.069	0.014
Q8LPE0	Putative blue light receptor	21	-1.069	0.014
A8J7M2	Pyrroline-5-carboxylate reductase (EC 1.5.1.2)	16	1.287	0.000
A8HXT4	Pyruvate carboxylase (Fragment)	26	-1.047	0.016
A8IW49	Pyruvate phosphate dikinase (EC 2.7.9.1)	16	1.222	0.000
A8J8P4	Ribosomal protein L34	7	-1.177	0.017
A8J0I0	Ribosomal protein L4	34	-1.107	0.001
A8J567	Ribosomal protein L7a	23	-1.148	0.001
A8J4Q3	Ribosomal protein S10	11	-1.134	0.016
D0FZF9	Ribulose biphosphate carboxylase large chain (EC 4.1.1.39) (Fragment)	75	-1.066	0.022
P00877	Ribulose biphosphate carboxylase large chain (RuBisCO large subunit) (EC 4.1.1.39)	81	-1.078	0.006
P23489	Ribulose biphosphate carboxylase/oxygenase activase, chloroplastic (RA) (RuBisCO activase)	21	-1.107	0.007
A8I9I9	Rieske ferredoxin	7	-1.274	0.021
Q6SA05	Rubisco activase	21	-1.107	0.007
A8J276	Rubredoxin	3	-1.802	0.004
A8HYU5	S-adenosylmethionine synthase (AdoMet synthase) (EC 2.5.1.6) (Methionine adenosyltransferase) (MAT)	21	1.138	0.001
A8IRK4	Sedoheptulose-1,7-bisphosphatase (EC 3.1.3.37)	28	1.190	0.000
A8IFC8	Selenium binding protein	8	1.302	0.001
A8JFK4	Serine hydroxymethyltransferase (EC 2.1.2.1)	33	1.125	0.004
A8J7F8	S-formylglutathione hydrolase (EC 3.1.2.12)	6	1.222	0.001
Q93Y52	Soluble inorganic pyrophosphatase 1, chloroplastic (EC 3.6.1.1) (Pyrophosphate phospho-hydrolase 1) (PPase 1)	11	1.117	0.006
Q4U1D9	Soluble starch synthase III	20	1.093	0.008
A8J5K8	Structural maintenance of chromosomes protein 6B	2	1.125	0.031
A8HX04	Succinate dehydrogenase [ubiquinone] iron-sulfur subunit, mitochondrial (EC 1.3.5.1)	12	-1.090	0.009
A8J9T5	Thiamine thiazole synthase, chloroplastic (Thiazole biosynthetic enzyme)	30	1.132	0.000
A8J6G0	Thylakoid lumenal protein	7	-1.143	0.014
A8HQP0	Transaldolase (EC 2.2.1.2)	12	-1.265	0.001
A8IAN1	Transketolase (EC 2.2.1.1)	62	1.089	0.001
A8J1C1	Ubiquitin-activating enzyme E1 (EC 6.3.2.19)	24	1.169	0.000
A8J9S9	UDP-glucose 4-epimerase	10	1.253	0.001
A2PZC3	UDP-glucose 6-dehydrogenase (EC 1.1.1.22)	14	1.231	0.000
A8J9I4	UDP-glucose 6-dehydrogenase (EC 1.1.1.22)	15	1.239	0.000

A8ITF3	UDP-glucose pyrophosphorylase	10	1.206	0.016
A2PZC0	Zygot-specific Zys3 like protein	12	1.214	0.001

**Table 11.3 Protein changes between 3 hour 0.2 M NaCl cultures and 18 hour 0.2 M NaCl cultures in *C. reinhardtii*.**

Accession number	Protein name	No. unique proteins	Fold change	P value
A8JFW4	1-deoxy-D-xylulose 5-phosphate synthase (EC 2.2.1.7) (Fragment)	18	-1.266	0.000
A8ILN4	1-hydroxy-2-methyl-2-(E)-butenyl 4-diphosphate synthase	29	-1.124	0.003
A8J3A4	26S proteasome regulatory subunit	20	1.140	0.003
D5LAZ2	294687m	9	1.173	0.013
O47027	30S ribosomal protein S2, chloroplastic	22	-1.156	0.012
Q08365	30S ribosomal protein S3, chloroplastic (ORF 712)	38	-1.151	0.012
P48270	30S ribosomal protein S4, chloroplastic	10	-1.155	0.023
A8HS48	40S ribosomal protein S3a	19	1.185	0.001
A8J1G8	40S ribosomal protein S6	24	1.239	0.001
A8JEV9	4-hydroxy-3-methylbut-2-enyl diphosphate reductase	9	-1.162	0.012
A8J5Z0	60S acidic ribosomal protein P0	34	-1.112	0.000
A8IUV7	60S ribosomal protein L13	20	1.190	0.002
A8J5F7	6-phosphogluconate dehydrogenase, decarboxylating (EC 1.1.1.44)	15	1.135	0.011
A8J6J6	Acetyl-CoA acyltransferase (EC 2.3.1.16)	23	1.181	0.002
A8HMQ1	Aconitate hydratase, mitochondrial (Aconitase) (EC 4.2.1.-)	53	-1.099	0.003
Q6UKY5	Acyl carrier protein	5	-1.563	0.034
A8J6A7	Adenylylphosphosulfate reductase	10	-1.195	0.005
A8ISN6	ADP-ribosylation factor-like protein 3	7	-1.212	0.026
A8J5Z8	Aldehyde dehydrogenase	7	1.274	0.011
Q1RS84	Aldehyde-alcohol dehydrogenase	51	1.106	0.003
A8IYK1	Alpha-1,4 glucan phosphorylase (EC 2.4.1.1)	34	1.147	0.000
Q2VA41	Alpha-1,4 glucan phosphorylase (EC 2.4.1.1)	34	1.147	0.000
Q2VA40	Alpha-1,4 glucan phosphorylase (EC 2.4.1.1)	34	1.240	0.000
A8IWJ3	Aminomethyltransferase (EC 2.1.2.10)	13	-1.184	0.001
A8IMY5	Anthranilate synthase, alpha subunit (Fragment)	16	-1.092	0.020
A8J129	Aspartate aminotransferase (EC 2.6.1.1)	20	-1.190	0.001
A8HXW8	Aspartate aminotransferase (EC 2.6.1.1)	8	-1.132	0.016
Q42687	ATP synthase delta chain, chloroplastic (F-ATPase delta chain)	18	-1.218	0.000
A8J785	ATP synthase subunit b', chloroplastic (ATP synthase F(0) sector subunit b') (ATPase subunit II)	15	-1.232	0.000
P06541	ATP synthase subunit beta, chloroplastic (EC 3.6.3.14) (ATP synthase F1 sector subunit beta) (F-ATPase subunit beta)	122	-1.081	0.016
P42380	ATP-dependent Clp protease proteolytic subunit (EC 3.4.21.92) (Endopeptidase Clp)	7	-1.224	0.012
P31178	Autolysin (EC 3.4.24.38) (Gamete lytic enzyme) (GLE) (Gametolysin)	8	-1.271	0.011
A8JB85	Autophagy-related protein	5	1.274	0.005
A8IT01	Carbonic anhydrase (EC 4.2.1.1)	28	-1.218	0.004
P20507	Carbonic anhydrase 1 (EC 4.2.1.1) (Carbonate dehydratase 1) (CA1) [Cleaved into: Carbonic anhydrase 1 large chain; Carbonic anhydrase 1 small chain]	28	-1.218	0.004
Q39588	Carbonic anhydrase, alpha type (Intracellular carbonic anhydrase, alpha type)	14	-1.202	0.007
A8HP36	Cell wall protein pherophorin-C2	21	-1.210	0.009
A8J1N4	Cell wall protein pherophorin-C24 (Fragment)	2	5.080	0.025

A8J094	Chitinase-related protein	12	1.087	0.020
Q8S567	Chlorophyll a/b-binding protein	13	-1.191	0.008
A8JF15	Chloroplast ATP synthase delta chain	18	-1.218	0.000
Q6J213	Chloroplast phytoene desaturase (Phytoene desaturase) (EC 1.3.-.-) (EC 1.3.99.-)	28	-1.125	0.007
Q6J216	Chloroplast phytoene synthase (Fragment)	8	-1.147	0.021
Q6J214	Chloroplast phytoene synthase (Phytoene synthase) (EC 2.5.1.32)	8	-1.147	0.021
A8IRJ7	Cilia- and flagella-associated protein 53	11	-1.122	0.027
A8JHC9	Citrate synthase	7	1.168	0.010
A8I972	ClpB chaperone, Hsp100 family	33	1.115	0.001
A8HYR2	Cobalamin-dependent methionine synthase (EC 2.1.1.13)	23	-1.160	0.002
A8JTT1	Cobalamin-dependent methionine synthase (Fragment)	18	-1.166	0.006
A8JH37	Cobalamin-independent methionine synthase (EC 2.1.1.14)	62	1.102	0.001
A8J6G4	Component of oligomeric golgi complex 5	6	1.265	0.045
A8IKK7	Copper target 1 protein	13	-1.163	0.005
Q84X75	CR051 protein (Predicted protein)	8	-1.191	0.028
A8IW43	Cullin	19	1.106	0.014
A8J9Y1	Cytochrome b6-f complex iron-sulfur subunit (EC 1.10.9.1)	18	-1.281	0.002
P49728	Cytochrome b6-f complex iron-sulfur subunit, chloroplastic (EC 1.10.9.1) (Plastohydroquinone:plastocyanin oxidoreductase iron-sulfur protein) (Rieske iron-sulfur protein) (ISP) (RISP)	18	-1.281	0.002
P15451	Cytochrome c	12	-1.523	0.000
A8JI07	Dual function alcohol dehydrogenase / acetaldehyde dehydrogenase	51	1.106	0.003
A8J637	Elongation factor Ts	47	-1.219	0.000
Q5QEB2	Elongation factor Ts	47	-1.219	0.000
P17746	Elongation factor Tu, chloroplastic (EF-Tu)	57	-1.197	0.002
O24450	Envelope protein	16	1.268	0.001
A8HX38	Eukaryotic translation elongation factor 1 alpha 1 (EC 3.6.5.3) (Eukaryotic translation elongation factor 1 alpha 2)	76	-1.119	0.001
A8I297	Eukaryotic translation initiation factor 5A (eIF-5A)	7	-1.277	0.004
A8JDR9	Fasciclin-like protein	8	1.380	0.005
Q9LD42	Fe-assimilating protein 1 (High-CO2 inducible, periplasmic protein)	5	-1.396	0.038
A8IYA1	Fe-assimilating protein 2	16	-1.608	0.000
Q8LL91	Ferroxidase-like protein (Multicopper ferroxidase)	18	-1.316	0.002
A8IHT2	Flagellar associated protein	8	-1.176	0.008
A8I7W0	Flagellar associated protein	17	-1.165	0.003
A8HW56	Flagellar associated protein (EC 3.6.1.3)	37	1.079	0.009
A8IZV9	Flagellar associated protein (Fragment)	37	1.185	0.001
A8I3Q0	Flagellar associated protein, transcriptional coactivator-like protein	7	-1.268	0.003
P12759	Flagellar radial spoke protein 3	8	-1.213	0.022
A8JCY4	Fructose-bisphosphate aldolase (EC 4.1.2.13)	12	1.138	0.009
A8HNE8	Geranylgeranyl reductase (EC 1.3.1.-)	29	-1.203	0.000
A8IE23	Glucose-6-phosphate isomerase (EC 5.3.1.9)	16	1.116	0.017
A8IRD5	Glutamate 5-kinase	7	1.521	0.003
A8JGD1	Glutamate dehydrogenase	14	1.174	0.006
A8HN52	Glutaredoxin, CGFS type	9	-1.217	0.001
A8JHR9	Glyceraldehyde-3-phosphate dehydrogenase (EC 1.2.1.-)	18	1.284	0.001
A8JHS0	Glyceraldehyde-3-phosphate dehydrogenase (EC 1.2.1.-)	18	1.284	0.001
P49644	Glyceraldehyde-3-phosphate dehydrogenase, cytosolic (EC 1.2.1.12)	18	1.284	0.001
A0A0B5KTL4	Glycerol-3-phosphate dehydrogenase [NAD(+)] (EC 1.1.1.8)	33	1.959	0.000
A8HNN4	Glycerol-3-phosphate dehydrogenase [NAD(+)] (EC 1.1.1.8)	33	1.959	0.000

A0A0B5KYA7	Glycerol-3-phosphate dehydrogenase [NAD(+)] (EC 1.1.1.8)	29	2.027	0.000
A8HNN6	Glycerol-3-phosphate dehydrogenase [NAD(+)] (EC 1.1.1.8) (Fragment)	27	2.073	0.000
Q945T2	GrpE protein homolog	16	-1.220	0.000
Q39568	G-strand telomere binding protein 1 (Gbp1p)	21	-1.166	0.002
A8HYV3	Heat shock protein 70B	62	1.077	0.003
Q39603	Heat shock protein 70B	62	1.077	0.003
A8ICF4	Heme oxygenase (EC 1.14.99.3)	8	-1.299	0.007
A8HN65	High light-induced nuclease	14	-1.124	0.009
A8HXE1	High mobility group protein	8	-1.174	0.003
A8J841	Hydroxymethylpyrimidine phosphate synthase	14	-1.154	0.012
A8I4F6	Imidazoleglycerol-phosphate dehydratase (EC 4.2.1.19)	3	-1.180	0.012
Q5W9T2	Lhc-like protein Lhl3 (Low molecular mass early light-induced protein)	13	-1.204	0.004
A8ITV3	Light-harvesting protein of photosystem I	13	-1.191	0.008
A8IT08	Low-CO2-inducible chloroplast envelope protein	16	1.268	0.001
A8J225	Low-CO2-inducible protein (Fragment)	14	1.240	0.025
Q93WE2	Magnesium chelatase H subunit (Magnesium chelatase H-subunit)	33	-1.213	0.000
A8I7P5	Magnesium chelatase subunit H	33	-1.213	0.000
Q9AR22	Magnesium-protoporphyrin IX monomethyl ester [oxidative] cyclase 2, chloroplastic (Mg-protoporphyrin IX monomethyl ester oxidative cyclase 2) (EC 1.14.13.81) (Copper target homolog 1 protein)	13	-1.163	0.005
A8JHU0	Malate dehydrogenase (EC 1.1.1.37)	33	-1.216	0.000
Q42686	Malate dehydrogenase, mitochondrial (EC 1.1.1.37)	33	-1.216	0.000
A8JII3	Matrix metalloproteinase	8	-1.271	0.011
A8I531	Mg-protoporphyrin IX chelatase (EC 6.6.1.1)	27	-1.094	0.002
A8J5T0	Mitochondrial cytochrome c	12	-1.523	0.000
A8JGD2	Mitochondrial NADH dehydrogenase	8	-1.151	0.010
A8IUU8	Mitogen activated protein kinase kinase kinase 10	3	-1.391	0.012
A8IZT9	Multicopper ferroxidase	18	-1.316	0.002
A8I893	NAD-dependent epimerase/dehydratase	16	1.670	0.000
A2PZD2	NAD-dependent epimerase/dehydratase (Predicted protein)	10	1.523	0.001
A8I629	Non-discriminatory gln-glu-trna synthetase (EC 6.1.1.17)	9	-1.144	0.014
A8JEV1	Oxygen evolving enhancer protein 3	39	-1.141	0.013
A8J0E4	Oxygen-evolving enhancer protein 1 of photosystem II	69	-1.145	0.000
A8IYH9	Oxygen-evolving enhancer protein 2 of photosystem II	57	-1.136	0.000
P12852	Oxygen-evolving enhancer protein 3, chloroplastic (OEE3)	39	-1.141	0.013
A8IRU6	Peptidyl-prolyl cis-trans isomerase, cyclophilin-type	32	-1.109	0.002
Q3HTK5	Pherophorin-C2 protein	21	-1.210	0.009
Q3HTK2	Pherophorin-C5 protein	4	-2.316	0.006
A8ICV4	Photosystem I 8.1 kDa reaction center subunit IV	8	-1.235	0.016
P12154	Photosystem I P700 chlorophyll a apoprotein A1 (EC 1.97.1.12) (PSI-A) (PsaA)	17	-1.261	0.003
P09144	Photosystem I P700 chlorophyll a apoprotein A2 (EC 1.97.1.12) (PSI-B) (PsaB)	12	-1.200	0.015
A8J4S1	Photosystem I reaction center subunit III	14	-1.289	0.001
P12356	Photosystem I reaction center subunit III, chloroplastic (Light-harvesting complex I 17 kDa protein) (P21 protein) (PSI-F)	14	-1.289	0.001
P12352	Photosystem I reaction center subunit IV, chloroplastic (PSI-E) (P30 protein) (Photosystem I 8.1 kDa protein)	8	-1.235	0.016
A8IFK0	Plasma membrane ATPase (EC 3.6.3.6)	17	-1.201	0.004
A8HVP7	Plastid ribosomal protein L10	13	-1.250	0.002
Q84U22	Plastid ribosomal protein L4 (Ribosomal protein L4)	12	-1.122	0.006
A8HTY0	Plastid ribosomal protein L7/L12	27	-1.192	0.006

Q70DX8	Plastid ribosomal protein S1 (Ribosomal protein S1 homologue)	15	-1.339	0.000
A8JDN8	Plastid ribosomal protein S16	8	-1.178	0.032
A8JGS2	Plastid ribosomal protein S17	10	-1.106	0.019
A8J8M5	Plastid ribosomal protein S5	27	-1.213	0.000
A8J5Y7	Plastid ribosomal protein S6	5	-1.618	0.006
A8I8A3	Plastid-specific ribosomal protein 3	10	-1.317	0.000
A8JH68	Plastocyanin	11	-1.283	0.011
P18068	Plastocyanin, chloroplastic (PC6-2)	11	-1.283	0.011
A8JFB1	Porphobilinogen deaminase	26	-1.192	0.002
A8JAQ2	Predicted protein	2	-1.411	0.032
A8IYJ6	Predicted protein	2	-1.351	0.016
A8ILP2	Predicted protein	6	-1.249	0.014
A8IMV0	Predicted protein	8	-1.231	0.006
A8HPE9	Predicted protein	9	-1.229	0.003
A8IBF4	Predicted protein	14	-1.208	0.021
A8JHB7	Predicted protein	26	-1.197	0.000
A8JHG9	Predicted protein	8	-1.164	0.019
A8IUB8	Predicted protein	4	-1.127	0.015
A8J8V6	Predicted protein	28	-1.113	0.012
A8IWL3	Predicted protein	26	1.107	0.002
A8HQ57	Predicted protein	12	1.142	0.022
A8HMMW6	Predicted protein	6	1.158	0.031
A8J9F0	Predicted protein	10	1.180	0.015
A8J5N1	Predicted protein	12	1.190	0.005
A8ITU2	Predicted protein	24	1.211	0.002
A8IYN6	Predicted protein	3	1.310	0.030
A8HPT6	Predicted protein	3	1.361	0.011
A8HTE5	Predicted protein	6	1.455	0.022
A8I804	Predicted protein	4	1.587	0.006
A8JCP3	Predicted protein	13	1.639	0.000
A8I2H7	Predicted protein	3	1.702	0.011
A8ISW1	Predicted protein (Fragment)	4	-1.641	0.018
A8I751	Predicted protein (Fragment)	7	-1.595	0.002
A8ISE3	Predicted protein (Fragment)	4	-1.185	0.010
A8JBI1	Predicted protein (Fragment)	8	-1.158	0.003
A8J0R6	Predicted protein (Fragment)	28	1.082	0.022
A8JCE1	Predicted protein (Fragment)	13	1.139	0.019
A8IUC1	Predicted protein (Fragment)	9	1.184	0.030
A8HZC0	Predicted protein (Fragment)	4	1.202	0.025
A8I114	Predicted protein (Fragment)	2	1.345	0.022
A8IBM2	Predicted protein of CLR family	6	1.323	0.035
A8IS98	PRLI-interacting factor L	9	-1.188	0.007
A8HQT1	Protein disulfide isomerase	14	1.126	0.004
A8IHI1	Protein disulfide isomerase (EC 5.3.4.1)	8	1.145	0.014
O48949	Protein disulfide-isomerase (EC 5.3.4.1)	32	1.158	0.002
Q9AXJ2	PsaN	10	-1.226	0.010
A8IMN8	PTEN PI-3 phosphatase	3	-1.362	0.017
A8J7M2	Pyrroline-5-carboxylate reductase (EC 1.5.1.2)	16	1.349	0.000
A8HXT4	Pyruvate carboxylase (Fragment)	26	-1.100	0.001

A8I6T5	R1 protein, alpha-glucan water dikinase	28	1.125	0.009
A8JCA4	RabGAP/TBC protein	3	1.077	0.032
A8J2J7	Radial spoke protein 3	8	-1.213	0.022
A8I8Z4	Ribosomal protein	20	-1.193	0.001
A8J1A3	Ribosomal protein L24	7	1.354	0.002
A8JHC3	Ribosomal protein S11	11	1.176	0.017
A8IGY1	Ribosomal protein S13	12	1.161	0.006
A8I4P5	Ribosomal protein S3	20	1.166	0.007
Q7Y258	Ribosomal protein S5	27	-1.213	0.000
D0FZF9	Ribulose biphosphate carboxylase large chain (EC 4.1.1.39) (Fragment)	75	-1.129	0.001
P00877	Ribulose biphosphate carboxylase large chain (RuBisCO large subunit) (EC 4.1.1.39)	81	-1.154	0.000
A8JGP9	Ribulose biphosphate carboxylase small chain (EC 4.1.1.39)	23	-1.356	0.000
P00873	Ribulose biphosphate carboxylase small chain 1, chloroplastic (RuBisCO small subunit 1) (EC 4.1.1.39)	23	-1.356	0.000
P08475	Ribulose biphosphate carboxylase small chain 2, chloroplastic (RuBisCO small subunit 2) (EC 4.1.1.39)	23	-1.357	0.000
P23489	Ribulose biphosphate carboxylase/oxygenase activase, chloroplastic (RA) (RuBisCO activase)	21	-1.108	0.002
Q6SA05	Rubisco activase	21	-1.108	0.002
A8J1A2	Serine/threonine-protein phosphatase (EC 3.1.3.16)	7	-1.138	0.023
Q39618	SF-assemblin	9	-1.128	0.017
Q546J6	SF-assemblin (Striated fiber assemblin)	9	-1.128	0.017
A8HQ72	SR protein factor	10	1.150	0.013
A8IHX1	Starch branching enzyme (EC 2.4.1.18)	12	1.207	0.002
A8IGH1	Superoxide dismutase (EC 1.15.1.1)	9	-1.193	0.012
A8I5N5	Tetrapyrrole-binding protein	6	-1.322	0.001
A8J9T5	Thiamine thiazole synthase, chloroplastic (Thiazole biosynthetic enzyme)	30	-1.147	0.002
A8IXV0	Thylakoid lumen protein	3	-1.586	0.010
A8J724	Transcriptional coactivator-like protein	16	1.118	0.015
A8JI60	Type-II calcium-dependent NADH dehydrogenase	14	-1.175	0.017
A8J914	UDP-glucose 6-dehydrogenase (EC 1.1.1.22)	15	1.562	0.000
A2PZC3	UDP-glucose 6-dehydrogenase (EC 1.1.1.22)	14	1.595	0.000
A8JC21	Uroporphyrinogen decarboxylase (EC 4.1.1.37)	12	-1.209	0.002
A8I647	Zeta-carotene desaturase (EC 1.3.5.6) (9,9'-di-cis-zeta-carotene desaturase)	9	-1.175	0.002
A2PZC0	Zygote-specific Zys3 like protein	12	1.196	0.002

**Table 11.4 Protein changes between 18 hour control (0 M NaCl) cultures and 18 hour 0.2 M NaCl cultures in *C. reinhardtii*.**

Accession number	Protein name	No. unique peptides	Fold change	P value
A8JFW4	1-deoxy-D-xylulose 5-phosphate synthase (EC 2.2.1.7) (Fragment)	18	-1.239	0.001
A8ILN4	1-hydroxy-2-methyl-2-(E)-butenyl 4-diphosphate synthase	29	-1.150	0.002
A8IV59	22 kDa translocon at the inner membrane of chloroplasts (Fragment)	6	-1.228	0.012
A8HVA6	26S proteasome regulatory subunit	14	1.130	0.003
A8IIP7	26S proteasome regulatory subunit	9	1.175	0.022
A8HWZ8	30S ribosomal protein S15	10	-1.434	0.001
O47027	30S ribosomal protein S2, chloroplastic	22	-1.148	0.007

Q08365	30S ribosomal protein S3, chloroplastic (ORF 712)	38	-1.094	0.017
P48267	30S ribosomal protein S7, chloroplastic	8	-1.218	0.009
Q6EMK7	38 kDa RNA-binding protein (Chloroplast-targeted RNA-binding protein) (RNA-binding protein RB38)	7	-1.344	0.001
A8J6Q7	3-deoxy-D-arabino-heptulosonate 7-phosphate synthetase (EC 2.5.1.54)	19	-1.137	0.004
A8JEF7	3-ketoacyl-CoA-synthase	10	-1.336	0.005
A8HS48	40S ribosomal protein S3a	19	1.195	0.004
A8IMP6	40S ribosomal protein S4	26	1.135	0.012
A8J1G8	40S ribosomal protein S6	24	1.388	0.000
A8HVQ1	40S ribosomal protein S8	13	1.137	0.021
A8JEV9	4-hydroxy-3-methylbut-2-enyl diphosphate reductase	9	-1.253	0.008
Q8HTL2	50S ribosomal protein L2, chloroplastic	16	-1.345	0.000
A8J5Z0	60S acidic ribosomal protein P0	34	-1.161	0.000
A8IUV7	60S ribosomal protein L13	20	1.167	0.011
A8J6J6	Acetyl-CoA acyltransferase (EC 2.3.1.16)	23	1.209	0.001
A8JHU1	Acetyl-coa carboxylase beta-carboxyltransferase subunit of plastidic multimeric ACCase (Fragment)	7	-1.253	0.013
A8HMQ1	Aconitate hydratase, mitochondrial (Aconitase) (EC 4.2.1.-)	53	-1.130	0.003
Q6UKY5	Acyl carrier protein	5	-2.096	0.007
A8IW34	Adenylosuccinate synthetase, chloroplastic (AMPSase) (AdSS) (EC 6.3.4.4) (IMP--aspartate ligase)	22	-1.288	0.000
A8J6A7	Adenylylphosphosulfate reductase	10	-1.234	0.001
A8ISN6	ADP-ribosylation factor-like protein 3	7	-1.482	0.012
Q19VH5	AGG3 (Flagellar flavodoxin)	9	-1.207	0.025
A8JFJ2	Alanine-glyoxylate transaminase	20	-1.141	0.007
A8J5Z8	Aldehyde dehydrogenase	7	1.271	0.010
Q2VA40	Alpha-1,4 glucan phosphorylase (EC 2.4.1.1)	34	1.122	0.001
A8IWJ3	Aminomethyltransferase (EC 2.1.2.10)	13	-1.427	0.000
A8JAG8	Argonaute-like protein	18	1.114	0.014
O49822	Ascorbate peroxidase (EC 1.11.1.11)	9	-1.191	0.015
A8I263	Aspartate aminotransferase (EC 2.6.1.1)	11	-1.134	0.016
A8I8Y6	ATM/ATR-like kinase	19	1.124	0.018
Q39595	ATP sulfurylase Ats1	14	-1.199	0.009
Q85KI7	ATP syntase-associated protein ASA1	28	-1.097	0.019
Q42687	ATP synthase delta chain, chloroplastic (F-ATPase delta chain)	18	-1.250	0.000
P07891	ATP synthase epsilon chain, chloroplastic (ATP synthase F1 sector epsilon subunit) (F-ATPase epsilon subunit)	7	-1.237	0.032
P12113	ATP synthase gamma chain, chloroplastic (F-ATPase gamma subunit)	29	-1.276	0.000
A8J785	ATP synthase subunit b', chloroplastic (ATP synthase F(0) sector subunit b') (ATPase subunit II)	15	-1.206	0.006
A8IXF1	ATP-sulfurylase	13	-1.205	0.010
P31178	Autolysin (EC 3.4.24.38) (Gamete lytic enzyme) (GLE) (Gametolysin)	8	-1.454	0.019
A8JGF4	Biotin carboxylase, acetyl-CoA carboxylase component	25	-1.113	0.019
A8I542	Calcium-transporting ATPase, endoplasmic reticulum-type	15	1.172	0.024
A8IDP6	Calmodulin	14	-1.288	0.008
P04352	Calmodulin (CaM)	14	-1.288	0.008
A6Q0K5	Calvin cycle protein CP12, chloroplastic (CP12 domain-containing protein) (Chloroplast protein 12)	11	-1.365	0.005
A8IT01	Carbonic anhydrase (EC 4.2.1.1)	28	-1.300	0.000
P20507	Carbonic anhydrase 1 (EC 4.2.1.1) (Carbonate dehydratase 1) (CA1) [Cleaved into: Carbonic anhydrase 1 large chain; Carbonic anhydrase 1 small chain]	28	-1.300	0.000
Q39588	Carbonic anhydrase, alpha type (Intracellular carbonic anhydrase, alpha	14	-1.135	0.030

	type)			
A8J1N4	Cell wall protein pterophorin-C24 (Fragment)	2	5.133	0.021
A8JFW5	Centriole proteome protein	5	-1.188	0.013
Q9FEH5	Chlamyopsin 2	15	-1.175	0.003
A8J270	Chlorophyll a-b binding protein of LHCII	45	1.144	0.003
Q9AXF6	Chlorophyll a-b binding protein of LHCII (Light-harvesting complex II protein)	50	1.148	0.001
Q8S3T9	Chlorophyll a-b binding protein of LHCII (Major light-harvesting complex II protein m9)	28	1.171	0.001
A8JF15	Chloroplast ATP synthase delta chain	18	-1.250	0.000
A8HXL8	Chloroplast ATP synthase gamma chain	29	-1.276	0.000
Q948V7	Chloroplast DNA recombination protein RECA	7	1.355	0.005
A8IA39	Chloroplast elongation factor G (EC 3.6.5.3)	29	-1.272	0.000
A2BCY1	Chloroplast nucleosome assembly protein-like (Nucleosome assembly protein) (Fragment)	15	-1.168	0.005
A8I670	Chloroplast RecA recombination protein	7	1.355	0.005
A8J264	Chlorophyll a-b binding protein of LHCII	46	1.138	0.004
A8J287	Chlorophyll a-b binding protein of LHCII type I, chloroplast	46	1.138	0.004
A8IRJ7	Cilia- and flagella-associated protein 53	11	-1.182	0.010
A8I4S9	Clathrin heavy chain	43	1.120	0.005
A8I1M5	CipD chaperone, Hsp100 family	8	1.152	0.014
A8HRR9	Coatomer subunit alpha	44	1.114	0.001
A8JEP9	Coatomer subunit beta (Beta-coat protein)	18	1.255	0.001
A8IM71	Coatomer subunit gamma	23	1.146	0.005
A8HYR2	Cobalamin-dependent methionine synthase (EC 2.1.1.13)	23	-1.141	0.003
A8JJT1	Cobalamin-dependent methionine synthase (Fragment)	18	-1.154	0.003
A8JH37	Cobalamin-independent methionine synthase (EC 2.1.1.14)	62	1.151	0.000
Q84X75	CR051 protein (Predicted protein)	8	-1.243	0.003
Q84X71	CR074 protein (Predicted protein)	16	-1.119	0.020
A8IW43	Cullin	19	1.127	0.010
A5YU13	CYP97C3	13	-1.176	0.005
A8J9Y1	Cytochrome b6-f complex iron-sulfur subunit (EC 1.10.9.1)	18	-1.423	0.001
P49728	Cytochrome b6-f complex iron-sulfur subunit, chloroplastic (EC 1.10.9.1) (Plastohydroquinone:plastocyanin oxidoreductase iron-sulfur protein) (Rieske iron-sulfur protein) (ISP) (RISP)	18	-1.423	0.001
P15451	Cytochrome c	12	-1.388	0.000
P23577	Cytochrome f	26	-1.178	0.012
C5HJ53	Cytochrome f	26	-1.178	0.012
A8JB14	Dihydroxyacetone kinase	7	1.233	0.023
A8I5K1	Dynamamin-related GTPase (EC 2.6.1.42)	13	1.232	0.004
A8J637	Elongation factor Ts	47	-1.211	0.000
Q5QEB2	Elongation factor Ts	47	-1.211	0.000
P17746	Elongation factor Tu, chloroplastic (EF-Tu)	57	-1.262	0.000
O24450	Envelope protein	16	1.390	0.001
A8HX38	Eukaryotic translation elongation factor 1 alpha 1 (EC 3.6.5.3) (Eukaryotic translation elongation factor 1 alpha 2)	76	-1.131	0.003
A8JDR9	Fasciclin-like protein	8	1.657	0.003
Q9LD42	Fe-assimilating protein 1 (High-CO2 inducible, periplasmic protein)	5	-1.197	0.026
A8IWK2	Ferredoxin thioredoxin reductase, catalytic chain (EC 1.18.-.-)	4	-1.368	0.031
A8JHB4	Ferredoxin-dependent glutamate synthase	47	-1.094	0.004
Q84X68	Flagella membrane glycoprotein 1B	28	-1.303	0.000
A8JG73	Flagellar associated protein	16	-1.430	0.000

A8I7W0	Flagellar associated protein	17	-1.281	0.000
A8JCA5	Flagellar associated protein	12	-1.139	0.016
A8IZV9	Flagellar associated protein (Fragment)	37	1.150	0.006
A8J0V2	Flagellar associated protein, calcium-transporting ATPase (EC 3.6.3.8) (Fragment)	11	1.119	0.018
A8I2Z6	Flagellar/basal body protein, PACRG-like protein	6	-1.270	0.009
A8HNE8	Geranylgeranyl reductase (EC 1.3.1.-)	29	-1.199	0.000
A8IRD5	Glutamate 5-kinase	7	1.639	0.012
A8HN52	Glutaredoxin, CGFS type	9	-1.303	0.000
A0A0B5KTL4	Glycerol-3-phosphate dehydrogenase [NAD(+)] (EC 1.1.1.8)	33	1.959	0.000
A8HNN4	Glycerol-3-phosphate dehydrogenase [NAD(+)] (EC 1.1.1.8)	33	1.959	0.000
A0A0B5KYA7	Glycerol-3-phosphate dehydrogenase [NAD(+)] (EC 1.1.1.8)	29	2.064	0.000
A8HNN6	Glycerol-3-phosphate dehydrogenase [NAD(+)] (EC 1.1.1.8) (Fragment)	27	2.109	0.000
A8IVM9	Glycine cleavage system, P protein (EC 1.4.4.2)	21	-1.132	0.005
Q6IV67	Glycogen synthase kinase 3 (EC 2.7.1.-)	14	-1.164	0.012
A8J2E9	Glycolate dehydrogenase	33	-1.134	0.000
Q0ZAZ1	Glycolate dehydrogenase	33	-1.134	0.000
Q945T2	GrpE protein homolog	16	-1.294	0.001
Q39568	G-strand telomere binding protein 1 (Gbp1p)	21	-1.196	0.002
A8IRX5	GTP-binding nuclear protein	6	-1.343	0.009
P25387	Guanine nucleotide-binding protein subunit beta-like protein	10	-1.198	0.013
A8J3P5	Heat shock protein 70E	26	-1.172	0.003
A8ICF4	Heme oxygenase (EC 1.14.99.3)	8	-1.409	0.004
A8HN65	High light-induced nuclease	14	-1.567	0.000
A8HXE1	High mobility group protein	8	-1.333	0.008
A8J3F0	High mobility group protein	8	-1.272	0.001
A8HRZ9	Histone H2A	5	-1.375	0.017
A8I826	Homoserine kinase (EC 2.7.1.39)	6	-1.144	0.018
A8J841	Hydroxymethylpyrimidine phosphate synthase	14	-1.352	0.000
A8IPI7	Hydroxypyruvate reductase	11	-1.200	0.009
Q5MAT3	Hydroxypyruvate reductase (Fragment)	11	-1.200	0.009
A8ICC8	Inorganic pyrophosphatase	11	-1.341	0.001
A8HR79	Inositol phosphatase-like protein	15	-1.181	0.015
A8J6V1	Isocitrate dehydrogenase, NAD-dependent (EC 1.1.1.41)	6	1.238	0.011
Q39577	Isocitrate lyase	24	-1.219	0.011
A8J244	Isocitrate lyase (EC 4.1.3.1)	26	-1.190	0.019
A8IXK0	Kinesin family member heavy chain	9	1.278	0.008
Q0Z9B8	LciD (Limiting CO2 inducible protein)	12	-1.136	0.023
A8HPJ2	Light-dependent protochlorophyllide reductase (EC 1.3.1.33)	20	-1.217	0.007
Q93WL4	Light-harvesting chlorophyll-a/b binding protein LhcII-1.3 (Light-harvesting complex II chlorophyll a-b binding protein M3)	52	1.131	0.004
Q93WE0	Light-harvesting chlorophyll-a/b binding protein LhcII-3 (Light-harvesting protein of photosystem II)	50	1.148	0.001
Q93VE0	Light-harvesting chlorophyll-a/b binding protein LhcII-4 (Light-harvesting complex II protein) (Major light-harvesting complex II protein m1)	40	1.147	0.004
Q75VY6	Light-harvesting chlorophyll-a/b protein of photosystem I (Light-harvesting protein of photosystem I)	9	-1.402	0.010
Q75VY7	Light-harvesting chlorophyll-a/b protein of photosystem I (Light-harvesting protein of photosystem I)	9	-1.347	0.019
A8IW39	LL-diaminopimelate aminotransferase	11	-1.173	0.004
A8IT08	Low-CO2-inducible chloroplast envelope protein	16	1.390	0.001
A8J225	Low-CO2-inducible protein (Fragment)	14	1.385	0.001

Q93WE2	Magnesium chelatase H subunit (Magnesium chelatase H-subunit)	33	-1.177	0.007
A8I7P5	Magnesium chelatase subunit H	33	-1.177	0.007
Q8S3U0	Major light-harvesting complex II protein m10	48	1.136	0.010
A8JHU0	Malate dehydrogenase (EC 1.1.1.37)	33	-1.253	0.001
Q42686	Malate dehydrogenase, mitochondrial (EC 1.1.1.37)	33	-1.253	0.001
A8JII3	Matrix metalloproteinase	8	-1.454	0.019
A8JG04	Membrane protein	9	-1.345	0.004
A8J3L9	Methylmalonate semi-aldehyde dehydrogenase	26	1.095	0.016
A8IMZ5	Mg-protoporphyrin IX chelatase (EC 6.6.1.1)	29	-1.252	0.000
A8J5T0	Mitochondrial cytochrome c	12	-1.388	0.000
A8IN92	Mitochondrial cytochrome c oxidase subunit	5	-1.394	0.011
A8HRZ4	Mitochondrial cytochrome c oxidase subunit 4, 13 kD	4	-1.451	0.019
A8ITL0	Mitochondrial F1F0 ATP synthase associated 60.6 kDa protein	28	-1.097	0.019
A8IFE2	Mitochondrial pyruvate dehydrogenase complex, E1 component, alpha subunit	9	1.154	0.009
A8HXM1	Mitochondrial ribosomal protein L29	7	-1.344	0.008
A8J2X6	N-acetyl-gamma-glutamyl-phosphate reductase	12	-1.202	0.003
A8JGR1	NaCl-inducible protein	4	-1.380	0.025
A8I893	NAD-dependent epimerase/dehydratase	16	1.665	0.000
A2PZD2	NAD-dependent epimerase/dehydratase (Predicted protein)	10	1.345	0.002
Q6V9B3	NADH:ubiquinone oxidoreductase 24 kD subunit (EC 1.6.5.3) (NADH:ubiquinone oxidoreductase 24 kDa subunit)	11	-1.188	0.004
Q6UP32	NADH:ubiquinone oxidoreductase B16.6 subunit (EC 1.6.5.3) (EC 1.6.99.3)	6	-1.159	0.014
Q6V9B1	NADH:ubiquinone oxidoreductase subunit 8 (EC 1.6.5.3)	3	-1.194	0.029
A8I629	Non-discriminatory gln-glu-trna synthetase (EC 6.1.1.17)	9	-1.179	0.023
A8J9H8	Nucleoside diphosphate kinase (EC 2.7.4.6)	14	-1.236	0.000
A8JH12	Nucleoside diphosphate kinase (EC 2.7.4.6)	10	-1.231	0.000
A8J513	Nucleosome assembly protein	22	-1.178	0.011
A8HPZ8	Oligoendopeptidase	10	-1.176	0.015
A8J827	Organellar class II aminoacyl tRNA synthetase	9	-1.113	0.012
A8JEV1	Oxygen evolving enhancer protein 3	39	-1.226	0.001
A8J0E4	Oxygen-evolving enhancer protein 1 of photosystem II	69	-1.290	0.000
A8IYH9	Oxygen-evolving enhancer protein 2 of photosystem II	57	-1.108	0.017
P12852	Oxygen-evolving enhancer protein 3, chloroplastic (OEE3)	39	-1.226	0.001
B1B601	Parkin-co-regulated gene product	6	-1.270	0.009
B5A8X8	PAS domain sensory protein FXL5	7	1.197	0.025
A8IW09	Peptidyl-prolyl cis-trans isomerase	5	-1.361	0.002
A8J3L3	Peptidyl-prolyl cis-trans isomerase	5	-1.266	0.017
A8JDL5	Peptidyl-prolyl cis-trans isomerase (PPIase) (EC 5.2.1.8)	11	-1.238	0.007
A8IRU6	Peptidyl-prolyl cis-trans isomerase, cyclophilin-type	32	-1.263	0.000
Q3HTK2	Pherophorin-C5 protein	4	-2.719	0.003
A8JC04	Phosphoglycerate kinase (EC 2.7.2.3)	36	-1.278	0.000
A8I6R4	Phosphoribosylformylglycinamide cyclo-ligase (EC 6.3.3.1)	6	-1.187	0.007
A8IH03	Phosphoserine aminotransferase (EC 2.6.1.52)	20	-1.261	0.002
A8ICV4	Photosystem I 8.1 kDa reaction center subunit IV	8	-1.349	0.000
A8J4S1	Photosystem I reaction center subunit III	14	-1.461	0.001
P12356	Photosystem I reaction center subunit III, chloroplastic (Light-harvesting complex I 17 kDa protein) (P21 protein) (PSI-F)	14	-1.461	0.001
P12352	Photosystem I reaction center subunit IV, chloroplastic (PSI-E) (P30 protein) (Photosystem I 8.1 kDa protein)	8	-1.349	0.000
A8HVJ9	Photosystem II stability/assembly factor HCF136 (Fragment)	11	-1.190	0.007

A8IXU7	Phototropin	21	-1.081	0.031
A8HVP7	Plastid ribosomal protein L10	13	-1.393	0.000
A8JAL6	Plastid ribosomal protein L15	15	-1.277	0.009
A8HNJ8	Plastid ribosomal protein L18	9	-1.248	0.009
A8JE35	Plastid ribosomal protein L3	13	-1.438	0.000
Q84U22	Plastid ribosomal protein L4 (Ribosomal protein L4)	12	-1.132	0.031
A8J503	Plastid ribosomal protein L6	13	-1.268	0.001
A8HTY0	Plastid ribosomal protein L7/L12	27	-1.257	0.001
A8IYS1	Plastid ribosomal protein L9	6	-1.365	0.014
Q70DX8	Plastid ribosomal protein S1 (Ribosomal protein S1 homologue)	15	-1.340	0.000
A8JDP6	Plastid ribosomal protein S13	8	-1.364	0.001
A8JDN8	Plastid ribosomal protein S16	8	-1.506	0.003
A8J5Y7	Plastid ribosomal protein S6	5	-1.433	0.002
A8I8A3	Plastid-specific ribosomal protein 3	10	-1.250	0.012
A8JH68	Plastocyanin	11	-1.629	0.001
P18068	Plastocyanin, chloroplastic (PC6-2)	11	-1.629	0.001
A8HME6	Polyadenylate-binding protein (PABP)	25	-1.235	0.000
O64985	Polyadenylate-binding protein (PABP)	20	-1.233	0.001
A8JFB1	Porphobilinogen deaminase	26	-1.500	0.000
A8ILP2	Predicted protein	6	-1.520	0.007
A8J5B8	Predicted protein	20	-1.432	0.014
A8I3P7	Predicted protein	3	-1.321	0.020
A8I5A0	Predicted protein	9	-1.310	0.013
A8HSU1	Predicted protein	11	-1.302	0.001
A8IAJ4	Predicted protein	6	-1.282	0.005
A8JDL8	Predicted protein	7	-1.242	0.014
A8IBF4	Predicted protein	14	-1.233	0.001
A8J7S1	Predicted protein	6	-1.225	0.014
A8JFZ2	Predicted protein	37	-1.205	0.000
A8J2Z8	Predicted protein	5	-1.192	0.031
A8JHB7	Predicted protein	26	-1.187	0.002
A8IS13	Predicted protein	9	-1.181	0.002
A8JH97	Predicted protein	14	-1.169	0.008
A8J2E5	Predicted protein	6	-1.154	0.007
A8JGL0	Predicted protein	4	-1.150	0.032
A8J4M0	Predicted protein	9	-1.140	0.023
A8IEC1	Predicted protein	16	-1.119	0.020
A8JAW4	Predicted protein	23	-1.095	0.012
A8HPF4	Predicted protein	19	1.099	0.021
A8IKB4	Predicted protein	13	1.133	0.010
A8HQ57	Predicted protein	12	1.167	0.020
A8JCP1	Predicted protein	3	1.170	0.019
A8IUT0	Predicted protein	5	1.188	0.033
A8IXA4	Predicted protein	7	1.191	0.008
A8IGN6	Predicted protein	6	1.201	0.014
A8HX54	Predicted protein	20	1.247	0.000
A8ITX5	Predicted protein	3	1.269	0.015
A8HX52	Predicted protein	14	1.269	0.000
A8I8L4	Predicted protein	5	1.283	0.020

A8JIW6	Predicted protein	6	1.285	0.016
A8IR20	Predicted protein	4	1.291	0.034
A8IKX4	Predicted protein	27	1.291	0.005
A8J7W8	Predicted protein	4	1.293	0.013
A8IJK6	Predicted protein	5	1.306	0.023
A8HMMW6	Predicted protein	6	1.320	0.002
A8JBW0	Predicted protein	5	1.323	0.007
A8HX50	Predicted protein	17	1.335	0.000
A8HQ79	Predicted protein	3	1.462	0.029
A8HTE5	Predicted protein	6	1.463	0.020
A8J5M3	Predicted protein	5	1.492	0.020
A8JCE0	Predicted protein	2	1.522	0.024
A8I804	Predicted protein	4	1.697	0.008
A8JCP3	Predicted protein	13	1.733	0.000
A8J400	Predicted protein	4	1.809	0.007
A8I751	Predicted protein (Fragment)	7	-1.664	0.002
A8ISE3	Predicted protein (Fragment)	4	-1.267	0.027
A8HWI9	Predicted protein (Fragment)	2	-1.251	0.007
A8J7J5	Predicted protein (Fragment)	11	-1.249	0.003
A8JFI7	Predicted protein (Fragment)	13	-1.237	0.027
A8IIE0	Predicted protein (Fragment)	5	-1.211	0.019
A8J0R6	Predicted protein (Fragment)	28	1.117	0.005
A8IWV9	Predicted protein (Fragment)	9	1.127	0.009
A8HP46	Predicted protein (Fragment)	5	1.127	0.024
A8JHT1	Predicted protein (Fragment)	16	1.146	0.027
A8IY01	Predicted protein (Fragment)	3	1.197	0.028
A8JCE1	Predicted protein (Fragment)	13	1.204	0.008
A8JAL9	Predicted protein (Fragment)	12	1.245	0.035
A8IJ16	Predicted protein (Fragment)	2	1.272	0.023
A8JA86	Predicted protein (Fragment)	3	1.283	0.020
A8IYD0	Predicted protein (Fragment)	5	1.453	0.018
A8JHP2	Predicted protein (Fragment)	4	1.560	0.015
A8IBM2	Predicted protein of CLR family	6	1.366	0.034
A8IS98	PRLI-interacting factor L	9	-1.196	0.005
A8J633	Prohibitin	13	1.123	0.025
Q39617	Protochlorophyllide reductase, chloroplastic (PCR) (EC 1.3.1.33) (NADPH-protochlorophyllide oxidoreductase) (POR)	20	-1.217	0.007
Q8LPD9	Putative blue light receptor	21	-1.081	0.031
Q8LPE0	Putative blue light receptor	21	-1.081	0.031
A8J816	Putative uncharacterized protein	5	1.806	0.018
A8J7M2	Pyrroline-5-carboxylate reductase (EC 1.5.1.2)	16	1.292	0.000
Q1RS83	Pyruvate formate-lyase	58	-1.223	0.000
A8J345	Pyruvate kinase (EC 2.7.1.40)	23	1.133	0.001
A8HMX2	Pyruvate-formate lyase (EC 2.3.1.54)	58	-1.223	0.000
A8I6T5	R1 protein, alpha-glucan water dikinase	28	1.182	0.005
A8J146	Rab GDP dissociation inhibitor protein	17	-1.145	0.002
A8J8Y1	Receptor of activated protein kinase C 1	10	-1.198	0.013
A8IRQ1	Ribose-5-phosphate isomerase (EC 5.3.1.6)	11	-1.130	0.026
A8I8Z4	Ribosomal protein	20	-1.236	0.000
A8HQ81	Ribosomal protein L11	11	-1.242	0.029

A8JI94	Ribosomal protein L22	14	1.203	0.004
A8J4Q3	Ribosomal protein S10	11	-1.160	0.001
A8JHC3	Ribosomal protein S11	11	1.323	0.004
A8IGY1	Ribosomal protein S13	12	1.211	0.014
A8HSU7	Ribosomal protein S16	16	1.218	0.001
A8HME4	Ribosomal protein S2	14	1.192	0.007
A8IJQ4	Ribosomal protein S23	8	1.293	0.006
A8I4P5	Ribosomal protein S3	20	1.250	0.002
P00877	Ribulose biphosphate carboxylase large chain (RuBisCO large subunit) (EC 4.1.1.39)	81	-1.110	0.001
P23489	Ribulose biphosphate carboxylase/oxygenase activase, chloroplastic (RA) (RuBisCO activase)	21	-1.186	0.003
A8I9I9	Rieske ferredoxin	7	-1.381	0.006
A8J5G1	RNA binding motif protein	5	-1.221	0.007
A8J8S4	RNA binding protein (Fragment)	9	-1.315	0.011
Q6SA05	Rubisco activase	21	-1.186	0.003
A8J276	Rubredoxin	3	-1.792	0.013
A8HYU5	S-adenosylmethionine synthase (AdoMet synthase) (EC 2.5.1.6) (Methionine adenosyltransferase) (MAT)	21	-1.293	0.000
A8JFY9	Serine glyoxylate aminotransferase (EC 2.6.1.45)	17	-1.177	0.010
A8JFZ0	Serine glyoxylate aminotransferase (EC 2.6.1.45)	17	-1.177	0.010
Q8W4V3	Serine hydroxymethyltransferase (EC 2.1.2.1)	36	-1.165	0.001
A8J1A2	Serine/threonine-protein phosphatase (EC 3.1.3.16)	7	-1.179	0.006
A8JBX4	Short-chain dehydrogenase/reductase SDR	8	1.195	0.027
A8JCM8	SM/Sec1-family protein	8	1.162	0.016
Q93Y52	Soluble inorganic pyrophosphatase 1, chloroplastic (EC 3.6.1.1) (Pyrophosphate phospho-hydrolase 1) (PPase 1)	11	-1.341	0.001
Q4U1D9	Soluble starch synthase III	20	1.197	0.000
A8J431	Stress-related chlorophyll a/b binding protein 2 (Stress-related chlorophyll a/b binding protein 3)	8	1.776	0.005
A8HX04	Succinate dehydrogenase [ubiquinone] iron-sulfur subunit, mitochondrial (EC 1.3.5.1)	12	-1.157	0.001
A8IGH1	Superoxide dismutase (EC 1.15.1.1)	9	-1.362	0.001
A8HP58	Thioredoxin m	11	-1.213	0.010
P23400	Thioredoxin M-type, chloroplastic (Trx-M) (Thioredoxin-CH2)	11	-1.213	0.010
A8HZZ1	Threonine synthase (EC 4.2.3.1)	23	-1.154	0.001
A8IXV0	Thylakoid lumen protein	3	-1.703	0.007
A8J1M9	Thylakoid lumenal 17.4 kDa protein	7	-1.460	0.003
A8HY43	Thylakoid lumenal protein	10	-1.237	0.011
A8JHA4	Transcription-coupled DNA repair protein (Fragment)	5	1.260	0.022
A8IK91	Translocon component Tic40-related protein	16	-1.176	0.016
A8JC42	Transmembrane ATPase (EC 3.6.3.14)	7	-1.154	0.027
A8JI60	Type-II calcium-dependent NADH dehydrogenase	14	-1.146	0.009
A8J7F2	Ubiquitin-protein ligase	7	1.333	0.006
A2PZC3	UDP-glucose 6-dehydrogenase (EC 1.1.1.22)	14	1.461	0.000
A8J914	UDP-glucose 6-dehydrogenase (EC 1.1.1.22)	15	1.478	0.000
A8J7D3	Uncharacterized protein	4	-1.148	0.012
A8I9S9	Uroporphyrinogen decarboxylase (EC 4.1.1.37)	5	-1.390	0.009
A8JC21	Uroporphyrinogen decarboxylase (EC 4.1.1.37)	12	-1.378	0.002
A8IW47	Vacuolar ATP synthase subunit E	11	-1.161	0.014
A8HQ97	Vacuolar ATP synthase subunit H	10	1.205	0.018
A8J087	Vasa intronic gene	18	-1.227	0.004

A8J8I6	VID72-domain protein	9	1.139	0.022
A8JGZ8	YCII-related protein	5	-1.167	0.023
A2PZC0	Zygote-specific Zys3 like protein	12	1.183	0.015

---

## 12 Appendix D: Supplementary Material from Chapter 5

### 12.1 Cell count data

#### 12.1.1 Cell count correlation with OD

Figure 12.1 shows the correlation of cell counts with optical density (750 nm and 600 nm), which was used to calculate cell densities in samples where OD was taken (see Section 5.5.1 for photosynthesis and respiration data). This shows that OD has a reliable linear relationship with cell number up to an OD of about 1.2 and that OD can be used as a reliable measure of culture growth and density. Choosing a wavelength where the absorbance of chlorophyll pigments is low, like 750 nm, is preferable, since differences between pigment contents will then not affect the proxy measure of cell density (Griffiths et al., 2011).

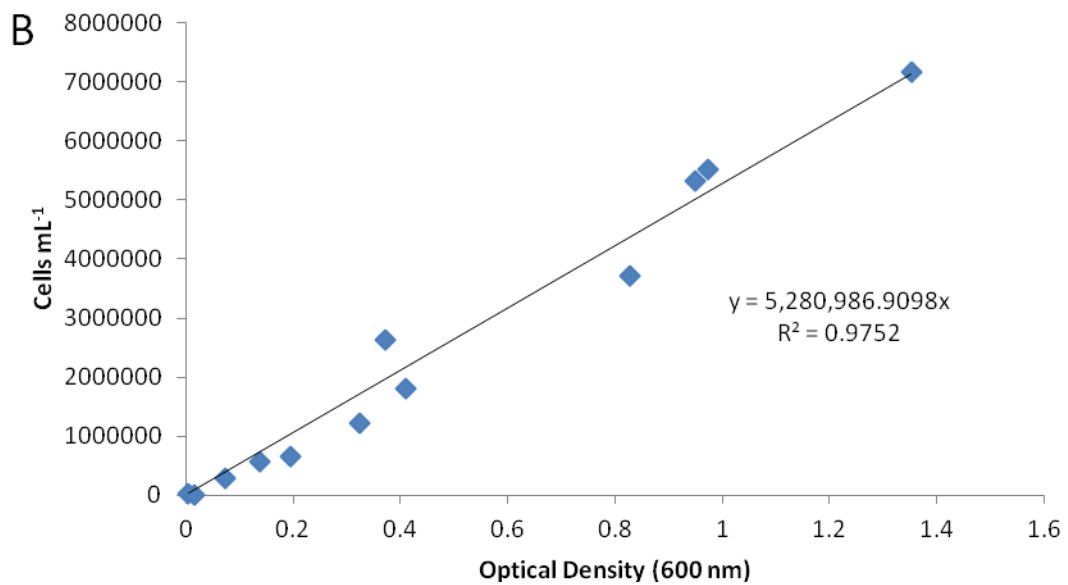
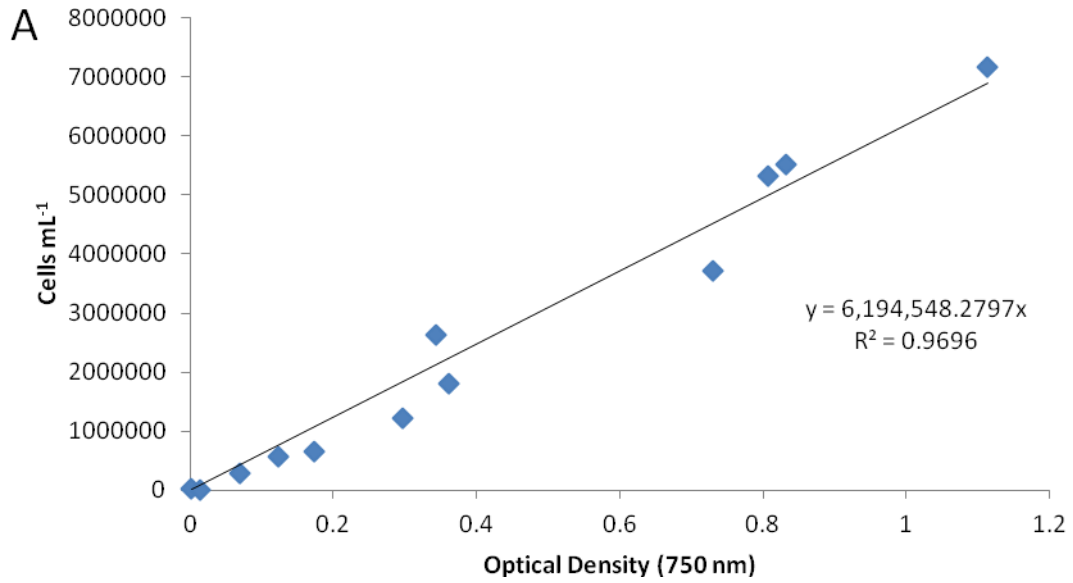


Figure 12.1 Optical density of *C. nivalis* cells at 750 nm (A) and 600 nm (B), correlated with cell count.

### 12.1.2 OD correlation with biomass

The correlations of optical density with biomass concentration in non salt stressed and 1.4 M salt stressed samples are shown in Figure 12.2 and Figure 12.3, respectively. Salt

stressed samples biomass concentration show a much better correlation with optical density ( $R^2=0.9121$ ) than non salt stressed biomass concentration does ( $R^2=0.6703$ ). The reasons for this are not clear. Optical density is therefore assumed to be a better proxy measure of cell density than. But due to changes in cell morphology under salt stress, biomass is used as a way to standardise measurements of lipid, carbohydrate and chlorophyll.

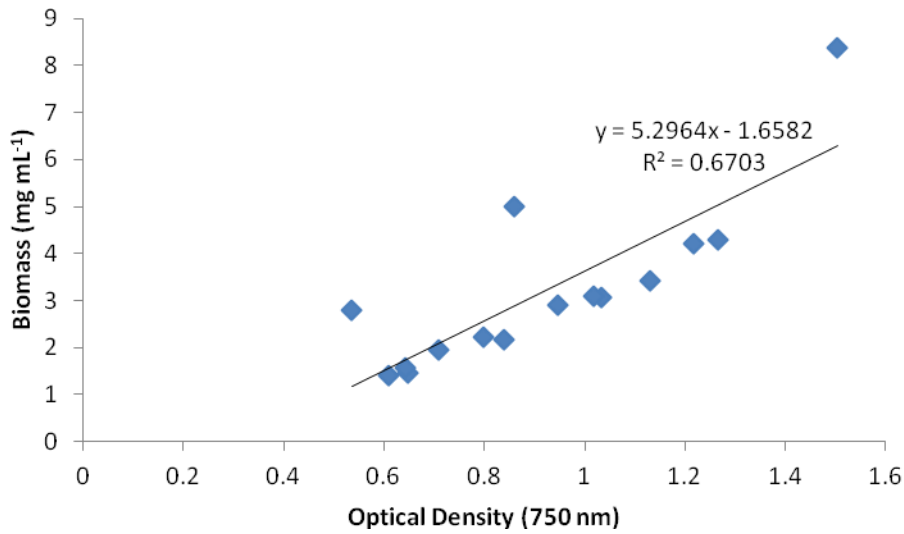


Figure 12.2 Correlation of *C. nivalis* OD (750 nm) with biomass in control (0 M NaCl) samples.

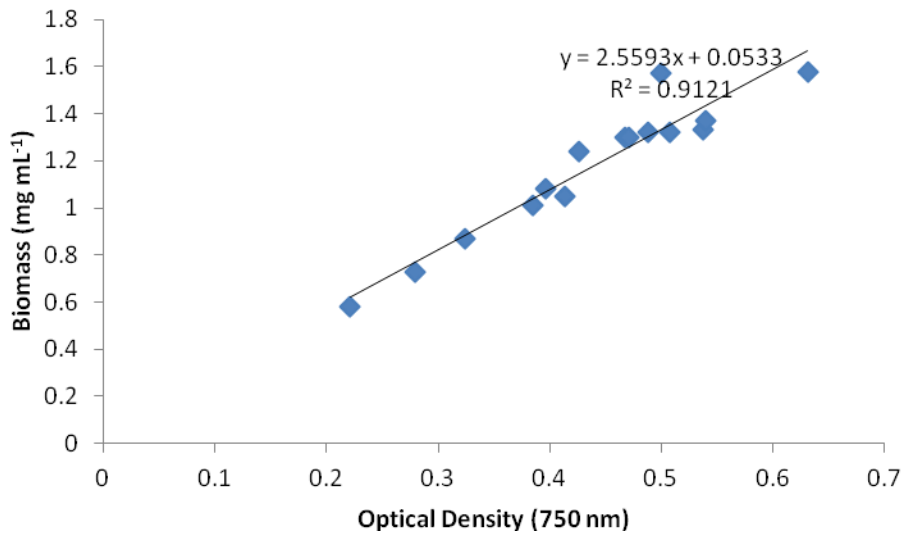


Figure 12.3 Correlation of OD (750 nm) with biomass in salt stressed (1.4 M NaCl) samples.

The correlation of cell count and OD was very good, ( $R=0.9752$  for 600 nm and  $R=0.9696$  for 750 nm) and therefore using OD as an indicator of culture density is a reliable method for measuring culture growth, which is much quicker than using cell numbers. Although biomass and cell count are not as well correlated in non salt stressed samples, biomass (dry cell weight) remains a good way to standardise the assays for subsequent measuring of pigment, carbohydrate and chlorophyll. Cell count can be misleading if cell size changes (Wood et al., 2005), whilst dry cell weight will take into account all the available biomass regardless of cell size or viability. Although it may be argued that one would not want to include non viable cells in a calculation, which biomass measurements would fail to take into account, the calculations of lipid, carbohydrate and pigment based on dry cell weight shows what percentage mass of a culture is the useful or desirable product. Cell counts are less intuitive in calculating the useful product content of a culture.

Kim et al. (2016a) found that salt stress had the effect of reducing cell counts, but increasing biomass production, due to the increasing of cell size. Therefore, using "per cell" measurements may not be the best way to measure the useful output from a culture,

since biomass will show a directly comparable measure of the algal material available. Biomass is often used as a standard way of normalising for lipid content (Bartley et al., 2013).

## 12.2 FAME profile for *C. nivalis* grown in 0.2 M NaCl conditions

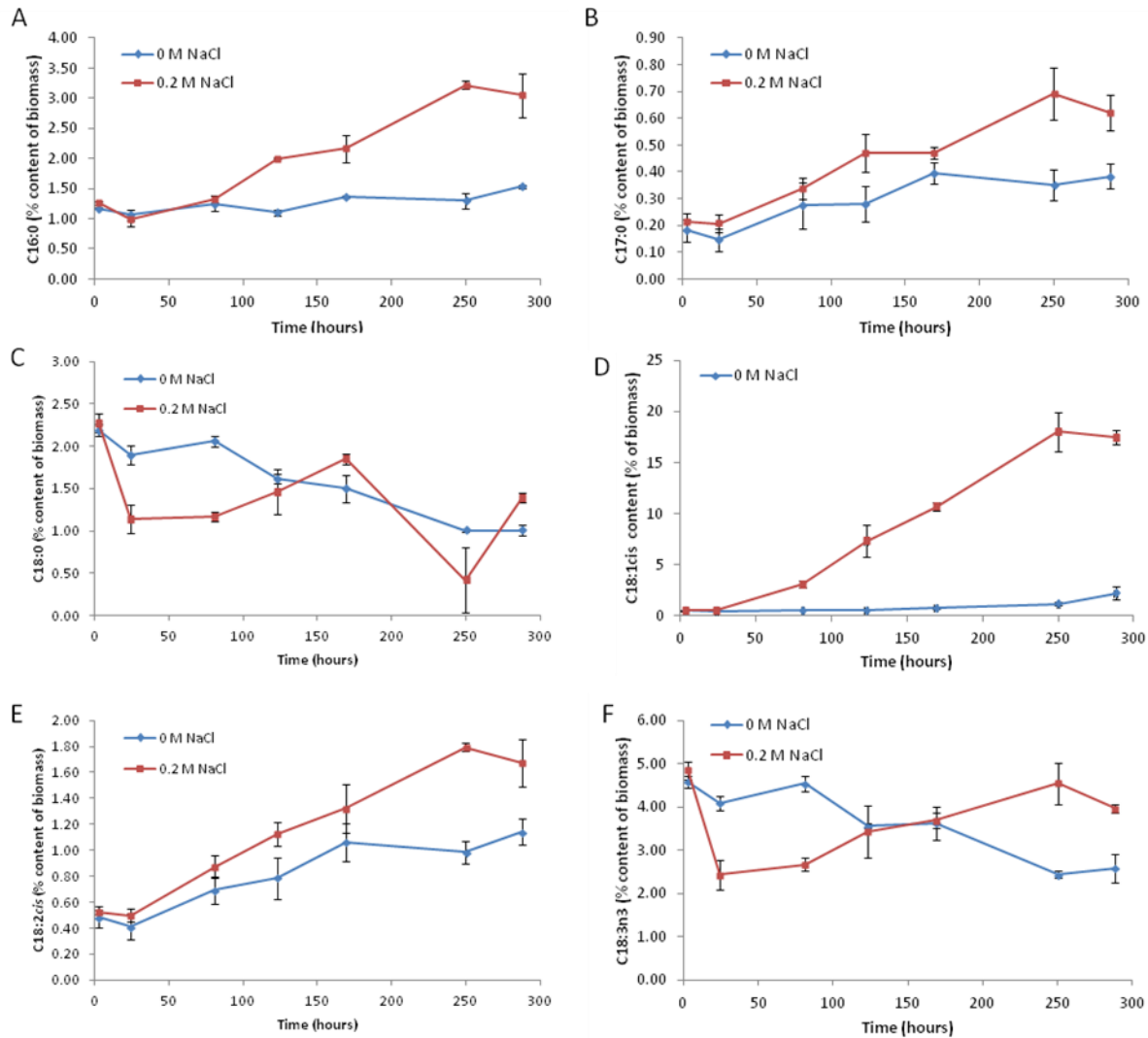


Figure 12.4 Amounts of individual FAMES detected in *C. nivalis* cultures in 0 and 0.2 M NaCl, in the first experimental run (n=3).

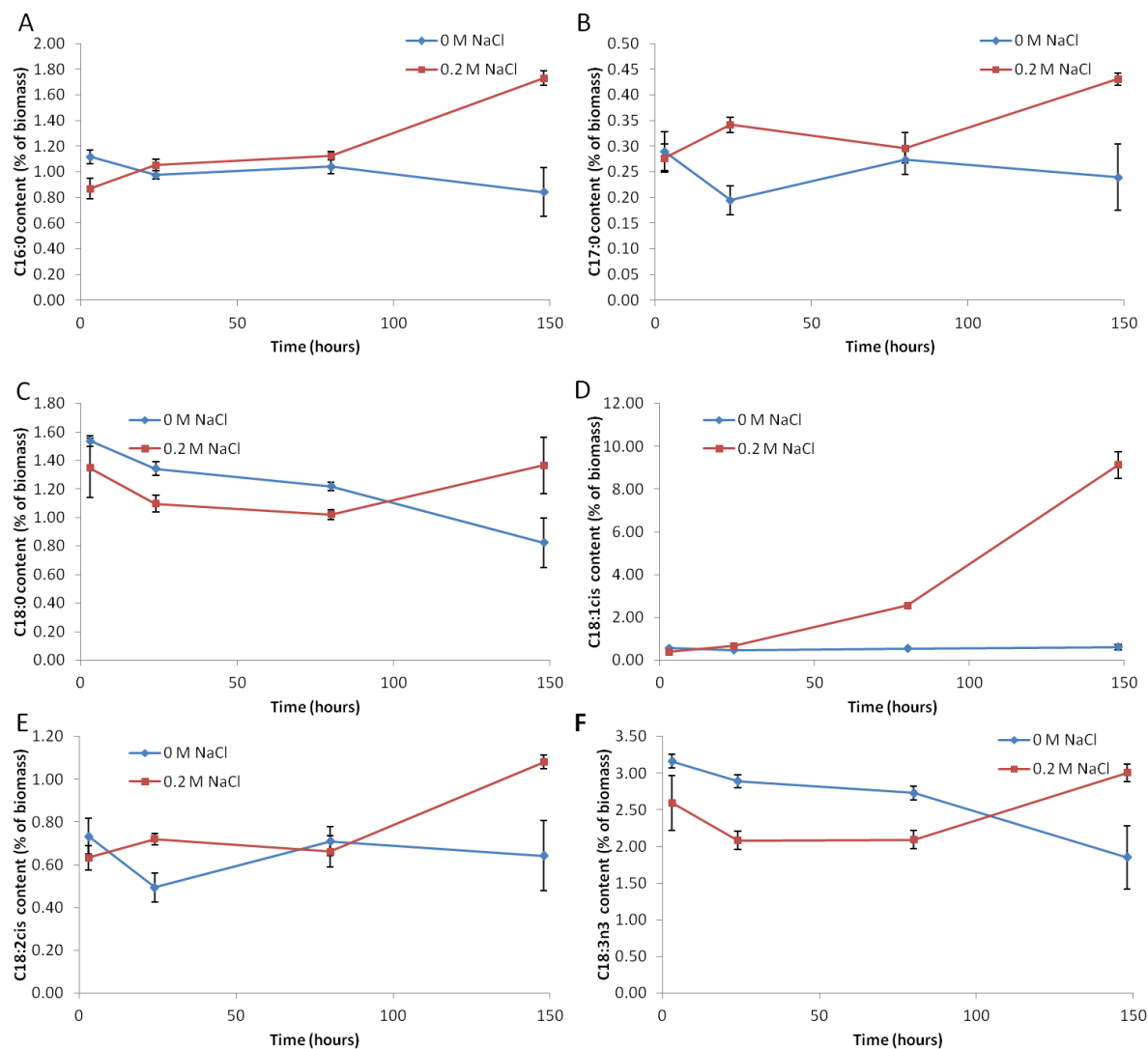


Figure 12.5 Amounts of individual FAMES detected in *C. nivalis* cultures in 0 and 0.2 M NaCl, in the second experimental run (n=3).

### 12.3 Preliminary investigation of proteomic identification of *C. nivalis* proteins using *C. reinhardtii* and *chlorophyta* databases

In preparation for potential quantitative proteomic investigation of *C. nivalis*, protein samples were extracted from cultures of *C. nivalis* grown as described in Section 2.3. The extracted protein was then analysed using the *C. reinhardtii* database, to explore the

possibility of using the *C. reinhardtii* genome to conduct proteomic investigation using *C. nivalis*.

### 12.3.1 Running *C. nivalis* through PEAKS using *C. reinhardtii* database - preliminary tests

The extracted *C. nivalis* protein samples were resolved by a 1D-SDS-PAGE for separation and digested then extracted using an in-gel digestion protocol. These samples were run on an Ultra High Resolution (UHR) Q-ToF maXis™ from Bruker (Bremen, Germany), online connected with Ultra High Performance Liquid Chromatography (uHPLC) Ultimate 3000 from Dionex (Surrey, UK). The 5176 resulting spectra obtained from the mass spectrometer were then processed and analysed using PEAKS software for *de novo* sequencing and matched with both the *C. reinhardtii* database and the Chlorophyta (green algae) database, using different stringencies to try to optimise data acquisition, as illustrated in Table 12.1. 167 proteins were identified using the *C. reinhardtii* database, whilst 285 were identified using the Chlorophyta database, making identifications belonging to the *C. reinhardtii* database account for 58% of the proteins identified when searching against all green algae databases.

Table 12.2 demonstrates the "masking" effect of the most abundant proteins dominating the detected spectra, demonstrating a general problem that low abundance proteins may not be detected in a sample, reducing the number of identifications obtained.

**Table 12.1 Summary statistics for protein detection using different search databases in PEAKS software.**

Database	Precursor Mass Error Tolerance	Fragment Mass Error Tolerance	Peptide spectrum matches (PSMs)	Peptide sequences	Proteins (with at least one unique peptide)	False Discovery Rate (FDR) (PSMs) %
<i>Chlamydomonas reinhardtii</i>	0.1 Da	0.1 Da	1028	328	167	4.8
<i>Chlamydomonas reinhardtii</i>	50ppm	0.1 Da	1019	327	170	4.8
Chlorophyta	0.1 Da	0.1 Da	1213	426	285	4.2

Chlorophyta	0.4 Da	0.3 Da	973	352	258	4.5
-------------	--------	--------	-----	-----	-----	-----

**Table 12.2** Examples of the top 5 most dominating proteins detected in the *C. nivalis* protein sample.

Spectra number	Percentage of total spectra	Protein name	Accession number
411	7.95%	Ribulose biphosphate carboxylase large	P00877 RBL_CHLRE
236	4.56%	ATP synthase subunit beta, chloroplastic	P06541 ATPB_CHLRE
67	1.29%	Photosystem II CP47 chlorophyll apoprotein	P37255 PSBB_CHLRE
66	1.28%	Geranylgeranyl reductase	tr A8HNE8 A8HNE8_CHLRE
55	1.06%	Photosystem II CP43 chlorophyll apoprotein	P10898 PSBC_CHLRE

To investigate which parts of the proteome are conserved between the two *Chlamydomonas* species, the detected proteins were run through KEGG mapping. The resulting successfully mapped proteins are displayed in Figure 12.6 and Figure 12.7, showing main metabolic pathways and photosynthesis pathways respectively. Identified proteins are highlighted in red. In the main metabolic pathways, only a few proteins involved in amino acid metabolism and energy metabolism were identified, especially in photosynthesis. No proteins relating to lipid metabolism were identified. Figure 12.7 shows the proteins conserved in photosynthesis in more detail.

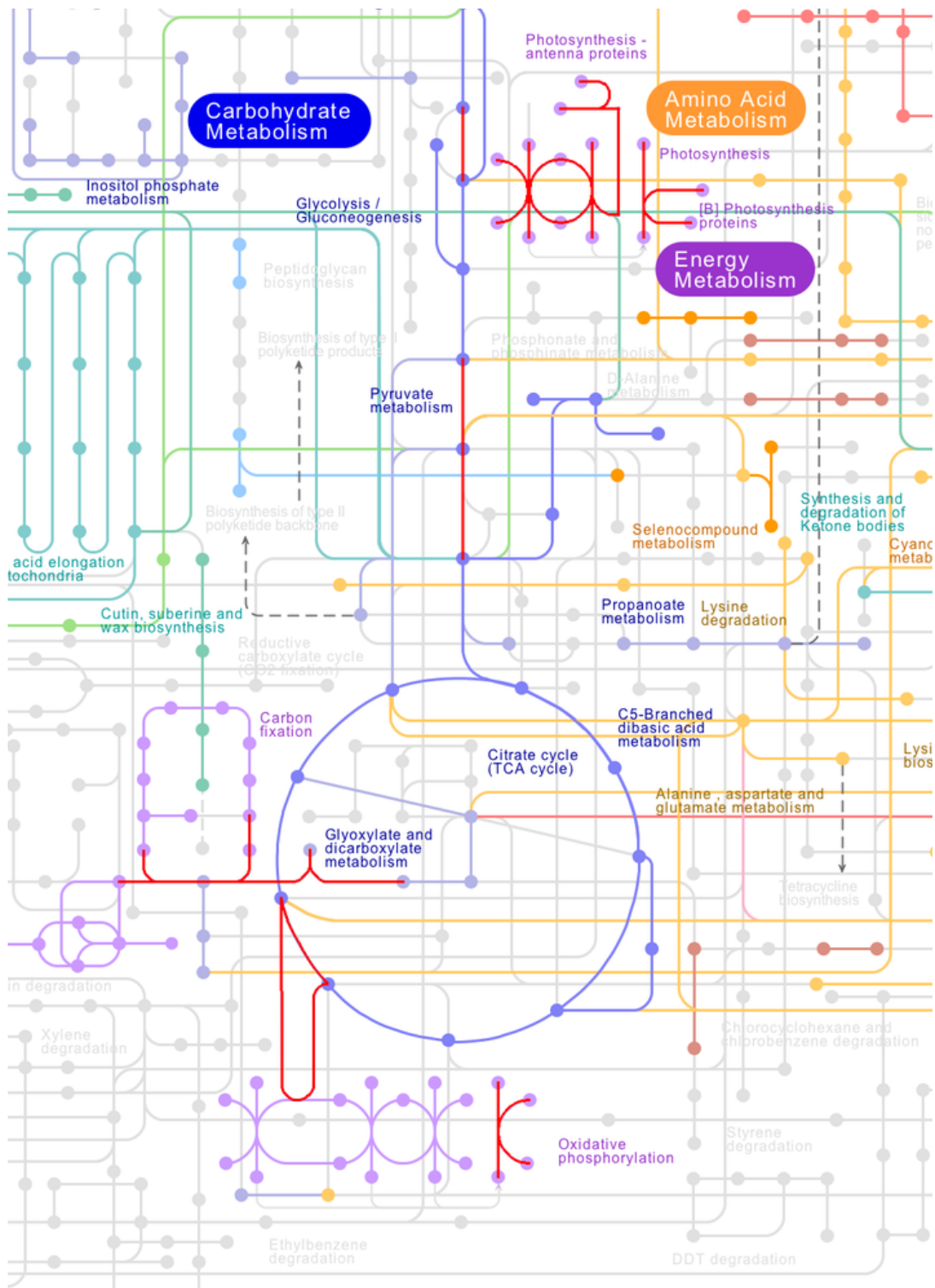
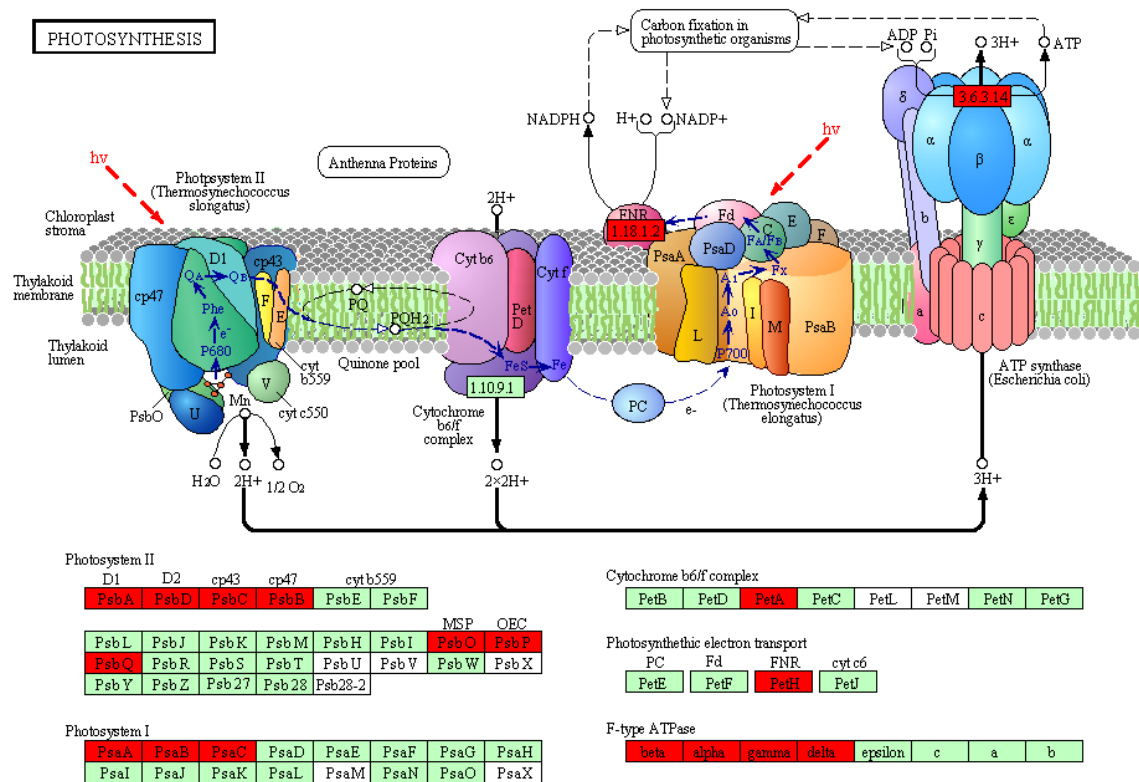


Figure 12.6 Proteins identified from *C. nivalis* (highlighted red) in *C. reinhardtii* main metabolic pathways in KEGG mapping, (26 proteins).



00195 1/15/14  
(c) Kanehisa Laboratories

**Figure 12.7** Proteins identified from *C. nivalis* (highlighted red) in *C. reinhardtii* photosynthesis pathway in KEGG mapping, (16 proteins).

Despite the limitations of the identification of *C. nivalis* proteins using *C. reinhardtii* database, it may still be possible to gather information from iTRAQ investigation of *C. nivalis* under salt stress and lipid producing conditions. The quantitative proteomic work following the initial identification investigation on *C. nivalis* was carried out on a more powerful MS. A combination of powerful MS analysis and homology based searching in PEAKS software meant that potentially more accurate identification results were found for this species.

## 12.4 Protein changes for iTRAQ experiments

Table 12.3 Protein changes between 3 hours 0.2 M NaCl cultures and 82 hour 0.2 M NaCl cultures for *C. nivalis*.

Accession number	Protein name	No. unique peptides	Fold change	P value
A8HMQ3	3,8-divinyl protochlorophyllide a 8-vinyl reductase	3	-1.902	0.010
P46295	40S ribosomal protein S14	4	-1.617	0.016
A8J576	40S ribosomal protein S27	4	-1.560	0.018
P47903	40S ribosomal protein S27	4	-1.560	0.018
E3SC50	40S ribosomal protein S9 (Fragment)	5	-1.546	0.015
Q8HTL2	50S ribosomal protein L2, chloroplastic	3	-1.796	0.009
A8JAV1	Actin	22	-1.220	0.012
P53498	Actin	22	-1.220	0.012
A2PZC1	Adrenodoxin reductase (Predicted protein)	6	-1.422	0.001
Q540H1	Alpha tubulin 1 (Alpha tubulin 2) (Alpha tubulin-2)	22	-1.949	0.000
Q2VA40	Alpha-1,4 glucan phosphorylase (EC 2.4.1.1)	3	1.237	0.010
P07891	ATP synthase epsilon chain, chloroplastic (ATP synthase F1 sector epsilon subunit) (F-ATPase epsilon subunit)	3	-1.830	0.017
P12113	ATP synthase gamma chain, chloroplastic (F-ATPase gamma subunit)	4	-1.996	0.003
Q96550	ATP synthase subunit alpha	20	-1.411	0.001
B7U1J0	ATP synthase subunit alpha, chloroplastic (EC 3.6.3.14) (ATP synthase F1 sector subunit alpha) (F-ATPase subunit alpha)	18	-1.828	0.000
P26526	ATP synthase subunit alpha, chloroplastic (EC 3.6.3.14) (ATP synthase F1 sector subunit alpha) (F-ATPase subunit alpha)	18	-1.828	0.000
A8J785	ATP synthase subunit b', chloroplastic (ATP synthase F(0) sector subunit b') (ATPase subunit II)	4	1.230	0.033
A8IQU3	ATP synthase subunit beta (EC 3.6.3.14)	26	-1.605	0.000
P06541	ATP synthase subunit beta, chloroplastic (EC 3.6.3.14) (ATP synthase F1 sector subunit beta) (F-ATPase subunit beta)	63	-1.697	0.000
P38482	ATP synthase subunit beta, mitochondrial (EC 3.6.3.14)	26	-1.605	0.000
A8IXZ0	Beta tubulin 1 (Beta tubulin 2)	37	-1.992	0.000
A8JGS8	Beta'-cop	8	-1.540	0.001
A8I7T8	Binding protein 1	39	-1.323	0.000
A8I7S9	Binding protein 2	37	-1.325	0.000
A8JGF4	Biotin carboxylase, acetyl-CoA carboxylase component	7	-1.479	0.002
A8JIB7	Chaperonin 60A	7	-1.450	0.002
A8JE91	Chaperonin 60B1	3	-1.830	0.014
A8ITH8	Chaperonin 60B2	10	-1.461	0.002
A8IMK1	Chaperonin 60C (Fragment)	6	-1.404	0.009
A8HXL8	Chloroplast ATP synthase gamma chain	4	-1.996	0.003
A8J2Z6	Chorismate synthase (EC 4.2.3.5)	4	-1.430	0.020
A8I4S9	Clathrin heavy chain	10	-1.404	0.008
A8I972	ClpB chaperone, Hsp100 family	14	1.267	0.000
A8JA18	ClpB chaperone, Hsp100 family	9	-1.606	0.001
A8HRR9	Coatomer subunit alpha	15	-1.342	0.012
A8IM71	Coatomer subunit gamma	8	-1.395	0.014
A8HYR2	Cobalamin-dependent methionine synthase (EC 2.1.1.13)	4	-1.637	0.010
A8JH37	Cobalamin-independent methionine synthase (EC 2.1.1.14)	5	1.111	0.007
A8IEE5	Cysteine synthase (EC 2.5.1.47)	5	-1.680	0.012
A8J7F6	Dihydrolipoamide acetyltransferase (EC 2.3.1.12)	4	-1.447	0.006
A8J1T4	Dihydrolipoyl dehydrogenase (EC 1.8.1.4)	3	1.110	0.033

A8I5K1	Dynamin-related GTPase (EC 2.6.1.42)	6	1.324	0.003
A8JHX9	Elongation factor 2 (EC 3.6.5.3)	13	-1.489	0.000
Q5QEB2	Elongation factor Ts	4	-1.320	0.008
P17746	Elongation factor Tu, chloroplastic (EF-Tu)	12	-1.533	0.001
A8IIL1	EMP/nonaspanin domain family protein	6	-1.651	0.001
A8JDR9	Fasciclin-like protein	3	1.282	0.023
A8JHB4	Ferredoxin-dependent glutamate synthase	6	-1.326	0.010
A8J6Y8	Ferredoxin--NADP reductase (EC 1.18.1.2)	8	-1.836	0.000
Q9S9E0	Ferredoxin--NADP reductase (EC 1.18.1.2)	8	-1.836	0.000
P53991	Ferredoxin--NADP reductase, chloroplastic (FNR) (EC 1.18.1.2)	8	-1.836	0.000
A8HW56	Flagellar associated protein (EC 3.6.1.3)	20	-1.283	0.011
A8HNE8	Geranylgeranyl reductase (EC 1.3.1.-)	4	-1.748	0.002
A8IE23	Glucose-6-phosphate isomerase (EC 5.3.1.9)	11	-1.590	0.000
A8JGD1	Glutamate dehydrogenase	4	-1.456	0.004
A8HP84	Glyceraldehyde-3-phosphate dehydrogenase (EC 1.2.1.-)	26	-1.529	0.000
A8JHR9	Glyceraldehyde-3-phosphate dehydrogenase (EC 1.2.1.-)	3	2.166	0.016
A8JHS0	Glyceraldehyde-3-phosphate dehydrogenase (EC 1.2.1.-)	3	2.166	0.016
P50362	Glyceraldehyde-3-phosphate dehydrogenase A, chloroplastic (EC 1.2.1.13) (NADP-dependent glyceraldehydophosphate dehydrogenase subunit A)	26	-1.529	0.000
P49644	Glyceraldehyde-3-phosphate dehydrogenase, cytosolic (EC 1.2.1.12)	3	2.166	0.016
A8HNN4	Glycerol-3-phosphate dehydrogenase [NAD(+)] (EC 1.1.1.8)	8	2.135	0.001
A8IVM9	Glycine cleavage system, P protein (EC 1.4.4.2)	4	-1.398	0.012
A8J2E9	Glycolate dehydrogenase	3	-1.611	0.013
Q0ZAZ1	Glycolate dehydrogenase	3	-1.611	0.013
P25387	Guanine nucleotide-binding protein subunit beta-like protein	6	-1.655	0.001
P25840	Heat shock 70 kDa protein	25	-1.359	0.000
A8JEU4	Heat shock protein 70A (EC 3.6.1.3)	34	-1.358	0.000
A8HYV3	Heat shock protein 70B	25	-1.340	0.004
Q39603	Heat shock protein 70B	25	-1.340	0.004
A8IZU0	Heat shock protein 70C	16	-1.336	0.006
A8J955	Kinesin-like calmodulin binding protein (Fragment)	9	-1.369	0.005
Q93WE2	Magnesium chelatase H subunit (Magnesium chelatase H-subunit)	5	-1.713	0.011
A8I7P5	Magnesium chelatase subunit H	5	-1.713	0.011
A8ICG9	Malate dehydrogenase (EC 1.1.1.37)	11	-1.340	0.003
Q8H0R8	Malate dehydrogenase (EC 1.1.1.37) (Fragment)	3	1.151	0.014
A8ILO8	Membrane AAA-metalloprotease (EC 3.4.24.-)	17	-1.558	0.000
A8I531	Mg-protoporphyrin IX chelatase (EC 6.6.1.1)	5	-1.711	0.016
I2FKQ9	Mitochondrial chaperonin 60	6	-1.404	0.009
A8ITL0	Mitochondrial F1F0 ATP synthase associated 60.6 kDa protein	7	1.152	0.017
A8IA86	Nucleolar protein, component of C/D snoRNPs	7	-1.464	0.019
A8JEV1	Oxygen evolving enhancer protein 3	5	-1.495	0.006
A8J0E4	Oxygen-evolving enhancer protein 1 of photosystem II	20	-1.864	0.000
P12853	Oxygen-evolving enhancer protein 1, chloroplastic (OEE1)	20	-1.864	0.000
A8IYH9	Oxygen-evolving enhancer protein 2 of photosystem II	10	-1.520	0.008
P11471	Oxygen-evolving enhancer protein 2, chloroplastic (OEE2)	10	-1.520	0.008
P12852	Oxygen-evolving enhancer protein 3, chloroplastic (OEE3)	5	-1.495	0.006
A8J282	Peptidyl-prolyl cis-trans isomerase (PPIase) (EC 5.2.1.8)	4	1.338	0.033
Q3HTK2	Pherophorin-C5 protein	3	-1.761	0.009
A8IZZ9	Phosphate acetyltransferase (EC 2.3.1.8)	3	1.192	0.019
A8IYP4	Phosphoribulokinase (EC 2.7.1.19)	18	-1.759	0.000

P19824	Phosphoribulokinase, chloroplastic (PRK) (PRKase) (EC 2.7.1.19) (Phosphopentokinase)	18	-1.759	0.000
Q00914	Photosystem I iron-sulfur center (EC 1.97.1.12) (9 kDa polypeptide) (PSI-C) (Photosystem I subunit VII) (PsaC)	5	-1.672	0.008
P12154	Photosystem I P700 chlorophyll a apoprotein A1 (EC 1.97.1.12) (PSI-A) (PsaA)	8	-1.823	0.000
P09144	Photosystem I P700 chlorophyll a apoprotein A2 (EC 1.97.1.12) (PSI-B) (PsaB)	9	-1.643	0.000
P10898	Photosystem II CP43 reaction center protein (PSII 43 kDa protein) (Protein CP-43) (Protein P6)	25	-1.623	0.000
P37255	Photosystem II CP47 reaction center protein (PSII 47 kDa protein) (Protein CP-47)	15	-1.583	0.000
P06007	Photosystem II D2 protein (PSII D2 protein) (EC 1.10.3.9) (Photosystem Q(A) protein)	27	-1.611	0.000
P07753	Photosystem II protein D1 (PSII D1 protein) (EC 1.10.3.9) (32 kDa thylakoid membrane protein) (Photosystem II Q(B) protein)	10	-1.840	0.000
A8HPE9	Predicted protein	5	-1.232	0.011
A8ITU2	Predicted protein	4	1.275	0.020
A8IWL3	Predicted protein	7	1.178	0.028
A8IX35	Predicted protein	5	1.464	0.006
A8J4Y6	Predicted protein	6	-1.458	0.001
A8JBL6	Predicted protein	6	1.254	0.026
A8JFZ2	Predicted protein	3	-1.618	0.013
A8JGL0	Predicted protein	2	-1.292	0.031
A8JH97	Predicted protein	4	1.096	0.024
A8IBY2	Predicted protein (Fragment)	11	-1.335	0.002
A8I8V6	Prohibitin	4	-1.624	0.003
A8J6K9	Proteasome subunit alpha type (EC 3.4.25.1)	2	-1.229	0.023
O48949	Protein disulfide-isomerase (EC 5.3.4.1)	8	1.184	0.009
A8J709	Protein phosphatase 2A regulatory subunit (EC 3.1.3.16)	5	-1.335	0.006
Q8LKK4	Protofilament ribbon protein of flagellar microtubules (RIB72 protein) (p72)	2	-1.127	0.016
A8IVR6	Pyruvate kinase (EC 2.7.1.40)	13	-1.297	0.002
A8J345	Pyruvate kinase (EC 2.7.1.40)	4	-1.301	0.021
A8I6T5	R1 protein, alpha-glucan water dikinase	8	1.244	0.006
A8J8Y1	Receptor of activated protein kinase C 1	6	-1.655	0.001
A8J0I0	Ribosomal protein L4	5	-1.572	0.014
A8HP90	Ribosomal protein L6	4	1.148	0.020
A8JDP4	Ribosomal protein L9	5	1.141	0.011
A8JHC3	Ribosomal protein S11	4	1.387	0.005
A8IGY1	Ribosomal protein S13	3	1.372	0.030
A8J768	Ribosomal protein S14	4	-1.617	0.016
A8I4P5	Ribosomal protein S3	7	-1.345	0.010
A8J2I5	Ribosomal protein S5	5	-1.693	0.016
A8JGF8	Ribosomal protein S9, component of cytosolic 80S ribosome and 40S small subunit	5	-1.546	0.015
P00877	Ribulose bisphosphate carboxylase large chain (RuBisCO large subunit) (EC 4.1.1.39)	83	-1.810	0.000
A8IT75	R-SNARE protein, VAMP72-family	2	1.249	0.026
Q42694	RuBisCO large subunit-binding protein subunit alpha, chloroplastic (60 kDa chaperonin subunit alpha) (CPN-60 alpha)	7	-1.450	0.002
A8I1Q9	Ser/thr protein kinase (Fragment)	4	-1.417	0.015
Q8W4V3	Serine hydroxymethyltransferase (EC 2.1.2.1)	4	-1.493	0.038
Q9XGU3	Serine/threonine-protein phosphatase (EC 3.1.3.16)	4	-1.452	0.017
A8HNE3	Serine/threonine-protein phosphatase (EC 3.1.3.16) (Fragment)	8	-1.548	0.000
A8HX04	Succinate dehydrogenase [ubiquinone] iron-sulfur subunit, mitochondrial (EC 1.3.5.1)	3	1.139	0.026

A8II42	T-complex protein 1 subunit gamma	4	-1.537	0.001
P09204	Tubulin alpha-1 chain	22	-1.949	0.000
P09205	Tubulin alpha-2 chain	21	-1.917	0.000
P04690	Tubulin beta-1/beta-2 chain (Beta-tubulin)	37	-1.992	0.000
A8J5P7	Ubiquinol:cytochrome c oxidoreductase 50 kDa core 1 subunit	6	-1.566	0.002
A2PZC2	UDP-Glucose:protein transglucosylase (UDP-glucose protein: protein transglucosylase)	14	-1.535	0.000
Q763T6	UDP-sulfoquinovose synthase	5	-1.275	0.014
A8IA45	Vacuolar ATP synthase subunit B	11	-1.543	0.002
A8I164	Vacuolar ATP synthase, subunit A	16	-1.454	0.000

**Table 12.4 Protein changes between 82 hour 0.2 M NaCl cultures and 170 hour 0.2 M NaCl cultures in *C. nivalis*.**

Accession number	Protein names	No. unique peptides	Fold change	P value
Q08365	30S ribosomal protein S3, chloroplastic (ORF 712)	8	-1.148	0.003
Q2VA40	Alpha-1,4 glucan phosphorylase (EC 2.4.1.1)	3	1.158	0.015
A8IWJ3	Aminomethyltransferase (EC 2.1.2.10)	7	-1.172	0.010
Q39595	ATP sulfurylase Ats1	5	1.279	0.029
A8J785	ATP synthase subunit b', chloroplastic (ATP synthase F(0) sector subunit b') (ATPase subunit II)	4	-1.251	0.026
Q6J213	Chloroplast phytoene desaturase (Phytoene desaturase) (EC 1.3.-.-) (EC 1.3.99.-)	5	-1.121	0.026
A8JA18	ClpB chaperone, Hsp100 family	9	1.322	0.015
A8HX38	Eukaryotic translation elongation factor 1 alpha 1 (EC 3.6.5.3) (Eukaryotic translation elongation factor 1 alpha 2)	4	-1.218	0.004
A8JHE3	Global transcription factor (Fragment)	2	1.154	0.017
A8HS14	Glucose-1-phosphate adenyltransferase (EC 2.7.7.27) (ADP-glucose pyrophosphorylase)	6	1.220	0.017
A8HXA6	Glutathione reductase	3	1.277	0.020
A8HNN4	Glycerol-3-phosphate dehydrogenase [NAD(+)] (EC 1.1.1.8)	8	1.192	0.006
A8JHB2	Iron-sulfur cluster assembly protein	4	1.284	0.029
A8I893	NAD-dependent epimerase/dehydratase	3	1.353	0.011
P11471	Oxygen-evolving enhancer protein 2, chloroplastic (OEE2)	4	-1.225	0.022
A8JDP6	Plastid ribosomal protein S13	7	-1.192	0.012
A8IX35	Predicted protein	5	1.375	0.003
A8HVG0	Predicted protein (Fragment)	4	-1.105	0.018
A8JG06	Programmed cell death protein 6-interacting protein	3	1.208	0.018
A8I9I9	Rieske ferredoxin	4	-1.219	0.027
A8IFZ9	Tryptophan synthase beta subunit	7	-1.380	0.021
A8J1C1	Ubiquitin-activating enzyme E1 (EC 6.3.2.19)	5	1.254	0.002

**Table 12.5 Protein changes between 3 hour 0.2 M NaCl cultures and 170 hour 0.2 M NaCl cultures in *C. nivalis*.**

Accession number	Protein name	No. unique peptides	Fold change	P value
A8JGV6	14-3-3 protein (EC 3.1.1.4)	25	-1.224	0.004
P52908	14-3-3-like protein	25	-1.224	0.004
A8JFW4	1-deoxy-D-xylulose 5-phosphate synthase (EC 2.2.1.7) (Fragment)	6	-1.223	0.021

A8HMQ3	3,8-divinyl protochlorophyllide a 8-vinyl reductase	3	-1.985	0.011
E3SC50	40S ribosomal protein S9 (Fragment)	5	-1.573	0.022
Q8HTL2	50S ribosomal protein L2, chloroplastic	3	-1.555	0.025
A8J5F7	6-phosphogluconate dehydrogenase, decarboxylating (EC 1.1.1.44)	5	1.216	0.024
A8J6J6	Acetyl-CoA acyltransferase (EC 2.3.1.16)	5	1.250	0.012
A8JAV1	Actin	22	-1.262	0.003
P53498	Actin	22	-1.262	0.003
A8IXE0	Adenosylhomocysteinase (EC 3.3.1.1)	19	-1.255	0.002
A2PZC1	Adrenodoxin reductase (Predicted protein)	6	-1.394	0.002
A8IJ19	Aldehyde dehydrogenase	4	1.306	0.023
Q540H1	Alpha tubulin 1 (Alpha tubulin 2) (Alpha tubulin-2)	22	-1.874	0.000
Q2VA40	Alpha-1,4 glucan phosphorylase (EC 2.4.1.1)	3	1.433	0.004
Q42687	ATP synthase delta chain, chloroplastic (F-ATPase delta chain)	4	-2.301	0.026
P07891	ATP synthase epsilon chain, chloroplastic (ATP synthase F1 sector epsilon subunit) (F-ATPase epsilon subunit)	3	-2.436	0.006
P12113	ATP synthase gamma chain, chloroplastic (F-ATPase gamma subunit)	8	-1.173	0.009
Q96550	ATP synthase subunit alpha	20	-1.482	0.000
B7U1J0	ATP synthase subunit alpha, chloroplastic (EC 3.6.3.14) (ATP synthase F1 sector subunit alpha) (F-ATPase subunit alpha)	18	-2.200	0.000
P26526	ATP synthase subunit alpha, chloroplastic (EC 3.6.3.14) (ATP synthase F1 sector subunit alpha) (F-ATPase subunit alpha)	18	-2.200	0.000
A8IQU3	ATP synthase subunit beta (EC 3.6.3.14)	26	-1.725	0.000
P06541	ATP synthase subunit beta, chloroplastic (EC 3.6.3.14) (ATP synthase F1 sector subunit beta) (F-ATPase subunit beta)	63	-1.812	0.000
P38482	ATP synthase subunit beta, mitochondrial (EC 3.6.3.14)	26	-1.725	0.000
A8IJ60	ATP-dependent Clp protease proteolytic subunit (EC 3.4.21.92)	3	-1.722	0.005
A8JB85	Autophagy-related protein	3	1.352	0.016
A8IXZ0	Beta tubulin 1 (Beta tubulin 2)	37	-1.966	0.000
A8JGS8	Beta'-cop	8	-1.545	0.002
A8I7T8	Binding protein 1	39	-1.301	0.000
A8I7S9	Binding protein 2	37	-1.303	0.000
A8JGF4	Biotin carboxylase, acetyl-CoA carboxylase component	7	-1.482	0.001
A8JIR0	Carbamoyl phosphate synthase, large subunit (EC 6.3.5.5)	17	-1.272	0.012
A8JIB7	Chaperonin 60A	7	-1.504	0.000
A8ITH8	Chaperonin 60B2	10	-1.476	0.004
A8IMK1	Chaperonin 60C (Fragment)	6	-1.471	0.000
A8JF15	Chloroplast ATP synthase delta chain	4	-2.301	0.026
A8HXL8	Chloroplast ATP synthase gamma chain	4	-2.060	0.008
A8J2Z6	Chorismate synthase (EC 4.2.3.5)	4	-1.566	0.006
A8I4S9	Clathrin heavy chain	10	-1.386	0.008
A8I972	ClpB chaperone, Hsp100 family	14	1.200	0.002
A8IM71	Coatomer subunit gamma	8	-1.377	0.026
A8HYR2	Cobalamin-dependent methionine synthase (EC 2.1.1.13)	4	-1.868	0.005
A8IEE5	Cysteine synthase (EC 2.5.1.47)	5	-1.859	0.013
A8ISA9	Cysteine synthase (EC 2.5.1.47)	6	-1.702	0.010
A8ISB0	Cysteine synthase (EC 2.5.1.47)	6	-1.702	0.010
O81523	Cysteine synthase (EC 2.5.1.47)	6	-1.702	0.010
A8IT25	Cytoplasmic DEXD/H-box RNA helicase	3	-1.283	0.023
A8J7F6	Dihydrolipoamide acetyltransferase (EC 2.3.1.12)	4	-1.621	0.003
A8I5K1	Dynamin-related GTPase (EC 2.6.1.42)	6	1.358	0.005
A8JHX9	Elongation factor 2 (EC 3.6.5.3)	13	-1.548	0.000

Q5QEB2	Elongation factor Ts	4	-1.340	0.001
P17746	Elongation factor Tu, chloroplastic (EF-Tu)	12	-1.739	0.000
A8IIL1	EMP/nonaspanin domain family protein	6	-1.430	0.027
A8IVW9	Eukaryotic initiation factor (Fragment)	3	-1.412	0.019
A8JHB4	Ferredoxin-dependent glutamate synthase	8	1.181	0.041
A8J6Y8	Ferredoxin--NADP reductase (EC 1.18.1.2)	8	-2.073	0.000
Q9S9E0	Ferredoxin--NADP reductase (EC 1.18.1.2)	8	-2.073	0.000
P53991	Ferredoxin--NADP reductase, chloroplastic (FNR) (EC 1.18.1.2)	8	-2.073	0.000
A8HW56	Flagellar associated protein (EC 3.6.1.3)	20	-1.254	0.005
A8HNE8	Geranylgeranyl reductase (EC 1.3.1.-)	4	-2.154	0.009
A8IE23	Glucose-6-phosphate isomerase (EC 5.3.1.9)	11	-1.671	0.000
A8JGD1	Glutamate dehydrogenase	4	-1.413	0.012
A8HP84	Glyceraldehyde-3-phosphate dehydrogenase (EC 1.2.1.-)	26	-1.682	0.000
A8JHR9	Glyceraldehyde-3-phosphate dehydrogenase (EC 1.2.1.-)	3	2.200	0.007
A8JHS0	Glyceraldehyde-3-phosphate dehydrogenase (EC 1.2.1.-)	3	2.200	0.007
P50362	Glyceraldehyde-3-phosphate dehydrogenase A, chloroplastic (EC 1.2.1.13) (NADP-dependent glyceraldehydephosphate dehydrogenase subunit A)	26	-1.682	0.000
P49644	Glyceraldehyde-3-phosphate dehydrogenase, cytosolic (EC 1.2.1.12)	3	2.200	0.007
A8HNN4	Glycerol-3-phosphate dehydrogenase [NAD(+)] (EC 1.1.1.8)	8	2.544	0.001
A8IVM9	Glycine cleavage system, P protein (EC 1.4.4.2)	4	-1.605	0.006
P25387	Guanine nucleotide-binding protein subunit beta-like protein	6	-1.852	0.007
P25840	Heat shock 70 kDa protein	25	-1.344	0.000
A8JEU4	Heat shock protein 70A (EC 3.6.1.3)	34	-1.334	0.000
A8HYV3	Heat shock protein 70B	25	-1.363	0.000
Q39603	Heat shock protein 70B	25	-1.363	0.000
A8IZU0	Heat shock protein 70C	16	-1.386	0.001
A8J1U1	Heat shock protein 90A	22	-1.189	0.006
Q66T67	Heat shock protein 90C	4	-1.543	0.013
A8JIN6	Histone H2B	4	-1.692	0.008
A8HVA3	Histone H4	6	-1.476	0.010
A8JIN9	Histone H4	6	-1.476	0.010
P50566	Histone H4	6	-1.476	0.010
A8JG03	Isopropylmalate dehydratase, large subunit	6	-1.390	0.005
A8J955	Kinesin-like calmodulin binding protein (Fragment)	9	-1.385	0.006
Q8H0R8	Malate dehydrogenase (EC 1.1.1.37) (Fragment)	3	1.265	0.007
A8ILO8	Membrane AAA-metalloprotease (EC 3.4.24.-)	17	-1.665	0.000
A8I531	Mg-protoporphyrin IX chelatase (EC 6.6.1.1)	5	-1.995	0.006
I2FKQ9	Mitochondrial chaperonin 60	6	-1.471	0.000
A8IKE3	Mitogen-activated protein kinase (EC 2.7.11.24)	3	-1.732	0.026
C0SPI7	Mitogen-activated protein kinase (EC 2.7.11.24)	3	-1.732	0.026
A8I893	NAD-dependent epimerase/dehydratase	3	1.565	0.010
A2PZD2	NAD-dependent epimerase/dehydratase (Predicted protein)	3	1.432	0.005
Q6V9A8	NADH:ubiquinone oxidoreductase 49 kD subunit (EC 1.6.5.3) (NADH:ubiquinone oxidoreductase 49 kDa ND7 subunit)	4	-1.584	0.017
A8IA86	Nucleolar protein, component of C/D snoRNPs	7	-1.718	0.012
A8JEV1	Oxygen evolving enhancer protein 3	5	-1.674	0.019
A8J0E4	Oxygen-evolving enhancer protein 1 of photosystem II	20	-2.186	0.000
P12853	Oxygen-evolving enhancer protein 1, chloroplastic (OEE1)	20	-2.186	0.000
A8IYH9	Oxygen-evolving enhancer protein 2 of photosystem II	10	-1.626	0.002
P11471	Oxygen-evolving enhancer protein 2, chloroplastic (OEE2)	10	-1.626	0.002

P12852	Oxygen-evolving enhancer protein 3, chloroplastic (OEE3)	5	-1.674	0.019
Q3HTK2	Pherophorin-C5 protein	3	-1.916	0.001
A8IZZ9	Phosphate acetyltransferase (EC 2.3.1.8)	3	1.176	0.010
A8IJJ8	Phosphoribosylaminoimidazole carboxylase, eukaryotic-type	4	1.155	0.032
A8IYP4	Phosphoribulokinase (EC 2.7.1.19)	18	-2.048	0.000
P19824	Phosphoribulokinase, chloroplastic (PRK) (PRKase) (EC 2.7.1.19) (Phosphopentokinase)	18	-2.048	0.000
Q00914	Photosystem I iron-sulfur center (EC 1.97.1.12) (9 kDa polypeptide) (PSI-C) (Photosystem I subunit VII) (PsaC)	5	-1.932	0.008
P12154	Photosystem I P700 chlorophyll a apoprotein A1 (EC 1.97.1.12) (PSI-A) (PsaA)	8	-1.864	0.000
P09144	Photosystem I P700 chlorophyll a apoprotein A2 (EC 1.97.1.12) (PSI-B) (PsaB)	9	-1.614	0.001
P10898	Photosystem II CP43 reaction center protein (PSII 43 kDa protein) (Protein CP-43) (Protein P6)	25	-1.824	0.000
P37255	Photosystem II CP47 reaction center protein (PSII 47 kDa protein) (Protein CP-47)	15	-1.693	0.000
P06007	Photosystem II D2 protein (PSII D2 protein) (EC 1.10.3.9) (Photosystem Q(A) protein)	27	-1.634	0.000
P07753	Photosystem II protein D1 (PSII D1 protein) (EC 1.10.3.9) (32 kDa thylakoid membrane protein) (Photosystem II Q(B) protein)	10	-1.727	0.000
A8JFB1	Porphobilinogen deaminase	8	-1.465	0.008
A8I804	Predicted protein	2	1.761	0.014
A8ITU2	Predicted protein	4	1.379	0.003
A8IX35	Predicted protein	5	2.012	0.002
A8J4Y6	Predicted protein	6	-1.262	0.013
A8J725	Predicted protein	4	1.145	0.019
A8IBY2	Predicted protein (Fragment)	11	-1.403	0.001
A8IKW9	Predicted protein (Fragment)	3	-1.433	0.016
A8IRE2	Proteasome subunit alpha type (EC 3.4.25.1)	2	-1.589	0.024
O48949	Protein disulfide-isomerase (EC 5.3.4.1)	8	1.237	0.004
A8J709	Protein phosphatase 2A regulatory subunit (EC 3.1.3.16)	5	-1.222	0.020
A8IVR6	Pyruvate kinase (EC 2.7.1.40)	13	-1.374	0.000
A8J345	Pyruvate kinase (EC 2.7.1.40)	4	-1.348	0.015
A8I6T5	R1 protein, alpha-glucan water dikinase	8	1.239	0.009
A8J8Y1	Receptor of activated protein kinase C 1	6	-1.852	0.007
A8I8Z4	Ribosomal protein	2	-2.062	0.031
A8J0I0	Ribosomal protein L4	5	-1.698	0.015
A8J567	Ribosomal protein L7a	4	-1.530	0.018
A8JDP4	Ribosomal protein L9	5	1.123	0.022
A8I4P5	Ribosomal protein S3	7	-1.682	0.004
A8J2I5	Ribosomal protein S5	5	-1.632	0.012
A8JGI9	Ribosomal protein S7	4	-1.560	0.007
A8JGF8	Ribosomal protein S9, component of cytosolic 80S ribosome and 40S small subunit	5	-1.573	0.022
P00877	Ribulose biphosphate carboxylase large chain (RuBisCO large subunit) (EC 4.1.1.39)	83	-1.991	0.000
P23489	Ribulose biphosphate carboxylase/oxygenase activase, chloroplastic (RA) (RuBisCO activase)	12	-1.555	0.015
Q6SA05	Rubisco activase	12	-1.555	0.015
Q42694	RuBisCO large subunit-binding protein subunit alpha, chloroplastic (60 kDa chaperonin subunit alpha) (CPN-60 alpha)	7	-1.504	0.000
A8I1Q9	Ser/thr protein kinase (Fragment)	4	-1.394	0.014
Q8W4V3	Serine hydroxymethyltransferase (EC 2.1.2.1)	4	-1.490	0.019
Q9XGU3	Serine/threonine-protein phosphatase (EC 3.1.3.16)	4	-1.582	0.011
A8HNE3	Serine/threonine-protein phosphatase (EC 3.1.3.16) (Fragment)	8	-1.581	0.000

A8HPL0	Splicing factor, component of the U5 snRNP and of the spliceosome	3	-1.575	0.025
A8J431	Stress-related chlorophyll a/b binding protein 2 (Stress-related chlorophyll a/b binding protein 3)	2	1.572	0.039
A8IAN1	Transketolase (EC 2.2.1.1)	26	-1.332	0.003
A8IFZ9	Tryptophan synthase beta subunit	7	-1.237	0.007
P09204	Tubulin alpha-1 chain	22	-1.874	0.000
P09205	Tubulin alpha-2 chain	21	-1.901	0.000
P04690	Tubulin beta-1/beta-2 chain (Beta-tubulin)	37	-1.966	0.000
A8J5P7	Ubiquinol:cytochrome c oxidoreductase 50 kDa core 1 subunit	6	-1.334	0.032
A8J1C1	Ubiquitin-activating enzyme E1 (EC 6.3.2.19)	5	1.198	0.013
A2PZC2	UDP-Glucose:protein transglucosylase (UDP-glucose protein: protein trans glycosylase)	14	-1.713	0.000
Q763T6	UDP-sulfoquinovose synthase	5	-1.289	0.012
A8IA45	Vacuolar ATP synthase subunit B	11	-1.439	0.012
A8I164	Vacuolar ATP synthase, subunit A	16	-1.380	0.000

**Table 12.6 Protein changes between 170 hour control cultures and 170 hour 0.2 M NaCl cultures in *C. nivalis*.**

Accession number	Protein name	No. unique peptides	Fold change	P value
A8JGV6	14-3-3 protein (EC 3.1.1.4)	25	-2.165	0.000
P52908	14-3-3-like protein	25	-2.165	0.000
A8HTX3	26S proteasome regulatory subunit	5	1.252	0.003
A8IIP7	26S proteasome regulatory subunit	13	-1.860	0.000
A8IR41	26S proteasome regulatory subunit	6	-1.972	0.002
A8IV67	26S proteasome regulatory subunit	6	-2.293	0.007
A8J8U1	26S proteasome regulatory subunit (Fragment)	3	-1.900	0.013
A8HMQ3	3,8-divinyl protochlorophyllide a 8-vinyl reductase	3	-2.294	0.018
A8I0I1	40S ribosomal protein S24	3	1.245	0.031
A8J1G8	40S ribosomal protein S6	5	1.524	0.005
A8J5F7	6-phosphogluconate dehydrogenase, decarboxylating (EC 1.1.1.44)	8	-1.361	0.009
Q8SAQ6	6-phosphogluconate dehydrogenase, decarboxylating (EC 1.1.1.44)	8	-1.361	0.009
A8J6J6	Acetyl-CoA acyltransferase (EC 2.3.1.16)	5	1.375	0.008
A8JAV1	Actin	22	-1.778	0.000
P53498	Actin	22	-1.778	0.000
A8IXE0	Adenosylhomocysteinase (EC 3.3.1.1)	19	-2.061	0.000
P51821	ADP-ribosylation factor 1	7	-1.921	0.003
A2PZC1	Adrenodoxin reductase (Predicted protein)	6	-2.143	0.000
Q540H1	Alpha tubulin 1 (Alpha tubulin 2) (Alpha tubulin-2)	22	-2.327	0.000
Q2VA40	Alpha-1,4 glucan phosphorylase (EC 2.4.1.1)	5	-1.688	0.003
A8IWJ3	Aminomethyltransferase (EC 2.1.2.10)	7	-1.223	0.023
P22675	Argininosuccinate lyase (ASAL) (EC 4.3.2.1) (Arginosuccinase)	3	-1.959	0.022
A8J506	Argininosuccinate synthase (EC 6.3.4.5)	8	-1.674	0.002
A8I8X8	ATP citrate lyase, subunit B (EC 2.3.3.8)	2	1.437	0.017
Q39595	ATP sulfurylase Ats1	4	-1.772	0.010
P07891	ATP synthase epsilon chain, chloroplastic (ATP synthase F1 sector epsilon subunit) (F-ATPase epsilon subunit)	3	-4.291	0.012
P12113	ATP synthase gamma chain, chloroplastic (F-ATPase gamma subunit)	4	-3.058	0.007
Q96550	ATP synthase subunit alpha	20	-1.967	0.000

B7U1J0	ATP synthase subunit alpha, chloroplastic (EC 3.6.3.14) (ATP synthase F1 sector subunit alpha) (F-ATPase subunit alpha)	18	-2.976	0.000
P26526	ATP synthase subunit alpha, chloroplastic (EC 3.6.3.14) (ATP synthase F1 sector subunit alpha) (F-ATPase subunit alpha)	18	-2.976	0.000
A81QU3	ATP synthase subunit beta (EC 3.6.3.14)	26	-2.329	0.000
P06541	ATP synthase subunit beta, chloroplastic (EC 3.6.3.14) (ATP synthase F1 sector subunit beta) (F-ATPase subunit beta)	63	-2.371	0.000
P38482	ATP synthase subunit beta, mitochondrial (EC 3.6.3.14)	26	-2.329	0.000
A81J60	ATP-dependent Clp protease proteolytic subunit (EC 3.4.21.92)	3	-2.952	0.002
A81XF1	ATP-sulfurylase	4	-1.772	0.010
A81XZ0	Beta tubulin 1 (Beta tubulin 2)	37	-2.124	0.000
A8JGS8	Beta'-cop	8	-2.108	0.000
A817T8	Binding protein 1	39	-1.817	0.000
A817S9	Binding protein 2	37	-1.812	0.000
A8JGF4	Biotin carboxylase, acetyl-CoA carboxylase component	7	-1.860	0.000
A81542	Calcium-transporting ATPase, endoplasmic reticulum-type	2	1.380	0.026
Q9STD3	Calreticulin	3	-2.097	0.018
A8HMC0	Calreticulin 2, calcium-binding protein	3	-2.097	0.018
A8JIR0	Carbamoyl phosphate synthase, large subunit (EC 6.3.5.5)	17	-2.023	0.000
Q695H0	CGMP-dependent protein kinase (EC 2.7.1.37) (cGMP-dependent protein kinase)	3	-2.572	0.021
A8JIB7	Chaperonin 60A	7	-1.740	0.000
A81TH8	Chaperonin 60B2	10	-1.998	0.000
A81MK1	Chaperonin 60C (Fragment)	6	-2.126	0.000
A8HXL8	Chloroplast ATP synthase gamma chain	4	-3.058	0.007
A8J2Z6	Chorismate synthase (EC 4.2.3.5)	4	-2.226	0.001
A8J2S0	Citrate synthase	4	-2.725	0.013
A814S9	Clathrin heavy chain	11	1.321	0.000
A81972	ClpB chaperone, Hsp100 family	9	-1.903	0.000
A8JA18	ClpB chaperone, Hsp100 family	9	-1.807	0.000
A8HRR9	Coatomer subunit alpha	15	-1.800	0.000
A81M71	Coatomer subunit gamma	8	-1.685	0.004
A8HYR2	Cobalamin-dependent methionine synthase (EC 2.1.1.13)	4	-2.231	0.004
A81EE5	Cysteine synthase (EC 2.5.1.47)	5	-2.553	0.005
A81SA9	Cysteine synthase (EC 2.5.1.47)	6	-2.629	0.001
A81SB0	Cysteine synthase (EC 2.5.1.47)	6	-2.629	0.001
O81523	Cysteine synthase (EC 2.5.1.47)	6	-2.629	0.001
A81T25	Cytoplasmic DEXD/H-box RNA helicase	3	-1.891	0.013
A8J7F6	Dihydrolipoamide acetyltransferase (EC 2.3.1.12)	4	-2.672	0.000
A8J1T4	Dihydrolipoyl dehydrogenase (EC 1.8.1.4)	3	1.149	0.023
A815K1	Dynamamin-related GTPase (EC 2.6.1.42)	6	1.464	0.007
A8JHX9	Elongation factor 2 (EC 3.6.5.3)	13	-2.017	0.000
P17746	Elongation factor Tu, chloroplastic (EF-Tu)	12	-1.674	0.002
A8JH98	Enolase (EC 4.2.1.11)	16	-1.628	0.000
A81232	Eukaryotic initiation factor	3	-2.049	0.010
A81VV9	Eukaryotic initiation factor (Fragment)	3	-2.256	0.006
A8HRF8	Eukaryotic translation initiation factor 3 subunit A (eIF3a) (Eukaryotic translation initiation factor 3 subunit 10)	4	1.303	0.012
A8JHB4	Ferredoxin-dependent glutamate synthase	6	-1.964	0.002
A8J6Y8	Ferredoxin--NADP reductase (EC 1.18.1.2)	8	-2.048	0.000
Q9S9E0	Ferredoxin--NADP reductase (EC 1.18.1.2)	8	-2.048	0.000
P53991	Ferredoxin--NADP reductase, chloroplastic (FNR) (EC 1.18.1.2)	8	-2.048	0.000

Q84X68	Flagella membrane glycoprotein 1B	4	-1.429	0.026
A8HW56	Flagellar associated protein (EC 3.6.1.3)	20	-1.996	0.000
A8IKQ0	Fructose-1,6-bisphosphatase (EC 3.1.3.11)	4	-1.771	0.002
Q42690	Fructose-bisphosphate aldolase 1, chloroplastic (EC 4.1.2.13)	3	-2.292	0.005
A8J3F9	GDP-D-mannose pyrophosphorylase	6	-2.103	0.000
A8HNE8	Geranylgeranyl reductase (EC 1.3.1.-)	4	-2.124	0.018
A8HS14	Glucose-1-phosphate adenyltransferase (EC 2.7.7.27) (ADP-glucose pyrophosphorylase)	6	1.199	0.013
Q9LLL6	Glucose-1-phosphate adenyltransferase (EC 2.7.7.27) (ADP-glucose pyrophosphorylase)	6	-1.653	0.001
A8IE23	Glucose-6-phosphate isomerase (EC 5.3.1.9)	11	-2.404	0.000
A8JGD1	Glutamate dehydrogenase	4	-1.950	0.005
A8IVZ9	Glutamine synthetase (EC 6.3.1.2)	4	-2.502	0.023
A8IW00	Glutamine synthetase (EC 6.3.1.2)	4	-2.502	0.023
Q42689	Glutamine synthetase, chloroplastic (EC 6.3.1.2) (GS2) (Glutamate-- ammonia ligase)	4	-2.502	0.023
A8HP84	Glyceraldehyde-3-phosphate dehydrogenase (EC 1.2.1.-)	26	-2.147	0.000
P50362	Glyceraldehyde-3-phosphate dehydrogenase A, chloroplastic (EC 1.2.1.13) (NADP-dependent glyceraldehydephosphate dehydrogenase subunit A)	26	-2.147	0.000
A8HNN4	Glycerol-3-phosphate dehydrogenase [NAD(+)] (EC 1.1.1.8)	8	2.648	0.001
A8IVM9	Glycine cleavage system, P protein (EC 1.4.4.2)	4	-2.973	0.008
A8IRX5	GTP-binding nuclear protein	5	-1.681	0.006
Q39570	GTP-binding protein YPTC4	10	-1.582	0.000
P25387	Guanine nucleotide-binding protein subunit beta-like protein	6	-2.430	0.000
P25840	Heat shock 70 kDa protein	25	-1.850	0.000
A8JEU4	Heat shock protein 70A (EC 3.6.1.3)	34	-1.880	0.000
A8HYV3	Heat shock protein 70B	25	-1.708	0.000
Q39603	Heat shock protein 70B	25	-1.708	0.000
A8IZU0	Heat shock protein 70C	16	-1.731	0.000
A8J1U1	Heat shock protein 90A	22	-1.848	0.000
A8I7T1	Heat shock protein 90B (Fragment)	5	-1.771	0.004
Q66T67	Heat shock protein 90C	4	-1.868	0.002
A8HRZ9	Histone H2A	4	-2.971	0.005
A8JIN6	Histone H2B	4	-4.409	0.001
A8HVA3	Histone H4	6	-2.710	0.000
A8JIN9	Histone H4	6	-2.710	0.000
P50566	Histone H4	6	-2.710	0.000
Q944M9	Iron-sulfur cluster assembly protein	4	1.311	0.006
A8JG03	Isopropylmalate dehydratase, large subunit	6	-1.531	0.016
A8J955	Kinesin-like calmodulin binding protein (Fragment)	9	-1.866	0.000
Q93WE2	Magnesium chelatase H subunit (Magnesium chelatase H-subunit)	5	-2.149	0.011
A8I7P5	Magnesium chelatase subunit H	5	-2.149	0.011
Q94FT3	Magnesium-chelatase subunit ChII, chloroplastic (Mg-chelatase subunit I-1) (EC 6.6.1.1) (Mg-protoporphyrin IX chelatase subunit ChII)	5	-1.638	0.017
A8ICG9	Malate dehydrogenase (EC 1.1.1.37)	11	-1.507	0.006
Q8H0R8	Malate dehydrogenase (EC 1.1.1.37) (Fragment)	3	1.298	0.023
P93106	Malate dehydrogenase (NAD-dependent malate dehydrogenase) (EC 1.1.1.37)	4	-2.252	0.020
A8IL08	Membrane AAA-metalloprotease (EC 3.4.24.-)	17	-1.771	0.000
A8I531	Mg-protoporphyrin IX chelatase (EC 6.6.1.1)	5	-2.222	0.003
A8IMZ5	Mg-protoporphyrin IX chelatase (EC 6.6.1.1)	5	-1.638	0.017
I2FKQ9	Mitochondrial chaperonin 60	6	-2.126	0.000

A8IKE3	Mitogen-activated protein kinase (EC 2.7.11.24)	3	-2.003	0.026
C0SPI7	Mitogen-activated protein kinase (EC 2.7.11.24)	3	-2.003	0.026
A8JCP5	NAD(P) transhydrogenase	10	1.203	0.009
A8I893	NAD-dependent epimerase/dehydratase	3	1.554	0.012
A2PZD2	NAD-dependent epimerase/dehydratase (Predicted protein)	3	1.474	0.010
Q6V9A8	NADH:ubiquinone oxidoreductase 49 kD subunit (EC 1.6.5.3) (NADH:ubiquinone oxidoreductase 49 kDa ND7 subunit)	4	-1.909	0.003
A8IA86	Nucleolar protein, component of C/D snoRNPs	7	-2.261	0.002
A8IID0	Nucleolar protein, component of C/D snoRNPs	2	-2.269	0.024
A8J9H8	Nucleoside diphosphate kinase (EC 2.7.4.6)	6	-1.584	0.001
A8JH12	Nucleoside diphosphate kinase (EC 2.7.4.6)	4	-1.585	0.003
A8J0E4	Oxygen-evolving enhancer protein 1 of photosystem II	20	-2.300	0.000
P12853	Oxygen-evolving enhancer protein 1, chloroplastic (OEE1)	20	-2.300	0.000
A8IYH9	Oxygen-evolving enhancer protein 2 of photosystem II	10	-2.072	0.001
P11471	Oxygen-evolving enhancer protein 2, chloroplastic (OEE2)	10	-2.072	0.001
A8IY43	Peptidyl-prolyl cis-trans isomerase (PPIase) (EC 5.2.1.8)	4	1.218	0.028
Q3HTK2	Pherophorin-C5 protein	3	-1.983	0.002
P81831	Phosphoenolpyruvate carboxylase 1 (PEP carboxylase 1) (PEPC 1) (PEPCase 1) (EC 4.1.1.31)	4	-2.116	0.018
Q6R2V6	Phosphoenolpyruvate carboxylase 2 (PEP carboxylase 2) (PEPC 2) (PEPCase 2) (EC 4.1.1.31)	3	-1.710	0.016
A8J8Z2	Phosphoglucomutase (EC 5.4.2.2)	5	1.127	0.026
A8JC04	Phosphoglycerate kinase (EC 2.7.2.3)	26	-1.554	0.004
Q548U3	Phosphoglycerate kinase (EC 2.7.2.3)	23	-1.506	0.009
P41758	Phosphoglycerate kinase, chloroplastic (EC 2.7.2.3)	23	-1.506	0.009
A8HVV5	Phosphoglycerate mutase (EC 5.4.2.1)	4	-1.586	0.002
A8HVV9	Phosphoglycerate mutase (EC 5.4.2.1)	4	-1.586	0.002
Q94KV1	Phosphoglyceromutase	4	-1.586	0.002
A8IYP4	Phosphoribulokinase (EC 2.7.1.19)	18	-3.650	0.000
P19824	Phosphoribulokinase, chloroplastic (PRK) (PRKase) (EC 2.7.1.19) (Phosphopentokinase)	18	-3.650	0.000
P13352	Photosystem I reaction center subunit VI, chloroplastic (PSI-H) (Light-harvesting complex I 11 kDa protein) (P28 protein)	3	-2.285	0.018
P10898	Photosystem II CP43 reaction center protein (PSII 43 kDa protein) (Protein CP-43) (Protein P6)	25	-1.469	0.008
P07753	Photosystem II protein D1 (PSII D1 protein) (EC 1.10.3.9) (32 kDa thylakoid membrane protein) (Photosystem II Q(B) protein)	10	-1.445	0.011
A8J503	Plastid ribosomal protein L6	5	-1.170	0.006
A8IYS1	Plastid ribosomal protein L9	2	-1.454	0.021
A8JFB1	Porphobilinogen deaminase	8	-1.440	0.013
A8HQ77	Predicted protein	2	-1.958	0.023
A8I804	Predicted protein	2	1.815	0.027
A8IBN3	Predicted protein	3	-1.665	0.028
A8IBV4	Predicted protein	7	1.193	0.004
A8IIB7	Predicted protein	2	-2.813	0.015
A8ITU2	Predicted protein	4	1.460	0.003
A8IWJ5	Predicted protein	4	-2.101	0.004
A8IWT7	Predicted protein	5	1.174	0.032
A8IX35	Predicted protein	5	1.666	0.021
A8J3F8	Predicted protein	3	1.241	0.029
A8J4Y6	Predicted protein	6	-2.007	0.001
A8J7F9	Predicted protein	3	-1.817	0.008
A8JBM7	Predicted protein	7	1.298	0.005

A8JG58	Predicted protein	6	1.125	0.020
A8HQ56	Predicted protein (Fragment)	2	1.224	0.016
A8IBY2	Predicted protein (Fragment)	11	-1.655	0.000
A8IKW9	Predicted protein (Fragment)	3	-1.778	0.003
A8JFI7	Predicted protein (Fragment)	4	-1.837	0.016
A8J633	Prohibitin	4	1.405	0.024
A8IRE2	Proteasome subunit alpha type (EC 3.4.25.1)	4	1.416	0.017
A8J6K9	Proteasome subunit alpha type (EC 3.4.25.1)	2	-2.939	0.022
A8HQT1	Protein disulfide isomerase	4	1.345	0.003
A8J709	Protein phosphatase 2A regulatory subunit (EC 3.1.3.16)	5	-1.578	0.001
A8IDT3	Putative uncharacterized protein	3	1.274	0.020
A8IVR6	Pyruvate kinase (EC 2.7.1.40)	13	-2.006	0.000
A8J345	Pyruvate kinase (EC 2.7.1.40)	4	1.273	0.018
A8HMX2	Pyruvate-formate lyase (EC 2.3.1.54)	7	-1.164	0.005
A8I6T5	R1 protein, alpha-glucan water dikinase	8	1.459	0.000
A8J146	Rab GDP dissociation inhibitor protein	4	-2.042	0.006
Q39572	Ras-related protein YPTC6	6	-1.461	0.005
A8J8Y1	Receptor of activated protein kinase C 1	6	-2.430	0.000
A8I8Z4	Ribosomal protein	2	-2.677	0.028
A8JI94	Ribosomal protein L22	3	1.452	0.005
A8J239	Ribosomal protein L23a	3	-2.276	0.016
A8J567	Ribosomal protein L7a	4	-2.002	0.006
A8JHC3	Ribosomal protein S11	4	1.397	0.007
A8JE07	Ribosomal protein S15a	3	-1.756	0.018
A8HSU7	Ribosomal protein S16	5	1.375	0.015
A8I4P5	Ribosomal protein S3	7	-1.471	0.006
A8J2I5	Ribosomal protein S5	5	1.366	0.009
A8JGI9	Ribosomal protein S7	4	-2.116	0.005
P00877	Ribulose biphosphate carboxylase large chain (RuBisCO large subunit) (EC 4.1.1.39)	83	-2.751	0.000
P23489	Ribulose biphosphate carboxylase/oxygenase activase, chloroplastic (RA) (RuBisCO activase)	12	-2.809	0.000
Q6SA05	Rubisco activase	12	-2.809	0.000
Q42694	RuBisCO large subunit-binding protein subunit alpha, chloroplastic (60 kDa chaperonin subunit alpha) (CPN-60 alpha)	7	-1.740	0.000
A8II71	RuvB-like helicase (EC 3.6.4.12)	5	-1.781	0.003
A8J4W8	RuvB-like helicase (EC 3.6.4.12)	4	-3.167	0.023
A8HYU5	S-adenosylmethionine synthase (AdoMet synthase) (EC 2.5.1.6) (Methionine adenosyltransferase) (MAT)	17	-1.432	0.000
A8JC30	Sar-type small GTPase	5	-1.832	0.005
A8JFY9	Serine glyoxylate aminotransferase (EC 2.6.1.45)	5	-1.592	0.002
Q8W4V3	Serine hydroxymethyltransferase (EC 2.1.2.1)	7	-1.154	0.002
A8JBP0	Serine/threonine-protein phosphatase (EC 3.1.3.16)	2	-2.863	0.035
Q9XGU3	Serine/threonine-protein phosphatase (EC 3.1.3.16)	4	-2.289	0.006
A8HNE3	Serine/threonine-protein phosphatase (EC 3.1.3.16) (Fragment)	8	-2.030	0.000
A8JCM8	SM/Sec1-family protein	2	1.323	0.033
A8IRT2	Small rab-related GTPase	6	-1.461	0.005
A8J195	Small rab-related GTPase	10	-1.582	0.000
Q4U1D9	Soluble starch synthase III	3	1.427	0.004
A8HPL0	Splicing factor, component of the U5 snRNP and of the spliceosome	3	-2.140	0.015
A8HW52	Starch branching enzyme (EC 2.4.1.18)	3	-2.318	0.008

A8IH77	Subunit H of photosystem I	3	-2.285	0.018
A8HX04	Succinate dehydrogenase [ubiquinone] iron-sulfur subunit, mitochondrial (EC 1.3.5.1)	3	-2.995	0.004
A8II42	T-complex protein 1 subunit gamma	4	-1.871	0.007
A8J014	T-complex protein, zeta subunit	3	-2.078	0.020
A8IAN1	Transketolase (EC 2.2.1.1)	26	-1.538	0.000
A8IFZ9	Tryptophan synthase beta subunit	7	-1.420	0.001
P09204	Tubulin alpha-1 chain	22	-2.327	0.000
P09205	Tubulin alpha-2 chain	21	-2.392	0.000
P04690	Tubulin beta-1/beta-2 chain (Beta-tubulin)	37	-2.124	0.000
A8J5P7	Ubiquinol:cytochrome c oxidoreductase 50 kDa core 1 subunit	6	-1.832	0.004
A8J1C1	Ubiquitin-activating enzyme E1 (EC 6.3.2.19)	5	1.097	0.017
A2PZC3	UDP-glucose 6-dehydrogenase (EC 1.1.1.22)	2	2.008	0.042
A2PZC2	UDP-Glucose:protein transglucosylase (UDP-glucose protein: protein trans glycosylase)	14	-2.510	0.000
Q763T6	UDP-sulfoquinovose synthase	5	-1.770	0.001
P36495	Uncharacterized membrane protein ycf78 (ORF-S) (ORF1995) (ORFA)	5	1.210	0.003
A8IA45	Vacuolar ATP synthase subunit B	11	-2.042	0.001
A8I164	Vacuolar ATP synthase, subunit A	16	-2.087	0.000

---